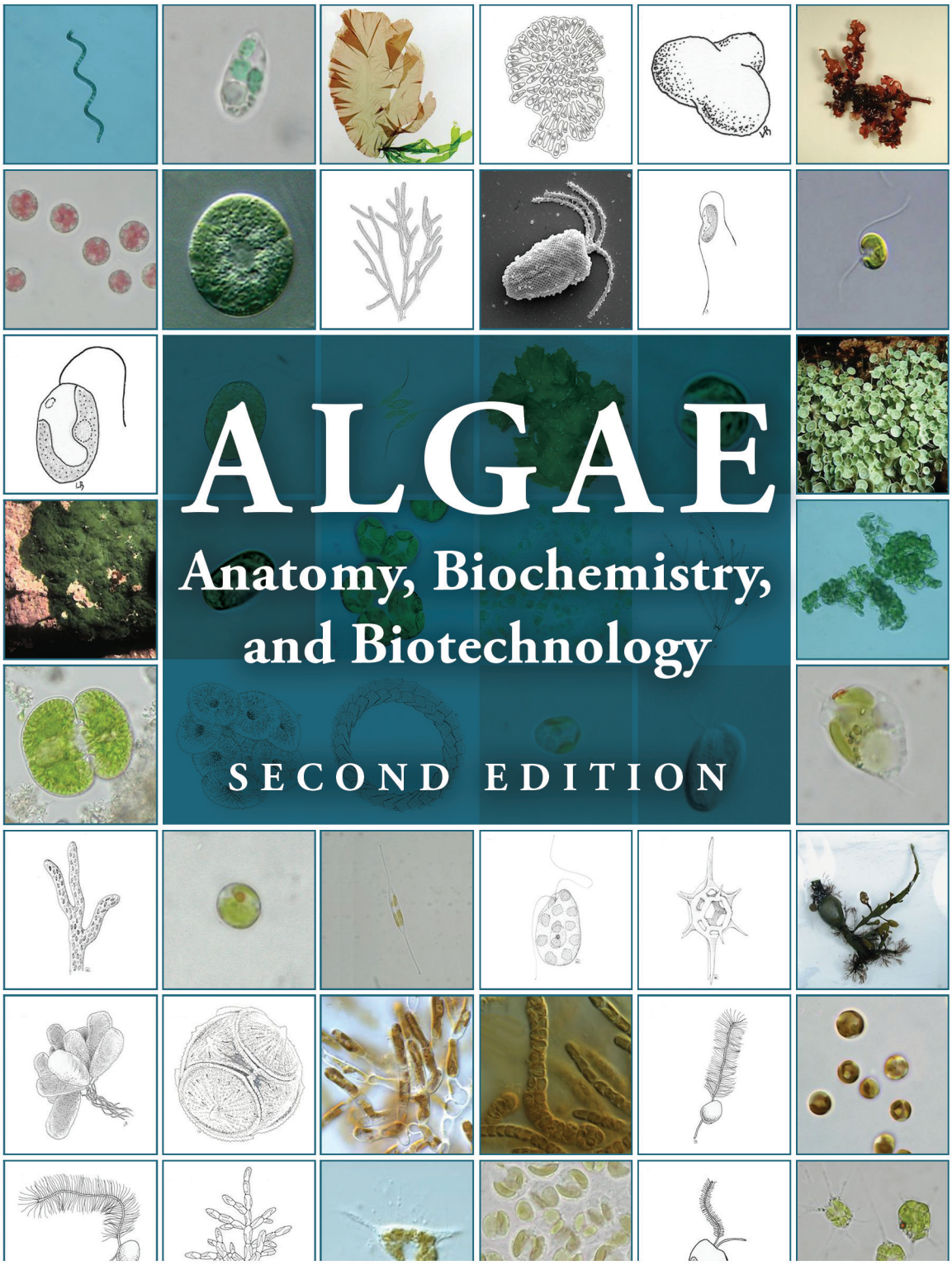

ALGAE

Anatomy, Biochemistry, and Biotechnology

SECOND EDITION

LAURA BARSANTI • PAOLO GUALTIERI

CRC Press
Taylor & Francis Group

ALGAE

ANATOMY, BIOCHEMISTRY, AND BIOTECHNOLOGY

SECOND EDITION

ALGAE

ANATOMY, BIOCHEMISTRY, AND BIOTECHNOLOGY

SECOND EDITION

LAURA BARSANTI • PAOLO GUALTIERI

Istituto di Biofisica
Pisa, Italy

CRC Press
Taylor & Francis Group
Boca Raton London New York

CRC Press is an imprint of the
Taylor & Francis Group, an **informa** business

CRC Press
Taylor & Francis Group
6000 Broken Sound Parkway NW, Suite 300
Boca Raton, FL 33487-2742

Version Date: 20130827

International Standard Book Number-13: 978-1-4398-6733-4 (eBook - PDF)

Alla Lilli, perché è sempre la mia mamma, anche se mi fa diventare matto come quando ero piccino [(ti voglio bene, mamma!)]

Paolo

To my mom, Silvana (1926–2008), and my dad, Renzo (1928–2009), because I know they are still watching over me, and to Bernard (1952–2011) pour son voyage en solitaire (nakupenda tarepanda)

Laura

Contents

Preface

In the seven years since the first edition of this book was published, we have built up a large amount of new material and data in the field of algology, based on our own experiences in reading, writing, and reviewing. With the aid of all this information, we have completely revised the book, introducing the following changes and additions:

- We have added 27 new figures for a total of 205 figures, many of them in color
- All the 38 tables have been revised and rewritten
- We have updated the literature in all chapters
- We wrote an entirely new chapter on how odd algae can be
- We have rewritten Chapter 1, updating the classification of algae and modifying the section on the endosymbiosis and origin of eukaryotic photosynthesis
- We have expanded Chapter 2, adding new types of root systems and algal swimming patterns and modifying the section on photoreception and photoreceptors
- We have updated Chapter 3, adding absorption spectra measured on samples from all algal divisions together with their decomposition in pigments. We have also added the absorption spectra of all the chlorophylls and the accessory pigments
- We have modified notation and wording of Chapters 4 and 5
- We have expanded section on collection storage and preservation in Chapter 6, adding new information on automatic algae recognition and classification
- We have rewritten Chapter 7, updating the section on algal toxins and algal bioactive molecules
- We have, of course, corrected the numerous errors present in the first edition (we do apologize for them), doing our best to avoid errors in this new edition

Like the previous edition, this book is written and designed for undergraduate and postgraduate students with a general scientific background, having their first academic experience with the world of algae, as well as researchers, teachers, and professionals in the field of phycology and applied phycology. Our major commitment is still the same, challenging and stimulating both students and teachers to move beyond the limit of the written page to further explore not only the topics highlighted in the book, but also all the new ideas that can spring to mind (we hope!) after reading each chapter.

Though updated, the bibliography is still by no means exhaustive; we have not attempted to be comprehensive and many excellent papers will be missing. Our intention was to put in only enough to lead the readers into the right part of the primary literature in a fairly directed manner and to provide a sort of orienteering compass in the "mare magnum" of scientific literature.

We are deeply grateful to the staff at CRC Press, Boca Raton, FL, particularly our patient and comprehensive editor John Sulzycki for trusting us enough to ask for a second edition and to the senior project coordinator Jill Jurgensen, who had to cope with all our e-mail.

Again, our sincere gratitude and a special thanks to Valter Evangelista for his skillful assistance and ability in preparing the final form of all the drawings and illustrations, and for his careful attention in preparing all the technical drawings of this second edition. We appreciate his efforts to keep pace with us both and to cope with our ever-changing demands and corrections and second thoughts without getting too upset. We know we have driven him crazy.

And we will always be grateful to Vincenzo Passarelli, who took care of the lab, making our work lighter and smoother. Next February he will retire, leaving our group after more than 30 years;

we have grown old together and we already know we will miss his smile, and his special trumpet-like whistling.

For the new illustrations present in the book, we are indebted to Luca Barsanti, brother of Laura and Maria Antonietta, who succeeded in realizing most of the drawing of our book before dying in February 2005. He made the drawing work in a wonderful way, confirming his artistic skill. Though almost eight years have passed by, and some snow has also fallen on his roof, he is still the same light-hearted and amusing company who delighted us during the preparation of the first edition. We will be always grateful to him.

Authors

Dr. Paolo Gualtieri graduated in biology and computer science from University of Pisa, Italy. At present, he is senior scientist at the Biophysics Institute of the National Council of Research (CNR) in Pisa, Italy, and adjunct professor of University of Maryland, University College, College Park, MA, USA. He is a professional orchestral trumpet player.

Dr. Laura Barsanti graduated in natural science from University of Pisa, Italy. At present, she is a scientist at the Biophysics Institute of the National Council of Research (CNR) in Pisa (Italy).

1 General Overview

DEFINITION

The term *algae* has no formal taxonomic standing; however, it is routinely used to indicate a polyphyletic (i.e., including organisms that do not share a common origin, but follow multiple and independent evolutionary lines), non-cohesive, and artificial assemblage of O_2-evolving, photosynthetic organisms (with several exceptions of colorless members undoubtedly related to pigmented forms). According to this definition, plants could be considered an algal division. Algae and plants produce the same storage compounds as well as use similar defense strategies against predators and parasites. A strong morphological similarity exists between some algae and plants; however, distinguishing algae from plants is quite easy since the similarities we have listed between algae and plants are much fewer than their differences. Plants show a very high degree of differentiation, with roots, leaves, stems, and xylem/phloem vascular network, their reproductive organs are surrounded by a jacket of sterile cells, they have a multicellular diploid embryo stage that remains developmentally and nutritionally dependent on the parental gametophyte for a significant period (and this feature is the source of the name embryophytes given to plants), and tissue-generating parenchymatous meristems at the shoot and root apices producing tissues that differentiate in a wide variety of shapes. Moreover, all plants have a digenetic life cycle, with an alternation between a haploid gametophyte and a diploid sporophyte. Algae do not have any of these features, they do not have roots, stems, leaves, nor well-defined vascular tissues, even though many seaweeds are plant-like in appearance and some of them show specialization and differentiation of their vegetative cells, they do not form embryos, their reproductive structures consist of cells that are all potentially fertile and lack sterile cells covering or protecting them, parenchymatous development is present only in some groups, and have both monogenetic and digenetic life cycles. Moreover, algae occur in dissimilar forms such as microscopic single cells, macroscopic multicellular loose or filmy conglomerations, matted or branched colonies, or more complex leafy or blade forms, which contrast strongly with uniformity in vascular plants. Evolution may have worked in two ways: one for shaping similarities and one for shaping differences. The same environmental pressure led to the parallel, independent evolution of similar traits in both plants and algae, while the transition from relatively stable aquatic environment to a gaseous medium exposed plants to new physical conditions that resulted in key physiological and structural changes necessary to be able to invade upland habitats and fully exploit them. The bottom line is that plants are a separate group with no overlapping with the algal assemblage.

The profound diversity of size ranging from picoplankton only 0.2–2.0 μm in diameter to giant kelps with fronds up to 60 m in length, ecology and colonized habitats, cellular structure, levels of organization and morphology, pigments for photosynthesis, reserve and structural polysaccharides, type of life history reflect the varied evolutionary origins of this heterogeneous assemblage of organisms, including both prokaryote and eukaryote species. The term *algae* refers to macroalgae and a highly diversified group of microorganisms known as microalgae. Estimates of the number of living algae varies from 30,000 to more than 1 million species, but most of the reliable estimates refer to the numbers given in AlgaeBase, which currently documents 32,260 species of organisms generally regarded as algae of an estimated 43,918 described species of algae, corresponding to about 73%. According to the AlgaeBase estimate of 28,500 species waiting for description, the total number of algal species is likely to be about 72,500, of which more than 20,000 will be diatomic.

CLASSIFICATION

Over the past 30 years, molecular phylogenetic studies have led to extensive modification of traditional classification schemes for algae; nowadays no easily definable classification system acceptable to all exists for this group of organisms, since taxonomy is under constant and rapid revision at all levels following everyday new genetic and ultrastructural evidence. Keeping in mind that the polyphyletic nature of the algal group is somewhat inconsistent with traditional taxonomic groupings, though they are still useful to define the general characteristics and levels of organizations, and aware of the fact that taxonomic opinion may change as information accumulates, we will adopt a tentative scheme of classification mainly based on the most recently published classifications. In particular, we will integrate the most recent publications on revised classifications of eukaryotes and specific groups to obtain a classification scheme highlighting the presence of algae in the four kingdoms of Bacteria, Plantae, Chromista, and Protozoa. The main purpose of the classification here reported is to categorize the diversity of the algae in a very practical manner, providing names useful for teaching students and searching the literature.

Prokaryotic members of this assemblage are grouped into the kingdom Bacteria, phylum Cyanobacteria, with the single class of Cyanophyceae. Members of the proposed division Prochlorophyta, considered artificial, are currently included in this class.

Eukaryotic members are grouped into the three kingdoms of Plantae, with four phyla, Chromista, with four phyla, and Protozoa, with two phyla. Table 1.1 shows the different classes comprised in the 11 phyla. Figure 1.1 shows examples of representatives of each class.

OCCURRENCE AND DISTRIBUTION

Algae can be aquatic or subaerial, when they are exposed to the atmosphere rather than being submerged in water. Aquatic algae are found almost everywhere from freshwater spring to salt lakes, with tolerance for a broad range of pH, temperature, turbidity, O_2, and CO_2 concentration. They can be planktonic, as most unicellular species do, living suspended throughout the lighted regions of all water bodies including under ice in polar areas. They can also be benthonic, attached to the bottom or living within sediments, limited to shallow areas because of the rapid attenuation of light with depth. Benthic algae can grow attached on stones (epilithic), on mud or sand (epipelic), on other algae or plants (epiphytic), or on animals (epizoic). In the case of marine algae, other terms can also be used to describe their growth habits, such as supralittoral, when they grow above the high-tide level, within the reach of waves and spray; intertidal, when they grow on shores exposed to tidal cycles; or sublittoral, when they grow in the benthic environment from the extreme low-water level to around 200-m deep, in the case of very clear water.

Oceans covering about 71% of the earth's surface contain more than 5000 species of planktonic microscopic algae, the phytoplankton, which forms the base of the marine food chain and produces roughly 50% of the oxygen we inhale. However, phytoplankton is not only a cause of life, but also sometimes a cause of death. When the population becomes too large in response to pollution with nutrients such as nitrogen and phosphate, these blooms can reduce the water transparency, causing the death of other photosynthetic organisms. They are often responsible for massive fish and bird kills, producing poisons and toxins. The temperate pelagic marine environment is also the realm of giant algae, the kelp. These algae have thalli up to 60-m long, and the community can be so crowded that it forms a real submerged forest; they are not limited to temperate waters, as they also form luxuriant thickets beneath polar ice sheets, and can survive at very low depth (more than 200 m), where the faint light is bluish-green and its intensity is only 0.0005% that of surface light. At these depths, the red part of the sunlight spectrum is filtered out from the water and not enough energy is available for photosynthesis. These algae can survive in the dark blue sea since they possess accessory pigments that absorb light in spectral regions different from those of the green chlorophylls *a* and *b* and channel this absorbed light energy into chlorophyll *a*, which is the only molecule able to convert sunlight

TABLE 1.1
Classification Scheme of the Different Algal Groups

	Kingdom	Subkingdom	Infrakingdom	Phylum	Class	Representative	Image
Prokaryota	Bacteria	Negibacteria		Cyanobacteria	Cyanophyceae	*Arthrospira*	1.1a
Eukaryota	Plantae	Biliphyta		Glaucophyta	Glaucophyceae	*Cyanophora*	1.1b
				Rhodophyta	Bangiophyceae	*Porphyra*	1.1c
					Compsopogonophyceae	*Erythrocladia*	1.1d
					Cyanidiophyceae	*Cyanodioschyzon*	1.1e
					Florideophyceae	*Phyllophora*	1.1f
					Porphyridiophyceae	*Porphyridium*	1.1g
					Rhodellophyceae	*Glaucosphaera*	1.1h
					Stylonematophyceae	*Stylonema*	1.1i
		Viridiplantae	Chlorophyta	Chlorophyta	Prasinophytes	*Pyramimonas*	1.1l
					Mamiellophyceae	*Crustomastix*	1.1m
					Nephroselmidophyceae	*Nephroselmis*	1.1n
					Pedinophyceae	*Pedinomonas*	1.1o
					Chlorodendrophyceae	*Tetraselmis*	1.1p
					Chlorophyceae	*Scenedesmus*	1.1q
					Ulvophyceae	*Ulva*	1.1r
					Trebouxiophyceae	*Chlorella*	1.1s
					Dasycladophyceae	*Acetabularia*	1.1t
					Palmophyllales	*Palmophyllum*	1.1u
			Streptophyta	Charophyta	Mesostigmatophyceae	*Mesostigma*	1.1v
					Chlorokybophyceae	*Chlorokybus*	1.1z
					Klebsormidiophyceae	*Klebsormidium*	1.1aa
					Charophyceae	*Nitella*	1.1ab
					Coleochaetophyceae	*Coleochaete*	1.1ac
					Zygnematophyceae	*Cosmarium*	1.1ad
	Chromista	Hacrobia		Haptophyta	Coccolithophyceae (Prymnesiophyceae)	*Umbellosphaera*	1.1ae
					Haptophyta incertae sedis	*Coronocyclus*	1.1af
					Pavlovophyceae	*Pavlova*	1.1ag

continued

TABLE 1.1 (continued)
Classification Scheme of the Different Algal Groups

Kingdom	Subkingdom	Infrakingdom	Phylum	Class	Representative	Image
			Cryptophyta	Cryptophyceae	*Rhodomonas*	1.1ah
	Harosa	Heterokonta	Ochrophyta	Chrysophyceae	*Ochromonas*	1.1ai
				Xanthophyceae	*Vaucheria*	1.1al
				Eustigmatophyceae	*Nannochloropsis*	1.1am
				Bacillariophyceae	*Cylindrotheca*	1.1an
				Raphidophyceae	*Heterosigma*	1.1ao
				Dictyochophyceae	*Distephanus*	1.1ap
				Phaeophyceae	*Ascophyllum*	1.1aq
				Pelagophyceae	*Chrysophaeum*	1.1ar
				Bolidophyceae	*Tetraparma*	1.1as
				Schizocladiophyceae	*Schizocladia*	1.1at
				Chrysomerophyceae	*Gyraudiopsis*	1.1au
				Picophagophyceae	*Picophagus*	1.1av
				Pinguiophyceae	*Pinguiococcus*	1.1az
				Placidiophyceae	*Placidia*	1.1ba
				Phaeothamniophyceae	*Phaeothamnion*	1.1bb
				Synchromophyceae	*Synchroma*	1.1bc
				Synurophyceae	*Synura*	1.1bd
				Aurearenophyceae	*Aurearena*	1.1be
			Cercozoa	Chlorarachniophyceae	*Gymnochlora*	1.1bf
Protozoa	Biciliata	Alveolata	Myzozoa	Dinophyceae	*Prorocentrum*	1.1bg
					Lepidodinium	1.1bh
	Eozoa	Euglenozoa	Euglenozoa	Euglenophyceae	*Euglena*	1.1bi
					Phacus	1.1bl
					Trachelomonas	1.1bm
					Peranema	1.1bn

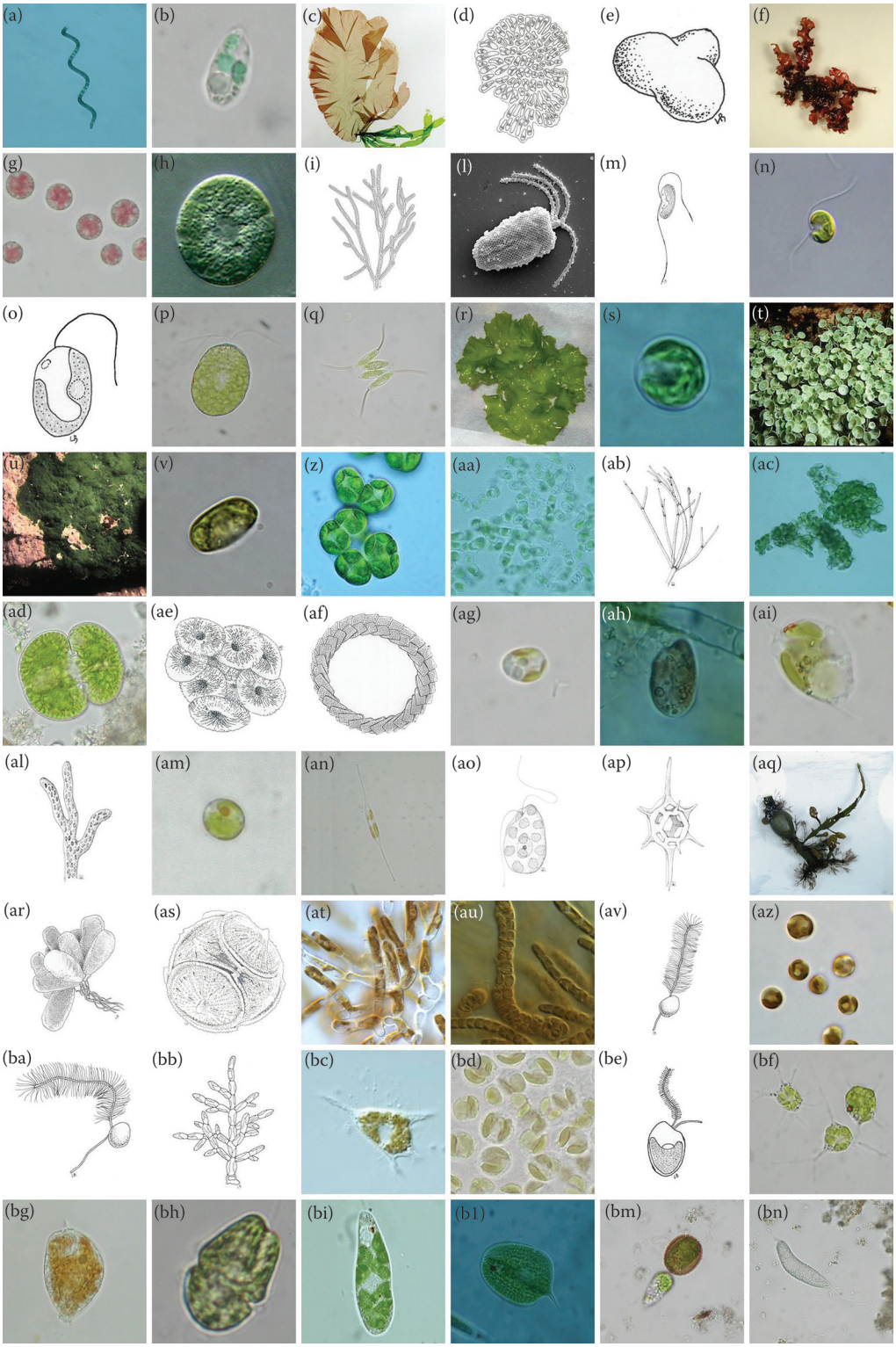

FIGURE 1.1 Examples of representatives of the different algal classes. See Table 1.1 for details. (Figures 1.1c, 1.1t, 1.1u—courtesy of Prof. Gianfranco Sartoni.)

TABLE 1.2
Distribution of Algal Divisions

		Habitat			
Phylum	**Common Name**	**Marine**	**Freshwater**	**Terrestrial**	**Symbiotic**
Cyanobacteria	Blue-green algae	Yes	Yes	Yes	Yes
Glaucophyta	n.a.	n.d.	Yes	Yes	Yes
Rhodophyta	Red algae	Yes	Yes	Yes	Yes
Chlorophyta	Green algae	Yes	Yes	Yes	Yes
Charophyta	n.a.	Yes	Yes	Yes	n.d.
Haptophyta	Coccolithophorids	Yes	Yes	Yes	Yes
Cryptophyta	Cryptomonads	Yes	Yes	n.d.	Yes
Ochrophyta	Golden algae Yellow-green algae Diatoms Brown algae	Yes	Yes	Yes	Yes
Cercozoa (Chlorarachniophyceae)	n.a.	Yes	n.d.	n.d.	Yes
Myzozoa (Dynophyceae)	Dinoflagellates	Yes	Yes	n.d.	Yes
Euglenozoa (Euglenophyceae)	Euglenoids	Yes	Yes	Yes	Yes

Note: n.a., not available; n.d., not detected.

energy into chemical energy. For this reason, the green of their chlorophylls is masked and they look dark purple. In contrast, algae that live in high-irradiance habitats typically have pigments that protect them against the photo-damages caused by the presence of singlet oxygen. It is the composition and amount of accessory and protective pigments that give algae their wide variety of colors and, for several algal groups, their common names such as brown algae, red algae, golden, and green algae. Internal freshwater environment displays a wide diversity of form of microalgae, although not exhibiting the phenomenal size range of their marine relatives. Freshwater phytoplankton and the benthonic algae form the base of the aquatic food chain.

A considerable number of subaerial algae have adapted to life on land. They can occur in surprising places such as tree trunks, animal fur, snow banks, hot springs, or even embedded within desert rocks. The activities of land algae are thought to convert rock into soil, to minimize soil erosion as well as to increase water retention and nutrient availability for plants growing nearby.

Algae also form mutually beneficial partnership with other organisms. They live with fungi to form lichens, or inside the cells of reef-building corals, in both cases providing oxygen and complex nutrients to their partner, and in return receiving protection and simple nutrients. This arrangement enables both partners to survive in conditions that they could not endure alone.

Chapter 8 will describe in detail some of the many and unusual interaction algae establish with different and distant environmental settings and other organisms, to highlight the extreme physiological variability and plasticity of this heterogeneous assemblage.

Table 1.2 summarizes the different types of habitat colonized by the algae of the divisions.

STRUCTURE OF THALLUS—CYTOMORPHOLOGICAL TYPES

An unrivalled diversity of morphological and cytological designs has evolved within algae, from microscopic unicells to macroscopic multicellular organisms, from simple filaments to giant-celled algae. Examples of the distinctive morphological characteristics within different groups are set forth in Table 1.3.

TABLE 1.3
Thallus Morphology in the Different Algal Divisions

Phylum	Unicellular and Nonmotile	Unicellular and Motile	Colonial and Nonmotile	Colonial and Motile	Filamentous	Siphonous	Parenchimatous
Cyanobacteria	*Synechococcus* *Prochloron*	n.d.	*Anacystis*	n.d.	*Calothrix* *Prochlorothrix*	n.d.	*Pleurocapsa*
Glaucophyta	*Glaucocystis*	*Cyanophora*	n.d.	n.d.	n.d.	n.d.	n.d.
Rhodophyta	*Phorphyridium*	n.d.	*Cyanoderma*	n.d.	*Goniotricum*	n.d.	*Palmaria*
Chlorophyta Charophyta	*Chlorella*	*Dunaliella*	*Pseudo-sphaerocystis*	*Volvox*	*Ulothrix*	*Bryopsis*	*Ulva*
Haptophyta	n.d.	*Chrysochromulina*	n.d.	*Corymbellus*	n.d.	n.d.	n.d.
Cryptophyta	n.d.	*Cryptomonas*	n.d.	n.d.	*Bjornbergiella*	n.d.	n.d.
Ochrophyta	*Triceratium*	*Ochromonas*	*Chlorobotrys*	*Synura*	*Ectocarpus*	*Vaucheria*	*Fucus*
Cercozoa (Chlorarachniophyceae)	n.d.	*Chlorarachnion*	n.d.	n.d.	n.d.	n.d.	n.d.
Myzozoa (Dynophyceae)	*Dinococcus*	*Gonyaulax*	*Gloeodinium*	n.d.	*Dinoclonium*	n.d.	n.d.
Euglenozoa (Euglenophyceae)	*Ascoglena*	*Phacus*	*Colacium*	n.d.	n.d.	n.d.	n.d.

Note: n.d., not detected.

Unicells and Unicell Colonial Type

Many algae are solitary cells, the unicell, with or without flagella, hence motile or nonmotile. *Nannochloropsis* (Ochrophyta) (Figures 1.1am and 1.2) is an example of a nonmotile unicell, while *Ochromonas* (Ochrophyta) (Figures 1.1ai and 1.3) is an example of a motile unicell. Other algae exist as aggregates of few or many single cells held together loosely or in a highly organized fashion, the colony. In this type of aggregate, cell number is indefinite, growth occurs by cell division of its components, there is no division of labor, and each cell can survive on its own. *Hydrurus* (Ochrophyta) (Figure 1.4) forms long and bushy nonmotile colonies with cells evenly distributed throughout a gelatinous matrix, while *Synura* (Ochrophyta) (Figures 1.1bd and 1.5) forms free-swimming colonies composed of cells held together by their elongated posterior ends. Another quite unusual example of colony is *Tetraflagellochloris mauritanica* (Chlorophyta) (Figure 1.6a and 1.6b): up to 12 cells can be arranged in groups, which are connected by intercellular diaphragms and cytoplasmic bridges, without sharing any common colonial boundary. When the number and arrangement of cells are determined at the time of origin of the colony and remain constant during

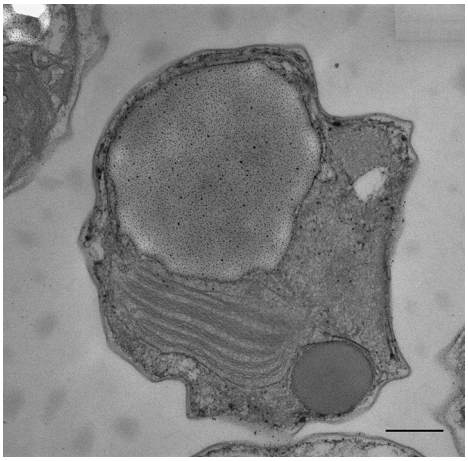

FIGURE 1.2 Transmission electron micrograph of a *Nannochloropsis* sp. nonmotile unicell. Scale bar: 0.5 µm.

FIGURE 1.3 *Ochromonas* sp. motile unicell. Scale bar: 4 µm.

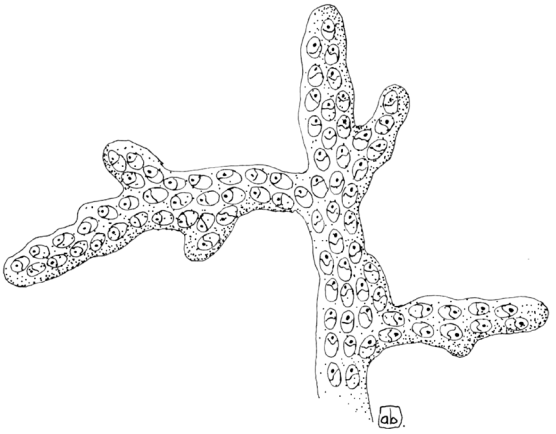

FIGURE 1.4 Nonmotile colony of *Hydrurus foetidus*.

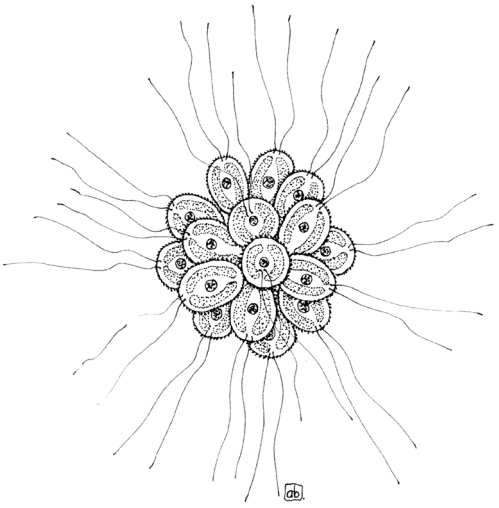

FIGURE 1.5 Free-swimming colony of *Synura uvella*.

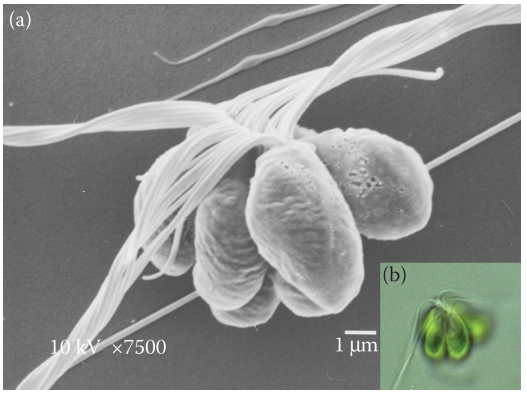

FIGURE 1.6 Free-swimming colony of *Tetraflagellochloris mauritanica*: (a) SEM image and (b) wide-field optical microscope image.

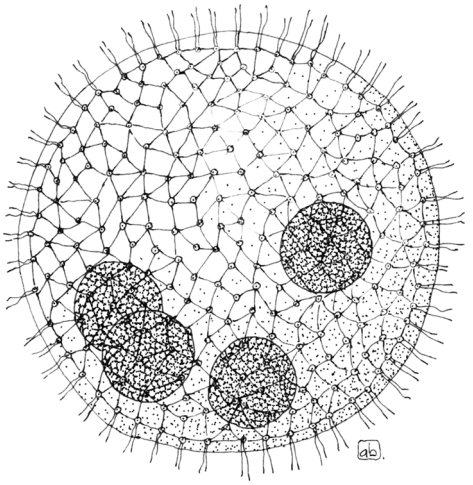

FIGURE 1.7 Motile coenobium of *Volvox aureus*.

the lifespan period of the individual colony, the colony is termed coenobium. *Volvox* (Chlorophyta) (Figure 1.7) with its spherical colonies composed of up to 50,000 flagellated cells interconnected by cytoplasmic bridges is an example of a motile coenobium, as well as *Eudorina* (Chlorophyta) (Figure 1.8). *Hydrodictyon* (Chlorophyta) with its flat plat-like networks of several thousand cells and *Pediastrum* (Chlorophyta) (Figure 1.9) with its flat colonies of cells characterized by spiny protuberances are examples of nonmotile coenobia.

Filamentous Type

Filaments result from cell division in the plane perpendicular to the axis of the filament and have cell chains consisting of daughter cells connected to each other by their end wall. Filaments can be simple as in *Oscillatoria* (Cyanobacteria) (Figure 1.10), *Spirogyra* (Chlorophyta) (Figure 1.11), or *Ulothrix* (Chlorophyta) (Figure 1.12), have false branching as in *Tolypothrix* (Cyanobacteria) (Figure 1.13) or *Scytonema* (Cyanobacteria) (Figure 1.14), or true branching as in *Cladophora* (Chlorophyta) (Figure 1.15). Filaments of *Stigonema ocellatum* (Cyanobacteria)

FIGURE 1.8 Motile coenobium of *Eudorina* sp. Scale bar: 10 μm.

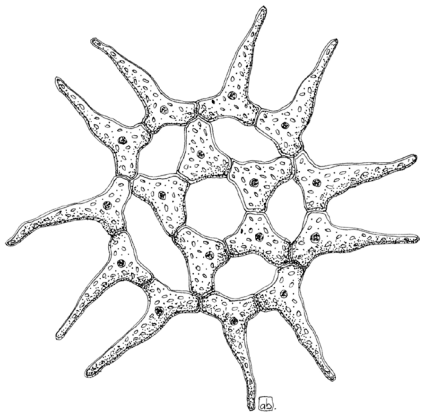

FIGURE 1.9 Nonmotile coenobium of *Pediastrum simplex*.

FIGURE 1.10 Simple filament of *Oscillatoria* sp.

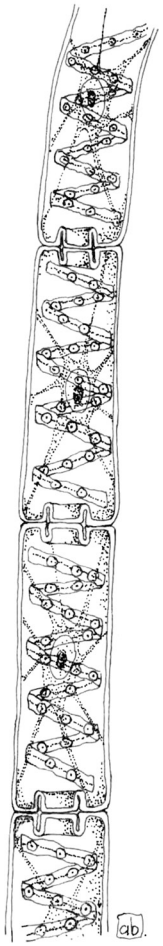

FIGURE 1.11 Simple filament of *Spirogyra* sp.

FIGURE 1.12 Simple filament of *Ulothrix variabilis*.

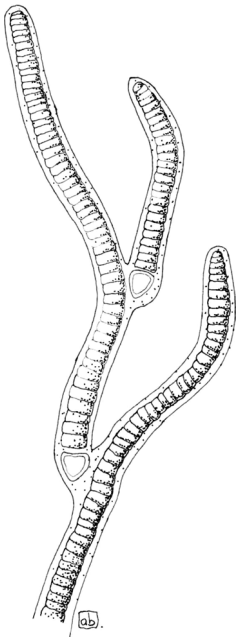

FIGURE 1.13 False branched filament of *Tolypothrix byssoidea*.

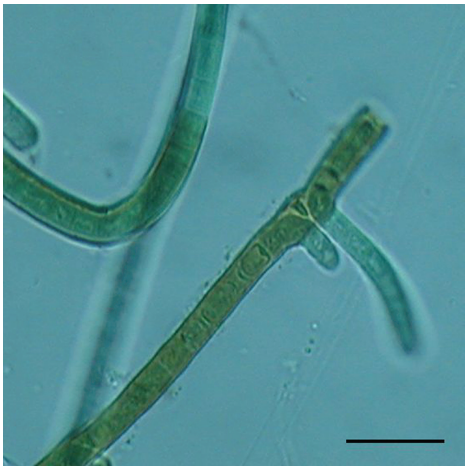

FIGURE 1.14 False branched filament of *Scytonema* sp. Scale bar: 50 µm.

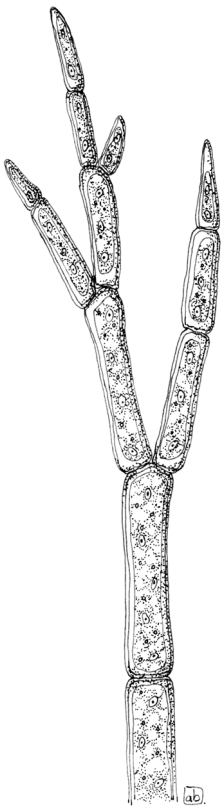

FIGURE 1.15 True branched filament of *Cladophora glomerata*.

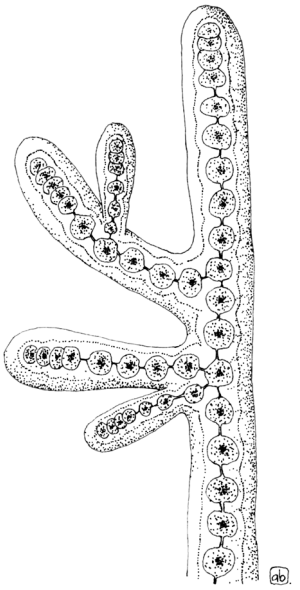

FIGURE 1.16 Uniseriate filament of *Stigonema ocellatum*.

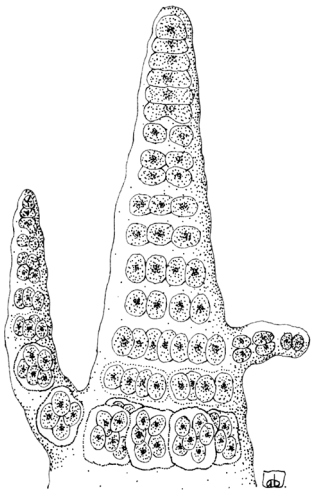

FIGURE 1.17 Pluriseraite filament of *Stigonema mamillosum*.

(Figure 1.16) consist of a single layer of cells and are called uniseriate, whereas those of *Stigonema mamillosum* (Cyanobacteria) (Figure 1.17) made up of multiple layers are called multiseriate.

Siphonocladous Type

The algae with this cytomorphological design have multicellular thalli, with a basically uniseriate filamentous, branched, or unbranched organization, composed of multinucleate cells as a consequence of uncoupled cell division and mitosis. The synchronously dividing nuclei are organized in nonmotile, regularly spaced nucleocytoplasmic domains that are maintained by perinuclear microtubule arrays. Despite lacking clear physical borders, such as a plasma membrane, these cytoplasmic domains behave like independent structural entities or pseudocells. This morphotype is present in members of the class Ulvophyceae (Chlorophyta) such as *Cladophora* sp. and *Anadyomene* sp.

Siphonous Type

Siphonous algae consist of a single giant tubular cell containing thousands to millions of nuclei dividing by asynchronous mitosis, and hence they are unicellular, but multinucleate (or coenocytic). No cross-walls are present and the algae often take the form of branching tubes. The sparsely branched tube of *Vaucheria* (Ochrophyta) (Figure 1.18) is an example of coenocyte or apocyte, a single cell containing many nuclei. *Bryopsis* (Chlorophyta) and *Acetabularia* sp. (Chlorophyta) (Figures 1.1t and 1.19) are other quite diverse examples; the first is a fern-like, asymmetrically branched, marine alga composed of a single, tubular-shaped cell which contains multiple nuclei and chloroplasts in a thin cytoplasmic layer surrounding a large central vacuole. The second is an umbrella-shaped alga, with a rhizoid, a stalk, and a cap-like whorl, growing in clusters attached on rocks. The single-compartment architecture of siphonous algae would suggest that they are particularly vulnerable to injury; but even if damage does occur, a complex, multistep wound response is triggered and a wound can be plugged in seconds, regenerating the lost tissue. Many species can even use a small bit of excised tissue to regenerate the rest of the plant. This ability offers these algae

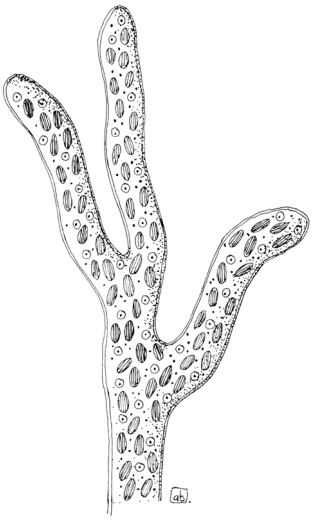

FIGURE 1.18 Siphonous thallus of *Vaucheria sessilis*.

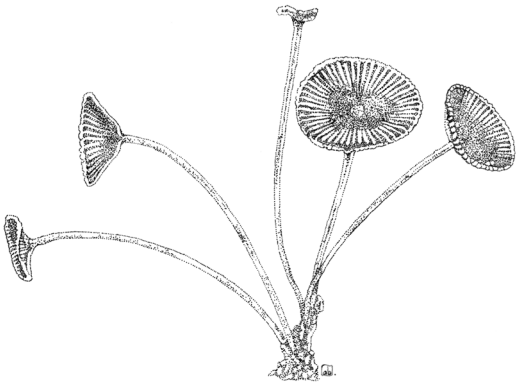

FIGURE 1.19 Portion of the thallus of *Acetabularia* sp.

considerable competitive advantage over other marine organisms. In some settings where they have been accidentally introduced, notably the Mediterranean Sea, certain species of siphonous green algae (e.g., *Caulerpa racemosa*; Figure 1.20) have proved all successful, displacing native marine flora over large areas.

Parenchymatous and Pseudo-Parenchymatous Type

These algae are mostly macroscopic with tissue of undifferentiated cells and growth originating from a meristem with cell division in three dimensions. In the case of parenchymatous algae, cells of the primary filament divide in all directions and any essential filamentous structure is lost. This tissue organization is present in *Ulva* (Chlorophyta) (Figure 1.1r), where the thallus is simply organized in a two-cell layered sheet and in many of the brown algae as *Laminaria* or *Fucus*. Pseudo-parenchymatous algae are made up of a loose or close aggregation of numerous, intertwined, branched filaments that collectively form the thallus, held together by mucilage, especially in red algae. Thallus construction is entirely based on a filamentous construction with little or no internal

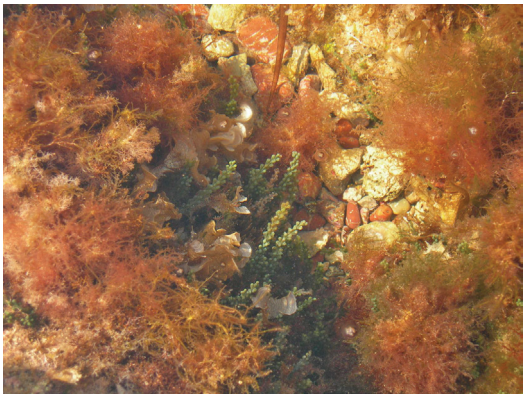

FIGURE 1.20 Frond of *Caulerpa racemosa*.

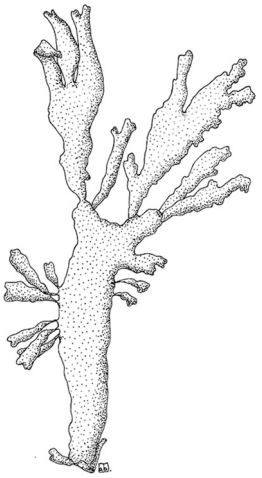

FIGURE 1.21 Pseudo-parenchymatous thallus of *Palmaria palmata*.

cell differentiation. *Palmaria* (Rhodophyta) (Figure 1.21) is a brown alga with a complex pseudo-parenchymatous structure.

Palmelloid Type

This type of thallus organization consists of nonmotile, quite independent cells embedded within a common mucilaginous matrix. The name comes from the similarity with the algae belonging to the genus *Palmella* (Chlorophyta) which form gelatinous colonies, with nonflagellate, spherical, or ellipsoid cells uniformly arranged at the peripheral matrix. The palmelloid type can be present as a temporary phase of the life cycle in some species and as permanent feature in others. Under unfavorable conditions, algae such as *Chlamydomonas* (Chlorophyta), *Haematococcus* (Chlorophyta), or *Euglena* (Euglenozoa) (Figure 1.22) lose their flagella, round off, and undergo successive divisions, while the cells secrete mucus. Once favorable conditions are restored, the mucilage dissolves and cells revert to the flagellate conditions.

In members of the genus *Tetraspora* (Chlorophyta), this organization is a permanent feature: colonies are vesicular and sac-like, containing many hundreds of cells at the periphery, with long pseudocilia extending beyond the mucilaginous matrix. The palmelloid organization is present

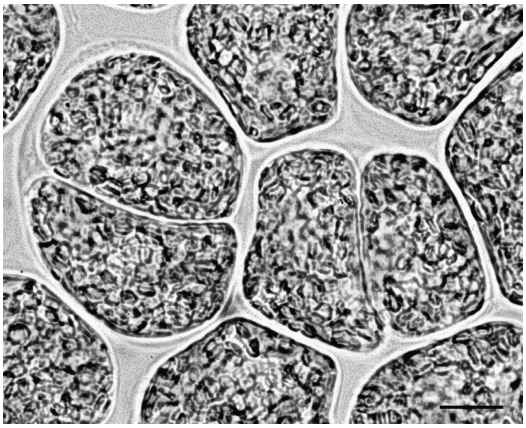

FIGURE 1.22 Palmelloid phase of *Euglena gracilis*. Scale bar: 5 μm.

also in the members of the Palmophyllales, an early-diverging chlorophytic lineage restricted to dimly lit habitats and deep water. These algae possess a unique type of multicellularity: they form well-defined macroscopic bodies composed of small spherical cells embedded in a firm gelatinous matrix.

NUTRITION

Following our definition of the term *algae*, most algal groups should be considered photoautotrophs, that is, depending entirely on their photosynthetic apparatus for their metabolic necessities, using sunlight as the source of energy, and CO_2 as the carbon source to produce carbohydrates and adenosine triphosphate. Most algal divisions contain colorless heterotrophic species that can obtain organic carbon from the external environment, either by taking up dissolved substances (osmotrophy) or by engulfing bacteria and other cells such as particulate prey (phagotrophy). There also exist some algae that cannot synthesize essential components such as the vitamins of the B_{12} complex, or fatty acids, and have to import them; these algae are defined auxotrophic.

However, it is widely accepted that algae use a complex spectrum of nutritional strategies, combining photoautotrophy and heterotrophy. This ability is referred to as mixotrophy. The relative contribution of autotrophy and heterotrophy to growth within mixotrophic species varies along a gradient from algae whose dominant mode of nutrition is phototrophy, through those for which phototrophy or heterotrophy provide essential nutritional supplements, to those for which heterotrophy is the dominant strategy. Some mixotrophs are mainly photosynthetic and only occasionally use an organic energy source. Others meet most of their nutritional demand by phagotrophy, but may use some of the products of photosynthesis from sequestered prey chloroplasts. Photosynthetic fixation of carbon as well as use of particulate food as a source of major nutrients (nitrogen, phosphorus, and iron) and growth factors (e.g., vitamins, essential amino acids, and essential fatty acids) can enhance growth, especially in extreme environments where resources are limited. Heterotrophy can be important for the acquisition of carbon when light is limiting and, conversely, autotrophy can maintain a cell during periods when particulate food is scarce.

On the basis of their nutritional strategies, we can classify algae into four groups:

1. *Obligate heterotrophic algae*: they are primarily heterotrophic, but are capable of sustaining themselves by phototropy when prey concentrations limit heterotrophic growth (e.g., *Gymnodium gracilentum*, Myzozoa);

2. *Obligate phototrophic algae*: their primary mode of nutrition is phototrophy, but they can supplement growth by phagotrophy and/or osmotrophy when light is limiting (e.g., *Dinobryon divergens*, Ochrophyta);
3. *Facultative mixotrophic algae*: they can grow equally well as photoautotrophs and as heterotrophs (e.g., *Fragilidium subglobosum*, Myzozoa);
4. *Obligate mixotrophic algae*: their primary mode of nutrition is phototrophy, but phagotrophy and/or osmotrophy provide substances essential for growth (in this group, we can include photoautoxotrophic algae) (e.g., *Euglena gracilis*, Euglenozoa).

REPRODUCTION

Methods of reproduction in algae may be vegetative by division of a single cell or fragmentation of a colony, asexual by production of motile spore, or sexual by union of gametes. Vegetative and asexual mode allows stability of an adapted genotype within a species from a generation to the next. Both modes provide a fast and economical means of increasing the number of individuals while restricting genetic variability. Sexual mode involves plasmogamy (union of cells), karyogamy (union of nuclei), chromosome/gene association, and meiosis, resulting in genetic recombination. Sexual reproduction allows for variation but is more costly, because of the waste of gametes that fail to mate.

Vegetative and Asexual Reproduction

Binary Fission or Cellular Bisection

It is the simplest form of reproduction; the parent organism divides into two equal parts, each having the same hereditary information as the parents. In unicellular algae, cell division may be longitudinal as in *Euglena* (Euglenozoa) (Figure 1.23) or transverse. The growth of the population follows a typical curve consisting of a lag phase, an exponential or log phase, and a stationary or plateau phase, where increase in density has leveled off (see Figure 6.3). In multicellular algae or in algal colonies, this process eventually leads to growth of the individual.

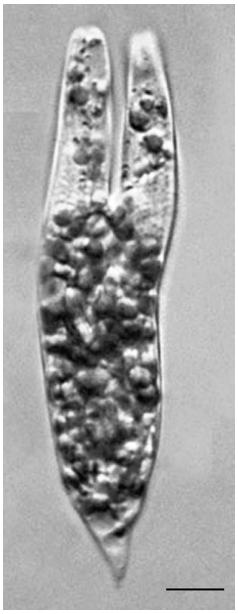

FIGURE 1.23 Cell division in *Euglena* sp. Scale bar: 5 μm.

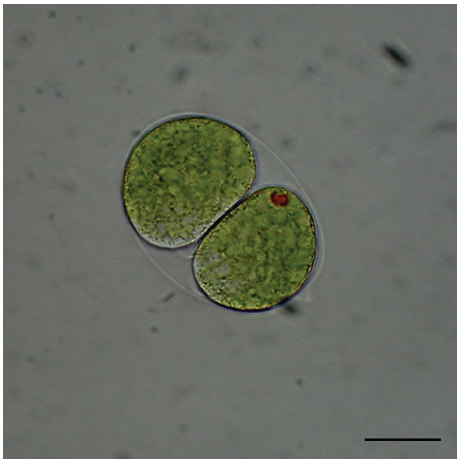

FIGURE 1.24 Zoospores of *Tetraselmis* sp. within the parental cell wall. Scale bar: 5 µm.

Zoospore, Aplanospore, and Autospore

Zoospores are flagellate motile spores that may be produced within a parental vegetative cell as in *Tetraselmis* (Chlorophyta) (Figure 1.24). Aplanospores are aflagellate spores that begin their development within the parent cell wall before being released; these cells can develop into zoospores. Autospores are aflagellate daughter cells that will be released from the ruptured wall of the original parent cell. They are almost perfect replicas of the vegetative cells that produce them and lack the capacity to develop in zoospospores. Examples of autospore-forming genera are *Nannochloropsis* (Ochrophyta) and *Chlorella* (Chlorophyta). Spores may be produced within and by ordinary vegetative cells or within specialized cells or structures called sporangia.

Autocolony Formation

In this reproductive mode, when the coenobium/colony enters the reproductive phase, each cell within the colony can produce a new colony similar to the one to which it belongs. Cell division no longer produces unicellular individuals but multicellular groups, a sort of embryonic colony that differs from the parent in cell size but not in cell number. This mode characterizes green algae such as *Volvox* (Chlorophyta; Figure 1.7) and *Pediastrum* (Chlorophyta; Figure 1.25). In *Volvox*, division is restricted to a series of cells which produce a hollow sphere within the parent colony, and with each mitosis each cell becomes smaller. The new colony everts, its cell forms flagella at their apical poles, and it is released by rupture of the parent sphere. In *Pediastrum*, the protoplast of some cells of the colony undergoes divisions to form biflagellate zoospores. These are not liberated but aggregate to form a new colony within the parent cell wall.

Fragmentation

A more or less random process whereby noncoenobic colonies or filaments break into two to several fragments having the capacity of developing into new individuals.

Resting Stages

Under unfavorable conditions, particularly of desiccation, many algal groups produce thick-walled resting cells, such as hypnospores, hypnozygotes, statospores, and akinetes.

Hypnospores and hypnozygotes, which have thickened walls, are produced ex novo by protoplasts which previously separated from the walls of the parental cells. Hypnospores are present in *Ulotrix* spp. (Chlorophyta) and *Chlorococcum* spp. (Chlorophyta), whereas hypnozygotes are

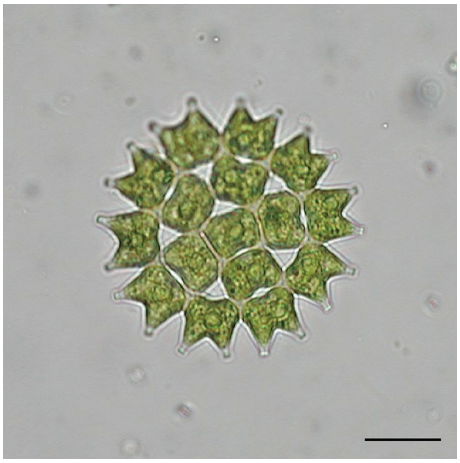

FIGURE 1.25 Nonmotile coenobium of *Pediastrum* sp. Scale bar: 100 µm.

FIGURE 1.26 Dinoflagellate hypnozygote. Scale bar: 10 µm.

present in *Spyrogyra* spp. (Chlorophyta) and Dinophyceae (Myzozoa) (Figure 1.26). Hypnospores and hypnozygotes enable these green algae to survive temporary drying out of small water bodies and also allow aerial transport from one water body to another, for instance, via birds. It is likely that dinoflagellate cysts have a similar function.

Statospores are endogenous cysts formed within the vegetative cell by member of Chrysophyceae such as *Ochromonas* spp. The cyst walls consist predominantly of silica and so are often preserved as fossils. These statospores are spherical or ellipsoidal, often ornamented with spines or other projections. The wall is pierced by a pore, sealed by an unsilicified bung, and a nucleus, chloroplasts and abundant reserve material lie within the cyst. After a period of dormancy, the cyst germinates and liberates its content in the form of one to several flagellated cells.

Akinetes is of widespread occurrence in the blue-green and green algae. They are essentially enlarged vegetative cells that develop a thickened wall in response to limiting environmental nutrients or limiting light. Figure 1.27 shows the akinetes of *Anabaena cylindrica* (Cyanophyta). They are extremely resistant to drying and freezing, as well as function as a long-term anaerobic

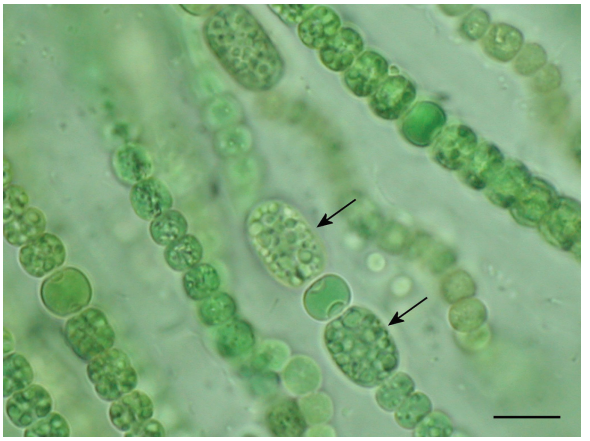

FIGURE 1.27 Akinetes (arrows) of *Anabaena* sp. Scale bar: 10 µm.

storage of the genetic material of the species. Akinetes can remain in sediments for many years, enduring very harsh conditions, and remain viable to assure the continuance of the species. When suitable conditions for vegetative growth are restored, the akinete germinates into new vegetative cells.

Sexual Reproduction

Gametes may be morphologically identical with vegetative cells or markedly differ from them, depending on the algal group. The main difference is obviously the DNA content which is haploid instead of diploid. Different combinations of gamete types are possible. In the case of isogamy, gametes are both motile and indistinguishable. When the two gametes differ in size, we have heterogamy. This combination occurs in two types: anysogamy, where both gametes are motile, but one is small (sperm) and one is large (egg); oogamy, when only one gamete is motile (sperm), which fuses with one nonmotile and very large (egg).

Algae exhibit three different life cycles with variation inside the different groups. The main difference is the point where meiosis occurs and the type of cells it produces, and whether or not there is more than one free-living stage present in the life cycle.

Haplontic or Zygotic Life Cycle

This cycle is characterized by a single predominant haploid vegetative phase, with the meiosis taking place upon germination of the zygote. *Chlamydomonas* (Chlorophyta) (Figure 1.28) exhibits this type of life cycle.

Diplontic or Gametic Life Cycle

This cycle has a single predominant vegetative diploid phase, and the meiosis gives rise to haploid gametes. Diatoms (Figure 1.29) and *Fucus* (Ochrophyta) (Figure 1.30) have a diplontic cycle.

Diplohaplontic or Sporic Life Cycles

These cycles present an alternation of generation between two different phases consisting of a haploid gametophyte and a diploid sporophyte. The gametophyte produces gametes by mitosis, and the sporophyte produces spores through meiosis. Alternation of generation in the algae can be isomorphic, in which the two phases are morphologically identical as in *Ulva* (Chlorophyta) (Figure 1.31) or heteromorphic, with predominance of the sporophyte as in *Laminaria* (Ochrophyta) (Figure 1.32), or with predominance of the gametophyte as in *Porphyra* (Rhodophyta) (Figure 1.33).

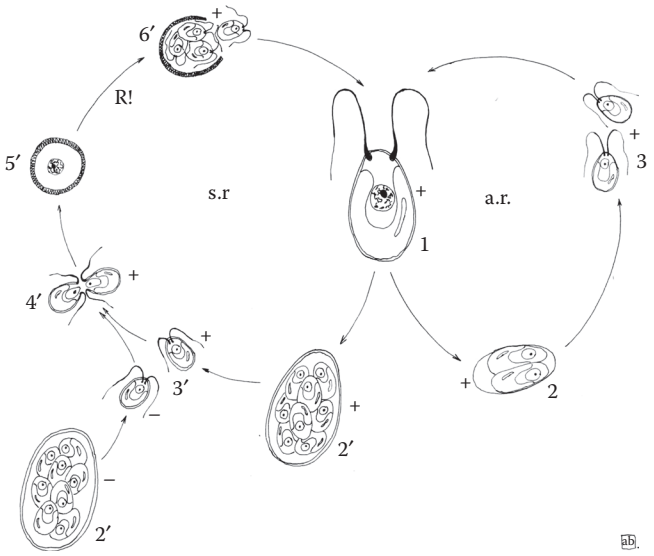

FIGURE 1.28 Life cycle of *Chlamydomonas* sp.: 1, mature cell; 2, cell-producing zoospores; 2′, cell-producing gametes (strain + and strain –); 3, zoospores; 3′, gametes; 4′, fertilization; 5′, zygote; 6′, release of daughter cells. R!: meiosis; a.r.: asexual reproduction; s.r.: sexual reproduction.

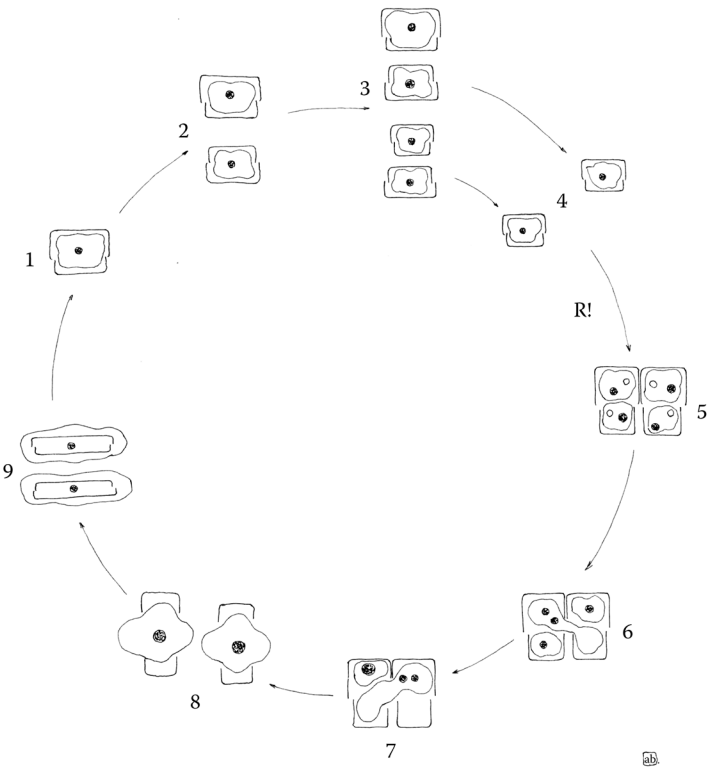

FIGURE 1.29 Life cycle of a diatom: 1, vegetative cell; 2–3, vegetative cell division; 4, minimum cell size; 5, gametogenesis; 6–7, fertilization; 8, auxospores; 9, initial cells. R!: meiosis.

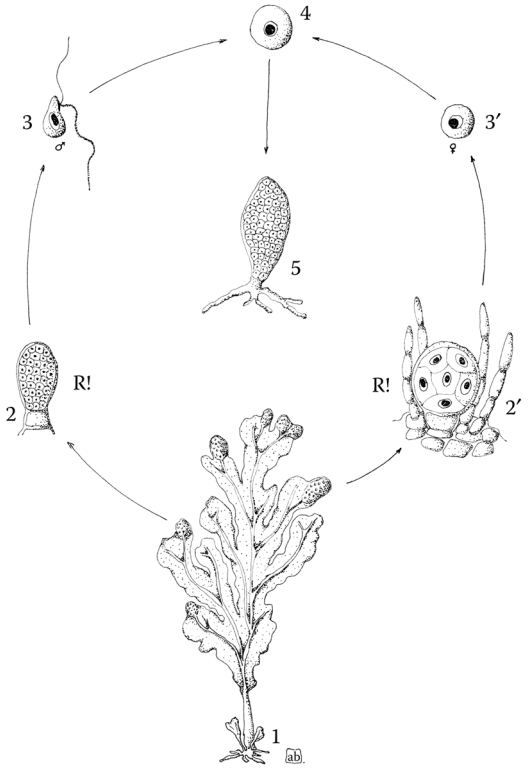

FIGURE 1.30 Life cycle of *Fucus* sp.: 1, sporophyte; 2, anteridium; 2′, oogonium; 3, sperm; 3′, egg; 4, zygote; 5, young sporophyte. R!: meiosis.

SUMMARIES OF THE 11 ALGAL PHYLA

Historically, the major groups of algae were classified on the basis of pigmentation, chemical nature of photosynthetic storage product, photosynthetic membrane (thylakoids) organization and other features of the chloroplasts, chemistry and structure of the cell wall, number, arrangement, and ultrastructure of flagella (if any), occurrence of any other special features, and sexual cycles. Recently revised classifications incorporate advances resulting from the widespread use of phylogenomic-scale phylogenetic analyses and massively increased taxon sampling in rRNA phylogenies. All these studies tend to assess the internal genetic coherence of the major phyla such as Cyanobacteria, Glaucophyta, Rhodophyta, Chlorophyta, Charophyta, Haptophyta, Cryptophyta, Ochrophyta, Cercozoa, Myzozoa, and Euglenozoa, confirming that these divisions are nonartificial. Table 1.4 attempts to summarize the main characteristics of the different algal groups.

Cyanobacteria

All blue-green algae (Figures 1.1a and 1.34) and prochlorophytes (Figure 1.35) are nonmotile Gram-negative eubacteria. In structural diversity, blue-green algae range from unicells to branched and unbranched filaments to unspecialized colonial aggregations and are possibly the most widely distributed of any group of algae. They are planktonic, occasionally forming blooms in eutrophic lakes and an important component of the picoplankton in both marine and freshwater systems; benthic, as dense mats on soil or in mud flats and hot springs, as the "black zone" high on the seashore, and as relatively inconspicuous components in most soils; and symbiotic in diatoms, ferns, lichens, cycads, sponges, and other systems. Numerically, these organisms dominate the ocean ecosystems.

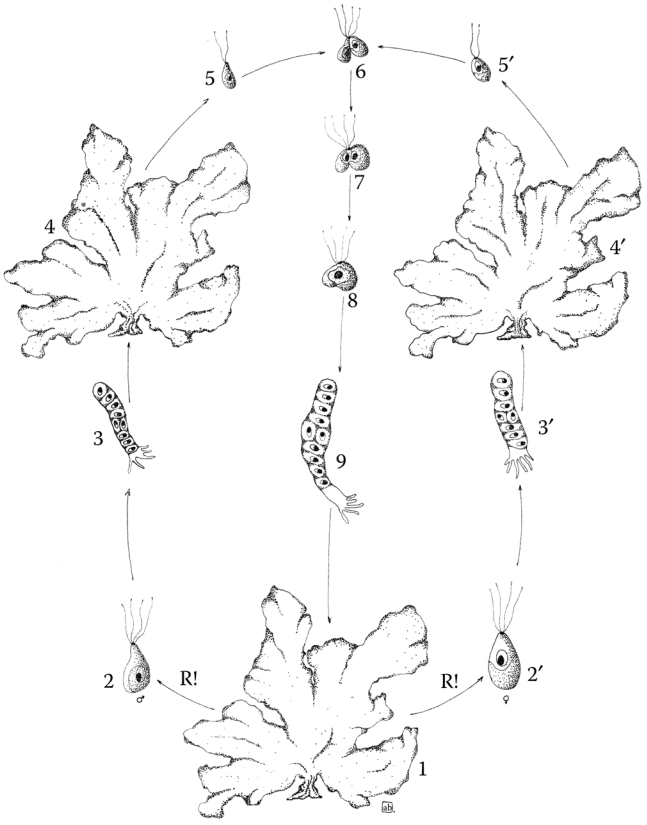

FIGURE 1.31 Life cycle of *Ulva* sp.: 1, sporophyte; 2, male zoospore; 2′, female zoospore; 3, young male gametophyte; 3′, young female gametophyte; 4, male gametophyte; 4′, female gametophyte; 5, male gamete; 5′, female gamete; 6–8, syngamy; 9, young sporophyte. R!: meiosis.

There are approximately 10^{24} cyanobacterial cells in the oceans. To put that in perspective, the number of cyanobacterial cells in the oceans is two orders of magnitude more than all the stars in the sky. Pigmentation of cyanobacteria includes both chlorophyll *a*, blue and red phycobilins (phycoerythrin, phycocyanin, allophycocyanin), and carotenoids. These accessory pigments lie in the phycobilisomes, located in rows on the outer surface of the thylakoids. Their thylakoids, which lie free in the cytoplasm, are not arranged in stacks, but singled and equidistant, in contrast to prochlorophytes and most other algae, but similar to Rhodopyta and Glaucophyta.

The reserve polysaccharide is cyanophycean starch, stored in tiny granules lying between the thylakoids. In addition, these cells often contain cyanophycin granules, that is, polymer of arginine and aspartic acid. Some marine species also contain gas vesicles used for buoyancy regulation. In some filamentous cyanobacteria, heterocysts and akinetes are formed. Heterocysts are vegetative cells that have been drastically altered (loss of photosystem II, development of a thick, glycolipid cell wall), to provide the necessary anoxygenic environment for the process of nitrogen fixation (Figure 1.36). Some cyanobacteria produce potent hepato- and neurotoxins.

Prochlorophytes can be unicellular or filamentous, and depending on the filamentous species, they can be either branched or unbranched. They exist as free-living components of pelagic nanoplankton and obligate symbionts within marine didemnid ascidians and holothurians and are mainly limited to living in tropical and subtropical marine environments, with optimal growth temperature at about 24°C. Prochlorophytes possess chlorophyll *a* and *b*, as euglenoids and land plants, but lack phycobilins, and this is the most significant difference between them and cyanobacteria, which

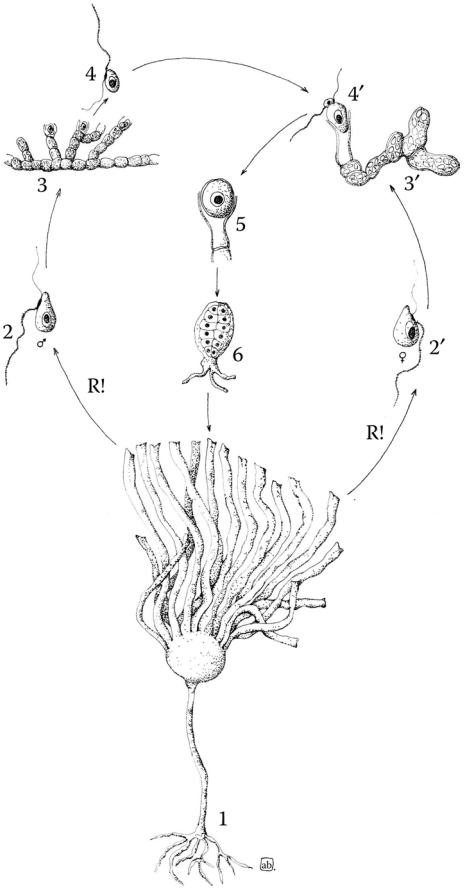

FIGURE 1.32 Life cycle of *Laminaria* sp.: 1, sporophyte; 2, male zoospore; 2′, female zoospore; 3, male gametophyte; 3′, female gametophyte; 4, sperm; 4′, egg and fertilization; 5, zygote; 6, young sporophyte. R!: meiosis.

extends the light-harvesting capacity of these algae into the blue and orange/red regions of the visible light spectrum. Other pigments are β-carotene and several xantophylls (zeaxanthin is the principal one). Their thylakoids, which lie free in the cytoplasm, are arranged in stacks. Prochlorophytes have a starch-like reserve polysaccharide. These prokaryotes contribute a large percentage of the total organic carbon in the global tropical oceans, making up from 25% to 60% of the total chlorophyll *a* biomass in the tropical and subtropical oceans. They are also able to fix nitrogen, though not in heterocysts. Both blue-green algae and prochlorophytes contain polyhedral bodies (carboxysomes) containing RuBisCo (ribulose-1,5-bisphosphate carboxylase/oxygenase, the enzyme that converts inorganic carbon into reduced organic carbon in all oxygen-evolving photosynthetic organisms) and have similar cell walls characterized by a peptidoglycan layer. Blue-green algae and prochlorophytes can be classified as obligate photoautotrophic organisms. Reproduction in both divisions is strictly asexual, by simple cell division, fragmentation of the colony, or filaments.

Glaucophyta

Glaucophyceae (Figures 1.1b and 1.37) are basically unicellular flagellates with a dorsiventral construction; they bear two unequal flagella, which are inserted into a shallow depression just below the apex of the cell. Glaucophyceae are rare freshwater inhabitants, sometimes collected from

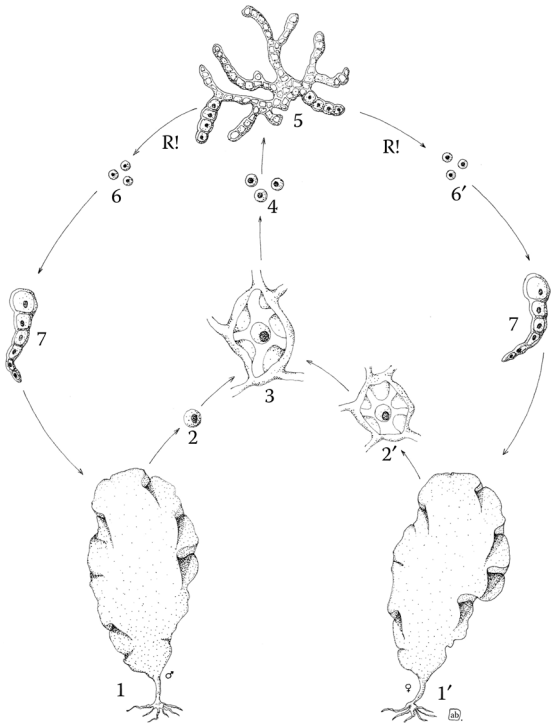

FIGURE 1.33 Life cycle of *Porphyra* sp.: 1, male gametophyte; 1′, female gametophyte; 2, sperm; 2′, egg; 3, fertilization and zygote; 4, spores; 5, sporophyte; 6, male spore; 6′, female spores; 7, young male gametophyte; young female gametophyte. R!: meiosis.

soil samples also. They possess only chlorophyll *a*; accessory pigments such as phycoerythrocyanin, phycocyanin, and allophycocyanin are organized in phycobilisomes. Carotenoids such as β-carotenes and xantophyll zeaxanthins are also present in their chloroplast. This unusual chloroplast lies in a special vacuole and presents a thin peptidoglycan wall located between the two plastid outer membranes. Thylakoids are not stacked. The chloroplast DNA is concentrated at the center of the chloroplast, where typical carboxysomes are present, which contain the RuBisCo enzyme. Starch is the reserve polysaccharide, which is accumulated in granular form inside the cytoplasm, but outside the chloroplast. Glaucophyceae live photoautotrophically with the aid of blue-green plastids often referred to as cyanelles. Cyanelles are presumed to be phylogenetically derived from endosymbiotic cyanobacterium. Sexual reproduction is unknown in this division.

Rhodophyta

This phylum is currently divided into two subphyla, Cyanidiophytina, with the single class of Cyanidiophyceae, and Rhodophytina with the remaining six classes. Red algae consist mostly of seaweed, but including genera of free-living unicellular microalgae. They inhabit prevalently marine ecosystems, but are also present in freshwater and terrestrial environment. The lack of any flagellate stages, the lack of centrioles, and the presence of accessory phycobiliproteins (allophycocyanin, phycocyanin, and phycoerythrin) organized in phycobilisomes (shared with Cyanobacteria, Cryptophyta, and Glaucophyta) are unique features of these algae; chlorophyll *a* is the only chlorophyll. Chloroplasts are enclosed by a double-unit membrane; thylakoids do not stack at all, but lie equidistant and singly within the chloroplast. One thylakoid is present around the periphery of the chloroplast, running parallel to the chloroplast's internal membrane. The chloroplastic DNA is

TABLE 1.4
Main Pigments, Storage Products, and Cell Coverings of the Algal Divisions

Phylum	Pigments (See Figures 3.5–3.9)				Storage Products
	Chlorophylls	Phycobilins	Main Carotenoids	Main Xantophylls	
Cyanobacteria	*a*, *b*	C-phycoerythrin C-phycocyanin Allophycocyanin	β-carotene	Myxoxanthin Zeaxanthin	Cyanophycin (arginine and aspartic acid) Cyanophycean starch (α-1,4-glucan)
Glaucophyta	*a*	Phycoerythrocyanin C-phycocyanin Allophycocyanin	β-carotene	Zeaxanthin	Starch (α-1,4-glucan)
Rhodophyta	*a*	B-phycoerythrin R-phycoerythrin R-phycocyanin Allophycocyanin	α- and β-carotene	Lutein	Floridean starch (α-1,4-glucan)
Chlorophyta	*a*, *b*	Absent	α-, β-, and γ-carotene	Lutein Prasinoxanthin	Starch (α-1,4-glucan)
Charophyta	*a*, *b*	Absent	α-, β-, and γ-carotene	Lutein Prasinoxanthin	Starch (α-1,4-glucan)
Haptophyta	*a*, c_1, c_2	Absent	α- and β-carotene	Fucoxanthin	Chrysolaminaran (β-1,3-glucan)
Cryptophyta	*a*, c_2	B-phycoerytrin (545) R-phycocyanin Allophycocyanin	α-, β-, and ε-carotene	Alloxanthin	Starch (α-1,4-glucan)
Ochrophyta	*a*, c_1, c_2, c_3	Absent	α-, β-, and ε-carotene	Fucoxanthin, violaxanthin	Chrysolaminaran (β-1,3-glucan)
Cercozoa (Chlorarachniophyceae)	*a*, *b*	Absent	Absent	Lutein, neoxanthin, violaxanthin	Paramylon (β-1,3-glucan)
Myzozoa (Dynophyceae)	*a*, c_1, c_2	Absent	β-carotene	Peridinin Fucoxanthin Diadinoxanthin Dinoxanthin Gyroxanthin	Starch (α-1,4-glucan)
Euglenozoa (Euglenophyceae)	*a*, *b*	Absent	β- and γ-carotene	Diadinoxanthin	Paramylon (β-1,3-glucan)

organized in blebs scattered throughout the whole chloroplast. The most important storage product is the floridean starch, an α-1,4-glucan polysaccharide, which is deposited in the cytoplasm. Grains of this starch are located only in the cytoplasm, unlike the starch grains produced in the Chlorophyta, which lie inside the chloroplasts. Most rhodophytes live photoautotrophically. In the great majority of red algae, cytokinesis is incomplete. Daughter cells are separated by the pit connection, a proteinaceous plug that fills the junction between cells; this connection successively becomes a plug. Species in which sexual reproduction is known generally have an isomorphic or heteromorphic diplohaplontic life cycle; haplontic life cycle is considered an exception.

The class Bangiophyceae includes all multicellular genera, in which the gametophyte has chloroplasts lacking a peripheral encircling thylakoid, and the Golgi is associated with both endoplasmic reticulum (ER) and mitochondrion. Many economically important genera found in intertidal and subtidal habitats, such as *Porphyra purpurea* and *P. umbilicalis*, belong to this class; they are harvested for human food across the North Atlantic and are under development as aquaculture crops for human and animal foods. *Porphyra* species (Figures 1.1c and 1.33) are important reference red algae because of their multicellularity, high stress tolerance (e.g., to heat, freezing, high light, osmotic stress, and desiccation), ancient fossil record of the Bangiales, and capacity to synthesize an array of storage carbohydrates and light-protection compounds. The life history of Bangiales such as *Porphyra* spp. involves an alternation between the economically important foliose blade (haploid gametophyte) and the microscopic, filamentous, diploid conchocelis phase.

The class Compsopogonophyceae includes microscopic filamentous algae (e.g., *Erythrocladia*; Figure 1.1d) to macroscopic multicellular species (e.g., *Compsopogon*). They live in coastal seawater or freshwater. They possess two distinctive ultrastructural characters in combination: the association of Golgi bodies with ER instead of mitochondria, typical of almost all red algae, and the presence of a peripheral encircling thylakoid in the chloroplast. The color of chloroplasts is variable from greenish blue to red. Asexual reproduction occurs by monospores generated by the oblique division of vegetative cells. Sexual reproduction and alternation of generations are reported in the Erythropeltidales.

The Cyanidiophyceae are all unicellular, spherical, or elliptical in shape, growing in volcanic and thermal areas under extremely low pH (0.05–5) and relatively high temperature (35–56°C). Unlike most eukaryotes, they are also capable of tolerating a large array of toxic chemical compounds such as sulfuric acid, arsenic, and other heavy metals. They reproduce by binary fission (*Cyanidioschyzon*; Figure 1.1e) or by formation of endospores (*Cyanidium*, *Galdieria*); they can be facultative heterotrophs or obligate photoautotrophs.

The Florideophyceae (Figures 1.1f and 1.38) includes all multicellular genera, both marine and freshwater, in which the gametophytes have chloroplasts with a peripheral encircling thylakoid, and the Golgi is associated with both ER and mitochondrion. The class contains species as seemingly different as the coralline algae, characterized for the presence of calcite and *Botryocladia*, known as sea-grapes, and parasitic taxa. These algae show a triphasic reproduction cycle: an isomorphic gametophyte and sporophyte generations are separated by the carposporophyte, a very different sporophyte that emerges from the development of the zygote. In general, carposporophyte is a set of small filaments that terminate in diploid spores, carpospores. These disperse and germinate to form the sporophyte. This is generally pseudoparenchymatous and identical to the gametophyte.

The three classes of Porphyridiophyceae (Figure 1.1g), Rhodellophyceae (Figure 1.1h), and Stylonematophyceae (Figure 1.1i) include the 10 recognized genera of unicellular red algae of the subphylum Rhodophytina. In the Porphyridiophyceae, the Golgi bodies are invariably associated with ER and a mitochondrion, while in the Rhodellophyceae the Golgi association can be either with ER or the functionally equivalent outer membrane of the nuclear envelope. The class Stylonematophyceae also includes pseudofilamentous or filamentous red algae. In the first two classes, reproduction occurs by cell division, while in the Stylonematophyceae reproduction occurs by both cell division and monospores.

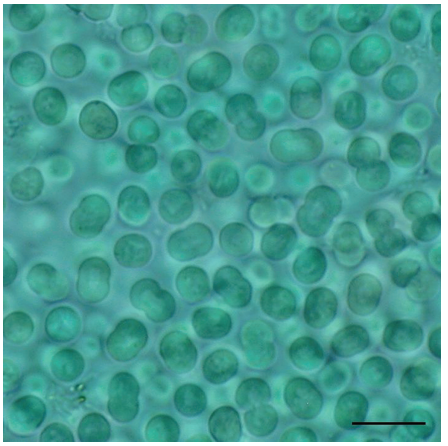

FIGURE 1.34 Cells of *Cyanothece* sp. Scale bar: 10 µm.

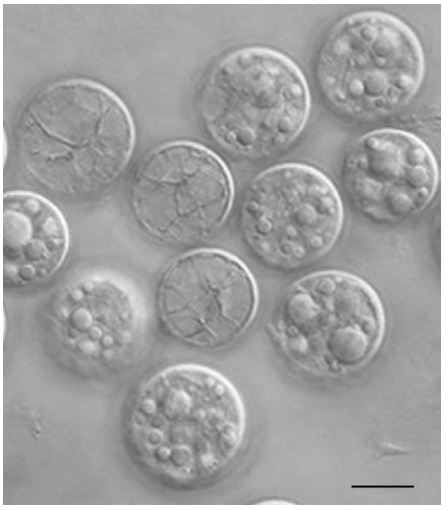

FIGURE 1.35 Cells of *Prochloron* sp. Scale bar: 10 µm.

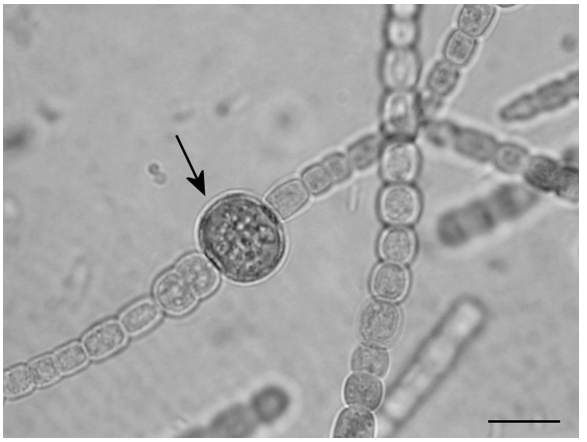

FIGURE 1.36 Heterocyst (arrow) of *Anabaena azollae*. Scale bar: 10 µm.

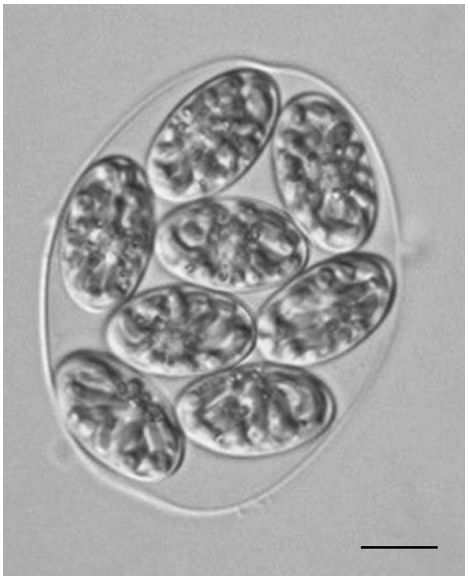

FIGURE 1.37 A group of eight autospores of *Glaucocystis nostochinearum* still retained within the parent cell wall. Scale bar: 10 μm.

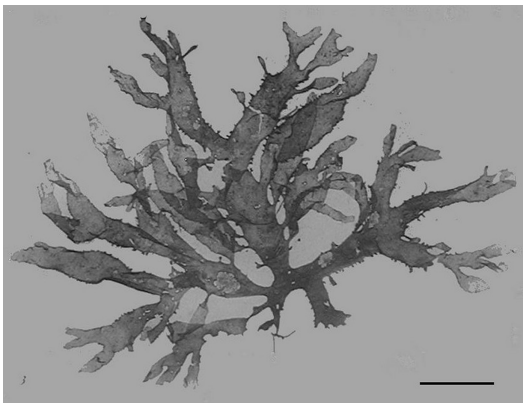

FIGURE 1.38 Frond of *Rhodophyllis acanthocarpa*. Scale bar: 5 cm.

Chlorophyta

Members of this phylum are common inhabitants of marine, freshwater, and terrestrial environments; within the phylum, a great range of somatic differentiation occurs, ranging from flagellates to complex multicellular thalli differentiated into macroscopic organs. The different level of thallus organization (unicellular, colonial, filamentous, siphonous, and parenchimatous) has traditionally served as the basis of classification of this division. Chlorophytes show a wide diversity in the number and arrangements of flagella associated with individual cells (one or up to eight, in the apical or subapical region). All members of the chlorophytes have motile stages with two or four anterior isokont flagella (i.e., flagella are of equal length and possess equivalent function), although algae with two flagella of slightly unequal lengths have been described. Flagella are characterized by a "stellate structure"-type flagellar transition region. Within the cell, the flagellar basal bodies are associated with four microtubular rootlets, cruciately arranged, which alternate between two and

higher numbers of microtubules, according to the formula X-2-X-2. When viewed from above the cell, the basal bodies and rootlets can have a perfect cruciate pattern, with the basal bodies directly opposed (DO) or they can be offset in a clockwise (CW) or counterclockwise (CCW) position.

According to the most recent classifications, Chlorophyta comprises the early-diverging prasinophytes, which gave rise to the core chlorophytes (including the early diverging Chloredendrophycae with the three major classes of Ulvophyceae, Trebouxiophyceae, and Chlorophyceae), to the Pedinophyceae, sister class to the core chlorophytes, and the recently proposed group Palmophyllales.

The prasinophytes, as presently conceived, include a heterogeneous assemblage of unicellular motile algae, either naked or covered on their cell body and flagella by nonmineralized organic scales (Figures 1.1l and 1.39). They are predominantly marine planktonic, but also include several freshwater representatives. At present, nine prasinophyte clades are recognized, two of which have been recently accommodated into the two classes of Mamiellophyceae and Nephroselmidophyceae. Mamiellophyceae (Figure 1.1m) are typically solitary cells, with one or two chloroplasts, mono- or biflagellate, with isokont or anisokont flagella. They may be scale-covered or naked. Nephroselmidophyceae (Figure 1.1n) are laterally compressed, scale-covered cells, with laterally inserted anisokont flagella, and possess a single cup-shaped chloroplast. Pedinophyceae (Figure 1.1o) are unicellular, monoflagellate asymmetrical algae, with CCW basal body orientation. Rigid or thin hair-like appendages are present on the flagellum. Chloredendrophyceae (Figure 1.1p) possess a pair of flagella inserted in a pit; basal body orientation is CCW. These algae are covered by organic scales, the outer layer of which is fused to form a theca. The class Chlorophyceae (Figure 1.1q) comprises mainly swimming cells with one or two pair of flagella, without mastigonemes. Cells can be naked or covered by a cell wall more or less calcified (Figure 1.40). Either DO or CW arrangements are present in the members of this class. Ulvophyceae morphologies range from microscopic unicellular to macroscopic multicellular plants and giant-celled organisms (Figures 1.1r, 1.41, and 1.42). Four main cytomorphological types can be distinguished: nonmotile uninucleate unicells; multicellular filaments or blades composed of multinucleate cells; multicellular bodies composed of multinucleate cells with nuclei organized in regularly spaced cytoplasmic domains; siphonous thalli consisting of a single giant tubular cell containing thousands to millions of nuclei. In some species, siphonous thalli are encrusted with calcium carbonate. The majority of Ulvophyceae are marine, but several members also occur in freshwater or damp subaerial habitats. All the algae of

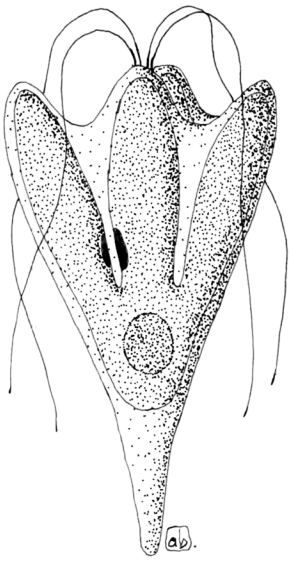

FIGURE 1.39 Unicell of *Pyramimonas longicauda*.

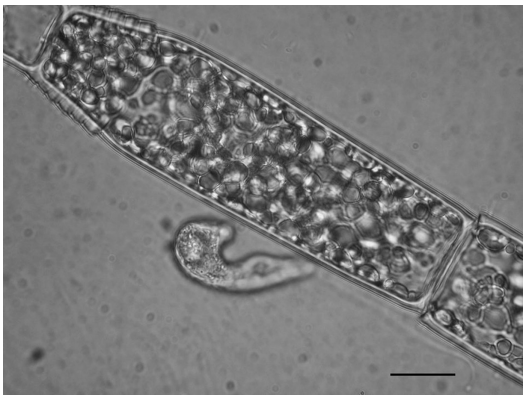

FIGURE 1.40 Filament of *Oedogonium* sp., with a *Peranema* sp. cell. Scale bar: 20 μm.

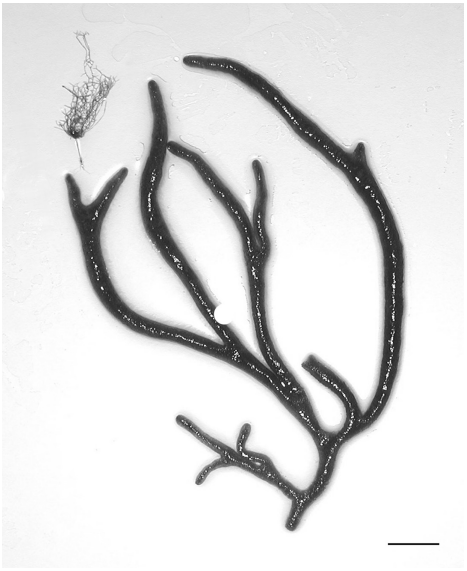

FIGURE 1.41 Thallus of *Codium* sp. Scale bar: 2 cm.

the class possess a CCW basal body orientation. The class Trebouxiophyceae (Figures 1.1s and 1.43) encompasses motile and nonmotile unicells, colonies, and multicellular filaments or blades from freshwater or terrestrial habitats, with some species present also in brackish or marine water. Several species are either symbiotic with fungi to form lichens or endosymbiotic with freshwater and marine protists, invertebrates, and plants. Swimming cells can have one or two pair of flagella without mastigonemes. All the algae of the class possess a CCW basal body orientation. The class Dasycladophyceae (Figures 1.1t and 1.19) contains algae characterized by a siphounous organization of the thallus, with numerous chloroplasts. This class is entirely marine.

As already stated, Palmophyllales (Figure 1.1u) are an early-diverging chlorophytic lineage; these algae are restricted to dimly lit habitats and deep water. They possess a unique type of multicellularity, forming well-defined macroscopic bodies composed of small spherical cells embedded in a firm gelatinous matrix.

Chlorophyta possess chlorophylls *a* and *b*, β- and γ-carotene, and several xantophylls as accessory pigments. Chloroplasts are surrounded by a two-membrane envelope without any ER membrane. Within the chloroplasts, thylakoids are stacked to form grana. Pyrenoids, where present,

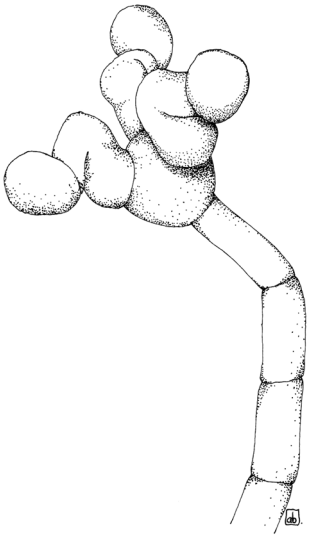

FIGURE 1.42 Thallus of *Trentepohlia arborum*.

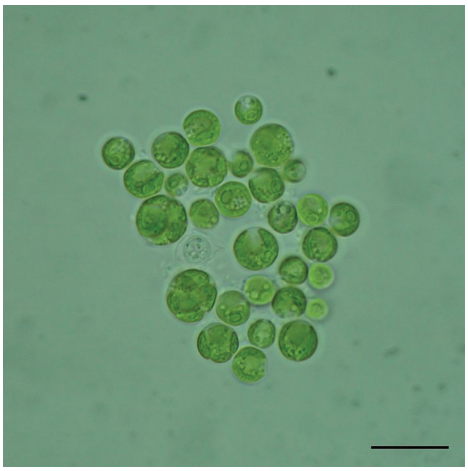

FIGURE 1.43 Group of *Chlorella* sp. cells. Scale bar: 10 μm.

are embedded within the chloroplast and often penetrated by thylakoids. The circular molecules of chloroplast DNA are concentrated in numerous small blobs (1–2 μm in diameter). The most important reserve polysaccharide is starch, which occurs as grains inside the chloroplasts; glucan or β-1,4 mannan can be present in the cell wall of some Ulvophyceae. Eyespot, if present, is located inside the chloroplast and consists of a layer of carotenoid-containing lipid droplets between the chloroplast envelope and the outermost thylakoids.

Charophyta

Charophytes are the organisms most closely related to land plants. The six groups of the phylum have been distinctly recognized on the basis of ultrastructural, biochemical, and molecular data. Mesostigmatophyceae (Figure 1.1v) and Chlorokybophyceae form the earliest branching

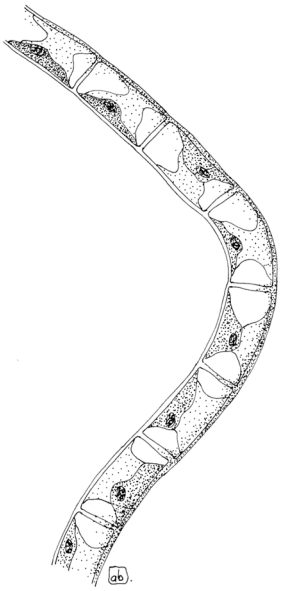

FIGURE 1.44 Filament of *Klebsormidium* sp.

streptophytes; the only genus of Mesostigmatophyceae is *Mesotigma* with two species, *M. viride* and *M. grande*. These isogamous algae are freshwater, scaly, asymmetrical, and unicellular biflagellate, and unlike other charophytes, possess two multilayered structures and an eyespot. Chlorokybophyceae (Figure 1.1z) consists of a sole representative, *Chlorokybus atmophyticus*, occurring in moist terrestrial habitats where it forms sarcinoid packets of a few cells enveloped in a common mucilaginous matrix, which reproduce asexually by asymmetrical motile spores possessing a single multilayered structure. Klebsormidiophyceae (Figure 1.1aa) represent the common ancestor of the remaining streptophytes, in which multicellularity evolved in the form of unbranched filaments (Figure 1.44). These freshwater or terrestrial algae, which can also form sarcinoid packets, reproduce by filament fragmentation and release of motile spores. Charophyceae (Figures 1.1ab and 1.45) are the most plant-like in appearance among the charophytes, because of the independent evolution of macrophytic forms. Thalli consist of a central stalk of large, elongated multinucleate cells and whorls of branches at nodes. All species are oogamous with motile sperm produced in complex antheridia. Coleochaetophyceae (Figure 1.1ac) range in morphology from branched filamentous algae to relatively complex discoid parenchymatous thalli. They may be epiphytic, endophytic, or loosely attached to submerged vascular plants or other substrates. They are oogamous, with biflagellate zoospore and sperm. The Zygnematophyceae (Figure 1.1ad) are the most species-rich clade of the Charophyta and the most morphologycally diverse. Thalli include nonmotile unicells, filaments, and small colonial forms (Figure 1.11). They possess an unusual mode of sexual reproduction by fusion of nonflagellate gametes. A very recent comprehensive genome scale analysis of 160 nuclear genes drawn from species distributed across all the charophyte groups supported the Zygnematophyceae as the closest living relative to land plants.

Haptophyta

This phylum contains only two classes: Coccolitophyceae (Prymnesiophyceae; Figures 1.1ae, 1.1af, and 1.46) and Pavlovophyceae (Figure 1.1ag). The great majority of these algae are unicellular, motile, palmelloid, or coccoid, but a few form colonies or short filaments. These algae are generally found in marine habitats, although there are a number of records from freshwater and terrestrial

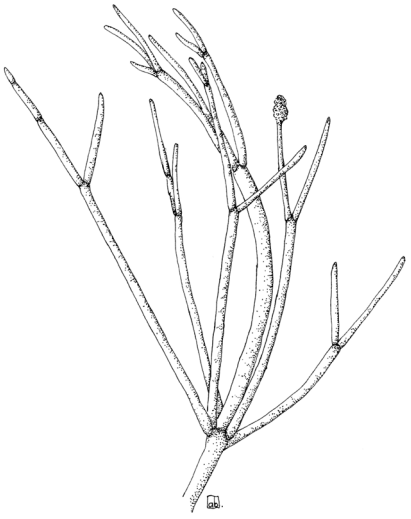

FIGURE 1.45 Thallus of *Nitella* sp.

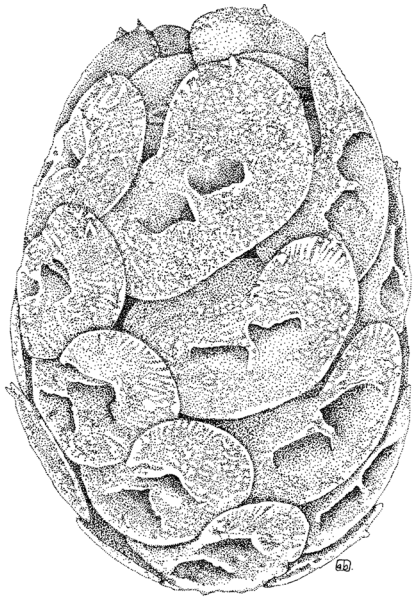

FIGURE 1.46 Unicell of *Helicosphaera carteri.*

environments. Flagellate cells bear two naked flagella, inserted either laterally or apically, which may have different lengths. A structure apparently found only in algae of this division is the haptonema, typically a long thin organelle reminiscent of a flagellum but with a different ultrastructure. The chloroplast contains only chlorophyll *a*, c_1, and c_2. The golden yellowish-brown appearance of chloroplast is due to the accessory pigments such as fucoxanthin, β-carotene, and other xanthins. Each chloroplast is enclosed within a fold of ER, which is continuous with the nuclear envelope. Thylakoids are stacked in threes and there are no girdle lamellae. The nucleic DNA is scattered throughout the chloroplast as numerous nucleoids. When present as in *Pavlova* (Figure 1.1ag), the eyespot consists in a row of spherical globules inside the chloroplast; no associated flagellar

swelling is present. The most important storage product is the polysaccharide chrysolaminarine. The cell surface is typically covered with tiny cellulosic scales or calcified scales bearing spoke-like fibrils radially arranged. Most haptophytes are photosynthetic, but heterotrophic nutrition is also possible. Phagothropy is present in the forms that lack a cell covering. A heteromorphic diplohaplontic life cycle has been reported, in which a diploid planktonic flagellate stage alternates with a haploid benthic filamentous stage.

Cryptophyta

The unicellular flagellate belonging to the division Cryptophyta are asymmetric cells dorsiventrally constructed (Figure 1.47). They are mostly biflagellated, with two unequal, hairy flagella, subapically inserted, emerging from above a deep gullet located on the ventral side of the cell. The wall of this gullet is lined by numerous ejectosomes similar to trichocysts. Cryptophytes are typically free-swimming in freshwater and marine habitats; palmelloid phases can also be formed, and some members are known to be zooxanthellae in host invertebrates or within certain marine ciliate.

These algae possess only chlorophyll *a* and c_2. Phycobilins are present in the thylakoid lumen rather than in phycobilisomes. The chloroplasts, one or two per cell, are bounded by four membranes. The outermost membrane is continuous with the nuclear envelope and its surface is studded with ribosomes. Between the inner and outer membrane pairs is the periplastidial compartment, which contains the nucleomorph, the relict nucleus of the eukaryotic endosymbiont. Thylakoids are arranged in pairs, with no girdle lamellae. The pyrenoid projects out from the inner side of the chloroplast. The chloroplast DNA is condensed in small nucleoids scattered inside the chloroplast. The reserve polysaccharide accumulates in the periplastidial space as starch granules. Sometimes an eyespot formed by spherical globules is present inside the plastid, but it is not associated with the flagella. The cell is enclosed in a stiff, proteinaceous periplast, made by polygonal plates. Most forms are photosynthetic, but there are some colorless, heterotrophic. The primary method of reproduction is simply by longitudinal cell division, but sexual reproduction has also been documented.

Ochrophyta

One of the defining features of the members of this division is that when two flagella are present, they are different. Flagellate stages, when present, are therefore termed heterokont, that is, they possess a long mastigonemate flagellum, which is directed forward during the swimming, and a

FIGURE 1.47 Unicell of *Cryptomonas* sp. Scale bar: 6 μm.

short smooth one that points backwards along the cell. These algae are mostly marine, but they can also be found in freshwater and terrestrial habitats. They show a preponderance of carotenoids over chlorophylls that result in all groups having golden rather than grass green hue typical of other major algal division. The members of this division possess chlorophylls *a*, c_1, c_2, and c_3 with the exception of the Eustigmatophyceae, Aurearenophyceae, and *Ochromonas* (Chrysophyceae) that have only chlorophyll *a*. The principal accessory pigments are β-carotene, fucoxantin, and vaucheriaxanthin. The chloroplast is surrounded by four membranes: the normal plastidial double-membrane envelope, surrounded by a periplastidial membrane and by rough ER, which may be continuous with the outer membrane of the nuclear envelope. The periplastidial membrane is considered to be the remnants of the eukaryotic endosymbiont's (a red alga) plasmalemma. The chloroplast interior is occupied by thylakoids, which are grouped into stacks of three, called lamellae. One lamella usually runs along the whole periphery of the chloroplast, and is termed girdle lamella, absent only in the Eustigmatophyceae. The chloroplastic DNA is usually arranged in a ring-shaped nucleoid. Dictyochophyceae species possess several nucleoids scattered inside the chloroplast. The main reserve polysaccharide is chrysolaminarin, a β-1,3-glucan, located inside the cytoplasm in special vacuoles. The eyespot consists of a layer of globules, enclosed within the chloroplast, and together with the photoreceptor, located in the smooth flagellum, forms the photoreceptive apparatus. The member of this phylum can grow photoautrophycally, but can also combine different nutritional strategy such as heterotrophy (phagotrophy). The Ochrophyta species that reproduce sexually have a haplontic (e.g., Chrysophyceae), diplontic (e.g., Bacillariophyceae), or diplohaplontic (e.g., Phaeophyceae) life cycles. Chrysophyceae are predominantly single-celled flagellate individuals, but also coccoid, filamentous, and parenchymatous (Figures 1.1ai and 1.3). Most of these algae lack cell walls and have flagella inserted apically or slightly subapically. Cell coverings, when present, include organic scales, organic lorica, and cellulose cell wall. Xanthophyceae can be unicellular coccoids or flagellate, ameboid, or filamentous, but the most distinctive species are siphonous (Figures 1.1al and 1.18). Most Xanthophyceae are freshwater or soil algae, but a few are marine. All known species of Eustigmatophyceae are green coccoid unicells either single, in pairs or in colonies, which exhibit little morphological diversity (Figures 1.1am and 1.2). They are found in fresh, brackish, and seawater, as well as soil environments. Bacillariophyceae or diatoms are a group of unicellular brown pigmented cells that are encased by a unique type of silica wall, composed of two overlapping frustules that fit together like a box and lid (Figures 1.1an, 1.48, and 1.49). They are both marine and freshwater. Raphidopyceae are all unicellular autotrophic cells (Figures 1.1ao and 1.50), relatively big in size (30–80 μm), and globoid to ovoidal elongated shaped. Sometimes, they show a more sharpened point with a curved dorsal side and a flat ventral

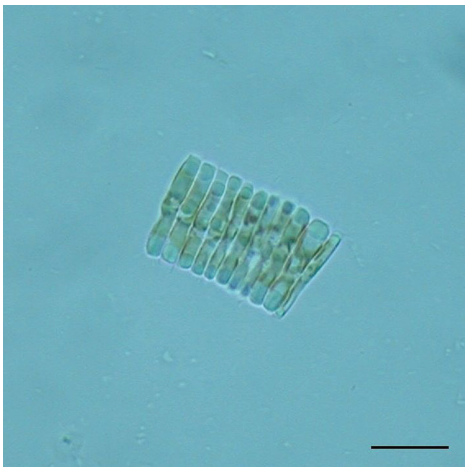

FIGURE 1.48 Marine diatom. Scale bar: 10 μm.

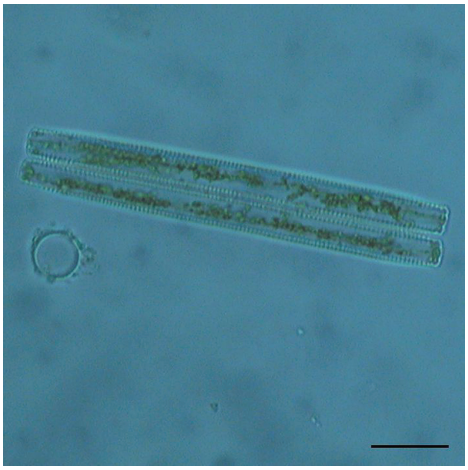

FIGURE 1.49 Freshwater diatom. Scale bar: 20 µm.

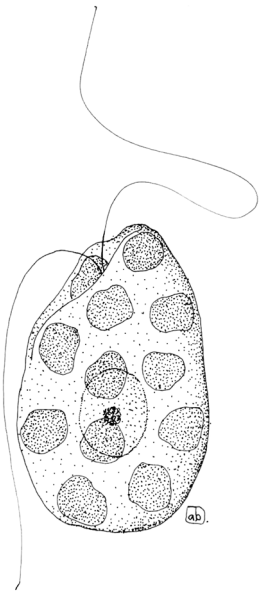

FIGURE 1.50 Unicell of *Heterosigma akashiwo.*

side. All the species lack a cell wall and they have no covering outside the cell membrane; consequently, the shape of the cell can vary with external conditions. They possess both trycocysts and mucocysts. Dictyochophyceae are naked unicells that bear a single flagellum, anteriorly directed, with mastigonemes (Figures 1.1ap and 1.51). The class includes the silicoflagellates, a group characterized by formation of a silicified skeleton, and organically scaled members. Phaeophyceae are multicellular, from branched filaments to massive, and complex parenchymatous kelp (Figures 1.1aq and 1.52). Flagellated stages possess two flagella usually laterally inserted, one anteriorly and one posteriorly directed. Cells show an alginate and cellulose wall. Pelagophyceae includes ciliated and coccoid members; cells can bear a single flagellum anteriorly directed, or two flagella, the second posteriorly directed (Figure 1.1ar). Bolidophyceae are flagellated picoplanktonic algae, considered as the closest, although separated lineage to diatoms (Figure 1.1as). Schizocladophyceae contains a

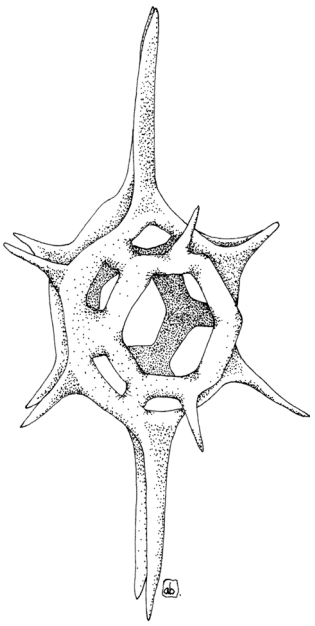

FIGURE 1.51 The silicoflagellate *Disthepanus speculum*.

FIGURE 1.52 Frond of *Bellotia eriophorum*. Scale bar: 5 cm.

single species, a marine filamentous alga isolated from the Tirrenian Sea; the cells possess a wall containing alginates but lacking cellulose (Figure 1.1at). Chrysomerophyceae are filamentous marine or brackish algae, epiphytic on halophytes, or algae (Figure 1.1au). Picophagophyceae contains both photosynthetic and nonphotosynthetic phagothrophs with filopodia or reticulopodia; the status of these algae as a distinct class has been questioned (Figure 1.1av). Pinguiophyceae are all single-celled microalgae from picoplankton size to over 40 μm (Figure 1.1az). They deserve mentioning because of the unusually high percentage of polyunsaturated fatty acids, especially eicosapentanoic acid

(20:5, *n*-3); this peculiarity is the basis for the choice of the Latin noun *pingue* (adj. fat) as the root for the class name. Placidiophyceae are kidney-shaped unicell with two flagella arising from a subapical region of the flattened ventral side. Cells that are usually attached to the substratum can glide or swim freely. They ingest prey particles on the posterior ventral side (Figure 1.1ba). Phaeothanmniophyceae can be filamentous (Figure 1.1bb), palmelloid, or coccoid; the vegetative cells are surrounded by a distinct cell wall of varying thickness. During cell division, an entirely new cell wall is formed inside the parent cell wall, that is, the new walls are formed by eleutheroschisis. Swimming stages have flagella inserted laterally. Synchromophyceae cell types can be sessile, migrating, and floating amoebae, surrounded by a lorica usually with one ostiole, through which reticulopodia protrude and fuse with neighboring cell to build up a meroplasmodium (Figure 1.1bc). The most striking and unique morphological feature of these algae is the aggregation of chloroplasts, each with two membranes, into groups of up to eight enclosed in a common periplastidial membrane and epiplastid rough ER. Synurophyceae are unicellular and colonial algae, important components of the species composition and biomass in freshwater environment worldwide (Figures 1.1bd and 1.5). A well-organized cell covering of siliceous, overlapping scales is characteristic of the class. These scales are morphologically unique for each species, and observations made with electron microscopy usually are required for species-level identification. They differ from closely related Chrysophyceae in the presence of only chlorophyll c_1, the parallel basal body orientation and the lack of eyespot. Aurearenophyceae (Figure 1.1be), a recently established class, are nonmotile algae, surrounded by a cell wall, with two unequal flagella lying inside the cell wall, or cells naked, motile, and biflagellate.

Cercozoa—Chlorarachniophyceae

Chlorarachniphyceae are naked, uninucleate cells that form a net-like plasmodium via filopodia (Figures 1.1bf, 1.53a, and 1.53b). The basic life cycle of these algae comprises ameboid, coccoid, and flagellate cell stages. The ovoid zoospores bear a single flagellum that during the swimming wraps around the cell. Chlorachniophytes are marine. They possess chlorophyll *a* and *b*. Each chloroplast has a prominent projecting pyrenoid and is surrounded by four envelope membranes. Thylakoids are grouped in stacks of 1–3. A nucleomorph is present between the second and third membranes of the chloroplast envelope. The origin of this organelle is different from the origin of the cryptophyte nucleomorph, since the chlorachniophytes came from a green algal endosymbiont. Paramylon (β-1,3-glucan) is the storage carbohydrate. They can phototrophic and phagotrophic, engulfing bacteria, flagellates, and eukaryotic algae. Asexual reproduction is carried out by either normal mitotic cell division or zoospore formation. Sexual reproduction characterized by heterogamy has been reported for only two species.

Myzozoa—Dinophyceae

Dinophyceae are typical unicellular flagellates, but can be also nonflagellate, ameboid, coccoid, palmelloid, or filamentous (Figures 1.1bg, 1.1bh, 1.54, and 1.55). Dinoflagellates have two flagella with independent beating pattern, one training, one girdling that confer characteristic rotatory swimming whirling motion. Flagella can be apically inserted (desmokont-type) or emerging from a region close to the midpoint of the ventral side of the cell (dinokont-type). Most dinoflagellates are characterized by cell-covering components that lie beneath the cell membrane. Around the cell, there is a superficial layer of flat, polygonal vesicles, which can be empty or filled with cellulose plates. In dinokont-type dinoflagellates, these thecal plates generally form a bipartite armor, consisting of an upper, anterior half and a lower, posterior half, separated by a groove known as cingulum, where the transversal flagellum is located (Figure 1.55). A smaller groove, the sulcus, extends posteriorly from the cingulum and hosts the longitudinal flagellum. The two flagella emerge from a pore located at the intersection of the two grooves. Very often dinoflagellates are important components of the microplankton of freshwater and marine habitats. Though most are too large (2–2000 μm) to be consumed by filter feeders, they are readily eaten by larger protozoa, rotifer, and planktivorous

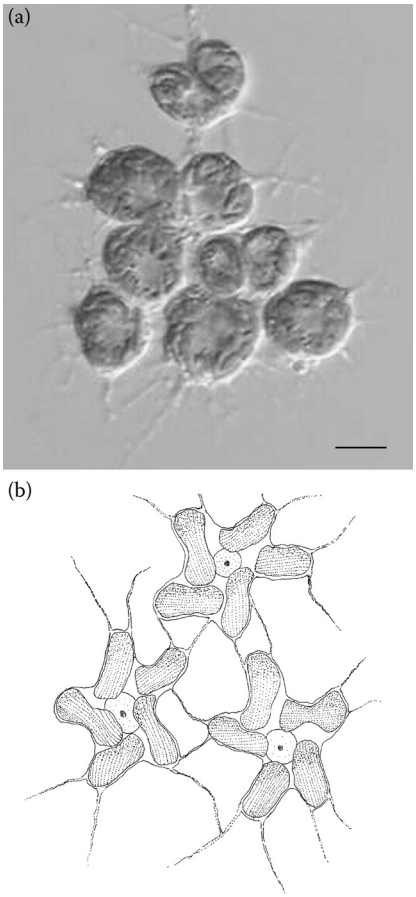

FIGURE 1.53 Plasmodial reticulum of *Chlorarachnion*: (a) bright-field microscope image and (b) schematic drawing. Scale bar: 4 μm.

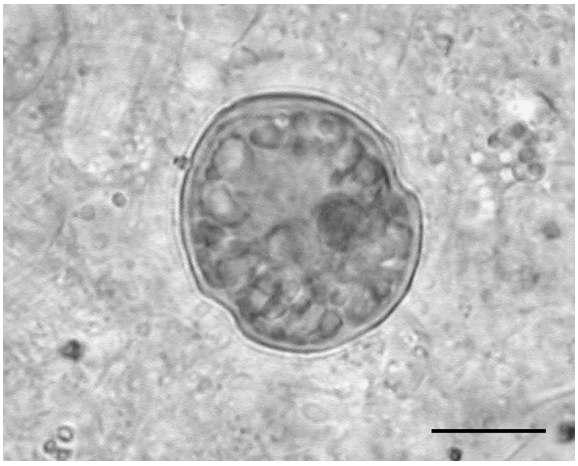

FIGURE 1.54 A marine dinoflagellate. Scale bar: 30 μm.

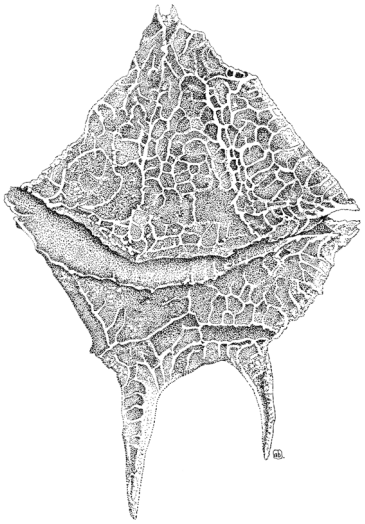

FIGURE 1.55 Dorsal view of *Gonyaulax* sp., a brackish water dinoflagellate.

fishes. Some dinoflagellates are invertebrate parasites, while others are endosymbionts (zooxanthellae) of tropical corals. Dinoflagellates possess chlorophylls *a*, c_1, and c_2, fucoxanthin, other carotenoids, and xanthophylls such as peridinin, gyroxanthin diester, dinoxanthin, diadinoxantin, and fucoxanthin. The chloroplasts, where present, are surrounded by three membranes. Within the chloroplasts typical pyrenoids are present, the thylakoids are for the most part united in a stack of 3. The chloroplast DNA is localized in small nodules scattered in the whole chloroplast. A really complex photoreceptive system is present in the dinophytes such as *Warnowia polyphemus*, *W. pulcra*, or *Erythropsidinium agile* consisting of a "compound eye" composed of a lens and a retinoid. Most dinoflagellates are distinguished by a dinokaryon, a special eukaryotic nucleus involving fibrillar chromosomes that remain condensed during the mitotic cycles. The principal reserve polysaccharide is starch, located as grains in the cytoplasm, but oil droplets are present in some genera. At the surface of the cell, there are trichocysts that discharge explosively when stimulated. Besides photoautotrophy, dinoflagellates exhibit an amazing diversity of nutritional types since about half of the known species lack plastids and are therefore obligate heterotrophic. Some are notorious for nuisance blooms and toxin production, and many exhibit bioluminescence. Dinophyceae have generally a haplontic life history.

Euglenozoa—Euglenophyceae

Euglenophyceae include mostly unicellular flagellates, although colonial species are common (Figures 1.1bi, 1.1bl, 1.1bm, 1.1bn, and 1.56). They are widely distributed, occurring in freshwater, but also brackish and marine waters, most soils and mud. They are especially abundant in highly heterotrophic environments. The flagella arise from the bottom of a cavity called reservoir, located in the anterior end of the cell. Cells can also ooze their way through mud or sand by a process known as metaboly, a series of flowing movements made possible by the presence of the pellicle, a proteinaceous wall that lies inside the cytoplasm. The pellicle can have a spiral construction and can be ornamented. The members of this division share their pigmentation with prochlorophytes, green algae, and land plants, since they have chlorophylls *a* and *b*, β- and γ-carotenes, and xanthins. However, plastids could be colorless or absent in some species. As in the Dinophyceae, the chloroplast envelope consists of three membranes. Within the chloroplasts, the thylakoids are usually in groups of 3, without a girdle lamella; pyrenoids may be present. The chloroplast DNA occurs

FIGURE 1.56 Unicell of *Euglena gracilis*. Scale bar: 10 µm.

as a fine skein of tiny granules. The photoreceptive system consisting of an orange eyespot located free in the cytoplasm and the true photoreceptor located at the base of the flagellum can be considered unique among unicellular algae. The reserve polysaccharide is paramylon, β-1,3-glucan stored in granules scattered inside the cytoplasm, and not in the chloroplasts such as the starch of the Chlorophyta. Though possessing chlorophylls, these algae are not photoautotrophic but rather obligate mixotrophic, because they require one or more vitamins of the B group. Some colorless genera are phagotrophic, with specialized cellular organelle for capture and ingestion of prey, while some other are osmotrophic. Some of the pigmented genera are facultative heterotrophic. Only asexual reproduction is known in this division. Euglenophyceae possess unique cellular and biochemical features that place these microorganisms closer to trypanosomes than to any other algal group.

ENDOSYMBIOSIS AND ORIGIN OF EUKARYOTIC PHOTOSYNTHESIS

The origin of cyanobacteria can be equated with the origin of aerobic photosynthesis around 2.8 billion years ago, in the Archaean Era of earth history. From that time to present, cyanobacteria have played fundamental roles in driving much of the ocean carbon, oxygen, and nitrogen fluxes, establishing a major turning point in the biogeochemistry of our planet. Prior to the appearance of these organisms, all photosynthetic organisms were anaerobic bacteria that used light to couple the reduction of carbon dioxide to the oxidation of low free energy molecules, such as H_2S or preformed organics. Cyanobacteria developed a key characteristic that distinguished them from their photosynthetic evolutionary precursors, that is the ability to extract electrons from water releasing oxygen as a byproduct, with the help of two photosystems linked in series. Oxygenic photosynthesis exploits the energy of visible light to oxidize water and simultaneously reduces CO_2 to organic carbon represented by $(CH_2O)_n$. Light energy is used as a substrate and chlorophyll *a* as a requisite catalytic agent.

Formally oxygenic photosynthesis can be summarized as

$$CO_2 + H_2O + \text{light} \xrightarrow{\text{Chlorophyll } a} (CH_2O)_n + O_2$$

Thanks to endosymbiosis, the photosynthetic trait was acquired in the founding group of photosynthetic eukaryotes, the Plantae or Archaeplastida, and spread to give rise to the wide variety of photosynthetic eukaryotes on earth today. The origin of plastids in eukaryotic cells about 1.8 billion years ago is one of the most profound effects of the endosymbiotic process. These organelles have been well established to have evolved from a single so-called "primary endosymbiotic event" involving the uptake of a β-cyanobacterium by a heterotrophic/phagotrophic eukaryote, whose ancestors had already acquired a mitochondrion via endosymbiosis of a proteobacterium. Plastid genomes rarely encode more than 200 proteins, which represent a small fraction of the proteins required for full functionality, and an even smaller fraction of the few thousand proteins found in

modern-day cyanobacteria. It is widely assumed that in the process of endosymbiosis, most endosymbiont genes were either lost together with the corresponding function or transferred to the host nucleus and merged into the chromosomes during the course of plastid integration. This migration of genes between two genomes is known as endosymbiotic gene transfer, a special case of horizontal gene transfer (HGT). Over time, some acquired targeting sequences that enabled their products synthesized on cytoplasmic ribosomes were targeted back to the organelle. In addition, some host genes acquired targeting sequences that enabled their products to be imported into the organelle. All these processes played a fundamental role in the integration of endosymbiont and host.

"Primary plastids" are surrounded by two bounding membranes and are only found in three major eukaryotic photosynthetic groups of Plantae, that is, Glaucophyta, Chlorophyta, and Rhodopyta.

Glaucophyta occupy a key position in the evolution of plastids; in fact, the plastids of glaucophytes contain chlorophyll *a*, present in cyanobacteria, and retain the remnant of a Gram-negative bacterial peptidoglycan wall that would have been between the two membranes of the cyanobacterial ancestor symbiont. The retention of this ancestral character is absent in both green and red plastids.

Chlorophyta (green algae and plants) constitute the second lineage of primary plastids. The simple two-membrane system surrounding the plastid, the congruence of phylogenies based on nuclear and organellar genes, and the antiquity of the green algae in the fossil record all indicate that the green algal plastid is of primary origin. In these chloroplasts, chlorophyll *b* was synthesized as a secondary pigment, phycobiliproteins were lost, and starch was stored. Another hypothesis suggested that the photosynthetic ancestor of green lineage was a prochlorophyte that possessed chlorophylls *a* and *b* and lacked phycobiliproteins.

The green lineage played a major role in oceanic food webs and the carbon cycle from about 2.2 billion years ago until the end-Permian extinction, approximately 250 million years ago. It was this similarity to the pigments of plants that led to the inference that the ancestors of land plants (i.e., embryophytes) would be among the green algae and is clear that phylogenetically plants are a group of green algae adapted to life on land.

The plastids of Rhodophyta (red algae) constitute the third primary plastid lineage. Like the green algae, the red algae are also an ancient group in the fossil record, and some of the oldest fossils interpreted as being of eukaryotic origin are often referred to the red algae, although clearly these organisms were very different from any extant alga. Like those of green algae, the plastids of red algae are surrounded by two membranes. However, they are pigmented with chlorophyll *a*, phycobiliproteins, organized into phycobilisomes, and are distinguished by the presence of phycoerithrin. Phycobilisomes are relatively large extrinsic antennas, water-soluble, and attached to the surface of the thylakoid membrane. Thylakoids with phycobilisomes do not form stacks like those in other plastids and consequently the plastids of red algae (and glaucophytes) bear an obvious ultrastructural resemblance to cyanobacteria.

Though the plastids of these three lineages are all primary plastids, that is, having only two membranes around them, they differ more noticeably in their light-harvesting machinery. Green algae and plants have membrane-intrinsic antenna proteins (members of the light-harvesting complex superfamily) that bind both chlorophylls *a* and *b* and are associated with both photosystems. Red algae have proteins of the same family that bind only chlorophyll *a* and are associated with photosystem I. Glaucophytes do not have this type of antenna, but along with the red algae they have phycobilisomes, extrinsic antennas which bind linear tetrapyrroles.

Molecular phylogeny supports two possible evolutionary scenarios for the branching order within Plantae, the red-first and glaucophyte-first hypotheses. The inability to unambiguously decide between these two using genome-wide analyses may be explained by the more than 1 billion years that have passed since primary endosymbiosis. The early period of Plantae evolution was likely characterized by a rapid radiation, reticulate evolution (by HGT) among taxa, and high rates of gene divergence, loss, and replacement that have diffused the evolutionary signal. This idea is supported by the findings regarding mitochondrial gene order and gene content that do not favor a particular order of branching.

As ancient as the primary endosymbiotic origin of plastid was (1.8 billion years ago), it is worth noting that cases of "recent" cyanobacterium–eukaryote endosymbiosis are known, for example, in the testate amoeba *Paulinella cromatophora* and the diatom *Rhopalodia gibba*. The photosynthetic consortium between *Paulinella* and an α-cyanobacterium was established 60 million years ago. This amoeba is surrounded by the cell wall called theca, which is composed of silica scales. Apart from typical eukaryotic organelles such as nucleus and mitochondria, it harbors two cyanobacterium-derived endosymbionts. The endosymbionts are photosynthetically active, deeply integrated with the host cell, and their genome has been reduced to one-third in comparison to their cyanobacterial ancestors. The pennate diatom *R. gibba* harbors endosymbionts closely related to extant cyanobacteria. Some of the closest free-living relatives of these so-called spheroid bodies are diazotrophic cyanobacteria of the *Cyanothece* sp. group. The spheroid bodies encode genes for nitrogen fixation and have the capacity to fix molecular nitrogen under light conditions only, unlike all other unicellular nitrogen-fixing cyanobacteria. Although the spheroid bodies are of cyanobacterial origin, they lack the typical photosynthetic pigmentation.

Plantae, that is, Glaucophyta, Chlorophyta, and Rhodopyta, represent just the beginning of the endosymbiosis story. In fact, while mitochondria originated once and have apparently never been lost, plastids have spread between eukaryotic lineages several times in events referred to as secondary and tertiary endosymbiosis, that is, the uptake and retention of a primary or secondary algal cell by another eukaryotic lineage.

Euglenozoa and Cercozoa derived from this primary plastid lineage by two separate secondary endosymbiosis acquiring the plastid by engulfing a green alga. Two independent lineages of green algae were captured by two distinct lineages of phagotrophic protists via secondary endosymbiosis; chloroplast genome analyses suggest that the chlorarachniophyte plastid is derived from a green alga belonging to the "core chlorophyte" group (Trebouxiophyceae, Ulvophyceae, Chlorophyceae), while the ancestor of the euglenophyte plastid is related to prasinophyte green algae. There is no strong similarity between the plastid of euglenids and chlorarachniophytes: euglenids have plastids bounded by three membranes and store paramylon in the cytosol, whereas chlorarachniophytes have plastids bounded by four membranes with a nucleomorph and store β-1,3-glucan in the cytosol.

Euglenozoa contains photoautotrophic species and species with different types of feeding strategies, osmotrophic (e.g., *Rhabdomonas*) or phagotrophic (e.g., *Peranema*). The plastids have been subsequently and independently lost in several branches within the phototrophic clade. Current knowledge on the phylogeny of euglenozoa implies that the secondary endosymbiotic event happened after the split of *Peranema*, but before the split of *Eutreptia* and *Eutreptiella*, which form the basal lineages of the phototrophic clade. Recently, a number of red algal origin genes have been identified in the photosynthetic *Euglena gracilis* as well as in the heterotrophic *Peranema*. It is likely that these genes have been acquired via eukaryote-to-eukaryote lateral gene transfer, giving rise to a complex pattern of genome mosaicism in euglenids. These genes may come from prey organisms, and the lineage of euglenids might have experienced a cryptic red algal plastid endosymbiosis before the current green algal plastid was established. Derived genes may have contributed to the successful integration and functioning of the green algal secondary plastid in modern-day euglenids.

Multiple red algal-derived Calvin cycle genes have been detected also in Cercozoa (Chlorarachniophyta) nuclear genomes. One possible explanation is that these genes were transferred from red alga prey organisms via HGT. The prey organism might have been captured by and retained in an ancestral and probably nonphotosynthetic chlorarachniophyte as an endosymbiont, which was then replaced by a green algal endosymbiont, giving rise to the extant secondary plastid in Chlorarachniophyta.

The plastid of cryptophytes, ochrophytes, dinoflagellates, and haptophytes likely arose from a single initial event of secondary endosymbiosis of a red alga with a nonphotosynthetic eukaryotic host.

The red alga eventually evolved chlorophyll *c* plastids and engaged in several subsequent higher-order endosymbiosis with phylogenetically diverse hosts (in an order still to be resolved), hence giving rise to all the extant photosynthetic lineages. The derivation of chlorophyll *c* containing plastids from the red algal lineage is still somewhat conjectural, but recent analyses of both gene sequences and gene content are consistent with this conclusion.

The cryptophytes were the first group in which secondary plastids were recognized, on the basis of their complex four-membrane structure. Like red algae, they have chlorophyll *a* and phycobiliproteins, but these are distributed in the intrathylakoidal space rather than in the phycobilisomes found in red algae, Glaucophyta, and Cyanophyta. In addition, cryptomonads possess a second type of chlorophyll, chlorophyll *c*, which is found in the plastids of the remaining red lineage clades, retain the nucleomorph, vestigial nucleus of their symbiont, and have starch the reserve polysaccharide of red algae in the periplastid space.

Ochrophyta (including kelps, diatoms, chrysophytes, and related groups), Haptophyta (the coccolithophorids), and probably those dinoflagellates (Myzozoa) pigmented with peridinin, have chlorophylls *a* and *c*, along with a variety of carotenoids. Stacked thylakoids are found in those lineages that lack phycobilisomes.

The plastid situation in dinoflagellate is exceptionally complex; most of the phototrophic species harbor a plastid of red algal origin bound by three membranes and characterized by the carotenoid peridinin, chlorophylls *a* and c_2. It has been speculated that the ancestral peridinin-containing chloroplast was replaced by one from a cryptophyte, a haptophyte, a diatom, or a green alga, that is, by additional endosymbiotic events, namely tertiary endosymbiosis in the first three cases, and serial secondary endosymbiosis for the green alga. All these symbiotic relationships have not reached the same level of permanence, and sometimes it is disputed whether the plastids are the traces of a stable symbiosis or rather they are kleptoplastids, that is, plastids obtained from ingested algal prey and retained, which may remain temporarily functional and be used for photosynthesis by the predator. In some cases, the endosymbiont is present in an almost unchanged form and was therefore established more recently (e.g., *Kryptoperidinium foliaceum*). In other cases, the symbiont has almost lost all organelles and only the chloroplast remains (e.g., peridinin-containing species, *Heterocapsa*, *Peridinium*), indicating an older, more well-established symbiosis.

Members of the Kareniaceae (*Karenia mikimotoi*, *Karlodinium micrum*) possess fucoxanthins as accessory pigment instead of peridinin; molecular data confirmed that the peridinin-containing chloroplast in this group has been superseded by a haptophyte-type-containing fucoxanthin. Other dinoflagellates such as *Dinophysis acuminata* have established a stable symbiosis with a cryptophyte symbiont, of which only the chloroplast remains, surrounded by three membranes. A diatom symbiont is present in a small group of closely related dinoflagellates named "dinotoms" consisting of only 10 species such as *Durinskia baltica*, *K. foliaceum*, *Peridinium quinquecorne*, and other species belonging to the genera *Galeidinium* and *Gymnodinium*. The endosymbionts have been shown to originate from three different diatom lineages, one pennate and two centric. Despite the loss of a distinctive cell wall, motility, and ability to divide mitotically, these endosymbionts have retained a large nucleus with vast amount of DNA, a large volume of cytoplasm, separate from the host by a single membrane, and their own mitochondria in addition to the chloroplasts. Another unique symbiosis is present in the dinoflagellate genus *Lepidodinium*; members of this genus such as *L. viride* (Figure 1.1bh; courtesy of Francisco Rodriguez Hernandez) and *Lepidodinium chlorophorum* (formerly *Gymnodinium chlorophorum*) possess green-colored plastids containing chlorophylls *a* and *b*. The pigment composition, phylogenetic analyses of plastid-encoded genes, and a survey of nuclear genes encoding plastid-targeted proteins in *L. chlorophorum* clearly indicated that the ancestral *Lepidodinium* cells replaced the original Chl-*a* + *c*-containing plastids with the Chl-*a* + *b*-containing plastids of an endosymbiotic green alga belonging to the core chlorophytes. Only the symbiont chloroplast

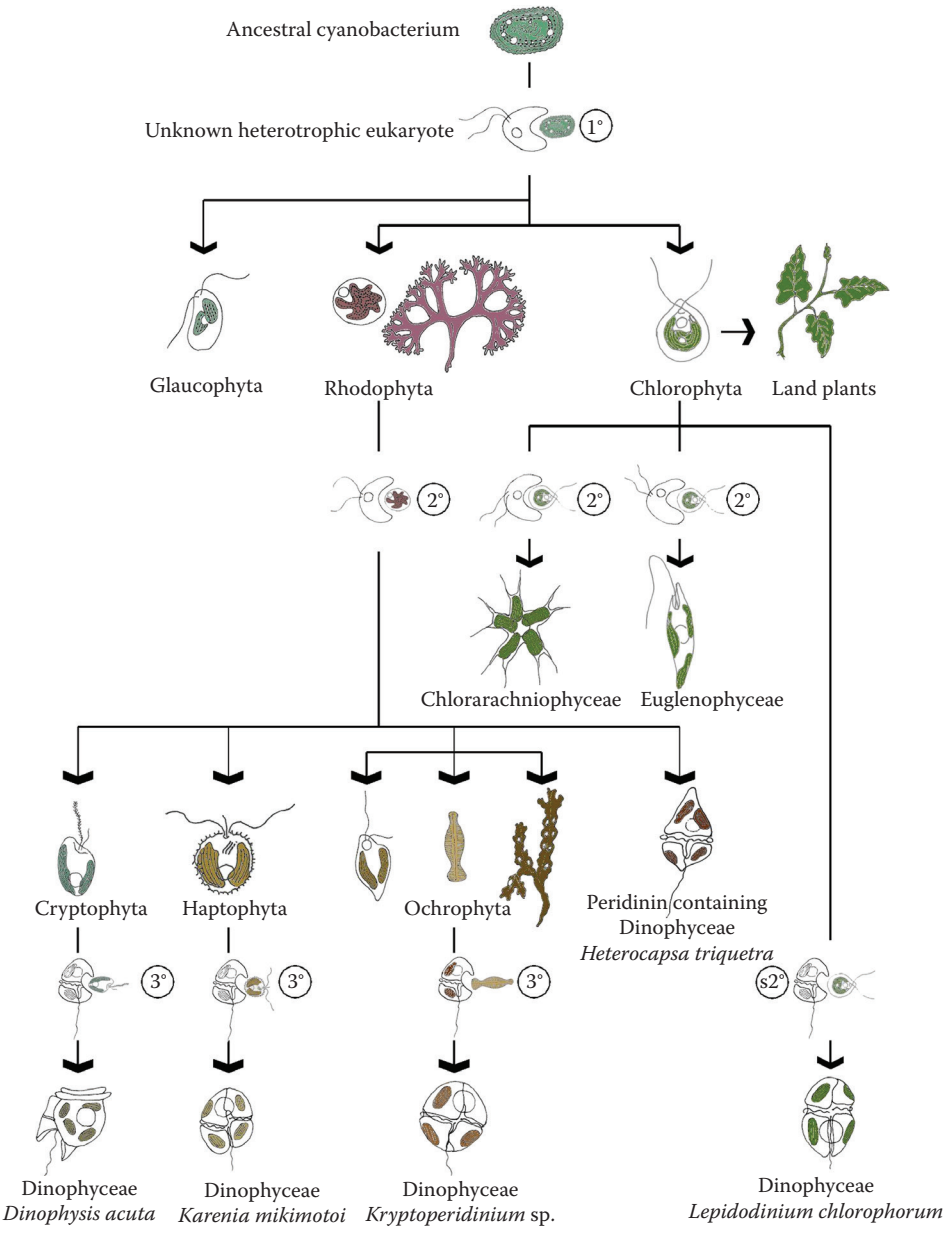

FIGURE 1.57 Hypothesis for algal evolution and endosymbiotic events. 1°, primary endosymbiosis; 2°, secondary endosymbiosis; s2°, serial secondary endosymbiosis; 3°, tertiary endosymbiosis.

remains in these dinoflagellates. A schematic drawing of the hypothesis of the different symbiotic events is shown in Figure 1.57.

SUGGESTED READING

Adl, S. M., Simpson, A. G. B., Lane, C. E., Lukeš, J., Bass, D., Bowser, S. S. et al. The revised classification of eukaryotes. *Journal of Eukaryotic Microbiology*, 59: 429–514, 2012.

Algaebase http://www.algaebase.org/

Andersen, R. A. Biology and systematics of heterokont and haptophyte algae. *American Journal of Botany*, 91: 1508–1522, 2004.

Archibal, J. M. The puzzle of plastid evolution. *Current Biology*, 19: R81–R88, 2009.

Bendif, E. M., Probert, I., Hervé, A., Billard, C., Goux, D., Lelong, C., Cadoret, J. P., and Véron, B. Integrative taxonomy of the Pavlovophyceae (Haptophyta): A reassessment. *Protist*, 162: 738–761, 2011.

Bhattacharya, D., Price, D. C., Yoon, H. S., Yang, E .C., Poulton, N. J., Andersen, R. A. et al. Single cell genome analysis supports a link between phagotrophy and primary plastid endosymbiosis. *Scientific Reports*, 2: 356, 2012.

Bold, H. C. and Wynne, M. J. *Introduction to the Algae—Structure and Reproduction*. Prentice-Hall, Englewood Cliffs, NJ, 1978.

Bourrelly, P. Les Algue d'eau douce. Initiation à la Systèmatique. Les algues verdes. Editions N. Boubèe, Paris, 1966.

Bourrelly, P. Les Algue d'eau douce. Initiation à la Systèmatique. Les algues jaunes et brunes. Editions N. Boubèe, Paris, 1968.

Bourrelly, P. Les Algue d'eau douce. Initiation à la Systèmatique. Eugleniens, Peridinies, Algues rouges et Algues bleues. Editions N. Boubèe, Paris, 1970.

Brodie, J. and Lewis, J. (Eds.). *Unravelling the Algae. The Past, Present and Future of Algal Systematic*. CRC Press, Taylor and Francis Group, Boca Raton, FL, 2007.

Burki, F., Okamoto, N., Pombert, J.-F., and Keeling, P. J. The evolutionary history of haptophytes and cryptophytes: Phylogenomic evidence for separate origins. *Proceedings of the Royal Society B: Biological Sciences*, 279(1736): 2246–2254, 2012.

Carr, N. G. and Whitton, B. A. *The Biology of Cyanobacteria*. Blackwell Scientific, Oxford, 1982.

Dorrell, R. G. and Smith, A. G. Do red and green make brown? Perspective on plastid acquisition within chromoalveolates. *Eukaryotic Cell*, 10(7): 856–868, 2011.

Facchinelli, F. and Weber, A. P. M. The metabolite transporters of the plastid envelope: An update. *Frontiers in Plant Science*, 2: 2011.

Garcia-Cuetos, L., Moestrup, Ø., Hansen, P. J., and Daugbjerg, N. The toxic dinoflagellate *Dinophysis acuminata* harbors permanent chloroplasts of cryptomonad origin, not kleptochloroplasts. *Harmful Algae*, 9(1): 25–38, 2010.

Graham, L. E. and Wilcox, L. W. *Algae*. Prentice-Hall, Upper Saddle River, NJ, 2000.

Green, B. After the primary endosymbiosis: An update on the chromalveolate hypothesis and the origins of algae with Chl *c*. *Photosynthesis Research*, 107(1): 103–115, 2011a.

Green, B. R. Chloroplast genomes of photosynthetic eukaryotes. *The Plant Journal*, 66: 33–44, 2011b.

Imanian, B., Pombert, J. F., Dorrell, R. G., Burki, F., and Keeling, P. J. Tertiary endosymbiosis in two dinotoms has generated little change in the mitochondrial genomes of their dinoflagellate hosts and diatom endosymbionts. *PLoS ONE*, 7: 1–13, 2012.

Janouškovec, J., Horák, A., Oborník, M., Lukeš, J., and Keeling, P. J. A common red algal origin of the apicomplexan, dinoflagellate, and heterokont plastids. *PNAS*, 15: 10949–10954, 2010.

Kai, A., Yoshii, Y., Nakayama, T., and Inouye, I. Aurearenophyceae classis nova, a new class of Heterokontophyta based on a new marine unicellular alga *Aurearena cruciata* gen. et sp. nov. inhabiting sandy beaches. *Protist*, 159(3): 435–457, 2008.

Kawachi, M., Inouye, I., Honda, D., O'Kelly, C. J., Bailey, J. C., Bidigare, R. R. et al. The Pinguiophyceae classis nova, a new class of photosynthetic stramenopiles whose members produce large amounts of omega-3 fatty acids. *Phycological Research*, 50(1): 31–47, 2002.

Keeling, P. J. The endosymbiotic origin, diversification and fate of plastids. *Philosophical Transactions of the Royal Society of London. Series B, Biological Sciences*, 365(1541): 729–748, 2010.

Keeling, P. J. The number, speed, and impact of plastid endosymbiosis in eukaryotic evolution. *Annual Review of Plant Biology*, 64: 27.1–27.25, 2013.

Kim, E. and Archibald, J. M. Plastid evolution: Gene transfer and the maintenance of "stolen" organelle. *BMC Biology*, 8: 73–76, 2010.

Kneip, C., Vobeta, C., Lockhart, P., and Maier, U. The cyanobacterial endosymbiont of the unicellular alga *Rhopalodia gibba* shows reductive genome evolution. *BMC Evolutionary Biology*, 8(1): 30, 2008.

Koch, C., Brumme, B., Schmidt, M., Flieger, K., Schnetter, R., and Wilhelm, C. The life cycle of the amoeboid alga *Synchroma grande* (Synchromophyceae, Heterokontophyta)—Highly adapted yet equally equipped for rapid diversification in benthic habitats. *Plant Biology*, 13(5): 801–808, 2011.

Lane, C. E. and Archibald, J. M. The eukaryotic tree of life: Endosymbiosis takes its TOL. *Trends in Ecology & Evolution*, 23(5): 268–275, 2008.

Leliaert, F., Smith, D. R., Moreau, H., Herron, M. D., Verbruggen, H., Delwiche, C. F., and De Clerck, O. Phylogeny and molecular evolution of the green algae. *Critical Reviews in Plant Sciences*, 31: 1–46, 2012.

Lukeš, J., Leander, B. S., and Keeling, P. J. Cascades of convergent evolution: The corresponding evolutionary histories of euglenozoans and dinoflagellates. *PNAS*, 106: 9963–9970, 2009.

Mackiewicz, P., Bodył, A., and Gagat, P. Protein import into the photosynthetic organelles of *Paulinella chromatophora* and its implications for primary plastid endosymbiosis. *Symbiosis*, 58(1–3): 99–107, 2012.

Marin, B. Nested in the Chlorellales or independent class? Phylogeny and classification of the Pedinophyceae (Viridiplantae) revealed by molecular phylogenetic analyses of complete nuclear and plastid-encoded rRNA operons. *Protist*, 163(5): 778–805, 2012.

Matsumoto, T., Ishikawa, S. A., Hashimoto, T. and Inagaki, Y. A deviant genetic code in the green alga-derived plastid in the dinoflagellate *Lepidodinium chlorophorum*. *Molecular Phylogenetics and Evolution*, 60(1): 68–72, 2011.

Miyagishima, S. Y. Mechanism of plastid division: From a bacterium to an organelle. *Plant Physiology*, 155(4): 1533–1544, 2011.

Moriya, M., Nakayama, T., and Inouye, I. A new class of the Stramenopiles, Placididea Classis nova: Description of *Placidia cafeteriopsis* gen. et sp. nov. *Protist*, 153(2): 143–156, 2002.

Nishitani, G., Nagai, S., Hayakawa, S., Kosaka, Y., Sakurada, K., Kamiyama, T. et al. Multiple plastids collected by the Dinoflagellate *Dinophysis mitra* through Kleptoplastidy. *Applied and Environmental Microbiology*, 78(3): 813–821, 2012.

Prescott, G. W. *Algae of the Western Great Lakes Area*. W.C. Brown, Dubuque, IA, 1962.

Qiu, D., Huang, L., Liu, S., and Lin, S. Nuclear, mitochondrial and plastid gene phylogenies of *Dinophysis miles* (Dinophyceae): Evidence of variable types of chloroplasts. *PLoS ONE*, 6(12): e29398, 2011.

Sheiner, L. and Striepen, B. Protein sorting in complex plastids. *Biochimica Biophysica Acta*, 1833: 352–359, 2013.

Tilden, J. E. *The Algae and Their Life Relations. Fundamentals of Phycology*. The University of Minnesota Press, Minneapolis, 1935.

Timme, R. E., Bachvaroff, T. R., and Delwiche, C. F. Broad phylogenomic sampling and the sister lineage of land plants. *PLoS ONE*, 27: 1–8, 2012.

Tirichine, L. and Bowler, C. Decoding algal genomes: Tracing back the history of photosynthetic life on Earth. *The Plant Journal*, 66: 45–57, 2011.

Van den Hoek, C., Mann, D. G., and Jahns, H. M. *Algae—An Introduction to Phycology*. Cambridge University Press, Cambridge, UK, 1995.

Xia, S., Zhang, Q., Zhu, H., Cheng, Y., Liu, G., and Hu, Z. Systematics of a kleptoplastidal dinoflagellate, *Gymnodinium eucyaneum* Hu (Dinophyceae), and its cryptomonad endosymbiont. *PLoS ONE*, 8(1): e53820, 2013.

Yamaguchi, H., Nakayama, T., Kai, A., and Inouye, I. Taxonomy and phylogeny of a new kleptoplastidal dinoflagellate, *Gymnodinium myriopyrenoides* sp. nov. (Gymnodiniales, Dinophyceae), and its cryptophyte symbiont. *Protist*, 162(4): 650–667, 2011.

Zapata, M., Fraga, S., Rodríguez, F., and Garrido, J. L. Pigment-based chloroplast types in dinoflagellates. *Marine Ecology Progress Series*, 465: 33–52, 2012.

Zechman, F. W., Verbruggen, H., Leliaert, F., Ashworth, M., Buchheim, M. A., Fawley, M. W. et al. An unrecognized ancient lineage of green plants persists in deep marine waters. *Journal of Phycology*, 46: 1288–1295, 2010.

2 Anatomy

CYTOMORPHOLOGY AND ULTRASTRUCTURE

The description of the algal cell will proceed from the outside structures to the inside components. Details will be given only for those structures that are not comparable with analog structures found in most animals and plants. The reader is referred to a general cell biology textbook for the structure not described in the following.

Outside the Cell

Cell surface forms the border between the external world and the inside of the cell. It serves a number of basic functions, including species identification, uptake and excretion/secretion of various compounds, protection against desiccation, pathogens, and predators, cell signaling, and cell–cell interaction. It serves as an osmotic barrier, preventing free flow of material, and as a selective barrier for the specific transport of molecules. Algae, besides naked membranes more typical of animal cells and cell walls similar to those of higher plant cells, possess a wide variety of cell surfaces. The terminology used to describe surface structure of cells of algae is sometimes confusing; to avoid this confusion, or at least to reduce it, we will adopt a terminology mainly based on that of Preisig et al. (1994).

Cell surface structures can be grouped into four different basic types:

- Simple cell membrane (Type 1)
- Cell membrane with additional extracellular material (Type 2)
- Cell membrane with additional intracellular material in vesicles (Type 3)
- Cell membrane with additional intracellular and extracellular material (Type 4)

Type 1—Simple Cell Membrane

This cell surface consists of a simple or modified plasma membrane. The unit membrane is a lipid bilayer, 7–8-nm thick, rich with integral and peripheral proteins. Several domains exist in the membrane, each distinguished by its own molecular structure. Some domains have characteristic carbohydrate coat enveloping the unit membrane. The carbohydrate side chains of the membrane, glycolipids, and glycoproteins form the carbohydrate coat. Difference in the thickness of plasma membrane may reflect differences in the distribution of phospholipids, glycolipids, and glycoproteins (Figure 2.1).

A simple plasma membrane is present in the zoospores and gametes of Chlorophyceae (Chlorophyta), Xanthophyceae (Ochrophyta), and Phaeophyceae (Ochrophyta), in the zoospores of the Eustigmatophyceae (Ochrophyta), and in the spermatozoids of Bacillariophyceae (Ochrophyta). This type of cell surface usually characterizes very short-lived stages and, in this transitory naked phase, the naked condition is usually rapidly lost once zoospores or gametes have ceased swimming and have become attached to the substrate, since wall formation rapidly ensues. A simple cell membrane covers the uninucleate cells that form the net-like plasmodium of the Chlorarachniophyceae (Cercozoa) during all their life history. Most Chrysophyceae occur as naked cells, whose plasma membrane is in direct contact with water, but in *Ochromonas*, the membrane is covered with both

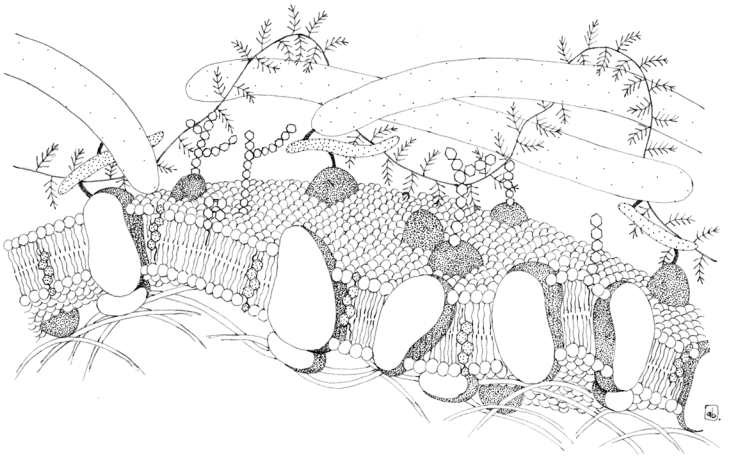

FIGURE 2.1 Schematic drawing of a simple cell membrane.

a carbohydrate coat and surface blebs and vesicles, which may serve to trap bacteria and other particles that are subsequently engulfed as food. The properties of the membrane or its domains may change from one stage in the life cycle to the next.

Type 2—Cell Surface with Additional Extracellular Material

Extracellular matrices occur in various forms and include mucilage and sheaths, scales, frustule, cell walls, loricas, and skeleta.

The terminology used to describe this membrane-associated material is quite confusing, and unrelated structures such as the frustule of diatoms, the fused scaled covering of some prasynophyceae, and the amphiesma of dinoflagellates have been given the same name, that is, theca. Our attempt has been to organize the matter in a less confusing way (at least in our opinion).

Mucilages and Sheaths

These are general terms for some sort of outer gelatinous covering present in both prokaryotic and eukaryotic algae. Mucilages are always present and we can observe a degree of development of a sheath that is associated with the type of the substrate the cells contact (Figure 2.2). All cyanobacteria secrete a gelatinous material, which, in most species, tends to accumulate around the cells or trichome in the form of an envelope or sheath. Coccoid species are thus held together to form colonies; in some filamentous species, the sheath may function in a similar manner, as in the formation of *Nostoc* balls, or in development of the firm, gelatinous hemispherical domes of the marine *Phormidium crosbyanum*. Most commonly, the sheath material in filamentous species forms a thick coating or a tube through which motile trichomes move readily. Sheath production is a continuous process in cyanobacteria, and variation in this investment may reflect different physiological stages or levels of adaptation to the environment. Under some environmental conditions, the sheath may become pigmented, although it is normally colorless and transparent. Ferric hydroxide or other iron or metallic salts as well as pigments originating within the cell may accumulate in the sheath. Only a few cyanobacterial exopolysaccharides have been defined structurally; the sheath of *Nostoc commune* contains cellulose-like glucan fibrils cross-linked with minor monosaccharides and that of *Mycrocystis flos-aquae* consists mainly of galacturonic acid, with a composition similar to that of pectin. Cyanobacterial sheaths appear as a major component of soil crusts found throughout the world, from hot desert to polar regions, protecting soil from erosion, favoring water retention and nutrient bio-mobilization, and affecting chemical weathering of the environment they colonize.

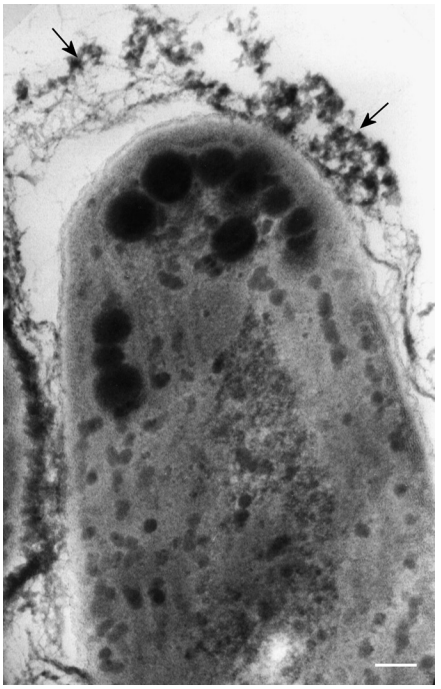

FIGURE 2.2 TEM image of the apical cell of *Leptolyngbya* spp. trichome in longitudinal section. The arrows point to the mucilaginous sheath of this cyanobacterium. Inside the cell, osmiophylic eyespot globules are present. Scale bar, 0.15 μm. (Courtesy of Prof. Patrizia Albertano.)

In eukaryotic algae, mucilages and sheaths are present in diverse divisions. The most common occurrence of this extracellular material is in the algae palmelloid phases, in which nonmotile cells are embedded in a thick, more or less stratified, sheath of mucilage. This phase is so called because it occurs in the genus *Palmella* (Chlorophyceae), but it is also present in other members of the same class, such as *Asterococcus* sp., *Hormotila* sp., and *Gloeocystis* sp. A palmelloid phase is also present in *Spirogyra* sp. (Zygnematophyceae), *Chroomonas* sp. (Cryptophyceae), *Gloeodinium montanum* vegetative cells (Dinophyceae) *Euglena gracilis* (Euglenophyceae) (Figure 1.22). Less common are the cases in which filaments are covered by continuous tubular layers of mucilages and sheath. It occurs in the filaments of *Geminella* sp. (Trebouxiophyceae). A more specific covering exists in the filaments of *Phaeothamnion* sp. (Phaeothamniophyceae), since under certain growth conditions, cells of the filaments dissociate and produce a thick mucilage that surround them in a sort of colony resembling the palmelloid phase.

Scales

Scales can be defined as organic or inorganic surface structures of distinct size and shape. Scales can be distributed individually or arranged in a pattern sometimes forming an envelope around the cell. They occur only in eukaryotic algae, in the divisions of Ochrophyta, Haptophyta, and Chlorophyta. They can be as large as the scales of Haptophyta (1 μm), but also as small as the scales of Prasynophytes (Chlorophyta) (50 nm). There are at least three distinct types of scales: nonmineralized scales, made up entirely of organic matter, primarily polysaccharides, which are present in the Prasynophytes (Chlorophyta); scales consisting of calcium carbonate crystallized onto an organic matrix, as the coccoliths produced by many Haptophyta; and scales constructed of silica deposited on a glycoprotein matrix, formed by some members of the Ochrophyta.

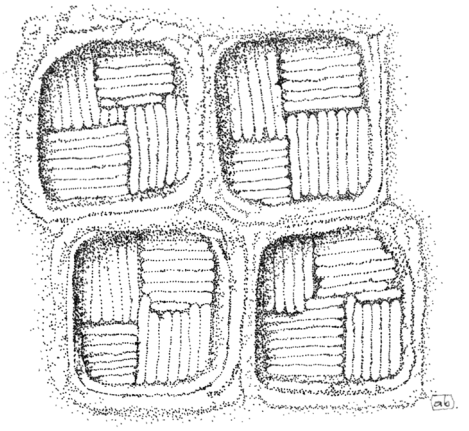

FIGURE 2.3 Box-shaped scales of the intermediate layer of *Pyramimonas* sp. cell body covering.

Most taxa of the Prasinophytes (Chlorophyta) possess several scale types per cell, arranged in 1–5 layers on the surface of the cell body and flagella, those of each layer having a unique morphology for that taxon. These scales consist mainly of acidic polysaccharides involving unusual 2-keto sugar acids, with glycoproteins as minor components. Members of the order Pyramimonadales such as *Pyramimonas* sp. exhibit one of the most complex scaly covering among the Prasinophytes. It consists of three layers of scales. The innermost scales are small, square, or pentagonal; the intermediate scales are either naviculoid or spider web-shaped or box-shaped (Figure 2.3); the outer layer consists of large basket or crown-shaped scales. It is generally accepted that scales of the Prasinophytes are synthesized within the Golgi apparatus; developing scales are transported through the Golgi apparatus by cisternal progression to the cell surface and released by exocytosis. In some genera such as *Tetraselmis* (Chlorodendrophyceae) and *Scherffelia* (Chlorodendrophyceae), the cell body is covered entirely by fused scales. The scales consist mainly of acidic polysaccharides. These scales are produced only during cell division. They are formed in the Golgi apparatus, and their development follow the route already described. After secretion, scales coalesce extracellularly inside the parental covering to form a new cell wall.

In the Haptophyta, cells are typically covered with external scales of varying degree of complexity, which may be unmineralized or calcified. The unmineralized scales consist largely of complex carbohydrates, including pectin-like sulfated and carboxylated polysaccharides, and cellulose-like polymers. The structure of these scales varies from simple plates to elaborate, spectacular spines and protuberances, as in *Chrysochromulina* sp. (Coccolithophyceae) (Figure 2.4), or to the unusual spherical or clavate knobs present in some species of *Pavlova* (Pavlovophyceae).

Calcified scales termed coccoliths are produced by the coccolithophorids, a large group of species within the Haptophyta. In terms of ultrastructure and biomineralization processes, two very different types of coccoliths are formed by these algae: heterococcoliths (Figure 2.5) and holococcoliths (Figure 2.6). Some life cycles include both heterococcolith- and holococcolith-producing forms. In addition, there are a few haptophytes that produce calcareous structures that do not appear to have either heterococcolith or holococcolith ultrastructure. These may be products of further biomineralization processes, and the general term nannolith is applied to them.

Heterococcoliths are the most common coccolith type, which mainly consist of radial arrays of complex crystal units. The sequence of heterococcolith development has been described in detail in *Pleurochrysis carterae* (Coccolithophyceae), *Emiliana huxleyi* (Coccolithophyceae), and the nonmotile heterococcolith phase of *Coccolithus pelagicus* (Coccolithophyceae). Despite the significant diversity in these observations, a clear overall pattern is discernible in all cases. The process commences with formation of a precursor organic scale inside Golgi-derived vesicles; calcification

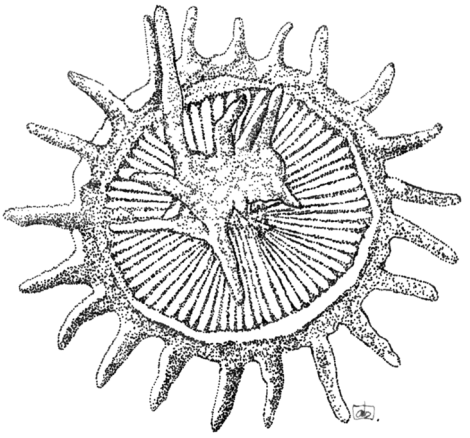

FIGURE 2.4 Elaborate body scale of *Chrysochromulina* sp.

occurs within these vesicles with nucleation of a protococcolith ring of simple crystals around the rim of the precursor base-plate scale. This is followed by growth of these crystals in various directions to form complex crystal units. After completion of the coccolith, the vesicle dilates, its membrane fuse with the cell membrane, and exocytosis occurs. Outside the cell, the coccolith joins other coccoliths to form the coccosphere, that is, the layer of coccoliths surrounding the cell (Figure 1.46).

Holococcoliths consist of large numbers of minute morphologically simple crystals. Studies have been performed on two holococcolith-forming species, the motile holococcolith phase of *C. pelagicus* and *Calyptrosphaera sphaeroidea*. As the heterococcoliths, the holococcoliths are also underlain by base-plate organic scales formed inside Golgi vesicles. However, holococcolith calcification is an extracellular process. Experimental evidences revealed that calcification occurs in a single highly regulated space outside the cell membrane, but directly above the stack of Golgi vesicles. This extracellular compartment is covered by a delicate organic envelope or "skin." The cell secretes calcite that fills the space between the skin and the base-plate scales. The coccosphere

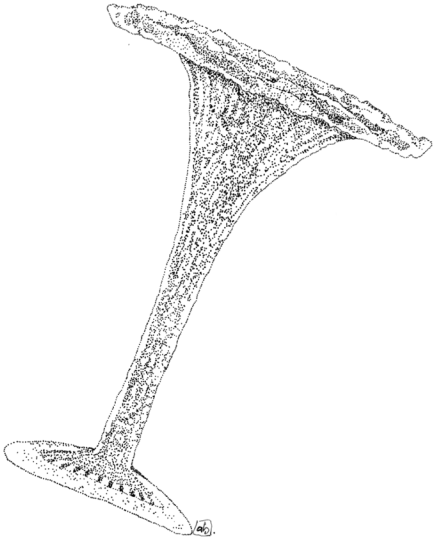

FIGURE 2.5 Heterococcolith of *Discosphaera tubifera*.

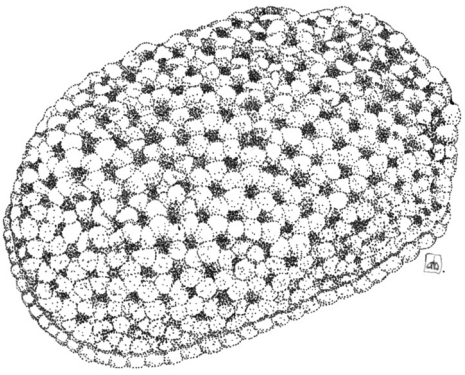

FIGURE 2.6 Holococcolith of *Syracosphaera oblonga*.

grows progressively outward from this position. As a consequence of the different biomineralization strategies, heterococcoliths are more robust than the smaller and more delicate holococcoliths.

Coccolithophorids, together with corals and foraminifera, are responsible for the bulk of oceanic calcification. Their role in the formation of marine sediment and the impact their blooms may exert on climate change will be discussed in Chapter 5.

Members of the Synurophyceae (Ochrophyta) such as *Synura* sp. and *Mallomonas* sp. are covered by armor of silica scales, with a very complicated structure. *Synura* scales consist of a perforated basal plate provided with ribs, spines, and other ornamentation (Figure 2.7). In *Mallomonas*, scales may bear long, complicated bristles (Figure 2.8). Several scale types are produced in the same cell, and deposited on the surface in a definite sequence, following an imbricate, often screw-like pattern. Silica scales are produced internally in deposition vesicles formed by the chrysoplast endoplasmic reticulum, which function as molds for the scales. Golgi body vesicles transporting material fuse with the scale-producing vesicles. Once formed, the scale is extruded from the cell and brought into correct position on the cell surface.

Frustule

This structure is present only in the Bacillariophyceae (Ochrophyta), commonly known as diatoms. The frustule is an ornate cell membrane made of amorphous hydrated silica, which displays intricate patterns and designs unique to each species. This silicified envelope consists of two overlapping valves, an epitheca and a slightly smaller hypotheca. Each theca is comprised of a highly patterned valve and one or more girdle bands (cingula) that extend around the circumference of the

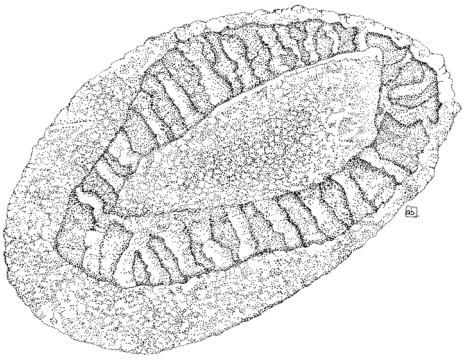

FIGURE 2.7 Ornamented body scale of *Synura petersenii*.

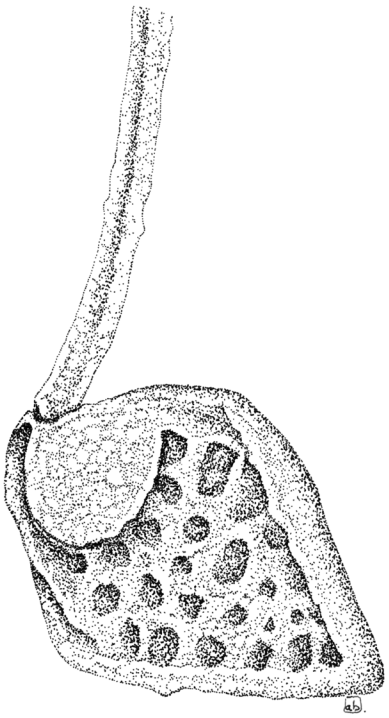

FIGURE 2.8 Body scale of *Mallomonas crassisquama*.

cell, forming the region of theca overlay. Extracellular organic coats envelop the plasma membrane under the siliceous frustule. They exist in the form of both thick mucilaginous capsules and thin tightly bound organic sheaths. The formation of the frustule occurs in the silica deposition vesicles, derived from the Golgi apparatus. The vesicles eventually secrete their finished product onto the cell surface in a precise position.

Diatoms can be divided artificially in centric and pennate according to the symmetry of their frustule. In centric diatoms, the symmetry is radial, that is, the structure of the valve is arranged in reference to a central point (Figure 2.9). However, within the centric series, there also oval,

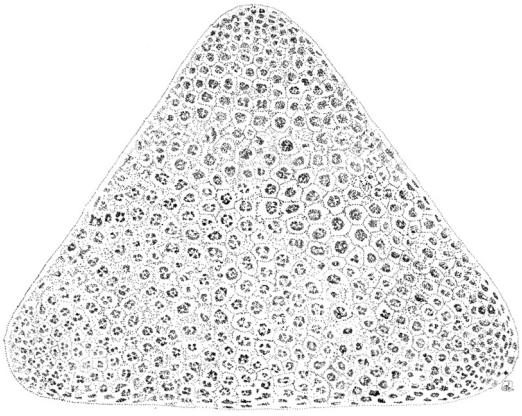

FIGURE 2.9 *Triceratium* sp., a centric diatom.

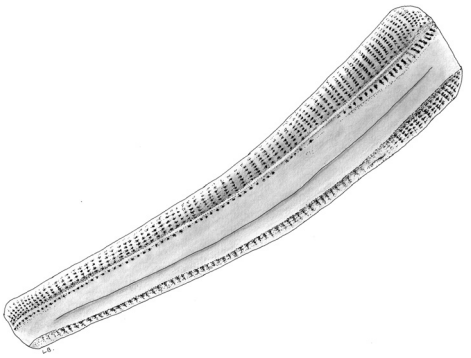

FIGURE 2.10 *Rhoicosphenia* sp., a pennate diatom.

triradiate, quadrate, and pentagonal variation of this symmetry, with a valve arranged in reference to two, three, or more points. Pennate diatoms are bilaterally symmetrical about two axes, apical and trans-apical, or only in one axis (Figure 2.10); some genera possess rotational symmetry (Figure 1.48). Valves of some pennate diatoms are characterized by an elongated fissure, the raphe, which can be placed centrally, or run along one of the edges. At each end of the raphe and at its center, there are thickening called polar and central nodules. Addiction details in the morphology of the frustule are the stria, lines composed of areolae, pores through the valve that can go straight through the structure, or can be constricted at one side. Striae can be separated by thickened areas called costae. Areolae are passageways for the gases, nutrient exchanges and mucilage secretion for movement, and attachment to substrates or other cells of colony. Other pores, also known as portules, are present on the surface of the valve. There are two types of portules: fultoportulae (Figure 2.11), found only in the order Thalassiosirales, and rimoportulae (Figure 2.12), which are universal. The structure of the fultoportulae is an external opening on the surface of the valve extended or not into a protruding structure (Figure 2.11). The other end penetrates the silica matrix and is supported with 2–5 satellite pores. The portules, themselves, function in the excretion of several materials, such as the β-chitin fibrils. These fibrils are manufactured in the conical invaginations in the matrix, under the portule. This may be the anchoring site for the protoplast. The rimoportula is similar to the

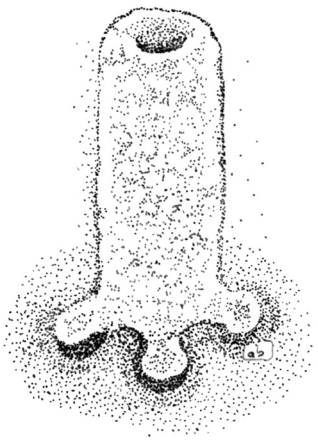

FIGURE 2.11 Fultoportula of *Thalassiosira* sp.

FIGURE 2.12 Rimoportula of *Stephanodiscus* sp.

fultoportulae, except that it has a simpler inner structure. The rimoportula does not have satellite pores in the inner matrix. However, the rimoportula does have some elaborate outer structures that bend, have slits, or are capped. Sometimes the valve can outgrow beyond its margin in structures called setae that help link adjacent cells into linear colonies as in *Chaetoceros* spp. or possesses protuberances as in *Biddulphia* spp., which allow the cells to gather in zigzag chains (Figure 2.13). In other genera such as *Skeletonema*, the valve presents a marginal ridge along its periphery consisting of long, straight spines, which make contact between adjacent cells, and unite them into filaments. Some genera also possess a labiate process, a tube through the valve with internally thickened sides that may be flat or elevated.

Diatoms are by far the most significant producer of biogenic silica, dominating the marine silicon cycle. It is estimated that over 30 million km^2 of ocean floor are covered with sedimentary deposits of diatom frustules. The geological and economical importance of these silica coverings as well as the mechanism of silica deposition will be discussed in Chapter 4.

Cell Wall

A cell wall, defined as a rigid, homogeneous, and often multilayered structure, is present in both prokaryotic and eukaryotic algae.

In Cyanobacteria, the cell wall lies between the plasma membrane and the mucilaginous sheath; its fine structure is of Gram-negative type. The innermost layer, the electron-opaque layer or peptidoglycan layer, overlays the plasma membrane, and in most cyanobacteria its width varies between 1 and 10 nm, but can reach 200 nm in some *Oscillatoria* species. Regularly arranged discontinuities are present in the peptidoglycan layer of many cyanobacteria; pores are located in single rows on either side of every cross-wall and are also uniformly distributed over the cell surface. The outer membrane of the cell wall appears as a double track structure tightly connected

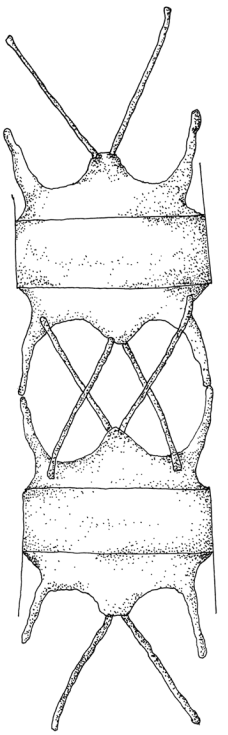

FIGURE 2.13 Cells of *Biddulphia* sp.

with the peptidoglycan layer; this membrane exhibits a number of evaginations representing sites of extrusion of material from the cytoplasm through the wall into the slime. The cell wall of genera such as *Prochloron* is comparable with that of the cyanobacteria in structure and contains muramic acid.

Eukariotic algal cell wall is always formed outside the plasmalemma and is in many respects comparable to that of higher plants. It is present in the Rhodophyta, Eustigmatophyceae (Ochrophyta) (Figure 2.14a and b), Phaeophyceae (Ochrophyta), Xanthophyceae (Ochrophyta), Chlorophyceae (Chlorophyta), and Charophyceae (Charophyta). Generally, cell walls are made up of two components, a microfibrillar framework embedded in an amorphous mucilaginous material composed of polysaccharides, lipids, and proteins. Encrusting substances such as silica, calcium carbonate, or sporopollenin may also be present. In the formation of algal cell walls, the material required are mainly collected into Golgi vesicles that then pass it through the plasma membrane, where enzyme complexes are responsible for synthesis of microfibrils, in a predeterminate direction.

In the Florideophyceae (Rhodophyta), the cell wall consists of more than 70% of water-soluble sulfated galactans such as agars and carrageenans, commercially very important in food and pharmaceutical industry, because of their ability to form gels. In the Phaeophyceae (Ochrophyta), cell wall mucilagine is composed primarily of alginic acid; the salts of this acid have valuable emulsifying and stabilizing properties. In the Xanthophyceae (Ochrophyta), the composition of the wall

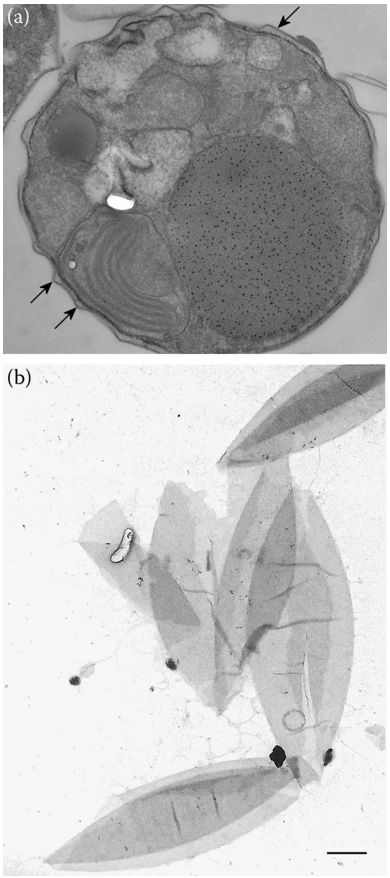

FIGURE 2.14 TEM image of *Nannochloropsis* sp. in transversal section: (a) arrows point to the cell wall and (b) negative staining of the shed cell walls. Scale bar, 0.5 μm.

is mainly cellulosic, while in the Chlorophyceae (Chlorophyta) xylose, mannose, and chitin may also be present in addition to cellulose. Some members of the Chlorophyceae (Chlorophyta) and Charophyceae (Charophyta) have calcified walls.

Lorica

These enveloping structures are present in some members of the class Chrysophyceae (Ochrophyta) such as *Dinobryon* sp., or *Chrysococcus* sp., and in some genera of the Chlorophyceae, such as *Phacotus*, *Pteromonas*, and *Dysmorphococcus.* These loricas are vase-shaped structure with a more or less wide apical opening, where the flagella emerge. These structures can be colorless, or dark and opaque due to impregnation of manganese and iron compounds. As can be expected, different shapes correspond to different species. In *Dinobryon* sp., the lorica is an interwoven system of fine cellulose or chitin fibrils (Figure 2.15). In *Chrysococcus* sp., it consists of imbricate scales. In *Phacotus*, the lorica is calcified, ornamented, and is composed of two cup-shaped parts that separate at reproduction. In *Pteromonas*, the lorica extends into a projecting wing around the cell and is composed of two shell-like portions joined at the wings (Figure 2.16).

Skeleton

A siliceous skeleton is present in a small group of marine organisms called silicoflagellates, belonging to the class Dictyocophyceae (Ochrophyta). This skeleton is placed outside the plasma membrane; it is a three-dimensional structure resembling a flat basket, which consists of a system of branched tubular elements bearing spinose endings (Figure 1.51). The protoplast is contained inside the basket and has a spongy or frothy appearance, with a central dense region containing the nucleus and the perinuclear dictyosomes, and numerous cytoplasmic pseudopodia extending outward and containing the plastids. Sometimes a delicate cell covering of mucilage can be detected.

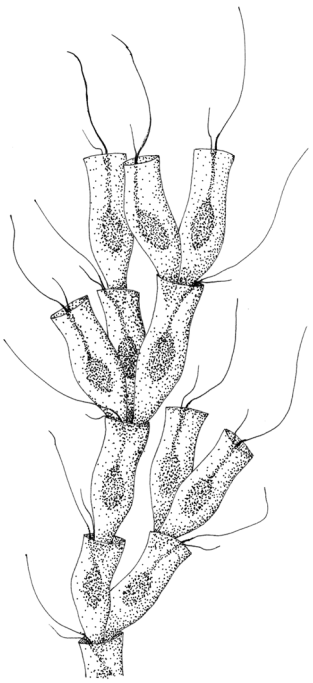

FIGURE 2.15 Tree-like arrangement of *Dynobrion* sp. cells showing their loricas.

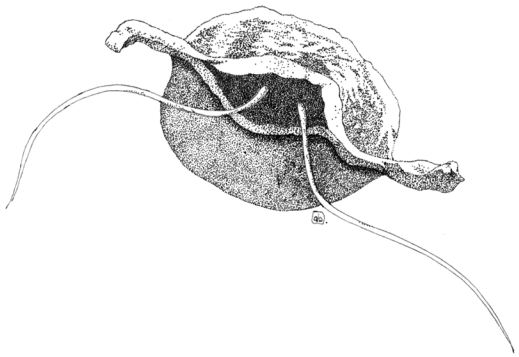

FIGURE 2.16 Lorica of *Pteromonas protracta*.

Type 3—Cell Surface with Additional Intracellular Material in Vesicles

In this type of cell surface, the plasma is underlined by a system of flattened vesicles. An example is the complex outer region of dinoflagellates (Dinophyceae) termed amphiesma. Beneath the cell membrane that binds dinoflagellate motile cells, a single layer of vesicles (amphiesmal vesicles) is almost invariably present. The vesicles may contain cellulosic plates (thecal plates) in taxa that are thus termed thecate, or armored; or the vesicles may lack thecal plates, such taxa being termed athecate, or unarmored or naked. In athecate taxa, the amphiesmal vesicles play a structural role. In thecate taxa, thecal plates, one of which occurs in each vesicle, adjoin one another tightly along linear plate sutures, usually with the margin of one plate overlapping the margin of the adjacent plate. Cellulosic plates vary from very thin to thick and can be heavily ornamented by reticula or striae; trichocyst pores, which may lie in pits termed areolae, penetrate most of them.

A separate layer internal to the amphiesmal vesicles may develop. It is termed pellicle, though in the case of dinoflagellates the term "pellicle" refers to a surface component completely different from the euglenoid pellicle, hence with a completely different accepted meaning, and in our opinion its use should be avoided. The layer consists primarily of cellulose, sometimes with a dinosporine component, a complex organic polymer similar to sporopollenin that makes these algae fossilizable. In some athecate genera, such as *Noctiluca* sp., this layer forms reinforce the amphiesma, and the cells are termed pelliculate. This layer is also sometimes present beneath the amphiesma, as in *Alexandrium* sp., or *Scrippsiella* sp., and forms the wall of temporary cysts.

According to Dodge and Crawford (1970), the amphiesma construction falls into eight reasonably distinct categories (Figure 2.17): (1) simple membrane underlain by a single layer of vesicles 600–800 nm in length, rather flattened, circular, or irregular in shape, with a gap of at least 40 nm between adjacent vesicles that may contain dense granular material; beneath the vesicles are parallel rows of microtubules which lie in groups of three; this simple arrangement is present in *Oxyrrhis marina*; (2) simple membrane underlain by closely packed polygonal (generally hexagonal) vesicles 0.8–1.2 μm in length, frequently containing fuzzy material; these vesicles and the cell membrane are occasionally perforated by trichocyst pores; beneath the vesicles lie microtubules in rows of variable number; this type of amphiesma is found in *Amphidinium carterae*; (3) as in category (2), but with plug-like structures associated with the inner side of the vesicles; these plugs are cylindrical structures 120-nm long and are arranged in single lines between single or paired microtubules; an example of this arrangement is present in *Gymnodinium veneficum*; (4) as in category (2), but with thin (about 20 nm) plate-like structure in the flattened vesicles; this amphiesma characterizes *Aureodinium pigmentosum*; (5) in this group, the vesicles contain plates of medium thickness (60 nm), which slightly overlap; in *Woloszynskia coronata*, the plates are perforated by trichocyst pores; (6) the plates are thicker (up to 150 nm), reduced in number with a marked diversity of form; each plate has two or more sides bearing ridges and the remaining sides have tapered flanges; where

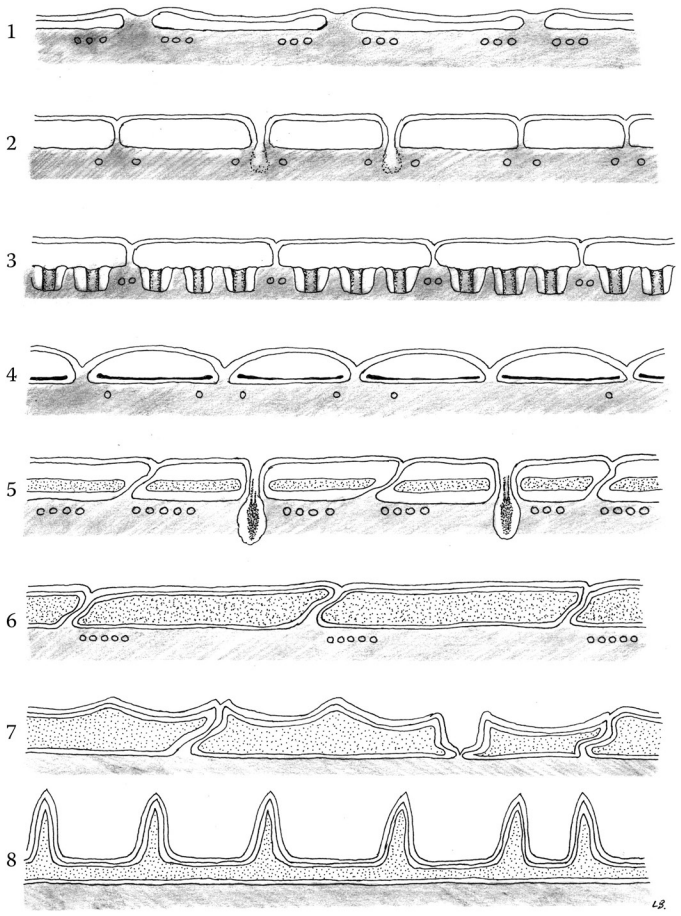

FIGURE 2.17 Diagram of the eight distinct category of the dinoflagellate amphiesma. See text for details.

the plates join, one plate bears a ridge and the opposite bears a flange; *Glenodinium foliaceum* belongs to this category; (7) the plates can be up to 25-µm large and up to 1.8-µm thick; they bear a corrugated flange on two or more sides, and a thick rim with small projections on the opposing edges; these plates may overlap to a considerable extent and their surfaces may be covered by a pattern of reticulations; a distinctive member of this category is *Ceratium* sp.; (8) amphiesma consisting of two large plates, with one or more small plates in the vicinity of the flagellar pores at the anterior end of the cell; plates can be very thin and perforated by two or three simple trichocyst pores as in *Prorocentrum nanum*, or thick and with a very large number (up to 60) of trichocyst pores as in *Prorocentrum micans*.

The arrangement of thecal plates is termed tabulation and is of critical importance in taxonomy of dinoflagellates. Tabulation can also be conceived of as the arrangement of amphiesmal vesicles with or without thecal plates. The American planktologist and parasitologist Charles Kofoid developed a tabulation system allowing reference to the shape, size, and location of a particular plate; plates were recognized as being in series relative to particular landmarks such as the apex, cingulum (girdle), and sulcus. His formulae (i.e., the listing of the total number of plates in each series) were especially useful for most gonyaulacoid and peridinioid dinoflagellates. Apart from some minor changes introduced afterwards, the Kofoid system is still the standard in the description of new taxa. Plates are numbered consecutively from that closest to the midventral position, continuing around to the cell left. A system of superscripts and other marks are used to designate the plate series. Two complete

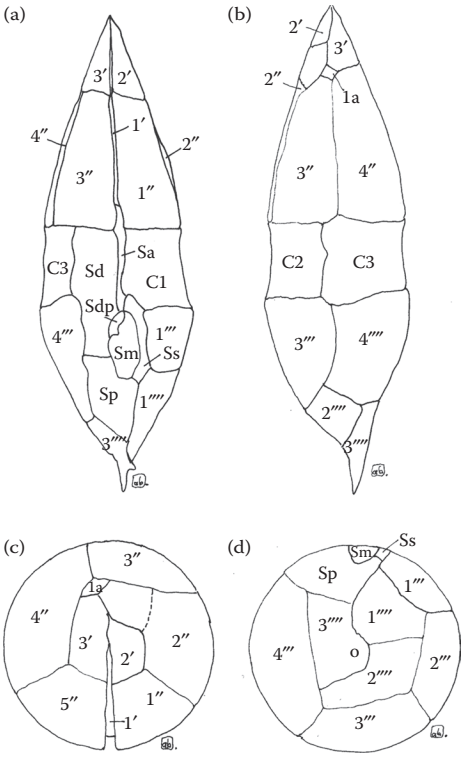

FIGURE 2.18 Line drawings of the thecal plate patterns of *Lessardia elongata* with the corresponding numeration: (a) ventral view; (b) dorsal view; (c) apical view; and (d) antiapical view. See text for details.

transverse series of plates are present in the epitheca: apical (′), and precingular (″), counted from the ventral side in a clockwise sequence. The hypotheca is also divided into two transverse series: postcingular (‴) and antapical (⁗). Some genera also possess an incomplete series of plates on the dorsal surface of the epitheca, termed anterior intercalary plates (a), and on the hypotheca, termed posterior intercalary plates (p). Cingular (C) and sulcal (S) plates are also identified (Figure 2.18). Thus, for example, the dinoflagellate *Proteperidinium steinii* has a formula 4′, 3a, 7″, 3C, 6S, 5‴, 2⁗, which indicates four apical plates, three anterior intercalary plates, seven precingular plates, three cingular plates, six sulcal plates, five postcingular plates, and two antapical plates.

Type 4—Cell Surface with Additional Extracellular and Intracellular Material

Both the surface structure of Cryptophyceae (Cryptophyta) and Euglenophyceae (Euglenozoa) can be grouped under this type.

The main diagnostic feature of the members of the Cryptophyceae is their distinctive kind of cell surface, colloquially termed periplast. Examples are *Chroomonas* (Figure 2.19) and *Cryptomonas*; in these algae, the covering consists of outer and inner components, present on both sides of the membrane but variable in their composition. The inner component is comprised of protein and may consist of fibril material, a single sheet or multiple plates having various shapes, hexagonal, rectangular, oval, or round. The outer component may have plates, heptagonal scales, mucilage, or a combination of any of these. The pattern of these plates can be observed on the cell surface when viewed with scanning electron microscope (SEM) and freeze-fracture transmission electron microscope (TEM), but it is not easily detectable under light microscopy view.

Euglenophyceae possess an unusual membrane complex called pellicle, consisting of the plasma membrane overlying an electron-opaque semicontinuous proteic layer made up of overlapping strips.

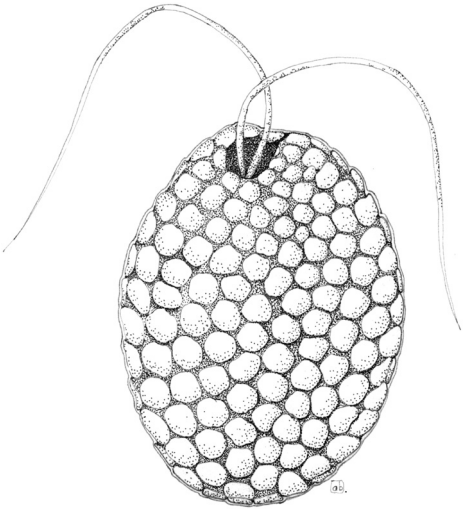

FIGURE 2.19 Periplast of *Chroomonas* sp.

These strips or striae can be described as long ribbons usually arising in the flagellar pocket and extending from the cell apex to the posterior. Each strip is curved at both its edges, and in transverse section it shows a notch, an arched, or a slightly concave ridge, a convex groove and a heel region where adjacent strips interlock and articulate. The strips can be arranged helically or longitudinally; the first arrangement, very elastic, is present in the "plastic euglenoids" (e.g., *Euglena*, *Peranema*, *Distigma*), either heterotrophic or phototrophic, where the strips are more than 16. Their relational sliding over one another along the articulation edges permit the cells to undergo "euglenoid movement" or "metaboly." This movement is a sort of peristaltic movement consisting of a cytoplasmic dilation forming at the front of the cell and passing to the rear. The return movement of the cytoplasm is brought about without dilation. The more rigid longitudinal arrangement is present in the "aplastic euglenoids" (e.g., *Petalomonas*, *Pleotia*, *Entosiphon*), all heterotrophic, where the strips are usually less than 12. These euglenids are not capable of metaboly.

The ultrastructure of the pellicular complex shows three different structural levels (Figure 2.20):

- The plasma membrane with its mucilage coating (first level)
- An electron-opaque layer organized in ridges and grooves (second level)
- The microtubular system (third level)

First Level

A dense irregular layer of mucilaginous glycoproteins covers the external surface of the cell. It has a fuzzy texture that, however, has a somehow ordered structure of orientated threads. Mucilage bodies present beneath the cell surface secrete the mucilaginous glycoproteins. The consolidation of the secretory products and their arrangement at one pole or round the periphery of the cell leads to the formation of peduncles (stalks of fixation) and other enveloping structures homologs to the loricas of Chrysophyceae and Chlorophyceae. Peduncles are present in *Colacium*, an euglenophyte that forms small arborescent colonies (Figure 2.21). Its cells, with reduced flagella, are attached by their anterior pole by a peduncle consisting of an axis of neutral polysaccharides and a cortex of acid polysaccharides. Loricas are present in *Trachelomonas* sp. (Figures 1.1bm and 2.22), *Strombomonas verrucosa* (Figure 2.23) and *Ascoglena*; they are very rigid, made up of mucilaginous filaments impregnated with ferric hydroxide or manganese compounds which confer an orange, brown to black coloration to

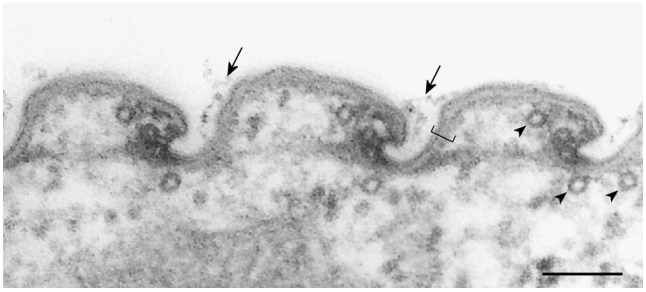

FIGURE 2.20 TEM image of the surface of *Euglena gracilis* in transverse section, showing the three different structural levels of the pellicle. Arrows point to the first level (mucus coating); a square bracket localizes the second level (ridges and grooves); arrowheads point the third level (microtubules). Scale bar, 0.10 μm.

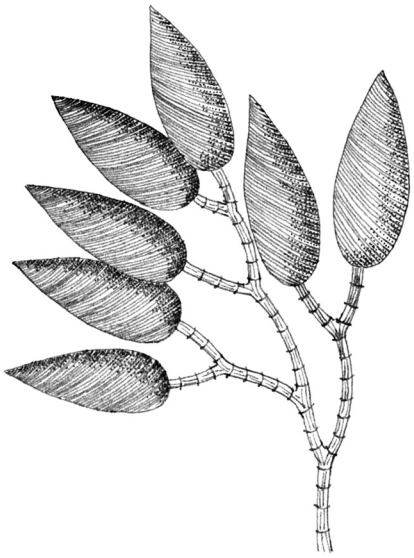

FIGURE 2.21 A small arborescent colony of *Colacium* sp. in which the cells are joined to one another by mucilaginous stalks.

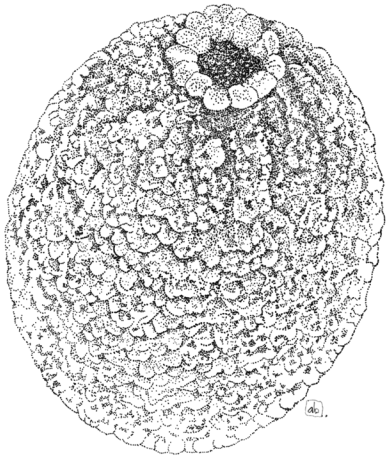

FIGURE 2.22 Lorica of *Trachelomonas* sp.

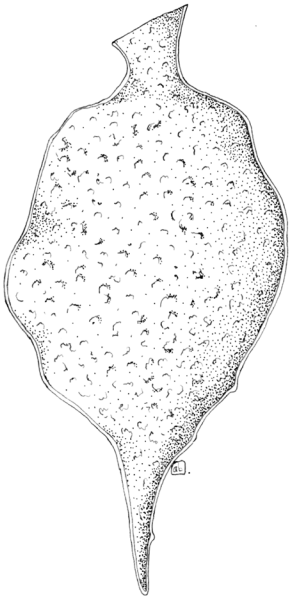

FIGURE 2.23 Lorica of *Strombomonas verrucosa*.

the structure. These loricas fit loosely over the body proper of the cell. They possess a sharply defined collar that tapers to a more or less wide apical opening, where the flagella emerge, or possess a wide opening in one pole and attached to a substrate at the other pole, as in *Ascoglena*.

Beneath the mucus coating, there is the plasma membrane (Figure 2.24). This cell membrane is continuous and covers the ridges and grooves on the whole cell and can be considered the external surface of the cell. The protoplasmic face (PF) of the plasma membrane shows that the strips are covered with numerous peripheral membrane proteins of about 10 nm.

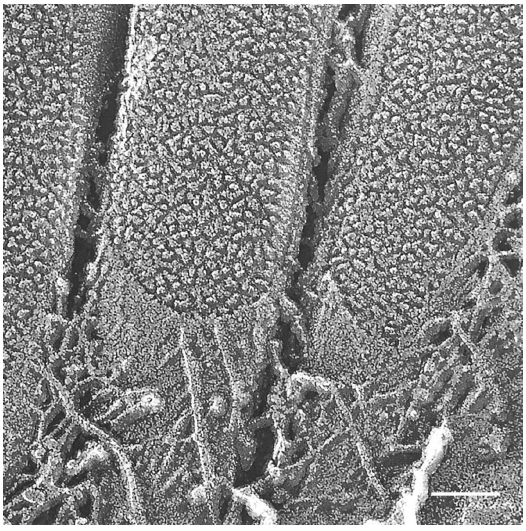

FIGURE 2.24 Deep-etching image of *Euglena gracilis* showing the mucus coating of the cell surface and the protoplasmic fracture of the cell membrane. Scale bar, 0.10 μm. (Courtesy of Pietro Lupetti.)

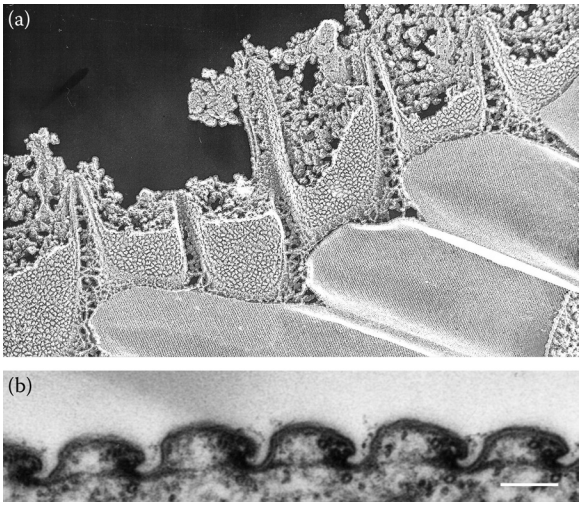

FIGURE 2.25 (a) Deep-etching image of *Euglena gracilis* showing the second structural level of the pellicular complex, showing the regular texture of the internal face of the pellicle stripes. (b) TEM image of the pellicle of *E. gracilis* in transverse section showing the transversal fibers connecting the edges of successive ridges. Scale bar, 0.10 μm.

Second Level

This peripheral cytoplasmic layer has a thickness that varies with the species. It consists of roughly twisted proteic fibers with a diameter from 10 to 15 nm arranged with an order texture or parallel striation (Figure 2.25a). The overall structure resembles the wired soul present in the tires, which gives the tire its resistance to tearing forces. Transversal fibers are detectable in some euglenoids, which connect the two longitudinal edges of the ridge of each strip (Figure 2.25b).

Third Level

There is a consistent number and arrangement of microtubules associated with each pellicular strip, which are continuous with those that line the flagellar canal and extend into the region of the reservoir. Within the ridge in the region of the notch, there are 3–5, usually 4, microtubules about 25-nm diameter running parallel along each strip. Two of these are always close together and are located immediately adjacent to the notch adhering to the membrane (Figure 2.20).

The lack of protein organization in the groove regions gives higher plasticity to these zones, and together with the presence of parallel microtubules in the ridge regions gives the characteristic pellucular pattern to the surface of euglenoids.

The solid structure of the pellicle confers a very high degree of flexibility and resistance to the cells. Our experience with *E. gracilis* allow us to say that this alga possesses one of the strongest covering present in these microorganisms. A pressure of more than 2000 psi (about 150 bar) is necessary to break the pellicular structure of this alga.

Flagella and Associated Structures

Flagella can be defined as motile cylindrical appendages found in widely divergent cell types throughout the plant and animal kingdom, which either move the cell through its environment or move the environment relative to the cell.

Motile algal cells are typically biflagellate, although quadriflagellate types are commonly found in green algae; it is generally believed that the latter have been derived from the former, and a

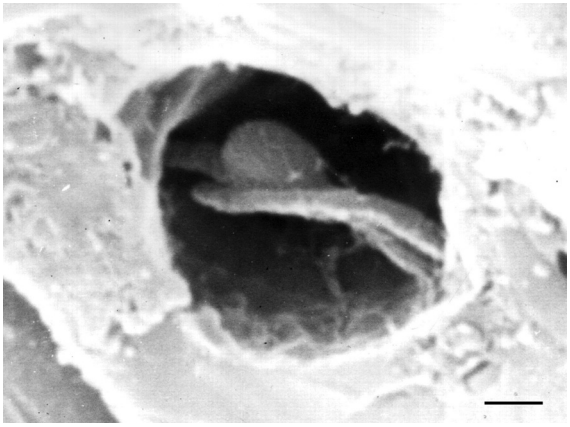

FIGURE 2.26 SEM image of the reservoir of *Euglena gracilis* in longitudinal section showing the locomotory emerging flagellum bearing the photoreceptor and the nonemerging flagellum reduced to a stub. Scale bar, 0.50 µm. (Courtesy of Franco Verni.)

convincing example of this derivation is *Polytomella agilis* (Chlorophyceae) from *Chlamydomonas* sp. (Chlorophyceae). A triflagellate type of zoospore such as that of *Acrochaete wittrockii* (Ulvophyceae) may have originated from a quadriflagellate ancestor by reduction, whereas the few uniflagellate forms are most likely descendant of biflagellated cells. Intermediate cases exist which carry a short second flagellum, as in *Mantoniella squamata* (Mamiellophyceae) or *Euglena gracilis* (Euglenophyceae), where one flagellum is reduced to a stub (Figure 2.26); in some species, one flagellum of the pair is reduced to a nonfunctional basal body attached to the functional one, as in the uniflagellate swarmer of *Dictyota dichotoma* (Phaeophyceae). A special case of multiflagellate alga is the naked zoospore of *Oedogonium* (Chlorophyceae), where the numerous flagella form a ring or crown around the apical portion of the cell (stephanokont zoospore).

The characteristics of the flagella in a pair, that is, relative length and surface features, have led to a specific nomenclature. When the two flagella differ in length and surface features, one being hairy and the other smooth, they are termed "heterokont." This term applies to all the members of the Ochrophyta. When the two flagella are equal in length and appearance, the term "isokont" is used (Figure 2.27), which applies to Haptophyta and to Chlorophyceae and Charopyceae. Within this group, there are few genera whose flagella differ in length, which are termed "anisokont."

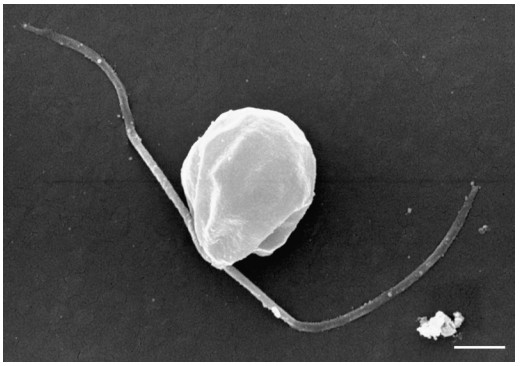

FIGURE 2.27 SEM image of an isokont cell (*Dunaliella* sp.). Scale bar, 3 µm.

Description of flagella anatomy will proceed from the outside to the inside, from the surface features and components to the axoneme and additional inclusions, to the structures anchoring the flagella to the cell.

Flagellar Shape and Surface Features

Deviations from the cylindrical shape are rare among the algae. Usually the flagellar membrane fits smoothly around the axoneme and a total diameter of 0.25–0.35 μm, excluding scales, hairs, etc, holds for most species. If extra material is present between the axoneme and the flagellar membrane, the flagellum diameter increases either locally as in the case of flagellar swellings, or through almost the entire length as in the case of paraxial rods. Minor deviations from the cylindrical shape are caused by small extensions of the membrane to form one or more longitudinal keels running the length of the flagellum. Greater extension of the membrane forms a ribbon or wing supported along the edge by a paraxial rod. More variations are present in the flagellar tip, since flagella can possess a hairpoint, that is, their distal part is thinner with respect to the rest of the flagellum, or be blunt-tipped, with an abundance of intermediates between these two types.

Flagellar surface is smooth in many algae, where only a simple plasma membrane envelopes the axoneme. Sometimes, however, a distinct, apparently homogeneous dense layer covers the flagellar membrane throughout (Figure 2.28). One of the two flagella of Ochrophyta is smooth; smooth flagella are present also in members of the Haptophyta, such as *Chrysochromulina parva* (Coccolithophyceae), and in many Chlorophyta, such as *Chlamydomonas reinhardtii* (Chlorophyceae).

Flagellar Scales

Flagella may bear a high variety of coverings and ornamentation, which often represents a taxonomic feature. The occurrence of flagellar scale follows that of cell body scales, since they are present only in eukaryotic algae, in the divisions of Ochrophyta, Haptophyta, and Chlorophyta. As for the cell body scales, they have a silica-based composition in the Ochrophyta, a mixed structure of calcium carbonate and organic matter in the Haptophyta, and a completely organic nature in the Chlorophyta.

Members of the Ochrophyta fall into two groups: one possessing exactly the same type of scale on both flagellar and body surface, while the other showing flagellar scales different in structure and arrangement from body scales. Example of the first group is *Sphaleromantis* sp.

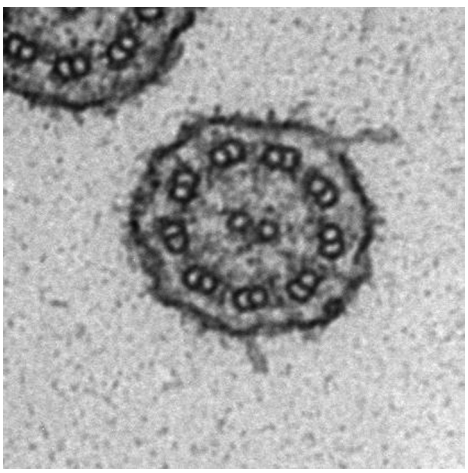

FIGURE 2.28 TEM image of a *Tetraflagellochloris mauritamca* flagellum in transverse section, showing the homogeneous fuzzy coating of its membrane. Scale bar, 0.10 μm.

(Chrysophyceae), whose flagella and cell body are closely packed with scales of very peculiar appearance, resembling the branched structure of a tree. Examples of the second group are *Mallomonas* sp. and *Synura* sp. (Synurophyceae); in both genera, flagellar scales are not arranged in a regular pattern, are very small (under 300 nm), and possess different morphological types, the most characteristic being the annular type. As the body scales, flagellar scales are produced in deposition vesicles, extruded from the cell and brought into correct position in relation to the other scales and the cell surface.

As said above, flagella of the Haptophyta are usually equal in length and appearance (isokont); however, members of the genus *Pavlova* (Pavlovophyceae) possess two markedly unequal flagella, the anterior one is much longer than the posterior, and carrying small, dense scales in the form of spherical or clavate knobs. These scales are often arranged in regular rows longitudinally, or can be randomly disposed on the flagellum. Scales are formed inside the Golgi apparatus and then released into the cell surface by fusion of the plasmalemma and the cisternal membrane.

Flagellar scales are known from many Chlorophyta, such as Prasinophytes, Chlorodendrophyceae, Nephroselmidophyceae, and Mamiellophyceae. These algae possess nonmineralized organic scales on their cell body and flagella, the same type of scale being rarely present on both surfaces. On the flagella, the scales are precisely arranged in parallel longitudinal rows, sometimes in one layer, two layers, or even three layers on top of each other. Each layer usually contains only one type of scales. The four flagella of *Tetraselmis* sp. (Chlorodendrophyceae) are covered by different types of scales: pentagonal scales attached to the flagellar membrane (Figure 2.29), rod-shaped scales covering the pentagonal scales, and hair scales organized in two rows on opposite side of the flagellum. A fourth type termed "knotted scales" is present only in some strains, but their precise arrangement is not known. In *Nephroselmis spinosa* (Nephroselmidophyceae), the flagellar surface is coated by two different types of scales arranged in two distinct layers. Scales of the inner layer, deposited directly on the membrane, are small and square, 40 nm across (Figure 2.30); scales of the outer layer are rod-shaped, 30–40-nm long, and are deposited atop the inner scales. As in *Tetraselmis*, hair scales of at least two different types are also present covering the flagella. In *Pyramimonas* sp. (Prasinophytes), the scales are extremely complex in structure and ornamentation, and belong to three different types. Minute pentagonal scales, 40-nm wide, form the layer covering the membrane, which in turn is covered by limuloid scales, 313-nm long and 190-nm wide, arranged in nine rows (Figure 2.31); each flagellum also bears two rows of almost opposite tubular hair scales, 1.3 μm long. Spider web scales with an ellipsoid outline are present in *Mamiella gilva* (Mamiellophyceae), which are ornamented by a radial spoke elongated into a conspicuous spine (Figure 2.32).

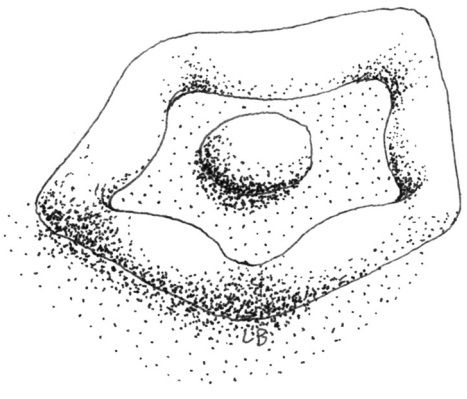

FIGURE 2.29 Pentagonal scale of the flagellar membrane of *Tetraselmis* sp.

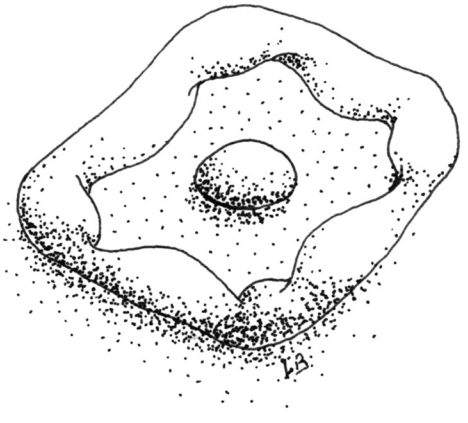

FIGURE 2.30 Square scale of the flagellar membrane of *Nephroselmis spinosa*.

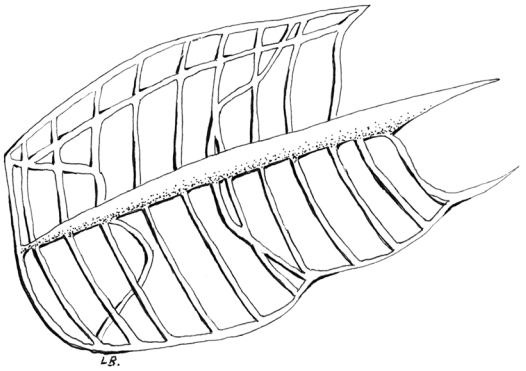

FIGURE 2.31 Limuloid scale of the flagellar membrane of *Pyramimonas* sp.

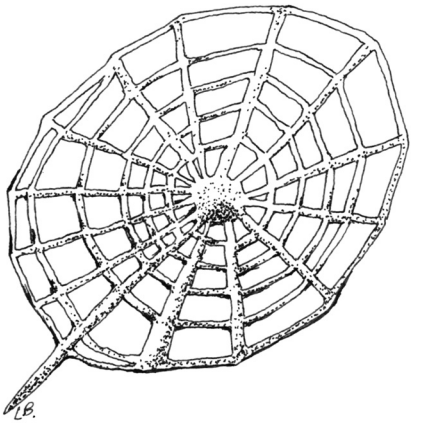

FIGURE 2.32 Spider web scale of the flagellar membrane of *Mamiella gilva*.

The scales are synthesized within the Golgi vesicles. The vesicles then migrate to the base of the flagella and from here are extruded and arranged on the flagella.

Flagellar Hairs

Flagellar hairs can be grouped into two types: tubular and nontubular (simple) hairs.

Tubular hairs consist of two or more distinct regions, at least one of which is thick and tubular, while the distal elements may be simpler. This type of hairs is further divided into cryptophycean hairs, tripartite hairs, and prasinophycean hairs.

The cryptophycean hairs are unique for arrangement to the Cryptophyceae (Cryptophyta), being attached in two opposite rows on the longer flagellum, and on a single row on the shorter one. On the long flagellum, the hairs consist of a tubular proximal part, 1.5–2.5-μm long, and a nontubular distal filament, 1 μm long, while the hairs on the shorter flagellum are shorter, 1–1.5-μm long, with a distal filament 1-μm long.

Tripartite hairs are the hair type of the Ochrophyta (Figure 2.33a and 2.33b). These hairs consist of three morphological regions, that is, a short basal region, a tubular hollow shaft, and a distal region. The basal part is 0.2–0.3-μm long and tapers towards the site of attachment to the flagellar membrane, at which point dense structures are present that connect the hairs to the peripheral axoneme microtubules. The hollow shaft shows a range of length from 0.7–0.8 to 2 μm and a diameter

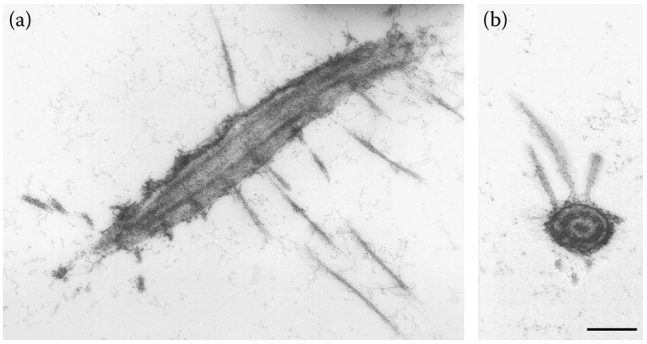

FIGURE 2.33 TEM image of the long trailing flagellum of *Ochromonas danica* in (a) longitudinal and (b) transverse sections, showing the tripartite hairs. Scale bar, 0.25 μm.

of about 16 nm. The distal parts of each hair, called terminal filaments or fibers, are extremely fragile, hence difficult to detect because readily shed during electron microscopy preparation. In some cases, they are organized in a 2 + 1 structure, that is, two short filaments 0.3-μm long and one long filament 1-μm long; however, differences exist in their number, length, and diameter.

Cells of the Prasinophytes carry hairs on all their flagella, whether one, two, four, or eight, which are very diverse in morphology. They can vary in length from 0.5 to 3 μm, and a single flagellum may carry more than one hair type. In *Pyramimonas orientalis*, both lateral and apical hairs are bipartite and of the same length, with the lateral hairs being divided into a short, thick base, of 160 nm, and a long, thin distal part, of 650 nm, and the apical hairs possessing a long thick base and a very short, thin tip. Another example of flagellar hairs is *Mantoniella* sp. (Mamiellophyceae), bearing hairs on the flagellar tip which are longer than those on the side. In *Nephroselmis* (Nephroselmidophyceae) and *Tetraselmis* (Chlorodendrophyceae), there is a single hair type divided into two regions of roughly the same length (0.5 μm).

Unlike tubular hairs, simple, nontubular hairs are not differentiated into regions; they are thin, and very delicate, probably consisting of a single row of subunits. These hairs occur in a variety of groups, but are unique in the Euglenophyceae and Dinophyceae, whose hairy coverings share certain features not known to occur in any other algal group.

In Euglenophyceae, long, simple hairs are arranged in a single row on the emergent part of the flagella. In general, with two emergent flagella, the hair covering is similar on the two flagella. In *Euglena gracilis*, these long hairs consist of a single filament 3–4-μm long, with a diameter of 10 nm, while in *Eutreptiella gymnastica*, they are 4–5-μm long and assembled in unilateral bundles. In addition to these long hairs, euglenoid flagella carry a dense felt of shorter hairs, which in *Euglena* are approximately half as long and half as thick as the long hairs. These short hairs, precisely positioned with respect to each other and to axonemal components, consist of a sheath about 240–300 nm in length, which represents the basic unit. The units, each formed by loops, side arms, and filaments lie parallel to each other in the longitudinal direction of the flagellum (Figure 2.34); two groups of short hairs are arranged helically on each narrow side of the flagellum, separated by each other by two membrane areas without hair attachments. In Dinophyceae, both the longitudinal and the transverse flagellum carry hairs, but unlike Euglenophyceae, the hairy coverings on the two flagella are different. The transverse flagellum carries unilateral hairs except in the proximal part; they are 2–4-μm long and arranged in bundles, each bundle consisting of differently sized hairs. In *Oxyrrhis marina*, hairs are of three different lengths, the

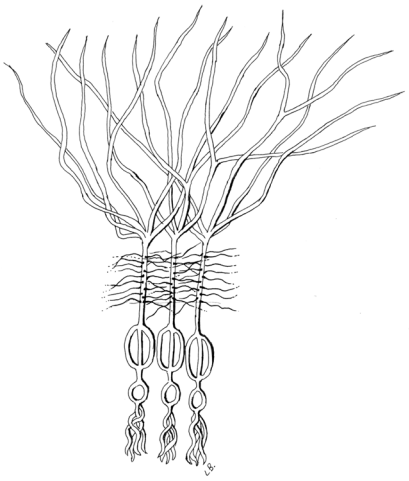

FIGURE 2.34 Short hairs of *Euglena* flagellum.

longest in the middle. Hairs on the longitudinal flagellum are shorter than those on the transverse flagellum (0.4–0.75 μm), but similar in diameter (10 nm).

Simple, nontubular hairs are present also in some Glaucophyta and Chlorophyta.

Flagellar Spines

Flagellar spines are a peculiarity of unknown function confined to male gametes of a few oogamous brown algae. The spermatozoids of *Dictyota* sp. (Phaeophyceae) are unique in possessing a longitudinal row of 12 very short spines on their single hairy flagella (these spermatozoids are basically biflagellate, but the second flagellum is reduced to its basal body only). Spines are absent on the distal 2.5–3 μm of the flagellum, and on the proximal 10 μm. In other Phaeophyceae such as *Himanthalia*, *Xiphophora*, and *Hormosira*, spermatozoids possess only a single spine, up to 1.0-μm long. In all these algae, each spine is made up of electron-dense material, located between the flagellar membrane and the peripheral axonemal doublets.

Internal Features of the Flagellum

Axoneme

The movements of the flagella are generated by a single functional unit, the axoneme, which consists of a long cylinder, from 10- to 100-μm long, 0.2-μm in diameter. Its structure, as seen in cross-sections by electron microscopy, is almost ubiquitous: it is made of nine equally spaced outer microtubule doublets (A and B) approximately 40 nm in diameter surrounding two central microtubules, the central pair (Figure 2.28). This arrangement is maintained by a delicate series of linkages to give the classical 9 + 2 pattern. The nine outer doublets are numbered starting from number 1 located in the plane orthogonal to the plane including the central pair, and counting clockwise when looking from the tip of the flagellum. The former plane allows the definition of the curvature directions during beating as left or right relatively to it. Doublets are transiently linked by outer/inner dynein arms (ODA and IDA) that represent the flagellar motor and permanently interconnected by nexin links; the radial spokes connect the central pair to the peripheral microtubules of the outer doublets. Divergence from the basic 9 + 2 pattern is rare, but include the spermatozoid of some centric diatoms (9 + 0) and the chlorophyta *Golenkinia minutissima* (9 + 1), as well as the haptonema of the Prymnesiophyceae (Figure 2.35). This structure develops between the two flagella of these algae, and it is sometimes longer than the flagella themselves. It resembles a flagellum, but contains a central shaft of 6–8 microtubules arranged in a cylinder, with no doublets. In transverse section, the microtubules are disposed in an arc of a circle or in a ring and are surrounded by a limb of the smooth endoplasmic reticulum. The distal part of the haptonema is fairly straightforward. It is surrounded by the plasma membrane, which is continuous over the tip of the haptonema and may be smooth, drawn into a tip, or form a spathulate projection.

The bulk of axonemal proteins (70%) is made of tubulins, the building blocks (heterodimers) that polymerize linearly to form microtubules. Those tubulins, which constitute the wall of microtubules, belong to the *a* and *b* families, whose sequences have been conserved during evolution (other families, *g*, *d*, *e*, are responsible for microtubule nucleation at the level of the basal bodies/centrosomes). A large molecular diversity among tubulins is generated by a series of post-translational modifications such as acetylation, detyrosylation, polyglutamylation, or polyglycylation. Tektin filaments are present at the junction between the A and B microtubules of each doublet. The internal and external arms that graft to the peripheral doublets represent 10–15% of the global protein mass of axonemes and are essentially formed by the "dynein-ATPases" motor (the Greek word "dyne" means force). Microtubular dyneins are large multimolecular complexes with a pseudo-bouquet shape and a molecular mass ranging from 1.4 MDa (bouquets with two heads) to 1.9 MDa (bouquets with three heads) for the whole molecule, and approximately 500 kDa for the largest subunits containing the ATP hydrolysis site. The size of both ODA and IDA is approximately 50 nm. Among

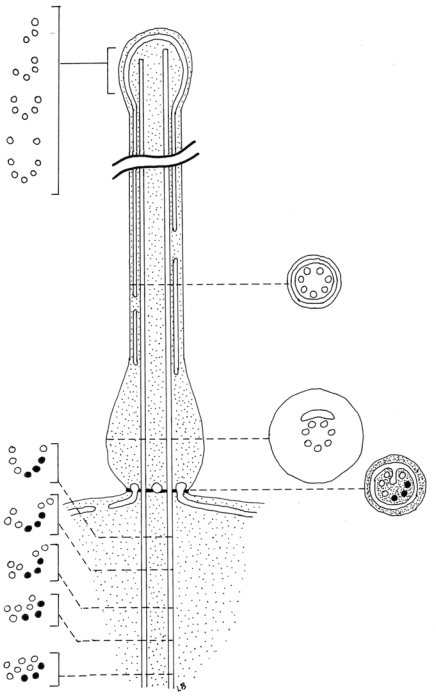

FIGURE 2.35 Schematic drawing of the generalized representation of the structure of the haptonema of *Chrysochromulina*.

the 250 different polypeptides present in the axoneme, as estimated by bidimensional electrophoresis, only a few have been associated with a function.

Paraxial Rod

In addition to the 9 + 2 axoneme, algal flagella may contain a number of other structures within the flagellar membrane. Among those extending through the entire length of the flagella, there is the paraxial rod, which is known only in the order of Pedinellales (Dictyochophyceae, Ochrophyta), and in members of the Euglenophyceae and Dinophyceae. Paraxial rod is also termed paraflagellar rod (PFR). PFRs are complex and highly organized lattice-like structures that run parallel to the axoneme. Among the different groups, PFRs are structurally and biochemically similar.

In the Pedinellales, the membrane of the single emergent flagellum is expanded into a sheath or fin supported along the edge by the rod, which is cross-banded. Thanks to the presence of the fin, these algae are excellent swimmers. Their axoneme beats in a distinct planar wave.

Paraflagellar structures of characteristic appearance are present in some dinoflagellates. A hollow cylinder with the wall composed of helically arranged filaments is present in the single emergent (longitudinal) flagellum of *Noctiluca* gametes and in the longitudinal flagellum of both *Gyrodinium lebouriae* and *Oxyrrhis marina*. This rod is about as big as the axoneme in diameter and runs along the axoneme to which it is attached for almost its entire length. The thin filaments (nanofilaments with a 2–4-nm diameter) of its highly geometrically organized network are periodically attached to some of the outer doublet microtubules of the axoneme, which in *O. marina* is doublet number 4. A different type of paraxial rod is present in the complex-shaped transverse flagellum of dinoflagellates. This rod takes a nearly straight path along the inner wall of the sulcus and is regularly banded in the transverse direction. In contrast, the axoneme itself is distinctly helical.

A rod is present in most members of Euglenophyceae. In genera with two emergent flagella, such as *Eutreptia* and *Eutreptiella*, both flagella carry a paraxial rod. In *Eutreptiella*, where the

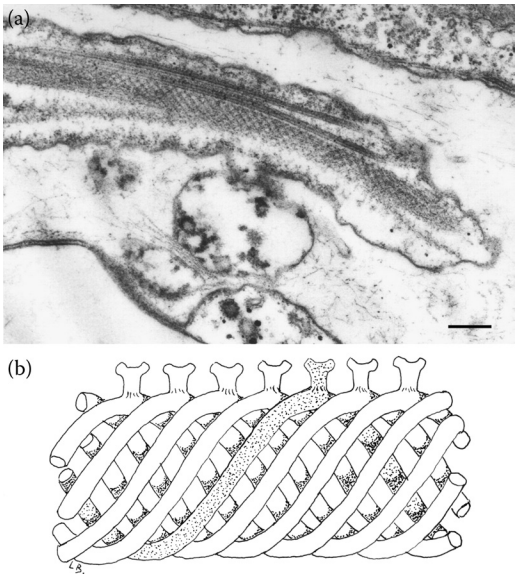

FIGURE 2.36 (a) TEM image of the locomotory flagellum of *Euglena gracilis* in longitudinal section. Arrows point to the PFR. (b) Schematic drawing of the PFR showing the coiled filaments and goblet-like projections. Scale bar, 0.40 μm.

two flagella differ in length, the rods also differ from each other in thickness and fine structure, the longer flagellum carrying a more complex rod than the shorter flagellum. In genera with a flagellar apparatus reduced to one long emergent flagellum and one short flagellum not extending beyond the reservoir region, only the emergent flagellum retains the rod, which extends its entire length. An example is *Euglena gracilis*; in this alga, the rod arises just above the flagellar transition zone and is located lateroventrally with respect to the axoneme and the cell body. In thin cross-sections of isolated and demembranated flagella, the rod appears hollow with an outer diameter of 90 nm. Images obtained from negative staining preparations show that the rod is made up of several coiled filaments, with a diameter of 22 nm, forming a 7-start left-handed helix with a pitch of 45° and a periodicity of 54 nm. Extending from the surface of the rod a series of goblet-like projections can be observed, which form the point of attachment between the rod and one of the axonemal doublet microtubules (Figure 2.36a and b). The PFR does not assume any consistent orientation with respect to the central-pair microtubules of the emergent flagellum.

Two major protein components of the PFR have been identified in euglenoids and dinoflagellates with a number of possible minor protein constituents. These major proteins (PFR_1 and PFR_2) migrate in the SDS–PAGE as a doublet of similar abundance. Depending on the organism, the mobility for PFR_1 ranges from 70 to 80 kDa, and for PFR_2 from 62 to 70 kDa. Coiled-coils are a common structural motif in the filament formed using the PFR_1 and PFR_2 proteins. Database searches reveal a 41-residue conserved region of the PFR_1/PFR_2 family that bears a significant relationship to a conserved motif within the central coiled-coil rod of tropomyosin.

Other Intraflagellar Accessory Structures

Other intraflagellar accessory structures are present in dinoflagellates besides the PFR, the so-called R fiber (Rf) and the so-called striated fiber (Sf). These structures do not show any kind of lattice or precisely organized structure. However, they deserve mentioning since they run for long distances along the axonemal structure and therefore are also candidates for modulating the axonemal beating, possibly by Ca^{2+}-dependent contraction or through dipole–dipole forces.

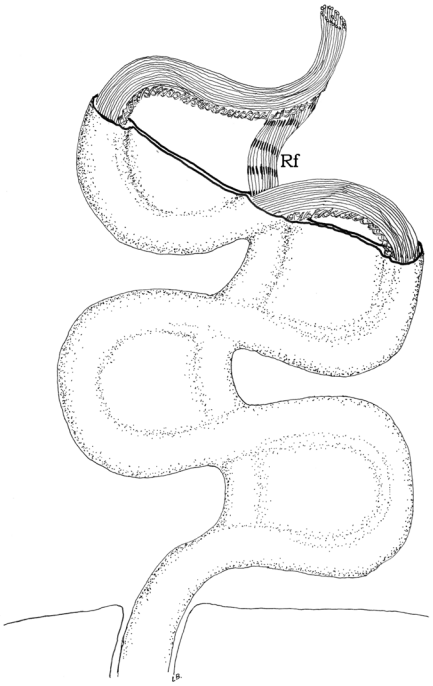

FIGURE 2.37 Schematic drawing of longitudinal flagellum of *Ceratium furca* during its contraction showing the striated Rf.

The Rf is made of thin filaments 2–4 nm in diameter. It may be as large as the axoneme or the PFR in diameter (300–500 nm), runs along the major part of the axoneme, and is attached to it via the PFR, the PFR linking the Rf to the axoneme. The Rf may contract and shows transversal striations of variable periodicities and thickness only during its contraction, but not in its relaxed or fully contracted state (Figure 2.37). The precise structure of the Rf varies according to the fixation conditions for TEM, mostly depending on the Ca^{2+} concentration, suggesting that its contractility is Ca^{2+}-dependent. In some dinoflagellates such as *Ceratium furca*, the Rf is a good candidate for the induction of the complete retraction of the longitudinal flagellum in the flagellar pocket, a movement that cannot be explained by the axoneme structure itself. In this retracted state, the Rf is contracted and the axoneme is highly folded (more tightly that during the usual flagellar beating). Therefore, the Rf could modulate the properties of the PFR and axoneme motility through constraints imposed to the PFR.

The so-called Sf is also made of thin filaments. It is much smaller than the PFR or the axoneme in diameter (about 35 nm) and runs along three-fourths of the axoneme. Its transversal striations suggest its implication in contractile processes that could modulate axonemal motility through gradual changes in the axonemal wavelength and/or amplitude.

Transition Zone

Although both the flagellar axoneme and the basal body that continues it are very constant in morphology among the different algae, the transition region where they meet varies considerably and is considered one of the most useful indicators of phylogenetic relationships. This region sometimes contains particular structures such as helices, star-shaped bodies, and transverse partitions referred to as basal plates. Five main types of transition zones may be distinguished, taking into account that secondary variations can appear within each zone.

Type 1 (Figure 2.38) appears the simplest, with only one basal plate situated at the level of the point of inflexion of the flagellar membrane. Immediately above it, the flagellum shows a slight

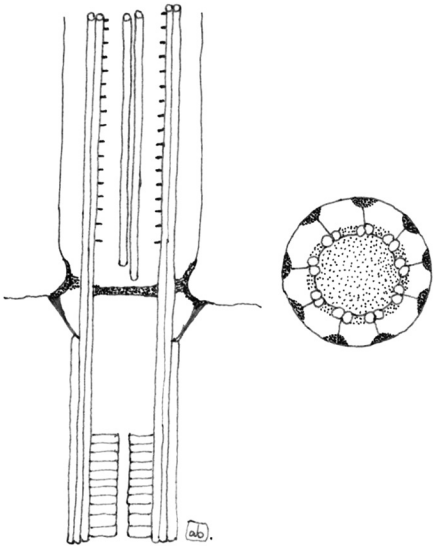

FIGURE 2.38 Type 1 transition zone (Phaeophyceae, Ochrophyta).

narrowing. Radial fibers connect the peripheral doublets with submembrane swellings. This type of transition zone is present in the Phaeophyceae (Ochrophyta).

In Type 2 (Figure 2.39), the basal plate is replaced by a sort of plug located beneath the point of inflexion of the flagellar membrane, far from the point of origin of the central pair of doublets. In this transition zone, the nine outer doublets show a strong dilatation, which leaves room for a fibrillar spiral suspended on the doublets by short spokes. The spiral can reach the central doublet or be much shorter. Each outer doublet is associated via other spokes with a thickening of the membrane, whose folding forms a star with nine characteristic arms (Figure 2.40a and b). This transition region

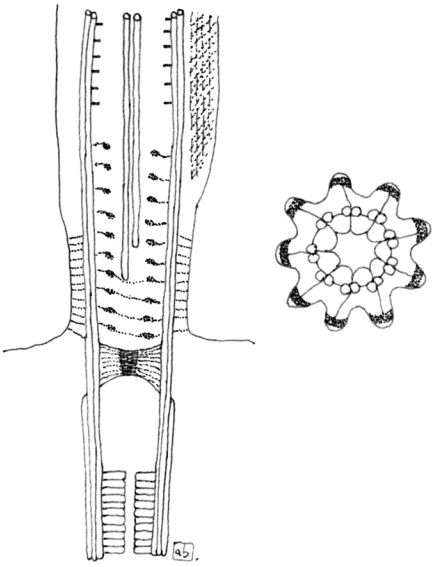

FIGURE 2.39 Type 2 transition zone (Euglenophyceae).

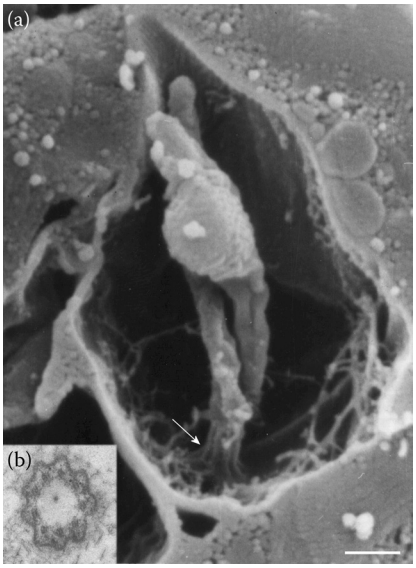

FIGURE 2.40 (a) SEM image of the reservoir region of *Euglena gracilis*, showing the two flagella arising from the bottom of the reservoir. The arrow points to the thickened folding of the flagellum membrane, typical of the transition zone. (b) TEM image of the transition zone in transverse section, showing the characteristic star configuration. Scale bar, 0.50 μm.

is typical of the Euglenophyceae. Among these algae, *Entosiphon sulcatum* is unique for its long transition region, the spiral of which surrounds the proximal 1 μm of the central doublet.

Type 3 transition regions possess a double system of complex plates. Variations exist due to the distance separating the plates or due to the presence of interposition material between them. In the Dinophyceae, the basal plate is duplicated and ring-shaped; above it, there are two median discs, the uppermost supporting the central doublet of the axoneme (Figure 2.41a). In the Cryptophyta, an apical plate is located at the level of the narrowing of the flagellum above the point of inflexion of the flagellar membrane; the central doublet is right above this plate. A second plate bearing a ring-shaped thickening is located beneath it. In *Cyanophora* (Glaucophyceae, Glaucophyta), the apical plate has the same localization present in Cryptophyta, but it is ring-shaped and traversed by the central doublet that continues toward the basal plate situated at the level of the point of inflexion of the flagellar membrane (Figure 2.41b). Further variations of this type are present in Haptophyta, where two widely spaced

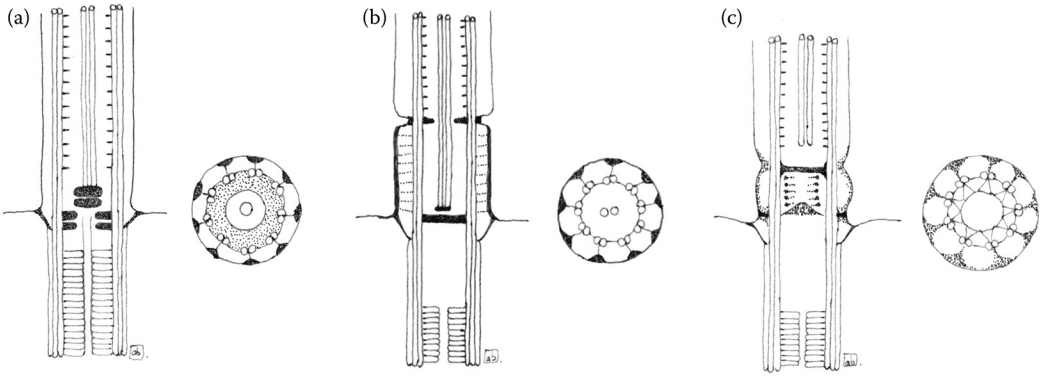

FIGURE 2.41 Type 3 transition zone of (a) Dinophyceae, (b) Glaucophyta, and (c) Haptophyta.

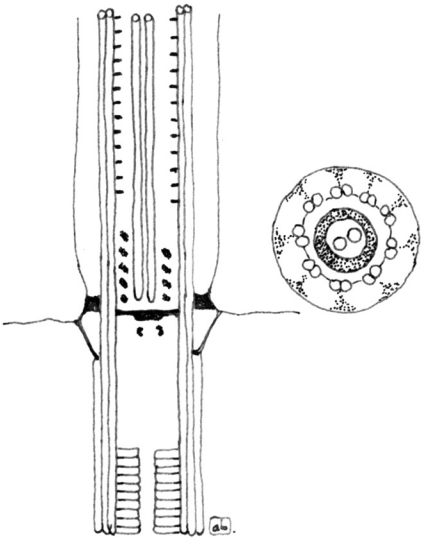

FIGURE 2.42 Type 4 transition zone of Chrysophyceae, Xanthophyceae, and Eustigmatophyceae (Ochrophyta).

plates are present, the apical below the central doublet. Each plate corresponds to a flagellar constriction, and the space between them possibly contains fibrillar material; in cross-section, a stellate structure is visible, the arm of which connect with the A-Tubules of the peripheral doublets (Figure 2.41c).

In Type 4 (Figure 2.42), there is only one basal plate situated at the point where the flagellum emerges, but this type of transition region is characterized by a very peculiar structure called "transitional helix." In longitudinal sections, this appears as a double row of punctae equidistant from the doublets, representing the four to six turns of a helix (Figure 2.43a and b). Some variations occur in the number of gyres, which in a short flagellum may be as low as 1. This helix is present in Chrysophyceae, Xanthophyceae, and Eustigmatophyceae (Ochrophyta).

Type 5 (Figure 2.44) is characterized by the so-called "stellate pattern"; typically, it is divided into a longer distal and a shorter proximal part, separated by a basal plate. In longitudinal section, the structure resembles an H, with the cross-bar located at a short distance above the cell surface (Figure 2.46a). Transversely, the cross-bar may or may not extend to the peripheral doublets of the axoneme. Variations regard the length of the proximal part, the location of the plate, and the appearance of additional rings. This transition zone is typical of Chlorophyta.

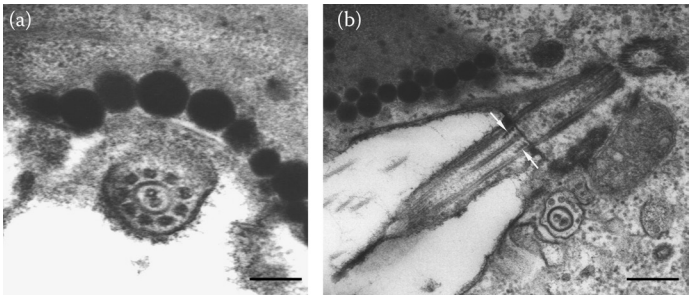

FIGURE 2.43 (a) TEM image of the transition zone of *Ochromonas danica* in transverse section, scale bar, 0.20 μm and (b) longitudinal section of the short flagellum of *Ochromonas*; arrows point to the double rows of punctae representing the turn of the helix. Scale bar, 0.40 μm.

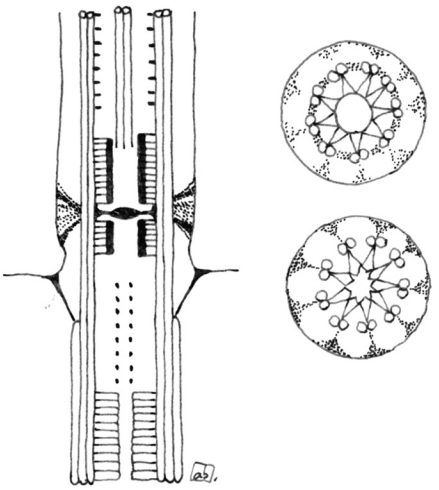

FIGURE 2.44 Type 5 transition zone (Chlorophyta).

Basal Bodies

A flagellum cannot be dissociated from its base, the basal body, or kinetosome. This structure has a cylindrical form, with an average diameter of 0.2 μm and a variable height (average 0.5 μm). The wall of the cylinder is discontinuous, consists of nine microtubular triplets tilted to the radii at an angle of 130°, and interconnected by transverse desmosomes. The complete tubule A consists of 13 protofilaments, and the incomplete tubules B and C have 10 protofilaments. The proximal part of the basal body contains a fibrogranular structure termed the cartwheel, composed of a longitudinal central tubule and nine series of spokes joined to the triplets. This structure seems to be present in nearly all species of algae, with variations reported mainly for the length of the basal body. While most green algae usually possess very short basal bodies (250–450 nm), those of the Prasinophytes are often twice as long (560–690 nm). Some members of the Haptophyta, such as *Chrysochromulina* (Coccolithophyceae), also possess very long basal bodies (850–875 nm), but this length can reach a value of 1300 nm in some Euglenophyceae such as *Entosiphon*.

In some Chlorophyta, two structures are present in association with the proximal ends of the basal bodies: the terminal cap and the proximal sheaths. The terminal cap is a more or less prominent electron-dense flap located at the anterior surface of the basal body, which folds over and covers in part its proximal end. The proximal sheath is located posterior to the proximal end of the basal body, can have a half-cylindrical shape or be wedge-shaped, narrow proximally, and broadening distally.

Variations in the number of basal bodies mainly reflect variations in the number of flagella. It is possible to distinguish:

1. Cells with only one basal body, carrying one flagellum; this situation is very rare and is present in the euglenophyte of uncertain affinity *Scytomonas pusilla*, and in the gametes of the diatoms *Lithodesmium* and *Biddulphia*.
2. Cells with two neighboring basal bodies, forming the so-called primordial pair, and indicated as 2A.
3. Cells with numerous basal bodies.

In the case of two basal bodies, two possibilities exist: only one basal body, generally situated close to the nucleus or linked to it, possesses a flagellum, as in the spores of *Hydrurus* (Chrysophyceae), or both basal bodies possess a flagellum. The latter is the most frequently occurring situation in flagellate algae. Most often the basal bodies are inclined towards each other; sometimes, they are perpendicular, or they may also be parallel facing the same directions or antiparallel

facing opposite directions. In the Glaucophyta, the two basal bodies are inclined toward each other; in the Heterokontophyta, they are parallel in the Chrysophyceae *Mallomonas* and *Synura,* almost perpendicular in *Ochromonas*, lie at an obtuse angle to each other in the Xanthophyceae and Phaeophyceae, are inclined to each other at an angle of about 90° in the Eustigmatophyceae and Raphidophyceae; in the Haptophyta, the angle between the two basal bodies can be acute or obtuse; in both Cryptophyceae and Euglenophyceae, the basal bodies are almost parallel, while in the Dinophyceae they lie at almost 180° to each other and slightly overlap. In the Chlorophyta, the angle between the two basal bodies can vary (about 90° in *Chlamydomonas* and 180° in *Acrosiphonia* zoid), and the couple can assume three different configurations:

1. 11 o'clock–5 o'clock configuration, in which the basal bodies are rotated anticlockwise relative to the ancestral configuration (Figure 2.45a).
2. 12 o'clock–6 o'clock ancestral configuration, in which the basal bodies are in line with each other (Figure 2.45b).
3. 1 o'clock–7 o'clock, in which the basal bodies are rotated clockwise relative to the ancestral configuration (Figure 2.45c).

The 11 o'clock–5 o'clock configuration is present in Ulvophyceae and Dasycladophyceae, while both the 12 o'clock–6 o'clock and 1 o'clock–7 o'clock configurations are present in the Chlorophyceae.

In the case of many basal bodies, the increase in their number and the corresponding increase in the number of flagella can result from

1. A replica of each basal body of the pair, as in the stephanokont zoospore of *Oedogonium* (Chlorophyceae).
2. Replica of the primordial pair, indicated by the formula $X \cdot 2A$, as in the dinoflagellate *Phaeopolykrikos* sp. (Dinophyceae), where the primordial pair has undergone four replicas ($4 \cdot 2A$).
3. Addition of new basal bodies in the surroundings of the primordial pair without there have been a replication of it, indicated by the formula $2A + N$; algae with four flagella, as *Tetraselmis suecica* (Chlorodendrophyceae) or *Pyramimonas lunata* (Prasinophytes), have a formula $2A + 2N$, while algae with eight flagella such as *Pyramimonas octopus* (Prasinophytes) are indicated by the formula $2A + 6N$.

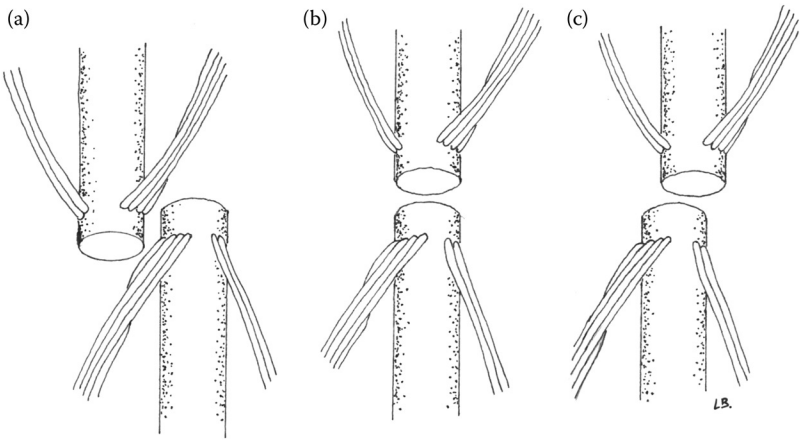

FIGURE 2.45 Schematic drawing of cruciate arrangements of basal bodies and roots of Chlorophyta. (a) 11 o'clock–5 o'clock type; (b) 12 o'clock–6 o'clock type; (c) 1 o'clock–7 o'clock type.

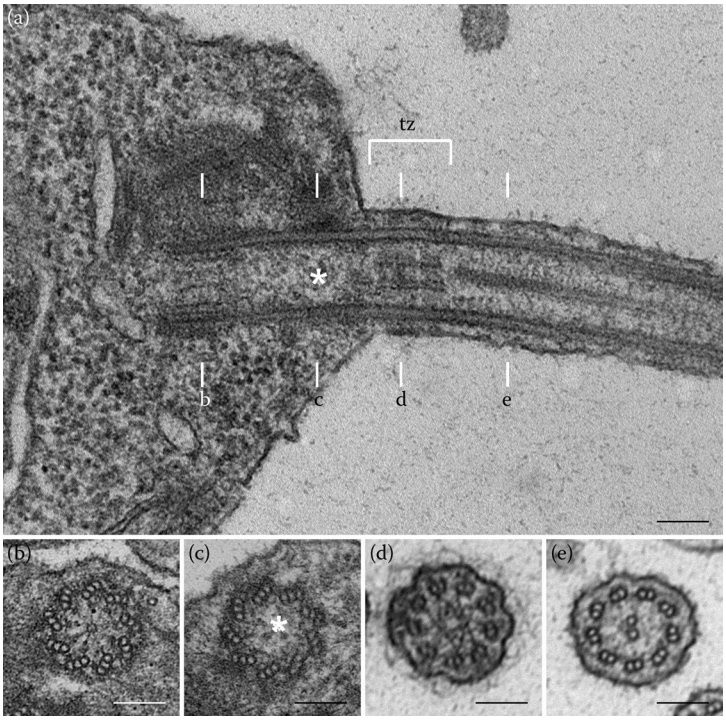

FIGURE 2.46 Longitudinal section of a flagellum of *Tetraflagellochloris mauritanica* between the basal body and the 9 + 2 axonemal structure. The level of each section in the series of transverse sections (b–e) is indicated in the longitudinal section (a). See text for details, scale bar, 0.5 μm.

Figure 2.46a shows an example of flagellum assemblage, relative to the longitudinal section of a flagellum of *Tetraflagellochloris mauritanica* (Chlorophyceae), in the region between the basal bodies and the 9 + 2 axonemal structure. The basal bodies are composed of nine tilted microtubular triplets with connections between the A- and C-tubules of adjacent triplets. At the proximal end of each basal body, the hub-and-spoke complex of the cartwheel is present (Figure 2.46b). This structure consists of a central hub with a central dot, and nine spokes that are connected to the A tubules by nine electron-dense knobs (Figure 2.46b). In the median longitudinal section, a series of projections seem to extend into the lumen of the basal body along the microtubular triplets, distally to the cartwheel. The lumen of the basal body is filled with filaments (asterisks, Figure 2.46a and c).

Distal to the end of the C-microtubules of the basal body is the transition zone (tz), which is characteristic of green algae (square brackets, Figure 2.46a).

This region contains two distinct stellate structures that are separated by the transitional plate. The stellate structure is formed by filaments that connect the A tubules of every third axonemal doublet with each other, constituting (as seen in transverse sections) a nine-pointed star with a central ring-like hub (Figure 2.46d). In longitudinal sections, the two stellate structures form an H-piece with uneven arms composed of the distal (~800-nm long) and proximal (~320-nm long) stellate structures and separated by the transitional plate (Figure 2.46a). Different from other chlorophycean algae such as *Chlamydomonas*, both the distal and the proximal stellate structures are attached to the same transitional plate, which in our preparation does not seem to extend to the microtubule doublets. Figure 2.46d shows a cross-section through the proximal stellate structure of the transitional region; projections attached to the A–B tubule junction extend to the flagellum membrane. Figure 2.46e shows the internal 9 + 2 structure of the axoneme.

Root System

All algal flagella appear to possess flagellar roots, that is, microtubular or fibrillar, often cross-banded structures, which extend from the basal bodies into the cytoplasm either underlying the plasma membrane or projecting into the cell and making contact with other organelles such as the nucleus, the mitochondria, the Golgi apparatus, or the chloroplasts. Diverse functions have been assigned to the flagellar roots: anchoring devices and/or stress absorbers; sensory transducers, skeletal, and organizational structures for morphogenetic processes.

The great diversity of morphology and arrangement of the flagellar root systems among the different algae make it necessary to describe them separately in each division. As said above, Cyanobacteria and Rhodophyta lack any flagellar apparatus, hence they will not be considered in the following.

Glaucophyta

In the cyanelle-containing genera *Gloeochaete* and *Glaucocystis*, four roots are arranged in a cruciate manner, that is, four roots spreading out more or less evenly from the basal bodies. All the four roots appear identical, each containing about 20 microtubules in *Glaucocystis*, and about 50 in *Gloeochaete*. In *Cyanophora*, the roots are two. In all the genera, each root contains a multilayered structure consisting of a band of microtubules which overlies several layers of parallel plates (Figure 2.47).

Chlorophyta—Charophyta

Flagellar apparatus of most green algae are characterized by a cruciate root system. A cruciate root system consists of four roots spreading out more or less evenly from the basal bodies and with opposite roots usually possessing identical numbers of microtubules. Since in most members of these two phyla, two of the roots are two-stranded, the general arrangement of microtubular root follows the X–2–X–2 system, with X varying from 3 to 8 microtubules.

The root system is cruciate with a 4–2–4–2 system in the tetraflagellate *Pyramimonas* (Prasinophytes) and *Tetraselmis* (Chlorodendrophyceae), a 4–2–0–0 system in *Mantoniella*

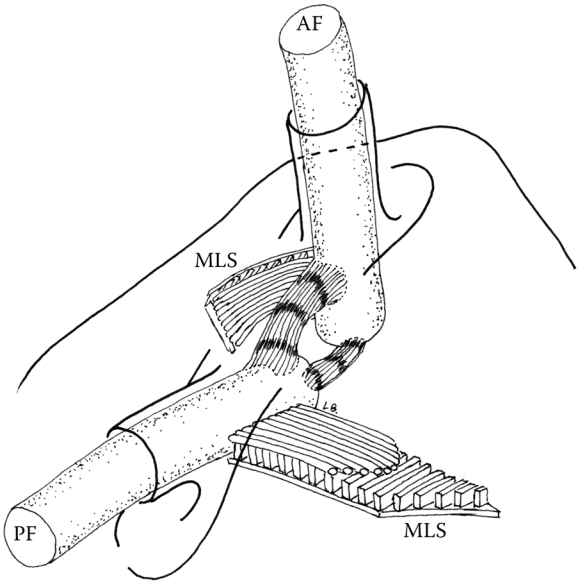

FIGURE 2.47 Root system of Glaucophyta. AF: anterior flagellum; PF: posterior flagellum; MLS: multilayered structure.

squamata (Mamiellophyceae), due to the reduction in one of the two flagella, and due to its lack of roots, a 4–3–0–(7–12) system in *Nephroselmis* (Nephroselmidophyceae), and a 4–6–4–6 system in *Mesostigma* (Mesostigmatophyceae). When four microtubular roots are present, as in *Pyramimonas*, they extend up to the sides of the flagellar pit toward the anterior of the cell, where they join the microtubules of the cytoskeleton, which radiate from the flagellar region below the membrane. An elaborate system of nonstriated fibers connects the basal bodies, which are associated with one or more rhizoplasts. These contractile structures extend from the proximal ends of the basal bodies down to the chloroplast, where they branch over the chloroplast surface and get in contact with it. Some tetraflagellate members of this class possess a synistosome, a fibrous band longitudinally striated connecting two of the basal bodies, and an asymmetrical structure termed lateral fibrous band, which forms an arc on one side of the four basal bodies. Proximal connective fibers may be present between the basal bodies. The microtubular root system of flagellate Chlorophyceae has the X–2–X–2 pattern except in the stephanokont reproductive cells of Oedogoniales. The roots diverge from the basal bodies and run beneath the cell membrane toward the posterior of the cell. Fibrous roots are generally present and associated with the 2-membered microtubular roots. Rhizoplasts extend from the basal bodies to the nucleus. The basal bodies are connected by a robust upper striated connective and two lower striated connectives (Figure 2.48).

In the stephanokont zoospore of *Oedogonium* sp., the flagellar bases are connected by a transversely striated fibrous band running around the top of the zoospore above the flagella. Three-membered microtubular roots perpendicular to the basal bodies depart from them and extend towards the posterior of the cell. Other striated components are present in close association with the microtubular roots.

The unusual root system of recently identified chlorophycean *T. mauritanica* deserves a more detailed description. The four basal bodies are arranged as two pairs in a nearly diamond shape; the two opposite basal bodies, numbers 1 and 2, are closer to each other than the other two, which are located on the sides of the first pair and do not touch (Figure 2.49). A complex system of striated roots and radiating microtubules occurs around the four basal bodies, anchoring the

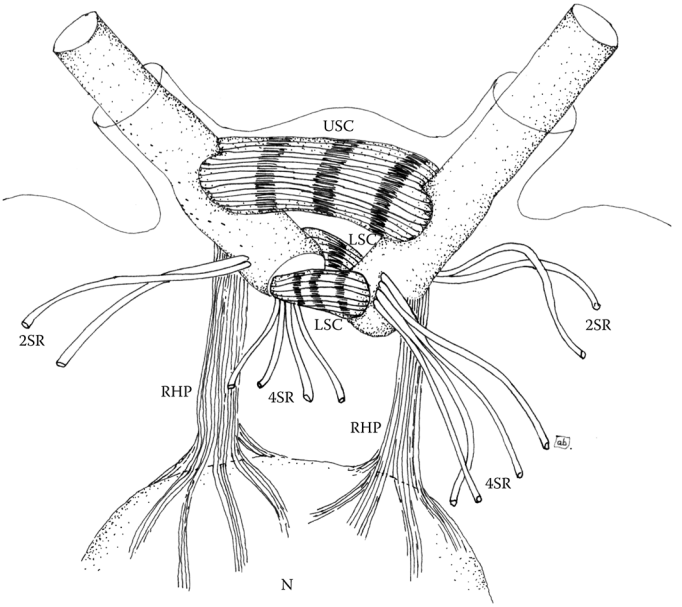

FIGURE 2.48 Root system of Chlorophyceae (Chlorophyta). 2SR, two-stranded roots; R4, four-stranded roots; RHP, rhizoplasts; N, nucleus; USC, upper striated connective; LSC, lower striated connectives.

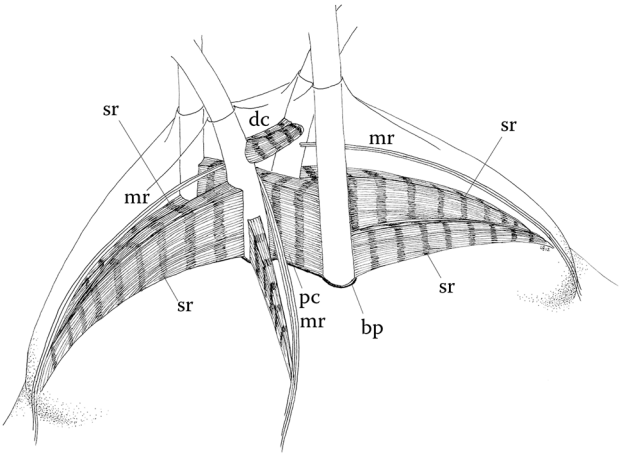

FIGURE 2.49 Schematic drawing of the posterior part of *Tetraflagellochloris mauritanica* illustrating the main components of the flagellar apparatus; sr, striated root; mr, microtubular root; dc, distal connection; pc, proximal connection; bp, basal plate. See text for details.

four flagella in the cell by a cruciate root system. One pair of striated roots, with one root more prominent than the other, originates at each of the two closer basal bodies (Figure 2.50a, white asterisk and white arrowhead, respectively). Smaller striated roots originate at the second pair of basal bodies (Figure 2.50b, arrowhead). In transverse and longitudinal sections, these striated roots reveal a periodicity of 300–330 nm (Figure 2.50c, asterisk) and a clear distal tapering where they underlie the plasmalemma (Figure 2.50c). Microtubular roots are also present: two-stranded microtubular roots (Figure 2.50e, arrows) and four-over-one roots (Figure 2.50f, arrow). The striated roots are closely associated with the microtubular roots (Figure 2.50c and d, arrow). In TEM and SEM images (Figure 2.51a and b), the tapered ends of the striated roots form two symmetrical shoulders in the posterior part of the cell, just below the flagellar emergence; the microtubular roots curve above the shoulders and down the sides of the cell for some distance. Basal bodies no. 1 and no. 2 lie in a V configuration (Figures 2.49 and 2.51c), while those of the other pair lie parallel to each other (Figures 2.49 and 2.51d). In the V configuration, the basal bodies are joined by a striated distal connection (Figure 2.51c, arrow) that is positioned immediately below the flagellar transition zone. The two basal bodies are joined at their bottom also by a basal plate (Figure 2.51c, double arrowheads). The basal bodies of the other flagellar pair show a similar connection system; a prominent proximal connection showing alternating electron-dense zones resembling a striation (Figure 2.51d, asterisk) and a basal plate (Figure 2.51c, arrowheads). The arrow in Figure 2.51d indicates the cross-sectioned connecting fiber that joins flagella no. 1 and no. 2. Immediately below the connecting fiber, the microtubular roots are visible (double asterisks).

The microtubular rootlets of the flagellate reproductive cells of Ulvophyceae follow the X–2–X–2 arrangement of most green algae, with X = 4 in *Ulva* and *Enteromorpha*, and X = 5 in *Ulothrix*. Striated bands connect the rootlets to the basal bodies, which are connected anteriorly by an upper connective; in some genera, additional striated bands between the basal bodies and striated component associated with the 2-membered root can be detected. In *Chaetomorpha*, X is 3, while in *Cladophora* X is 4. The microtubular rootlet systems of the biflagellate cells extends posteriorly nearly parallel to one another and to the basal body from which they arise. In the X-membered rootlets, an electron-dense strut or wing connects one of the uppermost microtubules to the subtending singlet, and the entire rootlet is usually subtended by a massive, more or less striated structure. The 2-membered rootlets may also be accompanied by such structures. An upper transversely striated connective links the basal bodies.

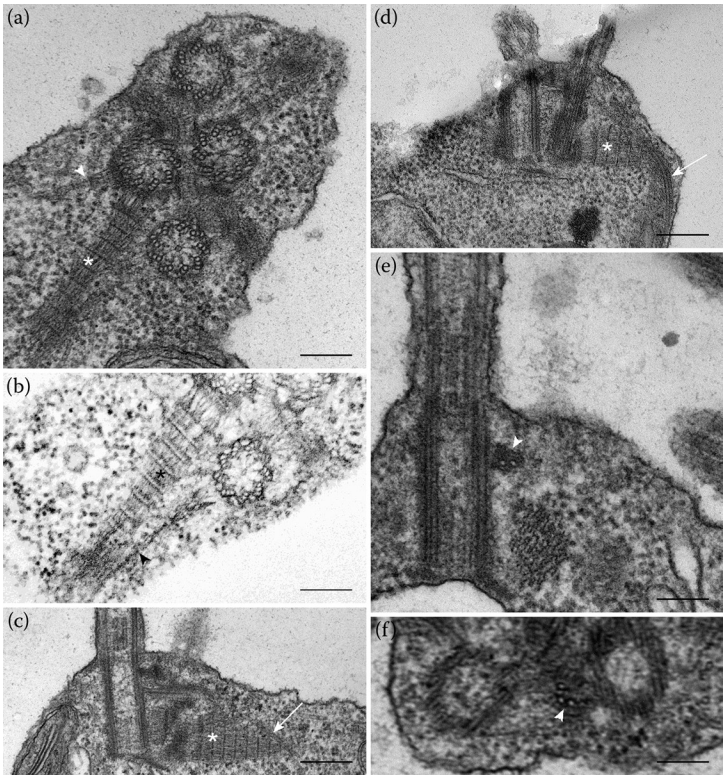

FIGURE 2.50 (a) TEM image of a transverse section of *Tetraflagellochloris mauritanica* showing the arrangement of the four basal bodies and the two striated roots originating at one basal body of the closer flagellar couple; arrowhead, minor root; asterisk, major root, scale bar, 1 μm; (b) similar section showing the smaller striated root (arrowhead) originating at one basal body of the more distant flagellar couple; asterisk, major root, scale bar, 1 μm; (c, d) TEM image of longitudinal sections of the posterior part of *T. mauritanica* cells showing the striated roots (asterisks) and the microtubular roots (arrow), scale bar: 1 μm; (e) two-stranded microtubular root (arrowhead), scale bar, 1 μm; (f) four-over-one microtubular root (arrowhead), scale bar, 1 μm.

The flagellar apparatus of the reproductive cells of the Bryopsidales (Ulvophyceae) is anchored in the cell by four microtubular roots following the usual X–2–X–2 pattern. Each of the microtubules in the rootlet may be subtended by an electron-dense wing. The basal bodies are connected anteriorly by a nonstriated upper connective, with a typically pronounced arched appearance. Transversely striated bands connecting the rootlets to the basal bodies are also present. Species exist in this class, which produce stephanokont zoospores with more than 30 flagella. In these cells, the basal bodies are connected by a nonstriated fibrous upper ring, which can be considered the result of the fusion of many nonstriated upper connectives. The proximal ends of the basal bodies are partially enclosed in a second lower ring of amorphous material. Four- and six-membered microtubular roots depart from between the basal bodies. The microtubular root system of the Trentepohliales (Ulvophyceae) motile cells (tetraflagellate zoospores and biflagellate gametes) does not follow the X–2–X–2 pattern, but shows a 6–4–6–4 arrangement in *Trentepohlia* sp. The dorsoventrally compressed form of the flagellate cells forces the basal bodies and the root system components in a flattened arrangement. Basal bodies are aligned perpendicular to the long axis of the cell, with a parallel or antiparallel arrangement, and the microtubular rootlets, especially in the gametes, extend posteriorly nearly parallel to one another and to the basal body from which they arise. Two of the rootlets (the 4-membered rootlets in *Trentepohlia* sp.) are associated with a complex columnar structure resembling the multilayered structure of the Charophyceae.

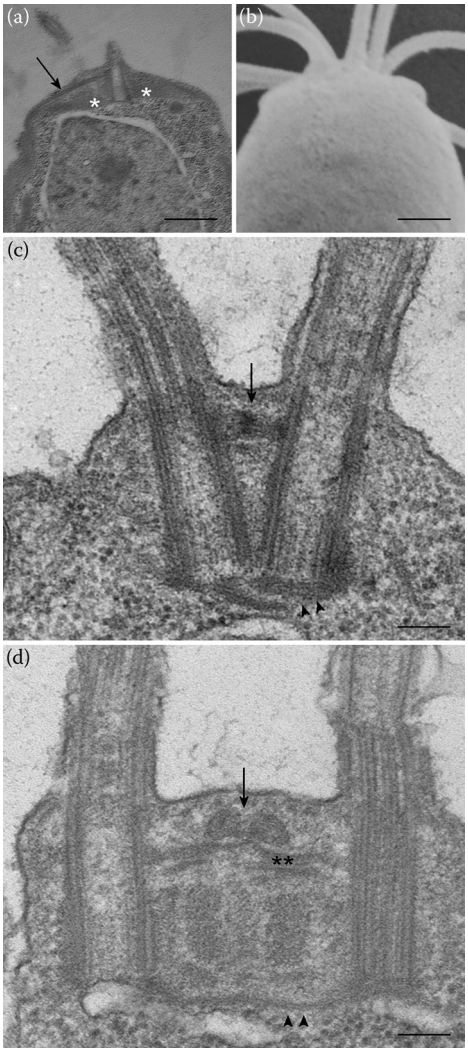

FIGURE 2.51 (a) TEM image of a longitudinal section of the posterior part of *Tetraflagellochloris mauritanica* showing the microtubular roots (arrow) in close association with the tapered ends of the striated roots, which form two symmetrical shoulders (asterisks), scale bar, 1 μm; (b) the posterior part of a cell visualized by SEM, showing the lateral wings formed by the association of microtubular roots and striated roots, scale bar, 1 μm; (c) V configuration of the basal bodies of the longer and closer flagellar pair; arrow: striated distal connecting fiber; double arrowheads: basal plate, scale bar, 1 μm; (d) as in (b), but showing the parallel configuration of the basal bodies of the shorter flagella; arrow: cross-sectioned striated distal connecting fiber; asterisk: proximal connection; double arrowheads: basal plate; double asterisks: microtubular roots, scale bar, 1 μm.

The root system and the associated structures of the biflagellate motile cells of Dasycladophyceae are scarcely distinguishable from those of the Ulvophyceae. The X–2–X–2 pattern is present, with the basal bodies and microtubular rootlets showing a flattened arrangement. A striated distal fiber connects the proximal ends of the basal bodies, from which two prominent rhizoplasts depart.

No flagellate reproductive cells are present in the Zygnematophyceae.

Biflagellate cells of Klebsormidiophyceae such as *Chaetosphaeridium* sp. and *Coleochaete* sp. are characterized by a unilateral construction, in which the two equal flagella emerge on one side of the cell, below the apex. A transversely striated connective links the basal bodies. The

system anchoring the flagella in the cell consists of a single lateral root of about 60 microtubules, which extend from the basal bodies along the cell side down to the posterior. At the level of the basal bodies, this broad root enters a multilayered structure in which the microtubules are located between two laminate plates.

In the biflagellate male gametes of the Charophyceae, the basal bodies are connected to each other by a conspicuous fibrous linkage; the root system consists of a main broad band of microtubules and a small secondary root.

A strongly suggested reading on this topic is the review by Moenstrup (1982).

Haptophyta

In the Haptophyta, there are different types of flagellar roots. Members of the order Pavlovales, such as *Pavlova* and *Diacronema*, possess a fibrous root, nonstriated, which extends from the base of the anterior flagellum and passes into the cell along the inner face of the nucleus, thus becoming progressively wider. In some species, another fibrous root originates at the base of the haptonema. Two microtubular roots extend from the base of the posterior flagellum: a seven-stranded root, which runs under the periplast, and a two-stranded root arising almost at right angles to the seven-stranded root, running inside the cell opposite to the haptonema. Fibrous connecting bands are present between the basal bodies (Figure 2.52). In the algae of the order Coccolithales, such as *Pleurochrysis*, the structure of the flagellar root system is more complex. Three main microtubular roots are associated with the two basal bodies, two broad roots, no. 1 and no. 2, arising near the left flagellum, and a smaller root, no. 3, arising near the right flagellum. Root no. 1 extends from the basal body up toward the cell apex and then curves backward to run inside the cell. A fibrous root is associated with root no. 1. Closely packed microtubules organized

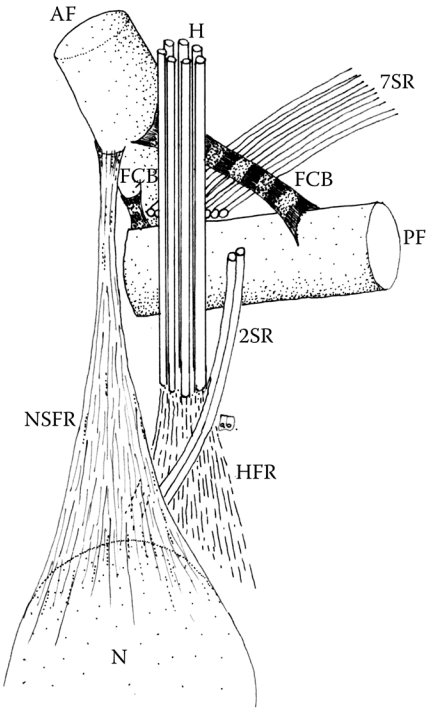

FIGURE 2.52 Root system of Pavlovales (Haptophyta). AF: anterior flagellum; PF: posterior flagellum; NSFR: nonstriated fibrous root; H: haptonema; HFR: haptonema fibrous root; 2SR: two-stranded root; 7SR: seven-stranded root; FCB: fibrous connecting band; N: nucleus.

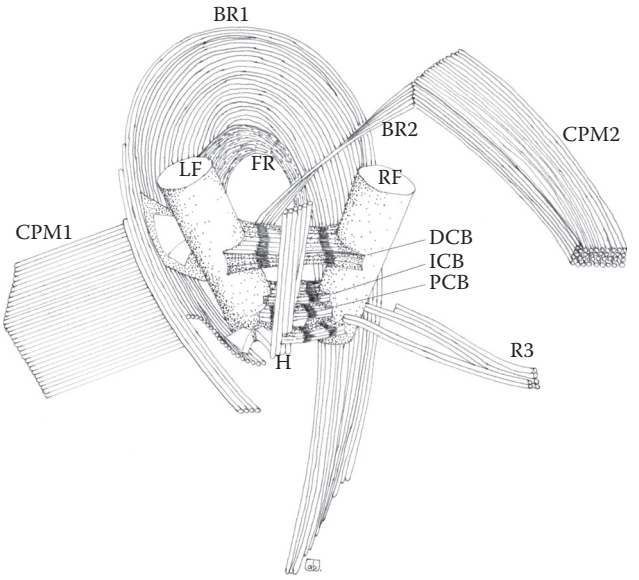

FIGURE 2.53 Root system of *Pleurochrysis* sp. (Haptophyta). LF: left flagellum; RF: right flagellum; H: haptonema; BR1, BR2: broad microtubular roots; FR: fibrous root; R3: small microtubule root; CPM1, CPM2: closely packed microtubules; DCB: distal connecting band; ICB: intermediate connecting band; PCB: proximal connecting band.

in a bundle branch off perpendicularly from both root no. 1 and root no. 2. The basal bodies are connected to each other by distal, intermediate, and proximal connecting bands. Accessory connecting bands link the haptonema to the basal bodies, and the left basal body to the broad microtubular root no. 1 (Figure 2.53).

Cryptophyta

The flagellar roots of these algae include two characteristic components, the rhizostyle and the compound rootlet. The rhizostyle is a posteriorly directed microtubular structure. It originates alongside the basal body of the dorsal flagellum and extends deep into the cell, parallel to the gullet, behind the layer of trichocysts, and ends in the posterior part of the cell. On the way, it runs through a groove in the nuclear surface. In many cryptomonads, such as *Chilomonas*, each of the rhizostyle microtubules bears a wing-like lamellar projection. The compound rootlet consists of a cross-banded fibrous band and microtubular roots. The fibrous band originates from the basal bodies of the dorsal flagellum, but perpendicularly to the rhizostyle. A microtubular root arises near the rhizostyle and passes between the basal bodies in close association with the fibrous band; a second microtubular root extends dorsolaterally in a curved path, and a third root, which can be very short, originates near the rhizostyle and extends anteriorly. In addition to this rootlet, a conspicuous 12-stranded microtubular root is present in *Chilomonas*, together with a mitochondrion-associated lamella root, while a delicated cross-banded anchoring fiber connecting one of the basal bodies to the ventral groove is present in *Cryptomonas*. The striated components of the root system have been shown to contain the contractile protein centrin (Figure 2.54).

Ochrophyta

The root system will be described for each class of this division, selecting when possible a genus representing the morphological cell type within the class.

The root system of *Ochromonas* can be considered the basic type of the Chrysophyceae. A single large cross-banded contractile root, termed rhizoplast, is typically present, associated with the basal

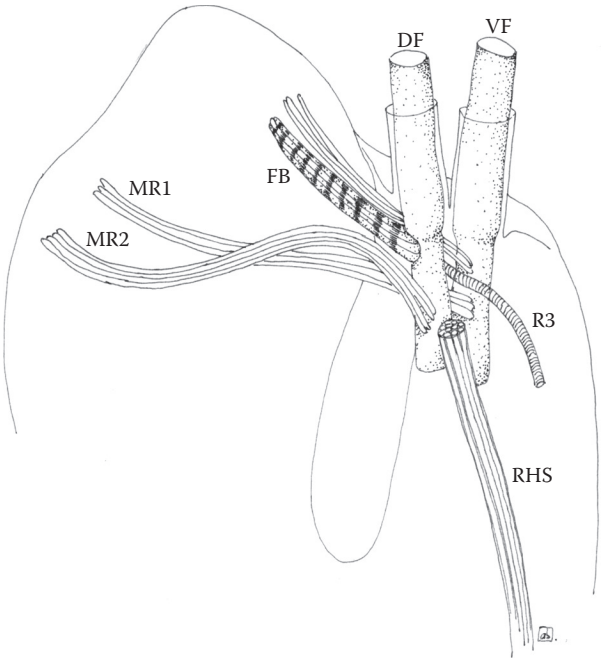

FIGURE 2.54 Root system of Chryptophyta. DF: dorsal flagellum; VF: ventral flagellum; RHS: rhizostyle; FB: fibrous band; MR1, MR2: microtubular roots; R3: root.

body of the longer pleuronematic flagellum. After leaving the basal body, this fibrous root passes closely against the edge of the chloroplast and reaches the tip of the pyriform nucleus. It then splits into several branches, ramifying over the nuclear surface, with some branches located in the narrow space between the nucleus and the associated Golgi body. Four microtubular roots, R1, R2, R3 and R4, anchor the two flagella in the cell, R1 and R2 associated with the basal body of the long pleuronematic flagellum, and R3 and R4 associated with the basal body of the short smooth flagellum. The three-stranded R1 describes an arc in the anterior part of the cell just beneath the cell membrane. The two-stranded R2 originates at the opposite side of the basal body, running along the cell membrane. R3 and R4, consisting of a species-specific number of microtubules, arise from the opposite sides of the basal body of the short flagellum and form a loop around and under this flagellum. R1 forms the base of attachment of numerous microtubules running toward the posterior end of the cell, with a cytoskeletal function (Figure 2.55).

No complete analysis of the flagellar root systems of Xanthophyceae exists. The typical root system as presently understood appears to consist of three different types of structures: a descending root originating near the basal bodies, resembling the rhizoplast in extending from the basal bodies along the nuclear surface, between the nucleus and the Golgi body, but differing in being unbranched, and in consisting of a succession of rectangular blocks rather than fibers as in the Chrysophyceae; a cross-banded fibrillar root composed of slightly curved bands, originating together with, but at right angles to the descending root, and terminating at the cell membrane; microtubular roots in various number near the basal bodies, each of which contains three or four microtubules. In *Vaucheria* (Xanthophyceae), the system is completely different; neither a descending root nor a cross-banded fiber is present, but its anterior protrusion is supported by a single broad microtubular root of 8–9 microtubules arranged in a row. This root originates near the base of the anterior pleuronematic flagellum, and from here passes forward along the cell membrane to the tip of the protrusion, turns around and runs back on the opposite side of the cell, again along the membrane.

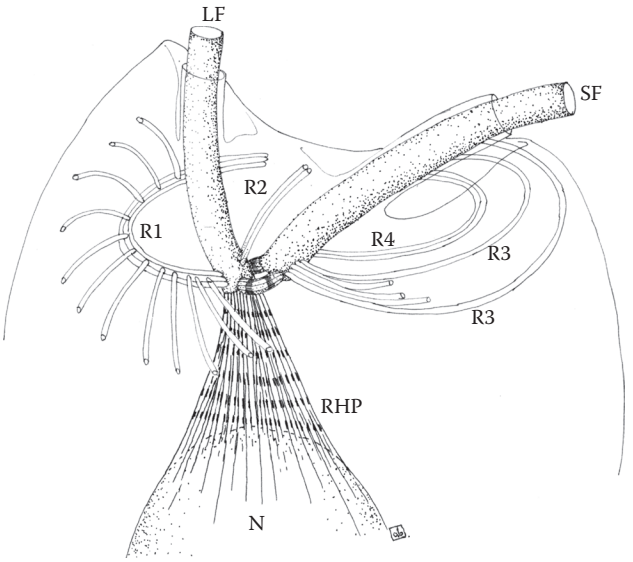

FIGURE 2.55 Root system of *Ochromonas* sp. (Ochrophyta). LF: long flagellum; SF: short flagellum; R1, R2, R3, R4: microtubular roots; RHP: rhizoplast; N: nucleus.

Only few data are available on the flagellar roots of Eustigmatophyceae. Both microtubular and cross-banded fibrillar types are present. The microtubular structures, consisting of 2–5 microtubules, arise close to the basal bodies and pass anteriorly and posteriorly in the cell. The cross-banded roots are narrow and pass from the region of the flagellar bases along the anterior flattened face of the nucleus.

The ultrastructure of the flagellar root system has been described only in one species of Bacillariophyceae, *Biddulphia laevis*. In the spindle-shaped spermatoids of this centric diatom, a system of microtubules radiates from the only basal body present into the cell, to form a cone on the anterior part of the nucleus, and at least some of these microtubules extend throughout the length of the cell. They appear to maintain the elongated shape of the nucleus and thus probably of the cell itself.

An elaborate root system connects the basal bodies to the anterior surface of the nucleus in the Raphidophyceae. In *Chattonella*, two or three roots have been described: one multilayered, associated with the pleuronematic flagellum, and one with the smooth flagellum. The latter is a band of 9–10 microtubules which extends from the anterior part of the cell, passing between the basal bodies, and joining with other microtubules before extending along the nucleus in a depression of its surface. A large number of distinctly cross-banded fibrous roots are also present, extending from the flagellar bases to ensheathe the anterior cone of the nucleus.

In the Phaeophyceae, the structure of the flagellar root system appears remarkably uniform. The main characteristic of the system is the root supporting the flat, elastic proboscis in spermatozoids of brown algae. In *Fucus*, this root is very broad, contains usually seven microtubules (but there can be up to 15 microtubules), which travel from the base of the anterior flagellum along the plasmalemma to the anterior end of the cell, where the proboscis is located. Here, they bend back and run along the cell membrane on the opposite side. A bypassing microtubular root, of about five microtubules, originates in the anterior part of the cell, runs along the proboscis root, bypasses the basal bodies, without contact, and continues toward the posterior part of the cell. Two other minor microtubular roots, consisting of only one microtubule, are present, one extending anteriorly, and the other posteriorly. The basal bodies are interlinked by three cross-banded connectives, the deltoid, the strap-shaped, and the button-shaped bands (Figure 2.56).

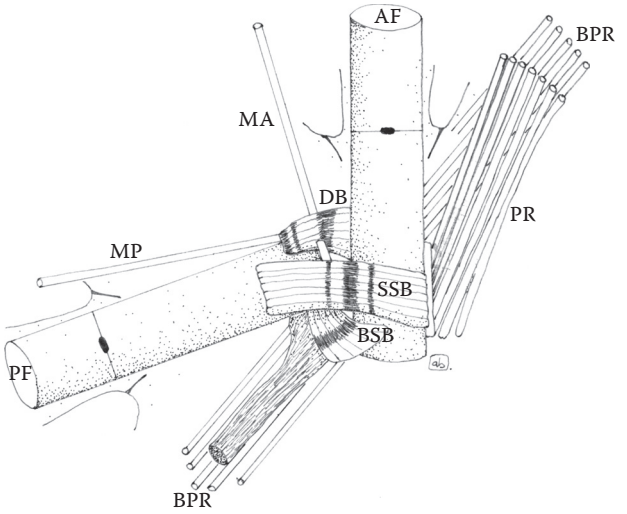

FIGURE 2.56 Root system of *Fucus* sp. (Ochrophyta). AF: anterior flagellum; PF: posterior flagellum; PR: proboscis root; BPR: bypassing microtubular root; MA: minor anterior root; MP: minor posterior root; DB: deltoid band; SSB: strap-shaped band; BSB: button-shaped band.

Cercozoa—Chlorarachniophyceae

The single flagellum of the ovoid zoospores of *Chlorarachion reptans* possesses a root system that consists of a microtubular component appearing as a 3 + 1 structure near the level of emergence of the flagellum, soon increasing to 8 + 1, and a second root with a homogeneous substructure that occupies a distinct concavity in the nuclear envelope.

In contrast to *C. reptans*, cells of *Bigelowiella natans* are basically biflagellate. The second flagellum, however, is exceptionally short and is represented only by a barren basal body inserted at approximately right angle to the emergent flagellum. In this alga, the four flagellar roots are represented by microtubular structures only with no cross-banded roots. A microtubular root is present on either sides of the long flagellum basal body; the largest and most conspicuous root, which attaches to the outside of the long flagellum basal body, is five-stranded and forms an "L" in the area between the nucleus and the plasma membrane. Just before terminating, this root becomes two-stranded. The second microtubular root associated with the long flagellum basal body emerges from the corner between the two basal bodies and is one-stranded. The third flagellar root emerges on the outside of the short basal body and it is three-stranded. The four microtubular roots are the most unusual; they are one-stranded and seem to emerge within the lumen to the short basal body next to the cartwheel structure (Figure 2.57).

Mizozoa—Dinophyceae

The root apparatus of these algae is quite complex for number and appearance of ancillary structures associated to the microtubular roots and for the spatial relationship between roots and other cell organelles. Minor features can be considered species-specific, whereas major components are common to almost all the dinoflagellates. The longitudinal basal body and the transverse basal body are interconnected by a small striated connective band. A multimembered microtubular root, the longitudinal root, originates on the left side of the longitudinal basal body and continues posteriorly along the sulcus. A cross-striated fibrous root, the transverse striated root, emanates from the left side of the transverse basal body and runs along the transverse flagellar canal and the cingulum. Striated connectives link the transverse striated root to both the longitudinal root, and the longitudinal basal body, and the proximal portion of the longitudinal

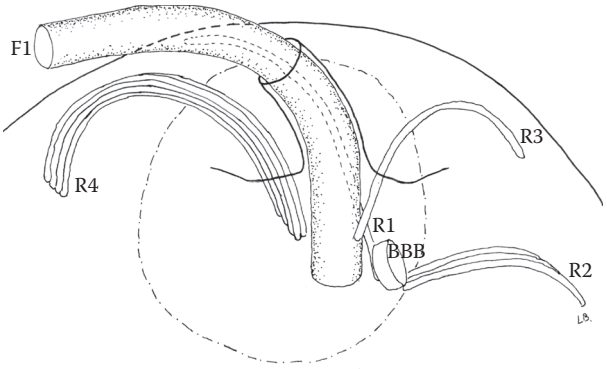

FIGURE 2.57 Root system of *Bigelowiella natans* (Chlorarachniophyceae). F1: main flagellum; BBB: barren basal body; R1, R2, R3, R4: microtubular roots.

basal body to the longitudinal root. The most distinct connective is a large electron-opaque fiber termed the nuclear fibrous connective, which links the proximal parts of the longitudinal root, the transverse striated root, and the transverse and longitudinal basal bodies with the nucleus. Fibrous rings with cross-striations, called fibrous collars, encircle the flagellar canals, the longitudinal striated collar less conspicuous than the transverse striated collar. A nonstriated fiber interconnects the two collars. The fibrous elements of this complex root apparatus are likely to contain centrin (Figure 2.58).

Euglenozoa—Euglenophyceae

Euglenoids show a rather uniform root structure, with one microtubular root opposite each basal body and a single microtubular root in between, termed dorsal, intermediate, and ventral roots (Figure 2.59). The dorsal root is anchored to the dorsal basal body at the side furthest from the ventral basal body; both the intermediate and ventral roots are associated with the ventral basal body at its dorsal and ventral side, respectively. In *Euglena mutabilis*, the dorsal and the intermediate roots consist of three microtubules, while the ventral root consists of five microtubules; in *E. gracilis*, the ventral root is formed by five microtubules as in *E. mutabilis*, while the microtubules of the dorsal root are more numerous. These roots extend from the basal bodies along the reservoir and into the cytoplasm, usually along the cell periphery, but in some species toward the nucleus. Flagellar roots are believed to play an important role in maintaining cell shape. In some species, the two flagellar basal bodies are connected by a conspicuous transversely striated connective.

Besides the intraflagellar accessory structures described above, euglenoids with two emergent flagella possess extra-flagellar accessory structures, the so-called rootlets. Two major classes of rootlets have been described: microtubular rootlets and filamentous rootlets. Microtubular rootlets are made of a usually complex and species-specific network (geometry, number of elements) anchoring the flagellar apparatus in the whole cell body. However, due to known functions of microtubules in other systems, these microtubules could not only play a role of an anchor, but also provide a stable oriented network along which cargos could be transported from inside the cell body to the flagellar apparatus.

The filamentous rootlets are made of filaments that can contain centrin. These appendages are attached to the pair of basal bodies located at the base of the flagella and extend inside the cytoplasm, usually in the direction of the nucleus or along the plasma membrane. Classically, they have been considered as anchoring structures providing the role of roots to the whole flagellar apparatus. However, they are also contractile structures, which may show transversal striations (centrin type, not assembling type) whose periodicity varies with their contraction state.

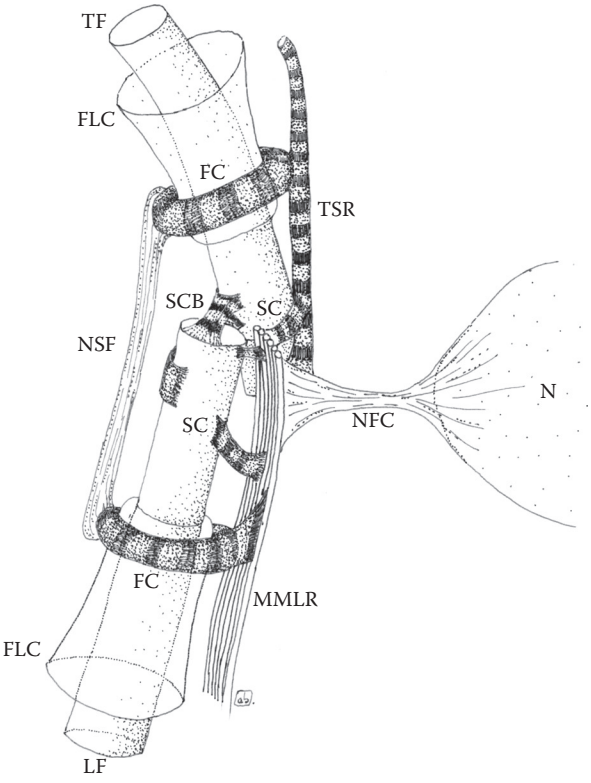

FIGURE 2.58 Root system of Dinophyceae. TF: transverse flagellum; LF: longitudinal flagellum; SCB: striated connective band; MMLR: multimembered longitudinal root; TSR: transverse striated root; SC: striated connectives; NFC: nuclear fibrous connective; N: nucleus; FC: fibrous collars; FLC: flagellar canals; NSF: nonstriated fiber.

How Algae Move

Cytoplasm, cell walls, and skeletons of algae have a density greater than the medium these organisms dwell in. The density of freshwater is 1.0 g cm^{-3} and that of seawater ranges from 1.021 to 1.028 g cm^{-3}, but most cytoplasmic components have a density between 1.03 and 1.10 g cm^{-3}, the silica forming the diatom frustule and the scales of Chrysophyceae have a density of 2.6 g cm^{-3}, and both calcite and aragonite of Haptophyta coccoliths reach an even higher value of 2.7 g cm^{-3}. With this density values, algae must inevitably sink. Therefore, one of the problems planktonic organisms face (organisms that wander in the water and/or are carried about by the movements of the water rather than by their own ability to swim) is how to keep afloat in a suitable attitude between whatever levels are suitable for their life. The phytoplankton must obviously remain floating quite close to the surface because only there is a sufficient illumination for photosynthesis. There are broadly two solutions by which algae can keep afloat and regulate their orientation and depth: a dynamic solution, obtaining lift by swimming, and a static solution, by buoyancy control, or through adaptations reducing sinking rates. In many cases, the two solutions function together.

Swimming

What does swimming mean? It means that an organism immersed in a liquid environment is able to sustain movement by deforming its body in a periodic way.

The algae are all good movers or better good swimmers. They swim more or less continuously and control their level chiefly by this means. For example, dinoflagellates, which can achieve speed

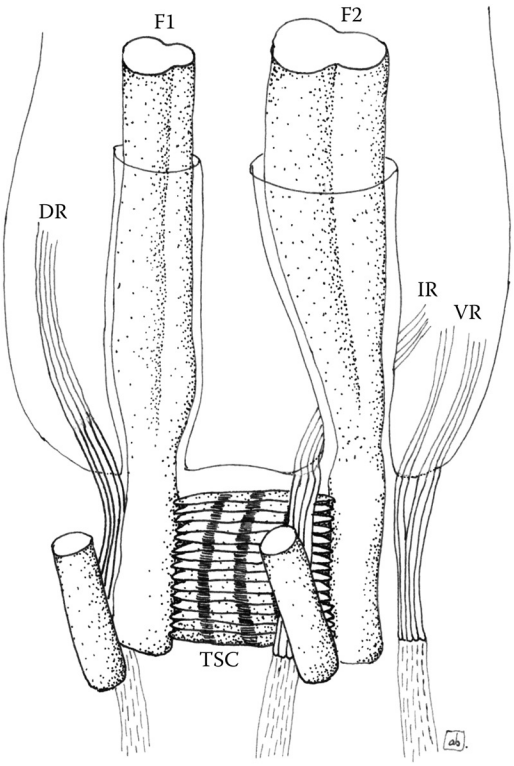

FIGURE 2.59 Root system of Euglenophyceae. F1, F2: flagella; DR: dorsal root; IR: intermediate root; VR: ventral root; TSC: transversely striated connective.

in the range 200–500 μm s^{-1}, are said to maintain themselves near the surface by repeated bursts of upward swimming, alternating with short intervals of rest during which they slowly sink. Motility is present in unicellular algae or colonies that are propelled by flagella; in some classes, it is confined only to gametes and asexual zoospores provided with flagella, which are used as a motor system for their displacement in the fluid medium.

In order to move through a fluid, the swimming cell must use its motor system to push a portion of the fluid medium in the direction opposite to that in which the movement is to take place.

The physics governing swimming at the micrometer scale experienced by algae is different from the physics of swimming at the macroscopic scale. Forward movement of a swimming alga is resisted by two things: the inertial resistance of the fluid that must be displaced, which depends upon the density of the fluid, and the viscous drag experienced by the moving organism, that is, the rearward force exerted on the organism by the fluid molecules adhering to its surface when it passes through the viscous fluid. The world of microorganisms is the world of low "Reynolds number," a world where inertia plays little role and viscous damping is paramount. The Reynolds number (R) is defined as the ratio of inertial and viscous forces; it depends on the size of the organism (related to the linear dimension, l), its velocity (u), and to the density (ρ) and viscosity (η) of the fluid medium according to the equation:

$$R = (\text{inertial forces})(\text{viscous forces})^{-1} = lu\mathtt{rh}^{-1}. \tag{2.1}$$

Since the ratio between the viscosity and the density is the kinematic viscosity ($\nu = \eta\rho^{-1}$ in $cm^2\ s^{-1}$), Equation 2.1 can be written as

$$R = luv^{-1} \tag{2.2}$$

In water, at 20°C the kinematic viscosity is 10^{-2} cm^2 s^{-1}.

A 50-μm long alga swimming at 10 μm s^{-1} has the minuscule Reynold's number of 5×10^{-4}, hence inertial effects are vanishing small and the major constraint is the viscous drag; this means that what an algae is doing at the moment is entirely determined by the forces that are exerted on it *at that moment*, and by nothing in the past. Therefore, when the flagellum stops, forward movement of the cell will cease abruptly without gradual deceleration.

Swimming strategies employed by larger organisms that operate at high Reynolds number, such as fish, birds, or insects, are ineffective at the small scale. Reynolds number might rise up to 10^5 for a fish that is 10 cm long and swims at 1 m s^{-1}. If the same fish would be swimming at the same Reynolds number of an alga, it would be as if it was swimming inside molasses. Any attempt to move by imparting momentum to the fluid, as is done in paddling, will be foiled by the large viscous damping. Therefore, microorganisms have evolved propulsion strategies that successfully overcome and exploit drag.

Another funny thing about motion at low Reynolds number is reciprocal motion. Since time does not matter, the deformation that produces the swimming must be asymmetrical. Therefore, the pattern of flagellar beating must be 3D and asymmetric, that is, the forward stroke should be different from the reverse.

For optimum propulsive efficiency, cell body size should be 15–40 times the flagellum radius (about 0.1 μm) and this ratio is present in many algae. When the cell body size is larger than predicted, as in *Euglena*, the effective radius of the flagellum is modified by simple, nontubular hairs.

Beat patterns of most smooth flagella (i.e., without hairs) are three-dimensional, and the analysis of the motion is far from straightforward. However, it is clear that the direction in which the microorganism moves is opposite to the direction in which the waves are propagated along the length of the flagellum, so that in almost all cases, when the cell body is to be pushed along, a wave must be initiated at the base of the smooth flagellum. Although basal initiation is more common than distal, both are known. The velocity of forward movement is always a small fraction of the velocity of the wave running along the flagellum, and its propulsive efficiency depends on the ratio of its amplitude and wavelength. Unlike smooth flagella, the propulsive force generated by a flagellum bearing tubular hairs is in the same direction of wave propagation. These stiff hairs remain perpendicular to the axis of the flagellum as it bends (Figure 2.60). A wave moving away from the cell body will cause the hairs to act as oars, and the overall effect will be to propel the cell flagellum first.

Control characteristics, and thus behavioral peculiarities, are connected with the functioning of the propelling structure of the cell. If the cell is asymmetric, it advances spinning along its axis; it can correct its trajectory only by sudden steering obtained by changing the insertion angle of flagella or by the stiffening of internal structures. This behavior can be attributed to all heterokont or uniflagellate algae. In the case of a symmetric cell, it can accomplish a gradual smooth correction of its trajectory going forward without spinning (or rotating with a very long period), and displacing the barycenter of the motor couple. This behavior can be attributed to all isokont cells.

Examples of main swimming patterns among algae will be described in the following.

In *Ochromonas* sp. (Ochrophyta), only the flagellum bearing hairs seems to be active during swimming (Figure 2.60). It is directed forward and executes simultaneous undulatory and helical waves that travel from its base to the tip. The resulting flagellum movements cause the whole body of the cell to rotate as it moves forwards. The shorter flagellum trails backward passively, lying against the cell; it is capable of acting as a rudder to steer the cells. The two rows of stiff hairs cause a reversal of the flagellum thrust. Water is propelled along the flagellum from the tip to the base, so that the cell is towed forward in the direction of the flagellum (Figure 2.61).

In desmokont dinoflagellates such as *Prorocentrum* sp., the longitudinal flagellum, which extends apically, beats with an anterior-to-posterior whipping action, generating a wave in a tip-to-base mode. The second flagellum, perpendicular to the first, is coiled and attached to the cell body except for the tip, which beats in a whiplash motion, while the attached part undulates (Figure 2.62). In

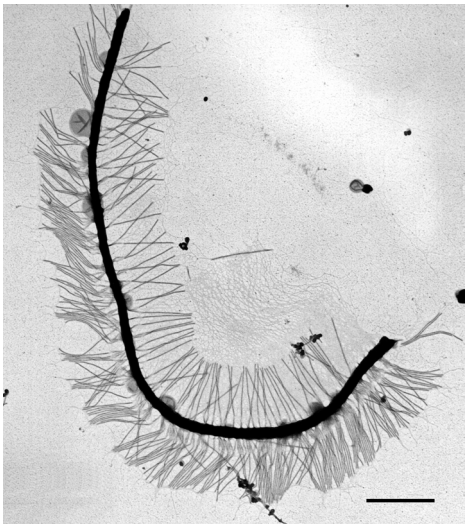

FIGURE 2.60 Negative staining of the trailing flagellum of *Ochromonas danica*. Scale bar, 1 μm.

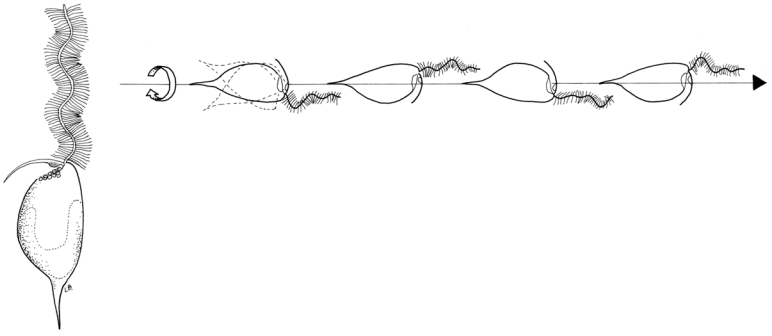

FIGURE 2.61 Swimming pattern of *Ochromonas danica*.

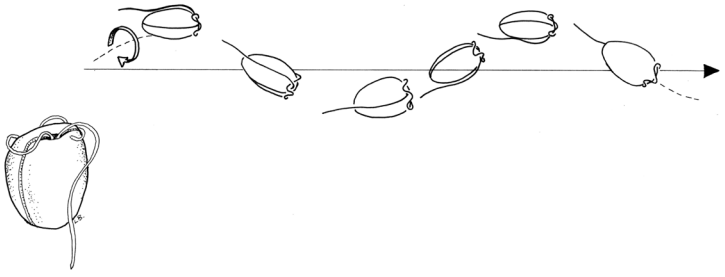

FIGURE 2.62 A desmokont dinoflagellate (*Prorocentrum* sp.) and its swimming pattern.

dinokont dinoflagellates, such as *Peridinium* sp. or *Gymnodinium* sp., the two flagella emerge at the intersection of the cingulum (transverse furrow) and sulcus (longitudinal sulcus). The longitudinal flagellum extends apically running in the sulcus and is the propelling and steering flagellum, while the ribbon-shaped transverse flagellum is coiled, lies perpendicular to the first and runs around the cell in the cingulum. It is thought to be responsible for driving the cell forward and it also

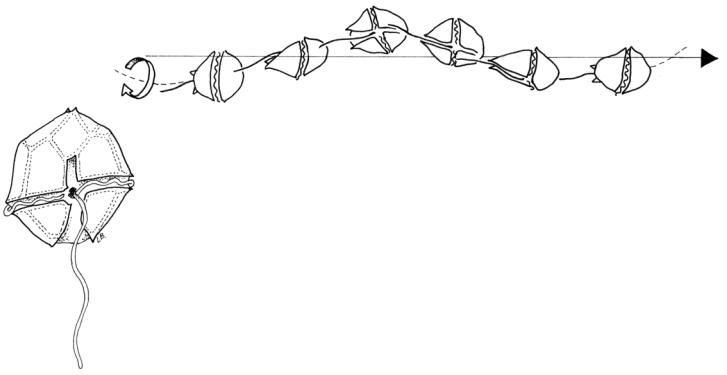

FIGURE 2.63 A dinokont dinoflagellate (*Peridinium* sp.) and its swimming pattern.

brings about rotation. The longitudinal flagellum beats with a planar waveform, which contributes to forward movement. The longitudinal flagellum can also reverse the swimming direction: it stops beating, points in a different direction by bending, and then resumes beating. This steering ability is related to change in orientation of basal bodies and contraction of the structures associated to the axoneme. In the transverse flagellum, a spiral wave generated in a base-to-tip mode is propagated along the axoneme, bringing about backward thrust and rotation and at the same time (Figure 2.63).

As said above, the emergent flagellum of *Euglena* sp. (Euglenophyceae) bears simple hairs 3–4-μm long. These long hairs are arranged in tufts of 3–4 and form a single row that runs along the flagellum spirally with a low pitch. The flagellar hairs increase the thrust of the flagellum against the surrounding water. During swimming, the long flagellum trails beside the cell body and performs helical waves, generated in a base-to-tip mode (Figure 2.64).

A peculiar swimming pattern is present in the ovoid zoospores of *Chlorarachnion reptans* and *Bigelowiella natans* (Chlorarachniophyceae), which bear a single flagellum inserted a little below the cell apex. This flagellum bears very delicate hairs markedly different from the tubular hairs of Heterokontophyta. During swimming, the flagellum wraps back around the cell in a downward spiral, lying in a groove along the cell body. The cells rotate around the longitudinal axis during swimming and the anterior or posterior end of the cell moves in either narrow or wide helical path that appears as a side-to-side rocking or wobbling (Figure 2.65).

In isokont biflagellate algae such as *Chlamydomonas* or *Dunaliella* (Chlorophyta), during the effective stroke, the flagella bend only at the base and push more water backward than adhering to them during the forward recovery stroke, thus bringing about net forward movement. While

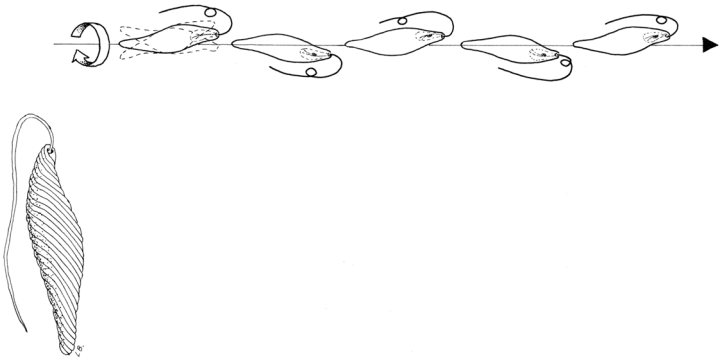

FIGURE 2.64 Swimming pattern of *Euglena gracilis.*

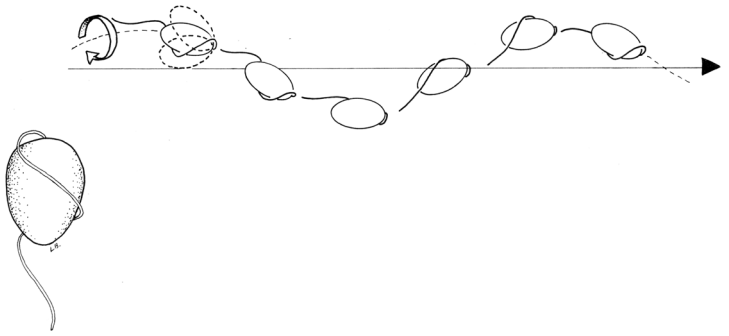

FIGURE 2.65 Swimming pattern of *Bigelowiella* sp.

swimming, these cells also rotate. Speeds ranging from 100 to 200 μm s^{-1} can be reached by these cells during forward swimming. Backward swimming is also possible, during which the flagella perform undulatory movements (Figure 2.66).

When the flagellar are four, and different in length (two shorter and two longer), as in *Tetraflagellochloris mauritanica* (Chlorophyceae), the swimming motion is more complex. This alga, which can be either single or in a group, shows a peculiar swimming motion, consisting of alternating short, rapid swimming phases and longer resting phases (maximum speed of about 200 μm s^{-1}). They swim mainly with the anterior end forward by beating the four flagella, which beat synchronously and unidirectionally behind the cell. The planar, undulatory waves propagate from the base and along the lengths of the four flagella, a swimming behavior considered quite primitive. Cells suddenly stop by throwing the flagella forward, which recover the bent configuration of the resting phase by assuming what appears to be a "braking" movement (Figure 2.67). The cells can also swim backward, although this motion seems to be used only during settling, with a ciliary beating that proceeds in fits and starts and appears to be rigid and limited to the part of the flagella distal to the bend.

An interesting question is why the algae swim?

All algae in an aquatic environment have a need to exchange molecules such as O_2, CO_2, NH_3 with environment. Since all solid boundaries in a liquid medium have associated with them a boundary layer in which water movement is reduced (due to the no-slip boundary), this layer will impede the nutrient uptake of the organisms by creating a small depleted layer around them. Turbulence is very ineffective in transporting nutrients toward such small organisms as the smallest length scale of turbulent eddies are in the order of several millimeters. Therefore, algae must rely on molecular diffusion to overcome the nutrient gradient across the boundary layer. Diffusion, that is, the slow mixing caused by the random motion of molecules, is important in the world of low Reynolds

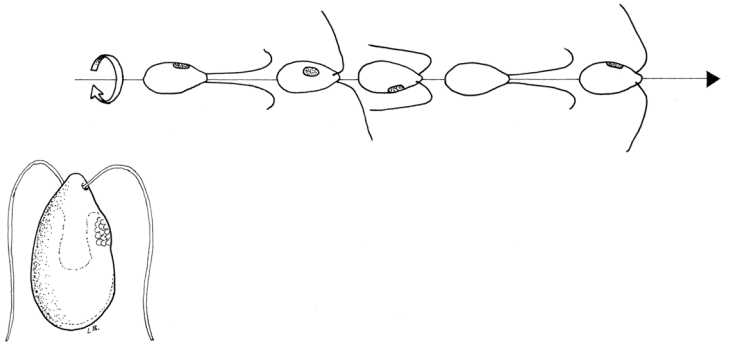

FIGURE 2.66 Swimming pattern of isokont biflagellate algae (*Dunaliella salina*).

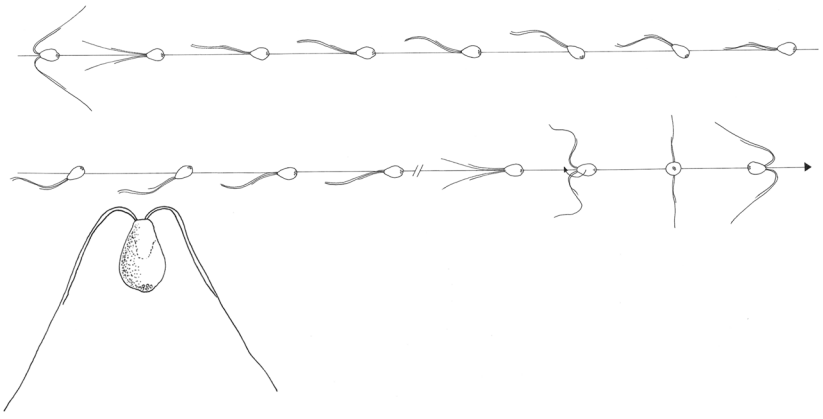

FIGURE 2.67 Swimming pattern of a quadriflagellate alga (*Tetraflagellochloris mauritanica*).

number, because of this world stirring is not any good. The alga's problem is not its energy supply; its problem is its environment. At low Reynolds number, you cannot shake off your environment. If you move, you take it along; it only gradually falls behind.

Algae use their motility (be it sinking or swimming) to generate movement relative to the water and hence replenish the boundary layer with nutrients. Depending on the size of the organism, the motive for swimming must differ; however, its effects differ significantly. For small algae in the 1–10-μm range, diffusion is about 100 times more effective in supplying nutrients than movement. This is often expressed as the Sherwood number (*S*):

$$\begin{aligned} S &= (\text{time for transport by diffusion})(\text{time for transport by movement})^{-1} \\ &= (L^2 D^{-1})(Lu^{-1})^{-1} = (Lu)^{-1} D, \end{aligned} \tag{2.3}$$

where *L* is the distance over which the nutrient is to be transported, *u* the water velocity, and *D* the diffusion constant.

For scale in the order of 1 μm, the ratio is $\approx 10^{-2}$. Diffusion is about 100 times faster than movement. Hence, in this world of low Reynolds numbers, nothing is gained by trying to reduce the diffusion barrier by generating turbulent advection. In this contest, the only possible advantage to the alga of undertaking locomotion is that it might encounter nutrients in a higher concentration. For this purpose, a helical swimming path is more useful than a straight one in spite of the longer distance for the same displacement. This is because a helical swimming path enables detection of 3D component of a gradient, whereas the straight path allows detection of only one dimension.

Purcell (1977) summarized it by saying that the organism does not move like a cow that is grazing on pasture, it moves to find a greener pasture.

Only the species that swim very fast such as the dinoflagellates (about 500 μm s^{-1}) can overcome the diffusion limitation. This high velocity should be related to the effective increase in the probability to catch more preys and therefore to the heterotrophy metabolism of the algal species.

Movements Other than Swimming

In some algae, movement cannot occur unless the cells are in contact with a solid substratum. This kind of movement, in some cases termed gliding, is present in cyanobacteria, in the red alga *Porphyridium* (Rhodophyta), in diatoms, and in some desmids (Chlorophyta).

The most efficient gliders among the cyanobacteria are found in the filamentous forms such as *Oscillatoria*, *Spirulina*, *Phormidium*, and *Anabaena*, which can travel at up to 10 μm s^{-1}. Some species, such as *Phormidium uncinatum* and *Oscillatoria*, rotate about their long axis while gliding; while others, such as *Anabaena variabilis* translate laterally. Other unicellular coccoid

cyanobacteria, such as *Synechocystis*, move by "twitching," a flagella-independent form of translocation over moist surfaces. This type of motility is analogous to social gliding motility (S-motility) in myxobacteria, which involves coordinated movements of cells close to each other (cell–cell interactions) and requires both Type IV pili operating in a manner similar to a grappling hook and fibrils (extracellular matrix material consisting of polysaccharides and proteins). While moving, cyanobacterial gliders secrete mucilage, or slime, which plays an active role in gliding. Mucilage is extruded from rows of fine pores clustered circumferentially around the septa. These pores are part of a larger structure called the junctional pore complex (JPC), which spans the entire cell wall, peptoglycan layer, and outer membrane. The channels formed by the JPCs are inclined relative to the cell axis, this angle providing directionality to the extruded slime, and are oppositely directed on either side of the septum. Propulsion of the filament results from the adherence of the slime to both the filament surface and the substratum, combined with its extrusion from a row of JPCs on one side of each septum. Switching slime extrusion to the JPCs on the other side of the septum would result in a reversal of the direction of gliding. In *P. uncinatum*, the pores are aligned in a single row, whereas in *A. variabilis* several rows of pores line both sides of the septum. The outer surface of gliding cyanobacteria consists of parallelly arranged fibrils of a glycoprotein known as oscillin, a Ca-binding protein required for motility. The surface striations formed by these fibrils would act as channels for the extruded slime to flow along. Therefore, if the fibrils are helically arranged, the cell will rotate as it glides; if the fibrils are aligned radially, the cell will not rotate. In all species studied to date, this correlation is consistent and provides a structural explanation for why some species rotate as they glide while others do not.

In diatoms, motility is restricted to pennate species possessing a raphe. These diatoms display a characteristic jerky movement forward or backward, with species-specific path patterns. The general velocity of their movement is 1–25 μm s^{-1}, but they can accelerate up to 100–200 μm s^{-1}. Raphid diatoms possess an actin-based cytoskeletal system located just beneath the plasma membrane at the raphe. Transmembrane components with an adhesive extracellular domain are connected to these actin bundles and their interaction is somehow involved in both adhesion and motility mechanisms. Microtubules are also present in this region; in addition, secretory vesicles containing polysaccharides often appear near the actin filaments at the raphe, providing the mucilage strands that project from the raphe and adhere to the substratum during the gliding process.

At least two models exist that provide reasonable explanation for diatom locomotion. In the first model, a force applied to the transmembrane protein–actin connectors, parallel to the actin bundles, would result in movement of the transmembrane proteins through the cell and the subsequent movement of the cell in the direction opposite to the force. In the second model, the energy required for motility would be generated by a conformational change of the adhesive mucilage on hydration that occurs when it is secreted from the raphe. In this model, the actin bundles restrict the secretion of mucilage to one end of the raphe, which generates a net force moving the cell over the site of secretion. In both models, the secreted mucilage plays a central role either by providing traction to translate the force into cell movement or by generating the energy through conformational changes on hydration.

A slow gliding movement over solid substrata has been observed in *Porphyridium* sp. (Rhodophyta) and in some desmids (Chlorophyta). In *Porphyridium*, the mucilage produced in mucilage sacs located inside the cell is excreted through the membrane. In desmids, mucilage is excreted through the cell wall by flask-shaped pores. As they move, these gliding cells leave behind a fibrillar mucilaginous trail, whose swelling by water pushes the cells forward.

Table 2.1 presents swimming and gliding speeds of some planktonic algae.

Buoyancy Control

The alternative to swimming is to float by means of some types of buoyancy device. In some of the attached brown algae of the seashore (*Fucus vesicolosus*, *Ascophyllum nodosum*, *Sargassum* sp., Ochrophyta), the fronds gain buoyancy from air bladders (pneumatocysts) within the thallus, which stands erect when submerged. Oxygen and nitrogen, in roughly the same proportion as in air,

TABLE 2.1
Swimming and Gliding Speeds of Some Planktonic Algae

Name	Mean Speed
Gymnodium gracilentum	500 μm*s^{-1}
Symbiodinium sp.	250 μm*s^{-1}
Tetraflagellochloris mauritanica	200 μm*s^{-1}
Tetraselmis suecica	180 μm*s^{-1}
Euglena gracilis	100 μm*s^{-1}
Chattonella sp.	120 μm*s^{-1}
Chlorarachnion reptans	110 μm*s^{-1}
Dunaliella salina	95 μm*s^{-1}
Ochromonas danica	80 μm*s^{-1}
Bigelowiella natans	70 μm*s^{-1}
Pavlova salina	50 μm*s^{-1}
Synechococcus	25 μm*s^{-1}
Oscillatoria spp.	10 μm*s^{-1}
Leptolyngbya spp.	0.004 μm*s^{-1}

form the bulk of the gas, but there are also small, variable amount of CO_2 and CO. Oxygen and CO_2 derive partly from the metabolic activities of the cells in the pneumatocyst wall, and diurnal changes in the composition and pressure of pneumatocyst gases have been shown. However, equilibration takes place between the gases in the pneumatocyst and in the surrounding water (or air). This is the source of nitrogen in the vesicles and also the major source of O_2 and CO_2. In *Enteromorpha* sp. (Chlorophyta), gas bubbles are entrapped in the central area of its tubular hollow thallus, which may aid in keeping the stipe upright by flotation. In other seaweeds such as *Codium fragile* (Chlorophyta), gas trapped among the filaments achieves the same buoyancy effect of pneumatocysts.

Buoyancy regulation in cyanobacteria involves production of intracellular gas-filled structures (also termed vacuoles), not delimited by membranes, and made up of assemblages of hollow cylinders, whose proteinaceous walls are permeable to gas, but not to water. The density of this structure is about 0.12 g cm^{-3}, about one-eighth of that of water, and if sufficient gas-filled structures are present in a cell, it can become positively buoyant. In cyanobacteria, buoyancy is regulated by varying gas-filled structure formation and cytoplasmatic composition through synthesis and breakdown of photosynthetic products. The production of gas-filled structures is induced by low-light conditions (e.g., in deep layers with insufficient light). Here, photosynthesis is reduced, osmotic pressure of newly synthesized sugars is small, and ballast materials such as carbohydrates are not produced at a high rate, and therefore they will not increase cell density, which in turn would increase sinking. Under these conditions, gas-filled structures can be produced at a high rate and cells increase their buoyancy. Conversely, if cell osmotic potential is high (high sugar production, increased amount of ballast in the form of secondary photosynthetic products), hence turgor pressure increases, it may collapse gas-filled structure, and cells become negatively buoyant sink in the water column. The rise in turgor pressure with light irradiance has been found in many cyanobacteria; however, for this rise to result in gas-filled structure regulation, the pressure reached must exceed the lowest pressure of gas-filled structures. This occurs, for example, in *Anabaena flos-aquae*, with a critical collapse pressure distributed about a mean of 6 bar. In *Trichodesmium* sp., gas-filled structures can withstand pressures of 12–37 bar depending on the species, and turgor pressure collapse is not possible as a buoyancy regulation mechanism in this genus; carbohydrate ballasting is considered the only plausible mechanism for rapid buoyancy shifts in this cyanobacterium.

Other algae obtain buoyancy from liquids of lower specific gravity than seawater or freshwater in a way similar to a bathyscaphe. Liquid-filled floats have the advantage of being virtually incompressible; but because of their higher density, they must comprise a much greater proportion of the organism's overall volume than is necessary with gas-filled floats if they are to give equivalent lifts. The large central vacuole of diatoms contains cell sap of reduced density, obtained by the selective accumulation of K^+ and Na^+, which replace the heavier divalent ions, conferring some buoyancy. In young, fast-growing cultures, diatom cells often remain suspended, or sink only very slowly, although in older cultures they usually sink more rapidly. Studies of the distribution of diatoms in the sea suggest that some species undergo diurnal changes of depth, usually rising nearer the surface during daylight and sinking lower in darkness, possibly due to slight alterations of their overall density effected by changes in specific gravity of the cell sap, or in some cases by formation or disappearance of gas vacuoles in the cytoplasm. The dinoflagellate *Noctiluca* also gain buoyancy from a high concentration of NH_4^+ ions in its large vacuoles, exclusion of relatively heavy divalent ions, especially sulfate, and a high intracellular content of Na^+ ions relative to K^+. As a result, the density of the cell sap in the vacuoles is less than that of seawater, and the cells can therefore be positively buoyant and float.

When buoyancy control is not possible by these mechanisms, algae can keep afloat and regulate their orientation and depth through adaptations reducing sinking rates. The rate at which a small object sinks in water varies with the amount by which its weight exceeds that of the water it displaces, and inversely with the viscous forces between the surface of the object and the water. The viscous forces opposing the motion are approximately proportional to the surface area, and therefore, other things being equal, the greater the surface area, the slower the sinking rate.

There are a number of structural features of planktonic organisms, which increase their surface area and must certainly assist in keeping them afloat. The majority of planktons are of small size, and therefore have a large surface-to-volume ratio. In many cases, modifications of the body surface increase its area with very little increase in weight. These modifications generally take two forms: a flattening of the body, or an expansion of the body surface into spines, bristles, knobs, wings, or fins.

A great range of flattened or elaborately ornamented shapes occur in diatoms such as *Chaetoceros* sp. In dinoflagellates, also, the cell wall is in some cases prolonged into spines (*Ceratium*) or wings (*Dinophysis*). Among the Chlorophyceae, the wall of the peripheral cells of *Pediastrum* colonies may bear clusters of very long and delicate chitinous bristles regarded as buoyancy devices. In *Scenedesmus* also, the cells are clothed by large number of bristles with a complex structure, which seem to help keep the cells in suspension.

Reduction of the sinking rate is also obtained by an increase in lipid content, which has a density of about 0.86 g cm^{-3}. Oil droplets are common inclusions in the cytoplasm of algae; lipids stored in this form are present in the Chrysophyceae and Phaeophyceae (Ochrophyta), and in the Haptophyta, Cryptophyta, and Dinophyceae. The thermal expansion of these compounds may be of some significance in effecting diurnal depth changes, through reduction of cell density, but without producing neutral buoyancy.

How a Flagellum Is Built: The Intraflagellar Transport

The mechanisms that determine and preserve the size and function of cellular organelles represent a fundamental question in cell biology up to now only partially understood, and flagella have provided a handy model system to investigate organelles' size-control analysis. It was discovered that flagella are dynamic structures and that flagellar length is regulated by a process called intraflagellar transport (IFT). IFT is a motile process within flagella in which large protein complexes move from one end of the flagellum to the other, and flagellar length is regulated by a balance between continuous assembly of tubulin at the tip of the flagellum, counterbalanced by continuous disassembly. According to Iomini et al. (2001), the IFT cycle consists of four phases. In phase I, which takes place in the basal body region of the flagellum, anterograde particles are assembled from retrograde

particles by remodeling and/or exchange of subunits with the cell body cytoplasm, with a concurrent decrease in number. In this phase, the precursors of the flagellar structures that make up the cargos are also loaded onto the particles. In phase II, the particles are transported from the base to the distal end of the flagellum by a heterometric kinesin II with a velocity of about 2 μm s^{-1}. In phase III, which occurs at the distal end of the flagellum, anterograde particles are remodeled into retrograde particles with a concurrent increase in number, probably upon or after unloading their cargo. Finally, in phase IV, retrograde particles are transported by a cytoplasmic flagellar dynein from the distal end back to the basal body region of the flagellum, with a velocity of about 3 μm s^{-1}, higher than that of anterograde particles.

How a Flagellar Motor Works

Movement can arise by shape change of permanently linked elements, by reversible interactions causing movement of elements relative to each other, by reversible assembly and disassembly, etc. all of which need energy input. We know that such changes can occur in proteins, the most likely molecules serving these locomotory functions in real movement system. But what drives and controls these changes? In principle, the problem is not difficult. Altering the ionic milieu, changing chemically or electrically its environment can in turn alter the tertiary and/or quaternary structure of a protein. In most control systems, if not all, a change in the environment brings about a change in the properties of the motor, acting either directly or indirectly on the component of the motor. We need only two proteins to make a motor using the sliding filaments mechanism, that is, a globular protein (such as tubulin) and an anchor protein (such as the dynein–dynactin complex). If the globular protein can polymerize, we can assemble it into a linear polymer that can be attached via the anchor protein to another structure some distance away. The transformation of chemical energy into mechanical work depends on a conformational change of the anchor protein, which uses the hydrolysis of ATP in ADP. Provided the anchor protein repeats the conformational change upon each monomer of the globular protein in turn, the "boat" can be hauled "hand over hand" toward the distant anchorage. Provided some kind of metachrony regulates adjacent motor molecules, we can link our small movements in a temporal series to amplify the amount of movement that can be achieved. Each step costs hydrolysis of one ATP molecule per anchor protein. The simplest and most obvious solution is either to have more than one anchor protein, or to have a dimer, working out-of-phase, being careful not to detach before the new attachment is formed. For instance, most (but not all) microtubular motors (dyneins, kinesins) work as dimers whose subunits walk along microtubule walls just like human legs walk on a surface. Once we have two hands to pull on the rope, we can indeed move hand over hand; the one-armed man cannot do more than pull once. The flagellum movements are due to the transient interaction between two anchored microtubules, coupled to a linkage control. The generation of sliding of adjacent doublets by flagellar dynein is combined to the resisting forces localized near the active sliding rows of dyneins. During the cycle of binding/release obtained by dynein conformational change coupled to ATP hydrolysis, chemical energy is converted into mechanical energy used for sliding. Owing to their regular spacing every 24 nm along the axoneme, several adjacent dyneins participate to this local sliding, and their functioning proceeds by local waves that propagate step by step all the way along the flagella. The postulated regulator has therefore to trigger the functioning of the different dyneins alternatively along the length as well as around the section of the axoneme, but its molecular nature remains unknown.

The model of Lindemann (1994) accounts for wave generation and propagation, regulated by geometrical constraints. This model, the so-called "geometric clutch," is based on the way a cylinder with nine generatrix (the nine outer doublets of the axoneme) changes form when submitted to bending. In the zone of curvature, the doublets located outside the curvature are brought apart, while the doublets located inside the curvature come closer to each other. This makes the corresponding dynein molecules efficient for sliding. In contrast, dynein molecules located outside the curvature are too far for binding to adjacent microtubules: no active sliding can occur in this

zone. This model is consistent with ultrastructural data of electron microscopy. As above, the functioning of the axonemal mechanics needs transient connections, which could possibly be disrupted by intrinsic proteolytic activities due to the combined activities of a protease/ligase system.

How a Paraxial Rod Works

Since the PFR and the axoneme are very tightly connected, both structures have to move together. It can be argued that the PFR contributes to regulate the flagellar movements. This could be done by providing a more rigid structure that can vary its stiffness in time, that is, modifying flagellum-beating pattern.

We need only one protein to build a device for information transfer and control, that is, a protein with two conformational, alternate states such as intermediate filament proteins, which can form lattice-like structures. The propagation of conformational changes along these proteins can be used to transport and/or transduce sensory information. Each protein can be considered as a dipole in one of the two possible states. We can imagine that the conformational change is transmitted by one dipole to the neighbor proteins as a wave. Therefore, a current flow through these lattice-like structures could be generated by the mobile electrons of the proteins that interact with their immediate neighbors via dipole–dipole forces.

The α-helical coiled-coil structural motif in the rod filament is well suited for electron propagation (Figure 2.36b). A current might be propagated distally, via PFR_1 and PFR_2 protein–protein charge transfers in the lattice-like rod filaments. The current flows through these lattice-like structures and the sole constraint is that each lattice site should possess a dipole moment proportional to the magnitude of the mobile charge unit and the distance over which it hops, that is, about 1–2 nm. This wave produces a contraction in the PFR and a varying internal resistance that modulates the flagellar beats. The contraction occurs by displacement of the goblet appendages of the PFR along the axonemal microtubules, which reduces the distance between the coiled filaments, hence generating longitudinal waves of contraction along the paraxial rod. The stiffening should swing the flagellum sideways, damping out some undulatory waves of the axoneme.

The Photoreceptor Apparata

In aquatic ecosystems, light is a physical factor of fundamental importance to both photosynthetic and (nonphotosynthetic) heterotrophic organisms. They are able to sense and respond to light stimuli, an ability essential to optimize physiological processes, and to time their lives to feeding, reproduction, defense, and virtually all their functions. One of the most striking responses is phototaxis, in which motile photosynthetic microorganisms adjust their swimming path with respect to incident light in a finely tuned manner. Many are the advantages of phototaxis: it allows photosynthetic organisms to position themselves for optimal light capture and efficient photosynthesis and facilitates avoidance responses in those situations where light is intense enough to damage pigments and chloroplasts. In the case of many sexually reproducing species, such as *Ulva* sp. (Chlorophyta), both female and male gametes show positive phototaxis, which may cause the colocalization of both gametes near the surface of seawater improving the possibility of encountering. On the other hand, zygotes usually become negatively phototactic, enabling them to swim towards the bottom of the seashore where they can find a suitable substratum. Also, nonphotosynthetic organisms (heterotrophic) have shown to benefit the ecological advantages of phototaxis. For example, the marine dinoflagellate predator *Oxyrrhis marina* can orient to light and is able to use photosensory response to locate patches of phytoplankton prey by detection of chlorophyll *a* fluorescence.

The full exploitation of light information necessitates proper perceiving devices, able to change the small signal represented by the light falling upon them in a larger signal and response of an entirely different physical nature, that is, these devices, termed photoreceptors, must act as sensors, to perceive wavelength and direction of light, as transducers, to convert the light signal not only into chemical

and/or electrical information, but also as amplifiers and eventually as transmitters. Hence, photoreceptors can be considered algal "eyes," with many similarities with the complex vision systems of higher organisms, since they do possess optics, photoreceptors, and signal transduction chain components.

The proper functioning of these basic visual systems relies on some necessary and universal structural, behavioral, and physiological features, such as the following:

- Shading device (structural)
- Photoreceptor and photoreceptive proteins (structural)
- Sampling strategies (behavioral)
- Trajectory control (behavioral)
- Signal transmission (physiological)

The shading device and the photoreceptor are the structural elements used to screen the environment and provide information about the intensity and directionality of the incident light. These two elements are always in close association. The shading device, termed eyespot, is usually an absorbing element that prevents light coming from certain direction from reaching the detector.

In flagellate algae, eyespot position is usually strictly defined with respect to the plane of beat of the flagella, though variation exists; however, along the longitudinal cell axis, the eyespot being located either more anteriorly or more posteriorly. The position of the eyespot gives the algae distinctive left–right asymmetry. The typical organization of the eyespot consists of a single layer of closely packed globules containing mainly carotenoids that can play the shading role, thanks to their strong absorbance in the 400–500-nm range.

The most common (and primitive) type of photoreceptor consists of extensive two-dimensional (2D) patches of photosensitive proteins, embedded in the plasma membrane in close association with the eyespot; the proteins have an ordered disposition in order to maximize light absorption. For detecting the direction of light of a specific spectral range, a photoreceptor demands a high packing density of chromophore molecules organized in a lattice structure, with high absorption cross-section of the chromophore, that is, high probability of photon absorption by the chromophore, and very low dark noise. The dark noise is the noise inherent in a receptor, constant, and independent of light level, which arises from the random thermal motions of the molecules. For detecting patterns of light, the number and location of photoreceptors, having fixed size and exposure time, must be viewed according to the pattern of motion of algae; therefore, the design of the photoreceptive apparatus in conjunction with the helical movement of the cell produces a highly directional optical device allowing effective tracking of the light direction. The function of photoreception is inseparable from the presence of photoreceptive proteins, but not necessarily from the presence of an eyespot; hence, when the eyespot is absent, its function must be performed by the whole algal body.

Only few photoreceptors can be identified by optical microscopy (Figure 1.56), whereas the eyespot is always easily recognizable because of its size and colour, usually orange-red (Figure 2.68).

FIGURE 2.68 Apical eyespot of *Tetraflagellochloris mauritanica*. Scale bar, 5 µm.

TYPES OF PHOTORECEPTIVE SYSTEMS

Depending on their organization and structure, photoreceptive systems can be grouped into three main types.

Type I

A single layer of photoreceptor molecules is present inside the whole-cell membrane or located in just the patch of membrane that covers the eyespot when present (Figure 2.69). Lacking the eyespot, the whole algal body performs the shading function. This means that this type of photoreceptive system could not be readily visible. This type of photoreceptive system is typical of Chlorophyta, but is present also in Cyanobacteria, Ochrophyta, Haptophyta, Cryptophyta, and Dinophyceae.

In Chlorophyta such as *Haematococcus* sp., *Spermatozopsis* sp., and *Dunaliella* sp., the eyespot is situated on one side of the cell, sometimes slightly protruding beyond the cell surface, as in the gametes of *Ulva*; its area can range from about 0.3 to 10 μm^2. The globules range from 80 to 190 nm in diameter and their number varies from 30 to approximately 2000. The most common organization consists of a single layer of closely packed globules lying between the outermost thylakoid and the two-layered chloroplast membrane. Additional layers of globules can be present underneath the first layer, individual layers subtended or not by a single thylakoid. In most species, the globules show a hexagonal packing, which enables the highest possible packing density. In both *Pandorina* and *Volvox* colonies, the eyespot of cells in the anterior of the colony are larger than those of the posterior, consisting of up to nine layers, marking the occurrence of some degree of colony polarity.

The photoreceptor of *Chlamydomonas reinhardtii* can be considered the model of Type I photoreceptor. The eyespot is about 1 μm in length, located at the equator of the cell, usually composed of two organized rows of carotenoid-filled lipid globules separated by thylakoid membranes, and packed under the chloroplast envelope. The layered structure of the shading organelle in this type of photoreceptor reflects orthogonal light toward the photoreceptor and blocks light originating from other directions. The photoreceptor of the green alga *Chlamydomonas* consists of an extensive 2D patch of photosensitive proteins in the plasma membrane that lies directly over the closely apposed chloroplast envelope at the level of the eyespot (Figure 2.69). This photoreceptor has been visualized by immunofluorescence microscopy.

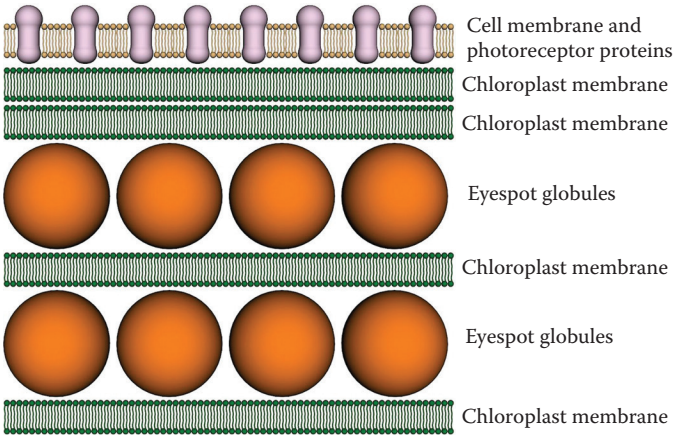

FIGURE 2.69 Schematic drawing of Type I photoreceptor system.

In Cyanobacteria, phototactic orientation has been described in *A. variabilis*, *Pseudoanabaena* sp., and *Phormidium*, although no defined structure for light sensing have been detected so far. The first identification of a complex photoreceptive system leading to the evidence of a photoreceptive protein was performed in *Leptolyngbya* sp. This deep red cyanobacterium lives in Roman hypogea at extremely low light intensity (10^{13} photons m^{-2} s^{-1}). It possesses an orange eyespot at the tip of the apical cell of the trichome. Electron microscopy revealed that this eyespot is characterized by osmiophilic globules of about 100 nm in diameter arranged in a peripheral cap extending 2–3 μm from the apex and with a possible layered pattern (Figure 2.2). Microspectrophotometric analysis of the tip of the apical cell of *Leptolyngbya* trichomes revealed a complex absorption spectrum with two main bands. The band centered at 456 nm is due to the absorption of the carotenoid present in the eyespot, whereas the band centered at 504 nm can be assigned to rhodopsin-like molecules packed in the plasma membrane of the tip of the apical cell.

In Ochrophyta, data exist indicating that the photoreceptor molecules are present inside the cell membrane of zygotes of the fucoid brown algae, *Fucus* sp. and *Silvetia compressa*. Experimental work confirmed this localization in *S. compressa* (Figure 2.70a), where a rhodopsin-like protein was identified in the zygote membrane (Figure 2.70b). Since no eyespot can be detected in these algal stages, the shading function is assigned to the whole-cell body.

In the Haptophyta, the eyespot is present only in some species of the order Pavlovales. It consists of a single layer of globules situated at the anterior end of one of the chloroplasts, beneath the posteriorly directed flagellum, at the level of its emersion from the cell. In these algae, the photoreceptor has not yet been localized, but we can presume it is positioned inside the membrane in close association with the eyespot.

In the Cryptophyta, the presence of an eyespot is limited to a small number of species belonging to the genus *Chroomonas*. The eyespot is situated at the center of the cell, within a conical lobe of the chloroplast. It consists of a single layer of about 35 closely packed globules, attached to the chloroplast envelope and the endoplasmic reticulum. Also in these algae, the photoreceptive proteins should be located inside the plasma membrane overlaying the eyespot.

In the Dinophyceae, the eyespot is chloroplastic in *Peridiniun* sp., consisting of a layer of globules under the chloroplast envelope, situated behind the longitudinal sulcus, and truly extraplastidic in *Woloszynskia coronata*, where it consists of an irregular cluster of globules located beneath the sulcus, and immediately adjacent to the subthecal microtubules. In the latter, neither a connection with the chloroplast nor membranes surrounding the eyespot are present. *Glenodinium foliaceum* and *Peridinium balticum* possess another type of eyespot. It is roughly a triangular body situated behind the sulcus and is an independent structure bounded by a three-membrane envelope. Basically, there are two layers of pigmented globules, separated by a vesicle of granular material. The eyespot can fold

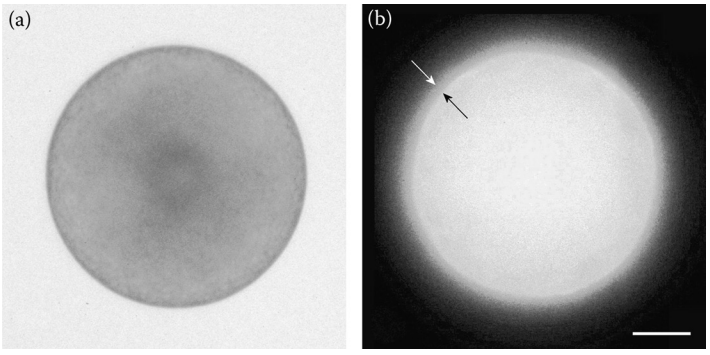

FIGURE 2.70 (a) A *Silvetia compressa* zygote in bright-field microscopy and (b) under fluorescence microscopy labeled with antirhodopsin antibody. The two arrows point to the cell membrane layer in which photoreceptive protein are located. Scale bar, 2 μm.

back upon itself, making more layers. In *Amphidinium lacustre*, the eyespot is an elongated structure located along the right edge of the sulcus. Its color is a shade of greenish-yellow rather than the reddish-orange color commonly found in eyespot; it consists of up to six flat rows of bric-like units, each row contained in a vesicle bounded by a unit membrane. No data exist on the photoreceptor location in these dinoflagellates, but the assumption is the same made for the Haptophyta and Cryptophyta, that is, photoreceptive proteins must be located inside the plasma membrane close to the eyespot.

A separate case is that of *Alexandrium hiranoi* and *Gymnodinium mikimotoi*. Both dinoflagellates show phototactic responses but lack a detectable eyespot, hence the shading function is performed by the cell body.

Type II

The photoreceptor consists of a multilayered membrane structure of photoreceptive protein. The eyespot is outwardly concave and is located close to this structure. This type of photoreceptive system is present in Ochrophyta and Euglenophyceae.

In Ochrophyta, complex photoreceptors, consisting of layered electron-dense material organized in a rounded, wedge-shaped or T-shaped organelle are present inside the smooth flagellum of the motile stages of Xanthophyceae, Eustigmatophyceae, and Phaeophyceae. In the Xanthophyceae, the eyespot consists of a single layer of about 40 globules located at one side of the anterior end of the chloroplast. It is contained by the outermost thylakoid of the chloroplast, bounded by the chloroplast envelope and its associated endoplasmic reticulum. The cell membrane above the eyespot forms a depression through which the posterior smooth flagellum passes. The eyespot depression accommodates the photoreceptor. In the Eustigmatophyceae, the prominent eyespot occupies nearly the whole anterior part of the cell, adjacent to the flagellar insertion. It consists of a somewhat irregular collection of globules situated in a slight bulge of the zoospore, but not enclosed by a membrane. The anterior hairy flagellum bears a photoreceptor swelling which fits alongside the eyespot. In the Phaeophyceae, the eyespot is situated in the posterior part of the cell, inside a strongly reduced chloroplast, and behind a depression of the cell surface through which the posterior flagellum runs. The eyespot appears concave in shape and prominent, containing a single layer of about 60 globules. The photoreceptor swelling is localized at level of the eyespot.

An example of Chrysophyceae photoreceptor can be found in *Ochromonas danica*: the eyespot located at the anterior end of the cell consists of a single layer of carotenoid globules contained by the outermost thylakoid of the chloroplast. The cell membrane above the eyespot forms a slight invagination; this depression accommodates the photoreceptor consisting of a 3D assemblage of proteins located inside the base of the smooth flagellum (Figure 2.71).

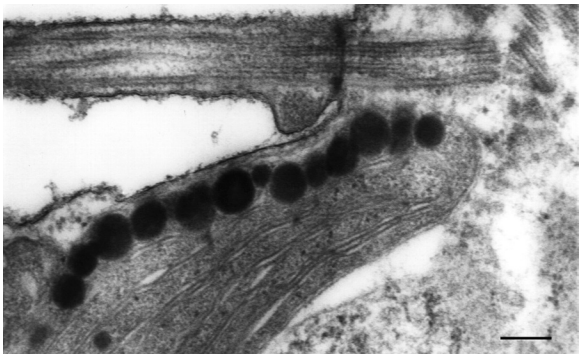

FIGURE 2.71 TEM image of the photoreceptive system of *O. danica* in longitudinal section, showing the photoreceptor inside the trailing flagellum. Scale bar, 0.30 μm.

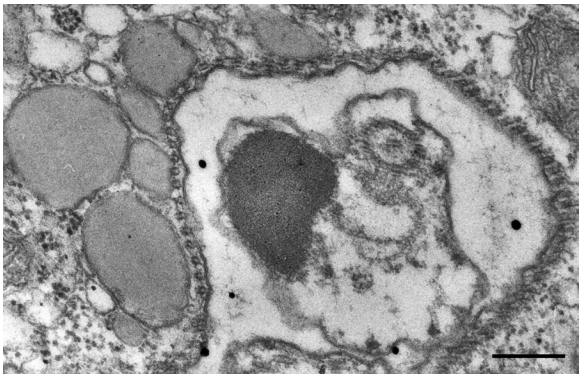

FIGURE 2.72 TEM image of the photoreceptive system of *Euglena gracilis* in transverse section, showing the photoreceptor and the PFR inside the trailing flagellum, and the eyespot in front of them inside the cell. Scale bar, 0.50 μm.

In the members of the Euglenophyceae, the eyespot consists of a loose collection of globules situated on the dorsal side of the reservoir, the anterior invagination characteristic of these organisms. The globules vary in size (from 240 to 1200 nm) and number, can lie in a single layer, or be bunched together. Individual globules may be membrane-bound, but there is never a membrane surrounding the whole complex, and no association with any chloroplast component is present. The position of the eyespot within the reservoir region can vary among the species, but it is always in front of the photoreceptor situated on the long or emergent flagellum (Figure 2.72). As example, the photoreceptor of *Euglena gracilis* will be described. This organelle is a 3D ordered assemblage of stacked membranes formed by 2D crystals of photoreceptive proteins. The organelle is located inside the membrane of the locomotory flagellum, connected to its axoneme by the paraxial rod. Figure 2.73a shows a portion of the photoreceptor at high magnification: the ordered disposition of the membrane layers is evident, made easily recognizable by osmium tetroxide staining of the phospholipid head groups. The periodicity is about 50 Å comparable to the distance between the hydrophilic head layers of a typical membrane bilayer. About 50 membrane layers are present in the photoreceptor. Electron micrograph of a negatively stained 2D lamellae, obtained by ionically induced uncoupling of the 3D compact structure of the photoreceptor, reveals stain excluding units protruding from the surface of the layer, arranged into a regular mesh (Figure 2.73b). After Fourier analysis, this mesh shows the ordered patches formed by the oligomers of the photoreceptive membrane spanning protein assembled in a hexagonal lattice as visible in the gray scale contour plot (Figure 2.73c), which is a magnification of the central zone of Figure 2.73b. The membrane layers composing the photoreceptor are characterized by in-plane hydrophobic interactions, while their closely stacked disposition is due to the interlayer interactions between charged protein extramembrane domains and the membrane in adjacent layers through charge density matching. About 10^6 photoreceptive proteins assembled in a hexagonal lattice span the membrane layers. Because of these characteristics, the photoreceptor of *Euglena* as a whole can be defined a "Type I" crystal, that is, an ordered assemblage of stacked membranes formed by 2D crystals of membrane proteins. The *Euglena* photoreceptor structure is an example of a perfect device to absorb light with a maximal cross-section (inset in Figure 2.73a). Figure 2.74 shows the isolated *Euglena* photoreceptor–PFR complex.

Type III

This organization is present only in some dinoflagellates of the order Warnowiales, such as *Nematopsides* sp. and *Erytropsidinium* sp. The photoreceptor system is very specialized and is

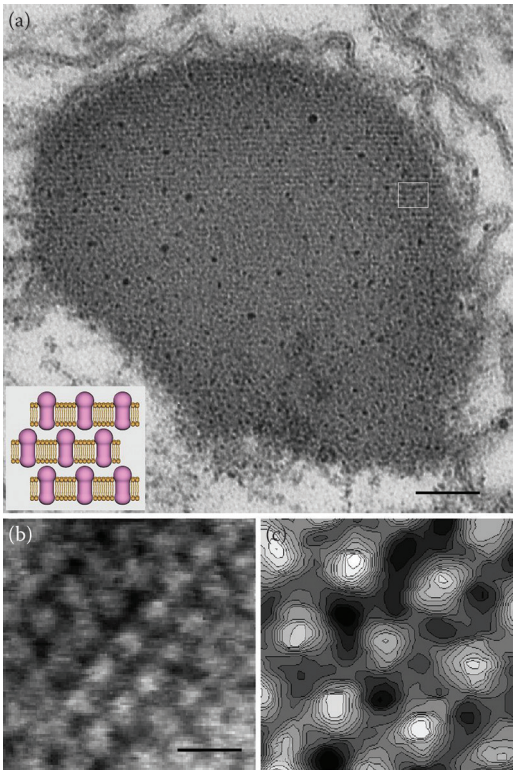

FIGURE 2.73 (a) TEM of a cross-section of the *Euglena gracilis* photoreceptor showing the fine structure of the organelle. Scale bar, 15 nm. Inset: Disposition of the photoreceptive proteins within the membrane layers of the *E. gracilis* photoreceptor. (b) Surface of a lamella showing the ordered pattern of protein oligomers. Scale bar, 10 nm. (c) Gray-scale contour plot of the central hexagon of (b).

termed ocellus. It is situated toward the left side of the ventral surface of the cell. It consists of a refractile structure termed hyalosome, thought to act as a lens, subtended by a domed pigmented part, divided into two sections, a retinoid and a pigmented cup. Between the lens and the retinoid is a chamber representing an invagination of the cell covering, which is lined by the cell membrane, and allows the contact of the ocellus with the external medium. The pigmented cup wrapping the

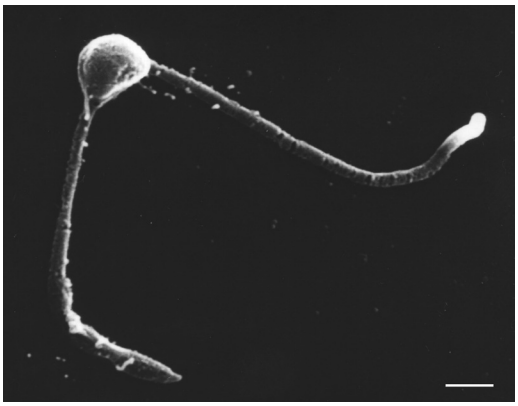

FIGURE 2.74 SEM image of the isolated photoreceptor–PFR complex of *Euglena gracilis.* Scale bar, 0.50 μm.

retinoid represents the eyespot and is made up of pigment containing droplets enclosed in a vesicular layer. Small droplets contain carotenoid pigments, whereas large droplets contain melanoid pigments. The retinoid is an extremely complex membranous construction made up of numerous regularly arranged layers giving an almost paracrystalline appearance.

No data are available on the structure and localization of the photoreceptive system in the divisions and classes of algae other than those listed above. It seems unlikely that Type II and III systems have not been identified so far in other algal groups, although it is more reasonable to assume that this lack of information is mainly due to the difficulty to reveal photoreceptor systems belonging to Type I. We can conclude that those algae should possess photoreceptor systems that can be taken back to Type I.

Photoreceptive Proteins

Over the past 10 years, genome sequencing and sequence comparison tools have revealed that genes encoding rhodopsin-like photoreceptive proteins are shared among distant taxa, in all three domains of life: Archaea, Eubacteria, and Eukarya. As far as algal world is concerned, reports from different research groups worldwide have provided examples of the broad distribution of Type I rhodopsin-based photoreceptors among the different algal division and allowed the assumption that these proteins are present in all the algae of the supergroups of Plantae (Glaucophyta, Rhodophyta, Chlorophyta) and Chromoalveolata (Haptophyta, Cryptophyta, Ochrophyta, and Dinophyceae), that is, those originating from a primary symbiotic event, and those originating from a secondary or tertiary symbiotic event. In fact, genes encoding functional rhodopsins probably related to photoreception or ionic transport have been detected in Cyanophyceae (prokaryotic algae), and Cryptophyceae, Glaucophyceae, Chlorophyceae, Dasycladophyceae, Mesostygmatophyceae, Mamiellophyceae, prasinophytes, Trebouxiophyceae, Coccolithophyceae, and Dinophyceae, all eukaryotic algae. The presence of an integral membrane protein in the membrane of the muroplast of *Cyanophora paradoxa*, a glaucophyte, the most primitive of all plastids, could indicate that the common primordial rhodopsin existed in preeukaryotic cells before the appearance of the first photosynthetic eukaryotic cell about 1.55×10^9 years ago (Figure 2.75). Moreover, spectroscopical and biochemical evidence of rhodopsin-based photoreceptor is available for algae belonging also to Euglenophyceae, Chrysophyceae, and Phaeophyceae.

All rhodopsins consist of a proteic part, the opsin, organized in seven transmembrane α-helices, and a light absorbing group, the retinal (i.e., the chromophore). The retinal is located inside a pocket of the opsin, approximately at its center. These proteins can be considered special for many reasons. First, retinal–opsin complex has an intense absorption band whose maximum can be shifted to the visible region of the spectrum, over the entire range from 380 to 640 nm. Second, light isomerizes the retinal inside the protein very efficiently and rapidly. This one-molecule isomerization, that is, the event initiating the vision reaction cascade, can be triggered almost exclusively by light. In the dark, it occurs about only once in a thousand years. Third, remarkable structural changes (movements of single α-helix) are produced by isomerization of retinal. Light is converted into atomic motion of sufficient magnitude to trigger a signal reliably and reproducibly. Fourth, the photocycle (the photoreceptive protein upon light excitation undergoes a series of conformational changes that can be driven back to the original conformational state) is very fast, and hence the intracellular photoreceptive machinery is immediately reset for a new response. Fifth, retinal is derived from β-carotene, a precursor with a widespread biological distribution.

Fundamental Behavioral and Physiological Features

The structural features described above should be accompanied by necessary behavioral and physiological characteristics (sampling strategies, trajectory control, and signal transmission).

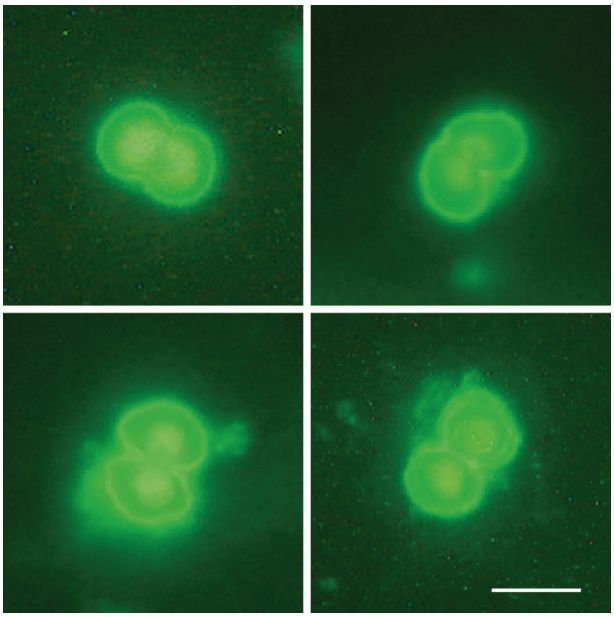

FIGURE 2.75 Immunofluorescence localization of the rhodopsin-like protein in *Cyanophora paradoxa* muroplasts. Scale bar, 5 μm.

Sampling Strategies

To determine the orientation of a stimulus field, an organism has to measure the stimulus intensity at different positions, that is, it should detect either spatial or temporal patterns of light. Femtoplankton (0.02–0.2 μm) is too small compared to the wavelength of light to create differential light intensity; hence, it cannot determine the direction of a light source. Still, femtoplankton microorganisms can use light, but can only measure its intensity and move in a light-intensity gradient. In contrast, phytoplankton dimensions are large enough to determine light direction and allow the scanning of the environment by means of their directionally sensitive receptor.

Two fundamental and alternative strategies exist for obtaining information on light direction: parallel sampling and sequential sampling. In parallel sampling, the stimulus is detected by multiple separated receptors positioned on different parts of the organism surface. In this case, the organism measures directly the spatial gradient by simultaneous comparison of light intensities at two different parts of its body (one instant mechanism). This strategy is present in the zygote of the brown alga *Silvetia compressa*; the photoreceptive system of the zygote is presumably the same as the egg before fertilization. The zygote absorbs or scatters more than 95% of the effective blue wavelengths within one cell diameter, thus creating a steep light gradient across the cells. Photoreceptors in or near the plasma membrane are activated differentially, and the cellular response to this gradient of photoreceptor activation is to organize an axis and germinate from the darkest point. Photopolarization is an early event, which has been observed 4 h after fertilization. The zygote produces a rhizoidal bulge at about 10 h after fertilization. Initially, any point on the cell surface is capable of becoming the germination site. The bulge elongates by tip growth (i.e., addition of new cell membrane and wall material by localized vesicle secretion), and about 18 h after fertilization the first cell division occurs. The plane of division is perpendicular to the growth axis, resulting in the formation of two highly asymmetrical cells with different developmental fates. The cell bearing the bulge will form the rhizoid, which will show negative phototaxis, while the other cell will form the thallus. Figure 2.76 shows the first steps of development of a *Silvetia* zygote from fertilization to rhizoid formation: changing of light direction causes a change in the rhizoid growth axis.

FIGURE 2.76 Parallel sampling used by *Silvetia* sp. zygote to orientate thallus-rhizoid growth direction. Light 2 is turned on after turning off Light 1.

In sequential sampling, the stimulus is detected by a single receptor as the cell changes its position in relation to the light source. In this situation, the organism measures directly a temporal gradient and then infers the spatial gradient from the information on the movements of the receptor (two-instant mechanism). This strategy is present in all the algae with a single photoreceptor. These algae have only a limited vision of the 3D world in which they navigate and cannot detect light directions by measuring light intensity at two different positions in the cell body. An example is *Leptolyngbya* sp., whose photoreceptor system has been described above. This cyanobacterium characterized by quite inflexible trichomes uses light to grow toward optimal light intensities, with a sort of oriented movement with respect to the stimulus direction. It changes the direction of the trichome by turning towards the light source at the level of the apical cell (Figure 2.77a and b), where both the photoreceptor and the eyespot are located (Figure 2.2). When the photoreceptor system is impaired, the movement becomes unguided and the trichomes appear disordered (Figure 2.77c). The simultaneous comparison of signals requires widely spaced receptors to detect intensity gradient, which makes large body size advantageous. On the other hand, sequential sampling requires a coherent pattern of movement. Many algae perform sequential sampling by swimming on helical paths along which their photoreceptor acts as a light antenna continuously searching space for bright spots. Sequential sampling also requires some form of memory to allow the comparison with previously recorded intensities.

Trajectory Control

Another fundamental distinction is based on whether an organism is able to make turns in its motion path, which will direct it toward its destination. Depending on the characteristic of the stimulus and

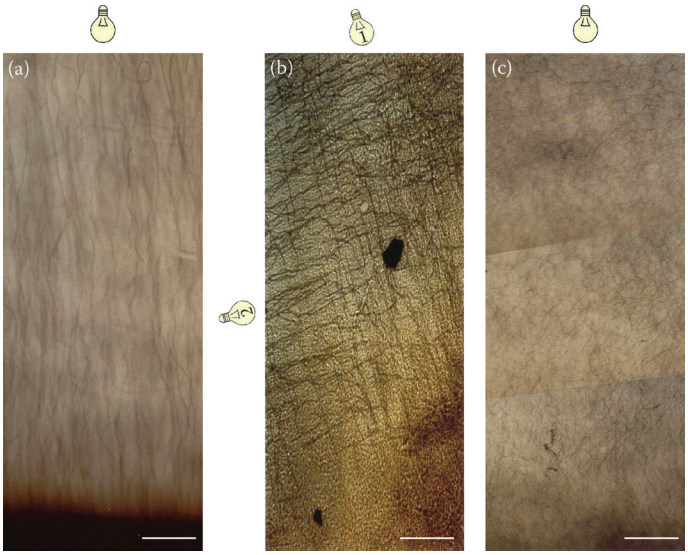

FIGURE 2.77 Sequential sampling by *Leptolyngbya*: refer to text for details. Light 2 is turned on after turning off Light 1. Scale bar, 60 mm.

the abilities of the microorganism, guiding may be either direct in the sense of taking a straight-line path to the destination or indirect, as in the case of a biased random walk, to reach the vicinity of the destination. Trajectory control characteristics, and thus behavioral peculiarities, are connected with both the shape of the cell and the functioning of the propelling structure of the algae, that is, the flagellum. If the cell is asymmetric, that is, if it possesses recognizable dorsal and ventral sides, then it advances spinning along its axis. It can correct its trajectory by either sudden steering obtained by changing the insertion angle of flagella, as, for example, *Ochromonas danica*, or stiffening of the flagellum via accessory structure of the axoneme, as *Euglena gracilis*. This behavior can be attributed to all heterokont and uniflagellate algae. In the case of a symmetric cell, it can accomplish a gradual smooth correction of its trajectory going forward without spinning (or rotating with a very long period) and displacing the barycenter of the motor couple, as *Dunaliella salina*. This behavior can be attributed to all isokont cells.

Signal Transmission

Signal transmission in algae is still a poorly investigated topic. Algae are aneural organisms, lacking any system for the transmission of the stimuli received from the outside. The information carried by light has to be translated into an organism-specific swimming control mechanism that allows orientation to the light with high fidelity. Hence, the light signal will be first transduced in an electric signal by means of electron or ion flux, and this electric signal will be transmitted to the algae motor apparatus, that is, the flagellum/flagella. It has been demonstrated that in *Chlamydomonas reinhardtii*, light absorbed by sensory rhodopsins initiates local photocurrents (a fast photocurrent and a slow photocurrent) in the eyespot region, presumably in the plasma membrane right above the eyespot, where the photosensitive proteins are located. At low intensities, sensory rhodopsins trigger a highly efficient biochemical amplification reaction which involves activation of yet unknown downstream elements and control of some diffusible messenger, a process analogous to vision in animals. At high light intensities, the second function of sensory rhodopsins, namely direct channel activity, begins to contribute to depolarization of the plasma membrane, which eventually allows motility responses. Biphasic photocurrents have been shown to exist also in other algae, such as *Volvox carteri* (Chlorophyta) and *Cryptomonas* sp. (Cryptophyta).

An Example: Photoreceptor and Photoreception in *Euglena*

As we have described in the previous section, in order for phototaxis (photoreception) to occur, proper perceiving devices (structural features) satisfying essential requirements are necessary together with specific behavioral and physiological features. In this section, we will use *Euglena* as an example to analyze how these structural, behavioral, and physiological aspects combine to achieve a concerted response to light stimuli. *Euglena* dwells in natural shallow ponds and uses sunlight as source of energy and information. Its chloroplasts are the energy-supplying devices, whereas the simple but sophisticated photoreceptive system already described is used as a light detector.

The photoreceptor ciliary line of evolution, which had its climax in the elaborate and remarkably complex vertebrate eye, originated from the photoreceptor of *Euglena*. According to the definition of the Swiss genetist Walter Gehring, the prototypical eye, which was presumably the common ancestor of all eyes, is a combination of a photoreceptor cell and a pigment cell, which achieves some directional selectivity by using screening pigment to block light coming from certain directions. The photoreceptor cell is located close to the effector and transmits the information conveyed by the light directly to it (without an intervening information-processing organelle). In the case of *Euglena*, the "eye" is formed within a single cell by the assembly of pigmented and photoreceptive molecules within that cell in two distinct organelles, namely the eyespot and the photoreceptor. In the following, we will describe and analyze the different components of this primitive eye to demonstrate how its simple design fits Gehring's definition.

As already said, the eyespot consists of a loose collection of globules situated on the dorsal side of the reservoir, always in front of the photoreceptor. The pigments present in the eyespot globules are carotenoids such as β-carotene, diatoxanthin, and diadinoxanthin. The absorption spectrum of the eyespot shows a unique and large band centered at 460 nm (Figure 2.78, orange line).

Euglena photoreceptor is located near the base of the locomotory flagellum. Its regular structure has already been described as "Type I" crystal, that is, an ordered assemblage of stacked membranes formed by 2D crystals of membrane proteins (Figure 2.73a). The spectral properties of this photoreceptor are quite more complex than those of the eyespot and support the presence of rhodopsin-like proteins. These proteins are characterized by optical bistability, that is, they possess two isomeric forms A and B, which interconvert along a photocycling path photochemically but not thermically. The absorption spectrum of A has a band centered at 498 nm (from now addressed as A_{498}) (Figure 2.78, green line); this is the dominant form in the photoreceptor under physiological conditions. The absorption spectrum of B has a band centered at 462 nm (from now addressed as B_{462}) (Figure 2.78, blue line). The absorption spectrum of the eyespot perfectly matches the absorption spectrum of the B_{462} form (Figure 2.78, orange line). A_{498} is the nonfluorescent form (hence, under physiological conditions, photoreceptor fluorescence is not observed), while B_{462} is the fluorescent form, energetically lower, which can be considered the signaling state of the protein. The presence of optically bistable proteins characterized by a fluorescent form is a common feature of euglenoid photoreceptors. Figure 2.79 shows the photocycle recorded on a single cell of *Euglena*, *Phacus*, and *Trachelomonas*. Optical bistability has recently been detected also in *Chlamydomonas* rhodopsin, indicating that this could be a property of the photoreceptive protein present in the algae.

The functioning of *Euglena* photoreceptor in nature can be described as in the following: the cells normally swim by rotating along a helicoidally path; during this motion, the photoreceptor proteins are in a photodynamic equilibrium in which A_{498} is the dominant isomer. The equilibrium is interrupted when the eyespot comes between the incoming light and the photoreceptor, thus screening the organelle (Figure 2.80). Owing to the superimposition of the absorption spectra of the eyespot and the isomer form B_{462}, only UV and green light illuminate the photoreceptor during the screening period, and the only possible transition is that of A_{498} to B_{462}. In detail, the photoisomerizable isomeric form A_{498} undergoes an intramolecular photoswitch, that is, A_{498} becomes B_{462} through an excited state, and contemporaneously an intermolecular and unidirectional Forster-type energy transfer (FRET) occurs, that is, the newly formed fluorescent B_{462} acts as an energy donor for the nearby protein in the A_{498} form, which acts as an energy acceptor. The intramolecular

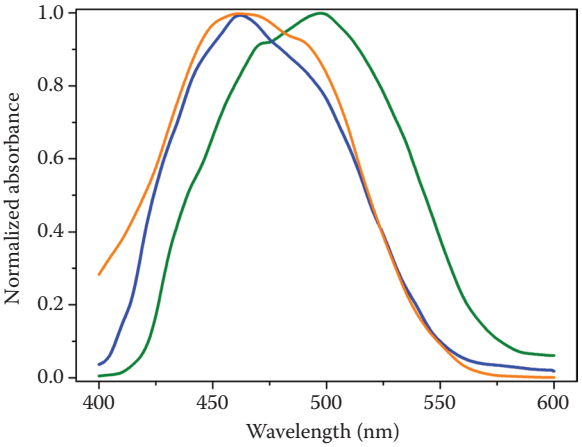

FIGURE 2.78 Absorption spectrum of eyespot of *Euglena gracilis* (orange line); absorption spectra of the A isomer (green line) and of B isomer (blue line).

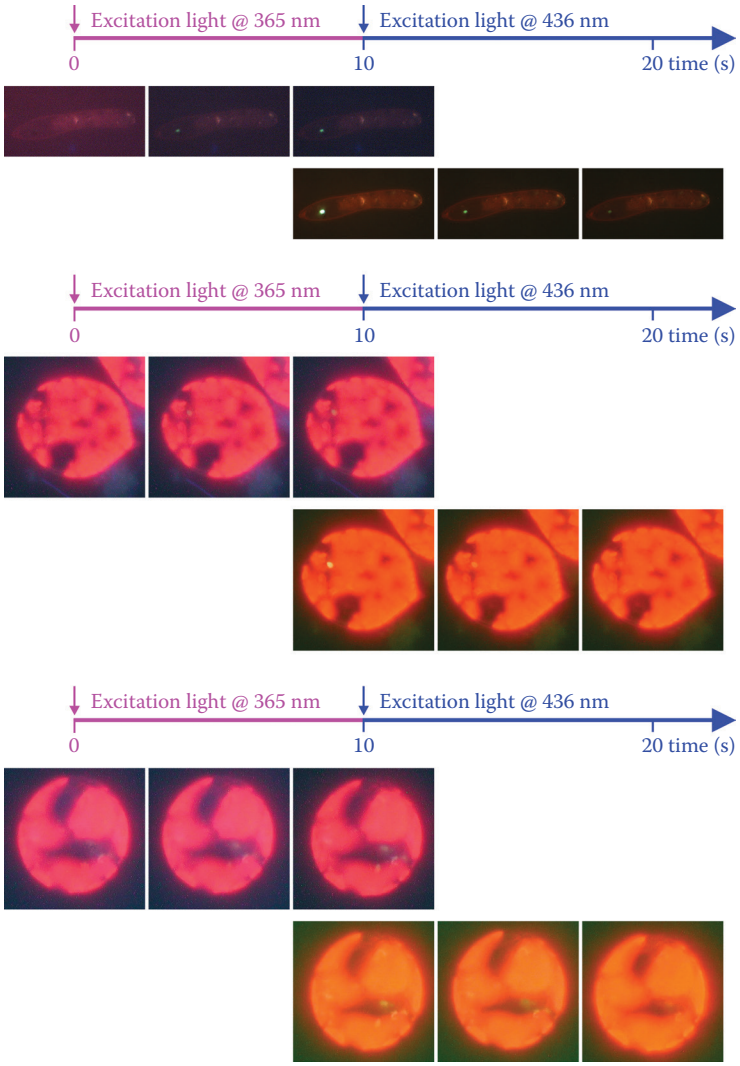

FIGURE 2.79 Photocycles recorded on *Euglena gracilis*, *Phacus* sp., and *Trachelomonas* sp.

switch and the FRET follow each other with a domino progression along the orderly organized and closely packed proteins in the layer(s) of the crystal structure of the photoreceptor (Figure 2.73), modulating the isomeric composition of the photoreceptive protein pool. As a consequence, B_{462}, the signaling state of the protein energetically lower than A_{498}, becomes the dominant isomer. It is worthwhile to highlight that the photoreceptive protein switches from a photoisomerizable device to a fluorescent dye.

The energy needed for the transition of the isomeric form A_{498} to B_{462} and the energy transferred from one protein to the nearby protein derives not only from the photons absorbed during the photoreceptor screening by the eyespot, but also from the photons absorbed by the photoreceptor in the no-screening period. These photons restore the photoreceptor isomeric composition with A_{498} as dominant isomer. Once the screening by the eyespot is over, the transition of B_{462} to A_{498} can again occur due to the full spectrum light (natural light) impinging on the photoreceptor, and the isomeric composition with A_{498} as dominant isomer is again restored.

How the signal generated by the photoreceptor drives the *Euglena* movement?

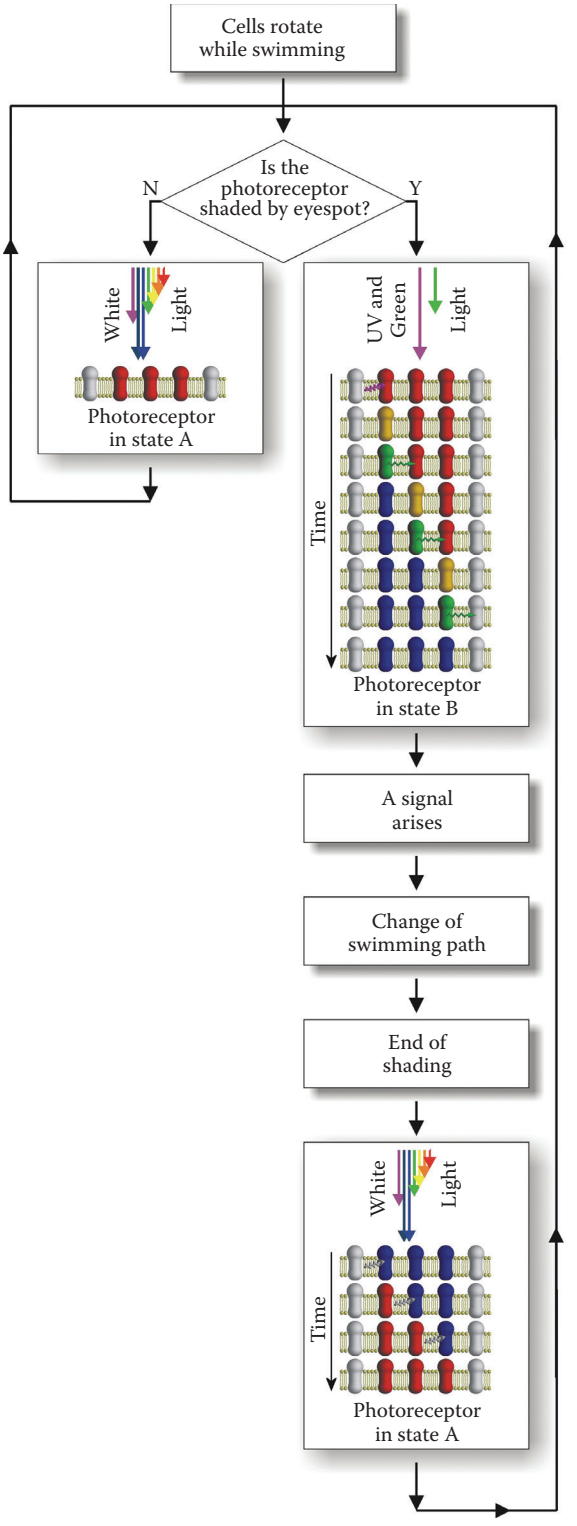

FIGURE 2.80 *Euglena gracilis* phototaxis flow chart.

As described above, changes in the motion trajectory by bending of the locomotory flagellum are due to the screening of the photoreceptor by the eyespot that changes the electrostatic field. The locomotory flagellum carries the paraxial rod (PAR; Figure 2.36a and b), a hollow rod-like structure with a diameter of 90 nm along the entire length. The PAR is the true effector. When the photoreceptor is screened by the eyespot, the signaling state of the protein becomes the dominant isomer and a change in the electrostatic field occurs. Since the photoreceptor and the paraxial rod are a structural unit (Figure 2.74), we can hypothesize that the photoelectric signal could be propagated through the paraxial rod filaments via charge transfer between rod proteins, modifying the pitch of its helix, which in turn modifies the distribution of the mass of the rod along the axoneme. This leads to a change in the motion wave running along the flagellum and eventually to a change in the swimming direction.

Chloroplasts

The photosynthetic compartment contains the pigments for absorbing light and channeling the energy of the excited pigment molecules into a series of photochemical and enzymatic reactions. These pigments are organized in proteic complexes embedded in the membrane of sac-like flat compressed vesicles known as the thylakoids. These vesicles are about 24-nm thick and enclose a space, termed lumen, 10-nm wide.

In prokaryotes, the thylakoids are free within the cytoplasm, whereas in eukaryotes they are enclosed within bounding membranes to form the chloroplast. The colorless matrix of the chloroplast is known as the stroma. Inside the chloroplast, thylakoids are organized into two different compartments, granal thylakoids, stacked into hollow disks termed grana, and stromal thylakoids forming multiple connections between the grana. All thylakoids surfaces run parallel to the plane of the maximum chloroplast cross-section. Chloroplasts contain nucleic acids and ribosomes. DNA is naked, that is, not associated with proteins, and occurs in two configurations: scattered, but not connected small nucleoids or as a peripheral ring. Chloroplasts are semiautonomous organelles that replicate their own DNA, and this replication is not linked to the division of the organelle. Synthesis of RNA and proteins is possible inside the chloroplast, though they are not strictly autonomous from the nuclear genome. The plastid genes are transcribed and translated within the plastids. The machinery of protein synthesis is, in any case, partially composed of imported nuclear gene products. In this respect, as in others, the chloroplast is no longer independent. Nevertheless, about half of the plastid genome consists of genes that contribute to the machine of gene expression, for example, genes for rRNA, tRNAs, RNA polymerase subunits, and ribosomal proteins. Plastids code for, and synthesize some proteins that are components for photosystems, and particular subunits of photosynthetic enzymes. The missing subunits of these complexes are coded in the nucleus and must be imported from the cytoplasm.

Chloroplast development and division (self-replication) may be coordinated with that of the cell or may proceed independently. They divide in mother cells and are inherited by daughter cells during vegetative division and usually only from the maternal side in sexual reproduction. The shape and the number of chloroplasts are extremely variable from the single cup-shaped chloroplast of *Dunaliella salina*, the ribbon-like chloroplast of *Spirogyra*, or stellate one of *Zygnema* to the numerous (about 10^8) ellipsoidal chloroplasts of *Acetabularia* giant cells.

The fact that algae of different divisions have different colors, due to the presence in the photosynthetic membrane system of a variety of pigments, might lead to the supposition that the photosynthetic membrane structures are variable. This is true since the features of photosynthetic membrane system represent a diagnostic important element at the class level. In this chapter, we will consider the structure, composition, and location of the photosynthetic membrane system in each algal division.

Cyanobacteria

The photosynthetic apparatus of these algae is localized on intracytoplasmic membranes termed thylakoids. The thylakoid membranes show considerable variations in structure and arrangements

depending on the species. The amount of thylakoid membranes per cell is also a variable due to their growth conditions and taxonomic specificity.

In most species, the thylakoids are arranged peripherally in 3–6 layers running parallel to the cell membrane, forming an anastomosing network of concentric shells. This peripheral region has been called chromatoplast, which is separated from the inner nucleoplasmic region called centroplasm. This type of thylakoid arrangement is characteristic of many unicellular and filamentous cyanobacteria, such as *Synechococeus planctibus*, and *Anabaena* sp. In some other organisms such as *Oscillatoria* and *Arthrospira*, the thylakoids are oriented perpendicular to the longitudinal cell wall. Radial arrangement is present in *Phormidium retzi*. Thylakoids are not always restricted to the cell periphery but can be found scattered throughout the cell as in *Gloeotrichia* sp. However, the arrangement of thylakoids can change from cell to cell and cell type (vegetative cells, heterocyst, akinete) within the same culture from parallel to a convoluted appearance. Thylakoids can fuse with each other and form an anastomosing network; unlike the chloroplasts of eukaryotic algae, the thylakoids of cyanobacteria form stacking regions only to a very limited extent. During cell division, the thylakoids have to be separated and divided into the daughter cells; generally, this division is an active process. Cell division starts by a centripetal growth of cytoplasmic membrane and peptidoglycan layer, to form the septum; the thylakoid cylinder is narrowed at the level of the cross-wall by invagination before the septum is formed. Proteins, lipids, carotenoids, and chlorophyll *a* are major components of thylakoids. On the outer surface of the thylakoids, regular rows of electron-dense granular structures are closely attached. These granules termed phycobilisomes, contain the light-harvesting phycobiliproteins, that is, allophycocyanin, phycocyanin, and phycoerythrin (Figure 2.81). The phycobilisome structure consists of a three-cylinder core of four stacked molecules of allophycocyanin, closest to the thylakoid membrane, on which rod-shaped assemblies of coaxially stacked hexameric molecules of only phycocyanin or both phycocyanin and phycoerythrin converge

FIGURE 2.81 TEM image of a cyanobacterium in longitudinal section, showing the thylakoid membranes with phycobilisomes. Scale bar, 0.20 μm. (Courtesy of Prof. Luisa Tomaselli.)

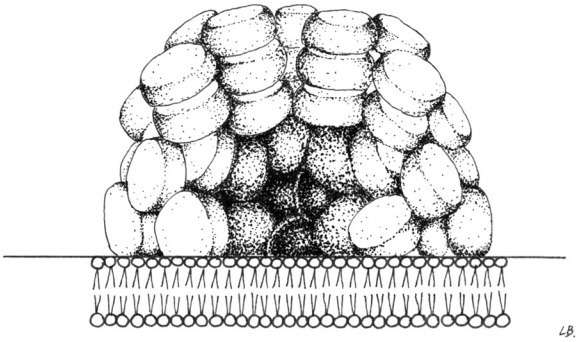

FIGURE 2.82 Schematic drawing of a phycobilisome.

(Figure 2.82). Phycobiliproteins are accessory pigment for the operation of photosystem II also in Glaucophyta, Cryptophyta, and Rhodophyta.

The thylakoid membranes of *Prochloron* are organized into stacked and unstacked regions reminiscent of the grana and stromal lamellae of higher plant chloroplasts. They differ from other cyanobacteria in that they contain chlorophyll *a/b* light-harvesting systems rather than phycobiliproteins organized in the phycobilisomes.

Glaucophyta

As already described in Chapter 1, these algae possess inclusion termed cyanelles that are probably symbiotic cyanobacteria functioning as chloroplasts (Figure 2.83). Each cyanelle, surrounded by a reduced peptoglycan cell wall (except in *Glaucosphaera* sp.), is enclosed in a vesicle of the host cytoplasm. Cyanelles do not fix molecular nitrogen in contrast with cyanobacteria; they contain polyphospate granules and a conspicuous central carboxisome similar to the pyrenoids of other algae. The thylakoids are not stacked but they are single and equidistant with a concentric arrangement. Cyanelle pigments are chlorophyll *a* and β-carotene, which represents the main carotenoid. Interthylakoidal phycobilisomes contain allophycocyanin and phycocianin. Phycoerythrin is absent from Glaucophyta but phycoerythrocyanin can be found in some species.

FIGURE 2.83 *Cyanophora paradoxa* isolated cyanelles. Scale bar, 5 μm.

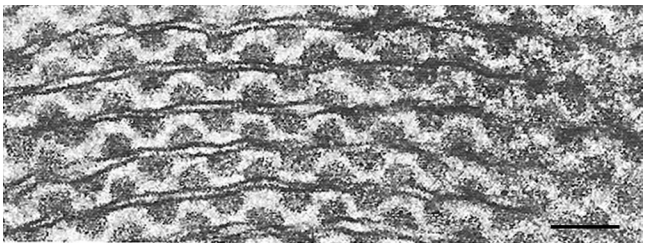

FIGURE 2.84 TEM image of rhodophyte thylakoid showing regularly arranged phycobilisomes. Scale bar, 0.05 μm.

Rhodophyta

Ultrastructurally, red algal chloroplasts are composed of a double-membraned envelope inside of which are one or more parallel, thylakoidal photosynthetic lamellae. These chloroplasts are not associated with the endoplasmic reticulum, a feature shared with Glaucophyta and Chlorophyta. Encircling thylakoids are present in all Florideophyceae, and in some taxa of Bangiophyceae while the thylakoids in the other red algae are equidistant and single, that is, not stacked, unlike any other group of eukaryotic algae (except Glaucophyta), and typically oriented parallel to each other. All thylakoids have phycobilisomes attached to their stromal surface, which contain the accessory phycobiliprotein pigments, that is, allophycocianin, phycocyanin, and five forms of phycoerythrin (Figure 2.84). Chlorophyll *a* is the only chlorophyll present in the thylakoid membrane, together with carotenoids such as β-carotene and lutein. Plastid number, shape, and position (many, discoid, and parietal) are rather uniform throughout the Florideophyceae, and pyrenoids may or may not be present. A single stellate plastid with a central pyrenoid is commonly associated with porphyridiophyceans, such as *Porphyridium* (Figure 2.85). DNA is organized into numerous nucleoids scattered throughout the chloroplast.

Chlorophyta—Charophyta

These algae are not uniform in the ultrastructure of chloroplast, still some generalization can be made. The chloroplasts of these algae are enclosed only by the double membrane of the chloroplast envelope; there is no additional envelope of endoplasmic reticulum or nuclear membrane. In this respect, they resemble Rhodophyta and Glaucophyta in the cell compartmentalization. The chloroplasts vary greatly in shape and size. In unicellular forms, the chloroplast is often cup-shaped with a thick base (*Dunaliella*); in filamentous forms, it is often ring- or net-shaped and lies against the cell

FIGURE 2.85 *Porphyridium cruentum* cells with a single stellate plastid. Scale bar, 1 μm.

wall (*Oedogonium*). More massive and elaborate plastids, lying along the longitudinal axis of the cell, are particularly characteristic of members of the Zygnematophyceae. Thylakoids are arranged in stacks of 2–6 or more; their multilayered arrangement may take on the appearance of grana with membrane interconnections, as in higher plants. Girdle lamellae are absent. One to several pyrenoids occur in most of the algae of this division embedded within the chloroplast and are often penetrated by thylakoids. The DNA organized in small nucleoids is distributed throughout the chloroplast matrix. Both chlorophyll *a* and *b* are present; accessory pigments include different xanthophylls such as lutein, zeaxantin, and violaxantin; β-carotene is always present together with other carotenoids.

Haptophyta

Cells of Haptophyceae species normally possess one or two chloroplasts containing thylakoids stacked in three to form lamellae. There is no girdle lamella. Spindle-shaped pyrenoids are commonly immersed within the chloroplast, penetrated by one or a few pairs of thylakoids, but in some genera they bulge from the inner face of the organelle. Both the chloroplast and the pyrenoid are surrounded by endoplasmic reticulum confluent with the nuclear envelope, the nucleus itself lying close to the chloroplast. Chlorophylls *a*, c_1, c_2 and in some genera also c_3 are found in the thylakoidal membranes together with carotenes, such as β-carotene, and xanthophylls, the most commonly occurring being fucoxanthin. DNA is organized into numerous nucleoids scattered throughout the chloroplast.

Cryptophyta

The chloroplasts of these algae, which are one or two per cell, are unusual in both their pigment composition and ultrastructure. Four membranes enclose these organelles: the inner pair forms the plastid envelope and the outer pair forms the plastid endoplasmic reticulum. This four-membrane configuration is common in chlorophyll *c*-containing algae. An expanded space is present between the plastid endoplasmic reticulum and the plastid envelope on its inward face. This compartment contains 80S ribosomes, starch grains, and the nucleomorph. Thylakoids inside the chloroplast are typically in pairs, although single thylakoids as well as large stacks have also been observed, with no girdle lamella. A pyrenoid is present, projecting from the inner side of the chloroplast. Cryptomonads are characterized by the presence of chlorophylls *a* and c_2, phycoerythrin, phycocyanin, allophycocyanin, carotenes, and several xanthophylls.

The phycobiliproteins differ from those in the red algae and cyanobacteria, since they are of lower molecular weight and do not aggregate to form discrete phycobilisomes, being localized within the lumen of the thylakoids. DNA is organized into numerous nucleoids scattered throughout the chloroplast.

Ochrophyta

Some ultrastructural features of the chloroplast compartments of these algae are common to all the 18 classes of the division, with few exceptions. Four membranes surround the chloroplasts, the outer two being the chloroplast endoplasmic reticulum, and the inner two being the chloroplast envelope. When the chloroplasts are located close to the nucleus, the chloroplast endoplasmic reticulum is continuous with the nuclear envelope. In the Xanthophyceae, this connection is not the rule. Thylakoids are grouped into lamellae of three, which are two in some Raphidophyceae, with varying degrees of coherence depending on the species. Thylakoids from adjacent lamellae frequently interconnect across the stroma. In all the classes, with the exception of Eustigmatophyceae and *Chattonella* (Raphidophyceae), one lamella runs around the periphery of the chloroplast beneath the chloroplast envelope, enclosing all the other lamellae. The lamella is called girdle lamella.

One or more plate-like (Chrysophyceae, Figure 2.86a and b; Eustigmatophyceae, Figure 2.87a and b), discoid (Xanthophyceae, Raphidophyceae, Dictyochophyceae), or ribbon-like (Phaeophyceae) plastids are typically present, often lobed, parietal, or located in close connection with the nucleus. In the Bacillariophyceae, chloroplasts are the most conspicuous feature, and their number and shape are consistent features of taxonomic importance. They may be rounded or lobed discs or large

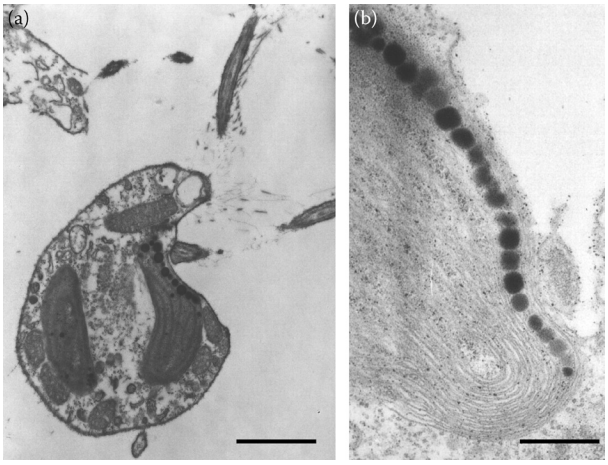

FIGURE 2.86 (a) TEM image of *Ochromonas danica* in longitudinal section, showing the chloroplast; scale bar, 3 μm. (b) TEM image of a chloroplast at higher magnification showing the thylakoid membrane and the eyespot globules; scale bar, 1 μm.

plate-like with or without lobed margins and may range from one to two, four, or more. A typical centric diatom has many disc-shaped plastids, arranged close to the periphery surrounding a large central vacuole or scattered throughout the cell. The raphid diatoms tend to have large chloroplasts (1–4) lying along the girdle with central nucleus flanked by two large vacuoles.

The chloroplast DNA is ring-shaped and located in the region between the girdle lamella and the others in all the classes, with the exception of the Eustigmatophyceae, where it is organized into many dot-like nucleoids, which may be united in a sort of reticulum. The main photosynthetic pigment is chlorophyll *a*, which is the only chlorophyll present in the Eustigmatophyceae, Aurearenophyceae and Ochromonas (Chrysophyceae). In addition, chlorophylls of the *c* group occur, both c_1 and c_2 (Chrysophyceae, Rhaphidophyceae, Phaeophyceae, Dictyocophyceae and only in extremely low concentrations in Xanthophyceae); only c_1 (synurophyceae), or only c_2 (Bacillariophyceae). The most important accessory pigment is fucoxanthin in Chrysophyceae, Bacillariophyceae, Dictyocophyceae, and Phaeophyceae; violaxanthin in Eustigmatophyceae, and vaucheriaxanthin in Xanthophyceae. Other accessory pigments are β-carotene and xanthophylls such as diadinoxanthin, heteroxanthin, vaucheriaxanthin, antheraxanthin, and lutein. In the Raphidophyceae, marine and

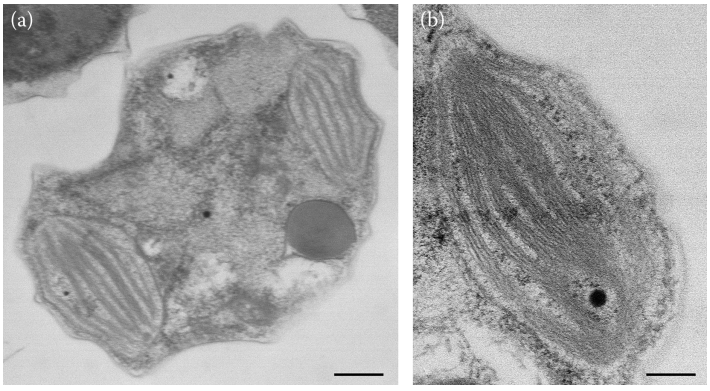

FIGURE 2.87 TEM image of *Nannochloropsis* sp.: (a) chloroplast in transverse section, scale bar, 0.50 μm and (b) chloroplast at higher magnification, scale bar, 0.10 μm.

freshwater species differ in their accessory pigments, marine species possessing mainly β-carotene, fucoxanthin, and violaxanthin, and freshwater species having β-carotene, diadinoxanthin, heteroxanthin, and vaucheriaxanthin.

Pyrenoids are present in all the classes, except in the zoospores of the Eustigmatophyceae, and in the freshwater species of Raphidophyceae. They are of a semi-immersed type, attached to the inner face of the chloroplast, pear-shaped in the Phaeophyceae, or stalked in the Eustigmatophyceae. They can be one or many (Bacillariophyceae and Phaeophyceae). No storage material or capping vesicles have been found to be associated with pyrenoids, but lipid or oil droplets normally distributed randomly in the chloroplast matrix are often concentrated at the periphery of the pyrenoid.

Cercozoa–Chlorarachniophyceae

Five to seven bilobed chloroplasts are present inside these algae in a peripheral position. Each chloroplast is bounded by a system of membranes that may appear either as four separate membranes, as a pair of membranes with a sort of flattened vesicles between them, or as three membranes. Four separate membranes are always found near the proximal end of the pyrenoid and over the pyrenoid itself. The outer pair of membranes, when four are present, is referred to as a type of chloroplast endoplasmic reticulum; however, the inner pair is interpreted as the chloroplast envelope. The thylakoids are often loosely stacked in three, with no girdle lamella. Each chloroplast bears a central, pear-shaped pyrenoid inward projecting. Around the pyrenoid, often tightly associated with it, there are vesicles containing β-1,3-glucan, which is the principal storage carbohydrate. A nucleomorph, which contains DNA and a nucleoulus-like body, is present between the second and third envelopes of each chloroplast, in a pocket located in the pyrenoid surface. Chloroplasts contain chlorophylls *a* and *b*, and xanthophylls.

Mizozoa-Dinophyceae

Chloroplasts may be present or absent in these algae, depending on the nutritional regimen. When present, they are characterized by triple-membrane envelopes not connected with the endoplasmic reticulum; thylakoids are usually in a group of three, unappressed, and girdle lamellae are generally absent. Pyrenoids show various types, stalked, or embedded within the chloroplast. DNA is organized into numerous nodules scattered throughout the chloroplast. About 50% of the dinoflagellates with plastids acquired them from a variety of photosynthetic eukaryotes by endosymbiosis (cf. Chapter 1). Hence, the pigments other than chlorophylls *a* and c_2 (e.g., carotenoids, xanthophylls) change among the different groups.

The most common chloroplast type is the peridinin-type plastid; an example is *Amphidinium carterae*, probably derived from the red lineage by secondary endosymbiosis, that is, through the uptake of primary plastid-containing endosymbiont. Other groups of dinoflagellates have plastids derived from a tertiary endosymbiotic event, that is, the uptake of a secondary plastid containing endosymbiont. Tertiary plastids are present in the toxic genus *Dinophysis*, characterized by two-membrane, cryptophyte-derived plastids, which contain phycobilin (phycoerythrin), and alloxanthin, a typical cryptophyte carotenoid; in other important species such as *Karenia* sp., *Gyrodinium aureolum* and *Gymnodinium galatheanum* with fucoxanthin as an accessory pigment, which possess haptophyte-derived plastids surrounded by two or four membranes; and in *Kryptoperidinium* sp. and close relatives, which have a five-membrane, diatom-derived plastid that includes a diatom nucleus of unknown complexity, and fucoxanthin as accessory pigment.

A serial secondary endosymbiosis (the uptake of a new primary plastid-containing endosymbiont) occurred in *Lepidodinium* chlorophorum and its close relatives, in which the peridinin plastid has apparently been replaced by a secondary plastid derived from a core chlorophyte alga containing chlorophylls a and b and surrounded by two membranes.

Noctiluca scintillans presents a completely different plastid situation: this large and conspicuous dinoflagellate, common in coastal areas worldwide, has both a completely heterotrophic form and a green "photosynthetic" form, harboring thousands of free-swimming cells of the prasinophyte *Pedinomonas noctilucae*.

TABLE 2.2
Possible Kleptoplastidic Dinoflagellates and Plastid Origin

Species	Habitat	Species of Plastid Origin	Source of Plastid	Detection
Gymnodinium acidotum	Freshwater	*Chroomonas* spp. (Cryptophyceae)	Direct ingestion	Microspectrophotometry
Amphidinium latum	Marine	Cryptophyceae	NA	TEM
Amphidinium poecilochroum	Marine	*Chroomonas* spp. (Cryptophyceae)	Direct ingestion	TEM
Cryptoperidiniopsis sp.	Marine	*Storeatula major* (Cryptophyceae)	Direct ingestion	TEM
Dinophysis acuminata	Marine	*Teleaulax amphioxeia* (Cryptophyceae)	*Myrionecta rubra*	PCR
Dinophysis mitra	Marine	Bacyllariophyceae	Unknown ciliate	PCR
Gymnodinium gracilentum	Marine	*Rhodomonas salina* (Cryptophyceae)	Direct ingestion	TEM
Pfiesteria piscicida	Marine	*Rhodomonas* sp. (Cryptophyceae)	Direct ingestion	TEM

In addition to dinoflagellates with permanent plastids, there are several taxonomic groups of dinoflagellates having kleptoplastids (stolen plastids), which are temporary but functional plastids captured from prey. Table 2.2 shows a list of possible kleptoplastidic dinoflagellates and their possible origin. Most of these dinoflagellates seem to prefer to retain kleptoplastids derived from cryptophytes. Among the most investigated cases is *Gymnodinium acidotum*; this dinoflagellate is characterized by the temporary retention of engulfed chloroplasts of a cryptophyte endosymbiont, *Chroomonas* spp. The exact identification of the prey was performed by microspectrophotometry. Figure 2.88a shows *Gymnodinium acidotum* and Figure 2.88b shows its absorption spectrum of its chloroplast. Figures 2.88d,g, and j show three possible preys present in the same environment, that is *Chroomonas* sp., an unknown cryptophyte, and *Cryptomonas* sp. The absorption spectra of their chloroplasts are shown in Figures 2.88e,h, and k. The difference spectra calculated between the absorption spectrum of the dinoflagellate and the absorption spectrum of the chloroplasts of the three preys are shown in Figures 2.88f,i, and l. Figure 2.88c shows the control difference spectrum. Since the difference spectra of Figures 2.88c and f are almost identical, it can be concluded that *Gymnodinium acidotum* preys only upon *Chroomonas* sp.

Euglenozoa

As in the Dinophyta, the chloroplast envelope consists of three membranes. Chloroplasts are typically many per cell and show considerable diversity of size, shape, and morphology (Figure 2.89a and b).

Five main types can be recognized:

1. Discoid chloroplasts with no pyrenoids (*Phacus*).
2. Elongated or shield-shaped chloroplasts with a central naked pyrenoid (*Trachelomonas*).
3. Large plated chloroplasts with the so-called double-sheeted pyrenoid, that is, a pyrenoid which carries a watch glass-shaped cup of paramylon on both plastid surfaces (*Euglena obtusa*).
4. Plated chloroplasts having a large pyrenoid projecting from the inner surface, which is covered by a cylindrical or spherical cup of paramylon (*Colacium*).
5. Chloroplast ribbons radiating from one, two, or three paramylon centers (*Eutreptia*).

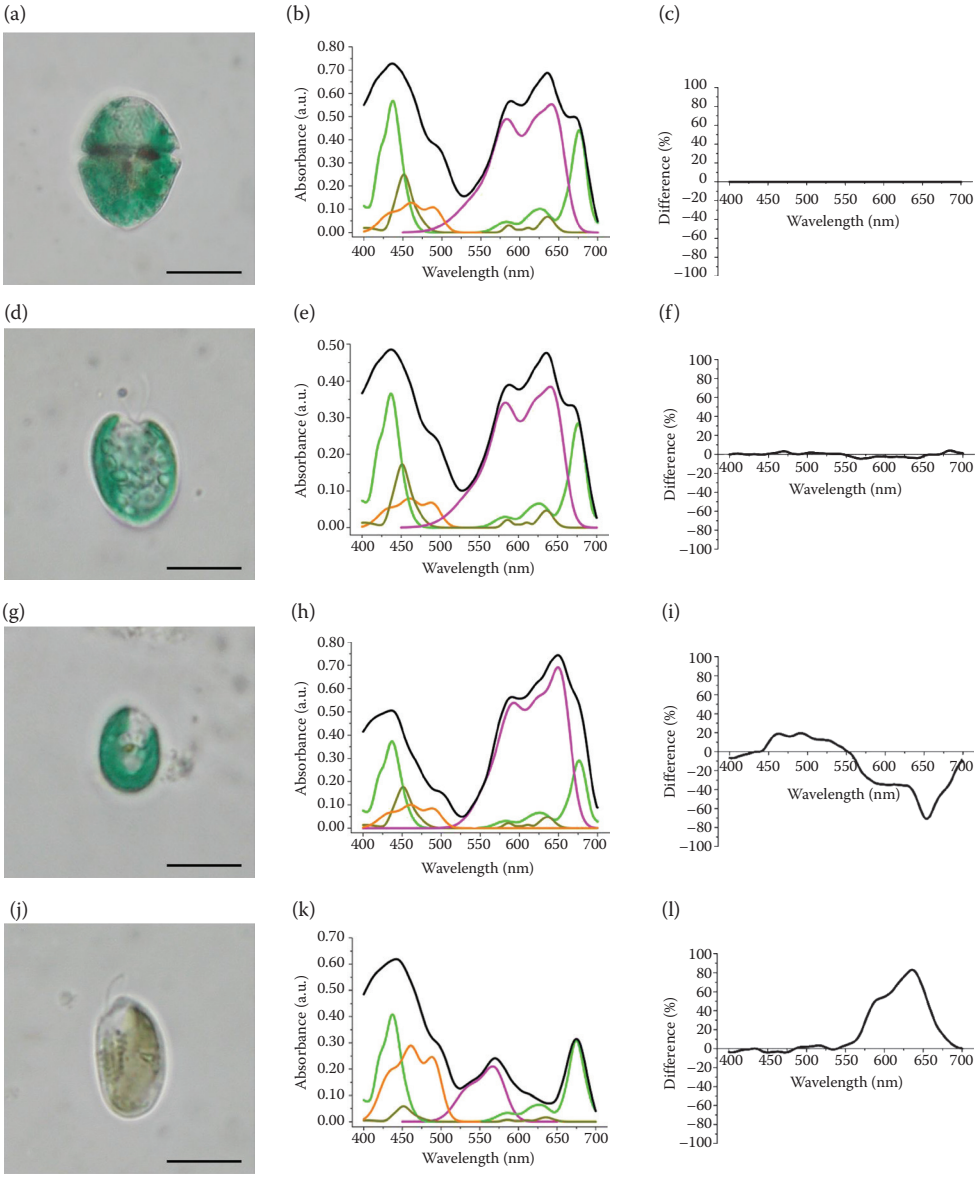

FIGURE 2.88 Absorption spectra of *G. acidotum* and its possible preys. See text for details, scale bar, 10 µm. Bright green line: chlorophyll *a*; dark green line: chlorophyll *b*; orange line: carotenoids and xanthophylls; purple lines: phycobiliproteins. (a) Scale bar, 10 µm; (b,c,d) scale bar, 5 µm.

The chloroplasts are never connected to the nucleus by the endoplasmic reticulum, and thylakoids are usually grouped in threes forming lamellae as in Ochrophyta and Dynophyta. Girdle lamellae are never found in this group. The photosynthetic pigments are chlorophylls *a* and *b* with carotenes and xanthophylls as accessory pigments. Chloroplast DNA occurs as tiny granules throughout the whole stroma.

The Nucleus, Nuclear Division, and Cytokinesis

An organized nucleus is absent in Cyanobacteria, where DNA molecules are free in the cytoplasm. The central region of those algae features the naked (without histone proteins) circular DNA genome,

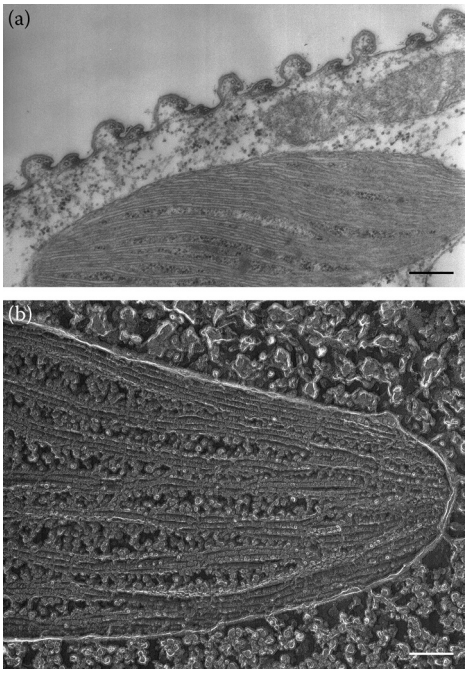

FIGURE 2.89 (a) TEM image of a chloroplast of *Euglena gracilis* in longitudinal section, scale bar, 0.10 μm. (b) Deep-etching image of a chloroplast of *E. gracilis*, scale bar, 0.05 μm.

which is not contained within a double membrane and consists of a single unbranched molecule. Transcription and translation processes are accomplished by the assistance of abundant 70S ribosomes located in the centroplasm. These ribosomes are smaller than their counterparts in the eukaryotic cytoplasm, but are typical of all prokaryotes, mitocondria, and chloroplasts. Cyanobacteria can only reproduce asexually, but appear to have some forms of genetic recombination possible, which are divided into two categories: transformation and conjugation. Transformation occurs when DNA is shed by one cell into the environment and is taken up by another cell and incorporated into its genome replacing homologous sections of DNA. The ability to be transformed by external DNA is species-specific and typically requires special environmental conditions. Conjugation is a "parasexual" process in which one of the partners develops a conjugation tube that connects to the recipient cell. Typically a plasmid (a small circle of DNA) from the donor cell passes through the conjugation tube. It is thought that genes for gas vacuolation, antibiotic resistance, and toxin production are carried on plasmids in cyanobacteria.

In eukaryotic algae, genetic information in the form of DNA, together with the controlling services for its selective expression, occurs in plastids (plastome), mitochondria (chondrome), and in the cell nucleus (genome). In the previous section, we have described organization and behavior of chloroplast DNA, which are similar to those of mitochondria. It is worthwhile to recall that plastid and mitochondrial genes and the way in which they are expressed have much in common with the system of gene expression of prokaryotes, and there are many plastid genes with extended introns that are very rare in prokaryotes. (Genes are mosaics of introns and exons. Introns are the DNA sequences of unknown function that are removed in the primary mRNA transcript. Exons are the DNA sequences that code for amino acids.)

In the nucleus of eukaryotic algae, long, linear, and unbranched molecules of DNA are associated with proteins and small amount of RNA. Two types of proteins are found: the relatively uniform histones (about 20), involved in the structural organization of the DNA, and the very variable

proteins involved in gene activity regulation, such as DNA and RNA polymerases. The DNA–protein complex, made up of repeating units termed nucleosomes, is known as chromatin, which is usually highly dispersed in the interphase nucleus. During mitosis and meiosis metaphases, the DNA–protein complexes are more helically condensed around the nucleosome and form the chromosomes, each chromosome consisting of a single DNA molecule.

The nucleus is surrounded by a two-membrane envelope continuous with the endoplasmic reticulum. Between the two membranes, there is a narrow perinuclear space about 20 nm wide. The nuclear envelope is perforated by numerous pores 60–100 nm in diameter. Nuclear pores have a complicated superstructure; they are not simply free openings, but are gateways in nuclear envelope through which the controlled transport of macromolecules (RNA, proteins) takes place. Pores can be arranged in straight lines as in *Bumilleria* (Xanthophyceae, Ochrophyta), in closely hexagonal groups as in *Prorocentrum* (Dinophyceae), or can be randomly distributed as in *Glenodinium* (Dinophyceae).

All algal nuclei possess nucleoli that vary in shape, size, and number in the different algal divisions. Nucleoli are dense concentrations of ribonucleoprotein-rich material, which are intimately associated with the specific region of the chromosomal DNA coding for ribosomal RNA. Nucleoli can be single and central as in *Cryptomonas* (Cryptophyta) or be more than 20 scattered in the nucleus as in *Euglena acus* (Euglenophyta).

In eukaryotic algae, the features of the interphase nucleus, DNA replication, and processes of transcription and translation in the expression of genetic information and cytokinesis are comparable to those of all the other eukaryotes. Exceptions to this rule will be described.

Rhodophyta

The basic features of mitosis and cytokinesis are the same throughout the division, though some variation may occur. Unlike other groups of eukaryotic algae, where the mitotic spindle is formed between two pairs of centrioles, one at each spindle pole, in red algae the poles of the spindle are marked by ring-shaped structures named polar rings. The absence of centrioles reflects the complete absence of flagella in the red algae. The chromosomal and interzonal microtubules do not converge toward the polar rings, so that the spindle poles are very broad. The nuclear envelope does not break down, though it is perforated by large holes, hence the mitosis is closed. The spindle persists for some time at early telophase, holding daughter nuclei apart; it collapses only at late telophase, when daughter nuclei are kept separated by a vacuole. Cytokinesis is by furrowing, but is typically incomplete; the furrow impinges upon the vacuole but leaves open a cytoplasmic connection between sibling cells. This connection is then filled and blocked by a proteinaceous stopper, named pit plug. The simplest type of pit plug consists only of a proteinaceous core; two- or one-layered caps partly composed of polysaccharides can border the core of both sides with different thicknesses. A cap membrane can be present between the two layers of the cap or bounding the plug core.

Chlorophyta—Charophyta

Nuclear and cell divisions have been intensively and extensively studied in the green algae at light microscopic and ultrastructural level, and several different patterns have been recognized. Two basic patterns have merged from these studies regarding nuclear and cell division in green algae:

1. Intranuclear mitosis, with the nuclear envelope closed at metaphase or open at the poles, interrupted by the microtubules of the spindle; other microtubules, transverse to the longitudinal axis of the spindle, are present at telophase and form the phycoplast; the latter functions somehow in cytokinesis, by furrowing or by cell-plate formation; the daughter nuclei at telophase are in close proximity.
2. The spindle and nuclear envelope are open and a phycoplast is absent; at telophase, the microtubules of the intranuclear spindle are persistent and a phragmoplast-like structure is organized as cytokinesis proceeds by furrowing.

Cylindrocapsa is an example of the first type; the parietal chloroplast divides before mitosis. Two pairs of centrioles are already present at the beginning of the interphase. In early prophase, the nuclear envelope is surrounded by one or two layers of endoplasmic reticulum, which is rough, that is, covered by ribosomes. Perinuclear microtubules appear around the nucleus and in late prophase they proliferate within the nucleus to form a tilted mitotic spindle between the pairs of centrioles lying at the spindle poles. At metaphase, the nuclear envelope is still intact and surrounded by the endoplasmic reticulum, so that mitosis is closed. The fully condensed chromosomes become aligned to form a distinct metaphase plate and have plate-like layered kinetochores. The nonpersistent telophase spindle soon degenerates, though a few microtubules can still be found around the re-formed nuclear envelopes. The pairs of centrioles migrate around the telophase nuclei, away from the former spindle poles, and toward the center of the equatorial plane, where they remain until after cytokinesis. Cisternae of endoplasmic reticulum proliferate in the narrow zone of cytoplasm present between the two daughter nuclei in the center of the cell. They bleb off smooth endoplasmic reticulum vesicles, which become aligned in the equatorial plane to form a cell plate of smooth vesicles. These vesicles coalesce to form a transverse system separating the daughter cells. Here, the vesicles accumulate within a phycoplast, that is, a plate of microtubules lying in the future plan of division. After completion of the transverse septum and the resultant separation of the daughter cells, a new cell wall is secreted around each daughter protoplast by exocytosis of Golgi-derived vesicles containing wall material. Each daughter cell thus gains a complete new wall; in the case of *Cylindrocapsa*, daughter cells remain united to form filaments, since the parental walls are persistent. In the case of other green algae with this type of mitosis and cytokinesis, daughter cells are liberated from the parent cell wall as nonflagellate autospores or as zoospores with centrioles ready to form flagella.

Coleochaete possess the second type of nuclear and cell division; the chloroplast begins to cleave at prophase; the single centriolar pair present during the interphase replicates at prophase and each of the two pairs takes up a position at one pole of the future spindle. Microtubules then form between the centriolar pairs, outside the envelope of the elongate prophase nucleus. The mitosis is open, since the nuclear envelope breaks down during metaphase; endoplasmic reticulum vesicles are present among the spindle microtubules. The chromosomes align in a distinct metaphase plate but the chromosomal microtubules do not attach to defined kinetochores. At early telophase, daughter nuclei become separated through elongation of the spindle, which is persistent during telophase and holds the nuclei far apart. By the end of the telophase, new microtubules proliferate and surround the spindle microtubules, forming the phragmoplast, which also includes actin filaments. Golgi-derived vesicles appear within the phragmoplast, guided by the microtubules and the filaments to the future plane of division, where they become arranged to form a cell plate. The vesicles contain cell-wall material, and their coalescence produces a transverse septum consisting of two cell membranes with the new transverse wall between them. Since the coalescence is not complete, connections leading to plasmodesmata are left between the daughter cells. This type of mitosis and cytokinesis is rare in the green algae, but is the common mode of division in plants such as bryophytes and tracheophytes.

Cryptophyta

These algae possess a peculiar organelle termed nucleomorph located in the space between the chloroplast endoplasmic reticulum and the chloroplast envelope. This organelle has a double membrane around it, pierced by pores, and contains both DNA and a nucleolus-like structure where rRNA genes are transcribed. The DNA is organized in three small chromosomes encoding genes for its own maintenance. It possesses the ability to self-replication, without forming a spindle during mitosis. It is considered a vestigial nucleus belonging to a photosynthetic eukaryotic symbiont of red algal ancestry.

Mizozoa—Dinophyceae

The dinoflagellate nucleus, known as dinokaryon, is bounded in the usual eukaryotic fashion by a nuclear envelope penetrated by pores. However, it possesses a number of unusual features, including

high amounts of DNA per cell (5–10 times the most common eukaryotic levels, up to a maximum of 200 pg in *Gonyaulax polyedra*). It is relatively large, often occupying about one-half of the volume of the cell. Nuclear shapes are variable, ranging from spheroid to U-, V-, or Y-shaped configurations. In most dinoflagellates, the chromosomes remain continuously condensed and visible, by both light and electron microscopy, during interphase and mitosis. Chromosome counts range from 12 to around 400, but may be variable within a species. A prominent nucleolus is also persistent. Each chromosome consists of a tightly super-coiled structure of DNA double helix. The permanent condensed chromosome shows a swirled, fibrillar appearance due to the naked DNA double helices (i.e., no histones are present). The 3–6-nm fibrils are packed in a highly ordered state, up to six levels of coiling. A small amount of basic protein is present in a few species, such as *O. marina*, but none of it corresponds in amino acid content to the histones normally present in eukaryotic chromosomes. A further peculiarity of dinoflagellate chromosomes is the high amount of calcium and other divalent metals, such as iron, nickel, or copper, which may play a role in chromosomal organization. In some dinoflagellate, such as *Noctiluca* and *Blastodinium*, the chromosomes undergo an expanded, decondensed change during interphase, and are termed noctikaryotic.

Dinoflagellate mitosis is also unusual. At the time of division, chromosomes divide longitudinally, the split starting at one end of the chromosome and moving along the entire length. The nucleus is invaded by cytoplasmic channels that pass from one pole to the other. Microtubules are present in these channels. The nuclear envelope and the nucleolus are persistent throughout nuclear division. The chromosomes upon dividing assume a V or Y configuration, and the apices of such chromosomes are closely associated with the nuclear envelope surrounding a cytoplasmic channel. This association suggests that the cytoplasmic channels serve as a mechanism for the movement of chromosomes.

The nuclear envelope persist during mitosis (closed mitosis), as it does in other algae, for example, Euglenophyceae and Raphidophyceae. However, with the exception of *Oxyrrhis marina*, where mitotic spindle is intranuclear, the chromosomes do not appear fibrillar, the mitosis strongly resembles that of *Euglena*, and the mitotic spindle is always extranuclear. The spindle microtubules pass through furrows and tunnels that form in the nucleus at prophase. No obvious spindle pole bodies other than concentric aggregation of Golgi bodies are present. Some microtubules contact the nuclear envelope, lining the tunnels at points where the chromosomes also contact. The chromosomes have differentiated dense regions inserted into the envelope.

Dinoflagellate cells undergo binary fission, and each daughter cell can retain half the parent cell wall, which splits along a predetermined fission line. This mode of reproduction is called "desmoschisis," and examples are *Ceratium* and many *Gonyaulax* species. In other dinoflagellates, daughter cells do not share the parent cell wall; this mode of division is called "eleutheroschisis." Binary fission may take place either inside the mother cell (many freshwater *Peridinium* species) or the protoplast may leave the mother cell wall before division through a hole or slit. In thecate species (many marine *Protoperidinium* species), the protoplast escapes after special thecal plates are dislocated through a hole. In several species, the protoplast has no flagella and deforms its cell wall during the escape from the mother theca; however, this is not a typical amoeboid stage. After cell division, each daughter cell produces a new cell wall or a new theca in thecate cells.

Euglenozoa—Euglenophyceae

In these algae, the interphase nucleus lies in the central or posterior region of the cell; it is spherical in most spindle-shaped species, and ovoid or long and narrow in elongate cells. In the largest species, the nucleus is at least 30×15 μm in dimensions, but in small species the spherical nucleus may be less than 2 μm in diameter. The chromosomes retain their condensed condition throughout interphase, appearing as granular or filamentous threads (Figure 2.90a and b). In some nuclei, the chromosomes radiate from the central endosome, while in others (even in the same species) they coil haphazardly throughout the nucleoplasm. Mitosis begins with a forward migration of the nucleus

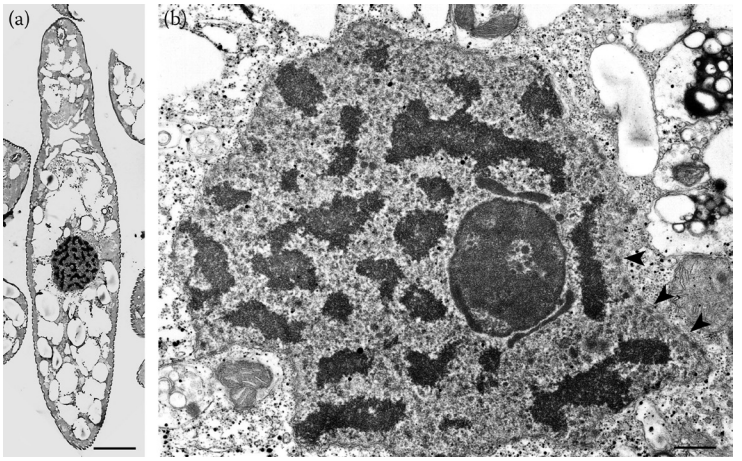

FIGURE 2.90 (a) TEM image of the WZSL mutant of *Euglena gracilis* in longitudinal section, showing the central nucleus with the condensed chromosomes, scale bar, 3 µm. (b) TEM image of the WZSL mutant of *E. gracilis* nucleus, showing the nucleoulus, the satellite nucleoli, and the nuclear membrane pores (arrowhead). Scale bar, 0.3 µm. (Courtesy of Giovanna Rosati.)

so that it comes to lie immediately posterior to the reservoir. In species with several endosomes in the interphase nucleus, these usually fuse to form a single body. The endosome then elongates along the divisions axis, perpendicular to the long axis of the cell, and the chromosomes orient into the metaphase position, following three main types of orientation:

1. Pairs of chromatids from late prophase orient into a circlet of single chromatids, separation and segregation having occurred during orientation (*Euglena gracilis*).
2. Pairs of chromatids from interphase and/or prophase come to lie along the division axis still as pairs, parallel to one another and to the elongated endosomes (*Euglena communis*, *Euglena viridis*).
3. Single chromosomes from prophase line up along the division axis and thereby undergo duplication into the pairs of chromatids of that mitosis (*Euglena acus*, *Euglena spirogyra*).

These different types overlap to a certain extent, species differing mainly in the time at which the double structure of the chromosomes first becomes microscopically visible. In all cases, the endosome continues to elongate and the chromatids segregate toward the ends of the endosome into two daughter groups. This stage, with most but not quite all of the daughter chromosomes separated, must be called metaphase in *Euglena*. During this early-to-late metaphase succession, the locomotor apparatus (flagella, photoreceptor, and eyespot) replicates and the reservoir divides. The daughter reservoirs open into the still single canal, but now each reservoir has its own contractile vacuole, eyespot, and flagella. Separation, segregation, and anaphasic movements of the chromatids are irregular, and this, coupled with a very low chromatid velocity, results in an extremely long anaphase. The end of the anaphase is marked by a sudden flowing to the poles of the central region of the elongated endosome, and the persistent nuclear envelope seals around the groups of chromatids and the daughter endosomes to form the telophase nuclei. Once telophase is established, with separate daughter nuclei, one of the two flagella in each daughter reservoir grows to emerge as a locomotory flagellum. A cleavage line is initiated between the now distinct daughter canals and progress helically backward to separate the daughter cells.

High chromosome numbers are the rule for species of Euglenophyceae, indicating a possible polyploidy.

Ejectile Organelles and Feeding Apparata

In this section, we will describe organelles that upon stimulation by contact, heat or chemicals discharge a structure, such as a tread or a tube from the surface of the cell. These organelles may serve for defense purposes or as feeding adjuvant.

Chlorophyta—Charophyta

Some *Pyramimonas* species (Prasinophytes) contain ejectile structures similar to the ejectosomes of Cryptophyta. In the undischarged state, they consist of a coiled ribbon, which upon discharge forms a hollow tube tapered at both ends.

Haptophyta

During its motile stage, *Phaeocystis* can eject ribbon-like filaments a few tens of nanometres wide and several tens of micrometers long. Their interconnections form a 5-branch star-like configuration (Figure 2.91). The winding of the filaments inside vesicles, as well as their axial twist, are probably the consequences of their biosynthesis within a confined space. As a result, the filaments behave like spring-coils whose stored energy is released once the vesicles are broken and the filaments ejected. Using electron diffraction techniques, the filaments have been unambiguously characterized as being made of α-chitin crystals, the polymer chain axis lying along the filament direction. These chains are antiparallelly arranged (allomorph) and this arrangement has never been reported before in the algal world.

Cryptophyta

These algae possess large refractile ejectosomes, lining the oral groove, and small ejectosomes scattered around the cell surface at the anterior corners of the periplast plates. An undischarged ejectosome

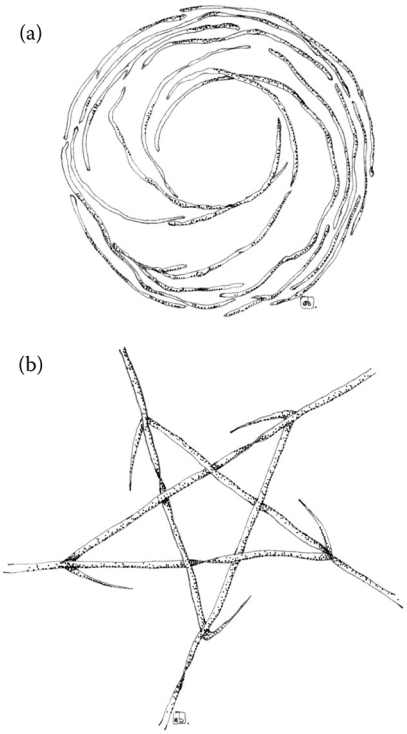

FIGURE 2.91 Ejectile organelles of *Phaeocystis* sp. Coiled filaments before release (a); star-like configuration after release (b).

is a tightly coiled, tapered ribbon that is wound with the wider end toward the outside; a smaller coil is attached to it and lies in the depression of the larger one. Prior to release, ejectosomes are enclosed within vesicles. The large ejectosomes are explosive organelles. If cryptophyte cells are irritated by mechanical or chemical stress, they escape the potentially lethal influences by discharging the ejectosomes: the cells jump backwards in fast zigzag movements through the water. When discharged, the ribbon unfurls, with the shorter segment forming a beak-like tip on the longer. The edges of the ribbon tend to curl inwards, producing circular and e-shaped profiles in cross-section (Figure 2.92).

Ochrophyta

Many species of Raphidophyceae have extrusome organelles that explode on strong stimulation throwing out up to 200-µm long slime threads. The material produced may surround a motile individual with mucilage so that it becomes palmelloid.

Cercozoa–Chlorarachmophyceae

Structures interpreted as ejectile organelles (extrusomes) are commonly seen in *Bigelowiella natans*. Each organelle resides in a vesicle and consists of two parts. The anterior part is very short, measuring approximately 0.15 µm in length, whereas the posterior part is approximately 0.55 µm long. The posterior part has a very distinct substructure, comprising a core surrounded by a less opaque cylinder. The cylinder is lined by a thin membrane-like structure, whereas the core comprises a thinner membranous structure surrounded by a more opaque one. The structure of the anterior part of the ejectile organelle is less well defined. Although it is clear that the membrane of the surrounding vesicle forms an indentation ring that separates the two parts of the ejectile organelle, the path of the membrane in this area is less clear. It appears that only the core of the organelle is discharged, the core apparently turning inside out during discharge. The surrounding cylinder seems to remain in place. The fate of the anterior part of the ejectile organelle after discharge has not been ascertained (Figure 2.93).

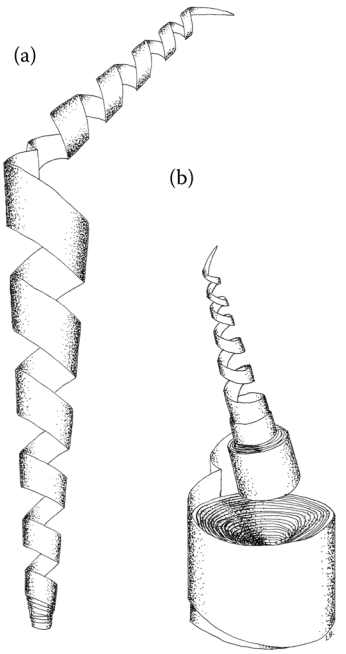

FIGURE 2.92 Ejectile organelles of a cryptophyte. Discharging ejectosome (a) and reel of an undischarged ejectosome just beginning to be pulled out (b).

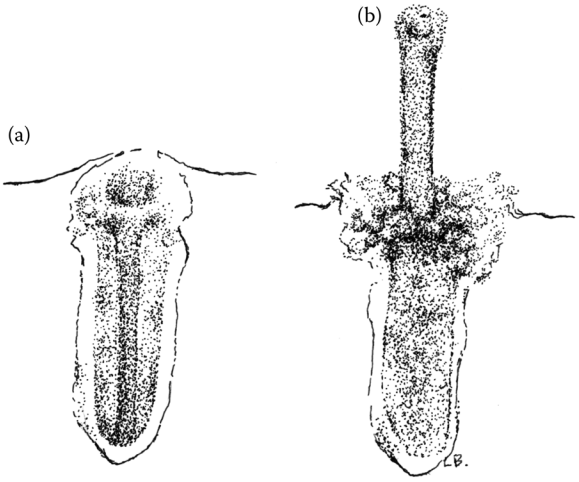

FIGURE 2.93 Ejectile organelle of *Bigelowiella natans* before (a) and during discharge (b).

Mizozoa—Dinophyceae

The most common type of extrusomes, of almost universal occurrence in the motile phase of these algae, are trichocysts, that is, rod-shaped bodies that, when mature, usually lie in the amphiesma perpendicular to the cell membrane (Figure 2.94). The shaft is paracrystalline, proteinaceous rod a few micrometers in length, rectangular in cross-section. At its distal end, it extends as a group of twisted fibers. The whole is enclosed within a membranous sac, and there is a sheating material between the rod and the membrane. The tip of the sac is in contact with the cell membrane, passing through the amphiesmal vesicles, and the thecal plates, if present. Thrichocysts are formed in the vicinity of the Golgi body and move to the cell periphery. They are discharged apparently by a rapid

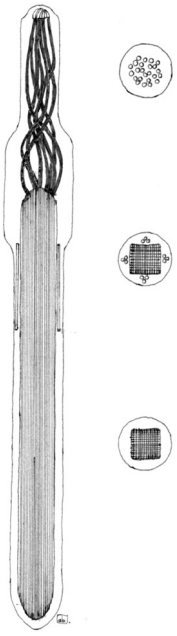

FIGURE 2.94 Undischarged trichocyst of *Goniaulax poliedra* in longitudinal and transverse sections.

hydration process, the discharged structures measuring up to 200 μm in length. Their function is unknown, but it is assumed to be defensive, excretory, or both.

A less ordered type of extrusomes in dinoflagellates is the mucocyst, a simple sac with granular content, associated with the release of mucoid material. They are located just beneath the cell membrane and are often aggregated in the region of the sulcus; their release in some species is correlated with the psamnophilous existence of these algae, facilitating the attachment of the cells to sand grains along the seashore.

More elaborate extrusomes termed nematocysts are found in genera such as *Polykrikos kofoidii* and *Nematodinium*; usually only about 8–10 nematocysts are present per cell. These organelles are larger than trichocysts and can reach 20 μm in length. They are conical, fluid-filled sacs with a capitated blunt end. Most of the body consists of a large posterior chamber, from which a smaller anterior chamber is isolated; the whole structure is capped by a lid-like operculum. A sharp stylet in the anterior chamber is connected to a tubular filament in the posterior chamber (Figure 2.95).

Feeding structures are present in dinoflagellates, depending on the type of feeding mechanisms present: feeding tube (peduncle, or tentacle) and feeding veil (pallium).

Tube feeding is commonly found among both naked and thecate species of dinoflagellates (e.g., *Dinophysis*, *Amphidinium*, *Gyrodinum*, and *Peridinopsis*). Cell membrane is extruded from the cell to form a tube, which can engulf whole cells or penetrate prey cell walls and suck in prey cytoplasm.

Pallium feeding has only been described for heterotrophic thecate species such as *Protoperidinium* and *Diplopsalis*. The prey is captured via a primary attachment filament; an extension of the cytoplasm then emerges from the region of the sulcus-cingulum, which encloses the prey as a veil (pallium). Enzymatic digestion of the prey cytoplasm is brought about inside the veil, and the products are then transported to the predator.

Direct engulfment is mainly found among naked species (e.g., *Gyrodinium*, *Gymnodinium*, *Noctiluca*); however, some thecate species have been shown to use this feeding mechanism as well. Feeding behavior in dinoflagellates involves several steps prior to actual ingestion, including precapture, capture, and prey manipulation. As feeding mechanisms allow the ingestion of relatively large preys, or parts thereof, dinoflagellates are regarded as raptorial feeders. While prey size plays an important role for the ability of dinoflagellates to ingest food, this cannot alone explain prey

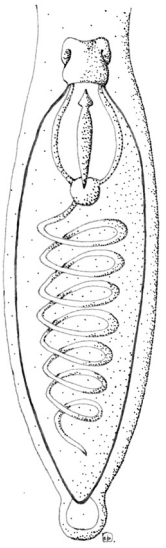

FIGURE 2.95 Nematocysts of *Polykrikos kofoidii*.

preferences actually found. Some dinoflagellate species can be very selective in their choice of prey, while others show a remarkable versatility.

Euglenozoa—Euglenophyceae

Trichocysts are present only in some phagotrophic species, such as *Entosiphon* and *Peranema trichophorum*. In *Peranema*, ejectile organelles or mucocysts are located beneath the cell surface, often subtending the pellicular articulations. In transverse sections, they appear as hollow tubes of amorphous material, with low electron density, enclosed within a vesicle bounded by single membrane, often found near the Golgi apparatus; or they show a content of greater density, and may subtend the pellicle or protrude through it. Mucocysts subtending the pellicular articulations are ejected from the cell through the grooves. They are characterized by three distinct regions: an inner tube 1.20-mm long and 1.18-mm wide with helical striations; an outer tube 0.77 mm long and 0.21-mm wide with a diamond-shaped pattern; and a dense middle band 0.07 mm in

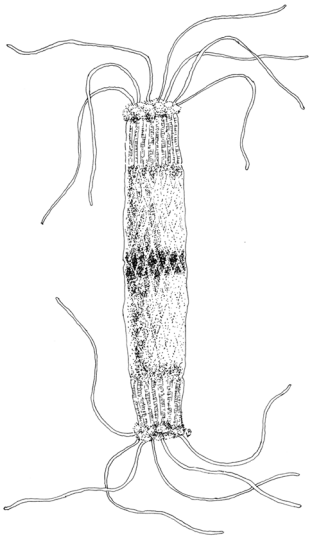

FIGURE 2.96 Ejected mucocyst of *P. trichophorum*.

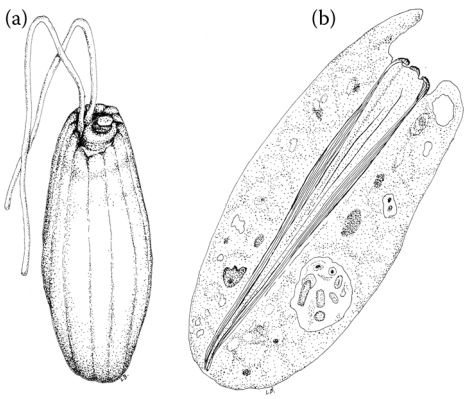

FIGURE 2.97 (a) Cell of *Entosiphon* sp. (b) Longitudinal section of the cell, showing the structure of the feeding apparatus.

width. Often a crown of dense fibrillar material occurs at the tips of the mucocyst. Small slime-extruding mucus bodies are the trichocyst counterparts commonly found in the nonphagotrophs (Figure 2.96).

A feeding apparatus is present in many Euglenophyceae, such as *Diplonema*, *Ploeotia*, *or Entosiphon*. In the latter (Figure 2.97a), it consists of a cytostome surrounded by four centrally located vanes (series of plicate folds or curved ribbons) and supported by rods composed of closely packed microtubules. Near the base of the feeding apparatus, one of the rods split giving rise to a total of three stout rods that extend nearly the length of the cell. At about one-third of the distance down the apparatus (from the anterior end), the number of microtubules per rod increases dramatically and then decreases in number toward the base giving the apparatus the overall appearance of a cone with one side open (Figure 2.97b). This feeding apparatus can be moved in and out, extending toward the anterior of the cell and then withdrawing down into the cell for a distance of 3–5 mm. This motion allows food to be drawn into the cell.

SUGGESTED READING

Albertano, P., Barsanti, L., Passarelli, V., and Gualtieri, P. A complex photoreceptive structure in the cyanobacterium *Leptolyngbya* sp., *Micron*, 31, 27, 2000.

Andersen, R.A. Biology and systematic of heterokont and haptophyte algae. *American Journal of Botany*, 91, 1508–1522, 2004.

Barlow, H.B. The physical limits of visual discrimination. In: *Photophysiology*, Giese A. (Ed.), Academic Press, New York, 1964.

Barsanti, V., Passarelli, V., Walne, P.L., and Gualtieri, P. In vivo photocycle of the *Euglena gracilis* photoreceptor. *Biophysical Journal*, 72, 545, 1997.

Barsanti, L., Evangelista, V., Passarelli, V., Frassanito, A.M., Coltelli, P., and Gualtieri, P. Microspectrophotometry as a method to identify kleptoplastids in the naked freshwater dinoflagellate *Gymnodinium acidotum*. *Journal of Phycology*, 45(6), 1304–1309, 2009.

Barsanti, L., Evangelista, V., Passarelli, V., Frassanito, A.M., and Gualtieri, P. Fundamental questions and concepts about photoreception and the case of *Euglena gracilis*. *Integrative Biology*, 4(1), 22–36, 2012.

Barsanti, L., Frassanito, A.M., Passarelli, V., Evangelista, V., Etebari, M., and Paccagnini, E. et al. *Tetraflagellochloris mauritanica* gen. et sp. nov. (Chlorophyceae), a new flagellated alga from the Mauritanian Desert: Morphology, ultrastructure, and phylogenetic framing. *Journal of Phycology*, 49(1), 178–193, 2013.

Beek, P.L. The long and the short, of flagellar length control. *Journal of Phycology*, 39, 837–839, 2003.

Bouck, G.B. The structure, origin, isolation and composition of the tubular mastigonemes of *Euglena gracilis*. *Journal Cell Biology*, 50, 362–384, 1971.

Bouck, G.B. and Ngo, H. Cortical structure and function in euglenoids with reference to trypanosomes, ciliates, and dinoflagellates. *International Review Cytology*, 169, 267–318, 1996.

Brett, S.J., Perasso, L., and Wetherbee, R. Structure and development of the cryptomonad periplast: A review. *Protoplasma*, 181, 106–122, 1994.

Buetow, D.E. (Ed). *The Biology of Euglena. Biochemistry*. Academic Press, New York, 1968a.

Buetow, D.E. (Ed). *The Biology of Euglena. General Biology and Ultrastructure*. Academic Press, New York, 1968b.

Buetow, D.E. (Ed). *The Biology of Euglena. Physiology*. Academic Press, New York, 1982.

Buetow, D.E. (Ed). *The Biology of Euglena. Subcellular Biochemistry and Molecular Biology*. Academic Press, New York, 1989.

Daugbjerg, N. *Pyramimonas tychotreta*, a new marine species from Antarctica: Light and electron microscopy of the motile stage and notes on growth rates. *Journal of Phycology*, 36, 160–171, 2000.

Dodge, J.H. *The Fine Structure of Algal Cells*. Academic Press, London, 1973.

Dodge, J. Photosensory systems in eukaryotic algae. In: Cronly-Dillon, J.R., and Gregory, R.L. (Eds.), *Evolution of the Eye and Visual System*. Macmillan, London, 1991.

Dodge, J.D. and Crawford, R.M. A survey of thecal fine structure in the Dinophyceae. *Botanical Journal of Linnean Society*, 63, 53–67, 1970.

Dusenbery, D.B. *Sensory Ecology*. Freeman Press, New York, 1992.

Ehlers, K. and Oster, G. On the mysterious propulsion of *Synechoccoccus*. *PLOS One*, 7(5), e36081, 2012.

Fenchel, T. How dinoflagellates swim. *Protist*, 152, 329–338, 2001.
Frassanito, A.M., Barsanti, L., Passarelli, V., Evangelista, V., and Gualtieri, P. A rhodopsin-like protein in *Cyanophora paradoxa*: Gene sequence and protein immunolocalization. *Cellular and Molecular Life Sciences*, 67, 965–971, 2010.
Fredrick, J.F. (Ed.). *Origins and Evolution of Eukaryotic Intracellular Organelles*. The New York Academy of Sciences, New York, 1981.
Gilson, P.R. and McFadden, G.I. Molecular, morphological and phylogenetic characterization of six chlorarachniophytes strains. *Phycological Research*, 47, 7–19, 1999.
Ginger, M.L., Portman, N., and McKean, P.G. Swimming with protists: Perception, motility and flagellum assembly. *Nature Reviews Microbiology*, 6, 838–850, 2008.
Grain, J., Mignot, J.P., and de Puytorac, P.. Ultrastructures and evolutionary modalities of flagellar and cyliary system in protists. *Biology of the Cell*, 63, 219–237, 1988.
Gregson, A.J., Green, J.C., and Leadbeater, B.S.C. Structure and physiology of Haptonema in *Chrisochromulina*. Fine structure of the flagellar/haptonematal root system in *C. acanthi* and *C. simplex*. *Journal of Phycology*, 29, 674–686, 1993a.
Gregson, A.J., Green, J.C., and Leadbeater, B.S.C. Structure and physiology of Haptonema in *Chrisochromulina*. Mechanism of haptonematal coiling and the regeneration process. *Journal of Phycology*, 29, 686–700, 1993b.
Gualtieri, P. Microspectroscopy of photoreceptor pigments in flagellated algae. *Critical Review Plant Science*, 9(6), 474–495, 1991.
Gualtieri, P. and Robinson, K.R. A rhodopsin-like protein in the plasma membrane of *Silvetia compressa* eggs. *Photochemistry Photobiology*, 75, 76, 2002.
Hackett, J.D., Anderson, D.M., Erdner, D.L., and Bhattacharya, D. Dinoflagellates: A remarkable evolutionary experiment. *American Journal of Botany*, 91, 1523–1534, 2004.
Harrison, F.W. and Corliss, J.O. *Microscopy Anatomy of Invertrebrate. Protozoa*. Wiley-Liss, New York, USA, 1991.
Hibbed, D.J. and Norris, R.E. Cytology and ultrastructure of *Chlorarachnion reptans* (Chlorarachniophyta divisio nova, Chlorarachniophyceae classis nova). *Journal of Phycology*, 20, 310–330, 1984.
Hilenski, L.L. and Walne, P.L. Ultrastructure of mucocysts in *Peranema trichophorum*. *Journal of Protozoology*, 30, 491–496, 1983.
Hoiczyk, E. and Hansel, A. Cyanobacterial cell walls: News from and unusual prokaryotic envelope. *Journal of Bacteriology*, 182, 1191–1199, 2000.
Honda, D. and Inouye, I. Ultrastructure and taxonomy of a marine photosynthetic stramenopile *Phaemonas parva* with emphasis on the flagellar apparatus architecture. *Phycological Research*, 50, 75–89, 2002.
Horiguchi, T. and Hoppenrath, M. *Haramonas viridis*, a new sand-dwelling raphidophyte from cold temperate waters. *Phycological Research*, 51, 61–67, 2003.
Hyams, J.S. The Euglena paraflagellar rod: Structure, relationship to the other flagellar components and preliminary biochemical characterization. *Journal of Cell Science*, 55, 199–210, 1982.
Inouye, I. and Hori, T. High-speed video analysis of the flagellar beat and swimming patterns of algae: Possible evolutionary trends in green algae. *Protoplasma*, 164, 54–69, 1991.
Iomini, C.V., Babaev-Khaimov, M., Sassaroli, D., and Piperno, G. Protein particles in *Chlamydomonas* flagella undergo a transport cycle consisting of four phases. *Journal of Cell Biology*, 153(1), 13–24, 2001.
Kantsler, V., Dunkel, J., Polin, M., and Goldstein, R.E. Ciliary contact interactions dominate surface scattering of swimming eukaryotes. *Proceedings of the National Academy of Sciences*, 110(4), 1187–1192, 2013.
Koch, D.L. and Subramanian, G. Collective hydrodynamics of swimming microorganisms: Living fluids. *Annual Review of Fluid Mechanics*, 43(1), 637–659, 2011.
Kugrens, P., Clay, B.L., and Lee, R.E. Ultrastructure and systematic of two new freshwater red cryptomonads, *Storeatula rhinosa*, and *Pyrenomonaas ovalis*. *Journal of Phycology*, 35, 1079–1089, 1999a.
Kugrens, P., Clay, B.L., Meyer, C.J., and Lee, R.E. Ultrastructure and description of *Cyanophora biloba* with additional observations on *C. paradoxa*. *Journal of Phycology*, 35, 844–854, 1999b.
Lakie, J.M. *Cell Movement and Cell Behaviour*. Allen and Unwin, London, 1986.
Lauga, E. and Powers, T.R. The hydrodynamics of swimming microorganisms. *Reports on Progress in Physics*, 72, 096601, 2009.
Lavau, S. and Wetherbee, R. Structure and development of the scale case of *Mallomonas adamas*. *Protoplasma*, 181, 259–268, 1994.
Leadbeater, B.S.C. and Green, J.C. (Eds.). *The Flagellates. Unit, Diversity and Evolution*. Taylor and Francis, London, 2000.

Leander, B.S. and Farmer, M.A. Comparative morphology of euglenid pellicle: Diversity of strip substructures. *Journal of Eukariotic Microbiology*, 48, 202–217, 2001.
Lima-de-Faria (Ed.). *Handbook of Molecular Cytology*. North-Holland Publishing Co., Amsterdam, The Netherlands, 1969.
Lobban, C.S. and Harrison, P.J. *Seaweed Ecology and Physiology*. Cambridge University Press, Cambridge, 1997.
Luck, M., Mathes, T., Bruun, S., Fudim, R., Hagedorn, R., Tran Nguyen, T.M., Kateriya, S., Kennis, J.T.M., Hildebrandt, P., and Hegemann, P. A Photochromic Histidine Kinase Rhodopsin (HKR1) that is bimodally switched by ultraviolet and blue light. *Journal of Biological Chemistry*, 287, 40083–40090, 2012.
Maga, J.A. and LeBowitz, J.H. Unravelling the kinetoplastid paraflagellar rod. *Trends Cell Biology*, 9, 409–413, 1999.
Marian, B. and Melkonian, M. Flagellar hairs in Prasinophytes: Ultrastructure and distribution on the flagellar surface. *Journal of Phycology*, 30, 659–678, 1994.
Maruyama, T. Fine structure of the longitudinal flagellum in *Ceratium tripos*, a marine dinoflagellate. *Journal Cell Science*, 58, 109–123, 1982.
Melkonian, M. (Eds.). *Algal Cell Motility*. Chapman & Hall, New York, 1992.
Melkonian, M. and Robenek, H. The eyespot apparatus of flagellated green algae: A critical review. In: Round, F.E., and Chapman, D.J. (Eds.), *Progress in Phycological Research*, Vol. 3. Biopress Ltd., Bristol, 1984, pp. 193–268.
Menzel, D. (Ed.). *The Cytoskeleton of the Algae*. CRC Press, Boca Raton, 1992.
Miyasaka, I., Nanba, K., Furuya, K., Nimura, Y., and A. Azuma. Functional roles of the transverse and longitudinal flagella in the swimming motility of Prorocentrum minimum. *Journal of Experimental Biology*, 207, 3055–3066, 2004.
Moenstrup, Ø. Flagellar structure in algae: A review, with new observations particularly on the Chrysophyceae, Phaeophyceae, Euglenophyceae, and Reckertia. *Phycologia*, 21, 4, 427–528, 1982.
Moenstrup, Ø. and Sengco, M. Ultrastructural studies on *Bigelowiella natans*, a Chlorarachniophyte flagellate. *Journal of Phycology*, 37, 624–646, 2001.
Niklas, K.J. The cell walls the bind the tree of life. *Bioscence*, 54, 831–841, 2004.
Nishitani, G., Nagai, S., Hayakawa, S., Kosaka, Y., Sakurada, K., Kamiyama, T et al. Multiple plastids collected by the dinoflagellate *Dinophysis mitra* through kleptoplastidy. *Applied and Environmental Microbiology*, 78(3), 813–821, 2012.
Norton, T.A. andersen, R.A., and Melkonian, M. Algal biodiversity. *Phycologia*, 35, 308, 1996.
Novarino, G. A companion to the identification of cryptomonad flagellates. *Hydrobiologia*, 502, 225–270, 2003.
O'Malley, S. and Bees, M.A. The orientation of swimming biflagellate in shear flows. *Bulletin of Mathematical Biol*ogy, 74, 232–255, 2012.
Parkinson, P.R. Ontogeny v. phylogeny: The strange case of the silicoflagellates. *Constancea*, 83, 1–29, 2002.
Patterson, D.J. and Larsen, J. *The Biology of Free-living Heterotrophic Flagellates*. Clarendon Press, Oxford, 1991.
Pickett-Heaps, J.D., Carpenter, J., and Koutoulis, A. Valve and seta (spine) morphogenesis in the centric diatom *Chaetoceros peruvianus*. *Protoplasma*, 181, 269–282, 1994.
Polin, M., Tuval, I., Drescher, K., Gollub, J.P., and Goldstein, R.E. *Chlamydomonas* swims with two "Gears" in a eukaryotic version of run-and-tumble locomotion. *Science*, 325(5939), 487–490, 2009.
Preisig, H.R. Siliceous structure and silicification in flagellate protists. *Protoplasma*, 181, 29–42, 1994.
Preisig, H.R. anderson, O.R., Corliss, J.O., Moestrup, Ø., Powell, M.J., Roberson, R.W., and Wetherbee, R. Terminology and nomenclature of protest cell surface structures. *Protoplasma*, 181, 1–28, 1994.
Purcell, E.M. Life at low Reynolds number. *American Journal of Physics*, 45(1), 3–11, 1977.
Rafai, S., Jibuti, L., and Peyla, P. Effective viscosity of microswimmer suspension. *Physical Review Letters*, 104, 098102, 2010.
Rave, J.A. and Brownlee, C. Understanding membrane function. *Journal of Phycology*, 37, 960–967, 2001.
Rizzo, P.J. Those amazing dinoflagellate chromosomes. *Cell Research*, 13, 215–217, 2002.
Rosati, G., Verni, F., Barsanti, L., Passarelli, V., and Gualtieri, P. Ultrastructure of the apical zone of *Euglena gracils*: Photoreceptor and motor apparatus. *Electron Microscopy Review*, 4, 319–342, 1991.
Sato, H., Greuet, C., Cachon, M., and Cosson, J. Analysis of the contraction of an organelle using its birefringency: The R-fibre of the *Ceratium flagellum*. *Cell Biology International*, 28, 387–396, 2004.
Solomon, C.M., Evelyn, J., Lessard, R., Keil, G., and Foy, M.S. Characterization of extracellular polymers of *Phaeocystis globosa* and *P. antarctica*. *Marine Ecology Progress Series*, 250, 81–89, 2003.
Taylor Max, F.J.R. Charles Atwood Kafoid and his dinoflagellate tabulation system: An appraisal and evaluation of the phylogenetic value of tabulation, *Protist*, 150, 213–220, 1999.

Ueki, N., Matsunaga, S., Inouye, I., and Hallmann, A. How 5000 independent rowers coordinate their strokes in order to row into the sunlight: Phototaxis in the multicellular green alga *Volvox*. *BMC Biology*, 8(1), 103, 2010.

Verspagen, J. M.H., Snelder, E.O.F.M., Visser, P.M., Huisman, J., Mur, L.R., and Ibelings, B.W. Recruitment of benthic microcystis to the water column: Internal buoyancy changes or resuspension? *Journal of Phycology*, 40, 260–270, 2004.

Westfall, J.A., Bradbury, P.C., and Townsend, J.W. Ultrastructure of the dinoflagellate *Polykrikos*. *Journal of Cell Science*, 63, 245–261, 1983.

Xia, S., Zhang, Q., Zhu, H., Cheng, Y., Liu, G., and Hu, Z. Systematics of a kleptoplastidal dinoflagellate, *Gymnodinium eucyaneum* Hu (Dinophyceae), and its cryptomonad endosymbiont. *PLoS ONE*, 8(1), e53820, 2013.

Young, J.R., Davis, S.A., Brown, P.R., and S. Mann. Coccolith ultrastructure and biomineralization. *Journal of Structural Biology*, 126, 195–215, 1999.

Zhang, F., Vierock, J., Yizhar, O., Fenno, L.E., Tsunoda, S., Kianianmomeni, A. et al. The microbial opsin family of optogenetic tools. *Cell*, 147, 1446–1457, 2011.

Zingone, A., Chretiennot-Dinet, M.J., Lange, M., and Medlin, L. Morphological and genetic characterization *Phaeocystis cordata* and *P. jahnii*, two new species from the Mediterranean Sea. *Journal of Phycology*, 35, 1322–1337, 1999.

3 Photosynthesis

LIGHT

The sun is the universal source of energy in the biosphere. Due to the nuclear fusion processes occurring in the sun, matter is changed into energy, which can be emitted into space in the form of electromagnetic radiation, having both wave and particle properties. Almost all light in the natural environment originates from the sun. Its spectral distribution (Figure 3.1, thin black line) is similar to that of an efficient radiant surface known as a blackbody at a temperature of 5800 K (Figure 3.1, thick black line) and ranges from short wavelength (10^{-6} nm, γ- and X-rays) to long wavelength (10^{15} nm, long radio waves) (Figure 3.2).

In passing through the atmosphere, a small portion of this light is absorbed and some is scattered. Short wavelengths are strongly scattered, and ozone absorption effectively eliminates wavelengths <300 nm (Figure 3.1, grey line). At longer wavelengths, water vapor, carbon dioxide, and oxygen absorb light significantly at particular wavelengths, producing sharp dips in the spectrum. At still-longer wavelengths, >4000 nm, all objects in the environment become significant sources of radiations, depending on their temperature, and surpass sunlight in intensity. These environmental characteristics restrict the range of electromagnetic radiation. About 99% of the sun's radiation that reaches the surface of the earth has a spectral range from ~300 nm (ultraviolet) to ~4000 nm (infrared) and is called the broadband or total solar radiation. Almost superimposable on the broadband radiation three spectral regions exist, which can be associated with specific phenomena, such as harmful and potentially mutagen ultraviolet radiation (UV, 100–400 nm), sight (visible light, 400–700 nm), and heat (infrared radiation, 700–4000 nm) (Figure 3.2).

Ultraviolet light is arbitrarily broken down into three bands, according to its anecdotal effects. UV-A (315–400 nm) is the least harmful and the most commonly found type of UV light, because it has the least energy. UV-A light is often called black light and is used for its relative harmlessness and its ability to cause fluorescent materials to emit visible light, thus appearing to glow in the dark. Most phototherapy and tanning booths use UV-A lamps. UV-B (280–315 nm) is typically the most destructive form of UV light, because it has enough energy to damage biological tissues, yet not quite enough to be completely absorbed by the atmosphere. UV-B is known to cause skin cancer. Since most of the extraterrestrial UV-B light is blocked by the atmosphere, a small change in the ozone layer could dramatically increase the danger of skin cancer. Short-wavelength UV-C (200–280 nm) is almost completely absorbed in air within a few hundred meters. When UV-C photons collide with oxygen molecules, the O–O bond is broken and the released O atom reacts with O_2 molecule (and for energetic reasons with a collision partner M) and forms ozone (O_3). UV-C is almost never observed in nature, since it is absorbed very quickly. Germicidal UV-C lamps are often used to purify air and water, because of their ability to kill bacteria.

The visible range extends from 400 to 700 nm, and these wavelengths are utilized for both vision and photosynthesis. The radiation utilized by oxygenic photosynthetic organisms is termed the photosynthetic active radiation (PAR). We will see in the following that this range has been expanded to 750 nm after the discovery of red-shifted chlorophylls.

Infrared light contains the least amount of energy per photon of any other band. Because of this, an infrared photon often lacks the energy required to pass the threshold of metabolic pathways. Little of the ultraviolet radiation (UV-A and UV-B) and infrared are utilized directly in photosynthesis.

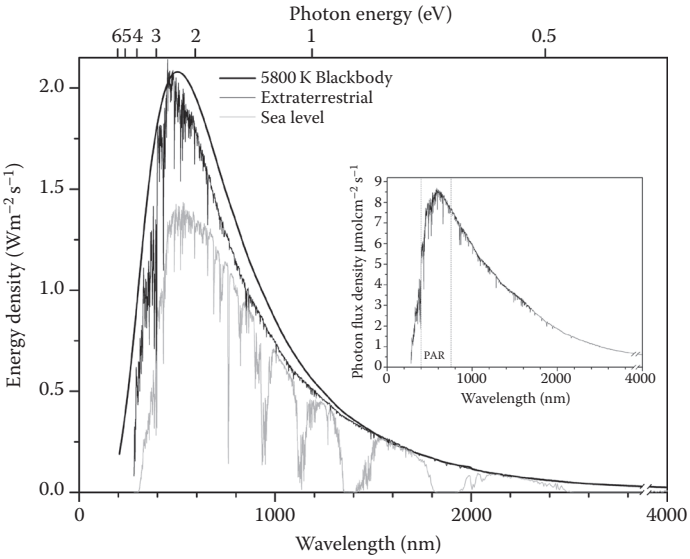

FIGURE 3.1 Spectral irradiance of the incoming sun radiation outside the atmosphere and at the sea level compared with that of a perfect blackbody at 5800 K. The curve in the inset is the photon flux density spectrum.

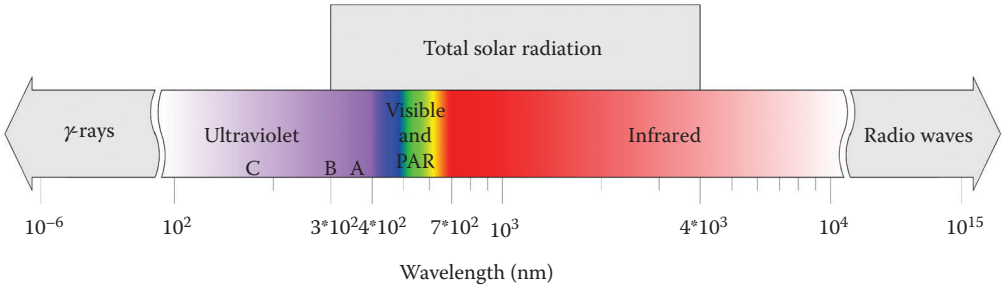

FIGURE 3.2 The electromagnetic spectrum, from γ-rays (10^{-6}) to radio waves (10^{15}).

The particles producing the electromagnetic waves are called photons or quanta. The energy (E) in joules (or watts per second) of a photon (or quantum) can be expressed by Planck's law:

$$E = hc\lambda^{-1}, \tag{3.1}$$

where h is Planck's constant (6.626×10^{-34} J s), c the speed of light (3×10^8 m s^{-1}), and λ the photon wavelength in meters (m). $c\lambda^{-1}$ represents the frequency υ of the photon.

According to this formula, the shorter the photon wavelength, the higher its energy; for example, the energy of a photon of 300 nm light is equal to 6.63×10^{-19} J, the energy of a photon of 400 nm light is equal to 4.97×10^{-19} J, the energy of a photon of 700 nm light is equal to 2.84×10^{-19} J, while the energy of a photon of 4000 nm light is equal to 0.49×10^{-19} J. It takes a larger number of longer-wavelength photons to supply a given quantity of energy than it does of shorter wavelength photons. This relationship has the effect of changing the shape of the curve represented in two different ways: the peak of the energy curve is at ~500 nm (Figure 3.1, thin black line), whereas the peak of the photon flux density curve is at ~700 nm (inset in Figure 3.1).

The energy of photons can also be expressed in terms of electron volts (eV). Absorption of a photon can lead to excitation of an electron and hence of a molecule. This excited electron acquires potential energy (capacity of producing chemical work) measured in eV. An electron volt is the

potential energy of 1 V gained by the excited electron, which is equal to 1.60×10^{-19} J. Thus, the energy of a photon of 300 nm light is equal to 4.14 eV (i.e., 6.63×10^{-19} J divided by 1.60×10^{-19} J), the energy of a photon of 400 nm light is equal to 3.11 eV, the energy of a photon of 700 nm light is equal to 1.77 eV, and the energy of a photon of 4000 nm light is equal to 0.30 eV.

The average intensity of the total solar radiation reaching the upper atmosphere is about 1.4 kW m^{-2} (UV, 8%; visible light, 41%; infrared radiation, 51%). The amount of this energy that reaches any one "spot" on the earth's surface will vary according to atmospheric and meteorological (weather) conditions, the latitude and altitude of the spot, and local landscape features that may block the sun at different times of the day. In fact, as sunlight passes through the atmosphere, some of it is absorbed, scattered, and reflected by air molecules, water vapor, clouds, dust, and pollutants from power plants, forest fires, and volcanoes. Atmospheric conditions can reduce solar radiation by 10% on clear, dry days, and by 100% during periods of thick clouds. At sea level, in an ordinary clear day, the average intensity of solar radiation is less than 1.0 kW m^{-2} (UV, 3%; visible light, 42%; infrared radiation, 55%). Penetrating water, much of the incident light is reflected from the water surface, more light being reflected from a ruffled surface than a calm one and reflection increases as the sun becomes lower in the sky (Table 3.1). As light travels through the water column, it undergoes a decrease in its intensity (attenuation) and a narrowing of the radiation band caused by the combined absorption and scattering of everything in the water column including water itself. In fact, different wavelengths do not penetrate equally; infrared light (700–4000 nm) penetrates least, being almost entirely absorbed within the top 2 m, and ultraviolet light (300–400 nm) is also rapidly absorbed. Within the visible spectrum (400–700 nm), red light is absorbed first, much of it within the first 5 m. In clear water, the greatest penetration is by the blue-green region of the spectrum (450–550 nm), while under more turbid conditions the penetration of blue rays is often reduced to a greater extent than that of the yellow-red wavelengths (550–700 nm). Depending on the conditions, 3–50% of incident light is usually reflected, and Lambert–Beer's law can describe mathematically the way the light decreases as a function of depth:

$$I_z = I_0 e^{-kz}, \tag{3.2}$$

where I_z is the intensity of light at depth z, I_0 the intensity of light at depth 0, that is, at the surface, and k the attenuation coefficient, which describes how quickly light attenuates in a particular body of water.

Algae use the light eventually available in two main ways:

- As information in sensing processes, supported by the photoreceptor systems, as already explained in Chapter 2.
- As energy in transduction processes, supported by chloroplasts in photosynthesis.

TABLE 3.1
Sunlight Reflected by Sea Surface

Angle between Sun Rays and Zenith	% of Reflected Light
0°	2
10°	2
20°	2.1
30°	2.1
40°	2.5
50°	3.4
60°	6
70°	13.4
80°	34.8
90°	100

Both types of processes depend on the absorption of photons by electrons of chromophore molecules with extensive systems of conjugated double bonds. These conjugated double bonds create a distribution of delocalized *pi* electrons over the plane of the molecule. Upon absorption of a photon in the range 400–700 nm, *pi* electrons can be driven to an available electronic "excited state" (an unoccupied orbital of higher energy, higher meaning the electron is less tightly bound). Only absorption of a photon in this range can lead to excitation of the electron and hence of the molecule, since the lower energy of an infrared photon could be confused with the energy derived by molecular collisions, eventually increasing the noise of the system and not its information; and the higher energy of an UV photon could dislodge the electron from the electronic cloud and destroy the molecular bonds of the chromophore. Charge separation is produced in the chromophore molecule elevated to the excited state by the absorption of a photon, which increases the capability of the molecule to perform work. In sensing processes, charge separation is produced by the photo-isomerization of the chromophore around a double bond, thus storing electrostatic energy, which triggers a chain of conformational changes in the protein that induces the signal transduction cascade. In photosynthesis, a charge separation is produced between a photo-excited molecule of a special chlorophyll (electron donor) and an electron-deficient molecule (electron acceptor) located within van der Waals distance, that is, a few angstrom (Å). The electron acceptor in turn becomes a donor for a second acceptor and so on; this chain ends in an electron-deficient trap. In this way, the free energy of the photon absorbed by the chlorophyll can thereby be used to carry out useful electrochemical work, avoiding its dissipation as heat or fluorescence. The ability to perform electrochemical work for each electron that is transferred is termed redox potential; a negative redox potential indicates a reducing capability of the system (the system possesses available electrons), while a positive redox potential indicates an oxidizing capability of the system (the system lacks available electrons).

Photosynthetic activity of algae, which roughly account for more than 50% of global photosynthesis, makes it possible to convert the energy of PAR into biologically usable energy, by means of reduction and oxidation reactions; hence, photosynthesis and respiration must be regarded as complex redox processes.

As shown in Equation 3.3, during photosynthesis, carbon is converted from its maximally oxidized state +4 in CO_2 to 0 in strongly reduced compounds such as carbohydrates $[CH_2O]_n$, using the energy of light:

$$nCO_2 + nH_2O + \text{light} \xrightarrow{\text{Chlorophyll } a} (CH_2O)_n + nO_2 \tag{3.3}$$

In this equation, light is specified as a substrate, chlorophyll *a* is a requisite catalytic agent, and $(CH_2O)_n$ represent the organic matter reduced to the level of carbohydrate. These reduced compounds may be re-oxidized to CO_2 during respiration, liberating energy. The process of photosynthetic electron transport takes place between +0.82 eV (redox potential of the H_2O/O_2 couple) and −0.42 eV (redox potential of the CO_2/CH_2O couple).

Approximately half of incident light intensity impinging on the earth surface (0.42 kW m^{-2}) belongs to PAR. In water, as explained above, the useful energy for photo-biochemical processes is even lower and distributed within a narrower wavelength range. About 95% of the PAR impinging on algal cells is lost mainly due to the absorption by components other than chloroplasts and to the ineffectiveness of the transduction of light energy into chemical energy. Only 5% of the PAR is used by photosynthetic processes. Despite this high energy waste, photosynthetic energy transformation is the basic energy-supplying process for algae.

PHOTOSYNTHESIS

Photosynthesis encompasses two major groups of reactions. Those in the first group, the "light-dependent reactions," involve the capture of the light energy and its conversion to energy currency as NADPH and ATP. These reactions are: absorption and transfer of photon energy, trapping of this energy, and generation of a chemical potential. The latter reaction follows two routes: the first

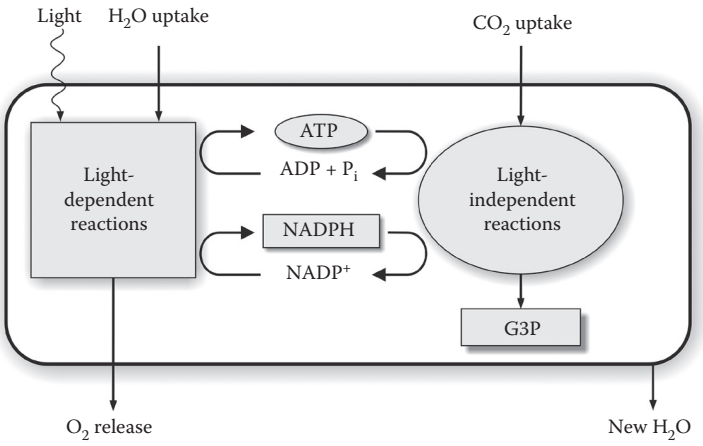

FIGURE 3.3 Schematic drawing of the photosynthetic machinery. ATP: adenosine triphosphate; ADP: adenosine diphosphate; P: phosphate; NADPH: nicotinamide adenine dinucleotide phosphate (reduced form); NADP: nicotinamide adenine dinucleotide; G3P: glyceraldehyde 3-phosphate.

one generates NADPH, thanks to the falling of the high-energy excited electron along an electron transport system; the second one generates ATP by means of a proton gradient across the thylakoid membrane. Water splitting is the source of both electrons and protons. Oxygen is released as a by-product of the water splitting. The reactions of the second group are the "light-independent reactions" and involve the sequence of reactions by which this chemical potential is used to fix and reduce inorganic carbon in triose phosphates (Figure 3.3).

LIGHT-DEPENDENT REACTIONS

Photosynthetic light reactions take place in thylakoid membranes where chromophore–protein complexes and membrane-bound enzymes are situated (Figure 3.4). The thylakoid membrane cannot be considered at all a rigid, immutable structure. It is rather a highly dynamic system, whose molecular compositions and conformation, including the spatial pattern of its components, can change very rapidly. This flexibility, is, however, combined with a high degree of order necessary for the energy-transforming processes.

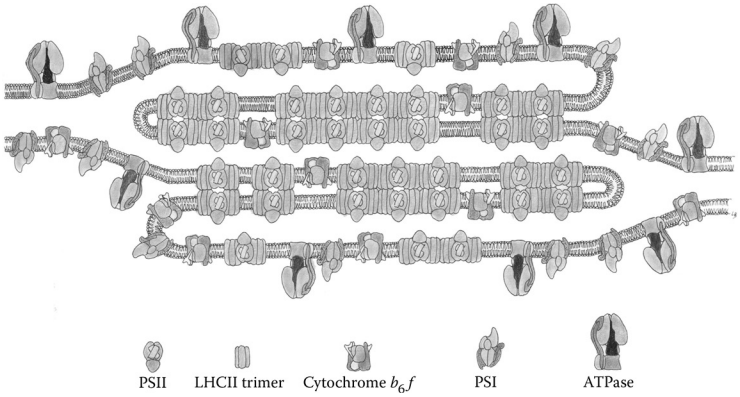

FIGURE 3.4 Model of the topology of chloroplast thylakoid membrane showing the disposition of the major intrinsic protein complexes, PSI, PSII, LHCII trimer, cytochrome b_6f dimer, and ATPase, according to Allen and Forsberg (2001).

Quantitative analysis established that the 7-nm-thick thylakoid membrane consists of ~50% lipids and 50% proteins. Galactolipids, a constituent that is specific of thylakoid membranes, make up ~40% of the lipid fraction. Chlorophylls, carotenoids, xanthophylls (when present), phycobilins (when present), phospholipids, sulfolipids, quinones, and sterols, all components occurring in a bound form, represent the remaining 10%.

Chlorophylls are the essential pigments of photosynthesis, for which they both harvest light and transduce it into chemical energy. There are five chemically distinct chlorophylls known to date, termed chlorophylls *a*, *b*, c_1, c_2, *d*, and *f*, which are present in light-harvesting complexes (LHCs) of oxygenic photosynthetic organisms (Figures 3.5 and 3.6). Chlorophyll *a* consists of a hydrophilic porphyrin head formed by four linked pyrrole rings with a magnesium atom chelated (Mg^{2+}) at the center and a hydrophobic phytol tail. Chlorophyll *b* possesses the same structure of chlorophyll *a*, but a keto group (–CH=O) is present in the second pyrrole ring instead of a methyl group ($–CH_3$). Chlorophyll *c* possesses only the hydrophilic porphyrin head without the phytol tail; chlorophyll c_2 differs from chlorophyll c_1 in possessing two vinyl groups ($–CH=CH_2$) instead of one. Chlorophyll *d* differs from chlorophyll *a* only in the C3 position at ring I, where a formyl group in chlorophyll *d* replaces the vinyl group in chlorophyll *a*. Chlorophyll *f* differs from chlorophyll *a* only in the C2 position at ring I, where a formyl group is present. Chlorophylls *a*, *b*, and *c* were identified in the nineteenth century, chlorophyll *d* was reported in 1943, but recognized only in 1996 in the cyanobacterium *Acaryochloris marina*, whereas chlorophyll *f* was discovered for the first time in the stromatolite-forming cyanobacterium *Halomicronema hongdechloris* in 2010.

Each chlorophyll has its own absorption spectrum (Figures 3.5 and 3.6). The discovery of the red-shifted chlorophylls *d* and *f* has expanded the portion of solar spectrum available for photosynthesis to 750 nm. This relatively modest increment (about 50 nm) increases the number of available photons by 19%.

Carotenoids are C_{40} hydrocarbon chains, strongly hydrophobic, with one or two terminal ionone rings, functioning as accessory pigments for energy capture and transfer and for also playing protection roles. Xanthophylls are carotenoid derivate with a hydroxyl group in the ring; they have a role in nonradiative dissipation of excess absorbed light energy (Figures 3.6 and 3.7). Phycobylins (Figure 3.8) possess the four pyrrolic rings linearly arranged, and unlike the chlorophylls they are strongly covalently bound to a protein. These are complex proteins often with more than one subunit, with more than one phycobilin as chromophore. Figure 3.9 shows the most common phycobiliproteins. They are considered accessory pigments for the operations of photosystem II (see the following paragraph). The organization of phycobiliproteins in the phycobilisome has been described in Chapter 2 (Figure 2.82).

The protein complex content consists mainly of the highly organized energy-transforming units, enzymes for the electron transport and ATP synthesis, more or less integrated into the thylakoid membrane. The energy-transforming units are two large protein complexes termed photosystems I (PSI) and II (PSII), surrounded by light-harvesting complexes (LHCs). Photons absorbed by PSI and PSII induce excitation of special chlorophylls *a*, P_{700} and P_{680} (P stands for the pigment and 700/680 stand for the wavelength in nanometer of maximal absorption), initiating translocation of an electron across the thylakoid membrane along organic and inorganic redox couples forming the electron transfer chains (ETCs). The main components of these chains are plastoquinones, cytochromes, and ferredoxin. This electron translocation process eventually leads to a reduction of $NADP^+$ to NADPH and to a transmembrane difference in the electrical potential and H^+ concentration, which drives ATP synthesis by means of an ATP synthase.

Thylakoid membranes are differentiated into stacked and unstacked regions. Stacking increases the amount of thylakoid membranes in a given volume. Both regions surround a common internal thylakoid space, but only unstacked regions make direct contact with the chloroplast stroma. The two regions differ in their content of photosynthetic assemblies; PSI and ATP synthase are located almost exclusively in unstacked regions, whereas PSII and LCHII are present mostly in stacked regions. This topology derives from protein–protein interactions rather than lipid bilayer

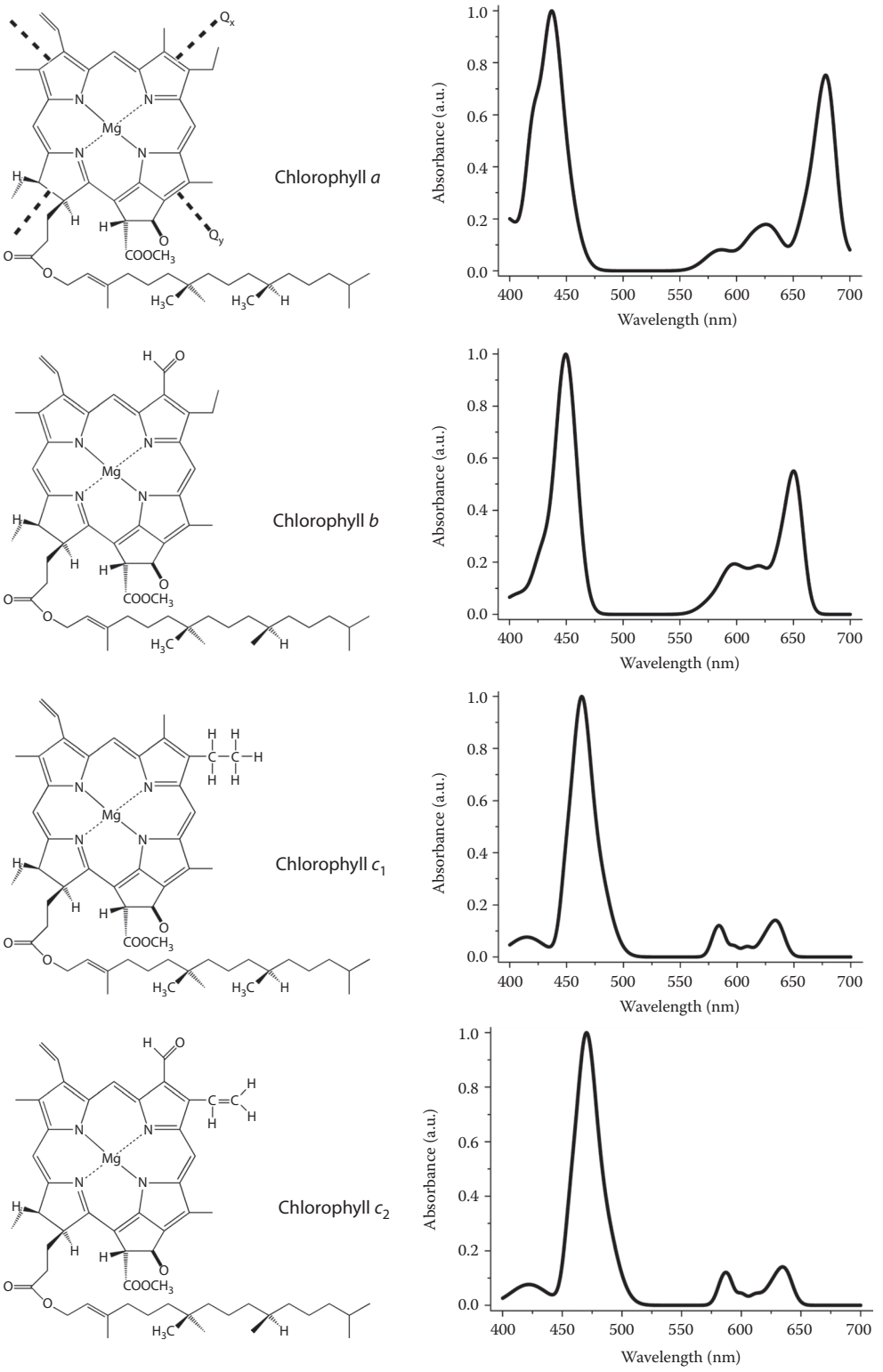

FIGURE 3.5 Structure of chlorophylls *a*, *b*, c_1, and c_2.

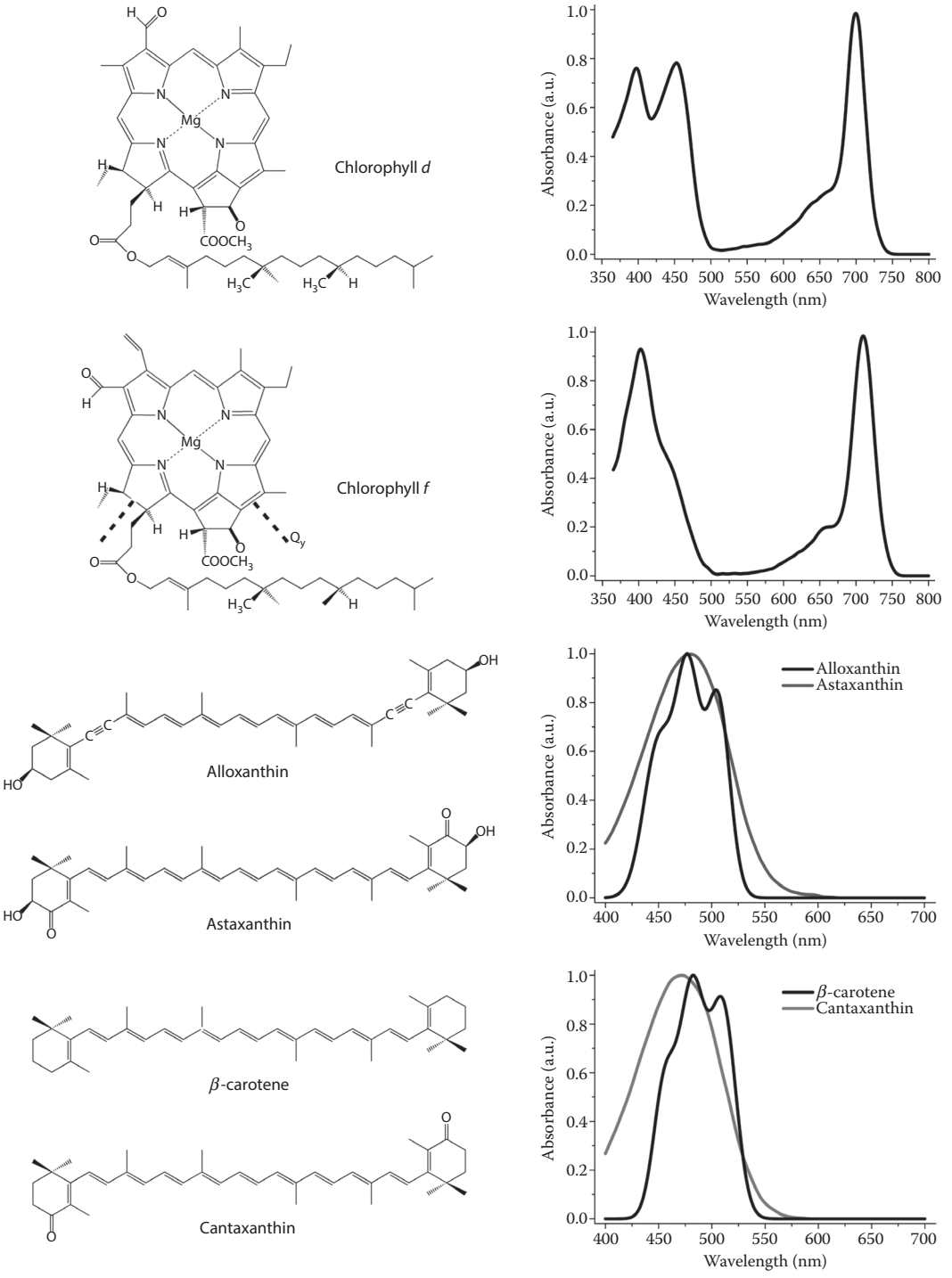

FIGURE 3.6 Structure of chlorophylls *d* and *f*, alloxanthin, astaxanthin, β-carotene, and cantaxanthin.

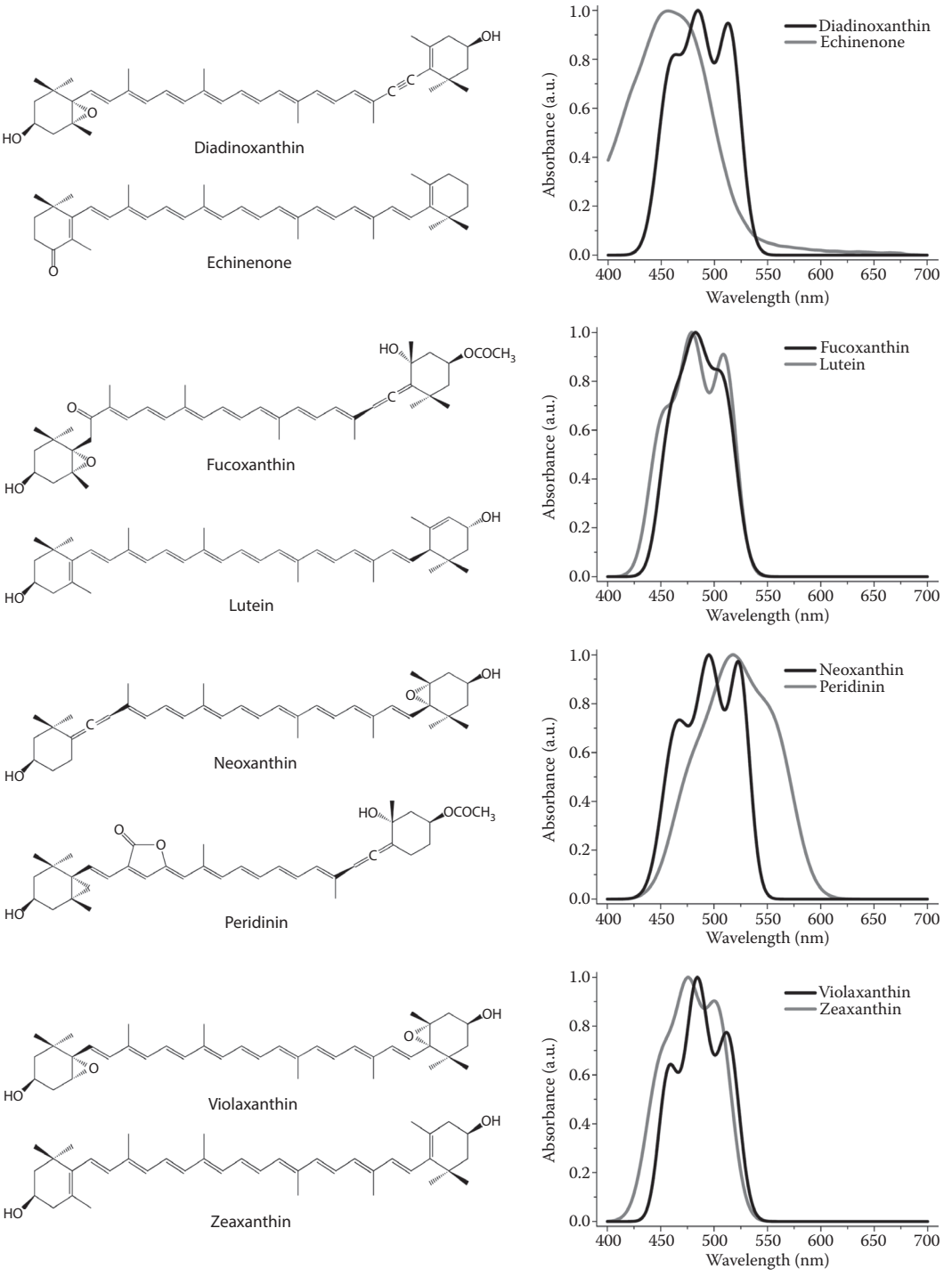

FIGURE 3.7 Structure of diadinoxanthin, echinenone, fucoxanthin, lutein, neoxanthin, peridinin, violaxanthin, and zeaxanthin.

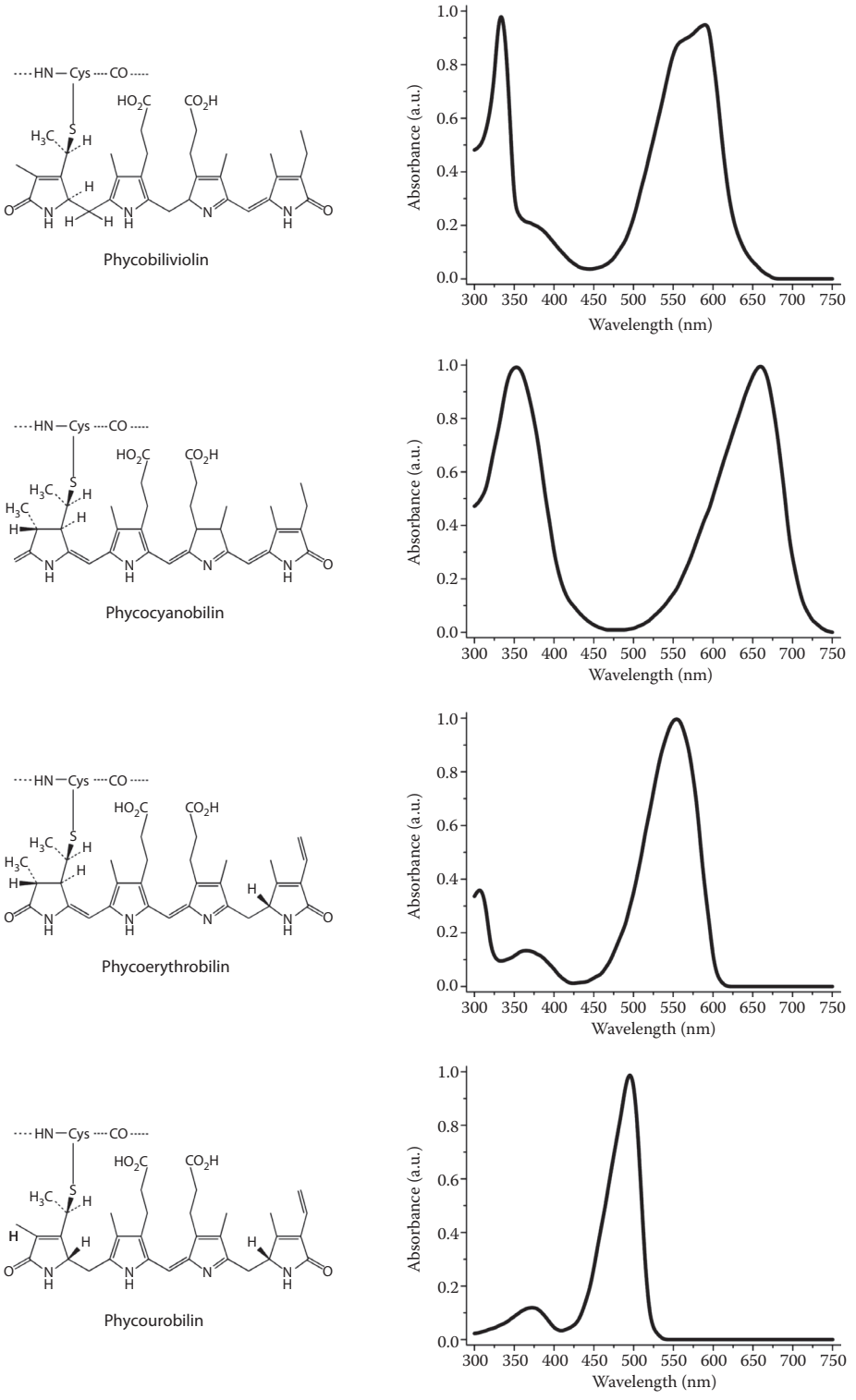

FIGURE 3.8 Structure of polypeptide-bound phycobiliviolin, phycocyanobilin, phycoerythrobilin, and phycourobilin.

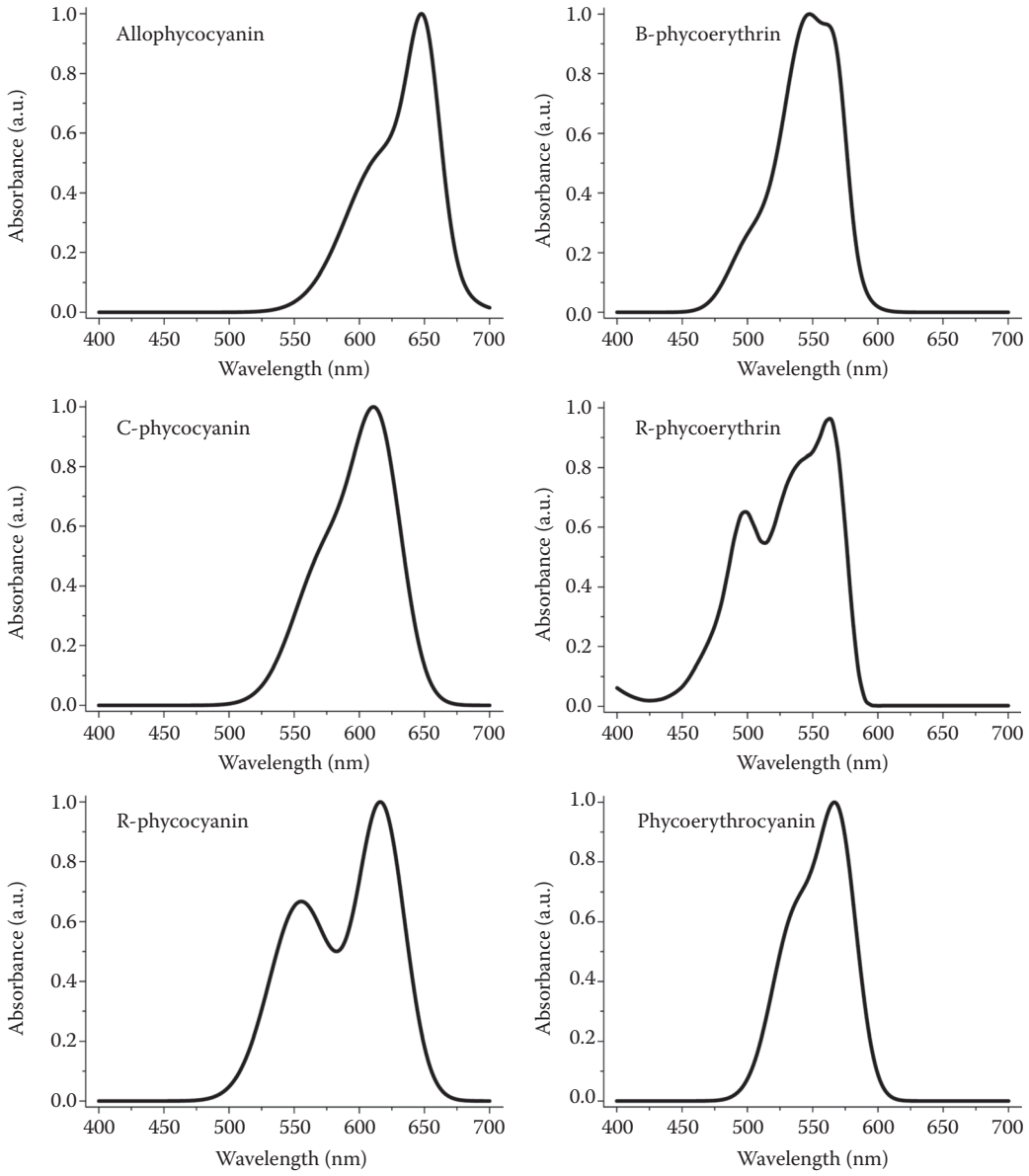

FIGURE 3.9 Structure of the main phycobiliproteins: allophycocyanin, C-phycocyanin, R-phycocyanin, B-phycoerythrin, R-phycoerythrin, and phycoerythrocyanin. The prefixes R, C, and B indicate the origins of proteins from Rhodophyta, Cyanobacteria, and Bangiales (Bangiophyceae, Rhodophyta), respectively.

interactions. A common internal thylakoid space enables protons liberated by PSII in stacked membranes to be utilized by ATP synthase molecules that are located far away in unstacked membranes. What is the functional significance of this lateral differentiation of the thylakoid membrane system? If both photosystems were present at high density in the same membrane region, a high proportion of photons absorbed by PSII would be transferred to PSI because the energy level of the excited-state P_{680*} relative to its ground-state P_{680} is higher than that of P_{700*} relative to P_{700}. A lateral separation of photosystems solve this problem by placing P_{680*} more than 100 Å away from P_{700}. The positioning of PSI in the unstacked membranes gives it direct access to the stroma for the reduction of $NADP^+$. In fact, the stroma-exposed surface of PSI, which contains the iron–sulfur proteins that

carry electrons to ferredoxin and ultimately to $NADP^+$, protrudes about 50 Å beyond the membrane surface and could not possibly be accommodated within the stacks, where adjacent thylakoids are separated by no more than 40 Å. It seems likely that ATP synthase is also located in unstacked regions to provide space for its large protruding portion and access to ADP. In contrast, the tight quarters of the appressed regions pose no problem for PSII, which interacts with a small polar electron donor (H_2O) and a highly lipid-soluble electron carrier (plastoquinone). According to the model of Allen and Forsberg (2001), the close appression of grana (stacks of thylakoids) membranes arises because the flat stroma-exposed surfaces of LCHII form recognition and contact surfaces for each other, causing opposing surfaces of thylakoids to interact. There is not steric hindrance to this close opposition of stacked grana membranes, because like LCHII, PSII itself presents a flat surface that protrudes no more than 10–20 Å beyond the membrane surface.

The functional significance of thylakoid stacking is presumably to allow a large, connected, light-harvesting antenna to form both within and between membranes. Within this antenna, excitation energy can pass between chlorophylls located in LCHII complexes that are adjacent to each other, both within a single membrane and between appressed membranes.

The degree of stacking and the proportion of different photosynthetic assemblies are regulated in response to environmental variables such as the intensity and spectral characters of incident light. The lateral distribution of LHC is controlled by reversible phosphorylation. At low light levels, LHC is bound to PSII. At high light levels, a specific kinase is activated by plastoquinol, and phosphorylation of threonine side chains of LHC leads to its release from PSII. The phosphorylated form of these light-harvesting units diffuses freely in the thylakoid membrane and may become associated with PSI to increase its absorbance coefficient (Figure 3.4).

Central to the photosynthetic process is PSII, which catalyzes one of the most thermodynamically demanding reactions in biology:

$$2H_2O \rightarrow 4e^- + 4H^+ + O_2 \tag{3.4}$$

that is, the photo-induced oxidation of water. PSII has the power to split water and use its electrons and protons to drive photosynthesis. The first ancestor bacteria carrying on anoxygenic photosynthesis probably synthesized ATP by oxidation of H_2S and FeS compounds abundant in the environment. The released energy could have been harnessed via production of a proton gradient, stimulating evolution of electron transport chains, and the reducing equivalents (electrons) generated used in CO_2 fixation and thence biosynthesis. This was the precursor of the PSI. About 2800 million years ago, the evolutionary pressure to use less strongly reducing (and therefore more abundant) source of electrons appears to have culminated in the development of the singularly useful trick of supplying the electrons to the oxidized reaction center from a tyrosine side chain, generating tyrosine cation radicals that are capable of sequential abstraction of electrons from water. Oxygenic photosynthesis, which requires the coupling in series of two distinct types of reaction centers (PSI and PSII) must have depended upon lateral transfer of genes between the evolutionary precursors of the modern sulfur bacteria (whose single reaction center resembles PSI) and those of purple bacteria (whose single reaction center resembles PSII). Thus, the cyanobacteria appeared. They were the first dominant organisms to use photosynthesis. As a by-product of photosynthesis, oxygen (O_2) was produced for the first time in abundance. Initially, oxygen released by photosynthesis was absorbed by iron (II), abundant in the sea, thus oxidizing it into insoluble iron (III) oxide (rust). Red "banded iron deposits" of iron (III) oxide are marked in marine sediments of ca. 2500 million years ago. Once most/all iron (II) had been oxidized to iron (III), then oxygen appeared in, and began to increase in the atmosphere, gradually building up from zero ca. 2500 million years ago to approximately present levels ca. 500 million years ago. This was the "oxygen revolution." Oxygen is corrosive, so prokaryotic life either became extinct or survived in anaerobic (oxygen-free) environments (and do so to this day), or evolved antioxidant-protective mechanisms. The latter could begin to use oxygen to pull electrons from organic molecules, leading to aerobic respiration. The respiratory electron

transport chain probably evolved from established photosynthetic electron transport, and the citric acid cycle probably evolved using steps from several biosynthetic pathways.

Hence, cyanobacteria marked the planet in a very permanent way and paved the way for the subsequent evolution of oxidative respiratory biochemistry. This change marks the end of the Archaean Era of the Precambrian time.

PSII and PSI: Structure, Function, and Organization

The PSII and PSI photosynthetic complexes are very similar in eukaryotic algae (and plants) and cyanobacteria, as are many elements of the light capture, electron transport, and carbon dioxide (CO_2) fixation systems. The PSI and PSII complexes contain an internal antenna-domain carrying light-harvesting chlorophylls and carotenoids both noncovalently bound to a protein moiety and a central core domain where biochemical reactions occur. In the internal antenna complexes, chlorophylls do most of the light harvesting, whereas carotenoids and xanthophylls mainly protect against excess light energy and possibly transfer the absorbed radiation. In all photosynthetic eukaryotes, PSI and PSII form a supercomplex since they are associated with an external antenna termed LHC. The main function of LHCs is the absorption of solar radiation and the efficient transmittance of excitation energy toward reaction center chlorophylls. LHCs are composed of a protein moiety to which chlorophylls and carotenoids are noncovalently bound. In eukaryotic algae, 10 distinct light-harvesting apoproteins (Lhc) can be distinguished. Four of them are exclusively associated with PSI (Lhca1–4), another four with PSII (Lhcb3–6), and two (Lhcb1 and Lhcb2) are preferentially but not exclusively associated with PSII, that is, they can shuttle between the two photosystems. The apoproteins are three membrane-spanning α-helices and are nuclear-encoded. LHCs are arranged externally with respect to the photosystems. In Cyanobacteria, Glaucophyta, Rhodophyta, and Cryptophyta, no LHCs are present and the light-harvesting function is performed by phycobiliproteins organized in phycobilisomes (Figure 2.82). These structures are peripheral to the thylakoid membranes in Cyanobacteria, Glaucophyta, and Rhodophyta (Figures 2.81 and 2.84) and localized within the lumen of thylakoids in Cryptophyta. The phycobilisome structure consists of a three-cylinder core of four stacked molecules of allophycocyanin, closed to the thylakoid membrane, on which rod-shaped assemblies of coaxially stacked hexameric molecules of only phycocyanin or both phycocyanin and phycoerythrin converge. Phycobilisomes are linked to the PSII but they can diffuse along the surface of the thylakoids, at a rate sufficient to allow movements from PSII to PSI within 100 ms. Though prokaryotes, *Prochlorococcus* sp., *Prochlorothrix* sp., and *Prochloron* sp. differ from other cyanobacteria in possessing an external chlorophyll *a* and *b* antenna, like eukaryotic algae, instead of the large extrinsic phycobilisomes.

PSII complex can be divided into two main protein superfamilies differing in the number of membrane-spanning α-helices, that is, the six-helix protein superfamily, which includes the internal antennae CP43 and CP47 (CP stands for chlorophyll–protein complex), and the five-helix proteins of the reaction center cores D1 and D2 (so-called because they were first identified as two *diffuse* bands by gel electrophoresis and staining), where ETC components are located. External antenna proteins of prochlorophytes belong to the six-helix CP43 and CP47 superfamily and not to the three-helix LHCs superfamily.

PSII is a homodimer, where the two monomers in the dimers are almost identical. The monomer consists of over 20 subunits. All the redox active cofactors involved in the activity of PSII are bound to the reaction center proteins D1 and D2. Closely associated with these two proteins are the chlorophyll *a* binding proteins CP43 and CP47, and the extrinsic luminally bound proteins of the oxygen-evolving complex. Each monomer also includes one heme *b*, one heme *c*, two plastoquinones, two pheophytins (a chlorophyll *a* without Mg^{2+}), one non-heme Fe and contains 36 chlorophylls *a* and 7 *all-trans* carotenoids assumed to be β-carotene molecules. Eukaryotic and cyanobacterial PSII are structurally very similar at the level of both their oligomeric states and organization of the transmembrane helices of their major subunits. The eukaryotic PSII dimer is flanked by two clusters of

Lhcb proteins. Each cluster contains two trimers of Lchb1, Lchb2, and Lchb3 and the other three monomers, Lchb4, Lchb5, and Lchb6.

The reactions of PSII are powered by light-driven primary and secondary electron-transfer processes across the reaction center (D1 and D2 subunits). Upon illumination, an electron is dislodged from the excited primary electron donor P_{680}, a chlorophyll *a* molecule located towards the luminal surface. The electron is quickly transferred toward the stromal surface to the final electron acceptor, a plastoquinone, via a pheophytin. After accepting two electrons and undergoing protonation, plastoquinone is reduced to plastoquinol, and it is then released from PSII into the membrane matrix. The cation P_{680}^{+} is reduced by a redox active tyrosine, which in turn is reduced by a Mn ion within a cluster of four. When the $(Mn)_4$ cluster accumulates four oxidizing equivalents (electrons), two water molecules are oxidized to yield one molecule of O_2 and four protons. All the redox active cofactors involved in the electron-transfer processes are located on the D1 side of the reaction center.

PSI complex possess only an 11-helix PsaA and PsaB protein superfamily. Each 11-transmembrane helices subunit has six N-terminal transmembrane helices that bind light-harvesting chlorophylls and carotenoids and act as internal antennae and five C-terminal transmembrane helices that bind Fe_4S_4 clusters as terminal electron acceptors. The N-terminal part of the PsaA and PsaB proteins are structurally and functionally homologs to CP43 and CP47 proteins of PSII; the C-terminal part of the PsaA and PsaB proteins are structurally and functionally homologs to D1 and D2 proteins of PSII. Eukaryotic PSI is a monomer that is loosely associated with the Lcha moiety, with a deep cleft between them. The four antenna proteins assemble into two heterodimers composed by Lhca1 and Lhca4, and homodimers composed by Lhca2 and Lhca3. These dimers create a half-moon-shaped belt that docks to PsaA and PsaB and to other 12 proteic subunits of the PSI, termed PsaC to PsaN that contribute to the coordination of antenna chromophores. On the whole, PSI binds approximately 200 chromophore molecules. The cyanobacterial PSI exists as a trimer. One monomer consists of at least 12 different protein subunits (PsaA, PsaB, PsaC, PsaD, PsaE, PsaF, PsaI, PsaJ, PsaK, PsaL, PsaM, and PsaX) coordinating more than 100 chromophores.

After primary charge separation initiated by excitation of the chlorophyll *a* pair P_{700}, the electron passes along the ETC consisting of another chlorophyll *a* molecule, a phylloquinone, and the Fe_4S_4 clusters. At the stromal side, the electron is donated by Fe_4S_4 to ferredoxin and then transferred to $NADP^{+}$ reductase. The reaction cycle is completed by re-reduction of P_{700}^{+} by plastocyanin (or the interchangeable cytochrome c_6) at the inner (lumenal) side of the membrane. The electron carried by plastocyanin is provided by PSII by way of a pool of plastoquinones and the cytochrome b_6f complex.

Photosynthetic eukaryotes such as Chlorophyta, Rhodophyta, and Glaucophyta have evolved by primary endosymbiosis involving a eukaryotic host and a prokaryotic endosymbiont. All other algae groups have evolved by secondary (or higher order) endosymbiosis between a simple eukaryotic alga and a nonphotosynthetic eukaryotic host. Although the basic photosynthetic machinery is conserved in all these organisms, it should be emphasized that PSI does not necessarily have the same composition and fine-tuning in all of them. The subunits that have only been found in eukaryotes, that is, PsaG, PsaH, and PsaN, have actually only been found in plants and in Chlorophyta. Other groups of algae appear to have a more cyanobacteria-like PSI. PsaM is also peculiar since it has been found in several groups of algae including green algae, in mosses and in gymnosperms. Thus, the PsaM subunit appears to be absent only in angiosperms. With respect to the peripheral antenna proteins, algae are in fact very divergent. All photosynthetic eukaryotes have Lhcs that belong to the same class of proteins. However, the Lhc*a* associated with PSI appear to have diverged relatively early and the stoichiometry and interaction with PSI may well differ significantly between species. Even the green algae do not possess the same set of four Lhc*a* subunits that is found in plants.

Are all these LHCs necessary? They substantially increase the light-harvesting capacity of both photosystems by increasing the photon-collecting surface with an associated resonance energy transfer to reaction centers, facilitated by specific pigment–pigment interactions. This process is related to the transition dipole–dipole interactions between the involved donor and acceptor antenna molecules that can be weakly or strongly coupled depending on the distance between and relative

orientation of these dipoles. The energy migrates along a spreading wave since the energy of the photon can be found at a given moment in one or the other of the many resonating antenna molecules. This wave describes merely the spread of the probability of finding the photon in different chlorophyll antenna molecules. Energy resonance occurs in the chromophores of the antenna molecules at the lowest electronic excited state available for an electron, since only this state has a life time (10^{-8} s) long enough to allow energy migration (10^{-12} s). The radiation-less process of energy transfer occurs toward pigments with lower excitation energy (longer-wavelength absorption bands). Within the bulk of pigment–protein complexes forming the external and internal antenna system, the energy transfer is directed to the chlorophyll *a* with an absorption peak at longest wavelengths. Special chlorophylls *a* (P_{680} at PSII and P_{700} at PSI) located in the reaction center cores represent the final step end of the photon trip, since once excited ($P_{680} + h\nu \rightarrow P_{680}^{*}$; $P_{700} + h\nu \rightarrow P_{700}^{*}$) they become redox active species ($P_{680}^{*} \rightarrow P_{680}^{+} + e^{-}$; $P_{700}^{*} \rightarrow P_{700}^{+} + e^{-}$), that is, each donor releases one electron per excitation and activates different electron transport chains.

It is worthwhile to emphasize that in the case of *Acaryochloris marina*, chlorophyll *a* is largely replaced by red-shifted chlorophyll *d* (it accounts for about 98% of the total chlorophylls) in the reaction centers and LHCs. Hence, the special chlorophylls in the case of this cyanobacteria will be P_{713} and P_{740}.

For an image gallery of the three-dimensional models of the two photosystems and LHCs in prokaryotic and eukaryotic algae, refer to the websites of Jon Nield and James Barber at the Imperial College of London (UK).

ATP Synthase

ATP production was probably one of the earliest cellular processes to evolve, and the synthesis of ATP from two precursor molecules is the most prevalent chemical reaction in the world. The enzyme that catalyzes the synthesis of ATP is the ATP synthase or F_0F_1–ATPase, one of the most ubiquitous proteins on earth. The F_1F_0–ATPases comprise a huge family of enzymes with members found not only in the thylakoid membrane of chloroplasts, but also in the bacterial cytoplasmic membrane and in the inner membrane of mitochondria. The source of energy for the functioning of ATP synthase is provided by photosynthetic metabolism in the form of a proton gradient across the thylakoid membrane, that is, a higher concentration of positively charged protons in the thylakoid lumen than in the stroma.

The F_0F_1–ATPase molecule is divided into two portions termed F_1 and F_0. The F_0 portion is embedded in the thylakoid membrane, while the F_1 portion projects into the lumen. Each portion is in turn made up of several different proteins or subunits. In F_0, the subunits are named *a*, *b*, and *c*. There is one *a* subunit, two *b* subunits, and 9–12 *c* subunits. The large *a* subunit provides the channel through which H^+ ions flow back into the stroma. Rotation of the *c* subunits, which form a ring in the membrane, is chemically coupled to this flow of H^+ ions. The *b* subunits are believed to help stabilize the F_0F_1 complex by acting as a tether between the two portions. The subunits of F_1 are called α, β, γ, δ, and ε. F_1 has three copies each of α and β subunits which are arranged in an alternating configuration to form the catalytic "head" of F_1. The γ and ε subunits form an axis that links the catalytic head of F_1 to the ring of *c* subunits in F_0. When proton translocation in F_0 causes the ring of *c* subunits to spin, the γ–ε axis also spins because it is bound to the ring. The opposite end of the γ subunit rotates within the complex of α and β subunits. This rotation causes important conformational changes in the β subunits resulting in the synthesis of ATP from ADP and P_i (inorganic phosphate) and to its release.

ETC Components

Components of the electron transport system in order are plastoquinone, cytochrome b_6f complex, plastocyanin, and ferredoxin. Each of the components of the electron transport chain has the ability to transfer an electron from a donor to an acceptor, though plastoquinone also transfers a proton. Each of these components undergoes successive rounds of oxidation and reduction, receiving an electron from the PSII and donating the electron to PSI.

Plastoquinone refers to a family of lipid-soluble benzoquinone derivatives with an isoprenoid side chain. In chloroplasts, the common form of plastoquinone contains nine repeating isoprenoid units. Plastoquinone possesses varied redox states, which together with its ability to bind protons and with its small size enables it to act as a mobile electron carrier shuttling hydrogen atoms from PSII to the cytochrome b_6f complex.

Plastoquinone is present in the thylakoid membrane as a pool of 6–8 molecules per PSII. Plastoquinone exists as quinone A (Q_A) and quinone B (Q_B); Q_A is tightly bound to the reaction center complex of PSII and it is immovable. It is the primary stable electron acceptor of PSII, and it accepts and transfers one electron at a time. Q_B is a loosely bound molecule, which accepts two electrons and then takes on two protons before it detaches and becomes Q_BH_2, the mobile reduced form of plastoquinone (plastoquinol). Q_BH_2 is mobile within the thylakoid membrane, allowing a single PSII reaction center to interact with a number of cytochrome b_6f complexes.

Plastoquinone plays an additional role in the cytochrome b_6f complex, operating in a complicated reaction sequence known as a Q-cycle. When Q_B is reduced in PSII, it not only receives two electrons from Q_A, but it also picks up two protons from the stroma matrix and becomes Q_BH_2. It is able to carry both electrons and protons (e^- and H^+ carrier). At the cytochrome b_6f complex level, it is then oxidized, but FeS and cytochrome b_6 can only accept electrons and not protons. So, the two protons are released into the lumen. The Q-cycle of the cytochrome b_6f complex is great because it provides extra protons into the lumen. Here two electrons travel through the two hemes of cytochrome b_6 and then reduce Q_B on the stroma side of the membrane. The reduced Q_B takes on two protons from the stroma, becoming Q_BH_2, which migrates to the lumen side of the cytochrome b_6f complex where it is again oxidized, releasing two more protons into the lumen. Thus the Q-cycle allows formation of more ATP. This Q-cycle links the oxidation of plastoquinol (Q_BH_2) at one site on the cytochrome b_6f complex to the reduction of plastoquinone at a second site on the complex in a process that contributes additional free energy to the electrochemical proton potential.

The cytochrome b_6f complex is the intermediate protein complex in linear photosynthetic electron transport. It essentially couples PSII and PSI and also provides the means of proton gradient formation by using cytochrome groups as redox centers in the electron transport chain, thereby separating the electron/hydrogen equivalent into its electron and proton components. The electrons are transferred to PSI via plastocyanin and the protons are released into the thylakoid lumen of the chloroplast. The electron transport from PSII to PSI via cytochrome b_6f complex occurs in about 7 ms, representing the rate-limiting step of the photosynthetic process.

The cytochrome b_6f exists as a dimer of 217 kDa. The monomeric complex contains four large subunits (18–32 kDa), including cytochrome f, cytochrome b_6, the Rieske FeS iron–sulfur protein (ISP), and subunit IV as well as four small hydrophobic subunits, PetG, PetL, PetM, and PetN. The monomeric unit contains 13 transmembrane helices: four in cytochrome b_6 (helices A–D); three in subunit IV (helices E–G); and one each in cytochrome f, the ISP, and the four small hydrophobic subunits PetG, PetL, PetM, and PetN. The monomer includes four hemes, one [2Fe-2S] cluster, one chlorophyll a, one β-carotene, one plastoquinone. The extrinsic domains of cytochrome f and the ISP are on the luminal side of the membrane and are ordered in the crystal structure. Loops and chain termini on the stromal side are less well ordered. The ISP contributes to dimer stability by domain swapping, its transmembrane helix obliquely spans the membrane in one monomer, and its extrinsic domain is part of the other monomer. The two monomers form a protein-free central cavity on each side of the transmembrane interface.

Cytochrome c_6 is a small soluble electron carrier. It is a highly α-helical heme-containing protein. It is located on the luminal side of the thylakoid membrane where it catalyzes the electron transport from the membrane-bound cytochrome b_6f complex to PSI. It is the sole electron carrier in some cyanobacteria.

Plastocyanin operates in the inner aqueous phase of the photosynthetic vesicle, transferring electrons from cytochrome f to PSI. It is a small protein (10 kDa) composed of a single polypeptide that is coded for in the nuclear genome. Plastocyanin is a β-sheet protein with copper as the central ion

that is ligated to four residues of the polypeptide. The copper ion serves as a one-electron carrier with a midpoint redox potential (0.37 eV) near that of cytochrome *f*. Plastocyanin shuttles electrons from the cytochrome b_6f complex to PSI by diffusion. Plastocyanin is more common in green algae and completely substitutes for cytochrome c_6 in the chloroplasts of higher plants. In cyanobacteria and green algae, where both cytochrome c_6 and plastocyanin are encoded, the alternative expression of the homologous protein is regulated by the availability of copper.

Ferredoxin is a small protein (11 kDa) and has the distinction of being one of the strongest soluble reductants found in cells (midpoint redox potential = −0.42 eV). The amino acid sequence for ferredoxin from different species is known as well as the three-dimensional structure. Plants contain different forms of ferredoxin, all of which are encoded in the nuclear genome. In some algae and cyanobacteria, ferredoxin can be replaced by a flavoprotein. Ferredoxin operates in the stromal aqueous phase of the chloroplast, transferring electrons from PSI to a membrane-associated flavoprotein, known as FNR. A 2Fe-2S cluster, ligated by four cysteine residues, serves as one-electron carrier.

Once an electron reaches ferredoxin, however, the electron pathway branches, enabling redox free energy to enter other metabolic pathways in the chloroplast. For example, ferredoxin can transfer electrons to nitrite reductase, glutamate synthase, and thioredoxin reductase.

Electron Transport: The Z-Scheme

The fate of the released electrons is determined by the sequential arrangement of all the components of PSII and PSI, which are connected by a pool of plastoquinones, the cytochrome b_6f complex and the soluble protein cytochrome c_6 and plastocyanin cooperating in series. The electrons from PSII are finally transferred to the stromal side of PSI and used to reduce $NADP^+$ to NADPH, which is catalyzed by ferredoxin-$NADP^+$ oxidoreductase (FNR). In this process, water acts as an electron donor to the oxidized P_{680} in PSII, and dioxygen (O_2) evolves as a by-product.

Photosystem II uses light energy to drive two chemical reactions: the oxidation of water and the reduction of plastoquinone. Photochemistry in PSII is initiated by charge separation between P_{680} and pheophytin, creating the redox couple P_{680}^+/$Pheo^-$. The primary charge separation reaction takes only a few picoseconds. Subsequent electron-transfer steps prevent the separated charges from recombining by transferring the electron from pheophytin to a plastoquinone molecule within 200 ps. The electron on Q_A^- is then transferred to the Q_B-site. As already stated, plastoquinone at the Q_B-site differs from plastoquinone at the Q_A-site in that it works as a two-electron acceptor and becomes fully reduced and protonated after two photochemical turnovers of the reaction center. The full reduction of plastoquinone at the Q_B-site requires the addition of two electrons and two protons. The reduced plastoquinone (plastoquinol, Q_3H_2) then unbinds from the reaction center and diffuses in the hydrophobic core of the membrane, after which an oxidized plastoquinone molecule finds its way to the Q_B-binding site and the process is repeated. Because the Q_B-site is near the outer aqueous phase, the protons added to plastoquinone during its reduction are taken from the outside the membrane. Electrons are passed from Q_3H_2 to a membrane-bound cytochrome b_6f, concomitant with the release of two protons to the luminal side of the membrane. The cytochrome b_6f then transfers one electron to a mobile carrier in the thylakoid lumen, either plastocyanin or cytochrome c_6. This mobile carrier serves as an electron donor to PSI reaction center, the P_{700}. Upon photon absorption by PSI, a charge separation occurs with the electron fed into a bound chain of redox sites: a chlorophyll *a* (A_0), a quinone acceptor (A_1), and then a bound Fe–S cluster, and then two Fe–S cluster in ferredoxin, a soluble mobile carrier on the stromal side. Two ferredoxin molecules can reduce $NADP^+$ to NADPH, via the flavoprotein ferredoxin–$NADP^+$ oxidoreductase. NADPH is used as a redox currency for many biosynthesis reactions such as CO_2 fixation. The energy conserved in a mole of NADPH is about 52.5 kcal, while in an ATP mole is 7.3 kcal.

The photochemical reaction triggered by P_{700} is a redox process. In its ground state, P_{700} has a redox potential of 0.45 eV and can take up an electron from a suitable donor, hence it can perform

an oxidizing action. In its excited state, it possesses a redox potential of more than −1.0 eV and can perform a reducing action donating an electron to an acceptor, and becoming P_{700}^+. The couple P_{700}/P_{700}^+ is thus a light-dependent redox enzyme and possesses the ability to reduce the most electron-negative redox system of the chloroplast, the ferredoxin–$NADP^+$ oxidoreductase (redox potential = −0.42 eV). On the other hand, P_{700} in its ground state (redox potential = 0.45 eV) is not able to oxidize, that is, to take electrons from water that has a higher redox potential (0.82 eV). The transfer of electrons from water is driven by the P_{680} at PSII, which in its ground state has a sufficiently positive redox potential (1.22 eV) to oxidize water. On its excited state, the P_{680} at PSII reaches a redox potential of about −0.60 eV that is enough to donate an electron to a plastoquinone (redox potential = 0 eV) and then via cytochrome b_6f complex to P_{700}^+ at PSI so that it can return to P_{700} and be excited once again. This reaction pathway is called the "Z scheme of photosynthesis," because the redox diagram from P_{680} to P_{700} looks like a big "Z" (Figure 3.10).

From this scheme, it is evident that only approximately one-third of the energy absorbed by the two primary electron donors P_{680} and P_{700} is turned into chemical form. A 680-nm photon has an energy of 1.82 eV, a 700-nm photon has an energy of 1.77 eV (total = 3.59 eV), that is, three times more than the energy sufficient to change the potential of an electron by 1.24 eV, from the redox potential of the water (0.82 eV) to that of ferredoxin–$NADP^+$ oxidoreductase (−0.42 eV).

It is worthwhile to emphasize that any photon that is absorbed by any chlorophyll molecules is energetically equivalent to a red photon since the extra energy of an absorbed photon of shorter wavelengths (<680 nm) is lost during the quick fall to the red energy level representing the lowest excited level.

Proton Transport: Mechanism of Photosynthetic Phosphorylation

The interplay of PSI and PSII leads to the transfer of electrons from H_2O to NADPH and the concomitant generation of proton gradient across the thylakoid membrane for ATP synthesis. The thylakoid space becomes markedly acidic, approaching pH 4. The light-induced transmembrane proton gradient is about 3.5 pH units. The generation of these protons follows two routes:

- Four protons are released in the thylakoid space for the splitting of two water molecules and the release of one oxygen molecule.
- The transport of four electrons through the cytochrome b_6f complex leads to the translocation of eight protons from the stroma to the thylakoid space.

Therefore, about 12 protons for each O_2 molecule released are translocated. The proton-motive force Δp, that is, the force created by the accumulation of hydrogen ions on one side of the thylakoid membrane, consists of a pH gradient contribution and a membrane-potential contribution. In chloroplasts, nearly all of Δp arise from the pH gradient, whereas in the mitochondria the contribution from the membrane potential is larger. This difference is due to the thylakoid membrane permeability to Cl^- and Mg^{2+}. The light-induced transfer of H^+ into the thylakoid space is accompanied by the transfer of either Cl^- in the same direction or Mg^{2+} in the opposite direction (1 per 2 H^+). Consequently, electrical neutrality is maintained and no membrane potential is generated. A pH of 3.5 units across the thylakoid membrane correspond to Δp of 0.22 V or a ΔG (change in Gibbs free energy) of −4.8 kcal/mol. The change in Gibbs free energy associated with a chemical reaction is a useful indicator of whether the reaction will proceed spontaneously. This energy is called free energy because it is the energy that will be released or freed up to do work. Since the change in free energy is equal to the maximum useful work which can be accomplished by the reaction, then a negative ΔG associated with a reaction indicates that it can happen spontaneously. About three protons flow through the F_0F_1 ATPase complex per ATP synthesized, which corresponds to a free energy input of 14.4 kcal per mole of ATP, but in which only 7.3 kcal are stored in the ATP molecule with a yield of about 50%. No ATP is synthesized if the pH gradient is less than two units because the gradient force

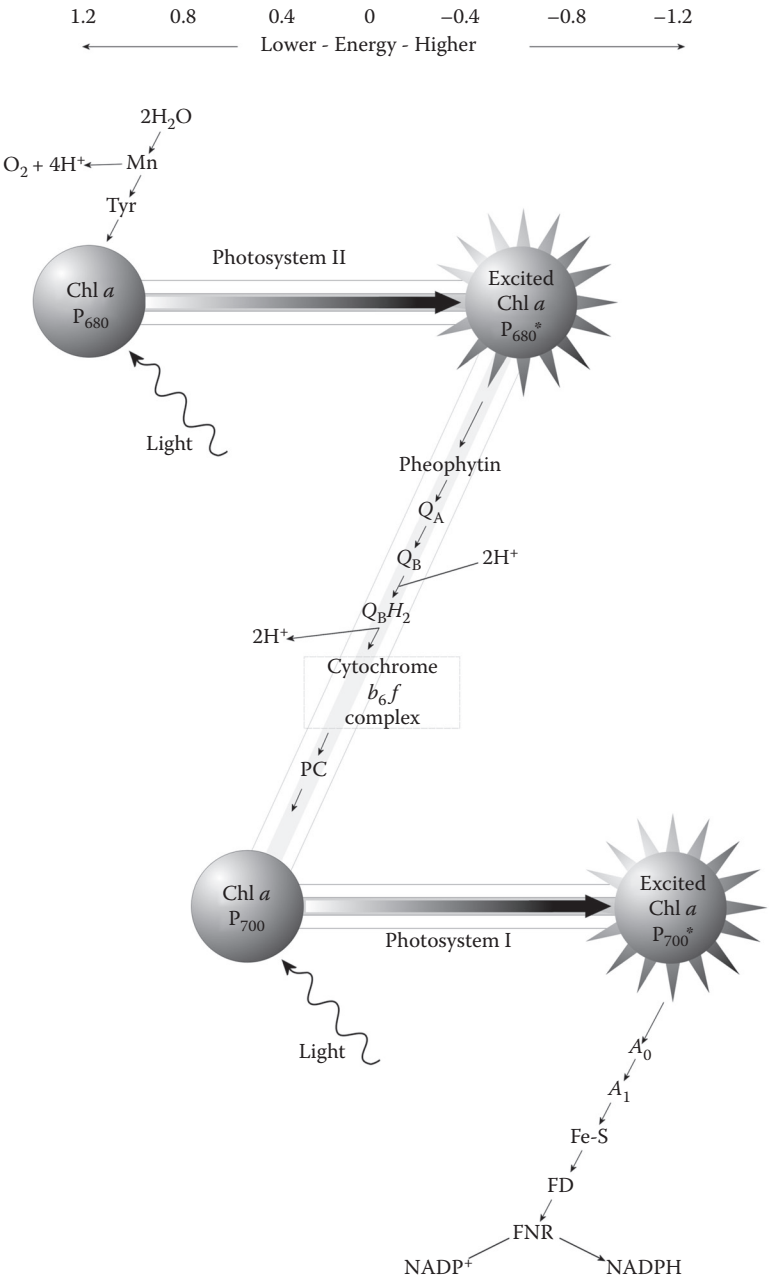

FIGURE 3.10 Schematic drawing of the Z scheme of photosynthetic electron transport, with the positions of the participants on the oxido-reduction scale.

is then too small. The newly synthesized ATP is released into the stromal space. Likewise, NADPH formed by PSI is released into the stromal space. Thus, ATP and NADPH, the products of light reactions of photosynthesis, are appropriately positioned for the subsequent light-independent reactions, in which CO_2 is converted into carbohydrates. The overall reaction can be expressed as

$$4NADP^+ + 2H_2O + 4ADP + 4P_i \xrightarrow{8\,\text{photons and } 4e^-} 4NADPH + 4ATP + O_2 \quad (3.5)$$

This equation implies that each H_2O is split in the thylakoids under the influence of light to give off $1/2O_2$ molecule and that the two electrons thus freed are then transferred to two molecules of $NADP^+$, along with H^+, to produce the strong reducing agent NADPH. Two molecules of ATP can be simultaneously formed from two ADP and two inorganic phosphates (P_i) so that the energy is stored in high-energy compounds. NADPH and ATP are the assimilatory power required to reduce CO_2 to carbohydrates in the light-independent phase. The generation of ATP following this route is termed noncyclic phosphorylation since electrons are just transported from water to $NADP^+$ and do not come back.

An alternative pathway for ATP production is cyclic phosphorylation, in which electrons from PSI cycle in a closed system through the phosphorylation sites and ATP is the only product formed. Electron arising from P_{700} are transferred to ferredoxin and then to the cytochrome b_6f complex. Protons are pumped by this complex as electrons return to the oxidized form of reaction center P_{700} through plastocyanine. This cyclic phosphorylation takes place when NADP is unavailable to accept electrons from reduced ferredoxin because of a very high ratio of NADPH to $NADP^+$.

The electrochemical potential of the proton gradient drives the synthesis of ATP through an ATP-synthase situated, as we have seen, anisotropically in the thylakoid membrane.

Pigment Distribution in PSII and PSI Super-Complexes of Algal Division

Absorption spectra can give us information about the spectral range in which pigment molecules organized in the thylakoid membranes capture photons. Absorption spectra in the visible range, from 400 to 700 nm, have been measured *in vivo* on photosynthetic compartments (thylakoid membranes, chloroplasts) of single cells belonging to each algal division. Each spectrum represents the envelope of the real absorption data and is coupled to the plot of the fourth-derivative absorption spectrum. This mathematical tool allows the resolution of absorption maxima relative to the different components of the pigment moiety characterizing the division, which cannot be detected in the envelope spectrum because of the overlapping of their multiple spectra. These components have been grouped and related to the following pigment classes: chlorophylls *a*, *b*, c_1 c_2, *d*, and *f*, carotenoids, xanthophylls, cytochromes, and phycobiliproteins. Each pigment possesses its own distinctive absorption spectrum in the visible range, which have been decomposed in its Gaussian bands and relative absorption maxima. By relating the absorption maxima resolved by means of fourth-derivative analysis with the absorption maxima of the Gaussian bands of the different pigments, it is possible to predict the presence of a specific pigment in an alga and to give an unknown alga a plausible taxonomic framing.

Chlorophylls and cytochromes always show the same absorption maxima independent of the algal division, though the intensity of their absorption bands may change; phycobiliproteins, carotenoids, and xanthophylls show a variable distribution of their single components, which is characteristic of each algal division. Figures 3.11 through 3.14 show the absorption spectra of the photosynthetic compartments in all the different algal divisions. The absorption spectrum of the tissue of a higher plant, a lawn daisy (*Bellis perennis*), is shown for highlighting the uniformity of the pigment distribution throughout the algal green lineage and plants (Figure 3.15).

It should be stressed that all the pigments other than chlorophyll *a* perform two main functions: protection of photosynthetic assemblies from photosensitization processes (mainly carotenoids); absorption of light at wavelengths other than those absorbed by chlorophyll *a* and transfer of its energy to P_{680} and P_{700}.

LIGHT-INDEPENDENT REACTIONS

We have seen that NADPH and ATP are produced in the light phase of photosynthesis. The next phase of photosynthesis involves the fixation of CO_2 into carbohydrates. Although many textbooks

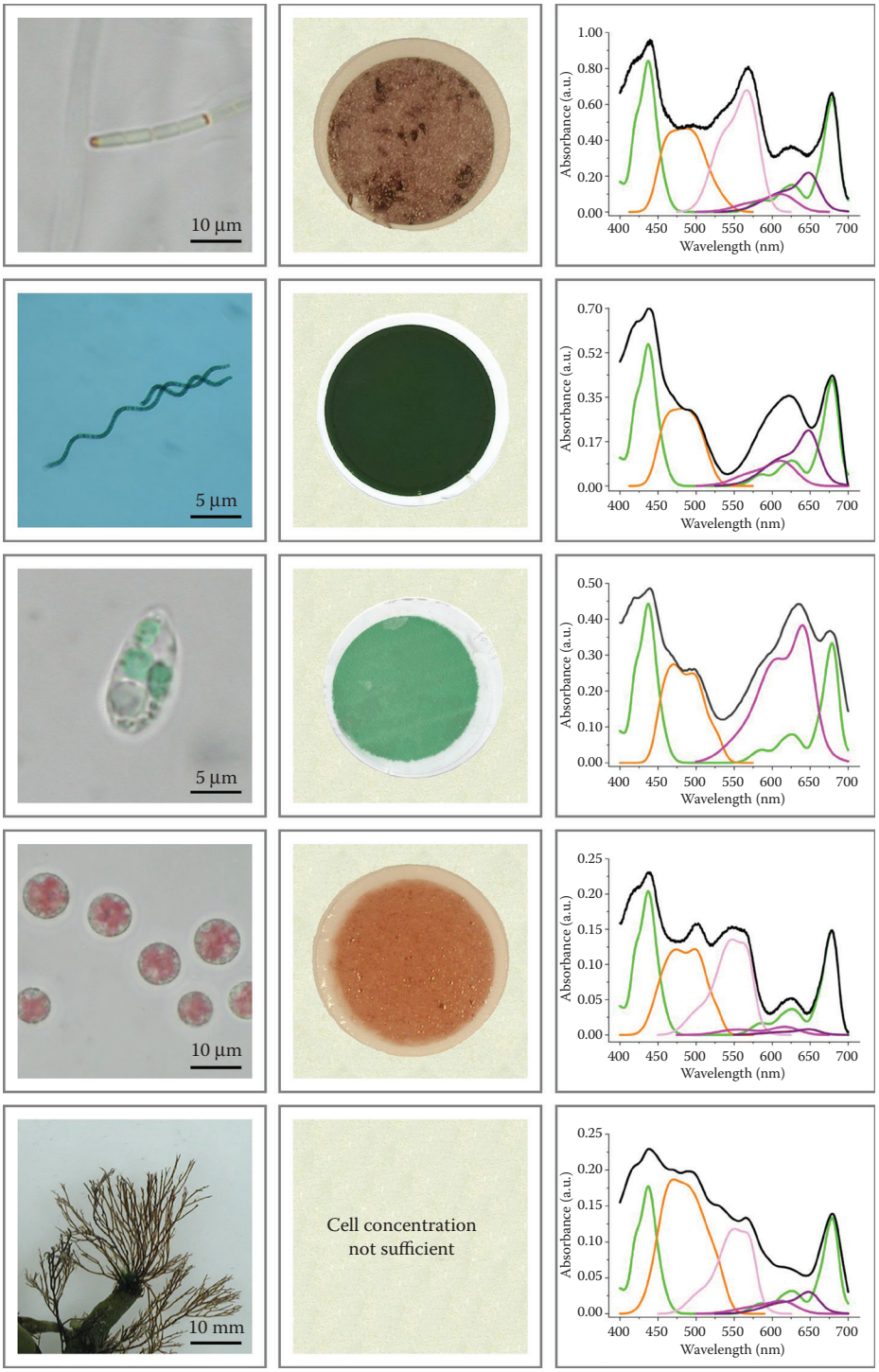

FIGURE 3.11 *In vivo* absorption spectra of photosynthetic compartments of *Leptolyngbya* (Cyanobacteria), *Arthrospira* (Cyanobacteria), *Cyanophora* (Glaucophyta), *Porphyridium* (Rhodophyta), *Polysiphonia lanosa* (Rhodophyta), from top to the bottom. Each series shows the sample, the color of the culture on filter, and the absorption spectrum. Bright green line: chlorophyll *a*; orange line: carotenoids and xanthophylls; purple lines: phycobiliproteins.

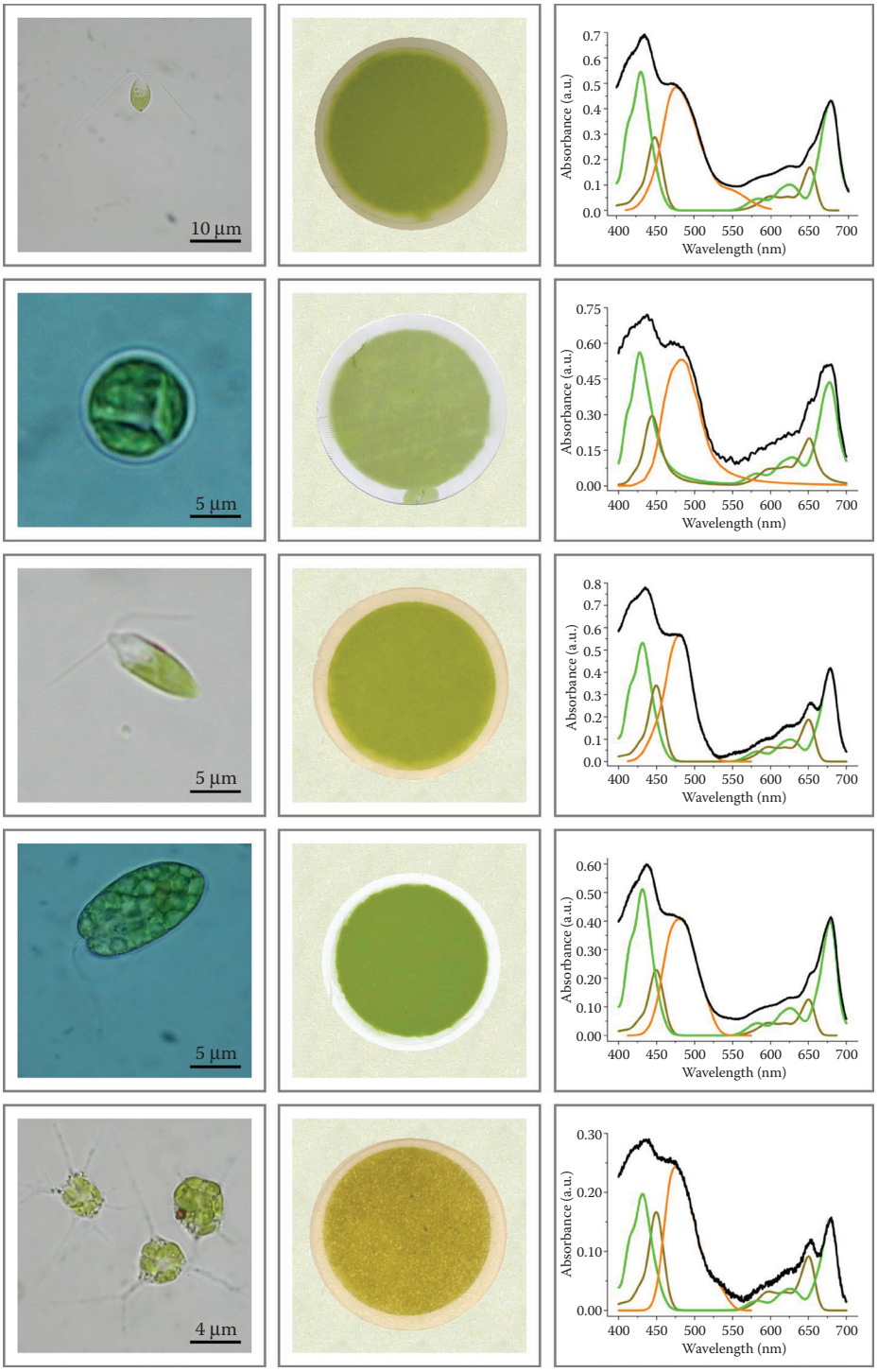

FIGURE 3.12 *In vivo* absorption spectra of photosynthetic compartments of *Tetraflagellochloris mauritanica* (Chlorophyta), *Chlorella* (Chlorophyta), *Dunaliella* (Chlorophyta), *Tetraselmis* (Chlorophyta), and *Gymnochlora* (Chlorarachniophyceae), from top to the bottom. Each series shows the sample, the color of the culture on filter, and the absorption spectrum. Bright green line: chlorophyll *a*; olive-green line: chlorophyll *b*; orange line: carotenoids and xanthophylls.

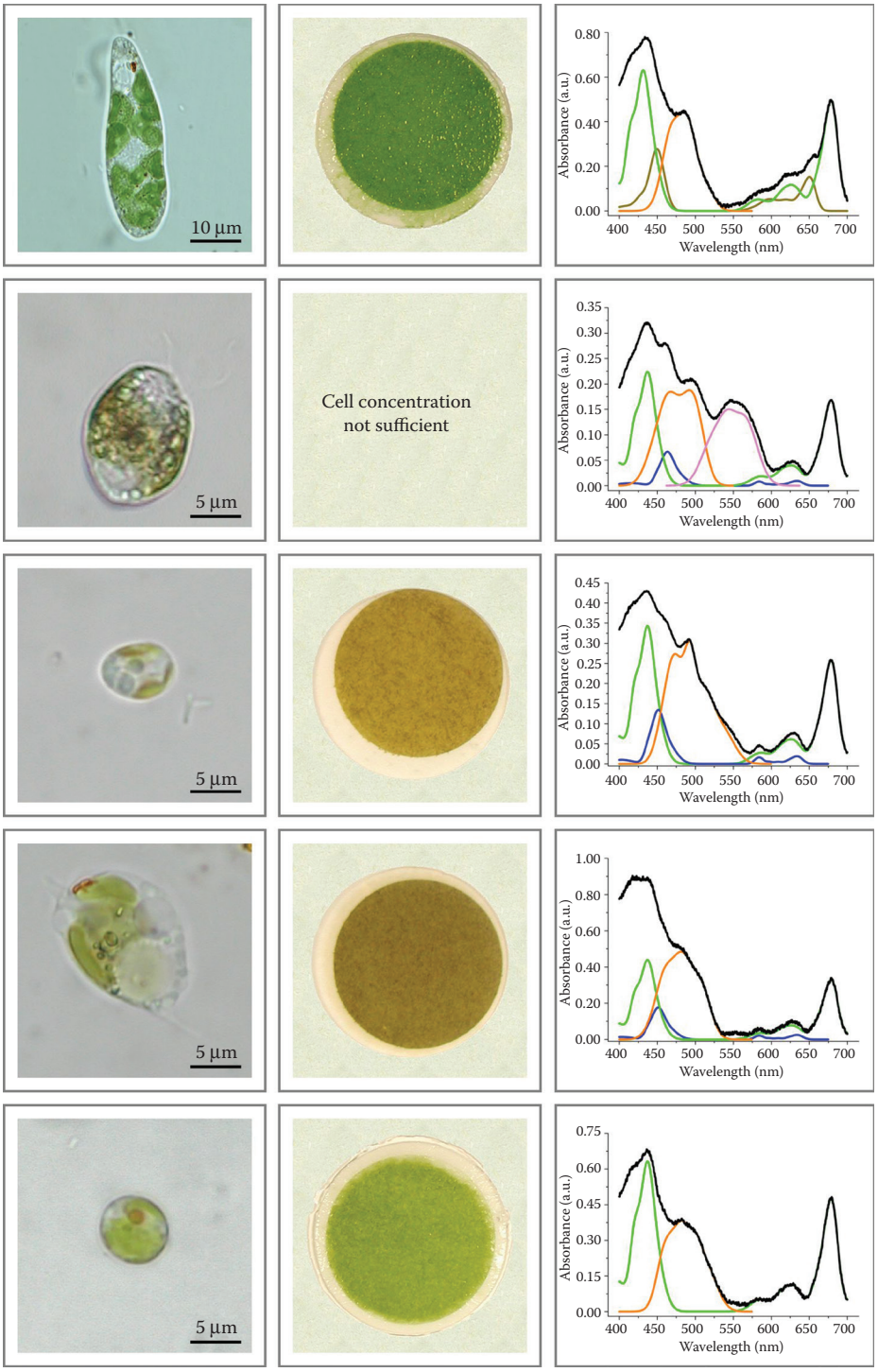

FIGURE 3.13 *In vivo* absorption spectra of photosynthetic compartments of *Euglena* (Euglenophyta), *Rhodomonas* (Cryptophyta), *Pavlova* (Haptophyta), *Ochromonas* (Ochrophyta), and *Nannochloropsis* (Ochrophyta), from top to the bottom. Each series shows the sample, the color of the culture on filter, and the absorption spectrum. Bright green line: chlorophyll *a*; olive-green line: chlorophyll *b*; blue line: chlorophyll *c*; orange line: carotenoids and xanthophylls; purple line: B-phycobiliprotein (545).

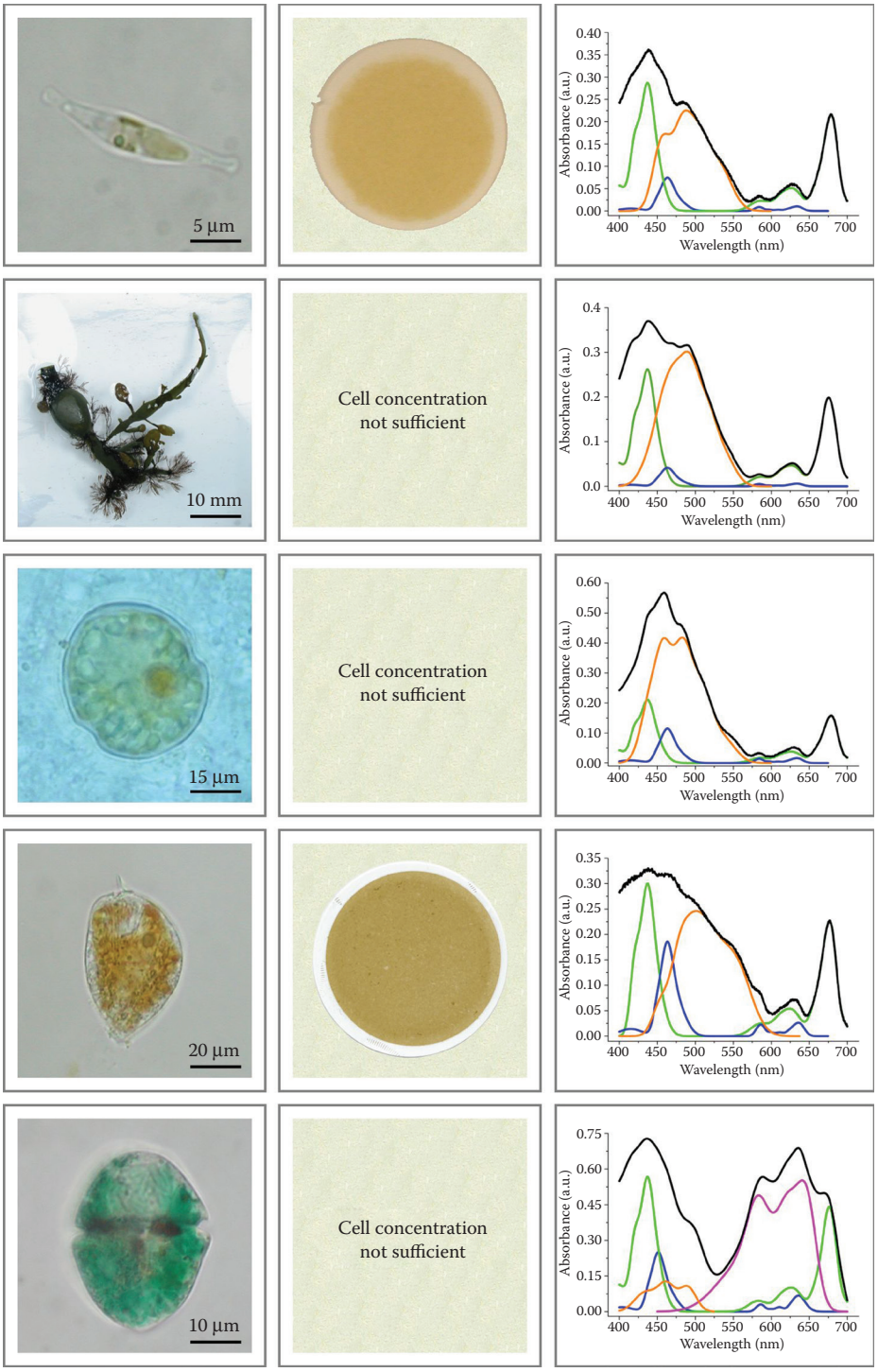

FIGURE 3.14 *In vivo* absorption spectra of photosynthetic compartments of *Phaeodactylum* (Ochrophyta), *Ascophyllum nodosum* (Ochrophyta), *Karenia* (Dinophyceae), *Prorocentrum* (Dinophyceae), *Gymnodinium* (Dinophyceae), from top to the bottom. Each series shows the sample, the color of the culture on filter, and the absorption spectrum. Bright green line: chlorophyll *a*; blue line: chlorophyll *c*; orange line: carotenoids and xanthophylls; purple line: R-phycocyanin (645).

FIGURE 3.15 *In vivo* absorption spectra of photosynthetic compartments of the lawn daisy *B. perennis* shown to highlight the uniformity of pigments distribution throughout the algae green lineage and plants. Bright green line: chlorophyll *a*; olive green line: chlorophyll *b*; orange line: carotenoids and xanthophylls.

state that glucose ($C_6H_{12}O_6$) is the major product of photosynthesis, the actual carbohydrate end-products are those listed in Table 1.4 (sucrose, paramylon, starch, etc.). The fixation of CO_2 takes place during the light-independent phase using the assimilatory power of NADPH and ATP in the chloroplast stroma (eukaryotic algae) or in the cytoplasm (prokaryotic algae). The light-independent reactions do not occur in the dark; rather they occur simultaneously with the light reactions. However, light is not directly involved. The light-independent reactions are commonly referred to as the Calvin–Benson–Bassham cycle (CBB cycle) after the pioneering work of its discoverers (Figure 3.16).

The first metabolite was a 3-carbon organic acid known as 3-phosphoglycerate (3-PG). For this reason, the pathway of carbon fixation in algae and most plants is referred to as C3 photosynthesis. Since the first product was a C3 acid, Calvin hypothesized that the CO_2 acceptor would be a C2 compound. However, no such C2 substrate was found. Rather, it was realized that the CO_2 acceptor

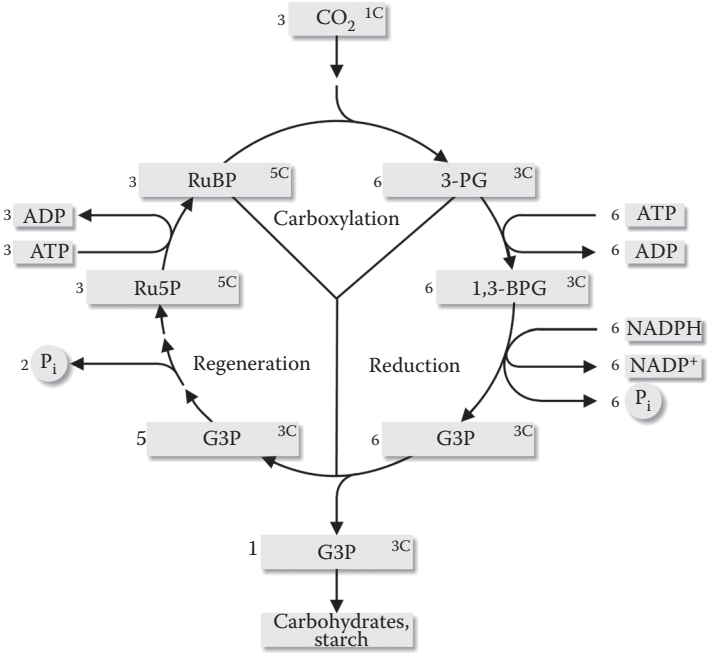

FIGURE 3.16 Schematic drawing of the three phases of the CBB cycle.

was a C5 compound, ribulose 1,5-bisphosphate (RuBP), and that the product of carboxylation was two molecules of 3-PG. This crucial insight allowed the pathway of carbon flow to be determined.

While the CBB cycle involves a total of 13 individual enzymatic reactions, only two enzymes are unique to this pathway: ribulose-1,5-bisphosphate carboxylase/oxygenase (RuBisCO) and phosphoribulokinase (PRK). All other enzymes involved also perform functions in heterotrophic metabolism. PRK catalyzes the phosphorylation of ribulose-monophosphate to ribulose-1,5-bisphosphate (RUBP). RUBP in turn is the substrate for RuBisCO, which catalyzes the actual carbon fixation reaction.

RuBisCO

The RuBisCO enzyme alone represents the most important pathway by which inorganic carbon enters the biosphere. It has also been described as the most abundant protein on earth. It is thought that as much as 95% of all carbon fixations by C3 organisms (that includes all phytoplankton) occur through RuBisCO.

RuBisCO is known to catalyze at least two reactions: the reductive carboxylation of ribulose 1,5-bisphosphate (RuBP) to form two molecules of 3-PG and the oxygenation of RuBP to form one molecule of 3-PG and one molecule of 2-phosphoglycolate.

The oxygenation of RuBP is commonly referred to as photorespiration and has traditionally been seen as a wasteful process, because the regeneration of RuBP in photorespiration leads to the evolution of CO_2 and requires free energy in the form of ATP. In addition, RuBisCO suffers from several other inefficiencies. Both reactions (carboxylation and oxygenation) occur in the same active site and compete, making the enzyme extremely sensitive to local partial pressures of CO_2 and O_2. RuBisCO makes up 20–50% of the protein in chloroplasts. It acts very slowly, catalyzing three molecules per second. This compares to 1000 molecules per second for typical enzymatic reactions. Large quantities are needed to compensate for its slow speed. Lastly, RuBisCO rarely performs its function at a maximum rate (K_{max}), since the partial pressure of CO_2 in the vicinity of the enzyme is often smaller than its Michaelis–Menten half-saturation constant (K_m). RuBisCO has been shown to occur in two distinct forms in nature termed Form I and II, respectively. Form I of the enzyme is an assemblage of eight 55-kDa large subunits (rbcL) and eight 15-kDa small subunits (rbcS). These subunits assemble into a 560-kDa hexadecameric protein-complex designated as L8S8. Most photosynthetic prokaryotes that depend on the CBB-cycle for carbon assimilation and all eukaryotic algae express a Form I type RuBisCO. The exception to this rule can be found in several marine dinoflagellates, which apparently contain a nuclear encoded Form II of RuBisCO. Form II of RuBisCO is a dimer of large subunits (L2) and is otherwise found in many photosynthetic and chemoautotrophic bacteria. Phylogenetic analysis of a large number of Form I rbcL DNA sequences revealed the division of Form I into four major clades referred to as IA, IB, IC, and ID. Form IA is commonly found in nitrifying and sulfur-oxidizing chemoautotrophic bacteria as well as some marine *Synechococcus* (marine type A) as well as all *Prochlorococcus* strains sequenced to date. All other cyanobacteria as well as all green algae possess a Form IB type enzyme. Form IC of rbcL is expressed by some photosynthetic bacteria such as hydrogen oxidizers. Form ID encompasses a diverse group of eukaryotic lineages including essentially all chromophytic, eukaryotic algae such as Rhodophyta, Bacillariophyceae, Raphidophyceae and Phaeophyceae.

The phylogeny of RuBisCO displays several interesting incongruences with phylogenies derived from ribosomal DNA sequences. This has led to the speculation that over evolutionary history, numerous lateral gene transfers may have occurred, transferring RuBisCO among divergent lineages. For example, the dinoflagellate *Gonyaulax polyhedra* contains a Form II RuBisCO most similar to sequences found in proteobacteria. Within the Form I clade, as many as six lateral transfers have been suggested to explain the unusual phylogeny observed among cyanobacteria, proteobacteria, and plastids. Some bacteria may have acquired a green-like cyanobacterial gene, while marine *Synechococcus* and *Prochlorococcus* almost certainly obtained their RuBisCO genes from a purple bacterium.

Three-dimensional structures of the RuBisCO enzyme are now known for a number of species, including *Synechococcus*, the green alga *Chlamydomonas reinhardtii*, and the red alga *Galdieria sulphuraria*. Based on these and other studies, it is now believed that the primary catalytic structure of RuBisCO is a dimer of two large subunits (L2). In Form I RuBisCO, four L2 dimers are cemented to form L8S8 hexadecameric superstructure, whereby the major contacts between the L2 dimers are mediated by the small subunits. A Mg^{2+} cofactor as well as the carbamylation of Lys201 is required for the activity of the enzyme. A loop in the beta barrel and two other elements of the large subunit, one in the N- and one in the C-terminus of the protein, form the active site in *Synechococcus*. Small subunits apparently do not contribute to the formation of the active site.

Calvin–Benson–Bassham Cycle

The reactions of the Calvin cycle can be thought of as occurring in three phases (Figure 3.16):

1. Carboxylation—fixation of CO_2 into a stable organic intermediate
2. Reduction—reduction of this intermediate to the level of carbohydrate
3. Regeneration—regeneration of the CO_2 acceptor

Carboxylation

Carboxylation involves the addition of one molecule of CO_2 to a 5-carbon "acceptor" molecule, ribulose biphosphate (RuBP). This reaction is catalyzed by the enzyme RuBisCO. Plants invest a huge amount of their available nitrogen into making this protein. As a result, RuBisCO is the most abundant protein in the biosphere. The resulting 6-carbon product splits into two identical 3-carbon products. These products are 3-PG. At this point in the cycle, CO_2 has been "fixed" into an organic product but no energy has been added to the molecule.

Reduction

The second step in the Calvin cycle is the reduction of 3-PG to the level of carbohydrate. This reaction occurs in two steps: (1) phosphorylation of 3-PG by ATP to form 1,3-biphosphoglycerate (1,3-BPG); (2) reduction of 1,3-BPG by NADPH to form glyceraldehyde-3-phosphate (G3P), a simple 3-carbon carbohydrate, and its isomers collectively called triose phosphates. This reaction requires both ATP and NADPH, the high-energy chemical intermediates formed in the light reactions.

The $NADP^+$ and ADP formed in this process return to the thylakoids to regenerate NADPH and ATP in the light reactions.

Regeneration

The final stage in the Calvin cycle is the regeneration of the CO_2 acceptor RuBP. This involves a series of reactions that convert triose phosphate first to the 5-carbon intermediate Ru5P (ribulose 5-phosphate), then phosphorylation of Ru5P to regenerate RuBP (ribulose-bisphosphate). This final step requires ATP formed in the light reactions.

Overall, for every three turns of the cycle, one molecule of product (triose phosphate) is formed ($3CO_2$:1G3P). The remaining 15 carbon atoms (5 G3P) re-enter the cycle to produce three molecules of RuBP.

The triose phosphate formed in the Calvin cycle can remain in the chloroplast where it is converted to starch. This is why chloroplasts form starch grains. Alternatively, triose phosphate can be exported from the chloroplast where it is converted to carbohydrates in the cytoplasm. Both reactions involve the release of phosphate. In the case of carbohydrates, the phosphate must be returned to the chloroplast to support continued photophosphorylation (ATP formation).

The net energy balance of six rounds of the Calvin cycle to produce 1 mol of hexose is thus:

$$6CO_2 + 18ATP + 12NADPH + 12H_2O \rightarrow C_6H_{12}O_6 + 18ADP + 18P_i + 12NADP^+ + 6H^+ \quad (3.6)$$

Photorespiration

Photosynthetic organisms must cope with a competing reaction that inhibits photosynthesis known as photorespiration. Unlike photosynthesis, this process involves the uptake of oxygen and the release of carbon dioxide.

Recall that mitochondrial respiration involves the uptake of O_2 and the evolution of CO_2 and is associated with the burning of cellular fuel to obtain energy in the form of ATP. In contrast, photorespiration starts in the chloroplast and actually wastes energy.

Photorespiration can be defined as the light-dependent uptake of O_2 in the chloroplast. It is caused by a fundamental "inefficiency" of RuBisCO.

During photosynthesis, RuBisCO catalyzes the carboxylation of RuBP to give two molecules of PGA. However, it can also catalyze the oxygenation of RuBP to give one molecule of PGA and one molecule of a 2-carbon compound called phosphoglycolate. This reaction occurs because O_2 can compete with CO_2 at the active site of RuBisCO. Since oxygenation of RuBP competes with carboxylation, it lowers the efficiency of photosynthesis. A significant portion (25%) of the carbon in phosphoglycolate is lost as CO_2. Algae must use energy to "recover" the remaining 75% of this carbon, which further limits the efficiency of photosynthesis.

If photorespiration lowers the yield of photosynthesis, why has such a process been maintained throughout the course of evolution? The answer to this intriguing question has to do with the origins of RuBisCO and the CBB cycle. RuBisCO is an ancient enzyme, having evolved over 2.5 billion years ago in cyanobacteria. During this period in earth's history, the atmosphere contained high levels of CO_2 and very little oxygen. Thus, photorespiration did not present a problem for early photosynthetic organisms. By the time oxygen accumulated to significant levels in the atmosphere (ironically, by the process of photosynthesis!), the catalytic mechanism of RuBisCO was apparently "fixed." In other words, since both O_2 and CO_2 compete for the same active site of the enzyme, algae could not decrease the efficiency of oxygenation without also decreasing the efficiency of carboxylation. To compensate, algae evolved an elaborate pathway, known as the photorespiratory pathway, to recover at least some of the carbon that would otherwise be lost. This pathway involved biochemical reactions in the chloroplasts, mitochondria, and peroxisomes. The importance of photorespiration is easily demonstrated by the fact that nearly all plants grow better under high CO_2 versus low CO_2. Conditions that favor carboxylation (photosynthesis) over oxygenation (photorespiration) include high CO_2, moderate light intensities, and moderate temperatures. Conditions that favor oxygenation over carboxylation include low CO_2 levels, high temperatures, and high light intensities.

THE ENERGY RELATIONSHIPS IN PHOTOSYNTHESIS: THE BALANCE SHEET

The consumption of a mole of glucose releases 686 kcal of energy. This value represents the difference between the energy needed to break the bonds of the reactants (glucose and oxygen) and the energy liberated when the bonds of the products (H_2O and CO_2) form. Conversely, the photosynthesis of a mole of glucose requires the input of 686 kcal of energy. The overall equation for each process is the same; only the direction of the arrow differs:

$$C_6H_{12}O_6 + 6O_2 \leftrightarrow 6H_2O + 6CO_2 \quad (3.7)$$

The average bond energies between common atoms are the following:

- C–H = 98 kcal/mol
- O–H = 110 kcal/mol
- C–C = 80 kcal/mol
- C–O = 78 kcal/mol
- H–H = 103 kcal/mol
- C–N = 65 kcal/mol
- O=O = 116 kcal/mol
- C=C = 145 kcal/mol
- C=O (as found in CO_2) = 98 kcal/mol

The 24 covalent bonds of glucose require a total of 2182 kcal to be broken. The six double bonds of oxygen require another 696. Thus, a grand total of 2878 kcal is needed to break all the bonds of the reactants in cellular respiration.

As for the products, the formation of six molecules of CO_2 involves the formation of 12 double polar covalent bonds each with a bond energy of 187 kcal; total = 2244 kcal. The formation of six molecules of H_2O involves the formation of 12 O–H bonds each with an energy of 110 kcal; total = 1320 kcal. Thus, a grand total of 3564 kcal is released as all the bonds of the products form.

Subtracting this from the 2878 kcal needed to break the bonds of the reactants, we arrive at −686 kcal, the free energy change in the oxidation of glucose. This value holds true whether we oxidize glucose quickly by burning it or in the orderly process of cellular respiration in mitochondria. The minus sign indicates that free energy has been removed from the system. The details of the energy budget are just the same. The only difference is that now it takes 3564 kcal to break the bonds of the reactants and only 2878 kcal are released in forming glucose and oxygen. So we express this change in free energy (+686 kcal) with a plus sign to indicate that energy has been added to the system. The energy came from the sun and now is stored in the form of bond energy that can power the needs of all life.

Photosynthetic reduction of CO_2 can be summarized by the equations:

$$2H_2O \rightarrow O_2 + 4H^+ + 4e^- \tag{3.8}$$

$$CO_2 + 4H^+ + 4e^- \rightarrow (CH_2O) + H_2O \tag{3.9}$$

Four electrons have to be transferred from water, through a redox span of 1.24 eV, to reduce one molecule of CO_2. The energy required for the reduction of 1 mol of CO_2 is therefore

$$4\,\text{mol} \times 6.02 \times 10^{23}\,\text{mol}^{-1} \times 1.24\,\text{eV} \times 1.60 \times 10^{-19}\,\text{J eV}^{-1} = 47.77 \times 10^4\,\text{J}\,(114.17\,\text{kcal}) \tag{3.10}$$

Theoretically, the energy requirement could be satisfied by the capture of 4 mol of photons of PAR light, say a red photon of 700 nm; the energy content of these photons will be

$$4\,\text{mol} \times 6.02 \times 10^{23}\,\text{mol}^{-1} \times 2.84 \times 10^{-19}\,\text{J} = 68.38 \times 10^4\,\text{J}\,(163.44\,\text{kcal}) \tag{3.11}$$

However, due to the thermodynamic losses during energy conversion, the fraction of absorbed photon energy converted in chemical energy seldom exceeds 0.35. Thus, 8 mol of photons are required for the reduction of 1 mol of CO_2:

$$8\,\text{mol} \times 6.02 \times 10^{23}\,\text{mol}^{-1} \times 2.84 \times 10^{-19}\,\text{J} = 136.76 \times 10^4\,\text{J} \times 0.35 = 47.86 \times 10^4\,\text{J}\,(114.40\,\text{kcal}) \tag{3.12}$$

A mole of glucose (formed by the addition of six CO_2 molecules) requires

$$6 \times 114.40 \text{ kcal} = 686.40 \text{ kcal} \tag{3.13}$$

This is the value calculated by taking into account the balance of the energy of bonds previously described.

SUGGESTED READING

Akutsu S., D. Fujinuma, H. Furukawa, T. Watanabe, M. Ohnishi-Kameyama, O. Hiroshi Ono et al. Pigment analysis of a chlorophyll *f*-containing cyanobacterium strain KC1 isolated from Lake Biwa. *Photomedicine and Photobiology*, 33, 35–40, 2011.

Allen J. F. and J. Forsberg. Molecular recognition in thylakoid structure and function. *Trends in Plant Science*, 6, 317–326, 2001.

Barber J. Photosystem II: A multisubunit membrane protein that oxidases water. *Current Opinion in Structural Biology*, 12, 523–530, 2002.

Bassi R. and S. Caffarri. Lhc proteins and the regulation of photosynthetic light harvesting function by xanthophylls. *Photosynthesis Research*, 64, 243–256, 2000.

Behrendt L., V. Schrameyer, K. Qvortrup, L. Lundin, S.J. Sørensen, A.W.D. Larkum et al. Biofilm growth and near-infrared radiation-driven photosynthesis of the chlorophyll *d*-containing cyanobacterium *Acaryochloris marina*. *Applied and Environmental Microbiology*, 78(11), 3896–3904, 2012.

Bibby T.S., J. Nield, F. Partensky, and J. Barber. Antenna ring around photosystem I. *Nature*, 413, 590, 2001.

Bibby T.S., J. Nield, M. Chen, A.W.D. Larkum, and J. Barber. Structure of a photosystem II supercomplex isolated from *Prochloron didemni* retaining its chlorophyll *a/b* light-harvesting system. *PNAS*, 100, 9050–9054, 2003.

Brettel K. and W. Leibl. Electron transfer in photosystem I. *Biochimica Biophysica Acta*, 1507, 100–114, 2001.

Catling, D.C., K.J. Zahnle, and C. McKay. Biogenic methane, hydrogen escape, and the irreversible oxidation of early Earth. *Science,* 293, 839–843, 2001.

Chen M. M. Schliep, R.D. Willows, Z.L. Cai, B.A. Neilan, and H. Scheer. A red-shifted chlorophyll. *Science*, 329(5997), 1318–1319, 2010.

Chen M. and R.E. Blankenship. Expanding the solar spectrum used by photosynthesis. *Trends in Plant Science*, 16(8), 427–431, 2011.

Chen M., Y. Li, D. Birch, and R.D. Willows. A cyanobacterium that contains chlorophyll *f*—A red-absorbing photopigment. *FEBS Letters*, 586(19), 3249–3254, 2012.

Chitnis P.R. Photosystem I: Function and physiology. *Annual Review Plant Molecular Biology*, 52, 593–626, 2001.

De Martino, A., D. Douady, M. Quinet-Szely, B. Rousseau, F. Crepineau, Kirk Apt, and L. Caron. The light harvesting antenna of brown algae. *European Journal of Biochemistry*, 267, 5540–5549, 2000.

Falkowski P.G., and J.A. Raven. *Aquatic Photosynthesis*. Blackwell Science, Oxford, UK, 1997.

Ferreira, K.N., T.M. Iverson, K. Maghlaoui, J. Barber, and S. Iwata. Architecture of the photosynthetic oxygen-evolving center. *Science,* 19(303), 1831–1838, 2004.

Germano M., A.E. Yakushevska, W. Keegstra, H.J. van Gorkom, J.P. Dekker, and E.J. Boekema. Supramolecular organization of photosystem I and light-harvesting complex I in *Chlamydomonas reinhardtii*. *FEBS Letters*, 525, 121–125, 2002.

Govindjee. Chlorophyll *a* fluorescence: A bit of basics and history. In G. Papageorgiou and Govindjee (Eds), *Chlorophyll a Fluorescence: A Probe of Photosynthesis*, pp. 2–42. Kluwer Academic Publishers, Dordrecht, The Netherlands, 2004.

Govindjee, J.F. Allen, and J.T. Beatty. Celebrating the millenium: Historical highlights of photosynthesis research, Part 3. *Photosynthesis Research*, 80, 1–13, 2004.

Hall D.O. and K.K. Rao. *Photosynthesis*. Cambridge University Press, Cambridge, UK, 1999.

Heathcote P., P.K. Fyfe, and M.R. Jones. Reaction centers: The structure and evolution of biological solar power. *Trends in Biochemical Sciences*, 27, 79–84, 2002.

Hohmann-Marriott M.F., and R.E. Blankenship. Evolution of photosynthesis. *Annual Review of Plant Biology*, 62(1), 515–548, 2011.

http://www.bio.ic.ac.uk/research/barber/people/jbarber.html

http://www.marine.usf.edu/microbiology/regulation-rubisco.shtml

http://www.life.uiuc.edu/govindjee/

Jiang J., H. Zhang, Y. Kang, D. Bina, C.S. Lo, and R.E. Blankenship. Characterization of the peridinin–chlorophyll *a*–protein complex in the dinoflagellate *Symbiodinium*. *Biochimica et Biophysica Acta (BBA)-Bioenergetics*, 1817(7), 983–989, 2012.

Jordan P., P. Fromme, H.T. Witt, O. Klukas, W. Saenger, and N. Krauß. Three-dimensional structure of cyanobacterial photosystem I at 2.5 Å resolution. *Nature*, 411, 909, 917, 2001.

Kamiya N. and J.-R. Shen. Crystal structure of oxygen-evolving photosystem II from *Thermosynechococcus vulcanus* at 3.7 Å resolution. *PNAS*, 100, 98–103, 2003.

Kargul J., J. Nield, and J. Barber. Three dimensional reconstruction of a light-harvesting complex I–photosystem I supercomplex from *Chlamydomonas reinhardtii*. *Journal of Biological Chemistry*, 278, 16135–16141, 2003.

Kramer D.M., T.J. Avenson, and G.E. Edwards. Dynamic flexibility in the light reaction of photosynthesis governed by both electron and proton transfer reaction. *Trends in Plant Science*, 9, 349–357, 2004.

Kurisu G., H. Zhang, J.L. Smith, and W.A. Cramer. Structure of the cytochrome b_6f complex of oxygenic photosynthesis: Tuning the cavity. *Science*, 302, 1009–1014, 2003.

Larkum A.W.D., J. Raven, and S. Douglas (Eds). *Photosynthesis of Algae*, Vol. 14, Govindjee, Series Editor. Kluwer Academic Publishers, Dordrecht, The Netherlands, 2003.

Larkum A.W.D. and M. Kühl. Chlorophyll *d*: The puzzle resolved. *Trends in Plant Science*, 10(8), 355–357, 2005.

Larkum A.W.D., M. Chen, Y. Li, M. Schliep, E. Trampe, J. West et al. A novel epiphytic chlorophyll *d*-containing cyanobacterium isolated from a mangrove-associated red alga. *Journal of Phycology*, 48(6), 1320–1327, 2012.

Laviale M. and J. Neveux. Relationships between pigment ratios and growth irradiance in 11 marine phytoplankton species. *Marine Ecology Progress Series*, 425, 63–77, 2011.

Li Y., N. Scales, R.E. Blankenship, R.D. Willows, and M. Chen. Extinction coefficient for red-shifted chlorophylls: Chlorophyll *d* and chlorophyll *f*. *Biochimica et Biophysica Acta-Bioenergetics*, 1817(8), 1292–1298, 2012.

Line, M.A. The enigma of the origin of life and its timing. *Microbiology,* 148, 21–27, 2002.

Markovic D. Energy storage in the photosynthetic electron-transport chain. An analogy with Michaelis–Menten kinetics. *Journal of Serbian Chemical Society*, 68, 615–618, 2003.

Mielke S.P., N.Y. Kiang, R.E. Blankenship, M.R. Gunner, and D. Mauzerall. Efficiency of photosynthesis in a Chl *d*-utilizing cyanobacterium is comparable to or higher than that in Chl *a*-utilizing oxygenic species. *Biochimica et Biophysica Acta-Bioenergetics*, 1807(9), 1231–1236, 2011.

Nelson N. and A. Ben-Shem. The complex architecture of oxygenic photosynthesis. *Nature Reviews Molecular Cell Biology*, 5, 1–12, 2004.

Nugent J.H.A. and M.C.W. Evans. Structure of biological solar energy converters—Further revelations. *Trends in Plant Sciences*, 9, 368–370, 2004.

Ort D.R., X. Zhu, and A. Melis. Optimizing antenna size to maximize photosynthetic efficiency. *Plant Physiology*, 155(1), 79–85, 2011.

Perrine Z., S. Negi, and R.T. Sayre. Optimization of photosynthetic light energy utilization by microalgae. *Algal Research*, 1(2), 134–142, 2012.

Pfannschmidt T. Chloroplast redox signal: How photosynthesis controls its own genes. *Trends in Plant Sciences*, 8, 33–41, 2003.

Raven J.A. Putting C in phycology. *European Journal of Phycology*, 32, 319–333, 1997.

Raven J.A. The cost of photoinhibition. *Physiologia Plantarum*, 142(1), 87–104, 2011.

Reed B. ATP synthase: Powering the movement of live. *Harvard Science Review*, Spring, 8–10, 2002.

Saenger W., P. Jordan, and N. Krauß. The assembly of protein subunits and cofactors in photosystem I. *Current Opinion in Structural Biology*, 12, 244–254, 2002.

Samsonoff W.A. and R. MacColl. Biliproteins and phycobilisomes from cyanobacteria and red algae at the extremes of habitat. *Archives of Microbiology*, 176, 400–405, 2001.

Schmid V.H.R., S. Potthast, M. Wiener, V. Bergauer, H. Paulsen, and S. Storf. Pigment binding of photosystem I in light-harvesting proteins. *Journal of Biological Chemistry*, 277, 37307–37314, 2002.

Stomp M., J. Huisman, F. de Jongh, A.J. Veraart, D. Gerla, M. Rijkeboer, B.W. Ibelings, U.I.A. Wollenzlen, and L.J. Stal. Adaptive divergence in pigment composition promotes phytoplankton biodiversity. *Nature*, 432, 104–107, 2004.

Tabita F.R. Microbial ribulose 1,5-bisphosphate carboxylase/oxygenase: A different perspective. *Photosynthesis Research*, 60:1–28, 1999.

Tice M.M. and D.R. Lowe. Photosynthetic microbial mats in the 3,416-Myr-old ocean. *Nature*, 431, 549–552, 2004.

Ting, C.S., G. Rocap, J. King, and S.W. Chisholm. Cyanobacterial photosynthesis in the ocean: The origins and significance of divergent light-harvesting strategies. *Trends in Microbiology*, 10, 134–142, 2002.

Tomo T., S.I. Allakhverdiev, and M. Mimuro. Constitution and energetics of photosystem I and photosystem II in the chlorophyll *d*-dominated cyanobacterium *Acaryochloris marina*. *Journal of Photochemistry and Photobiology B: Biology*, 104(1–2), 333–340, 2011.

Towe K.M., D. Catling, K. Zahnle, and C. McKay. The problematic rise of archean oxygen. *Science,* 295, 1419a, 2002.

Walker J.E. (Ed). The mechanism of F_1F_0-ATPase. *Biochimica Biophysica Acta*, 1458, 221–510, 2000.

Wynn-Williams D.D., H.G.M. Edwards, E.M. Newton, and J.M. Holder. Pigmentation as a survival strategy for ancient and modern photosynthetic microbes under high ultraviolet stress on planetary surfaces. *International Journal of Astrobiology*, 1, 39–49, 2002.

Zhu X.G., S.P. Long, and D.R. Ort. What is the maximum efficiency with which photosynthesis can convert solar energy into biomass? *Current Opinion in Biotechnology*, 19(2), 153–159, 2008.

Zouni A., H.-T. Witt, J. Kern, P. Fromme, N. Krauß, W. Saenger, and P. Orth. Crystal structure of photosystem II from *Synechococcus elongates* at 3.8 Å resolution. *Nature*, 409, 739–743, 2001.

4 Working with Light

HOW LIGHT BEHAVES

In Chapter 3, we have already described the dual nature of light, defining it as electromagnetic radiation with particle and wave properties. Light consists of tiny packets or particles termed photons that propagate through space as electromagnetic waves. Whether it be transmitted to a radio from the broadcast station, heat radiating from the oven, furnace, or fireplace, x-rays of teeth, or the visible and ultraviolet light emanating from the sun, the various forms of electromagnetic radiation all share fundamental wave-like properties. Every form of electromagnetic radiation, including visible light, oscillates in a periodic fashion with peaks and valleys, and displays a characteristic amplitude, wavelength, and frequency. The standard unit of measure for all electromagnetic radiation is the magnitude of the wavelength (λ) and is measured by the distance between one wave crest and the next. Wavelength is usually measured in nanometers (nm) for the visible light portion of the spectrum. Each nanometer represents one-thousandth of a micrometer. The corresponding frequency (ν) of the radiation wave, that is, the number of complete wavelengths that passes a given point per second, is proportional to the reciprocal of the wavelength. Frequency is usually measured in cycles per second or Hertz (Hz). Thus, longer wavelengths correspond to lower frequency radiation and shorter wavelengths correspond to higher frequency radiation. A wave is characterized by a velocity (the speed of light) and phase. If two waves arrive at their crests and troughs at the same time, they are said to be in phase.

An electromagnetic wave, although it carries no mass, does carry energy. The amount of energy carried by a wave is related to the amplitude of the wave (how high is the crest). A high-energy wave is characterized by high amplitude; a low-energy wave is characterized by low amplitude. The energy transported by a wave is directly proportional to the square of the amplitude of the wave. The electromagnetic wave does not need any medium for its sustainability; unlike sound, light can travel in the vacuum.

During their traveling, light waves interact with matter. The consequences of this interaction are that the waves are either scattered or absorbed. In the following, we describe the principal behaviors of light.

SCATTERING

Scattering is the process by which small particles suspended in a medium of a different density diffuse a portion of the incident radiation in all directions. In scattering, no energy transformation results, there is only a change in the spatial distribution of the radiation (Figure 4.1).

In the case of solar radiation, scattering is due to its interaction with gas molecules and suspended particles found in the atmosphere. Scattering reduces the amount of incoming radiation reaching the earth's surface since significant proportion of solar radiation is redirected back to space. The amount of scattering that takes place depends upon two factors: wavelength of the incoming radiation and the size of the scattering particle or gas molecule. For small particles compared to the visible radiation, Rayleigh's scattering theory holds. It states that the intensity of scattered waves roughly in the same direction of the incoming radiation is inversely proportional to the fourth power of the wavelength. In the earth's atmosphere, the presence of a large number of small particles compared to the visible radiation (with a size of about 0.5 μm) causes shorter

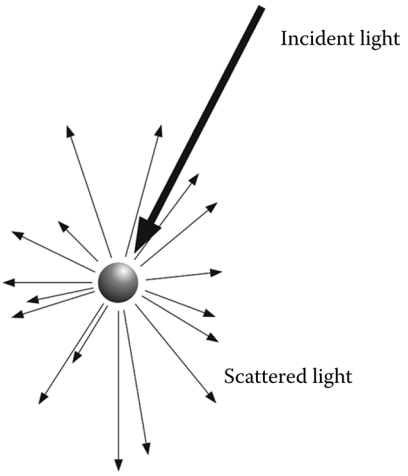

FIGURE 4.1 Light interaction with matter: the scattering process.

wavelengths of the visible range to be more intensely diffused. This factor causes our sky to appear blue because this color corresponds to those wavelengths. When the scattering particles are very much larger than the wavelength, the intensity of scattered waves roughly in the same direction of the incoming radiation become independent of wavelength and for this reason, the clouds, made of large raindrops, are white. If scattering did not occur in our atmosphere, the daylight sky would be black.

ABSORPTION

Some molecules have the ability to absorb incoming light. Absorption is defined as a process in which light is retained by a molecule. In this way, the free energy of the photon absorbed by the molecule can be used to carry out work, either emitted as fluorescence or dissipated as heat.

The Lambert–Beer law is the basis for measuring the amount of radiation absorbed by a molecule, a subcellular compartment, such as a chloroplast or a photoreceptive apparatus and a cell, such as a unicellular alga (Figure 4.2). A plot of the amount of radiation absorbed (absorbance, A_λ)

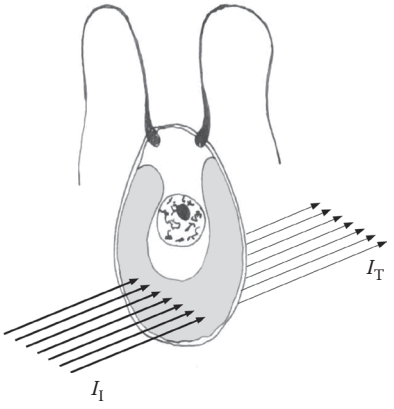

FIGURE 4.2 Light absorption by a unicellular alga; I_I: light incident on the cell; I_T: light transmitted by the cell.

TABLE 4.1
Relationship between Transmitted Light Percentage and the Absorbance Value

Transmittance	Absorbance
100	0.000
90	0.045
80	0.096
70	0.154
60	0.221
50	0.301
40	0.397
30	0.522
20	0.698
10	1.000
1	2.000
0.1	3.000

as a function of wavelengths is called a spectrum. The Lambert–Beer law states that the variation in the intensity of the incident beam as it passes through a sample is proportional to the concentration of that sample and its thickness (path length). We have adopted this law to measure the absorption spectra in all algal photosynthetic compartments presented in Chapter 3.

The Lambert–Beer law states the logarithmic relationship between absorbance and the ratio between the incident (I_I) and the transmitted light (I_T). In turn, absorbance is linearly related to the pigment concentration C (mol L^{-1}), the path length l (cm), and the molar extinction coefficient ε_λ, which is substance-specific and is a function of the wavelength:

$$A_\lambda = \log\left(\frac{I_I}{I_T}\right) = \varepsilon_\lambda Cl. \tag{4.1}$$

Table 4.1 shows the comparison between transmitted light and absorbance values.

INTERFERENCE

Electromagnetic waves can superimpose. Scattered waves, all of which usually have the same frequency, are particularly susceptible to the phenomenon of interference, in which waves can get added constructively or destructively. When two waves, vibrating in the same plane, meet and the crests of one wave coincide with the crests of the other wave, that is, they are in phase, then constructive interference occurs. Therefore, the amplitude of the wave has been increased and this results in the light appearing brighter. If the two waves are out of phase, that is, if the crests of one wave encounter the troughs of the other, then destructive interference occurs. The two waves cancel each other out, resulting in a dark area (Figure 4.3). The interference of scattered waves gives rise to reflection, refraction, diffusion, and diffraction phenomena.

REFLECTION

Reflection results when light is scattered in the direction opposite to that of incident light. Light reflecting off a polished or mirrored flat surface obeys the law of reflection: the angle between the incident ray and the normal to the surface (θ_I) is equal to the angle between the reflected ray and

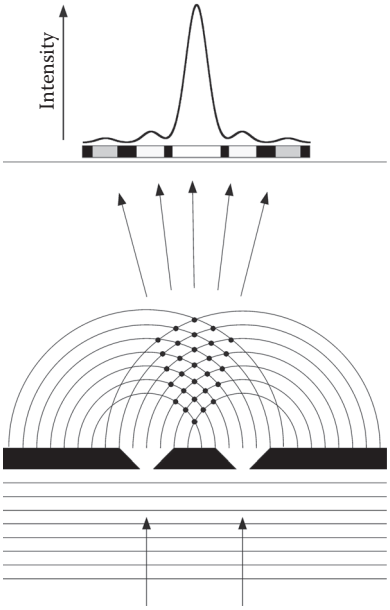

FIGURE 4.3 Interference of light passing through two narrow slits, each acting as a source of waves. The superimposition of waves produces a pattern of alternating bright and dark bands. When crest meets crest or trough meets trough, constructive interference occurs, which makes bright bands; when crest meets trough, destructive interference occurs, which creates dark bands. The dots indicate the points of constructive interference. The light intensity distribution shows a maximum that corresponds to the highest number of dots.

the normal (θ_R). This kind of reflection is termed specular reflection. Most hard-polished (shiny) surfaces are primarily specular in nature. Even transparent glass specularly reflects a portion of incoming light. Diffuse reflection is typical of particulate substances such as powders. If you shine a light on baking flour, for example, you will not see a directionally shiny component. The powder will appear uniformly bright from every direction. Many reflections are a combination of both diffuse and specular components and are termed spread (Figure 4.4), such as that performed by the blooms of the haptophyte emiliana huxley (cf. Chapter 5).

Now we will turn our attention to the topic of curved mirrors, especially curved mirrors that have the shape of spheres—the spherical mirrors. Spherical mirrors can be thought of as a portion of a sphere that was sliced away and then silvered on one of the sides to form a reflecting surface. Concave mirrors were silvered on the inside of the sphere and convex mirrors were silvered on the outside of the sphere (Figure 4.5). If a concave mirror were thought to have been a slice of a sphere, then there would be a line passing through the center of the sphere and attaching to the mirror in the exact center of the mirror. This line is known as the principal axis. The center of the sphere from which the mirror was sliced is known as the center of curvature of the mirror. The point on the mirror's surface where the principal axis meets the mirror is known as the vertex. The vertex is the geometric center of the mirror. Midway between the vertex and the center of curvature is the focal point. The distance from the vertex to the center of curvature is known as the radius of curvature. The radius of curvature is the radius of the sphere from which the mirror was cut. Finally, the distance from the mirror to the focal point is known as the focal length. The focal point is the point in space at which light incident towards the mirror and traveling parallel to the principal axis will meet after reflection. In fact, if some light from the sun was collected by a concave mirror, then it would converge at the focal point. Because the sun is at such a large distance from the earth, any

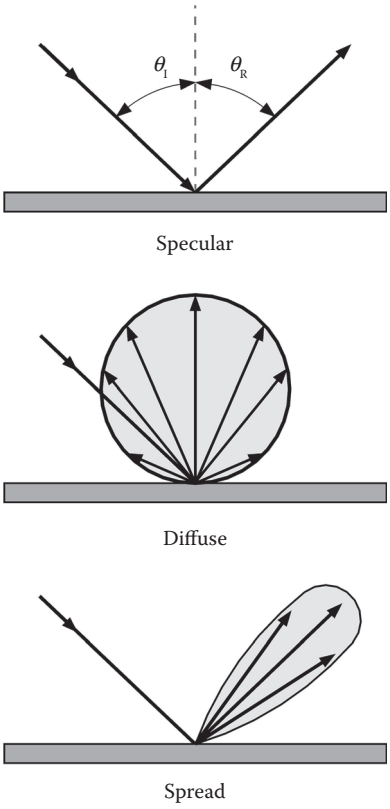

FIGURE 4.4 Different types of reflection; θ_I, angle of incidence; θ_R, angle of reflection.

light rays from the sun that strike the mirror will essentially be traveling parallel to the principal axis. As such, this light should reflect through the focal point.

Unlike the concave mirror, a convex mirror can be described as a spherical mirror with silver on the outside of the sphere. In convex mirrors, the focal point is located behind the convex mirror, and such a mirror is said to have a negative focal length value. A convex mirror is sometimes referred to as a diverging mirror due to its ability to take light from a point and diverge it. Any incident ray traveling parallel to the principal axis on the way to a convex mirror will reflect in a manner that its extension will pass through the focal point. Any incident ray traveling towards a convex mirror such that its extension passes through the focal point will reflect and travel parallel to the principal axis.

REFRACTION

Refraction results when light is scattered in the same direction as that of incident light but when passing between dissimilar materials, the rays bend and change their velocities slightly. Refraction is dependent on two factors: the incident angle θ, that is, the angle between the incident light and the normal to the surface, and the refractive index, n of the material, defined as the ratio between the velocity of the wave in vacuum, c_v, and the velocity of the wave in the medium, c_s:

$$n = \frac{c_v}{c_s}. \tag{4.2}$$

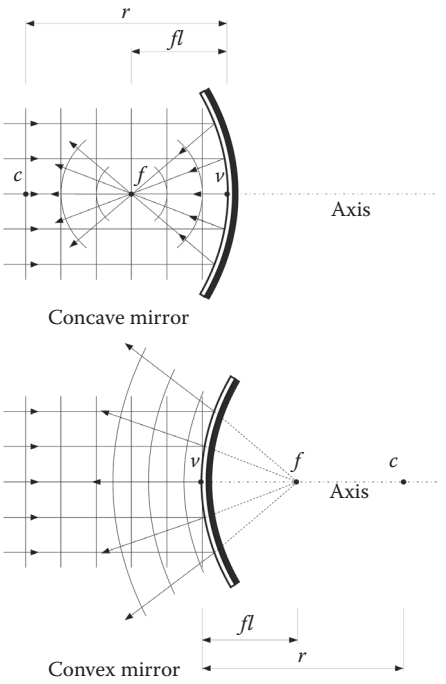

FIGURE 4.5 Curved mirrors; *c*, center of curvature of the mirror; *v*, vertex or geometric center of the mirror; *f*, focal point; *r*, radius of curvature; *fl*, focal length.

The refraction results in the following relationship termed Snell's law:

$$ {}_1n_2 = \frac{\sin\theta_1}{\sin\theta_2}, \tag{4.3} $$

where ${}_1n_2$ is the refractive index while passing from medium 1 to medium 2 and θ_1 and θ_2 are the angles between the direction of the propagated waves and the normal to the surface separating the two media.

For a typical air–water boundary ($n_{air} = 1$, $n_{water} = 1.333$), a light ray entering the water at 45° from normal travels through the water at 32.11° (Figure 4.6).

The refractive index decreases with increasing wavelength. This angular dispersion causes blue light to refract more than red, causing rainbows and allowing prisms to separate the spectrum (dispersion). Table 4.2 shows the refractive index of some common materials.

DISPERSION

Dispersion is a phenomenon that causes the separation of a light into components with different wavelengths, due to their different velocity in a medium other than vacuum. As a consequence, the white light traveling through a triangular prism is separated into its color components, the spectrum of light. The red portion of the spectrum deviates less than the violet from the direction of propagation of the white light (Figure 4.7).

DIFFRACTION

Light waves change the propagation direction when they encounter an obstruction or edge, such as a narrow aperture or slit (Figure 4.8). Diffraction depends on both wavelength of incoming

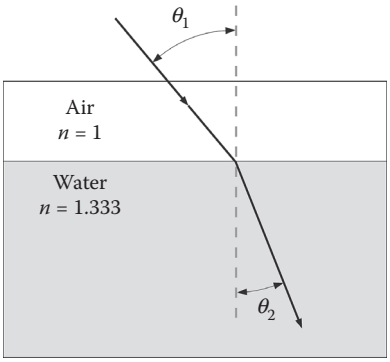

FIGURE 4.6 Refraction of a light ray passing from a medium with a lower refractive index (air) to a medium with a higher refractive index (water). θ_1, angle of incidence; θ_2, angle of refraction.

radiation (λ) and obstruction or edge dimensions, a. It is negligible when a/λ is sufficiently large and becomes more and more important when the ratio tends to zero. This effect is almost absent in most optical systems, such as photographic and video cameras, with a large a/λ, but is very important in all microscopes, where diffraction limits the resolution that microscope can ultimately achieve (a/λ tends to zero). The resolution is the smallest distance between two points to discriminate them as separate.

TABLE 4.2
Refractive Index of Some Common Materials

Material	Index
Vacuum	1.000
Air at STP	1.00029
Water at 0°	1.333
Water at 20°	1.332
Ice	1.309
Glycerin	1.473
Oil	1.466–1.535
Fluorite	1.434
Quartz	1.544
Glass, fused silica	1.459
Glass, Pyrex	1.474
Glass, crown (common)	1.520
Glass, flint 29% lead	1.569
Glass, flint 55% lead	1.669
Glass, flint 71% lead	1.805
Glass, arsenic trisulfide	2.040
Polypropylene	0.900
Polycarbonate	1.200
Plexiglas	1.488
Plastic	1.460–1.55
Nylon	1.530
Teflon	2.200
Salt	1.516

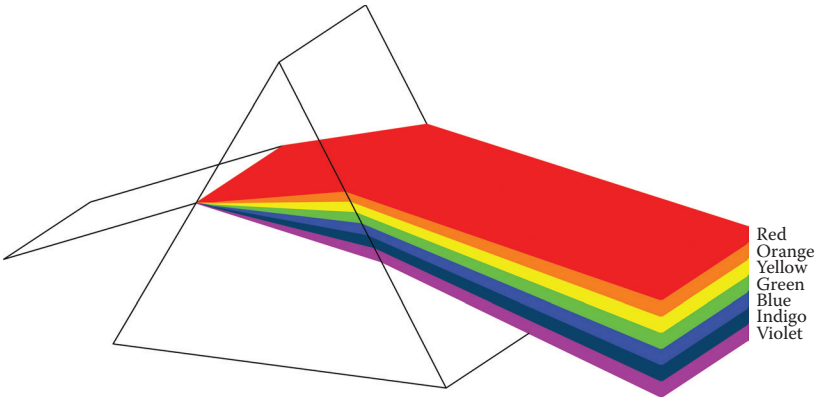

FIGURE 4.7 Dispersion of white light through a prism: the red portion of the spectrum deviates less than the violet from the direction of propagation of white light.

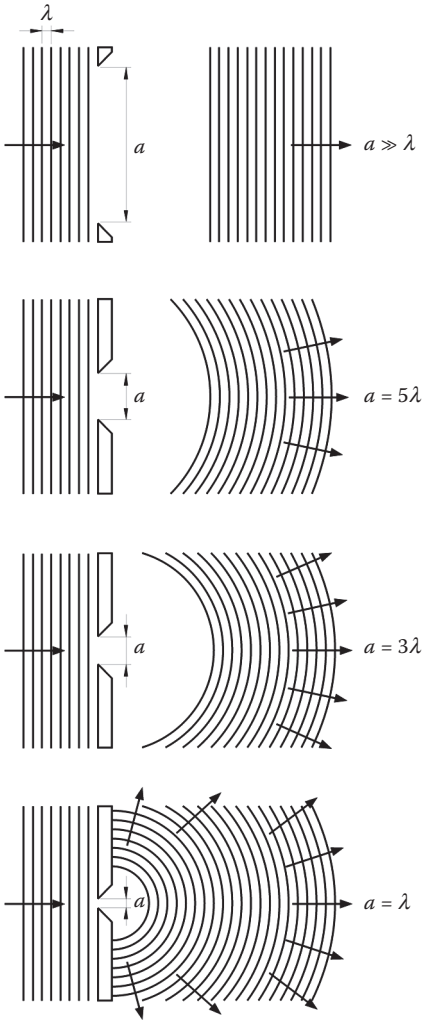

FIGURE 4.8 Diffraction of light from different width apertures; the effect increases with decreasing aperture width.

FIELD INSTRUMENTS: USE AND APPLICATION

Almost all light in the natural environment originates from the sun. Its spectral distribution is similar to that of an efficient radiant surface known as a blackbody at a temperature of 5800°C, which ranges from 100 to 4000 nm (Figure 3.1).

While passing through the atmosphere, a small portion of this light is absorbed and some is scattered. Short wavelengths are strongly scattered, and ozone absorption effectively eliminates wavelengths less than 300 nm. At longer wavelengths, water vapor, carbon dioxide, and oxygen absorb light significantly at particular wavelengths, producing sharp dips in the spectrum. At still-longer wavelengths, beyond 4000 nm, all objects in the environment become significant sources of radiations, depending on their temperature, and surpass sunlight in intensity. These characteristics of the environment restrict the range of electromagnetic radiation. Solar radiant energy that reaches the surface of the earth has a spectral range from about 300 nm (ultraviolet) to about 4000 nm (infrared). Photosynthetically active radiation (PAR) occurs between approximately 400 and 750 nm and is less than 50% of the total energy impinging on the earth's surface (Figure 3.2).

Before describing the detectors used in the field application, a short lexicon of the terms and the conversion units on light measurements would be very useful because of the plethora of confusing terminology and units.

RADIOMETRY

Radiometry is the science of measuring light in any portion of the electromagnetic spectrum. In practice, the term is usually limited to the measurement of infrared, visible, and ultraviolet light using optical instruments, such as radiation thermocouples, bolometers, photodiodes, photosensitive dyes and emulsions, vacuum phototubes, charge-coupled devices, etc.

MEASUREMENT GEOMETRIES: SOLID ANGLES

One of the key concepts to understanding the relationships between measurement geometries is that of the solid angle, ω. This can be defined as the angle that, seen from the center of the sphere, includes a given area on the surface of that sphere. The value of a solid angle is numerically equal to the size of the area on the surface of the sphere, A, divided by the square of the radius, r, of that sphere:

$$\mathrm{w} = \frac{A}{r^2}. \tag{4.4}$$

The value of a solid angle is given in steradian. A sphere of radius r and surface of $4\pi r^2$ will contain 4π steradians. The steradian is a dimensionless quantity.

A surface can be described as a continuum of infinitesimal points, each occupying an infinitesimal area, dA,

$$\mathrm{dw} = \frac{\mathrm{d}A}{r^2}, \tag{4.5}$$

where dω is the differential solid angle of the elemental cone containing a ray of light that is arriving at or leaving a infinitesimal surface dA. The symbol d stands for differential, the operator that reduces the applied variable to an infinitesimal quantity.

Most radiometric measurements do not require an accurate calculation of the spherical surface area. Flat area estimates can be substituted for spherical area when the solid angle is less than 0.03 steradians, resulting in an error of <1%. This roughly translates to a distance at least 5 times greater

than the largest dimension of the detector. When the light source is the sun, flat area estimates can be substituted for a spherical area.

RADIANT ENERGY

Light is radiant energy. When light is absorbed by a physical object, its energy is converted into some other form. Visible light causes an electric current to flow in a light detector when its radiant energy is transferred to the electrons as kinetic energy.

Radiant energy (denoted as Q) is measured in joules (J).

SPECTRAL RADIANT ENERGY

A broadband source such as the sun emits electromagnetic radiation throughout most of the electromagnetic spectrum. However, most of its radiant energy is concentrated within the PAR. A single-wavelength laser, on the other hand, is a monochromatic source; all of its radiant energy is emitted at one specific wavelength.

From this, we can define spectral radiant energy, which is the amount of radiant energy per unit wavelength interval at wavelength λ and is defined as

$$Q_\lambda = \frac{dQ}{d\lambda}. \tag{4.6}$$

Spectral radiant energy is measured in joules per nanometer (J nm^{-1}).

RADIANT FLUX (RADIANT POWER)

Energy per unit time is power, which we measure in joules per second (J s^{-1}), or watts (W). Light "flows" through space and so radiant power is more commonly referred to as the flow rate of radiant energy with respect to time or radiant flux. It is defined as

$$\Phi = \frac{dQ}{dt}, \tag{4.7}$$

where Q is the radiant energy and t the time.

In terms of a light detector measuring PAR, the instantaneous magnitude of the electric current is directly proportional to the radiant flux. The total amount of current measured over a period of time is directly proportional to the radiant energy absorbed by the light detector during that time.

For phycological purpose, radiant flux is expressed also as μmol of photons per second.

SPECTRAL RADIANT FLUX (SPECTRAL RADIANT POWER)

Spectral radiant flux at wavelength λ is radiant flux per unit wavelength interval. It is defined as

$$\Phi_\lambda = \frac{d\Phi}{d\lambda} \tag{4.8}$$

and is measured in watts per nanometer (W nm^{-1}).

RADIANT FLUX DENSITY (IRRADIANCE AND RADIANT EXITANCE)

Radiant flux density is the radiant flux per unit area at a point on a surface. Radiant flux density is measured in watts per square meter (W m^{-2}).

There are two possible conditions. The flux can be arriving at the surface in which case the radiant flux density is referred to as irradiance. Irradiance is defined as

$$E = \frac{d\Phi}{dA}, \tag{4.9}$$

where Φ is the radiant flux arriving at the infinitesimal area dA.

Since irradiance is the radiant flux per unit area, it can be expressed as mole of photons per area per unit time (μmol m^{-2} s^{-1}). Modern instruments measure *in situ* irradiance directly in these units.

The flux can also be leaving the surface due to emission or reflection. The radiant flux density is referred to as radiant exitance. As with irradiance, the flux can leave in any direction above the surface. The definition of radiant exitance is

$$M = \frac{d\Phi}{dA}, \tag{4.10}$$

where Φ is the radiant flux leaving the infinitesimal area dA.

Typical Values for Irradiance	(in W m^{-2})
Sunlight	1000
Skylight	100
Overcast daylight	10
Moonlight	0.001
Starlight	0.0001

SPECTRAL RADIANT FLUX DENSITY

Spectral radiant flux density is radiant flux per unit wavelength interval at wavelength λ. When the radiant flux arrives at the surface, it is called spectral irradiance and is defined as

$$E_\lambda = \frac{dE}{d\lambda}. \tag{4.11}$$

When the radiant flux leaves the surface, it is called spectral radiant exitance and is defined as

$$M_\lambda = \frac{dM}{d\lambda}. \tag{4.12}$$

Spectral radiant flux density is measured in watts per square meter per nanometer (W m^{-2} nm^{-1}).

RADIANCE

Imagine a ray of light arriving at or leaving a point on a surface in a given direction. Radiance is simply the amount of radiant flux contained in this ray (a cone of solid angle dω). If the ray intersects a surface at an angle θ with the normal to that surface, and the area of intersection with the surface has an infinitesimal cross-sectional area dA, the cross-sectional area of the ray is dA cos θ. The radiance of this ray is

$$L = \frac{d^2\Phi}{dA\, d\omega \cos\theta}. \tag{4.13}$$

Radiance is measured in watts per square meter per steradian (W m^{-2} sr^{-1}).

Unlike radiant flux density, the definition of radiance does not distinguish between flux that arrives at or leaves a surface.

Another way of looking at radiance is to note that the radiant flux density at a point on a surface due to a single ray of light arriving (or leaving) at an angle θ to the normal to that surface is $d\Phi/dA \cos \theta$. The radiance at that point for the same angle is then $d^2\Phi/(dA\, d\omega \cos \theta)$, or radiant flux density per unit solid angle.

The irradiance, E, at any distance from a uniform extended area source is related to the radiance, L, of the source by the following relationship, which depends only on the subtended central viewing angle, θ, of the radiance detector:

$$E = \pi L \sin^2(\theta/2). \tag{4.14}$$

Radiance is independent of distance for an extended area source, because the sampled area increases with distance, cancelling inverse square losses. The inverse square law defines the relationship between the irradiance from a point source and the distance d. It states that the intensity per unit area is inversely proportional to the square of the distance. In other words, if you measure 16 W m^{-2} at 1 m, you will measure 4 W m^{-2} at 2 m, and can likewise calculate the irradiance at any other distance. The following alternate form is often more convenient:

$$E_1 d_1^{\,2} = E_2 d_2^{\,2}. \tag{4.15}$$

SPECTRAL RADIANCE

Spectral radiance is the radiance per unit wavelength interval at wavelength λ. It is defined as

$$L_\lambda = \frac{d^3\Phi}{dA\, d\omega \cos\theta\, d\lambda} \tag{4.16}$$

and is measured in watts per square meter per steradian per nanometer (W m^{-2} sr^{-1} nm^{-1}).

RADIANT INTENSITY

We can imagine a small point source of light that emits radiant flux in every direction. The amount of radiant flux emitted in a given direction can be represented by a ray of light contained in an elemental cone. This gives us the definition of radiant intensity:

$$I = \frac{d\Phi}{d\omega}, \tag{4.17}$$

where $d\omega$ is the infinitesimal solid angle of the elemental cone containing the given direction. From the definition of an infinitesimal solid angle, we obtain

$$I = r^2\left(\frac{d\Phi}{dA}\right) \quad \text{or} \quad I = r^2 E \quad \text{or} \quad E = \frac{I}{r^2}, \tag{4.18}$$

where the infinitesimal surface area dA is on the surface of a sphere centered on the source and at a distance r from the source and E is the irradiance of that surface. More generally, the radiant flux will intercept dA at an angle θ from the surface normal. This gives us the inverse square law for point sources:

$$E = \frac{I_\theta \cos\theta}{d^2}, \tag{4.19}$$

where I_θ is the intensity of the source in the θ-direction and d the distance from the source to the surface element dA. Radiant intensity is measured in watts per steradian (W sr^{-1}).

Combining the definitions of radiance (Equation 4.13) and radiant intensity (Equation 4.17) gives us an alternative definition of radiance:

$$L = \frac{\mathrm{d}I_\theta}{\mathrm{d}A\cos\theta}, \tag{4.20}$$

where $\mathrm{d}I_\theta$ is the infinitesimal intensity of the point source in the θ-direction with the surface normal.

SPECTRAL RADIANT INTENSITY

Spectral radiant intensity is the radiant intensity per unit wavelength interval at wavelength λ. It is defined as

$$I_\lambda = \frac{\mathrm{d}I}{\mathrm{d}\lambda} \tag{4.21}$$

and measured in watts per steradian per nanometer (W sr^{-1} nm^{-1}).

PHOTOMETRY

Photometry is the science of measuring visible light in units that are weighted according to the sensitivity of the human eye. It is a quantitative science based on a statistical model of the human visual response to light under carefully controlled conditions. We cannot apply this model to the "perception" of light by algae, since we should substitute the sensitivity of the algal photoreception systems for that of the human eye.

For the human perception, the CIE (Commission International d'Eclairage) photometric curves (photopic and scotopic) provide a weighting function that can be used to convert radiometric into photometric measurements. In a scotopic curve, yellowish-green light receives the greatest weight because it stimulates the eye more than blue or red light of equal radiant power ($\lambda_{max} = 555$ nm) (Figure 4.9 and Table 4.3), whereas in a photopic curve blue-green light receives the greatest weight because it stimulates the eye more than other lights of equal radiant power ($\lambda_{max} = 507$ nm) (Figure 4.9 and Table 4.3). For algae, action spectroscopy may be used for a similar purpose even though the spectra so far measured are contradictory, not very accurate, and very often are difficult to interpret (Figure 4.9).

LUMINOUS FLUX (LUMINOUS POWER)

Luminous flux is radiant flux weighted to match the eye response of the "standard observer." Its unit of measurement is the lumen. The lumen (lm) is the photometric equivalent of the watt and is defined as 1/683 watts of radiant power at a frequency of 540×10^{12} Hz, or better at a wavelength of 555 nm.

LUMINOUS INTENSITY

The luminous intensity is the luminous flux emitted from a point source per unit solid angle into a given direction. The luminous intensity is measured in candela (the Latin word for "candle"). Together with the CIE photometric curve, the candela provides the weighting factor needed to convert between radiometric and photometric measurements. The candela (cd) is the luminous intensity, in a given direction, of a source that emits monochromatic radiation with a frequency of 540×10^{12} Hz ($\lambda = 555$ nm) and has a radiant intensity of 1/683 W sr^{-1} in that direction.

TABLE 4.3
Luminous Efficacy of the Eye at the Different Wavelengths Tabulated for Both the Light-Adapted (Photopic) Vision and the Dark-Adapted (Scotopic) Vision

λ (nm)	Photopic Luminous Sensitivity	Photopic lm W^{-1} Conversion	Scotopic Luminous Sensitivity	Scotopic lm W^{-1} Conversion
380	0.000039	0.027	0.000589	1.001
390	0.000120	0.082	0.002209	3.755
400	0.000396	0.270	0.009290	15.793
410	0.001210	0.826	0.034840	59.228
420	0.004000	2.732	0.096600	164.220
430	0.011600	7.923	0.199800	339.660
440	0.023000	15.709	0.328100	557.770
450	0.038000	25.954	0.455000	773.500
460	0.060000	40.980	0.567000	963.900
470	0.090980	62.139	0.676000	1149.200
480	0.139020	94.951	0.793000	1348.100
490	0.208020	142.078	0.904000	1536.800
500	0.323000	220.609	0.982000	1669.400
507	0.444310	303.464	**1.000000**	**1700.000**
510	0.503000	343.549	0.997000	1694.900
520	0.710000	484.930	0.935000	1589.500
530	0.862000	588.746	0.811000	1378.700
540	0.954000	651.582	0.650000	1105.000
550	0.994950	679.551	0.481000	817.700
555	**1.000000**	**683.000**	0.402000	683.000
560	0.995000	679.585	0.328800	558.960
570	0.952000	650.216	0.207600	352.920
580	0.870000	594.210	0.121200	206.040
590	0.757000	517.031	0.065500	111.350
600	0.631000	430.973	0.033150	56.355
610	0.503000	343.549	0.015930	27.081
620	0.381000	260.223	0.007370	12.529
630	0.265000	180.995	0.003335	5.670
640	0.175000	119.525	0.001497	2.545
650	0.107000	73.081	0.000677	1.151
660	0.061000	41.663	0.000313	0.532
670	0.032000	21.856	0.000148	0.252
680	0.017000	11.611	0.000072	0.122
690	0.008210	5.607	0.000035	0.060
700	0.004102	2.802	0.000018	0.030
710	0.002091	1.428	0.000009	0.016
720	0.001047	0.715	0.000005	0.008
730	0.000520	0.355	0.000003	0.004
740	0.000249	0.170	0.000001	0.002
750	0.000120	0.082	0.000001	0.001
760	0.000060	0.041	0.000001	0.001
770	0.000030	0.020	0.000001	0.001

Note: The table also shows the conversion factors to use when reporting the photometric units (luminous flux) in radiometric units (radiant flux). See text for details.

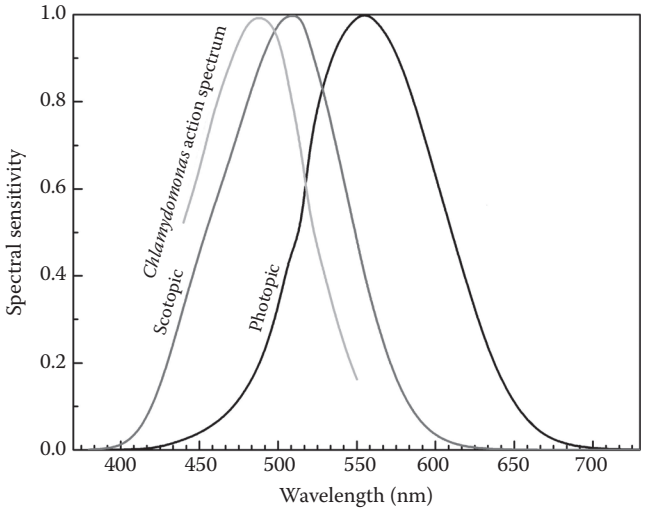

FIGURE 4.9 Curves of spectral sensitivity for the scotopic (dark-adapted) and photopic (light-adapted) human vision compared with the action spectrum of *Chlamydomonas*.

If a light source is isotropic, that is, its intensity does not vary with direction, then the relationship between lumens and candelas is 1 cd = 4π lm. In other words, an isotropic source having a luminous intensity of 1 candela emits 4π lumens into space, which just happens to be 4π steradians. We can also state that 1 cd = 1 lm sr, analogous to the equivalent radiometric definition. If a source is not isotropic, the relationship between candelas and lumens is empirical. A fundamental method used to determine the total flux (lumens) is to measure the luminous intensity (candelas) in many directions using a goniophotometer, and then numerically integrate over the entire sphere. Since 1 steradian has a projected area of 1 m^2 at a distance of 1 m, a 1 cd light source will duly produce 1 lm m^{-2} (Figure 4.10).

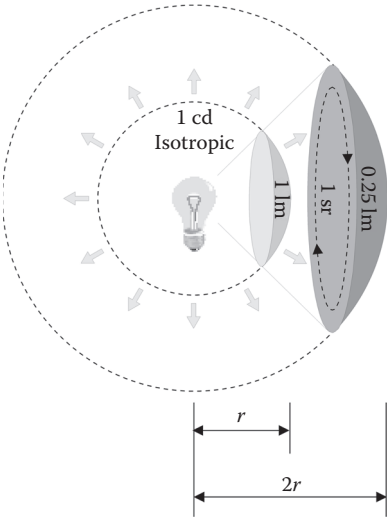

FIGURE 4.10 Luminous intensity: a 1-cd light source emits 1 lm per steradian in all directions (isotropically). According to the inverse square law, the intensity is inversely proportional to the square of the distance, that is, at a distance of 2*r* from the source; the intensity will be equal to 1/4 lm sr^{-1}.

Typical Values for Luminous Intensity	(in cd)
Flashtube	1,000,000
Automobile headlamp	100,000
100 W incandescent bulb	100
Light-emitting diode (LED)	0.0001

LUMINOUS ENERGY

Luminous energy is photometrically weighted radiant energy. It is measured in lumen per second (lm s^{-1}).

LUMINOUS FLUX DENSITY (ILLUMINANCE AND LUMINOUS EXITANCE)

Luminous flux density is photometrically weighted radiant flux density. Illuminance is the photometric equivalent of irradiance, whereas luminous exitance is the photometric equivalent of radiant exitance.

Luminous flux density is measured in lux (lx) or lumens per square meter (lm m^{-2}).

Typical Values for Illuminance	(in lux)
Sunlight	100,000
Skylight	10,000
Overcast daylight	1000
Moonlight	0.1
Starlight	0.01.

LUMINANCE

Luminance is photometrically weighted radiance. In terms of visual perception, we perceive luminance. It is an approximate measure of how "bright" a surface appears when we view it from a given direction. Luminance used to be called "photometric brightness." Luminance is measured in lumens per square meter per steradian (lm m^{-2} sr^{-1}).

LAMBERTIAN SURFACES

A Lambertian surface is referred to as a perfectly diffusing surface, which adheres to Lambert's cosine law. This law states that the reflected or transmitted luminous intensity in any direction from an element of a Lambertian surface varies as the cosine of the angle between that direction and the normal of the surface. The intensity I_θ of each ray leaving the surface at an angle θ from the ray in a direction perpendicular to the surface (I_n) is given by

$$I_\theta = I_n \cos\theta. \tag{4.22}$$

Therefore, even if the luminous intensity decrease with a factor cos θ from the normal, the projected surface decreases with the same factor; as a consequence, the radiance (luminance) of a Lambertian surface is the same regardless of the viewing angle, and is given by

$$L = \frac{dI_n \cos\theta}{dA \cos\theta} = \frac{dI_n}{dA}. \tag{4.23}$$

It is worthwhile to note that in a Lambertian surface the ratio between the radiant exitance and the radiance is π and not 2π:

$$\frac{M}{L} = \mathrm{p}. \tag{4.24}$$

This equation can be easily derived. Suppose we place an infinitesimal Lambertian emitter dA on the inner surface of an imaginary sphere S. The inverse square law (Equation 4.15) provides the irradiance E at any point P on the inner surface of the sphere. However, $d = D \cos \theta$, where D is the diameter of the sphere. Thus

$$E = \frac{I_{\mathrm{q}}}{D^2 \cos \mathrm{q}} \tag{4.25}$$

and from Lambert's cosine law (Equation 4.22), we have

$$E = \frac{I_{\mathrm{n}}}{D^2}, \tag{4.26}$$

which simply says that the irradiance (radiant flux density) of any point P on the inner surface of S is a constant.

This is interesting. From the definition of irradiance (Equation 4.9), we know that $\Phi = EA$ for constant flux density across a finite surface area A. Since the area A of the surface of a sphere with radius r is given by

$$A = 4\mathrm{p}r^2 = \mathrm{p}D^2, \tag{4.27}$$

we have

$$\Phi = EA = \mathrm{p}I_{\mathrm{n}}. \tag{4.28}$$

Given the definition of radiant exitance (Equation 4.10) and radiance for a Lambertian surface (Equation 4.23), we have

$$M = \frac{\mathrm{d}\Phi}{\mathrm{d}A} = \mathrm{p}L. \tag{4.29}$$

This explains, clearly and without resorting to integral calculus, where the factor of π comes from.

UNITS CONVERSION

Radiant and Luminous Flux (Radiant and Luminous Power)

- 1 J (joule) = 1 W s (watt second)
- 1 W (watt) = 683.0 lm (photopic) at 555 nm = 1700.0 lm (scotopic) at 507 nm
- 1 lm = 1.464×10^{-3} W at 555 nm = $1/4\pi$ candela (cd) (only if isotropic)
- 1 lm s^{-1} (lumen seconds^{-1}) = 1.464×10^{-3} J at 555 nm

A monochromatic point source with a wavelength of 510 nm with a radiant intensity of 1/683 W sr^{-1} has a luminous intensity of 0.503 cd, since the photopic luminous efficiency at 510 nm is 0.503.

A 680-nm laser pointer with the power of 5 mW produces 0.005 W * 0.017 * 683 lm W^{-1} = 0.058 lm, while a 630-nm laser pointer with a power of 5 mW produces 0.905 lm, a significantly greater power output.

Determining the luminous flux from a source radiating over a spectrum is more difficult. It is necessary to determine the spectral power distribution for the particular source. Once that is done, it is necessary to calculate the luminous flux at each wavelength or at regular intervals for continuous spectra. Adding up the flux at each wavelength gives a total flux produced by a source in the visible spectrum.

A standard incandescent lamp produces a continuous spectrum in the visible region, and various intervals must be used to determine the luminous flux. For sources like a mercury vapor lamp, however, it is slightly easier. Mercury emits light primarily in a line spectrum. It emits radiant flux at six primary wavelengths. This makes it easier to determine the luminous flux of this lamp versus the incandescent.

Generally, it is not necessary to determine the luminous flux for yourself. It is commonly given for a lamp based on laboratory testing during manufacture. For instance, the luminous flux for a 100-W incandescent lamp is approximately 1700 lm. We can use this information to extrapolate the flux for similar lamps. Thus, the average luminous efficacy for an incandescent lamp is about 17 lm W^{-1}. We can now use this as an approximation for similar incandescent sources at various wattages.

Irradiance (Flux Density)

- 1 W m^{-2} = 10^{-4} W cm^{-2} = 6.83×10^2 lx at 555 nm
- 1 lm m^{-2} = 1 lux = 10^{-4} lm cm^{-2}
- 1 photon at 400 nm = 4.96×10^{-19} J
- 1 W m^{-2} at 400 nm = 1 J m^{-2} s^{-1} = 3.3 µmol m^{-2} s^{-1} = 3.3 µEinsten m^{-2} s^{-1}
- 1 photon at 500 nm = 3.97×10^{-19} J
- 1 W m^{-2} at 500 nm = 1 J m^{-2} s^{-1} = 4.2 µmol m^{-2} s^{-1} = 4.2 µEinsten m^{-2} s^{-1}
- 1 photon at 600 nm = 3.31×10^{-19} J
- 1 W m^{-2} at 600 nm = 1 J m^{-2} s^{-1} = 5.0 µmol m^{-2} s^{-1} = 5.0 µEinsten m^{-2} s^{-1}
- 1 photon at 700 nm = 2.83×10^{-19} J
- 1 W m^{-2} at 700 nm = 1 J m^{-2} s^{-1} = 5.9 µmol m^{-2} s^{-1} = 5.9 µEinsten m^{-2} s^{-1}

Radiance

- 1 W m^{-2} sr^{-1} = 6.83×10^2 lm m^{-2} sr^{-1} = 683 cd cm^{-2} at 555 nm

Radiant Intensity

- 1 W sr^{-1} = 12.566 W (isotropic) = 4π W = 683 cd at 555 nm

Luminous Intensity

- 1 lm sr = 1 cd = 4π lm (isotropic) = 1.464×10^{-3} W sr^{-1} at 555 nm

Luminance

- 1 lm m^{-2} sr^{-1} = 1 cd m^{-2} = 10^{-4} lm cm^{-2} sr^{-1} = 10^{-4} cd cm^{-2}

Geometries

Converting between geometry-based measurement units is difficult and should be attempted only when it is impossible to measure in the actual desired units. You must be aware of what each of the

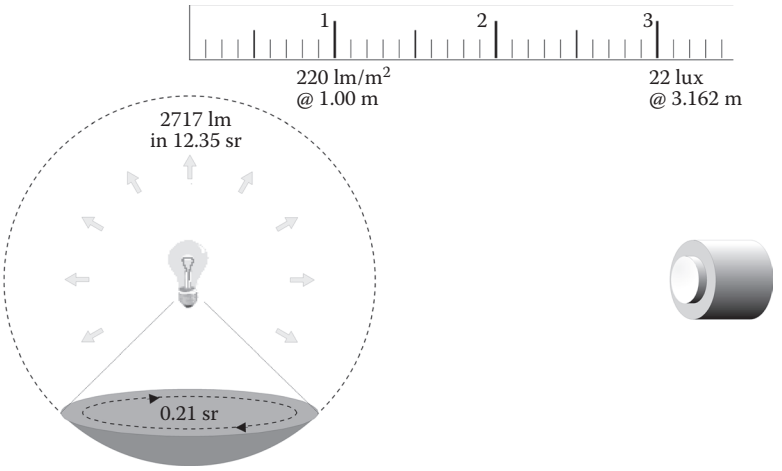

FIGURE 4.11 Example of conversion between lux and lumen.

measurement geometries implicitly assumes before you can convert. The example below shows the conversion between lux and lumens.

If you measure 22.0 lux from a light bulb at a distance of 3.162 m, how much light, in lumens, is the bulb producing? Assume that the lamp is an isotropic point source, with the exception that the base blocks a 30° solid angle.

Using Equation 4.15, the irradiance at 1.0 m is

$$E_{1.0\,\mathrm{m}} = \left(\frac{3.162}{1.0}\right)^2 \times 22.0 = 219.96\,\mathrm{lm\,m^{-2}}.$$

Based on steradian definition (Equation 4.4), we know that 1 sr cuts off a spherical surface area of 1 m^2 at a distance of 1 m from the source. Therefore, 220 lm m^{-2} corresponds to 220 lm sr^{-1}. The solid angle of the lamp is equal to $2\pi h\ r^{-1}$ (Equation 4.4), where h is the height of the spherical calotte and corresponds to 2π [1–cos(360 – 30/2)] = 12.35 sr, while the shadowed solid angle corresponds to 0.21 sr. Therefore, the total lumen output will be 220 lm sr^{-1} 12.35 sr = 2717 lm (Figure 4.11).

PAR DETECTORS

Photosynthetic irradiance is the radiant flux density of PAR and is expressed as the radiant energy (400–700 nm) incident on a unit of surface per unit time. A PAR detector is typically an irradiance detector that is equally sensitive to light between 400 and 750 nm and insensitive to light outside this region. Irradiance is now internationally expressed in moles of photons per unit area and per unit time as µmol m^{-2} s^{-1} (formerly µEinsten m^{-2} s^{-1}), where 1 µmol (µEinsten) corresponds to 1 micromole of photons, that is, 6.02×10^{17} photons, at a given wavelength. Modern instruments measure *in situ* irradiance flux densities directly in µmol m^{-2} s^{-1}.

In terms of collector geometry, a PAR detector is usually equipped with either a planar (cosine) or a spherical (scalar) collector. A planar or 2π collector measures PAR in a 180° arc, while a spherical or 4π collector measures the light impinging from all directions on a single point (Figure 4.12).

The irradiance impinging on the surface of the water or sediment is commonly measured with a planar detector. Spherical detectors provide a measurement of the amount of light available for

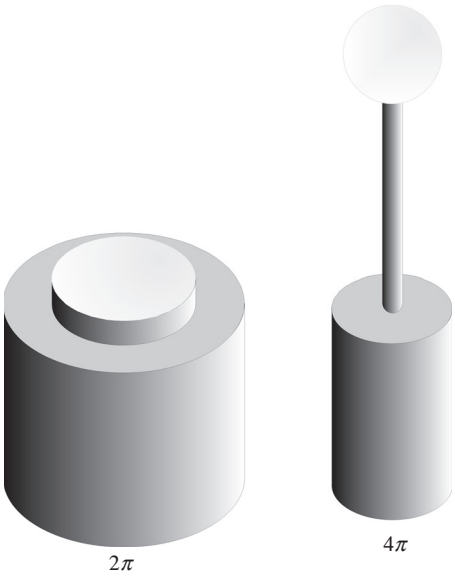

FIGURE 4.12 Examples of PAR detectors equipped with a planar 2π collector or with a spherical 4π collector.

photosynthesis by phytoplankton suspended in the water column. A leaf resembles a small planar collector, whereas algae resemble small spherical collectors.

Direct solar radiation reaching the water surface varies with the angular height of the radiation and therefore, with time of day, season, and latitude. The quantity and quality of light also vary with the molecular transparency of the atmosphere and the distance the light must travel through it; therefore, it varies with altitude and meteorological conditions. In water, upwelling (bottom-reflected radiance) and downwelling (depth-attenuated radiance) irradiance are usually quantified using paired cosine collectors mounted on a frame that is lowered in the water column. Spherical collectors are also mounted on a frame and lowered into the water to obtain light profiles. For photophysiological studies, spherical collectors provide a realistic measure of the total amount of PAR available for photosynthesis in a water body.

Accurate measurement of photosynthetic radiation is essential for controlled environmental research. The most common method of measuring PAR gives equal value, that is, equal energy content, to all photons with wavelength between 400 and 750 nm and is referred to as the photosynthetic photon flux (PPF) measured in $\mu mol\ m^{-2}\ s^{-1}$. The ideal PPF sensor would respond equally to all photons between 400 and 750 nm. However, photosynthesis is also driven by photons with wavelength below 400 nm and above 750 nm, and photons of different wavelength induce an unequal amount of photosynthesis. For these reasons, an accurate measurement of PAR should follow the relative quantum efficiency (RQE) curve, which weights the photosynthetic value of all photons with wavelength from 360 to 760 nm. The RQE resembles the absorption spectrum of the absorbing algal structures. A sensor that responds according to this curve measures yield photon flux (YPF) in micromoles per square meter per second, the same unit of PPF.

Detectors designed to measure YPF or PPF are commercially available. Both types consist of an optical diffuser collector (planar or spherical) and multiple spectral filters in front of a broad-spectrum photovoltaic detector.

Planar detectors measure only unreflected sunlight. They should possess cosine-corrected response; since the light impinging on the measurement plane is proportional to the cosine of the angle at which the light is incident, the response of the detector must also be proportional to the

cosine of the incidence angle (see Equation 4.22). An integrating sphere measures both unreflected and all the scattered sunlight; it needs no correction since it is the ideal cosine detector, responding equally to light coming from all directions.

The peak responsivity and bandwidth of a detector can be controlled through the use of filters. Filters can suppress out-of-band light but cannot boost signal and can restrict the spatial responsivity of the detector. Filters operate either by absorption or by interference. Colored glass filters are doped with materials that selectively absorb light by wavelength and obey the Lambert–Beer law. The peak transmission is inherent to the additives, while bandwidth is dependent on thickness. Interference filters, which select very narrow bandwidths, rely on thin layers of dielectric to cause constructive interference between the wavefronts of the incident white light. So, by varying filter thickness, we can selectively modify the spectral responsivity of a detector to match a particular function. Pass-band filters are often used to select a specific wavelength radiation. Any of these filter types can be combined to form a composite filter that matches a particular photobiological process. Multiple filters cemented in layers give a net transmission equal to the product of the individual transmissions. The detector's overall spectral sensitivity is equal to the product of the responsivity of the detector and the transmission of the filters. Given a desired overall sensitivity and known detector responsivity, we can then solve for the ideal filter transmission curve.

Different measurement geometries necessitate specialized input optics. Radiance and luminance measurements require a narrow viewing angle (<4°) in order to satisfy the conditions underlying the measurement units. Power measurements, on the other hand, require a uniform response to radiation regardless of input angle to capture all the light.

THE PHOTOSYNTHESIS–IRRADIANCE RESPONSE CURVE (*P* vs. *E* CURVE)

The *P* versus *E* curve or the light-response curve shows how photosynthetic rate varies with increasing irradiance. The rate of photosynthesis can be measured as net O_2 evolution or as carbon fixation per chlorophyll *a* units, measured as mg C * (mg chlorophyll *a*)$^{-1}$ h^{-1}. This curve describes a complex multistep process that depends upon several limiting factors. Three regions are present in the curve: a light-limited region, a light-saturated region, and a light-inhibited region. The basic description of the *P–E* curves requires a nonlinear mathematical function to account for the light saturation effects. Quite a few such functions have been employed with varying degrees of success, such as rectangular hyperbola, and quadratic, exponential, and hyperbolic tangent.

In our opinion, the rectangular hyperbolic function such as the Michaelis–Menten formulation that describes the nutrient uptake kinetics is quite suitable to describe the dynamic relationship between photosynthetic rate and irradiance, though the Michaelis–Menten formulation shows a much less sharper transition from the limited region to the saturated region. The *P–E* curve (without the light-inhibited) region can be described with the following rectangular hyperbolic function:

$$P_E = \frac{P_{max} E_1}{K_m + E_1}, \tag{4.30}$$

where P_E is the photosynthetic rate at any irradiance E, E_λ the spectral irradiance (in μmol m^{-2} s^{-1}) and K_m is the half-saturation constant when $P_E = P_{max}/2$ (Figure 4.13a).

In the light-limited region, that is, at low irradiance levels, the rate of photon absorption determines the rate of steady-state electron transport from H_2O to CO_2. In the light-limited region, the available light is insufficient to support the maximum potential rate of the light-dependent reactions and thus limits the overall rate of photosynthesis. In this region, P_E can be described as

$$P_E = E_1 \mathtt{a}, \tag{4.31}$$

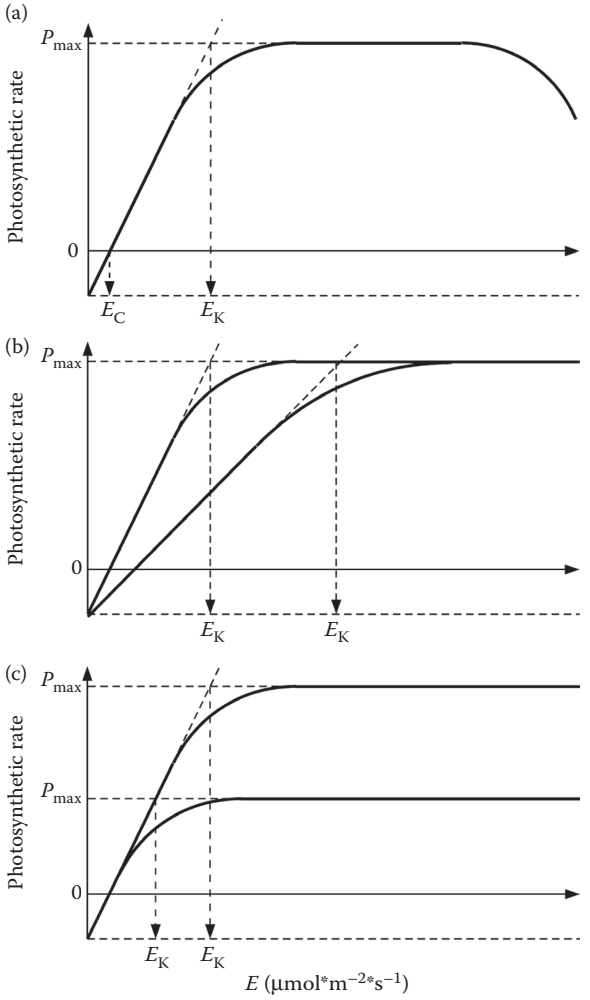

FIGURE 4.13 Photosynthesis–irradiance response curves; E_C, irradiance compensation point; E_K, saturating irradiance; P_{max}, maximum photosynthetic rate. (a) Typical plot; (b) comparison of two curves with different slopes: keeping constant the number of photosynthetic units, but increasing the functional absorption cross-section, the slope increases; (c) comparison of two curves with different maximum photosynthetic rate: increasing the number of photosynthetic units P_{max} increases.

where E_λ is the spectral irradiance and α a measure of "photosynthetic efficiency" or how efficiently solar energy is converted into chemical energy. α represents the slope of the P vs E curve at low light levels, that is, the initial linear part of the curve estimated as

$$(\text{mg chlorophyll } a)^{-1}\,\text{h}^{-1}\,\mu\text{mol}\,\text{m}^{-2}\,\text{s}^{-1}$$

α takes into account that the light absorbed by the algal cell is proportional to the functional absorption cross-section (σ_{PSII}) of the PSII (the effective area that a molecule presents to an incoming photon and that is proportional to the probability of absorption) and to the number of photosynthetic units (n):

$$\mathtt{a} = \mathtt{s}_{PSII} n \tag{4.32}$$

Equation 4.31 shows that the photosynthetic rate is linearly proportional to irradiance at low irradiance levels. The greater the slope (α), the more efficient is the photosynthetic process (Figure 4.13b). By keeping the number of photosynthetic units constant but increasing the functional absorption cross-section the slope will increase. The slope can be normalized to chlorophyll biomass and, if so, a superscript "B" is added to denote this normalization: α^B. In this case, the curve dimensions are O_2 evolved (or C fixed) per unit chlorophyll *a* and quanta per unit area.

At very low irradiance level, the rate of oxygen consumption will be greater than the rate of oxygen evolution; hence, respiration is greater than photosynthesis and net oxygen evolution will be negative. Therefore, the *P–E* curve does not pass through the origin. The irradiance value on the *X*-axis at which photosynthesis balances respiration is called the light compensation point (E_c). Therefore, Equation 4.30 becomes

$$P_E = \frac{P_{max}(E_1 - E_C)}{K_m + (E_1 - E_C)} \tag{4.33}$$

This phenomenon (chlororespiration) is more pronounced in cyanobacteria, where the photosynthetic and respiratory pathways share common electron carriers (cytochromes). The irradiance levels needed to reach the compensation point (E_C) are about 10 μmol m^{-2} s^{-1} for shallow water, but are much lower in dim habitats.

As irradiance increases, more ATP and NADPH are produced, and the overall rate of photosynthesis becomes increasingly nonlinear rising towards its maximum or saturation level, P_{max} (light-saturated photosynthesis per unit of chlorophyll *a*). This pattern will continue until some other factors become limiting. By definition, in the light-saturated region, the rate of photon absorption exceeds the rate of steady-state electron transport from H_2O to CO_2. Saturating irradiance, E_K, is defined at the point at which the extrapolated initial slope crosses P_{max}:

$$E_K = \frac{P_{max}}{a} \tag{4.34}$$

E_K represents an optimum on the photosynthesis irradiance curve.

Light-saturated photosynthetic rate is independent of the functional absorption cross-section of the photosynthetic apparatus and is related only to the number of photosynthetic unit (*n*) and its steady-state electron turnover rate through the PSII reaction center ($1/\tau_{PSII}$):

$$P_{max} = n\left(\frac{1}{t_{PSII}}\right). \tag{4.35}$$

This equation says that increasing the number of photosynthetic units (but not their size) P_{max}, that is, the saturation level, increases, and that P_{max} cannot be derived from measurements of light absorption (Figure 4.13c). In other words, above the saturation point (E_K), the light-dependent reaction is producing more ATP and NADPH than that can be used by the light-independent reaction for CO_2 fixation, that is, increasing irradiance no longer causes any increase in the photosynthetic rate. Above E_K and under normal condition, availability of CO_2 is the limiting factor, since the concentration of CO_2 in the atmosphere is very low (0.035%, v/v).

Saturating irradiances show some correlation with habitat, but generally, they are low compared with full sun. Intertidal species require 400–600 μmol m^{-2} s^{-1} (ca. 10% of the full sun irradiance), upper and midsublittoral species 150–250 μmol m^{-2} s^{-1} and deep sublittoral species less than 100 μmol m^{-2} s^{-1}. Diatoms under ice, saturate at 5 μmol m^{-2} s^{-1}.

Further increase in irradiance beyond light saturation can lead to a reduction in the photosynthetic rate from the maximum saturation level. This reduction, which is dependent on both the

irradiance and the duration of the exposure, is often termed photoinhibition. Photoinhibition can be thought as a modification of P_{max} either by a reduction in the number of photosynthetic units or by an increase in the maximum turnover rate (Equation 4.35); thus, photoinhibition leads to a reduction in the photochemical efficiency of PSII, through a reduction in the population of functional (O_2 evolving) reaction centers. Increasing irradiance levels increase the probability that more than one photon, two, for example, strike the same reaction centers at the same time. The added energies of two blue photons, for example, could be very harmful since the resulting energy will correspond to a UV photon and could damage the chromophores.

PHOTOACCLIMATION

Photoacclimation is a complex light response that changes cellular activities on many time scales.

The aquatic environment presents a highly variable irradiance (E) field with changes occurring over a wide range of time scales. For example, changes in E on short time scales can result from focusing and defocusing of radiation by waves at the surface. Longer time-scale changes can result from variable cloud cover or turbulent motion that transports phytoplankton across the exponential E gradient of the surface mixed layer. In a well-mixed surface layer, phytoplankton experiences long periods of low E interspersed by short periods of saturating or even supersaturating E. The diurnal solar cycle causes changes in E on even longer time scales. To cope with the highly variable radiation environment, phytoplankton has developed numerous strategies to optimize photosynthesis, while minimizing susceptibility to photodamage. Photosynthetic acclimation to E over time scales of hours to days proceeds through changes in cellular pigmentation or structural characteristics, for example, size and number of photosynthetic units. On shorter time scales, cells adjust photon utilization efficiencies by changing the distribution of harvested energy between photosystems (state transitions) or by dissipating excess energy through nonphotochemical processes, for example, xanthophyll cycle or photoinhibition.

Therefore, photoacclimation involves change in the macromolecular composition in the photosynthetic apparatus. It is relatively easy to observe acclimation in unicellular algae and seaweeds, where chlorophylls per cell or per unit surface area can increase five-to-ten-fold as irradiance decrease. The response is not a linear function of irradiance; rather at extremely low light levels, cells often become a bit chlorotic, and on exposure to slightly higher (but still low) irradiance, chlorophyll reaches the maximum. Increase in irradiance leads to a decrease in the cellular complement of chlorophylls until a minimum value is reached. The absolute irradiance levels that induce this effect are species-specific and chlorotic response is not universal. The changes in pigmentation resulting from photoacclimation have profound consequences for light absorption properties of the cells. First, cells acclimated to high irradiance levels generally have high carotenoid concentration relative to chlorophyll a. Carotenoids such as β-carotene and zeaxanthin do not transfer excitation energy to the reaction centers and consequently act to screen the cell from excess light. Some xantophylls such as lutein transfer excitation energy but with reduced efficiency, and therefore effectively reduce the functional absorption cross-section of the associated photosystem. Because these carotenoids absorb light without a concomitant increase in the functional cross-section of PSII, organisms acclimated to high irradiance levels often have lower maximum quantum yield of photosynthetic O_2 evolution. Second, when cells acclimate to low irradiance levels, the subsequent increase in pigmentation is associated with a decrease in functional optical absorption section normalized to chlorophyll a. This effect is due primarily to the self-shading of the chromophores between layers of thylakoids membranes and is inversely proportional to the number of membranes in the chloroplast, that is, the more the membranes, the lower is the optical cross-section. Thus, as cells accumulate chlorophyll, each chlorophyll molecule becomes less effective in light absorption; a doubling of cellular chlorophyll does not produce a doubling in the rate of light absorption. The reduction in the chlorophyll-specific optical absorption cross-section can be visualized considering the fate of photons incident on two

stacks of thylakoid membranes: one is a thin stack from a cell acclimated to high irradiance levels and the second is a thick stack from a cell acclimated to low irradiance levels. The probability of a photon passing through a thick stack of membranes without being absorbed is small compared with a thin stack of membranes. This so-called "package effect" reduces the effectiveness of increased pigmentation in harvesting light and has important implications for the capital costs of light harvesting, that is, the investments in the physical structures of the organism required for the metabolic processes. The diminution in the optical absorption cross-section with increased chlorophyll is also a function of cell size: the larger the cell, the more important this effect. At some point, a cell is, for most practical purposes, optically black, and further increases in pigment levels confer no advantage in light absorption.

There are two basic photoacclimation responses in algae. In one, acclimation is accomplished primarily by changes in the number of photosynthetic reaction centers, while the effective absorption cross-section of the reaction centers remains relatively constant. The second is characterized by relatively large changes in the functional size of the antennae serving the reaction centers, while the number of reaction centers remains relatively constant. Complementary changes in either of the responses produce the same effect on the initial slope of the photosynthesis-irradiance curve. As the functional size of the antenna serving PSII, and not the number of reaction centers, determines the light-saturation parameter, organisms that vary the cross-section would tend to have more control over this parameter, as long as the turnover time remains constant.

SUGGESTED READING

Adir N., Zer H., Shochat S., and I. Ohad. Photoinhibition, a historical perspective. *Photosynthetic Research*, 76, 343–370, 2003.

Barnes, C., Tibbitts T., Sager J., Deitzer G., Bubenheim D., Koerner G., and Bugbee B. Accuracy of quantum sensor measuring yield photon flux and photosynthetic photon flux. *HortScience*, 28, 1197–1200, 1993.

Behrenfeld, M.J., Prasil O., Babin M., and F. Bruyant. In search of a physiological basis for covariations in light-limited and light-saturated photosynthesis. *Journal of Phycology*, 40, 4–25, 2004.

Blanchard G.F., Guarini J.-M., Dang C., and P. Richard. Characterizing and quantifying photoinhibition in intertidal microphytobenthos. *Journal of Phycology*, 40, 692–696, 2004.

Buhrer H. Light within algal cultures: Implications from light intensity within a lens. *Aquatic Science*, 62, 91–103, 2000.

Dusenbery, D.B. *Sensory Ecology—How an Organism Acquires and Responds to Information*. W.H. Freeman and Co., New York, 1992.

Havelkova-Dousova H., Prasil O., and Behrenfeld M.J. Photoacclimation of *Dunaliella tertiolecta* (Chlorophyceae) under fluctuating irradiance. *Photosynthetica*, 42, 273–281, 2004.

http://hyperphysics.phy-astr.gsu.edu/hbase/hframe.html

http://www.4colorvision.com/files/photopiceffic.htm

http://www.4colorvision.com/files/scotopiceffic.htm

http://www.biospherical.com/Index.htm

http://www.cvrl.org/

http://www.fb.u-tokai.ac.jp

http://www.helios32.com/Measuring%20Light.pdf

http://www.helios32.com/Thinking%20Photometrically%20II.pdf

http://www.intl-light.com/ildocs/handbook.pdf

http://www.konicaminoltaeurope.com/products/industrial/en/support/brochure/download/pdfs/the_language_of_light.pdf

http://www.licor.com/

http://www.optics.arizona.edu/

http://www.plantphys.net/

Jones H.G., Archer N., Rotenberg E., and Casa R. Radiation measurement for plant ecophysiology. *Journal of Experimental Botany*, 54, 879–889, 2003.

Levi, L. *Applied Optics—A Guide to Optical System Design*, Vols. I and II. John Wiley and Sons, Inc., New York, 1980.

Lobban C.S. and Harrison P.J. *Seaweed Ecology and Physiology*. Cambridge University Press, NY, 1994.

MacIntyre H.L., Kana T.M., Anning T., and Geider R.J. Photoacclimation of photosynthesis irradiance response curves and photosynthetic pigments in microalgae and cyanobacteria. *Journal of Phycology*, 38, 17–38, 2002.

Singsaas E.L., Ort D.R., and De Lucia E.H. Variation in measured values of photosynthetic quantum yield in ecophysiological studies. *Oecologia*, 128, 15–23, 2001.

5 Biogeochemical Role of Algae

THE ROLE OF ALGAE IN BIOGEOCHEMISTRY

Biogeochemical cycling can be defined as the movement and exchanging of both matter and energy between the four different components of the earth, namely the atmosphere (the air envelope that surrounds the earth), the hydrosphere (includes all the earth's water that is found in streams, lakes, seas, soil, groundwater, and air), the lithosphere (the solid inorganic portion of the earth, including the soil, sediments, and rock that forms the crust and upper mantle, and extends about 80-km deep), and the biosphere (all the living organisms, plants, and animals). The four spheres are not mutually exclusive, but overlap and intersect in a quite dynamic way. Soils contain air and exchange gases with the atmosphere, thus causing the geosphere and atmosphere to overlap; but as they also contain water, the geosphere and hydrosphere too overlap. Dust from the geosphere and water from the hydrosphere occur in the atmosphere. Organisms are present in water bodies, soils, aquifers, and the atmosphere, so the biosphere overlaps with the other three spheres. Chemical elements are cyclically transferred within and among the four spheres, with the total mass of the elements in all of the spheres being conserved, though chemical transformations can change their form.

The biogeochemical cycle of any element describes pathways which are commensurate with the movement of the biologically available form of that element throughout the biosphere (where the term "biological availability" is used to infer the participation of a substance in a "biological" reaction as opposed to its simple presence in biota).

The most efficient cycles are often equated with a high atmospheric abundance of the element. These cycles ensure a rapid turnover of the element and have the flexibility to process the element in a number of different forms or phases (i.e., solid, liquid, and gaseous). Except in a few rare but interesting situations (e.g., geothermal/tectonic systems), all biogeochemical cycles are driven directly or indirectly by the radiant energy of the sun. Energy is absorbed, converted, temporarily stored, and eventually dissipated, essentially in a one-way process (which is fundamental to all ecosystem function). In contrast to energy flow, materials undergo cyclic conversions. Through geologic time, biogeochemical cycling processes have fundamentally altered the conditions on earth in a unidirectional manner, most crucially by decomposition of abiotically formed organic matter on the primitive earth by early heterotrophic forms of life, or changing the originally reducing atmosphere to an oxidized one via the evolution of oxygenic phototrophs. Contemporary biogeochemical cycles, however, tend to be cycling rather than unidirectional, leading to dynamic equilibria between various forms of cycled materials.

Like all organisms, algae provide biogeochemical as well as ecological services; that is, they function to link metabolic sequences and properties to form a continuous, self-perpetuating network of chemical element fluxes. They have played key roles in shaping earth's biogeochemistry and contemporary human economy, and these roles are becoming ever more significant as human impacts on ecosystems result in massive alteration of biogeochemical cycling of chemical elements. Just think about the earth's initial atmosphere, 80% N_2, 10% CO/CO_2, 10% H_2 (by volume): no free O_2 appeared until the development of oxygenic photosynthesis by cyanobacteria, transforming the atmosphere composition in the actual 78% N_2, 21% O_2, 0.036% CO_2, and other minor gases (by volume). Or the petroleum and natural gas we consume as fuels, plastics, dyes, etc. in our everyday life; these fossilized hydrocarbons are mostly formed by the deposition of organic matter consisting of the remains of several freshwater marine microalgae from the classes Eustigmatophyceae,

Dinophyceae, and Chlorophyceae. These remains contain bacterially and chemically resistant, high aliphatic biopolymers (algaenans) and long-chain hydrocarbons that are selectively preserved upon sedimentation and diagenesis and make a significant contribution to kerogens, a source of petroleum under appropriate geochemical condition. Moreover, we are still using the remains of calcareous microorganisms, deposited over millions of years in ancient ocean basins, for building material. Diatomaceous oozes are mined as addictives for reflective paints, polishing materials, abrasives, and for insulation. The fossil organic carbon, skeletal remains, and oxygen are the cumulative remains of algae export production that has occurred uninterrupted for more than 3 billion years in the upper ocean.

99.9% of the biomass of algae is accounted for by six major elements such as carbon (C), oxygen (O), hydrogen (H), nitrogen (N), sulfur (S), and phosphorus (P), plus calcium (Ca), potassium (K), sodium (Na), chlorine (Cl), magnesium (Mg), iron (Fe), and silicon (Si). The remaining elements occur chiefly as trace elements, because they are needed only in catalytic quantities.

All elements that become incorporated into organic material are eventually recycled, but on different time scales. The process of transforming organic materials back to inorganic forms of elements is generally referred to as mineralization. It takes place throughout the water column as well as on the bottom of water bodies (lakes, streams, and seas), where much of the detrital material from overlying waters eventually accumulates. Recycling of minerals may take place relatively rapidly (within a season) in the euphotic zone (i.e., the portion of water column supporting net primary production), or much more slowly (over geological time) in the case of refractory materials which sink and accumulate on the seabed. In the water column, where there is usually plenty of oxygen, decomposition of organic material takes place via oxidative degradation through the action of heterotrophic bacteria. Carbon dioxide and nutrients are returned for re-utilization by the phytoplankton. Ecologically, the most important aspect of recycling in the water bodies is the rate at which growth-limiting nutrients are recycled. Among the nutrients that can be in short supply, nitrate (NO_3^-), iron (bioavailable Fe), phosphate (PO_4^{3-}), and dissolved silicon ($Si(OH)_4$) are most often found in concentration well below the half-saturation levels required for the maximum phytoplankton growth. In particular, algae are important for the biogeochemical cycling of the chemical elements they uptake, assimilate, and produce such as carbon, oxygen, nitrogen, phosphorus, silicon, and sulfur.

We will now briefly consider some of the aspects of these elements in relation to biosynthesis and photosynthesis.

LIMITING NUTRIENTS

Among the elements required for algal growth, there are some that can become limiting factors. The original notion of limitation was introduced by von Liebig more than a century ago to establish a correlation between the yield of a crop and the elemental composition of the substrate required for the synthesis of that crop. Von Liebig stated that if one crop nutrient is missing or deficient, plant growth will be poor, even if the other elements are abundant. That nutrient will be defined "limiting nutrient." This concept has become to be known as Liebig's "Law of the Minimum." Simply stated, Liebig's law means that growth is controlled not by the total of nutrients available but by the nutrient available in the smallest quantity with respect to the requirements of the plant. Liebig likens the potential of a crop to a barrel with staves of unequal length. The capacity of this barrel is limited by the length of the shortest stave and can only be increased by lengthening that stave. When that stave is lengthened, another one becomes the limiting factor.

The concentration of a nutrient will give some indication whether or not the nutrient is a limiting factor, but the nutrient's supply rate or turnover time is more important in determining the magnitude or degree of limitation. For example, if the concentration of a nutrient is a limiting factor, but the supply rate is slightly less than the uptake rate by the algae, then the algae will only be slightly nutrient-limited. Not all the algae are limited by the same nutrient, but it occurs at the species level,

for example, all the diatoms are limited by silicate. Moreover, there is a considerable variation in the degree, kind, and seasonality of nutrient limitation, which is related not only to variations in riverine input, but also to conditions and weather in the outflow area.

In general, growth rate of a population of organisms would be proportional to the uptake rate of that one limiting factor. Nutrient-limited growth is usually modeled with a Monod (or Michaelis–Menten) equation:

$$\mu = \frac{\mu_{max}[LN]}{[LN] + K_m} \tag{5.1}$$

where μ is the specific growth rate of population as a function of [LN], [LN] is the concentration of limiting nutrient, μ_{max} is the maximum population growth rate (at "optimal" conditions), and K_m is the Monod coefficient, also called the half-saturation coefficient because it corresponds to the concentration at which μ is one-half of its maximum. When the concentration of limiting nutrient [LN] equals K_m, the population growth rate is $\mu_{max}/2$.

As [LN] increases, μ increases and so the algal population (number of cells) increases. Beyond a certain [LN], μ tends asymptotically to its maximum (μ_{max}), and the population tends to its maximum yield. If this concentration is not maintained, primary productivity returns to a level comparable to that prior to the nutrient enrichment rapidly. This productivity variation is the seasonal blooming. Normal becomes abnormal when there is a continuous over-stimulation of the system by excess supply of one or more limiting nutrients, which leads to intense and prolonged algal blooms throughout the year. The continuous nutrient supply sustains a constant maximum algal growth rate (μ_{max}). Therefore, instead of peaks of normal blooms, followed by periods when phytoplankton is less noticeable, we have a continuous primary production. When this occurs, we refer to it as eutrophication. In this process, the enhanced primary productivity triggers various physical, chemical, and biological changes in autotroph and heterotroph communities, as well as changes in processes in and on the bottom sediments and changes in the level of oxygen supply to surface water and oxygen consumption in deep waters. Eutrophication is considered to be a natural aging process for lakes and some estuaries, and it is one of the ways in which a water body (lake, rivers, and seas) transforms from a state where nutrients are scarce (oligotrophic), through a slightly richer phase (mesotrophic) to an enriched state (eutrophic).

Eutrophication can result in a series of undesirable effects. Excessive growth of planktonic algae increases the amount of organic matter settling to the bottom. This may be enhanced by changes in the species composition and functioning of the pelagic food web by stimulating the growth of small flagellates rather than larger diatoms, which leads to lower grazing by copepods and increased sedimentation. In areas with stratified water masses, the increase in oxygen consumption can lead to oxygen depletion and changes in community structure or death of the benthic fauna. Bottom dwelling fish may either die or escape. Eutrophication can also promote the risk of harmful algal blooms that may cause discoloration of the water, foam formation, death of benthic fauna and wild or caged fish, or shellfish poisoning of humans. Increased growth and dominance of fast growing filamentous macroalgae in shallow sheltered areas is yet another effect of nutrient overload which will change the coastal ecosystem, increase the risk of local oxygen depletion, and reduce biodiversity and nurseries for fish.

Human activities can greatly accelerate eutrophication by increasing the rate at which nutrients and organic substances enter aquatic ecosystems from their surrounding watersheds, for example, introducing in the water bodies detergents and fertilizers very rich in phosphorus. The resultant aging, which occurs through anthropogenic activity, is termed cultural eutrophication.

Globally, nitrogen and phosphorus are the two elements that immediately limit, in a Liebig sense, the growth of photosynthetic organisms. Silicon could also become a more generally limiting nutrient, particularly for diatom growth. These nutrients are present in algal cells in a species-specific structural ratio, the so-called *Redfield ratio*, which determines the nutrient requirement of the

species, and the value of which depends on the conditions under which species grow and compete. Consequently, the species composition of an environment will be determined not only by nutrient availability, but also by their proper relationship, since changes in nutrient ratio cause shifts in phytoplankton communities and subsequent trophic linkages. Nitrogen generally limits overall productivity in the marine system. Nitrogen limitation occurs most often at higher salinities and during low flow periods. However, since marine system is in stoichiometric balance, any nutrient can become a limiting factor. Phosphorus limitation occurs most often in freshwater system, in environments of intermediate salinities, and along the coasts during periods of high freshwater input. The occurrence of silicon limitation appears to be more spatially and temporally variable than phosphorus or nitrogen limitation and is more prevalent in spring than summer.

In the case of phosphorus, the limitation of algal growth can be at least twofold. First, there is limitation of nucleic acid synthesis. This limitation can be at the level of genome replication or at the level of RNA synthesis (a form of transcriptional control). The limitation can affect photosynthetic energy conversion by reducing the rate of synthesis of proteins in the photosynthetic apparatus, which is effectively a negative feedback on photosynthesis. This inhibition of protein synthesis may thus have effects on cell metabolism and oxidative stress similar to those for inhibition of protein synthesis under N limitation, except that the effect is indirect and less immediate. Secondly, a more immediate response to phosphorus limitation is on the rate of synthesis and regeneration of substrates in the Calvin–Benson cycle, thereby reducing the rate of light utilization for carbon fixation. Cells can also undergo a decrease in membrane phospholipids; moreover, the inability to produce nucleic acids under P limitation limit cell division, leading to an increased cell volume.

On a biochemical level, nitrogen limitation directly influences the supply of amino acids, which in turn limits the translation of mRNA and hence reduces the rate of protein synthesis. Under nitrogen-limited conditions also, the efficiency of PSII decreases, primarily as a consequence of thermal dissipation of absorbed excitation energy in the pigment bed. This appears to be due mainly to a decrease in the number of PSII reaction centers relative to the antennae. The functional absorption cross-section of PSII increases under nitrogen-limiting conditions, while the probability of energy transfer between PSII reaction center decreases. From a structural point of view, the reaction centers behave as if they were energetically isolated with a significant portion of the light-harvesting antenna disconnected from the photochemical processes. As nitrogen limitation leads to a reduction of growth and photosynthetic rates, it also leads to a reduction in respiratory rates. The relationship between the specific growth rate and specific respiration rate is linear with a positive intercept at zero growth, which is termed "maintenance respiration." The molecular basis of the alterations is unclear; however, the demands for carbon skeletons and ATP, two of the major products of the respiratory pathways, are markedly reduced if protein synthesis is depressed.

The requirement for silicon for construction of the diatom frustule makes this group uniquely subject to silicate limitation. Since silicic acid uptake, silica (SiO_2) frustule formation, and the cell division cycle are all tightly linked, under silica limitation, the diatom cell cycle predominantly stops at the G_2 phase, before the completion of cell division. Thus, an inhibition of cell division linked to an inability to synthesize new cell-wall material under silicon limitation can lead to an increase in the volume per cell. This increase could also be partly explained by the formation of auxospores with a larger cell diameter.

ALGAE AND THE PHOSPHORUS CYCLE

The phosphorus cycle is the simplest of the biogeochemical cycles. Phosphorus is the eleventh-most abundant mineral in the earth's crust and does not exist in a gaseous state. Natural inorganic phosphorus deposits occur primarily as phosphate, that is, a phosphorous atom linked to four oxygen atoms, in the mineral apatite. The heavy molecule of phosphate never makes its way into the atmosphere; it is always part of an organism, dissolved in water, or in the form of rock. Cycling processes of phosphorus are the same in both terrestrial and aquatic systems. When rock with

phosphate is exposed to water (especially water with a little acid in it), the rock is weathered out and goes into solution. Autotrophs (algae and plants) assimilate this dissolved phosphorus up and alter it to organic phosphorus using it in a variety of ways. It is an important constituent of lipid portion of cell membranes, many coenzymes, DNA, RNA, and, of course ATP. Heterotrophs obtain their phosphorous from the autotrophs they eat. When heterotrophs and autotrophs die (or when heterotrophs defecate), the phosphate may be returned to the soil or water by the decomposers. There, it can be taken up by other autotrophs and used again. This cycle will occur again and again until at last the phosphorous is lost at the bottom of the deepest parts of the ocean, where it becomes part of the sedimentary rocks forming there. If the rock is brought to the surface and weathered, this phosphorous will be released. During the natural process of weathering, the rocks gradually release the phosphorus as phosphate ions that are soluble in water and the mineralized phosphate compounds breakdown. Phosphates PO_4^{3-} are formed from this element. Phosphates exist in three forms: orthophosphate, metaphosphate (or polyphosphate), and organically bound phosphate, each compound containing phosphorous in a different chemical arrangement. These forms of phosphate occur in living and decaying plant and animal remains, as free ions or weakly chemically bounded in aqueous systems, chemically bounded to sediments and soils, or as mineralized compounds in soil, rocks, and sediments.

Orthophosphate forms are produced by natural processes, but major man-influenced sources include: partially treated and untreated sewage, runoff from agricultural sites, and application of some lawn fertilizers. Orthophosphate is readily available to the biological community and typically found in very low concentrations in unpolluted waters. Poly-forms are used for treating boiler waters and in detergents. In water, they are transformed into orthophosphate and made available for autotrophs uptake. The organic phosphate is the phosphate that is bound or tied up in autotrophs, waste solids, or other organic material. After decomposition, this phosphate can be converted to orthophosphate.

Algae and plants are the key elements to passing on phosphates to other living organisms, but their importance in phosphorus cycling is connected mainly to the impact of this element on their growth. As already remarked, both phosphorus and nitrogen are among the nutrients that can become limiting factors, and hence an overloading of these two elements leads to dramatic changes in the structure and functioning of an ecosystem.

Phosphorus, in the form of orthophosphate, is generally considered the main limiting nutrient in freshwater aquatic systems; that is, if all the phosphorus is used, autotroph growth will cease, no matter how much nitrogen is available. In phosphorus-limited systems, excess phosphorus will trigger eutrophic condition. In these situations, the natural cycle of the nutrient becomes overwhelmed by excessive inputs, which appear to cause an imbalance in the "production versus consumption" of living material (biomass) in an ecosystem. The system then reacts by producing more phytoplankton/vegetation than can be consumed by ecosystem. This overproduction triggers the series of events determining the aging process of the water body.

Under aerobic conditions, as water plants and algae begin to grow more rapidly than normal, there is also an excess die off of the plants and algae as sunlight is blocked at lower levels. Bacteria try to decompose the organic waste, consuming oxygen, and releasing more phosphate which is known as "recycling" or "internal cycling." Some of the phosphate may be precipitated as iron phosphate and stored in the sediment where it can then be released if anoxic conditions develop. In deeper environments, the phosphate may be stored in the sediments and then recycled through the natural process of lithophication, uplift, and erosion of rock formations. In anaerobic conditions, as conditions worsen as more phosphates and nitrates may be added to the water, all of the oxygen may be used up by bacteria in trying to decompose all of the waste. Different bacteria continue to carry on decomposition reactions; however, the products are drastically different. The carbon is converted into methane gas instead of CO_2; sulfur is converted into hydrogen sulfide gas. Some of the sulfide may be precipitated as iron sulfide. Under anaerobic conditions, the iron phosphate precipitated in the sediments may be released from the sediments making the phosphate bioavailable. This is a key

component of the growth-and-decay cycle. The water body may gradually fill with decaying and partially decomposed plant materials to make a swamp, which is the natural aging process. The problem is that this process can be significantly accelerated by human activities.

Phosphates were once commonly used in laundry detergents, which contributed to excessive concentrations in rivers, lakes, and streams. Most detergents no longer contain phosphorous. Currently, the predominant outside sources of phosphorus are agricultural and lawn fertilizers and improperly disposed animal wastes.

ALGAE AND THE NITROGEN CYCLE

The growth of all organisms depends on the availability of mineral nutrients, and none is more important than nitrogen, which is required in large amounts as an essential component of peptides, proteins, enzymes, chlorophylls, energy-transfer molecules (ATP, ADP), genetic materials (RNA, DNA), and other cellular constituents.

Nitrogen is present in all the four different spheres of the earth: the lithosphere contains about 98% of the global N (1.7×10^{17} tons), distributed among its different compartments (soils and sediments of the crust, mantle, and core). The core and the mantle have been estimated to contain a total of over 1.6×10^{17} tons of N. However, this N is not readily available to be cycled in the near-surface earth environment. Some periodically enters the atmosphere and hydrosphere through volcanic eruptions, primarily as ammonia (NH_3) and nitrogen (N_2) gas. Most of the remainder (~2%, 4×10^{15} tons) is found in the atmosphere, where nitrogen gas (N_2) comprises more than 78% of the volume. The hydrosphere and the biosphere together contain relatively little N compared with the other spheres (~0.015%, 3×10^{12} tons).

Nitrogen has many chemical forms, both organic and inorganic, in the atmosphere, biosphere, hydrosphere, and lithosphere. It occurs in the gas, liquid (dissolved in water), and solid phases. N can be associated with carbon (organic species) and with elements other than carbon (inorganic species). Important inorganic species include nitrate (NO_3^-), nitrite (NO_2^-), nitric acid (HNO_3), ammonium (NH_4^+), ammonia (NH_3), the gas N_2, nitrous oxide (N_2O), nitric oxide (NO), and nitrogen dioxide (NO_2). Most organic N species in the four spheres are biomolecules, such as proteins, peptides, enzymes, and genetic material. The presence of these many chemical forms make the N cycle more complex with respect to the cycle of other nutrients. The key processes linking the major pathways of the nitrogen cycle are the following:

- N-fixation, that is, reduction of atmospheric N_2 into ammonia NH_3
- Assimilation, that is, conversion of NO_3^- and NH_4^+ to organic nitrogen
- Mineralization, or ammonification, that is, conversion of organic nitrogen to NH_4^+
- Nitrification, that is, conversion of NH_4^+ to NO_2^- and successively NO_3^-
- Denitrification, that is, conversion of NO_3^- to gaseous forms of nitrogen (NO, N_2O, N_2)

Though complex microbial relationships regulate these processes, we can assume that fixation, mineralization, nitrification, and denitrification are carried out almost exclusively by bacteria, whereas algae play a main active role only in nitrogen fixation and assimilation. Greatly simplifying the overall nitrogen cycle, and from an algal point of view, atmospheric molecular nitrogen is converted by prokaryotic algae (cyanobacteria) to compounds such as ammonia (fixation), which are in part directly converted into amino acids, proteins, and other nitrogen-containing cell constituents of the fixators, and in part excreted into the open environment. Eukaryotic algae, unable to perform fixation, incorporate fixed nitrogen, either ammonium or nitrate, into organic N compounds by assimilation. When organic matter is degraded, organic compounds are broken down into inorganic compounds such as NH_3 or NH_4^+ and CO_2 through the mineralization process. The resultant ammonium can be nitrified by aerobic chemoautotrophic bacteria that use it as electron donor in the respiration process. The cycle is completed by denitrification carried out by usually facultative anaerobic bacteria that reduce nitrate

used as an electron acceptor in respiration to nitrogen gas. We must stress that a realistic depiction of the N cycle would have an almost infinite number of intermediary steps along the circumference of a circle, connected by a spiderweb of internal, crisscrossing complex connections.

It is one of nature's great ironies that though all life forms require nitrogen compounds, the most abundant portion of it (98%) is buried in the rocks, and therefore deep and unavailable, and the rest of nitrogen, the N_2 gas (2%), can be utilized only by very few organisms. This gas cannot be used by most organisms because the triple bond between the two nitrogen atoms makes the molecule almost inert. In order for N_2 to be used for growth, this gas must be "fixed" in the forms directly accessible to most organisms, that is, ammonia and nitrate ions.

A relatively small amount of fixed nitrogen is produced by atmospheric fixation (5–8%) by means of the high temperature and the pressure associated with lightning. The enormous energy of this phenomenon breaks nitrogen molecules and enables their atoms to combine with oxygen in the air forming nitrogen oxides. These molecules dissolve in rain, forming nitrates that are carried to the earth. Another relatively small amount of fixed nitrogen is produced industrially (industrial fixation) by the Haber-Bosch process, in which atmospheric nitrogen and hydrogen (usually derived from natural gas or petroleum) can be combined to form ammonia (NH_3) using an iron-based catalyst, at very high pressures and a temperature of about 600°C. Ammonia can be used directly as a fertilizer, but most of it is further processed to urea $(NH_2)_2CO$ and ammonium nitrate (NH_4NO_3).

The major conversion of N_2 into ammonium, and then into proteins, is a biotic process achieved by microorganisms, which represents one of the most metabolically expensive processes in biology. Biological nitrogen fixation can be represented by the following equation, in which 2 mol of ammonia (but in solution, ammonia exists only as an ammonium ion, that is, $NH_3 + H_2O \leftrightarrow NH_4^+ + OH^-$) are produced from 1 mol of nitrogen gas, at the expense of 16 mol of ATP and a supply of electrons and protons (hydrogen ions):

$$N_2 + 8H^+ + 8e^- + 16ATP \rightarrow 2NH_3 + H_2 + 16ADP + 16P_i \tag{5.2}$$

All known nitrogen-fixing organisms (diazotrophs) are prokaryotes, and the ability to fix nitrogen is widely, though paraphyletically, distributed across both the bacterial and archaeal domains. In cyanobacteria, nitrogen fixation is an inducible process, triggered by low environmental levels of fixed nitrogen.

The capacity of nitrogen fixation in diazotrophs relies solely upon an ATP-hydrolyzing, redox-active enzyme complex termed nitrogenase. In many of these organisms, nitrogenase comprises about 10% of total cellular proteins and consists of two highly conserved components, an iron protein (Fe-protein), and a molybdenum-iron protein (MoFe-protein). The Fe-protein is a γ_2 homodimer composed of a single Fe_4S_4 cluster bound between identical 32–40 kDa subunits. The Fe_4S_4 cluster is redox-active and is similar to those found in small molecular weight electron carrier proteins such as ferredoxins. It is the only known active agent capable of obtaining more than two oxidative states and transferring electrons to the MoFe-protein. The MoFe-protein is a $\alpha_2\beta_2$ heterotetramer; the ensemble is approximately 250 kDa. The α subunit contains the active site for dinitrogen reduction, typically a $MoFe_7S_9$ metal cluster (termed FeMo cofactor), although some organisms contain nitrogenases, wherein Mo is replaced by either Fe or V. These so-called alternative nitrogenases are found only in a limited subset of diazotrophs and, in all cases studied so far, are present secondarily to the MoFe-nitrogenase. The MoFe-nitrogenase has been found to be more specific for and more efficient in binding N_2 and reducing it to ammonia than either of the alternative nitrogenases. The catalytic efficiency of these alternative nitrogenases is lower than that of the MoFe-nitrogenase. In addition to variations in metal cofactors, the nitrogenase complex is nonspecific and reduces triple and double bond molecules other than N_2. These include hydrogen azide, nitrous oxide, acetylene, and hydrogen cyanide. The nonspecificity of this enzyme and the alternative nitrogenases containing other metal cofactors implicate the role of varying environmental pressures on the evolutionary

history of nitrogenase that could have been selected for different functions of the ancestral enzyme. The nitrogenase enzyme system is extremely O_2-sensitive, since oxygen not only affects the protein structure, but also inhibits the synthesis of nitrogenase in many diazothrops. The repression is both transient (lasting only a few hours) and permanent. The reactions occur while N_2 is bound to the nitrogenase enzyme complex. The Fe-protein is first reduced by electrons donated by ferredoxin. Then the reduced Fe-protein binds ATP and reduces the MoFe-protein, which donates electrons to N_2, producing diimide (HN=NH). In two further cycles of this process (each requiring electrons donated by ferredoxin), HN=NH is reduced to imide ($H_2N–NH_2$), which in turn is reduced to $2NH_3$. Depending on the type of microorganism, the reduced ferredoxin which supplies electrons for this process is generated by fermentation or photosynthesis and respiration.

As already stated, nitrogenase is highly sensitive to molecular oxygen (*in vitro* it is irreversibly inhibited by exposure to O_2). Therefore, during the course of planetary evolution, cyanobacteria have co-evolved with the changing oxidation state of the ocean and atmosphere to accommodate the machinery of oxygenic photosynthesis and oxygen-sensitive N_2 fixation within the same cell and/or colony of cells. Since nitrogen fixation occurs in a varied metabolic context in both anaerobic and aerobic environments, strategies have followed a very complex pattern of biochemical and physiological mechanisms for segregation that can be simplified in some spatial and/or temporal separation of the two pathways.

Nitrogenase is an ancient enzyme that almost certainly arose in the Archean ocean before the oxidation of the atmosphere by oxygenic photoautotrophs. An attractive hypothesis of the development of biological nitrogen fixation is that it arouse in response to changes in atmospheric composition that resulted in the reduction of the production of abiotically fixed nitrogen. On the early earth, concentrations of CO_2 in the atmosphere were high, because of oxidation of CO produced by impacts of extraterrestrial bodies and only slow removal of CO_2 by weathering (the continents were smaller at this time, meaning that a smaller area of minerals was exposed for weathering). With these CO_2 conditions, the initial production rate of NO was estimated to be about 3×10^{11} g year^{-1}. Atmospheric CO_2 levels declined with time; however, the impact rate dropped and the continents grew. A rise in atmospheric CH_4 produced by methanogenic, methane-generating, bacteria may have warmed the Archaean earth and speeded the removal of CO_2 by silicate weathering. As this happened, the production rate of NO by lightning dropped to below 3×10^9 g year^{-1} because of the reduced availability of oxygen atoms from the splitting of CO_2 and H_2O. The resulting crisis in the availability of fixed nitrogen for organisms triggered the evolution of biological nitrogen fixation about 2.2 billion years ago. Under the prevailing anaerobic conditions of that period in earth's history, anaerobic heterotrophs, such as *Clostridium*, developed. With the evolution of cyanobacteria and the subsequent generation of molecular oxygen, oxygen-protective mechanisms would be essential. A semitemporal separation of nitrogen fixation and oxygenic photosynthesis combined with spatial heterogeneity was the first oxygen-protective mechanism developed by marine cyanobacteria such as *Trichodesmium* sp. and *Katagnymene* sp. A full temporal separation, in which nitrogen is only fixed at night, then developed in unicellular diazotrophs and in some nonheterocystous filamentous diazotrophs (e.g., *Oscillatoria limosa* and *Plectonema boryanum*). Finally, in yet other filamentous organisms, complete segregation of N_2 fixation and photosynthesis was achieved with the cellular differentiation and evolution of heterocystous cyanobacteria (e.g., *Nostoc* and *Anabaena*).

The nonheterocystous filamentous cyanobacteria *Trichodesmium* sp. and *Katagnymene* sp., unlike all other nonheterocystous species, fix nitrogen only during the day. Nitrogenase is compartmentalized in 15–20% of the cells in *Trichodesmium* sp., and 7% of the cells in *Katagnymene* sp. often arranged consecutively along the trichome, but active photosynthetic components (PSI, PSII, RuBisCo, and carboxysomes) are found in all cells, even those harboring nitrogenase. A combined spatial and temporal segregation of nitrogen fixation from photosynthesis and a sequential progression of photosynthesis, respiration, and nitrogen fixation over a diel cycle are the strategies used by these cyanobacteria. These pathways are entrained in a circadian pattern that is ultimately controlled

by the requirement for an anaerobic environment around nitrogenase. Light initiates photosynthesis, providing energy and reductants for carbohydrate synthesis and storage, stimulating electron cycling through PSI, and poising the plastoquinone (PQ) pool at reduced levels. High respiration rates early in the photoperiod supply carbon skeletons for amino acid synthesis (the primary sink for fixed nitrogen) but simultaneously reduce the PQ pool further. Linear electron flow to PSI is never abolished. The reduced PQ pool leads to a down-regulation of PSII, which opens a window of opportunity for N_2 fixation during the photoperiod, when oxygen consumption exceeds oxygen production. As the carbohydrate pool is consumed, respiratory electron flow through the PQ pool diminishes, intracellular oxygen concentrations rises, the PQ pool becomes increasingly oxidized, and net oxygenic production exceeds consumption. Nitrogenase activity is lost until the following day.

A full temporal separation between oxygenic photosynthesis and nitrogen fixation occurs in *P. boryanum* and *O. limosa*. Transcription of nitrogenase and photosynthetic genes are temporally separated within the photoperiod, that is, nitrogenase is expressed primarily during the night. Nitrogenase is contained in all cells in equal amounts. The onset of nitrogen fixation is preceded by a depression in photosynthesis that establishes a sufficiently low level of dissolved oxygen in the environment. *Plectonema* sp. has a versatile physiology that allows it to reversibly modulate uncoupling of the activity of the two photosystems in response to intracellular nitrogen status. *Oscillatoria* sp. initiate nitrogen fixation in the dark and perform it primarily in the absence of light.

In nonheterocystous cyanobacteria such as the filamentous *Symploca* sp. and *Lyngbya maiuscola*, and the unicellular *Gloeothece* sp. and *Cyanothece* sp., the temporal separation does not need for a microaerobic environment. *Phormidium* sp. and *Pseudoanabaena* sp. are other examples of cyanobacteria fixing only under microanaerobic conditions. Under contemporary oxygen levels, all of these organisms are relegated to narrow environmental niches.

In heterocystous cyanobacteria, such as *Anabaena* sp. and *Nostoc* sp., a highly refined specialization spatially separates oxygenic photosynthesis from N_2 fixation. Here, nitrogenase is confined to a micro-anaerobic cell, the heterocyst, characterized by a thick membrane that slows the diffusion of O_2, high PSI activity, loss of division capacity, absence of PSII (that splits the water forming O_2), and variation of phycobiliproteins content. This cell differentiates completely and irreversibly 12–20 h after combined nitrogen sources are removed from the medium. The development of these cells, formed at intervals between vegetative cells, is a primitive form of cell differentiation. In this process, all PSII activity is gradually lost, and the proteins involved in oxygenic photosynthesis are degraded, while PSI activity is maintained. Simultaneously, the production of active nitrogenase is triggered. Nitrogen fixation is localized specifically in heterocysts, and light is used for cyclic electron flow around PSI to maintain a supply of ATP for the process. The primary organic nitrogen product (glutamate) is exported to adjacent vegetative and photo-oxygenic cells, while carbon skeletons, formed by the respiratory and photosynthetic processes in the latter cells, are translocated to the heterocysts. In some heterocystous cyanobacteria such as *Anabaena variabilis*, under anaerobic conditions, a different Mo-dependent nitrogenase can be synthesized inside vegetative cells. This nitrogenase is expressed shortly after nitrogen depletion, but prior to heterocyst formation, and can support the fixed N needs of the filaments independent of the nitrogenase in the heterocysts. Figure 5.1 shows the position of a heterocyst (H), and the akinetes (A) formed adjacent to it in a filament of *Anabaena* sp. The absorption spectra measured by microspectrophotometry on these cells and a vegetative cell (V) are shown on the right side of the figure. The absorption spectrum of the heterocyst indicates that phycobiliproteins are lacking at this stage of development.

The biotic nitrogen fixation is estimated to produce about 1.7×10^8 tons per year of ammonia, while atmospheric and industrial nitrogen fixation produce about 1.7×10^7 tons per year of ammonia.

For all eukaryotic algae, the only forms of inorganic nitrogen that are directly assimilable are nitrate (NO_3^-), nitrite (NO_2^-), and ammonium (NH_4^+). The more highly oxidized form, nitrate, is the most thermodynamically stable form in oxidized aquatic environments and hence is the predominant form of fixed nitrogen in aquatic ecosystems, though not necessarily the most readily available form. Following translocation across the plasmalemma (which is an energy-dependent process), the

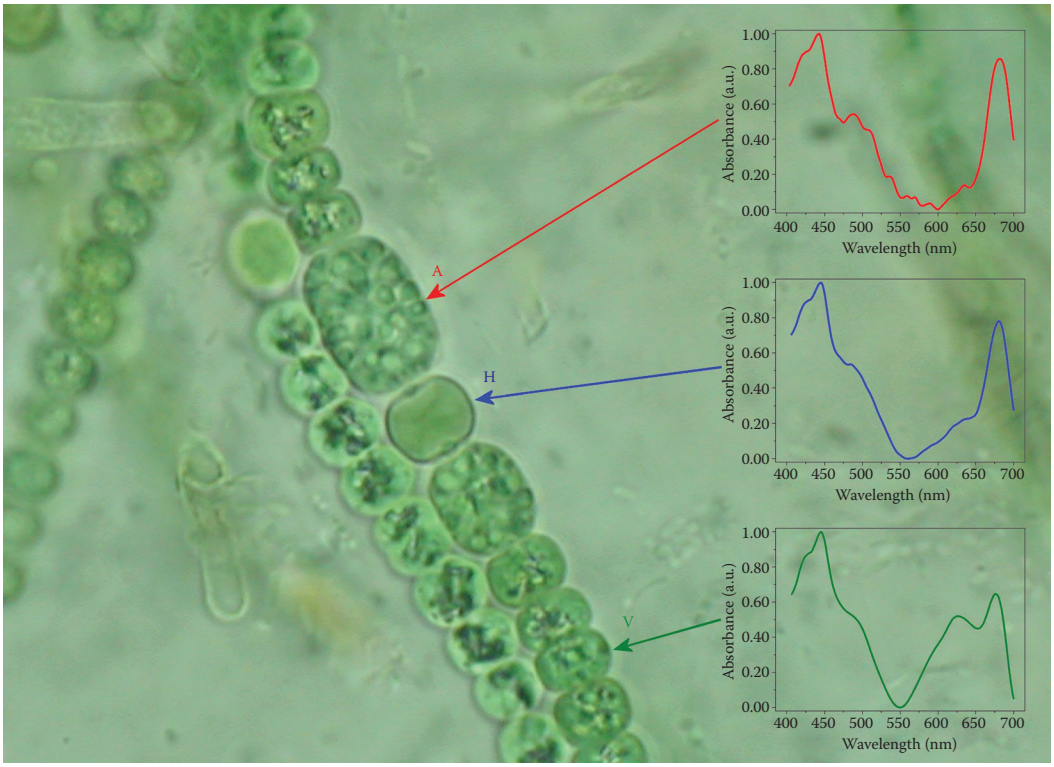

FIGURE 5.1 Position of a heterocyst (H) and the akinetes (A) formed adjacent to it in a filament of *Anabaena* sp. The absorption spectra measured by microspectrophotometry on these cells and a vegetative cell (V) are shown on the right side of the figure. The absorption spectra of the heterocyst and akinete indicate that phycobiliproteins are lacking at this stage of development.

assimilation of NO_3^- requires chemical reduction to NH_4^+. This process is mediated by two enzymes, namely nitrate reductase and nitrite reductase. Nitrate reductase is located in the cytosol and uses NADPH to catalyze the two-electron transfer:

$$NO_3^- + 2e^- + 2H^+ \rightarrow NO_2^- + H_2O \tag{5.3}$$

In cyanobacteria, nitrate reductase is coupled to the oxidation of ferredoxin rather than a pyridine nucleotide as in eukaryotic algae. The nitrite formed by nitrate reductase is reduced in a six-electron transfer reaction:

$$NO_2^- + 6e^- + 8H^+ \rightarrow NH_4^+ + 2H_2O \tag{5.4}$$

Nitrite reductase utilizes ferredoxin in both cyanobacteria and eukaryotic algae; in the latter, the enzyme is localized in the chloroplasts. In both cyanobacteria and eukaryotic algae, photosynthetic electron flow is an important source of reduced ferredoxin for nitrite reduction. The overall stoichiometry for the reduction of nitrate to ammonium can be written as

$$NO_3^- + 8e^- + 10H^+ \rightarrow NH_4^+ + 3H_2O \tag{5.5}$$

The incorporation of ammonium into amino acids is primarily brought about by the sequential action of glutamine synthetase (GS) and glutamine 2-oxoglutarate aminotransferase (GOGAT).

Ammonium assimilation by GS requires glutamate as substrate and ATP, and catalyzes the irreversible reaction:

$$\text{glutamate} + NH_4^+ + \text{ATP} \rightarrow \text{glutamine} + \text{ADP} + P_i \quad (5.6)$$

The amino nitrogen of glutamine is subsequently transferred to 2-oxoglutarate, and reduced, forming 2 moles of glutamate:

$$\text{2-oxoglutarate} + \text{glutamine} + \text{NADPH} \rightarrow 2[\text{glutamate}] + NADP^+ \quad (5.7)$$

Both GS and GOGAT are found in chloroplasts, although isoenzymes (multiple forms of an enzyme with the same substrate specificity, but with genetic differences in their primary structures) of both enzymes may also be localized in the cytosol. Whatever the location of the enzymes, however, glutamate must be exported from the chloroplast to the cytosol where transamination reaction (the reversible transfer of an amino group of a specific amino acid to a specific keto acid, forming a new keto acid and a new amino acid) can proceed, thereby facilitating the syntheses of other amino acids.

ALGAE AND THE SILICON CYCLE

The biogeochemical cycle of silicon (Si) might be interpreted as those processes that link sources and sinks of silicic acid [$Si(OH)_4$]. Silicic acid is the only precursor in the processing and deposition of silicon in biota. The biogeochemical cycle of silicon does not facilitate a high biospheric abundance of the element; in fact, silicon cycle differs from the cycles of carbon, nitrogen, and sulfur and it is similar to phosphorus in that there is no atmospheric reservoir. The silicon cycle, like those for phosphorus and the divalent metals calcium and magnesium, has a significant abiotic drain. The cycle actually consists of two parts: the terrestrial or freshwater cycle and the marine cycle, the former feeding the latter. However, its replenishment can occur only via the marine sedimentary cycle. This is dependent upon geotectonic processes, such as mountain building and subduction, and, as such, will incur delays of tens to hundreds of millions years before marine silicon is returned to the terrestrial environment.

The substantial losses of biospheric silicic acid to abiotic sinks may be compensated for in nature by its overall abundance in the earth's crust. It is the second most abundant element in the lithosphere (28%), iron being the first one (35%). It is found in the earth's crust in silicate minerals, the most prevalent of which are quartz, the alkali feldspars, and plagioclase. The latter two minerals are aluminosilicates and contribute significantly to the aluminum content of the crust. All of these minerals are broken down by the process of weathering. Important feedback exists between autotrophs (algae and plants), weathering, and CO_2.

The dominant form of weathering is the carbonation reaction involving carbonic acid (H_2CO_3), which results in enhanced removal of CO_2 from the atmosphere, because the net effect of silicate mineral weathering is to convert soil carbon, derived ultimately from photosynthesis, into dissolved HCO_3^-. On a geological timescale, this transfer has an important control on the CO_2 content of the atmosphere and hence global climate. Weathering is a complex function of rainfall, runoff, lithology, temperature, topography, vegetation, and magnitudes. Algae, plants, and their associate microbiota directly affect silicate mineral weathering in several ways: by generation of organic substances, known as *chelates*, that have the ability to decompose minerals and rocks by the removal of metallic *cations*; by modifying pH through production of CO_2 or organic acids such as acetic, citric, phenolic, etc., and by altering the physical properties of a soil, particularly the exposed surface areas of minerals, and the residence time of water. The significance of this natural process for biota can be found in the detailed geochemistry of the weathering reactions and, in particular, in the rates at

which these reactions occur. The rate of mineral weathering is dependent upon a number of factors including the temperature, pH, and ionic composition of the solvent (or leachate) and hydrogeological parameters such as water flow.

Silicification occurs in three clades of photosynthetic heterokonts: Chrysophyceae (Parmales), Bacillariophyceae, and Dictyochophyceae, with diatoms being the world's largest contributors to biosilicification. Since amorphous silica (SiO_2) is an essential component of the diatom cell wall, silicon availability is a key factor in the regulation of diatom growth in nature; in turn, the use of silicon by diatoms dominates the biogeochemical cycling of silicon in the sea, with each atom of silicon weathered from land passing through a diatom an average of 39 times before burial in the seabed.

Several thousand million years ago, little if any of the life on earth was involved in the processing of silicic acid to amorphous silica ($SiO_2 \cdot nH_2O$). The concentration of silicic acid in the aqueous environment was high, in the order of millimolar, and reflected equilibration according to the dominant mineral weathering reactions at that time. The prevalence of these environments rich in silicic acid is indicated in the fossil record by evidence of blue-green algae found encased in silica cherts. It is important to recognize that implicit in this observation is the acceptance that early biochemical evolution proceeded within environments which, relative to the conditions which prevail today, were extremely rich in silicic acid. Concomitant with the advent of dioxygen, and its subsequent gradual increase in atmospheric concentration from approximately 1% toward the today level of 21%, there occurred an increasing number of organisms within which silicic acid was processed to silica. The most important of these, in terms of their diversity, ubiquity (both freshwater and marine species), and biomass, were the diatoms. The diatoms are characterized by a silica frustule which surrounds their cell wall. Silicic acid is freely diffusible across the cell walls and membranes and, in most cell types of most organisms, the intracellular concentration of silicic acid equilibrates with the extracellular environment according to a "Donnan equilibrium" (the equilibrium characterized by an unequal distribution of diffusible ions between two ionic solutions separated by a membrane which is impermeable to at least one of the ionic species present). However, while the intracellular concentration of the silicic acid in the diatom has not been measured, it is likely that it is under kinetic as opposed to thermodynamic control and that it is maintained at an extremely low level, probably <1 μmol. This kinetic control of the intracellular silicic acid concentration may be achieved through the condensation and polymerization of silicic acid in a number of chemical (e.g., pH-controlled) and physical (e.g., membrane-bound) compartments eventually resulting in amorphous silica. This biogenic silica is then deposited in a controlled manner to form the intricate and elaborate silica frustules. How all of these remarkable feats of chemistry are achieved within the diatom remains largely unknown. However, what is known, and is becoming more apparent, is the formative role played by diatoms and other silica-forming organisms, such as silicoflagellates, radiolarian, and sponges, in the biogeochemical cycle of silicon.

The reactions of condensation of silicic acid and subsequent polymerization to form biogenic silica eventually (i.e., upon the death of the organism) result in a net loss of silicic acid to the biosphere. The rate of the forward reaction (condensation and polymerization) is orders of magnitude higher than that of the reverse (regeneration of silicic acid pool) with the result that concomitant with the rise of the diatoms and other silica-forming organisms there was a significant reduction in the environmental silicic acid concentration. Silica frustules are formed in a matter of hours to days, whereas the rate at which silicic acid is returned to the biosphere through the dissolution of the frustules of dead diatoms as they sink in the water column is in the order of 10^{-9} μmol m^{-2} s^{-1}. In addition, the dissolution of these sinking frustules can be greatly influenced by the chemistry of the water column. For example, the frustule is a highly adsorptive surface and is implicated in the removal of metal ions, for example, aluminum, from the water column. These adsorptive processes tend to stabilize the frustule surface toward dissolution, thereby reducing the amount of silicic acid returned to the biosphere during sedimentation. Once the silica frustules have settled to the bottom, their silica enters the sedimentary cycle whereupon it is unlikely to reappear in the biosphere for tens of millions of years.

The biologically induced dramatic decline in the environmental silicic acid concentration had the effect of accelerating the rate of mineral weathering. This, in turn, consumed more carbon dioxide and precipitated a gradual reduction in the atmospheric concentration of this "greenhouse" gas. The impact of the emergence of diatoms and other silica-forming organisms, and then the spread of rooted vascular plants, on the biogeochemical cycle of silicon contributed significantly to the global cooling which has resulted in the climate of today. The diatoms, in particular, are extremely successful organisms and will continue to deposit silica frustules of varying silica content at micromolar concentrations of environmental silicic acid. In this way, they are a continuous accelerant of mineral weathering almost regardless of how low the environmental silicic acid concentration may fall. From the advent of the silica-forming organisms, the process of biochemical evolution has continued in silicon-replete, though no longer of millimolar concentration, environments. Diatoms in sedimentary deposits of marine and continental, especially lacustrine, origin belong to different geologic ranges and physiographic environments. Marine diatoms range in age from Early Cretaceous to Holocene, and continental diatoms range in age from Eocene to Holocene; however, most commercial diatomites, both marine and lacustrine, were deposited during the Miocene. Marine deposits of commercial value generally accumulated along continental margins with submerged coastal basins and shelves where wind-driven boundary currents provided the nutrient-rich upwelling conditions capable of supporting a productive diatom habitat. Commercial freshwater diatomite deposits occur in volcanic terrains associated with events that formed sediment-starved drainage basins. Generally, marine habitats are characterized by stable conditions of temperature, salinity, pH, nutrients, and water currents, in contrast to lacustrine habitats, which are characterized by wide variations in these conditions. Marine deposits generally are of higher quality and contain larger resources, owing to their greater areal extent and thickness, whereas most of the world's known diatomites are of lacustrine origin.

Unlike many other algae, the division cycles of which are strongly coupled to the diel light cycle, diatoms are capable of dividing at any point of the diel cycle. This light independence extends to their nutrient requirements, with nitrate and silicic acid uptake and storage continuing during the night through the use of excess organic carbon synthesized during the day. Moreover, the silica frustule has recently been shown to play a role in CO_2 acquisition, which indicates that Si limitation can induce CO_2 limitation in diatoms. Specifically, the silica frustule facilitates the enzymatic conversion of bicarbonate to CO_2 at the cell surface by serving as a pH buffer, thus enabling more efficient photosynthesis. This control by diatoms and the reduction in silicate input from rivers due to cooling and drying of the climate offers a feedback mechanism between climate variability, diatom productivity, and CO_2 exchange. These features of diatom physiology almost certainly contribute to the *in situ* observation that diatoms have greater maximum growth rates relative to comparable algae. Further, so long as silicic acid is abundant (and other nutrients nonlimiting), diatoms are found to dominate algal communities. Diatoms are estimated to contribute up to 45% of total oceanic primary production, making them major players in the cycling of all biological elements. They globally uptake and process 240 Tmol Si $year^{-1}$. Nowadays, risk to diatoms comes from both climate forced impacts and anthropogenic sources. Reduced input of silicate due to damming of rivers and changes in water-use patterns, and increased input of inhibitory levels of ammonium to estuaries and adjacent coastal waters affect diatom success. The high ammonium concentrations prevalent in some estuaries, a result of anthropogenic inputs from sewage-treatment plants and agricultural runoff inhibit the uptake of nitrate by diatoms which draw primarily on nitrate for high growth rates.

Aside from their role in the silicon cycle, the diatoms have also attracted attention because of their importance to the export of primary production to the ocean's interior. Aggregation and sinking is an important aspect in the life history of many diatom species, and high sinking velocities, whether as individuals, aggregates, or mats, allow diatoms to rapidly transport material out of the surface mixed layer. Additionally, mesozooplankton grazers that consume diatoms produce large, fast-sinking fecal pellets. These processes remove nutrients and carbon from the productive surface waters before they can be remineralized, making the diatoms crucial to "new" (or export)

production. So long as silicic acid is available, diatoms act as a conduit for nutrients and carbon to deep waters, contrasting with the production of other algae which "traps" nutrients in a regeneration loop at the surface.

Though diatoms are by far the most important organisms that take up silicic acid to form their encasing structures, silicoflagellates also deserve mentioning. These unicellular heterokont algae belong to a small group of siliceous marine phytoplankton. Silicoflagellates live in the upper part of the water column and are adapted for life in tropical, temperate, and frigid waters. Silicoflagellates have a multistage life-cycle, not all stages of which are known. The best-known stage consists of a naked cell body with a single anterior flagellum and numerous plastids contained within an external lateral skeleton. This skeleton is composed of hollow beams of amorphous silica, forming a network of bars and spikes arranged to form an internal basket. The siliceous skeleton of silicoflagellates is very susceptible to dissolution and therefore their preservation is often hindered by diagenetic processes; moreover, their abundance is relatively low compared to that of other siliceous microfossils, since they form a small component of marine sediments; both these reasons make their presence rare in the sedimentary record.

ALGAE AND THE SULFUR CYCLE

Sulfur is an essential element for autotrophs and heterotrophs. In its reduced oxidation state, the nutrient sulfur plays an important part in the structure and function of proteins. Three amino acids found in almost all proteins (cysteine, cystine, and methionine) contain carbon-bounded sulfur. Sulfur is also found in sulfolipids, some vitamins, sulfate esters, and a variety of other compounds.

In its fully oxidized state, sulfur exists as sulfate and is the major cause of acidity in both natural and polluted rainwater. This link to acidity makes sulfur important to geochemical, atmospheric, and biological processes such as the natural weathering of rocks, acid precipitation, and rates of denitrification. Sulfur cycle is also one of the main elemental cycles most heavily perturbed by human activity. Estimates suggest that emissions of sulfur to the atmosphere from human activity are at least equal or probably larger in magnitude than those from natural processes. Like nitrogen, sulfur can exist in many forms: as gases or sulfuric acid particles. The lifetime of most sulfur compounds in the air is relatively short (e.g., days). Superimposed on these fast cycles of sulfur are the extremely slow sedimentary-cycle processes or erosion, sedimentation, and uplift of rocks containing sulfur. Sulfur compounds from volcanoes are intermittently injected into the atmosphere, and a continual stream of these compounds is produced from industrial activities. These compounds mix with water vapor and form sulfuric acid smog. In addition to contributing to acid rain, the sulfuric acid droplets of smog form a haze layer that reflects solar radiation and can cause a cooling of the earth's surface. While many questions remain concerning specifics, the sulfur cycle, in general, and acid rain and smog issues, in particular, are becoming major physical, biological, and social problems.

The sulfur cycle can be thought of as beginning with the gas sulfur dioxide (SO_2) or the particles of sulfate (SO_4^{2-}) compounds in the air. These compounds either fall out or are rained out of the atmosphere. Algae and plants take up some forms of these compounds and incorporate them into their tissues. Then, as with nitrogen, these organic sulfur compounds are returned to the land or water after the algae and plants die or are consumed by heterotrophs. Bacteria are important here as well since they can transform the organic sulfur to hydrogen sulfide gas (H_2S). In the oceans, certain phytoplankton can produce a chemical that transforms organic sulfur to SO_2 that resides in the atmosphere. These gases can re-enter the atmosphere, water, and soil, and continue the cycle.

All living organisms require S as a minor nutrient, in roughly the same atom proportion as phosphorus. Sulfur is present in freshwater algae at a ratio of about 1 S atom to 100 C atoms (0.15–1.96% by dry weight), and the S content varies with species, environmental conditions, and season. Vascular plants, algae, and bacteria (except some anaerobes that require S^{2-}) have the ability to take up, reduce, and assimilate SO_4^{2-} into amino acids and convert SO_4^{2-} into ester sulfate compounds.

Reduced volatile sulfur compounds, which are released to the oxygen-rich atmosphere, are chemically oxidized during their atmospheric lifetime and end up finally as SO_2 (oxidation state +4) and sulfuric acid (H_2SO_4) and particulate SO_4^{2-} (oxidation state +6) and methane sulfonate (oxidation state +6). It is mainly these compounds that are removed from the atmosphere and brought back to the earth by dry and wet depositions.

Since the oxidation state of sulfur in H_2SO_4 (+6) is the most stable under oxic conditions, sulfate is the predominant form of sulfur in oxic waters and soils. Thus, the reduction of sulfate to a more reduced sulfur species is a necessary prerequisite for the formation of volatile sulfur compounds and their emission to the atmosphere. Biochemical processes which lead to this reduction can be considered as the driving force of the atmospheric sulfur cycle.

Two types of biochemical pathways of sulfate reduction are important in the global cycles: dissimilatory and assimilatory sulfate reduction. Dissimilatory reduction of sulfate is a strictly anaerobic process that takes place only in anoxic environments. Sulfate-reducing bacteria reduce sulfate and other sulfur oxides to support respiratory metabolism, using sulfate as a terminal electron acceptor instead of molecular oxygen. Since the process is strictly anaerobic, dissimilatory sulfate reduction occurs largely in stratified, anoxic water basins and in sediments of wetlands, lakes, and coastal marine ecosystems. The process is particularly important in marine ecosystems, including salt marshes, because sulfate is easily available due to its high concentration in seawater (28 mM; 900 mg L^{-1}).

In contrast to animals, which are dependent on organo-sulfur compounds in their food to supply their sulfur requirement, other biota (bacteria, cyanobacteria, fungi, eukaryotic algae, and vascular plants) can obtain sulfur from assimilatory sulfate reduction for synthesis of organo-sulfur compounds. Sulfate is assimilated from the environment, reduced inside the cell, and fixed into sulfur-containing amino acids and other organic compounds. The process is ubiquitous in both oxic and anoxic environments. Most of the reduced sulfur is fixed by the intracellular assimilation process and only a minor fraction of the reduced sulfur is released as volatile gaseous compounds, as long as the organisms are alive. However, after death of the organisms, microbial degradation liberates reduced sulfur compounds (mainly in the form of hydrogen sulfide (H_2S) and dimethyl sulfide (DMS), but also as organic sulfides) to the environment. During this stage, volatile sulfur compounds may escape to the atmosphere. However, as with sulfides formed from dissimilatory sulfate reduction, the sulfides released during decomposition are chemically unstable in an oxic environment and are re-oxidized to sulfate by a variety of microorganisms.

Sulfate is taken up into the cell by an active transport mechanism and inserted into an energetically activated molecule, APS (adenosine-5′-phosphosulfate), which can be further activated at the expense of one more ATP molecule to PAPS (3′-phosphoadenosine-5′-phosphosulfate). It is then transferred to a thiol carrier (a molecule with a –SH group) and reduced to the –2 oxidation state. In contrast to nitrate assimilation, where the various intermediates are present free in the cytoplasm, sulfur remains attached to a carrier during the reduction sequence. In a final step, the carrier-bound sulfide reacts with *O*-acetyl-serine to form cysteine. Cysteine serves as the starting compound for the biosynthesis of all other sulfur metabolites, especially the other sulfur-containing amino acids homocysteine and methionine. Cysteine and methionine are the major sulfur amino acids and represent a very large fraction of the sulfur content of biological materials.

One aspect of the sulfur metabolism of algae deserves special mention because of its atmospheric consequences: many types of marine algae including planktonic algae, such as prymnesiophytes, dinoflagellates, diatoms, chrysophytes, and prasinophytes, and macroalgae, such as chlorophytes and rhodophytes, produce large amount of dimethylsulfonium propionate (DMSP) from sulfur-containing amino acids (methionine). DMSP is the precursor of DMS, its enzymatic cleavage product, which is a gas with a strong smell, and in turn is a major source of atmospheric sulfur. Marine organisms generate about half the biogenic sulfur emitted to the atmosphere annually, and the majority of this sulfur is produced as DMS. Because reduced sulfur compounds such as DMS are rapidly oxidized to sulfur dioxides that function as cloud condensation nuclei, the production of

DMS can potentially affect climate on a global scale. DMS has also a peculiar role: birds use DMS as a foraging cue, as algae being consumed by fish release DMS, as consequence bringing the presence of the fish to the attention of the birds.

DMSP can function as osmoregulator, buoyancy controller, cryoprotectant, and antioxidant. Freshwater algae do not produce DMSP, since, being an osmolyte, it has no significance in freshwater systems. It has also been postulated that DMSP production is indirectly related to the nitrogen nutrition of algae, with DMSP being a store for excess sulfate taken up while assimilating the molybdenum necessary to synthesize nitrate reductase or nitrogenase (this could also be true for vascular plants with high nitrate-reductase activities or with symbiotic nitrogen-fixing bacteria). The cleavage of DMSP by means of the enzyme DMSP lyase produces gaseous DMS and acrylic acid. DMSP can also be released from phytoplankton cells during senescence, whereas zooplankton grazing on healthy cells is thought to facilitate the release of DMSP from ruptured algal cells during sloppy feeding. Once released from algal cells, DMSP undergoes microbially mediated conversion by cleavage into gaseous DMS and acrylate.

It had been known for many years that the global budget of sulfur could not be balanced without a substantial flux of this element from the oceans to the atmosphere and then to land. Once emitted from the sea, DMS is transformed in the atmosphere by free radicals (particularly hydroxyl and nitrate) to form a variety of products, most importantly sulfur dioxide and sulfate in the form of small particles. As already stated, these products are acidic and are responsible for the natural acidity of atmospheric particles; activities of human in burning fossil fuels add further sulfur acidity to this natural process. In addition, the sulfate particles (both natural and manmade) can alter the amount of radiation reaching earth's surface both directly by scattering of solar energy and indirectly by acting as the nuclei on which cloud droplets form (cloud condensation nuclei, CCN), thereby affecting the energy reflected back to space by clouds (denser cloud albedo). The reduction in the amount of sunlight that reaches the earth surface leads to the consequent reduction of global temperature. This drop in temperature is suggested to cause a decrease in the primary production of DMSP (in other words, DMS). Thus, DMS is considered to be counteractive to the behavior of green house gases such as CO_2 and CH_4. Removal of the algae-DMS-derived sulfur from the air by rain and deposition of particles is a significant source of this biologically important element for some terrestrial ecosystems.

ALGAE AND THE OXYGEN–CARBON CYCLES

The oxygen and carbon cycles are closely related, because they are directly associated with photosynthesis and respiration processes.

The natural oxygen cycle is determined by the aerobic respiration of glucose (taking place in all living organisms), which consumes oxygen in free form (O_2) using it as an electron sink and produces carbon dioxide and water, and by the photosynthesis, which consumes carbon dioxide and water to produce carbohydrates and molecular oxygen as a by-product, as we have seen in Chapter 3.

Today oxygen constitutes about 21% of the atmosphere, 85.8% of the ocean, and 46.7% by volume of the earth's crust. It has not always been like that. The primordial atmosphere of the earth is thought to have contained mainly CO_2, N_2, H_2O, and CO with traces of H_2, HCN, H_2S, and NH_3, but to have been devoid of O_2 (only small amounts were derived from the photolysis of water), thus being neutral to mildly reducing. Today, the atmosphere contains 78% N_2, 21% O_2, and 0.036% CO_2 by volume and is strongly oxidizing. All of the molecular oxygen present in the earth's atmosphere has been produced as the result of oxygenic photosynthesis, the source of the original O_2 being photosynthetic activity in the primordial oceans. The development of aquatic photosynthesis coincided with a long and reasonably steady drawdown of atmospheric CO_2, from concentration approximately 100-fold higher than in the present-day atmosphere to approximately half of the present levels. This drawdown was accompanied by a simultaneous evolution of oxygen from nil to approximately 21%, comparable to that of the present day. The current atmospheric oxygen concentration is maintained

in equilibrium between the production by photosynthesis and the consumption by respiration, with annual fluctuations of ±0.002%. Over geological time scales, the drawdown of CO_2 was not stoichiometrically proportional to the accumulation of O_2 because photosynthesis and respiration are but two of the many biological and chemical processes that affect the atmospheric concentrations of these two gases. The removal rate of CO_2 from the atmosphere by photosynthesis on land is about 60 gigatons C year^{-1}, worldwide. The concentration of oxygen in the oceans (85.8%) is influenced horizontally and vertically by physical features such as the thermocline (i.e., a layer in a large body of water, such as a lake, that sharply separates regions differing in temperature), which isolates deep water from exchange with the atmosphere and can be a zone of significant decomposition causing an oxygen minimum. Oxygen is only sparingly soluble in water (oxygen solubility is inversely proportional to the temperature) and diffuses about 10^4 times more slowly in water than air. Deep water masses are produced at the sea surface in the polar zones where cooling gives rise to increased gas solubility and convection currents. These waters remain largely intact and move through the ocean basins with their oxygen concentration decreasing with time due to the decomposition of organic matter.

Carbon, the key element of all life on earth, has a complex global cycle that involves both physical and biological processes, made up of carbon flows passing back and forth among four main natural reservoirs of stored carbon: the atmosphere, storing 735 gigatons (0.0011%) of the world's carbon as carbon dioxide (CO_2), carbon monoxide (CO), methane (CH_4), longer chain volatile hydrocarbons, and halogen compounds (CFC and HCFC compounds); terrestrial biosphere, storing 2000 gigatons (0.0032%) of the world's carbon as compounds such as fats, carbohydrates, and proteins; the hydrosphere, storing 39,000 gigatons (0.063%) of the world's carbon, as dissolved carbon dioxide; the lithosphere, storing 1000 gigatons (0.002%) of the world's carbon in the form of fossils (e.g., oil, natural gas, lignite, and coal), and 62,000,000 gigatons (99.9%) in sedimentary rocks (e.g., limestone and dolomite). Carbon is also present in the mineral soil, in the bottom sediments of water bodies, in peat in bogs and mires, in the litter and humus, which contain 3000 gigatons (0.0048%) of the world's carbon.

Carbon dioxide enters the ocean from the atmosphere because it is highly soluble in water; in the sea, free dissolved CO_2 combines with water and ionizes to form bicarbonate and carbonate ions, according to the following equilibrium:

$$\begin{array}{ccccc} & & CO_2 + OH^- & & \\ & & \updownarrow & & \\ CO_2 + H_2O & \leftrightarrow & H_2CO_3 & \leftrightarrow & HCO_3^- + H^+ \\ & & \updownarrow & & \\ & & CO_3^{2-} + H^+ & & \end{array} \qquad (5.8)$$

These ions are bound forms of carbon dioxide and they (especially bicarbonate) represent by far the greatest proportion of dissolved carbon dioxide in seawater. On average, there are about 45 mL of total CO_2 in 1 L of seawater, but because of the equilibrium chemical reactions shown above, nearly all of this occurs as bound bicarbonate and carbonate ions which thus act as a reservoir of free CO_2. The amount of dissolved CO_2 occurring as gas in 1 L of seawater is about 0.23 mL. When free CO_2 is removed by photosynthesis, the reaction shifts to the left and the bound ionic forms release more free CO_2; so, even when there is a lot of photosynthesis, carbon dioxide is never a limiting factor to plant production. Conversely, when CO_2 is released by the respiration of algae, plants, bacteria, and animals, more bicarbonate and carbonate ions are produced.

According to the general chemical reactions shown above, the pH of seawater is largely regulated by the concentrations of bicarbonate and carbonate, and the pH is usually 8 ± 0.5. The seawater acts as a buffered solution, since when CO_2 is added to seawater due to mineralization processes and respiration, the number of hydrogen ions increases and the pH goes down (the solution becomes more acidic). If CO_2 is removed from water by photosynthesis, the reverse happens and the pH is elevated.

Some marine organisms combine calcium with carbonate ions in the process of calcification to manufacture calcareous skeletal material. Calcium carbonate ($CaCO_3$) may either be in the form of calcite or aragonite, the latter being a more soluble form. After death, this skeletal material sinks and is either dissolved, in which case CO_2 is again released into the water, or it becomes buried in sediments, in which case the bound CO_2 is removed from the carbon cycle. The amount of CO_2 taken up in the carbonate skeletons of marine organisms has been, over geological time, the largest mechanism for absorbing CO_2. At present, it is estimated that about 50×10^{15} tons of CO_2 occurs as limestone, 12×10^{15} tons in organic sediments, and 38×10^{12} tons as dissolved inorganic carbonate.

Calcification is not confined to a specific phylogenetically distinct group of organisms, but evolved (apparently independently) several times in marine organisms. Carbonate sediments blanket much of the Atlantic Basin and are formed from the shells of both coccolithophorids and foraminifera. As the crystal structure of the carbonates in both groups is calcite (as opposed to the more diagenically susceptible aragonite), the preservation of these minerals and their co-precipitating trace elements provides an invaluable record of ocean history. Although on geological time scales, huge amounts of carbon are stored in the lithosphere as carbonates, on ecological time scales, carbonate formation depletes the oceans of Ca^{2+}, and in so doing, potentiates the efflux of CO_2 from the oceans to the atmosphere. This calcification process can be summarized by the following reaction:

$$Ca^{2+} + 2HCO_3^- \leftrightarrow CaCO_3 + CO_2 + H_2O \tag{5.9}$$

Among the marine organisms responsible for calcification, coccolithophores play a major role, especially *Emiliania huxleyi*. When the blooms of this haptophyte appear over large expanses of the ocean (white water phenomenon), myriad effects on the water and on the atmosphere above can be observed. Although each cell is invisibly small, there can be as many as a thousand billion billion (10^{21}) of them in a large bloom, and the population as a whole has an enormous impact. *E. huxley* blooms are processed through the food web, with viruses, bacteria, and zooplankton all contributing to the demise and decomposition of blooms. Some debris from the bloom survives to sink to the ocean floor, taking chemicals out of the water column. While they live and when they die, the phytoplankton cells leak chemicals into the water. A bloom can be thought of as a massive chemical factory, extracting dissolved carbon dioxide, nitrate, phosphate, etc. from the water, and at the same time injecting other chemicals such as oxygen, ammonia, DMS, and other dissolved organic compounds into the water. This chemical factory pumps large volumes of organic matter and calcium carbonate into the deep ocean and to the ocean floor. Some of this calcium carbonate eventually ends up as chalk or limestone marine sedimentary rocks, perhaps to cycle through the earth's crust and to reappear millions of years later as mountains, hills, and cliffs. Coccolithophorids are primarily found at low abundance in tropical and subtropical seas, and at higher concentrations at high latitudes in midsummer, following diatom blooms. Hence, export of inorganic carbon by diatoms in spring at high latitudes can be offset by an efflux of carbon to the atmosphere with the formation of coccolithophore blooms later in the year.

The contemporary ocean export of organic carbon to the interior is often associated with diatom blooms. This group has only risen to prominence over the past 40 million years.

Coccolithophorid abundance generally increases through the Mesozoic and undergoes a culling at the Cretaceous/Tertiary (K/T) boundary, followed by numerous alterations in the Cenozoic. The changes in the coccolithophorid abundances appear to trace eustatic sea-level variations, suggesting that the transgressions lead to higher calcium carbonate fluxes. In contrast, diatom sedimentation increases with regressions and since the K/T impact, diatoms have generally replaced coccolithophorids as ecologically important eukaryotic phytoplankton. On much finer time scales, during the Pleistocene, it would appear that interglacial periods favor coccolithophorid abundance, while glacial periods favor diatoms. The factors that lead to glacial–interglacial variations between these

two functional groups are relevant to elucidating their distributions in the contemporary ecological setting of the ocean.

Coccolithophores influence regional and global temperature, since they can affect ocean albedo and ocean heat retention, and can have a greenhouse effect. Coccoliths do not absorb photons, but they are still optically important since they act like tiny reflecting surfaces, diffusely reflecting the photons.

A typical coccolith bloom (containing 100 mg m^{-3} of calcite carbon) can increase the ocean albedo from 7.5 to 9.7%. If each bloom is assumed to persist for about a month, then an annual coverage of 1.4×10^6 km^2 will increase the global annual average planetary albedo by

$$(9.7 - 7.5) \times \left(\frac{1}{12}\right) \times \left(\frac{1.4}{510}\right) = 0.001\% \tag{5.10}$$

where 510×10^6 km^2 is the surface area of the earth.

This is a lower bound on the total impact, because light-scattering of sub-bloom coccolith concentration will have an impact, over much larger areas (estimated maximum albedo impact = 0.21%). A 0.001% albedo change corresponds to a 0.002 W m^{-2} reduction in incoming solar energy, whereas an albedo change of 0.21% causes a reduction of 0.35 W m^{-2}. These two numbers can be compared to the forcing due to anthropogenic addition of CO_2 since the 1700s, estimated to be about 2.5 W m^{-2}. Coccolith light scattering is therefore a factor of only secondary importance in the radiative budget of the earth. However, the scattering caused by coccoliths causes more heat and light than usual to be pushed back into the atmosphere; it causes more of the remaining heat to be trapped near to the ocean surface and only allows a much smaller fraction of the total heat to penetrate to deeper in the water. Because it is the near-surface water that exchanges heat with the atmosphere, all three of the effects just described conspire to mean that coccolithophore blooms may tend to make the overall water column dramatically cooler over an extended period, even though this may initially be masked by a warming of the surface skin of the ocean (the top few meters).

All phytoplankton growth removes CO_2 into organic matter and reduces atmospheric CO_2 (by means of photosynthesis). However, coccolithophores are unique in that they also take up bicarbonate, with which to form the calcium carbonate of their coccoliths (calcification process). The coccolithophorid blooms are responsible for up to 80% of surface ocean calcification. In the equilibrium of calcification process, an increase in CO_2 concentration leads to calcium carbonate dissolution, whereas a decrease in CO_2 levels achieves the reverse. While photosynthetic carbon fixation decreases the partial pressure of CO_2 as dissolved inorganic carbon is being utilized, conditions favoring surface calcification by coccolithophorid blooms contribute to the increase of dissolved CO_2.

The relative abundance of the components of the carbonate system (CO_2, H_2CO_3, HCO_3^-, and CO_3^{2-}) depends on pH, dissolved inorganic carbon, and the total alkalinity, and the equilibrium between the components can shift very easily from being in one of these dissolved forms to being in another. How much of the total carbon is in each form is determined mainly by the alkalinity and by the water temperature. When the seawater carbon system is perturbed by coccolithophore cells removing HCO_3^- to form coccoliths, this causes a rearrangement of how much carbon is in each dissolved form, and this rearrangement takes place more or less instantaneously. The removal of two molecules of HCO_3^- and the addition of one molecule of CO_2 change the alkalinity and this indirectly causes more of the dissolved carbon to be pushed into the CO_2 form. Although the total dissolved carbon is obviously reduced by removal of dissolved carbon (bicarbonate ions) into solid calcium carbonate, yet the total effect, paradoxically, is to produce more dissolved CO_2 in the water. In this way, coccolithophore blooms tend to exacerbate global warming by causing increased atmospheric CO_2 (greenhouse effect), rather than to ameliorate it, as is the case when dissolved CO_2 goes into new organic biomass. However, recent work shows that additional properties of coccoliths may make the situation yet more complicated. Coccolith calcite is rather dense (2.7 kg L^{-1} compared to seawater density of 1.024 kg L^{-1}) and the presence of coccoliths in zooplankton fecal pellets and

marine snow (the two main forms in which biogenic matter sinks to the deep ocean) causes them to sink more rapidly. Slow-sinking organic matter may also adhere to the surfaces of coccoliths, hitching a fast ride out of the surface waters. If organic matter sinks faster, then there is less time for it to be attacked by bacteria and so more of the locked-in carbon will be able to escape from the surface waters, depleting the surface CO_2. Probably this co-transport of organic matter with coccoliths offsets the atmospheric CO_2 increase that would otherwise be caused and makes coccolithophore blooms act to oppose global warming, rather than to intensify it.

SUGGESTED READING

Ærtebjerg G., J. Carstensen, K. Dahl, J. Hansen, K. Nygaard, B. Rygg et al. *Eutrophication in Europe's Coastal Waters*. Topic Report 7/2001. European Environment Agency, Copenhagen, 2001.

Anbar A.D. and A.H. Knoll. Protezoic ocean chemistry and evolution: A bioorganic bridge? *Science*, 297, 1137–1142, 2002.

Berman-Frank I., P. Lundgren, Y. Chen, H. Kupper, Z. Kolber, B. Bergman, and P. Falkowski. Segregation of nitrogen fixation and oxygenic photosynthesis in the marine cyanobacterium *Thricodesmium*. *Science*, 294, 1534–1537, 2001.

Berman-Frank I., P. Lundgren, and P. Falkowski. Nitrogen fixation and photosynthetic oxygen evolution in cyanobacteria. *Research in Microbiology*, 154, 157–164, 2003.

Bjerrum C. J. and D. E. Canfield. Ocean productivity before about 1.9 Gyr ago limited by phosphorus adsorption onto iron oxides. *Nature*, 417, 159–162, 2002.

Bucciarelli E. and W. G. Sunda. Influence of CO_2, nitrate, phosphate, and silicate limitation on intracellular dimethylsulfoniopropionate in batch cultures of the coastal diatom *Thalassiosira pseudonana*. *Limnology and Oceanography*, 48, 2256–2265, 2003.

Capone D. G., J. P. Zehr, H. W. Paerl, B. Bergman, and E.J. Carpenter. *Tricodesmium*, a globally significant marine cyanobacterium. *Science*, 276, 1221–1229, 1997.

Conley, D. J. Biochemical nutrient cycles and nutrient management strategies. *Hydrobiologia*, 410, 87–96, 2000.

Conley, D. J. Terrestrial ecosystems and the global biogeochemical silica cycle. *Global Biogeochemical Cycles*, 16, 1121–1128, 2002.

Cottingham, P., B. Hart, H. Adams, J. Doolan, P. Feehan, N. Grace et al. Quantifying nutrient–algae relationships in freshwater systems. Outcomes of a workshop held at Monash University on the 8th August 2000. CRCFE Technical Report 8. CRCFE, Canberra, 2000.

Dismukes G. C., V. V. Klimov, S. V. Baranov, N. Kozlov Yu, J. DasGupta, and A. Tyryshkin. Special feature: The origin of atmospheric oxygen on Earth: The innovation of oxygenic photosynthesis. *PNAS*, 98, 2170–2175, 2001.

Edwards A. M., T. Platt, and S. Sathyendranath. The high-nutrient, low-chlorophyll regime of the ocean: Limits on biomass and nitrate before and after iron enrichment. *Ecological Modeling*, 171, 103–125, 2004.

Exley, C. Silicon in life: A bioinorganic solution to bioorganic essentiality. *Journal of Inorganic Biochemistry*, 69, 139–144, 1998.

Falkowski P. G. Rationalizing elemental ratio in unicellular algae. *Journal of Phycology*, 36, 3–6, 2000.

Fasham, M. J. R. *Ocean Biogeochemistry*. Springer, Berlin, 2003.

Gabric A., W. Gregg, R. Najjar, D. Erickson, and P. Matrai. Modeling the biogeochemical cycle of dimethylsulfide in the upper ocean: A review. *Chemosphere-Global Change Science*, 3, 377–392, 2001.

Gallon J. R. N_2 fixation in phototrophs: Adaptation to a specialized way of life. *Plant and Science*, 230, 39–48, 2001.

Galloway, J. N., J. D. Aber, J. W. Erisman, S. P. Seitzinger, R. W. Howarth, E. B. Cowling, and B. J. Cosby. The nitrogen cascade. *Bioscience*, 53, 341–356, 2003.

Galloway, J. N., F. J. Dentener, D. G. Capone, E. W. Boyer, R. W. Howarth, S. P. Seitzinger et al. Nitrogen cycles: Past, present and future. *Biogeochemistry*, 70, 153–226, 2004.

Holloway J. A. M. and R. A. Dahlgren. Nitrogen in rock: Occurrences and biogeochemical implications. *Global Biogeochemical Cycles*, 16, 1118–1134, 2002.

Horwarth, R. W., J. W. B. Stewart, and M. V. Ivanov. Sulfur cycling on the continent. *Scope*, 48, 27–61, 1992.

http://www.environment-agency.gov.uk/

http://www.ewater.canberra.edu.au/domino/html/Site-CRCFE/CRCFE_WebSite.nsf

http://www.globalchange.umich.edu/

http://history.nasa.gov/CP-2156/contents.htm

http://www.icsu-scope.org/
http://www.icsu-scope.org/downloadpubs/scope13/
http://www.icsu-scope.org/downloadpubs/scope48/
http://www.icsu-scope.org/downloadpubs/scope54/
http://www.mp-docker.demon.co.uk/environmental_chemistry/topic_4b/index.html
http://www.physicalgeography.net/
http://www.soes.soton.ac.uk/staff/tt/eh/biogeochemistry.html
http://www.sws.uiuc.edu/nitro/nitrodesc.asp

Hughes, C., M. Johnson, R. Von Glasow, Chance, R. Lee, S. Gareth et al. Climate-induced change in biogenic bromine emissions from the Antarctic marine biosphere. *Global Biogeochemical Cycles*, 26, GB3019, 2012.

Inokuchi, R., K. Kuma, T. Miyata, and M. Okada. Nitrogen-assimilating enzymes in land plants and algae: Phylogenic and physiological perspectives. *Physiologia Plantarum*, 116, 1–11, 2002.

Kasamatsu N., T. Hirano, S. Kudoh, T. Odate, and M. Fukuchi. Dimethylsulfopropionate production by psychrophilic diatom isolates. *Journal of Phycology*, 40, 874–878, 2004.

Klausmeier C. A., E. Litchman, T. Daufresne, and S. A. Levin. Optimal nitrogen-to-phosphorus stoichiometry of phytoplankton. *Nature*, 429, 171–174, 2004.

Kumazawa, S., S. Yumura, and H. Yoshisuji. Photoautrophic growth of a recently isolated N_2-fixing marine non-heterocystous filamentous cyanobacterium, *Symploca* sp. *Journal of Phycology*, 37, 482–487, 2001.

Lee P. A. and S. J. de Mora. Intracellular dimethylsulfoxide in unicellular marine algae: Speculation on its origin and possible biological role. *Journal of Phycology*, 35, 8–18, 1999.

Letscher R. T., D. A. Hansell, C. A. Carlson, R. Lumpkin, and A. N. Knapp. Dissolved organic nitrogen in the global surface ocean: Distribution and fate. *Global Biogeochemical Cycles*, 27, 141–153, 2013.

Litchman E., D. Steiner, and P. Bossard. Photosynthetic and growth response of three freshwater algae to phosphorus limitation and daylenght. *Freshwater Biology*, 48, 2141–2148, 2003.

Lomans B. P., A. J. P. Smolders, L. M. Intven, A. Pol, H. J.M. Op de Camp, and C. van der Drift. Formation of dimethyl sulfide and methanethiol in anoxic freshwater sediments. *Applied and Environmental Microbiology*, 63, 4741–4747, 1997.

Lomans B. P., C. van der Drift, A. Pol, and H. J. M. Op den Camp. Microbial cycling of volatile organic sulfur compounds. *Cellular and Molecular Life Sciences*, 59, 575–588, 2002.

Lundgren P., E. Soderback, A. Singer, E. J. Carpenter, and B. Bergman. *Katagnymene*: Characterization of a novel marine diazotroph. *Journal of Phycology*, 37, 1052–1062, 2001.

Misra H. S., Khairnar, and S. K. Mahajan. An alternate photosynthetic electron donor system for PSI supports light dependent nitrogen fixation in a non-heterocystous cyanobacterium, *Plectonema boryanum*. *Journal of Plant Physiology*, 160, 33–39, 2003.

NASA's Earth Science Enterprise Research Strategy for 2000–2010. Biology and biogeochemistry NASA research on the biology and biogeochemistry of ecosystems and the global carbon cycle aims to understand and predict how terrestrial and marine ecosystems are changing. http://earth.nasa.gov/visions/researchstrat/

Navarro-Gonzales R., C. P. McKay, and D. N. Mvondo. A possible nitrogen crisis for Archean life due to reduced nitrogen fixation by lightning. *Nature*, 412, 61–64, 2001.

Otsuki T. A study of the biological CO_2 fixation and utilization system. *The Science of Total Environment*, 27, 121–125, 2201.

Raven J. A. and P. G. Falkowki. Oceanic sinks for atmospheric CO_2. *Plant and Cell Environment*, 22, 741–755, 1999.

Raven J. A. and A. M. White. The evolution of silicification in diatoms: Inesplicable sinking and sinking as escape? *New Phytologist*, 162, 45–61, 2004.

Raymond, J., J. L. Siefert, C. R. Staples, and R. E. Blankenship. The natural history of nitrogen fixation. *Molecular Biology and Evolution*, 21, 541–554, 2004.

Sarmiento J. L. and N. Gruber. *Ocean Biogeochemical Dynamics*. Princeton University Press, Princeton, NJ, 2004.

Sarmiento, J. L., S. C. Wofsy, E. Shea, A. S. Denning, W. Easterling, C. Field et al. *A U.S. Carbon Cycle Science Plan*. University Corporation for Atmospheric Research, Boulder, CO, 1999.

Seibach J. (Ed.). *Cellular Origin and Life in Extreme Habitats*, Vol. 3. Kluwer Academic Publishers, Dordrecht, The Netherlands, 2002.

Seitzinger S. P., R. W. Sander, and R. Styles. Bioavailability of DON from natural and antropogenic sources to estuarine plankton. *Limnology and Oceanography*, 47, 353–366, 2002.

Sharpley A. N., T. Daniel, T. Sims, J. Lemunyon, R. Stevens, and R. Parry. Agricultural phosphorus and eutrophication. Agricultural Research Service ARS-149. United States Department of Agriculture, 2003.

Sunda W., D. J. Kleber, R. P. Keine, and S. Huntsman. An antioxidant function for DMSP and DMS in marine algae. *Nature*, 418, 317–320, 2002.

The Open University. *Ocean Chemistry and Deep-Sea Sediments*. Butterorth-Heinemann, Oxford, 2001.

Toggweller J. R. An ultimately limiting nutrient. *Nature*, 400, 511–512, 1999.

Tyrrel T. The relative influence of nitrogen and phosphorus on oceanic primary production. *Nature*, 400, 525–531, 1999.

Van Alstyne K. L., and L. T. Houser. Dimethylsulfide release during macroinvertebrate grazing and its role as an activated chemical defense. *Marine Ecology Progress Series*, 250, 175–181, 2003.

Voss M. and S. Hietanen. The depth of nitrogen cycling. *Nature*, 493, 616–618, 2013.

Wolfe G. V., M. Steinke, and G. O. Kirst. Grazing-activated chemical defence in a unicellular marine algae. *Nature*, 387, 894–897, 1997.

Yool A. and T. Tyrrel. Role of diatoms in regulating the ocean's silicon cycle. *Global Biogeochemical Cycles*, 17, 1103–1124, 2003.

6 Algal Culturing

COLLECTION, STORAGE, AND PRESERVATION

Algae grow in almost every habitat in every part of the world. They can be found on very different natural substrates, from animals (snails, crabs, sloths, turtles, etc. are algal hosts) to plants (tree trunks, branches and leaves, water plants, and macroalgae), from springs and rivers to hypersaline lagoons and salt lakes. They also colonize artificial habitats, such as dams and reservoirs, fountains and pools, and cans, bottles, plant pots, or dishes all allow algae to extend their natural range. The ubiquity of these organisms together with the plasticity of their metabolic requirements makes many algal species easily available for investigation, collection, or simple observation.

Floating microalgae can be collected with a mesh net (e.g., with 25–30-μm pores) or, if in sufficient quantity (i.e., coloring the water), by simply scooping a jar through the water. A small amount of the bottom sediments will also provide many of the algal species that live in or on these sediments. Some algae live attached to other types of substrates, such as dead leaves, twigs, and any underwater plants that may be growing in the water. Macroalgae and the attached microalgae can either be collected by hand or by using a knife, including part or all of the substrate (rock, plant, wood, etc.) if possible. Algae growing on soil are difficult to collect and study, many requiring culturing before sufficient and suitable materials are available for identification.

Any sample should be labeled with standard information such as the locality, date of collection, and as many of the following features as possible: whether the water is saline, brackish, or fresh; whether the collection site is terrestrial, or a river, stream, or lake; whether the alga is submerged during water level fluctuations or floods; whether the water is muddy or polluted; whether the alga is free floating or attached, and if the latter, the type of substrate to which it is attached; and the color, texture, and size of the alga. Algae can be stored initially in a glass jar, a plastic bottle, or a bag, or in a vial with some water from the collecting site. The container should be left open or only half-filled with liquid, and wide shallow containers are better than narrow deep jars. If refrigerated or kept on ice soon after collecting, most algae can be kept alive for short periods (a day or two). If relatively sparse in the sample, some algae can continue to grow in an open dish stored in a cool place with reduced light. For long-term storage, specimens can be preserved in liquid, dried, or made into a permanent microscope mount. Even with ideal preservation, examination of fresh material is sometimes essential for an accurate determination. Motile algae must be examined particularly, while flagella and other delicate structures remain intact, since any kind of preservation procedure causes the detachment of the flagella.

Commercial formalin (40% formaldehyde in water), diluted between 1/10 and 1/20 with the collecting medium, is the most commonly used fixative. As formaldehyde is considered carcinogenic, any contact with skin, eyes, and air passages should be avoided. This compound when mixed with other chemicals such as glacial acetic acid and alcohol (FAA 1–1–8 by volume: 40% formaldehyde 1: glacial acetic acid 1: 95% alcohol 8) gives better preservation results for some of the more fragile algae, whereas the standard alcohol and water mix (e.g., 70% ethyl alcohol) will ruin all but the larger algae. However, FAA may cause thin-walled cells to burst.

Color is an important taxonomic characteristic, especially for cyanobacteria, and formalin is a good preservative for green algae, cyanobacteria, and dinoflagellates because cell color remains intact if samples are stored in the dark. Algae can be kept in diluted formalin for a number of years,

but the solution is usually replaced by 70% ethyl alcohol with 5% glycerin (the latter to prevent any accidental drying out).

Lugol's solution is the preferred preservative commonly used for short-term (e.g., a few months, but possibly a year or more) storage of microalgae. It is excellent for preserving chrysophytes but it makes the identification of dinoflagellates difficult, if not impossible. Samples can be preserved and kept in dark bottles away from light for as long as 1 year in Lugol's solution (0.05–1% by volume). The solution is prepared by dissolving 20 g of potassium iodide and 10 g of iodine crystals in 180 mL of distilled water and by adding 20 mL of glacial acetic acid. Note that Lugol's solution is affected by light and has a shelf-life of about 6 months.

Dried herbarium specimens can be prepared by "floating out" similar to aquatic flowering plants. Ideally, fresh specimens should be fixed prior to drying. Most algae will adhere to absorbent herbarium paper. Smaller, more fragile specimens or tangled, mat-forming algae may be dried onto mica or cellophane. After "floating out," most freshwater algae should not be pressed but simply left to air-dry in a warm dry room. If pressed, they should be covered with a piece of waxed paper, plastic, or muslin cloth so that the specimen does not stick to the drying paper during pressing.

To examine a dried herbarium specimen, a few drops of water are added to the specimen to make it swell and lift slightly from the paper. This makes it possible to remove a small portion of the specimen with forceps or a razor-blade.

Observations (preferably including drawings or photographs) based on living material are essential for the identification of some genera and a valuable adjunct to more leisurely observations on preserved material for other genera. The simplest method is to place a drop of the water including the alga onto a microscope slide and carefully lower a coverslip onto it. It is always tempting to put a large amount of the alga onto the slide, but smaller fragments are much easier to view under a microscope. Microalgae may be better observed using the "hanging drop method," that is, a few drops of the sample liquid are placed on a coverslip which is turned over onto a ring of paraffin wax, liquid paraffin, or a "slide ring."

A permanent slide can be prepared using staining materials such as aniline blue (1% aqueous solution, pH 2.0–2.5), toluidine blue (0.05% aqueous solution, pH 2.0–2.5), and potassium permanganate ($KMnO_4$; 2% aqueous solution), which are useful stains for macroalgae (different stains suit different species) and Indian Ink, which is a good stain for highlighting mucilage and some flagella-like structures. Staining time ranges from 30 s to 5 min (depending on the material), after which the sample is rinsed in water. Mounting is achieved by adding a drop or two of glycerin solution (75% glycerin and 25% water) to a small piece of the sample placed on a microscope slide, then carefully lowering the coverslip. Sealing with nail polish is essential. This method is unsuitable for most unicellular algae, which should be examined fresh or in temporary mounts of liquid-preserved material.

Magnifications of between 40× and 1000× are required for the identification of all but a few algal genera. A compound microscope with 10× to 12× eyepiece and 4× to 10× to 40× objectives is therefore an essential piece of equipment for anyone wishing to discover the world of algal diversity. An oil immersion 100× objective would be a useful addition, particularly when aiming at identifying samples to species level. Phase-contrast or interference microscopy (e.g., Nomarski) can improve the contrast for bleached or small specimens. A dissecting microscope providing 20×, 40× up to 60× magnifications is a useful aid but is secondary to a compound microscope. A camera lucida attachment is helpful for producing accurate drawings, whereas an eyepiece micrometer is important for size determinations. Formulas for calculating biomass for various phytoplankton shapes using geometric forms and measurements and shape code for each taxa exist in the literature and are routinely used in the procedure for phytoplankton analysis that require biovolume calculations (Table 6.1). Scanning and transmission electron microscopes are beyond the reach of all except specialist institutions; however, they are an essential tool for identifying some of the very small algae, and also for investigating the details of their ultrastructure.

In an attempt to speed up the time-consuming procedure of classification by optical microscopy, several kinds of automatic analysis and microalgae identification methods were set up. They include,

TABLE 6.1
Shape Codes and Corresponding Dimensions Required for Calculating Biovolumes of Various Phytoplankton Species

		Dimensions Required			
Shape	**Code**	**Length**	**Width**	**Depth**	**Diameter**
Cone	CON	L	W		
Cylinder	CYL	L	W	DP	D
Dumbell box	DBB	L	W	DP	
Dumbell	DBL	L	W	DP	
Diamond box	DMB	L	W	DP	
Fusiform	FUS	L	W		
Ovoid box	OVB	L	W	DP	
Ovoid	OVO	L	W		
Rectangular box	RTB	L	W	DP	
Sphere	SPH				D
Teardrop	TRP	L	W		

for example, a method based on algal cell morphology identification, absorption spectroscopy, fluorescence spectroscopy, high-performance liquid chromatographic method, flow cytometric method, and gene probe method. Though automated classification of microalgae is a rather active field of research, commercial developments are limited.

Pioneering attempts in automatic classification of microalgal images were able to distinguish between few species of distinct size and shape using simple geometric features. To achieve higher classification accuracy, a hundreds of features, such as shape, moments, texture, and contours, and several classifiers, such as decision trees, Bayesian statistics, ridge linear regression, neural network, fuzzy logic, and genetic algorithm, were used. Unfortunately, most of the existing research systems are still adapted to identify few specific types of algae. This is mainly due to the difficulties in choosing the correct feature pattern. The previously described techniques are very complex and limited in their applicability; very recently, an innovative software methodology that combines robust image segmentation, shape features extraction, centroid distance spectrum calculation, and characteristic color (i.e., pigment signature) determination which can offer a reliable, real-time recognition of multialgal samples has been developed. Introducing a categorization parameter never used before, that is, centroid distance spectrum calculation and the pigment fingerprint of each alga, combined with a very simple technology, this methodology has the capacity to obtain real-time recognition accuracy comparable to that obtained by a phycologist. This methodology needs only a simple hardware platform, which integrates an optical microscope equipped with a color CCD digital camera, a personal computer, and a commercial software such as Matlab. Images are processed according to the following flow of 5 operations:

1. *Image Acquisition* For image acquisition, slides from algae samples are prepared without any kind of processing or fixation. All the color images are acquired with the highest accuracy, because image processing can remove unwanted information, not add new information. All the objects present in the microscope field images undergo real-time processing. Those corresponding to objects other than algae, such as debris, particles, detritus, overlapping cells, are discarded.
2. *Contours Detection* The amount of data of the acquired images is reduced by representing the algae with lengths and contours as descriptors.

3. *Centroid Distance Spectrum Calculation* To obtain invariant features for translation, rotation, and scaling, the contour is normalized, oriented following the maximum Feret diameter, and its points uniformly resampled.
4. *Characteristic Color Identification* The color having greater Euclidean distance corresponds to the chloroplast domain and is defined the alga characteristic color, that is, the color that represents the pigment signature of each algal group.
5. *Classification of Images* All the features measured by the operations described so far are used to classify the microalgae according to a Classifier Algorithm that assign the sample to a specific database class. Each database class corresponds to an alga taxonomically recognized by the expert at the genus and/or species level. The accuracy of the correct number of database classes and the correct assignment of the images to the different database classes using this methodology are close to 97%. Figure 6.1 shows the results of the application of the algorithms for contour detection on *Gymnodinium acidotum* (Myzozoa, Dinophyceae) and characteristic color identification on *Cyanophora paradoxa* (Glaucophyceae).

CULTURE TYPES

A culture can be defined as an artificial environment in which the algae grow. Theoretically, culture conditions should resemble the alga's natural environment as far as possible; actually, many significant differences exist, most of which are deliberately imposed. In fact, following isolation from the natural environment, algal strains are maintained under largely artificial conditions of media composition, light, and temperature. The imposition of an artificial environment on a cell population previously surviving under complex, fluctuating conditions and following a seasonal life cycle inevitably causes a period of physiological adaptation and/or selection, during which population growth will not occur or is very slow.

Although contaminated algal cultures have previously been satisfactory for certain applications and experiments, modern experimental methods and application demand contaminants not to be present, and taxonomy and growth characteristics of the strains to be defined. Hence, for most purposes, algal cultures are maintained as unialgal, contaminant-free, or axenic stocks. "Unialgal" cultures contain only one kind of alga, usually a clonal population (but that may contain bacteria, fungi, or protozoa), whereas "axenic" cultures should contain only one alga and no bacteria, fungi, or protozoa.

To obtain a unialgal culture, a species must be isolated from all the rest; three major techniques borrowed from microbiology are available for obtaining unialgal isolates: streaking and successive plating on agar media; serial dilution; and single-cell isolations using capillary pipettes. Streaking is useful for single-celled, colonial, or filamentous algae that will grow on agar surface. Filaments can be grabbed with a slightly curved pipette tip and dragged through soft agar (>1%) to remove contaminants. It is best to begin with young branches or filament tips that have not yet been extensively epiphytized.

Many flagellates, however, as well as other types of algae must be isolated by single-organism isolations or serial-dilution techniques. A particularly effective means of obtaining unialgal cultures is isolation of zoospores immediately after they have been released from parental cell walls, but before they stop swimming and get attached to a surface. Recently released zoospores are devoid of contaminants, unlike the surfaces of most algal cells, but catching zoospores requires a steady hand and experience.

Sterile cultures of microalgae may be obtained from specialized culture collections. Alternatively, axenic cultures can be obtained by treating isolated algae to an extensive washing procedure and/or with one or more antibiotics. Resistant stages such as zygotes or akinetes can be treated with bleach to kill epiphytes and then planted on agar for germination. It is usually necessary to try several different concentrations of bleach and times of exposure to find a treatment that will kill epiphytes without harming the alga. When diatoms represent the contaminating species, addition of

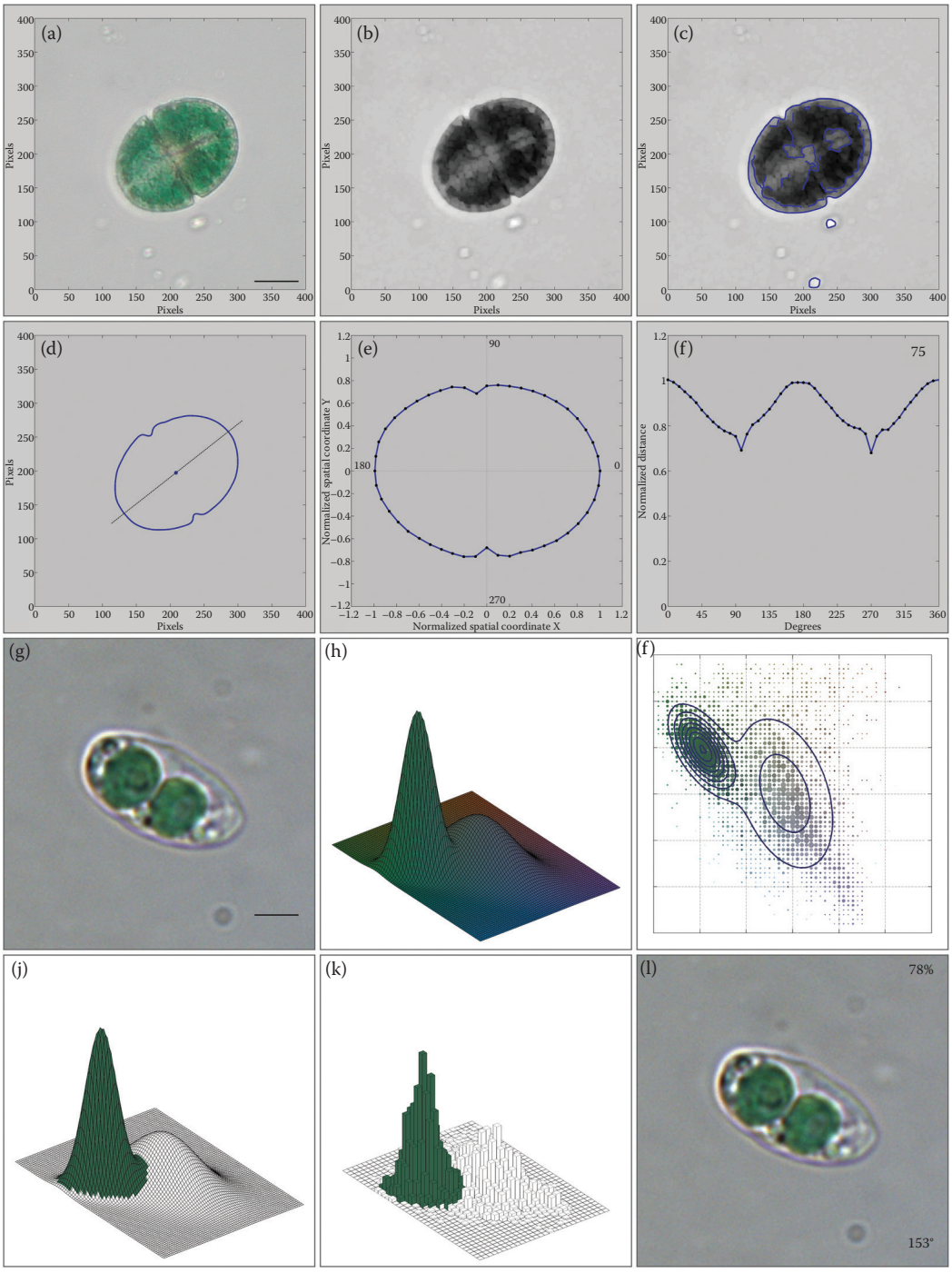

FIGURE 6.1 Results of the application of the algorithm for centroid distance spectrum calculation on *Gymnodinium acidotum* (a–f) and application of the algorithm for characteristic color calculation on *Cyanophora paradoxa* (g–l). Figure 6.1a, scale bar: 10 µm; Figure 6.1g, scale bar: 5 µm.

low concentrations (5 mg/L) of germanium dioxide, GeO_2, to a culture medium can inhibit diatom growth, since it disrupts silica deposition.

"Cleaning," previously contaminated cultures, is a skilful and time-consuming process and could take several years in sizeable collections. Extensive measures must be taken to keep pure unialgal cultures chemically and biologically clean. Chemical contamination may have unquantifiable, often deleterious, and therefore undesirable effects on algal growth. Biological contamination of pure algal cultures by other eukaryotes and prokaryotic organisms in most cases invalidates experimental work and may lead to the extinction of the desired algal species in culture through out-competition or grazing. In practice, it is very difficult to obtain bacteria-free (axenic) cultures, and although measures should be taken to minimize bacterial numbers, a degree of bacterial contamination is often acceptable.

If biological contaminants appear in a culture, the best remedy is to isolate a single cell from the culture with a micropipette and try to establish a new, clean clonal culture. Alternatively, the culture can be streaked on an agar plate hoping to attain a free of contaminants colony. Neither of these methods works well, however, for eliminating bacteria that attach firmly to the surface of microalgae. Placing a test tube of microalgal culture in a low-intensity 90 kHz s^{-1} ultrasonic water bath for varying lengths of time (a few seconds to tens of minutes) can sometimes physically separate bacteria without killing the algae, making it easier to obtain an axenic culture by micropipette isolation. Often, however, to achieve an axenic culture, antibiotics must be added to the growth medium to discourage growth of contaminating cyanobacteria and other bacteria. Best results appear to occur when an actively growing culture of algae is exposed to a mixture of penicillin, streptomycin, and gentamycin for around 24 h. This drastically reduces the growth of bacteria while allowing the microalgae to continue to grow, increasing the chances of obtaining an axenic cell when using micropipette or agar streaking isolation. Different algal species tolerate different concentrations of antibiotics, so a range of concentrations should be used (generally 50–500‰, w/v). Other antibiotics, such as chloramphenicol, tetracycline, and bacitracin, can also be used. Antibiotic solutions should be made with filter-sterilized (0.2-µm filter units) distilled water into sterile tubes and stored frozen until use. Another approach is to add a range of antibiotic concentrations to a number of subcultures and then select the culture that has surviving algal cells but no surviving bacteria or other contaminants. Sterility of cultures should be checked by microscopic examination (phase-contrast) and by adding a small amount of microalgal culture to sterile bacterial culture medium (e.g., 0.1% peptone) and observing regularly for bacterial growth. Absence of bacterial growth does not, however, ensure that the microalgal culture is axenic, since the majority of bacteria do not respond to standard enrichments. In reality, there is no way of demonstrating that a microalgal culture is completely axenic. In practice, therefore, axenic usually means "without demonstrable unwanted prokaryotes or eukaryotes." Some microalgal cultures may die when made axenic, probably due to the termination of obligate symbiotic relationships with bacteria.

The collection of algal strains should be carefully protected against contamination during handling and poor temperature regulation. To reduce risks, two series of stocks are often retained, one which supplies the starter cultures for the production system and the other which is only subjected to the handling necessary for maintenance. Stock cultures are kept in test tubes at a light intensity of about 1.5 W m^{-2} and at a temperature of 16–19°C. Constant illumination is suitable for the maintenance of flagellates, but may result in decreased cell size in diatom stock cultures. Stock cultures are maintained for about a month and then transferred to create a new culture line.

CULTURE PARAMETERS

A culture has three distinct components: the culture medium contained in a suitable vessel; the algal cells growing in the medium; air, to allow exchange of carbon dioxide between medium and atmosphere.

For strictly autotrophic alga, all that is needed for growth are light, CO_2, water, nutrients, and trace elements. By means of photosynthesis, the alga will be able to synthesize all the biochemical compounds necessary for growth. Only a minority of algae is, however, autotrophic; many are unable to synthesize certain biochemical compounds (e.g., certain vitamins) and will require these to be present in the medium (for obligate mixotropy condition, see Chapter 1).

The most important parameters regulating algal growth are nutrient quantity and quality, light, pH, turbulence, salinity, and temperature. Optimal parameters as well as the tolerated ranges are species-specific; the different parameters may be interdependent and a parameter that is optimal for one set of conditions is not necessarily optimal for another.

Temperature

The temperature at which cultures are maintained should ideally be as close as possible to the temperature at which the organisms were collected; for example, polar organisms (<10°C), temperate (10–25°C), tropical (>20°C). Most commonly cultured species of microalgae tolerate temperatures between 16°C and 27°C, although this may vary with the composition of the culture medium, the species, and strain cultured. An intermediate value of 18–20°C is most often employed. Temperature-controlled incubators usually use constant temperature (transfers to different temperatures should be conducted in steps of 2°C per week), although some models permit temperature cycling. Temperatures less than 16°C will slow down growth, whereas those higher than 35°C are lethal for a number of species.

Light

As for plants, light is the source of energy, which drives photosynthetic reactions in algae and in this regard intensity, spectral quality, and photoperiod need to be considered. Light intensity plays an important role, but the requirements greatly vary with the culture depth and the density of the algal culture: at higher depths and cell concentrations, the light intensity must be increased to penetrate through the culture. Too high light intensity (e.g., direct sunlight, small container close to artificial light) may result in photo-inhibition. Most often employed light intensities range between 100 and 200 $\mu E\ s^{-1}\ m^{-2}$, which corresponds to about 5–10% of full daylight (2000 $\mu E\ s^{-1}\ m^{-2}$). Moreover, overheating due to both natural and artificial illumination should also be avoided.

Light may be natural or supplied by fluorescent tubes emitting either in the blue or in the red light spectrum, as these are the most active portions of the light spectrum for photosynthesis. Light intensity and quality can be manipulated with filters. Many microalgal species do not grow well under constant illumination, although cultivated phytoplankton develops normally under constant illumination, and hence a light/dark (LD) cycle is used (maximum 16:8 LD, usually 14:10 or 12:12).

pH

The pH range for most cultured algal species is between 7 and 9, with the optimum range being 8.2–8.7, though there are species that dwell in more acid/basic environments. Complete culture collapse due to the disruption of many cellular processes can result from a failure to maintain an acceptable pH. The latter is accomplished by aerating the culture. In the case of high-density algal culture, the addition of carbon dioxide allows to correct for increased pH, which may reach limiting values of up to pH 9 during algal growth.

Salinity

Marine algae are extremely tolerant to changes in salinity. Most species grow best at salinity slightly lower than that of their native habitat, which is obtained by diluting seawater with tap water. Salinities of 20–24 $g\ L^{-1}$ are found to be optimal.

Mixing

Mixing is necessary to prevent sedimentation of the algae, to ensure that all cells of the population are equally exposed to the light and nutrients, to avoid thermal stratification (e.g., in outdoor cultures) and to improve gas exchange between the culture medium and the air. The latter is of primary importance as the air contains the carbon source for photosynthesis in the form of carbon dioxide. For very dense cultures, the CO_2 originating from the air (containing 0.03% CO_2) bubbled through the culture is limiting and pure carbon dioxide may be supplemented to the air supply (e.g., at a rate of 1% of the volume of air). CO_2 addition furthermore buffers the water against pH changes as a result of the CO_2/HCO_3^- balance.

Mixing of microalgal cultures may be necessary under certain circumstances: when cells must be kept in suspension in order to grow (particularly important for heterotrophic dinoflagellates); in concentrated cultures to prevent nutrient limitation effects due to stacking of cells and to increase gas diffusion. It should be noted that in the ocean, algae cells seldom experience turbulence and hence mixing should be gentle. Depending on the scale of the culture system, mixing is achieved by stirring daily by hand (test tubes, Erlenmeyer's), aerating (bags, tanks), or using paddle wheels and jet pumps (ponds). Not all algal species can tolerate vigorous mixing. The following methods may be used: bubbling with air (may damage cells), plankton wheel or roller table (about 1 rpm), and gentle manual swirling. Most cultures do well without mixing, particularly when not too concentrated, but when possible, gentle manual swirling (once a day) is recommended.

CULTURE VESSELS

Culture vessels should have the following properties: nontoxic (chemically inert); reasonably transparent to light; easily to clear and sterilize; providing a large surface-to-volume ratio (depending on organism).

Certain materials which could potentially be used for culture vessels may leach chemicals into the medium with a deleterious effect on algal growth. The use of chemically inert materials is particularly important when culturing oceanic plankton and during isolation. Recommended materials for culture vessels and media preparation include

- Borosilicate glass
- Polycarbonate
- Teflon
- Polystyrene

Culture vessels are usually borosilicate glass conical flasks (narrow- or wide-mouth Erlenmeyer flasks) of various volume (from tens of milliliters to 3–5 L) or test tubes for liquid culture, and agar cultures. Borosilicate glass flasks and tubes, which have been shown to inhibit growth of some species, can be replaced by more expensive transparent polycarbonate vessels, which offer excellent clarity and good physical strength. Like borosilicate, polycarbonate is autoclavable, but it is expensive and becomes cloudy and cracks with repeated autoclaving, undergoing some loss of mechanical strength. Teflon is very expensive, and it is used only for media preparation, and polystyrene, the cheaper alternative to Teflon and polycarbonate, is not autoclavable. Polystyrene tissue culture flasks can be purchased as single-use sterile units (Iwaki, Nunc, and Corning) and used for transport purposes.

The vessels are capped by nonadsorbent cotton-wool plugs, which will allow gas transfer but prevent entry of microbial contaminants. A more efficient and costly way of capping is to use foam plugs or silicone bubble stoppers (bungs), which also allow efficient gas transfer; they are reusable and autoclavable. Glass, polypropylene, or metal covers and caps are also used for flasks and tubes.

Materials which should generally be avoided during microalgal culturing include all types of rubber and PVC.

MEDIA CHOICE AND PREPARATION

The correct maintenance of algal strains is dependent on choice of growth media and culture parameters. Two approaches are possible for selection of media composition:

- Theoretically, it is better to work on the principle that if the alga does not need the addition of any particular chemical substance to the culture media (i.e., if it has no observable positive effect on growth rate), do not add it.
- In practice, it is often easier to follow well-known (and presumably, therefore, well tested) media recipes, and safer to add substances "just in case" (provided they have no observable detrimental effect on algal growth).

When choosing a culture medium, the natural habitat of the species should be considered in order to determine its environmental requirements. It is important to know whether the environment is eutrophic, hence nutrient-rich, or oligotrophic, hence nutrient-poor, and whether the algae belong to an *r*-selected or a *k*-selected species. *r*-Selected species are characterized by a rapid growth rate, autotrophic metabolism, and a wide environmental plasticity, whereas *k*-selected species show a slow growth rate, mixotrophic, or photoheterotrophic metabolism, and a low environmental tolerance.

The media recipes currently available are not always adequate for many species, and the exact choice for a particular species therefore is dependent on trial and error. It must be remembered that there are (within limits) no right and wrong methods in algal culturing; culture media have been only developed trying out various additions, usually based on theoretical considerations. Refinement of media composition for laboratory-maintained algal cultures have been the object of research for several decades, resulting in many different media recipes reported in the literature and used in different laboratories.

Media can be classified as defined or undefined. Defined media, which are often essential for nutritional studies, have constituents that are all known and can be assigned a chemical formula. Undefined media, on the other hand, contain one or more natural or complex ingredients, for example, agar, or liver extract and seawater, the composition of which is unknown and may vary. Defined and undefined media may further be subdivided into freshwater or marine media.

In choosing or formulating a medium, it may be important to decide whether it is likely to promote heavy bacterial growth. Rich organic media should be avoided unless the algae being cultivated are axenic. For contaminated cultures, mineral media should be used. These may contain small amount of organic constituents, such as vitamins or humic acids and, in either case, provide insufficient carbon for contaminating organisms to outgrow the algae.

Culture collections have attempted to rationalize the number of media recipes and to standardize recipes for algal strain maintenance. In particular, the use of undefined biphasic media (soil/water mixture) is declining, due to lack of reproducibility in media batches and occasional contamination of the media from soil samples.

Media may be prepared by combining concentrated stock solutions which are not combined before use, to avoid precipitation and contamination. Reagent grade chemicals and bidistilled (or purer) water should be used to make stock solutions of enrichments. Gentle heating and/or magnetic stirring of stock solutions can be used to ensure complete dissolution. When preparing a stock solution containing a mixture of compounds, each compound has to be dissolved individually in a minimal volume of water before mixing, then combined with the others and the volume diluted to the needed amount.

Another practical way of preparing artificial defined media is to mix the ingredients together and dry them prior to long-term storage. Constituents are added sequentially to distilled water, smallest

quantities first, for obtaining a solution and finally a stiff slurry. Prior to the addition of the major salts, the pH is adjusted to be between 4 and 5. The mixture is then transferred to a clean desiccator of suitable size and the final additions are made. The well-stirred slurry is vacuum-dried, and the dry mixture is then stored with calcium chloride as a desiccant. It can be stored for some years if kept dry.

Solid media are usually prepared using 1.0–1.5% (w/v) agar, tubes being rested at an angle of 30° during agar gelation to form a slope that increases the surface area available for growth.

As said above, media are sterilized either by autoclaving at 126°C (20 min, 1 atm pressure), or by filtration, using 0.2-μm pore cellulose nitrate or acetate sterile filters. Generally, subculturing is performed using aseptic microbiological techniques; laminar flow cabinets, equipped with Bunsen flame, microbiological loops, and glass or plastic sterile pipettes are required.

Freshwater Media

Freshwater media are generally selected because they possess characteristics similar to the natural environment or they differentially selected for a specific algal component of the habitat. Artificial media, with known chemical composition, are often employed as additives to natural media with an unknown chemical composition, such as lake water, to enrich them. They are often used to simulate diverse nutritional or physical requirements of a particular species or groups of species, especially when the exact nutritional requirements are unknown.

Media are generally prepared from premixed stock solutions. Aliquots from these stocks are measured and added to a given volume of water. Some, however, must be prepared by weighting or measuring the desired components and adding them directly to a given volume of liquid. Accuracy in measuring liquid aliquots from stock solution or water, and weighing of chemicals is essential. Improper procedures may result in precipitation of one or more of the components of the medium, such as nitrates and phosphates, or failure of some of the constituents to go into solutions.

Stock solution can be prepared and stored at low temperature in tightly sealed glassware, since evaporation may alter initial concentrations.

Water generally employed for freshwater media should belong to one of the following types: copper-distilled water, single distilled water, double distilled water, membrane-filtered water, and deionized water. In most laboratories, single- or double-distilled water is routinely used, which can be deionized by passing it through a prepacked deionizing column.

Freshwater media can be "defined" and "undefined." Defined medium such as Sueoka's or Bold Basal Medium has been proved successful for many algal classes. Most of these defined media can be used for additional algal groups by adding a variety of other components or modifying the amounts of certain reagents. These "undefined" media often have the advantage of supporting the growth of a large number of different algal species, but, when highly organic, they also have the disadvantage of encouraging more bacterial growth respect to strictly inorganic media.

Some of the most commonly used freshwater media, defined and undefined, are listed in Tables 6.2 through 6.12.

Marine Media

Seawater is an ideal medium for growth of marine species, but it is an intrinsically complex medium, containing over 50 known elements in addition to a large but variable number of organic compounds. Usually, it is necessary to enrich seawater with nutrients such as nitrogen, phosphorus, and iron. Synthetic formulations have been designed primarily to provide simplified, defined media. Marine species generally have fairly wide tolerances, and difficulties attributed to media can frequently be related to problems of isolation, conditions of manipulations and incubation, and physiological state of the organism. A single medium will generally serve most needs of an

TABLE 6.2
BG11 Medium Composition

Reagents	Per Liter
$NaNO_3$[a]	1.5 g
$K_2HPO_4 \cdot 3H_2O$	0.004 g
$MgSO_4 \cdot 7H_2O$	0.075 g
$CaCl_2 \cdot 2H_2O$	0.027 g
Citric acid ($C_6H_8O_7$)	0.006 g
Ammonium ferric citrate ($C_6H_8O_7 \cdot x\text{Fe} \cdot y\text{NH}_3$)	0.006 g
Na_2Mg-EDTA	0.001 g
Na_2CO_3	0.02 g
Microelement stock solution	1 mL

Microelement Stock Solution	Per Liter
H_3BO_3	2.860 g
$MnCl_2 \cdot 4H_2O$	1.810 g
$ZnSO_4 \cdot 7H_2O$	0.222 g
$Na_2MoO_4 \cdot 2H_2O$	0.390 g
$CuSO_4 \cdot 5H_2O$	0.079 g
$Co(NO_3)_2 \cdot 6H_2O$	0.0494 g

pH 7.4

[a] To be omitted for N_2-fixing cyanobacteria.

TABLE 6.3
Diatom Medium Composition

Reagents	Per Liter
$Ca(NO_3)_2 \cdot 4H_2O$	20 mg
KH_2PO_4	12.4 mg
$MgSO_4 \cdot 7H_2O$	25 mg
$NaHCO_3$	15.9 mg
FeNa–EDTA	2.25 mg
Na_2–EDTA	2.25 mg
H_3BO_3	2.48 mg
$MnCl_2 \cdot 4H_2O$	1.39 mg
$(NH_4)_6Mo_7O_{24} \cdot 4H_2O$	1.0 mg
Biotin (vitamin B_7)	0.04 mg
Thiamine HCl (vitamin B_1)	0.04 mg
Cobalamin (vitamin B_{12})	0.04 mg
$Na_2SiO_3 \cdot 9H_2O$	57 mg

pH 6.9

TABLE 6.4
DY-III Modified Medium Composition

Reagents	**Per Liter**
$MgSO_4 \cdot 7H_2O$	50 mg
KCl	3 mg
NH_4Cl	2.68 mg
$NaNO_3$	20 mg
H_3BO_3	0.8 mg
Na_2 EDTA $\cdot 2H_2O$	8 mg
$Na_2SiO_3 \cdot 9H_2O$	14 mg
$FeCl_3 \cdot 6H_2O$	1 mg
$CaCl_2$	75 mg
MES buffer	200 mg
Microelement stock solution	1 mL
Vitamin solution	1 mL
Microelement Stock Solution	**Per Liter**
$MnCl_2 \cdot 4H_2O$	200 mg
$ZnSO_4 \cdot 7H_2O$	40 mg
$CoCl_2 \cdot 6H_2O$	8 mg
$Na_2MoO_4 \cdot 6H_2O$	20 mg
$Na_3VO_4 \cdot nH_2O$	2 mg
H_2SeO_3	2 mg
Vitamin Solution	**Per Liter**
Biotin (vitamin B_7)	0.5 μg
Thiamine HCl (vitamin B_1)	100 mg
Cobalamin (vitamin B_{12})	0.5 mg
pH 6.7	

TABLE 6.5
Aaronson's Medium Composition

Reagents	**Per Liter**
NH_4Cl	0.5 g
KH_2PO_4	0.3 g
$MgSO_4 \cdot 7H_2O$	1.0 g
$MgCO_3$	0.4 g
$C_6H_9NO_6$ (nitrilotriacetic acid)	0.2 g
$CaCO_3$	0.05 g
$C_5H_9NO_4$ (glutamic acid)	3.0 g
Glucose	10.0 g
Arginine	0.4 g
Hystidine monocloride	0.4 g
Biotin (vitamin B_7)	0.00001 g
Thiamine HCl (vitamin B_1)	0.001 g
Microelement stock solution	10 mL
Microelement Stock Solution	**Per Liter**
$Fe(NH_4)_2(SO_4)_2 \cdot 6H_2O$	0.5 g
H_3BO_3	0.025
$MnSO4 \cdot H_2O$	0.125 g
$CoSO_4 \cdot 7H_2O$	0.025 g
$CuSO_4 \cdot 5H_2O$	0.020 g
$ZnSO_4 \cdot H_2O$	0.25 g
$(NH_4)_6Mo_7O_{24} \cdot 4H_2O$	0.0125 g
$Na_3VO_4 \cdot 16H_2O$	0.025 g
pH 5.0	

TABLE 6.6
Cramer and Myers Modified Medium Composition

Reagents	Per Liter
$(NH_4)_2HPO_4$	1 g
KH_2PO_4	1 g
$MgSO_4 \cdot 7H_2O$	0.2 g
$CaCl_2$	0.02 g
$Na_3C_6H_5O_7 \cdot 2H_2O$ (sodium citrate)	0.8 g
$Fe_2(SO_4)_3 \cdot nH_2O$	3 mg
$MnCl_2 \cdot 4H_2O$	1.8 mg
$CoSO_4 \cdot 7H_2O$	1.5 mg
$ZnSO_4 \cdot 7H_2O$	0.4 mg
$Na_2MoO_4 \cdot 2H_2O$	0.2 mg
$CuSO_4 \cdot 5H_2O$	0.02 mg
H_3BO_3	2.48 mg
Carbon Sources (Choose One)	
$C_6H_{12}O_6$ (glucose)[a]	10 g
$C_4H_6O_4$ (succinic acid)[a]	5 g
$C_5H_9NO_4$ (glutammic acid)[a]	5 g
$C_2H_3O_2Na \cdot 5H_2O$ (sodium acetate)[b]	1.64 g
Thiamine HCl (vitamin B_1)	0.5 mg
Cobalamin (vitamin B_{12})	0.02 mg

[a] pH 3.4
[b] pH 6.8

TABLE 6.7
Sueoka's Medium Composition

Reagents	**Per Liter**
Beijerinck's solution	5 mL
Phosphate solution	5 mL
Hutner's trace elements	1 mL
Beijerinck's Solution	**Per Liter**
NH_4Cl	100 g
$MgSO_4 \cdot 7H_2O$	4 g
$CaCl_2 \cdot 2H_2O$	2 g
Phosphate Solution	**Per Liter**
KH_2PO_4	144 g
K_2HPO_4	288 g
Hutner's Trace Elements	**Per Liter**
H_3BO_3	11.4 g
$MnCl_2 \cdot 4H_2O$	5.06 g
Na_2-EDTA	50 g
$CuSO_4 \cdot 5H_2O$	1.57 g
$ZnSO_4 \cdot H_2O$	22 g
$CoCl_2 \cdot 6H_2O$	1.61 g
$FeSO_4 \cdot 7H_2O$	4.99 g
$(NH_4)_6Mo_7O_{24} \cdot 4H_2O$	1.10 g

pH 6.8

TABLE 6.8
Bold Basal Medium Composition

Reagents	**Per Liter**
KH_2PO_4	175 mg
$CaCl_2 \cdot 2H_2O$	25 mg
$MgSO_4 \cdot 7H_2O$	75 mg
$NaNO_3$	250 mg
K_2HPO_4	75 mg
NaCl	25 mg
H_3BO_3	11.42 mg
Microelement stock solution	1 mL
Solution 1	1 mL
Solution 2	1 mL
Microelement Stock Solution	**Per Liter**
$ZnSO_4 \cdot 7H_2O$	8.82 g
$MnCl_2 \cdot 4H_2O$	1.44 g
MoO_3	0.71 g
$CuSO_4 \cdot 5H_2O$	1.57 g
$Co(NO_3)_2 \cdot 6H_2O$	0.49 g
Solution 1	**Per Liter**
Na_2–EDTA	50 g
KOH	3.1 g
Solution 2	**Per Liter**
$FeSO_4$	4.98 g
H_2SO_4 (conc.)	1 mL

pH 6.8

TABLE 6.9
MES–Volvox Medium Composition

Reagents	Per Liter
MES buffer	1.95 g
$Ca(NO_3)_2 \cdot 4H_2O$	117.8 mg
$Na_2C_3H_9O_6P \cdot 5H_2O$ (sodium glycerolphosphate)	60 mg
$MgSO_4 \cdot 7H_2O$	40 mg
KCl	50 mg
NH_4Cl	26.7 mg
Biotin (vitamin B_7)	0.0025 mg
Cobalamin (vitamin B_{12})	0.0015 mg
Microelement stock solution	6 mL
Microelement Stock Solution	**Per Liter**
Na_2–EDTA	750 mg
$FeCl_3 \cdot 6H_2O$	97 mg
$MnCl_2 \cdot 4H_2O$	41 mg
$ZnCl_2$	5 mg
$CoCl_2 \cdot 6H_2O$	2 mg
$Na_2MoO_4 \cdot 2H_2O$	4 mg

pH 6.7

TABLE 6.10
Jaworski's Medium (JM) Composition

Reagents	Per Liter
$MgSO_4 \cdot 7H_2O$	50 mg
$Ca(NO_3)_2 \cdot 4H_2O$	20 mg
$NaNO_3$	80 mg
$Na_2HPO_4 \cdot 12H_2O$	36 mg
$NaHCO_3$	15.9 mg
KH_2PO_4	12.8 mg
H_3BO_3	2.48 mg
FeNa-EDTA	2.25 mg
Na_2-EDTA	2.25 mg
$MnCl_2 \cdot 4H_2O$	1.39 mg
$(NH_4)_6Mo_7O_{24} \cdot 4H_2O$	1 mg
Cobalamin (vitamin B_{12})	0.04 mg
Tiamina HCl (vitamin B_1)	0.04 mg
Biotin (vitamin H)	0.04 mg

pH 6.5

TABLE 6.11
CY-II *Cyanophora paradoxa* Medium Composition

Reagents	Per Liter
$NH_4C_2O_3H_3$	200 mg
$FeCl_3$	1 mg
$CaCl_2 \cdot 2H_2O$	50 mg
KCl	30 mg
$MgSO_4 \cdot 7H_2O$	100 mg
$Na_2C_3H_9O_6P \cdot 5H_2O$ (sodium glycerolphosphate)	50 mg
Tris-base (pH 7.2)	333 mg
Cobalamin (vitamin B_{12})	1 µg
PII metal mix	10 mL
Vitamine solution	5 mL
PII Metal Mix	**Per Liter**
Na_2-EDTA $\cdot 2H_2O$	10 mg
$MnCl_2 \cdot H_2O$	0.4 mg
$ZnSO_4 \cdot 7H_2O$	0.05 mg
$FeCl_3 \cdot 6H_2O$	0.1 mg
H_3BO_3	2 mg
$CoCl_2 \cdot 7H_2O$	0.01 mg
Vitamine Solution	**Per Liter**
Biotin (vitamin B_7)	1 µg
Thiamine HCl (vitamin B_1)	0.5 mg
Folic acid	2 µg
Nicotin acid	0.1 mg
Calcium pantothenate	0.1 mg
PABA (*para*-amino benzoic acid)	10 µg
Thymine	3 mg
Inositol	5 mg
pH 7.6	

TABLE 6.12
Zarrouk's Medium Composition

Reagents	**Per Liter**
$NaHCO_3$	16.8 g
K_2HPO_4	0.5 g
$NaNO_3$	2.5 g
K_2SO_4	1.0 g
NaCl	1.0 g
$MgSO_4 \cdot 7H_2O$	0.2 g
$CaCl_2 \cdot 2H_2O$	0.04 g
$Fe_2SO_4 \cdot 7H_2O$	0.01 g
EDTA	0.08 g
Microelement stock solution	1 mL
Microelement Stock Solution	**Per Liter**
H_3BO_3	2.86 g
$MnCl_2 \cdot 4H_2O$	1.81 g
$ZnSO_4 \cdot 4H_2O$	0.222 g
Na_2MoO_4	0.0177 g
$CuSO_4 \cdot 5H_2O$	0.079 g
pH 9	

investigator. Many media are only major variations of some widely applicable, and often equally effective. Whatever the choice, a medium should be as simple as possible in composition and preparation.

Media for the culture of marine phytoplankton consist of a seawater base (natural or artificial), which may be supplemented by various substances essential for microalgal growth, including nutrients, trace metals and chelators, vitamins, soil extract, and buffer compounds.

The salinity of the seawater base should first be checked (30–35‰ for marine phytoplankton), and any necessary adjustments (addition of fresh water/evaporation) made before addition of enrichments.

Seawater, stock solutions of enrichments, and the final media must be sterile in order to prevent (or more realistically minimize) biological contamination of unialgal cultures. Autoclaving is a process that has many effects on seawater and its constituents, potentially altering or destroying inhibitory organic compounds, as well as beneficial organic molecules. Because of the steam atmosphere in an autoclave, CO_2 is driven out of the seawater and the pH is raised to about 10, a level that can cause precipitation of the iron and phosphate added in the medium. Some of this precipitate may disappear upon re-equilibration of CO_2 on cooling, but both the reduced iron and phosphate levels and the direct physical effect of the precipitate may limit algal growth. The presence of ethylenediaminetetraacetic acid (EDTA) and the use of organic phosphate may reduce precipitation effects. Addition of 5% or more of distilled water may also help in reducing precipitation (but may affect final salinity). The best solution, however, if media are autoclaved, is to sterilize iron and phosphate (or even all media additions) separately and add them aseptically afterwards.

Some marine microalgae grow well on solid substrate. A 3% high-grade agar can be used for the solid substrate. The agar and culture medium should not be autoclaved together, because toxic breakdown products can be generated. The best procedure is to autoclave 30% agar in deionized water in one container and nine times as much seawater base in another. After removing from the autoclave, sterile nutrients are added aseptically to the water, which is then mixed with the molten agar. After mixing, the warm fluid is poured into sterile Petri dishes, where it solidifies when it cools. The plate is inoculated by placing a drop of water containing the algae on the surface of the agar, and streaking with a sterile implement. The plates are then maintained under standard culture conditions.

SEAWATER BASE

The quality of water used in media preparation is very important. Natural seawater can be collected near shore, but its salinity and quality is often quite variable and unpredictable, particularly in temperate and polar regions (due to anthropogenic pollution, toxic metabolites released by algal blooms in coastal waters). The quality of coastal water may be improved by ageing for a few months at 4°C (allowing bacteria degradation), by autoclaving (heat may denature inhibitory substances), or by filtering through acid-washed charcoal (which absorbs toxic organic compounds). Most coastal waters contain significant quantities of inorganic and organic particulate matter, and therefore must be filtered before use (using, e.g., Whatman no. 1 filter paper).

The low biomass and continual depletion of many trace elements from the surface waters of the open ocean by biogeochemical processes makes this water much cleaner, and therefore preferable for culturing purposes. Seawater can be stored in polyethylene carboys, in cool dark conditions.

Artificial seawater, made by mixing various salts with deionized water, has the advantage of being entirely defined from the chemical point of view, but it is very laborious to prepare and often do not support satisfactory algal growth. Trace contaminants in the salts used are at rather high concentrations in artificial seawater because so much salt must be added to achieve the salinity of full-strength seawater. Commercial preparations are available which consists of synthetic mixes of the major salts present in natural sea water, such as sea salts produced by Tropic Marine® in Germany and by Instant Ocean in Virgina (USA).

NUTRIENTS, TRACE METALS, AND CHELATORS

The term "nutrient" is colloquially applied to a chemical required in relatively large quantities, but can be used for any element or compound necessary for algal growth.

The average concentrations of constituents of potential biological importance found in typical seawater is shown in Table 6.13. These nutrients can be divided into three groups, I, II, and III, with decreasing concentration.

- *Group I*: concentrations of these constituents exhibit essentially no variation in seawater, and high algal biomass cannot deplete them in culture media. These constituents do not,

TABLE 6.13
Average Concentration of Typical Seawater Constituents

Element	Average Molar Concentration (Range in Brackets)
	Group I
Na^+	4.7×10^{-1}
K^+	1.02×10^{-2}
Mg^{2+}	5.3×10^{-2}
Ca^{2+}	1.03×10^{-2}
Cl^-	5.5×10^{-1}
SO_4^{2-}	2.8×10^{-2}
HCO_3^-	2.3×10^{-3}
BO_3^{3-}	4.2×10^{-4}
	Group II
Br^-	8.4×10^{-4}
F^-	6.8×10^{-5}
IO_3^-	4.4×10^{-7}
Li^+	2.5×10^{-5}
Rb^+	1.4×10^{-6}
Sr^{2+}	8.7×10^{-5}
Ba^{2+}	1×10^{-7}
MoO_4^{2-}	1.1×10^{-7}
VO_4^{3-}	2.3×10^{-8}
CrO_4^{2-}	4×10^{-9}
AsO_4^{3-}	2.3×10^{-8}
SeO_4^{2-}	1.7×10^{-9}
	Group III
NO_3^-	3×10^{-5} (10^{-8} to 4.5×10^{-5})
PO_4^{3-}	2.3×10^{-6} (10^{-7} to 3.5×10^{-6})
Fe^{3+}	1×10^{-9} (10^{-10} to 10^{-7})
Zn^{2+}	6×10^{-9} (5×10^{-11} to 10^{-7})
Mn^{2+}	5×10^{-10} (2×10^{-10} to 10^{-6})
Cu^{2+}	4×10^{-9} (5×10^{-10} to 6×10^{-9})
Co^{2+}	2×10^{-11} (10^{-11} to 10^{-10})
SiO_4^{4-}	1×10^{-4} (10^{-7} to 1.8×10^{-4})
Ni^{2+}	8×10^{-9} (2×10^{-9} to 1.2×10^{-8})

therefore, have to be added to culture media using natural seawater, but do need to be added to deionized water when making artificial seawater media.

- *Group II*: these elements also have quite constant concentrations in seawater or vary by a factor <5. Because microalgal biomass cannot deplete their concentrations significantly, they also do not need to be added to natural seawater media. Standard artificial media (and some natural seawater media) add molybdenum (as molybdate), an essential nutrient for algae, selenium (as selenite), which has been demonstrated to be needed by some algae, as well as strontium, bromide, and fluoride, all of which occur at relatively high concentrations in seawater, but none of which has been shown to be essential for microalgal growth.
- *Group III*: microalgae need all these elements (silicon is needed only by diatoms and some chrysophytes, and nickel is only known to be needed to form urease when algae are using urea as a nitrogen source). These nutrients are generally present at low concentrations in natural seawater, and since microalgae take up substantial amounts of them, concentrations vary widely (generally by a factor of 10–1000). All of these nutrients (except silicon and nickel in some circumstances) generally need to be added to culture media in order to generate significant microalgal biomass.

Nitrate is the nitrogen source most often used in culture media, but ammonium can also be used, and indeed it is the preferential form for many algae since it does not have to be reduced prior to amino acid synthesis, the point of primary intracellular nitrogen assimilation into the organic linkage. Ammonium concentrations >25 μM are, however, often reported to be toxic to phytoplankton, hence, ammonium concentrations should be kept low.

Inorganic (ortho)phosphate, the phosphorus form preferentially used by microalgae, is most often added to culture media, but organic (glycero)phosphate is sometimes used, particularly when precipitation of phosphate is anticipated (e.g., when nutrients are autoclaved in the culture media rather than separately). Most microalgae are capable of producing cell-surface phosphatases that allow them to utilize this and other forms of organic phosphate as a phosphorus source.

The trace metals which are essential for microalgal growth are incorporated into essential organic molecules, particularly a variety of coenzyme factors that enter into photosynthetic reactions. The concentrations (or more accurately the biologically available concentrations) of Fe, Mn, Zn, Cu, and Co (and sometimes Mo and Se) in natural waters may be limiting factors to algal growth. Little is known about the complex relationships between chemical speciation of metals and biological availability. It is thought that molecules complexing with metals (chelators) influence the availability of these elements. Chelators act as trace metal buffers, maintaining constant concentrations of free ionic metal. It is the free ionic metal, not the chelated metal, which influences microalgae, either as a nutrient or as a toxin. Without proper chelation, some metals (such as Cu) are often present at toxic concentrations, and others (such as Fe) tend to precipitate and become unavailable to phytoplankton. In natural seawater, dissolved organic molecules (generally present at concentrations of 1–10 mg L^{-1}) act as chelators. The most widely used chelator in culture media additions is EDTA, which must be present at high concentrations since it mostly complexes with Ca^{2+} and Mg^{2+}, present in large amounts in seawater. EDTA may have an additional benefit of reducing precipitation during autoclaving. High concentrations have, however, occasionally been reported to be toxic to microalgae. As an alternative, the organic chelator citrate is sometimes utilized, having the advantage of being less influenced by Ca^{2+} and Mg^{2+}. The ratio of chelator:metal in culture medium ranges from 1:1 in f/2 to 10:1 in K medium. High ratios may result in metal deficiencies for coastal phytoplankton (i.e., too much metal is complexed), and many media therefore use intermediate ratios.

In today's aerobic ocean, iron is present in the oxidized form as various ferric hydroxides and thus it is rather insoluble in seawater. Although concentrations of nitrogen, phosphorus, zinc, and manganese in deep water are similar to plankton elemental composition, there is proportionally 20

times less iron in deep water than is apparently needed, leading to the suggestion that iron may be the ultimate geochemically limiting nutrient to phytoplankton in the ocean. Very little is known about iron in seawater or phytoplankton uptake mechanisms due to the complex chemistry of the element. Iron availability for microalgal uptake seems to be largely dependent on levels of chelation. It is highly recommended that iron be added as the chemically prepared chelated iron salt of EDTA rather than as iron chloride or other iron salts; the formation of iron chelates is relatively slow, and iron hydroxides will form first in seawater, leading to precipitation of much of the iron in the culture medium.

Apparently as a result of the extreme scarcity of copper in anaerobic waters, copper was not utilized by organisms until the earth became aerobic and copper increased in abundance. Consequently, copper does not seem to be an obligate requirement, algae either not needing it or needing in such a small amount that free ionic copper concentrations in natural seawater are sufficient to maintain maximum growth rates. Copper may indeed be toxic, particularly to more primitive algae, and hence copper, if added to culture media at all, should be kept at low concentrations.

The provision of manganese, zinc, and cobalt in culture medium should not be problematical since even fairly high concentrations are not known to be toxic to algae.

VITAMINS

Many planktonic algae are auxotrophic for one or more vitamins, that is, they lack one or more vitamin biosynthetic pathways and therefore must gather essential vitamins from the environment. Possession of a biosynthetic pathway means independence, at the cost of synthesis. A survey conducted on more than 300 algal species has shown that more than half required cobalamin (vitamin B_{12}); about 20% of microalgal species need thiamine (vitamin B_1), and <5% need biotin (vitamin B_7) (Figure 6.2).

Cobalamin (vitamin B_{12}) is a cobalt-containing tetrapyrrole related to chlorophyll and heme. Cobalamin acts as a cofactor for enzymes that catalyze either rearrangement-reduction reactions or methyl-transfer reactions. In bacteria, there are more than 20 cobalamin-dependent enzymes,

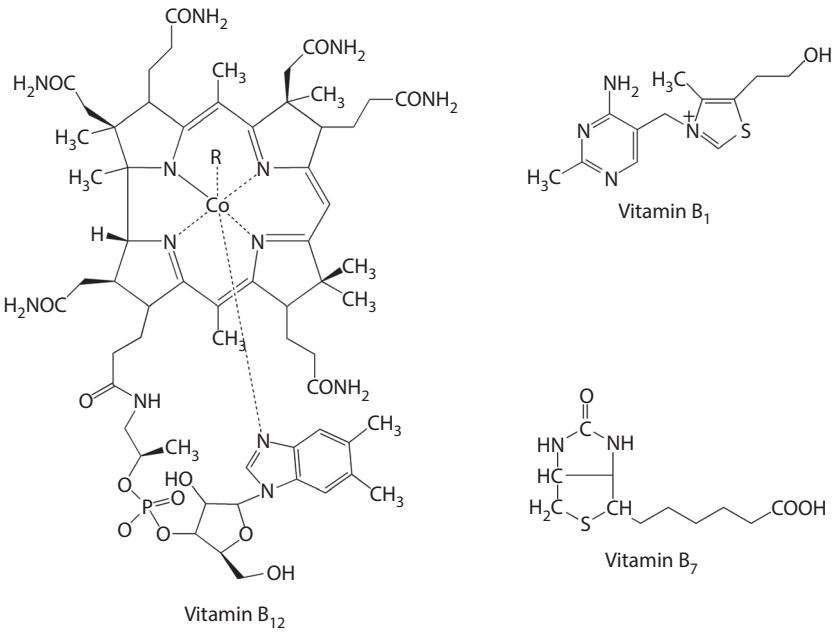

FIGURE 6.2 Structure of cobalamin (vitamin B_{12}), thiamine (vitamin B_1), and biotin (vitamin B_7).

including those important for methanogenesis, but in eukaryotes there are many fewer. Higher plants have no cobalamin-dependent enzymes and so neither utilize nor synthesize cobalamin.

Cobalamin appears to be important in transferring methyl groups and methylating toxic elements such as arsenic, mercury, tin, thallium, platinum, gold, and tellurium.

Biotin (vitamin B_7) is a cofactor for several essential carboxylase enzymes, including acetyl coenzyme A (CoA) carboxylase, which is involved in fatty acid synthesis, and so is universally required. The molecule consists of an imidazole ring fused to a sulfur-containing tetrahydrothiophene ring with a fatty acid side chain. In eubacteria, the first precursor for biotin synthesis is pimeloyl-CoA but the source of this differs among different species.

Like biotin, thiamine (vitamin B_1) also plays a pivotal role in intermediary carbon metabolism. The active form of the vitamin is thiamine pyrophosphate (TPP), which is essential for all organisms. The cofactor associates with a number of enzymes involved in primary carbohydrate and branched-chain amino acid metabolism, including pyruvate dehydrogenase, transketolase, α-ketoacid decarboxylase, and α-ketoacid oxidase. Thiamine consists of a thiazole and a pyrimidine moiety, which are produced in separate branches of the biosynthetic pathway before being coupled together to produce thiamine phosphate. This is then further phosphorylated to produce the active cofactor TPP.

It is recommended that these vitamins are routinely added to seawater media. No other vitamins have ever been demonstrated to be required by any photosynthetic microalga.

SOIL EXTRACT

Soil extract has historically been an important component of culture media. It is prepared by heating, boiling, or autoclaving a 5–30% slurry of soil in freshwater or seawater and subsequently filtering out the soil. The solution provides macronutrients, micronutrients, vitamins, and trace metal chelators in undefined quantities, each batch being different, and hence having unpredictable effects on microalgae. With increasing understanding of the importance of various constituents of culture media, soil extract is less frequently used.

BUFFERS

The control of pH in culture media is important since certain algae grow only within narrowly defined pH ranges and also to prevent the formation of precipitates. Except under unusual conditions, the pH of natural seawater is around 8. Because of the large buffering capacity of natural seawater due to its bicarbonate buffering system (refer to Chapter 5), it is quite easy to maintain the pH of marine culture media. The buffer system is overwhelmed only during autoclaving, when high temperatures drive CO_2 out of solution and hence cause a shift in the bicarbonate buffer system and an increase in pH, or in very dense cultures of microalgae, when enough CO_2 is taken up to produce a similar effect.

As culture medium cools after autoclaving, CO_2 reenters solution from the atmosphere, but certain measures must be taken if normal pH is not fully restored:

- the pH of seawater may be lowered prior to autoclaving (adjustment to pH 7–7.5 with 1 M HCl) to compensate for subsequent increases;
- certain media recipes include additions of extra buffer, either as bicarbonate, Tris (Tris-hydroxymethyl-aminomethane), or glycylglycine to supplement the natural buffering system. Tris may also act as a Cu buffer, but has occasionally been cited for its toxic properties to microalgae such as *Haematococcus* sp. Glycylglycine is rapidly metabolized by bacteria and hence can only be used with axenic cultures. These additions are generally not necessary if media are filter-sterilized, unless very high cell densities are expected;
- the problem of CO_2 depletion in dense cultures may be reduced by having a large surface area of media exposed to the atmosphere relative to the volume of the culture, or

by bubbling with either air (CO_2 concentration 0.03%) or air with increased CO_2 concentrations (0.5–5%). Unless there is a large amount of biomass taking up the CO_2, the higher concentrations could actually cause a significant decline in pH. When bubbling is employed, the gas must first pass through an in line 0.2-μm filter unit (e.g., Millipore Millex GS) to maintain sterile conditions. For many microalgal species, aeration is not an option since the physical disturbance may inhibit growth or kill cells.

Some of the most commonly used marine media, defined and undefined, are listed in Tables 6.14 through 6.21. Table 6.22 indicates the algal classes that have been successfully cultured in the media included in this chapter.

For a full range of possible media, refer to the catalog of strains from culture collections present all over the world, such as:

- SAG (Experimentelle Phykologie und Sammlung von Algenkulturen, University of Gottigen, http://www.epsag.uni-goettingen.de/).
- UTEX (Culture Collection of Algae at the University of Texas at Austin, http://www.utex.org).
- CCAP (Culture Collection of Algae and Protozoa, Argyll, Scotland, http://www.sams.ac.uk/ccap).
- UTCC (University of Toronto Culture Collection of Algae and Cyanobacteria, http://www.phycol.ca/).
- CCMP (The Provasoli-Guillard National Center for Culture of Marine Phytoplankton, Maine, https://ncma.bigelow.org/).
- CSIRO (CSIRO Collection of Living Microalgae, Tasmania, http://www.csiro.au/Organisation-Structure/National-Facilities/Australian-National-Algae-Culture-Collection.aspx).
- PCC (Pasteur Culture Collection of Cyanobacteria, http://www.pasteur.fr/recherche/banques/PCC/).

STERILIZATION OF CULTURE MATERIALS

All vessels used for culture purpose should be scrubbed (abrasive brushes not appropriate for most plastics) and soaked with warm detergent (not domestic detergents, which leave a residual film on culture ware, but phosphate-free laboratory detergent), then rinsed extensively with tap water. After soaking in 10% HCl for 1 day–1 week (not routinely necessary, but particularly important for new glass and polycarbonate material), vessels should be rinsed extensively with distilled and finally bidistilled water, and left inverted to dry in a clean, dust-free place, or in an oven.

Sterilization can be defined as a process which ensures total inactivation of microbial life and should not be confused with disinfection, which is defined as an arbitrary reduction of bacterial numbers. The primary purpose of sterilization is to prevent contamination by unwanted organisms, but it may also serve to eliminate unwanted chemicals. Sterilization can be obtained by means of several methods, the choice depending not only on the purpose and the material used, either empty glassware/plasticware or medium-containing vessels, but also on the facilities available in a laboratory.

Several methods are available for sterilization of material, some of which can be used also for growth media:

- Gas such as ethylene oxide, EtO, finds the best application on heat-sensitive equipment on which steam autoclaving (sterilization with heat) cannot be performed. EtO sterilizes by alkylation, it substitutes for hydrogen atoms on molecules such as proteins and DNA,

TABLE 6.14
Walne's Medium Composition

Reagents	Per Liter Seawater
Solution A	1.0 mL
Solution C	0.1 mL
Solution D (to add for diatoms)	2.0 mL
Solution A	**Per Liter**
$FeCl_3 \cdot 6H_2O$	1.3 g
$MnCl_2 \cdot 4H_2O$	0.4 g
H_3BO_3	33.6 g
Na_2-EDTA	45.0 g
$NaH_2PO_4 \cdot 2H_2O$	20.0 g
$NaNO_3$	100.0 g
Solution B	1 mL
Solution B	**Per 100 mL**
$ZnCl_2$	2.1 g
$CoCl_2 \cdot 6H_2O$	2.0 g
$(NH_4)_6Mo_7O_{24} \cdot 4H_2O$	0.9 g
$CuSO_4 \cdot 5H_2O$	2.0 g
Concentrated HCl	10 mL
Solution C	**Per 200 mL**
Thiamine HCl (vitamin B_1)	0.2 g
Cobalamin (vitamin B_{12})	10 mg
Solution D	**Per Liter**
$Na_2SiO_3 \cdot 5H_2O$	40.0 g

TABLE 6.15
ASN-III Medium Composition

Reagents	Per Liter Seawater
NaCl	25 g
$MgCl_2 \cdot 6H_2O$	2 g
$MgSO_4 \cdot 7H_2O$	3.5 g
$NaNO_3$	0.75 g
$K_2HPO_4 \cdot 3H_2O$	0.02 g
KCl	0.5 g
$CaCl_2 \cdot 2H_2O$	0.5 g
$C_6H_8O_7$ (citric acid)	0.003 g
$C_6H_8O_7 \cdot x\text{Fe} \cdot y\text{NH}_3$ (ammonium ferric citrate)	0.003 g
Na_2Mg-EDTA	0.0005 g
Na_2CO_3	0.02 g
Microelement stock solution	1 mL
Microelement Stock Solution	**Per Liter**
H_3BO_3	2.860 g
$MnCl_2 \cdot 4H_2O$	1.810 g
$ZnSO_4 \cdot 7H_2O$	0.222 g
$Na_2MoO_4 \cdot 2H_2O$	0.390 g
$CuSO_4 \cdot 5H_2O$	0.079 g
$Co(NO_3)_2 \cdot 6H_2O$	0.0494 g

pH 7.5

TABLE 6.16
CHU-11 Medium Composition

Reagents	Per Liter Seawater
$MgSO_4 \cdot 7H_2O$	0.075 g
$CaCl_2 \cdot 2H_2O$	0.036 g
$NaNO_3$	1.5 g
$K_2HPO_4 \cdot 3H_2O$	0.04 g
Na_2CO_3	0.02 g
$Na_2SiO_3 \cdot 9H_2O$	0.58 g
$C_6H_8O_7$ (citric acid)	0.006 g
$C_6H_8O_7 \cdot x\text{Fe} \cdot y\text{NH}_3$ (Ammonium ferric citrate)	0.006 g
Na_2Mg-EDTA	0.001 g
Microelement stock solution	1 mL
Microelement Stock Solution	**Per Liter**
H_3BO_3	0.5 g
$MnCl_2 \cdot 4H_2O$	2 g
$Zn(NO_3)_2 \cdot 6H_2O$	0.5 g
$Na_2MoO_4 \cdot 2H_2O$	0.025 g
$CuCl_2 \cdot 2H_2O$	0.025 g
$Co(NO_3)_2 \cdot 6H_2O$	0.025 g
$VOSO_4 \cdot 6H_2O$	0.025 g
HCl 1 M	3 mL
pH 7.5	

TABLE 6.17
PCR-S11 Medium Composition

Reagents	Per Liter Seawater
$(NH_4)_2SO_4$	2.68 mg
Na_2-EDTA/$FeCl_3$	8 mg
Na_2PO_4 (pH 7.5)	14 mg
HEPES-NaOH (pH 7.5)	200 mg
Microelement stock solution	0.5 mL
Microelement Stock Solution	**Per Liter**
H_3BO_3	18.549 mg
$MnSO_4 \cdot H_2O$	10.140 mg
$ZnSO_4 \cdot 7H_2O$	1.725 mg
$(NH_4)_6Mo_7O_{24} \cdot 4H_2O$	0.494 mg
$CuSO_4 \cdot 5H_2O$	0.749 mg
$Co(NO_3)_2 \cdot 6H_2O$	0.873 mg
$VSO_5 \cdot 5H_2O$	0.098 mg
$Na_2WO_4 \cdot 2H_2O$	0.198 mg
KBr	0.714 mg
KI	0.498 mg
$Cd(NO_3)_2 \cdot 6H_2O$	0.925 mg
$NiCl_2 \cdot 6H_2O$	0.713 mg
$Cr(NO_3)_3 \cdot 9H_2O$	0.240 mg
SeO_2	0.333 mg
$KAl(SO_4)_2 \cdot 12H_2O$	2.846 mg
Cobalamin (vitamin B_{12})	10 µg
pH 7.5	

TABLE 6.18
f/2 Medium Composition

Reagents	Per Liter Seawater
$NaNO_3$	0.075 g
$NaH_2PO4 \cdot H_2O$	0.005 g
Microelement stock solution	1 mL
Vitamin solution	1 mL
Microelement Stock Solution	**Per Liter**
$FeCl_3 \cdot 6H_2O$	3.150 g
Na_2-EDTA	4.160 g
$MnCl_2 \cdot 4H_2O$	0.180 g
$CoCl_2 \cdot 6H_2O$	0.010 g
$CuSO_4 \cdot 5H_2O$	0.010 g
$ZnSO_4 \cdot H_2O$	0.022 g
$Na_2MoO_4 \cdot 2H_2O$	0.006 g
Vitamin Solution	**Per Liter**
Biotin (vitamin B_7)	0.5 mg
Thiamine HCl (vitamin B_1)	100 mg
Cobalamin (vitamin B_{12})	0.5 mg

pH 8.0 adjust with 1 M NAOH or HCl

TABLE 6.19
K Medium Composition

Reagents	Per Liter Seawater
$NaNO_3$	75 mg
$Na_2C_3H_9O_6P \cdot 5H_2O$ (sodium glycerolphosphate)	2.16 mg
NH_4Cl	2.67 mg
Tris-base (pH 7.2)	121.1 mg
Microelement stock solution	1 mL
Vitamin solution	1 mL
Microelement Stock Solution	**Per Liter**
FeNa-EDTA	4.3 g
Na_2-EDTA $\cdot 2H_2O$	37.22 g
$CuSO_4 \cdot 5H_2O$	4.9 mg
$MnCl_2 \cdot 4H_2O$	178.2 mg
$ZnSO_4 \cdot 7H_2O$	22 mg
$Na_2MoO_4 \cdot 2H_2O$	6.3 g
H_2SeO_3	1.29 µg
$FeCl_3 \cdot 6H_2O$	3.15 g
$CoCl_2 \cdot 6H_2O$	11.9 mg
Vitamin Solution	**Per Liter**
Biotin (vitamin B_7)	0.1 mg
Thiamine HCl (vitamin B_1)	200 mg
Cobalamin (vitamin B_{12})	1 mg

pH 7.2

TABLE 6.20
Johnson's Medium Composition

Reagents	Per Liter Seawater
$Mg_2Cl_2 \cdot 6H_2O$	1.5 g
$Mg_2SO_4 \cdot 7H_2O$	0.5 g
KCl	0.2 g
$CaCl_2$	0.2 g
KNO_3	1 g
$NaHCO_3$	0.043 g
KH_2PO_4	0.035 mg
$NH_4Mo_7O_{24} \cdot 4H_2O$	0.38 mg
$CuCl_2 \cdot 2H_2O$	0.041 mg
$MnCl_2 \cdot 4H_2O$	0.41 mg
$ZnCl_2$	0.041 mg
VOCl2	0.041 mg
$FeCl_3 \cdot 6H_2O$	2.44 mg
$CoCl_2 \cdot 6H_2O$	0.015 mg
H_3BO_3	0.61 mg
EDTA	1.89 mg
Tris-base (pH 7.5)	2.45 g

pH 7.5

TABLE 6.21
ESAW Medium Composition

Reagents	Per Liter
NaCl	21.19 g
Na_2SO_4	3.55 g
KCl	0.599 g
Na_2HCO_3	0.174 g
KBr	0.0863 g
H_3BO_3	0.023 g
NaF	0.0028 g
$MgCl_2 \cdot 6H_2O$	9.592 g
$CaCl_2 \cdot 2H_2O$	1.344
$SrCl_2$	0.0218
$NaNO_3$	46.7 mg
$NaH_2PO_4 \cdot H_2O$	3.09 mg
$Na_2SiO_3 \cdot 9H_2O$	30 mg
Metal Stock I	1 mL
Metal Stock II	1 mL
Vitamin solution	1 mL
Metal Stock I	**Per Liter**
Na_2-EDTA $\cdot 2H_2O$	3.09 g
$FeCl_3 \cdot 6H_2O$	1.77 g
Metal Stock II	**Per Liter**
Na_2- EDTA $\cdot 2H_2O$	2.44 g
$ZnSO_4 \cdot 7H_2O$	0.073 g
$CoSO_4 \cdot 7H_2O$	0.016 g
$MnSO_4 \cdot 4H_2O$	0.54 g
$Na_2MoO_4 \cdot 2H_2O$	1.48 mg
Na_2SeO_3	0.173 mg
$NiCl_2 \cdot 6H_2O$	1.49 mg
Vitamin Solution	**Per Liter**
Biotin (vitamin B_7)	1 mg
Thiamine HCl (vitamin B_1)	100 mg
Cobalamin (vitamin B_{12})	2 mg

pH 8.2

TABLE 6.22
Media Listed in This Chapter and the Corresponding Cultured Algal Groups

Medium	Group Cultured
BG11 Medium	Freshwater and soil Cyanophyceae
Diatom Medium	Freshwater Bacillariophyceae
DY-III Medium	Freshwater Chrysophyceae
Aaronson's Medium	*Ochromonas* sp.
Cramer and Myers Medium	Euglenophyceae
Sueoka's Medium	Freshwater Chlorophyceae
Bold Basal Medium	Broad spectrum medium for freshwater Chlorophyceae, Xantophyceae, Chrysophyceae, Cyanophyceae
MES-Volvox Medium	Broad spectrum medium for freshwater algae
Jaworski's Medium (JM)	Broad spectrum medium for freshwater algae
CY-II- Medium	*Cyanophora paradoxa* (Glaucophyceae)
Zarrouk's Medium	Mass production of *Arthrospira* sp.
Walne's Medium	Broad spectrum medium for marine algae (especially designed for mass culture)
ASN-III Medium	Marine Cyanobacteria
CHU-11 Medium	Marine Cyanobacteria
PCR-S11 Medium	*Prochloron* (Cyanophyceae)
f/2 Medium	Broad spectrum medium for coastal algae
Johnson's Medium	Halophilic algae (e.g. Dunaliella sp.)
K Medium	Broad spectrum medium for oligotrophic marine algae
ESAW Medium	Broad spectrum medium for costal and open ocean algae

and, by attaching to these molecules and disrupting them, EtO stops these molecules' normal life-supporting functions. This method is widely used for the sterilization of medical devices, but it is not a routinely available technique for algology laboratories. Moreover, EtO is a potent carcinogen.

- Dry heat; some laboratory use dry heat to sterilize empty vessels, putting the material in an oven for at least 3–4 h at 160°C; however, only higher temperature (200–250°C) guarantee an effective result. Vessels are covered with aluminum foil to maintain sterility on removal from the oven. This procedure is suitable only for few materials that stand high temperatures, such as glass, Teflon, silicone, metal, cotton, etc.
- Autoclaving (moist heat) is the most widely used technique for sterilizing culture media and vessels and is the ultimate guarantee of sterility (including the destruction of viruses). A commercial autoclave is best, but pressure cookers of various sizes are also suitable. Sterility requires 15 min at 1–2 bar pressure and a temperature of 121°C in the entire volume of the liquid (i.e., longer times for larger volumes of liquid; approximately 10 min for 100 mL, 20 min for 2 L, 35 min for 5 L). Flasks containing media should be no more than half full and should be left partially open or plugged with cotton wool or covered with aluminum foil or paper, since for sterility the steam must penetrate the material. Autoclave steam may introduce chemical contaminants; empty glass and polycarbonate vessels should be autoclaved containing a small amount of bidistilled water that is poured out (thus diluting contaminants) under sterile conditions immediately prior to use. Vessels should never be closed, because of the risk of implosion, using cotton wool bungs, or leaving screw caps slightly open. Ensure the heating elements are covered with distilled water, and the escape valve should not be closed until a steady stream of steam is observed. After autoclaving, the

pressure release valve should not be opened until the temperature has cooled to below 80°C. Autoclave steam may contaminate the media (i.e., with trace metals from the autoclave tubing). Autoclaving also produces leaching of chemicals from the medium receptacle into the medium (silica from glass bottles, toxic chemicals from plastics). Autoclaving in well-used Teflon or polycarbonate vessels reduces leaching of trace contaminants.

- Pasteurization (heating to 90–95°C for 30 min) of media in Teflon or polycarbonate bottles is a potential alternative, reducing the problems of trace metal contamination and alteration of organic molecules inherent with autoclaving. Pasteurization does not, however, completely sterilize seawater containing media; it kills all eukaryotes and most bacteria, but some bacterial spores probably survive. Heating to 90–95°C for at least 30 min and cooling, repeated on two or more successive days (tyndallization) may improve sterilization efficiency; it is assumed that vegetative cells are killed by heat and heat-resistant spores will germinate in the following cool periods and be killed by subsequent heating.
- Ultraviolet radiation (240–280 nm) is not often used for culture materials, because very high intensities are needed to kill everything in a medium such as seawater (1200-W lamp, 2–4 h for culture media in quartz tubes). Such intense UV light necessarily alters and destroys the organic molecules in seawater and generates many long-lived free radicals and other toxic reactive chemical species. Therefore, seawater exposed to intense UV light must be stored for several days prior to use, to allow for the level of these highly reactive chemical species to decline.
- Sterile filtration is probably the best method of sterilizing certain media, especially seawater-based media, without altering their chemistry, as long as care is taken not to contaminate the seawater with a dirty filter apparatus. Sterilization efficiency is, however, to some extent, reduced compared with heat sterilization methods. Membrane filters of 0.2-µm porosity are generally considered to yield water free of bacteria, but not viruses. 0.1-µm filters can be used, but the time required for filtration of large volumes of culture media may be excessively long. The filtration unit must be sterile: for small volumes (<50 mL) presterilized single-use filter units for syringe filtration (e.g., Millipore Millex GS) can be used; for volumes up to 1 L reusable autoclavable self-assembly filter units (glass or polycarbonate) with 47-mm cellulose ester sterile membrane filters (e.g., Millipore HA) can be used with suction provided by a vacuum pump; for larger volumes, in-line systems with peristaltic pump and cartridge filters may be the best option. Filter units (particularly disposable plastic systems) and the membrane filters themselves can also leak toxic compounds into the filtrate. The first portion of filtrate (e.g., 5% of volume to be filtered) should be discarded to alleviate this problem.

Most stock solutions of culture medium additions can be sterilized separately by autoclaving, although vitamin stock solutions are routinely filtered through 0.2-µm single-use filter units (e.g., Millipore Millex GS), since heat sterilization will denature these organic compounds. Filter sterilization of all additions may reduce uncertainties about stability of the chemical compounds and contamination from autoclave steam, but absolute sterilization is not guaranteed. Stock solutions can be stored in ultraclean sterile glass, polycarbonate, or Teflon tubes/bottles. In order to minimize effects of any microbial contaminations, all stock solutions should be stored in a refrigerator at 4°C, except vitamin stocks, which are stored frozen at –20°C and thawed immediately prior to use.

CULTURE METHODS

Algae can be produced according to a great variety of methods, from closely controlled laboratory methods to less predictable methods in outdoor tanks. Indoor culture allows for control over illumination, temperature, nutrient level, contamination with predators and competing algae, whereas

outdoor algal systems, though cheaper, make it very difficult to grow specific algal cultures for extended periods. Open cultures such as uncovered ponds and tanks (indoors or outdoors) are more readily contaminated than closed culture vessels such as tubes, flasks, carboys, bags, etc. Axenic cultivation can be also chosen, by using algal cultures free of any foreign organisms such as bacteria, but this cultivation is expensive and difficult, since it requires a strict sterilization of all glassware, culture media, and vessels to avoid contamination. These constraints make it impractical (and very expensive) for commercial operations. On the other hand, nonaxenic cultivation, though cheaper and less laborious, are more prone to crash, less predictable, and often of inconsistent quality.

Different types of algal cultures are used worldwide; the most routinely adopted being batch, continuous and semicontinuous, ponds, and photobioreactors.

Batch Cultures

The most common culture system is the batch culture, due to its simplicity and low cost. This is a closed system, volume-limited, in which there is no input or output of materials, that is, resources are finite. The algal population cell density increases constantly until the exhaustion of some limiting factor, while other nutrient components of the culture medium decrease over time. Any products produced by the cells during growth also increase in concentration in the culture medium. Once the resources have been utilized by the cells, the cultures die unless supplied with a new medium. In practice, this is done by subculturing, that is, transferring a small volume of existing culture to a large volume of fresh culture medium at regular intervals. In this method, algal cells are allowed to grow and reproduce in a closed container. A typical batch culture set-up can be a 250-mL Erlenmeyer's culture flask with a cotton/gauze bung; in some cases, the bung can be fitted with a Pasteur pipette and air is bubbled into the culture to maintain high levels of oxygen and carbon dioxide and provide mixing.

Batch culture systems are highly dynamic. The population shows a typical pattern of growth according to a sigmoidal curve (Figure 6.3a), consisting of a succession of six phases, characterized by variations in the growth rate (Figure 6.3b); the six phases are summarized in Table 6.23.

The growth curve, relatively to the phases 3–5, without the lag, acceleration, and crash phases, can be described with a rectangular hyperbolic function similar to the Michaelis–Menten formulation

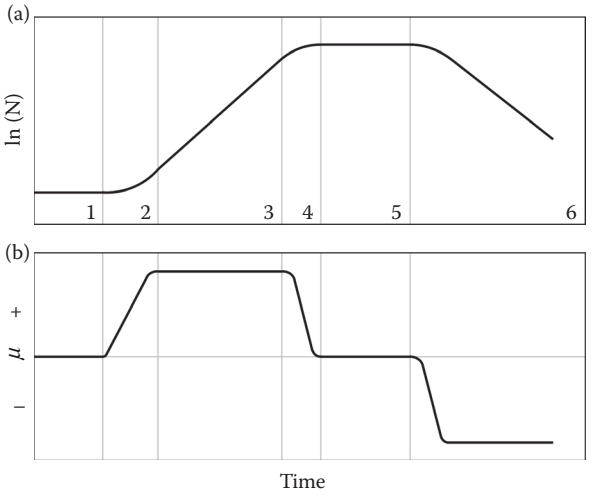

FIGURE 6.3 (a) Growth curve of an algal population under batch culture conditions. (b) Corresponding variations of the growth rate.

TABLE 6.23
Description of the Six Successive Phases of Growth for an Algal Population under Batch Culture Conditions

Phase	Growth	Growth Rate Interpretation	Description
1	Lag	Zero	Physiological adaptation of the inoculum to changing conditions
2	Acceleration	Increasing	Trivial
3	Exponential	Constant	Population growth changes the environment of the cells
4	Retardation	Decreasing	Effects of changing conditions appear
5	Stationary	Zero	One or more nutrients (or light) are exhausted down to the threshold level of the cells
6	Decline	Negative	The duration of stationary phase and the rate of decline are strongly dependent on the kind of organisms

that describe the nutrient uptake kinetics and the dynamic relationship between phosynthetic rate and irradiance.

After the inoculum, growth does not necessarily start right away, since most cells may be viable, but not in condition to divide. The interval necessary for the transferred cells to adapt to the new situation and start growing is the first phase of the growth curve, the lag phase. This lag or induction phase is relatively long when an algal culture is transferred from a plate to liquid culture. Cultures inoculated with exponentially growing algae have short lag phases, which can seriously reduce the time required for up-scaling. The lag in growth is attributed to the physiological adaptation of the cell metabolism to growth, such as the increase in the levels of enzymes and metabolites involved in cell division and carbon fixation. During this phase, the growth rate is zero.

After a short phase of growth acceleration, characterized by a continuously increasing growth rate, up to its maximum value, which is achieved in the following exponential phase, the cell density increases as a function of time t according to the exponential function:

$$N_2 = N_1 \, e^{m(t_2 - t_1)}, \tag{6.1}$$

where N_2 and N_1 are the number of cells at two successive times t_2 and t_1, respectively, and μ is the growth rate. During this phase, the growth rate reached is kept constant. The growth rate is mainly dependent on algal species and cultivation parameters, such as light intensity, temperature, nutrient availability, etc.

The exponential growth phase normally lasts for a very short period, since cells start to shade each other as their concentration increases. Hence, the culture enters the phase of retardation and the cell growth rate decrease because mainly light, but also because of nutrients, pH, carbon dioxide, and other physical and chemical factors begin to limit growth. Following this phase, the cell population continues to increase, but the growth rate decreases until it reaches zero, at which point the culture enters the stationary phase, during which the cell concentration remains constant at its maximum value. The final stage of the culture is the death or "crash" phase, characterized by a negative growth rate; during this phase, water quality deteriorates, mainly due to catabolite accumulation, and nutrients are depleted to a level incapable of sustaining growth. Cell density decreases rapidly and the culture eventually collapses.

In practice, culture crashes can be caused by a variety of reasons, including the depletion of a nutrient, oxygen deficiency, overheating, pH disturbance, or contamination. The key to the success

of algal production is maintaining all cultures in the exponential phase of growth. Also, the nutritional value of the produced algae is inferior once the culture is beyond phase 4 due to reduced digestibility, deficient composition, and possible production of toxic metabolites.

In batch cultures, cell properties such as size, internal nutrient composition, and metabolic function vary considerably during the above growth phases. This often makes interpretation of the results difficult. During the exponential growth phase, cell properties tend to be constant. However, this phase usually lasts only for a short period of time, and if one wishes to estimate growth rates of the exponential phase of batch cultures, daily sampling appeared to be insufficient to allow for a reasonably accurate estimate. Moreover, the accuracy of growth rate determination is highest in artificial, defined media when compared to cells grown in natural surface water media.

A significant advantage of batch culture systems is their operational simplicity. The culture vessels most often consist of an Erlenmeyer flask with a sample-to-flask volume ratio of about 0.2, in order to prevent carbon dioxide limitation. This volume ratio is only critical if the flasks are shaken by hand once a day during the culturing run. If the flasks are cultured on a rotating shaker table, a sample-to-flask volume ratio of 0.5 is permitted.

Batch culture systems are widely applied because of their simplicity and flexibility, allowing to change species and to remedy defects in the system rapidly. Although often considered as the most reliable method, batch culture is not necessarily the most efficient method. Batch cultures are harvested just prior to the initiation of the stationary phase and must thus always be maintained for a substantial period of time past the maximum specific growth rate. Also, the quality of the harvested cells may be less predictable than that in continuous systems and, for example, vary with the timing of the harvest (time of the day, exact growth phase).

Another disadvantage is the need to prevent contamination during the initial inoculation and early growth period. Because the density of the desired phytoplankton is low and the concentration of nutrients is high, any contaminant with a faster growth rate is capable of outgrowing the culture. Batch cultures also require a lot of labor to harvest, clean, sterilize, refill, and inoculate the containers.

Continuous Cultures

In continuous cultures, resources are potentially infinite: cultures are maintained at a chosen point on the growth curve by the regulated addition of fresh culture medium. In practice, a volume of fresh culture medium is added automatically at a rate proportional to the growth rate of the alga, while an equal volume of culture is removed. This method of culturing algae permits the maintenance of cultures very close to the maximum growth rate, since the culture never runs out of nutrients.

Fresh growth medium is stored in a large vessel. Air is pumped into the airspace in this medium vessel. This air pressure will push the medium through a tube which is connected to the culture vessel. By opening and closing the clamp on this medium line, one can add medium to the culture vessel. Air is also pumped into the culture vessel, passes down a long glass tube to the bottom of the culture, and bubbles up. This keeps the culture well suspended as well as high in oxygen and CO_2. The air flowing into the culture vessel flows out through an outflow tube. As fresh medium is added, the level of the liquid in the culture vessel rises; when the level reaches the bottom of the outflow tube, old medium and cells flow out of the culture vessel into a waste flask. There is another glass tube in the culture vessel, the sample port. When a sample of cells from the culture vessel is needed, the clamp on the sample port can be opened up and medium and cells flow out.

Continuous culture systems have been widely used to culture microbes for industrial and research purposes. The early development of a continuous culture system can be traced back to the 1950s, when the first chemostat, also called bactogen, was developed.

Batch and continuous culture systems differ in that in a continuous culture system, nutrients are supplied to the cell culture at a constant rate, and in order to maintain a constant volume, an equal volume of cell culture is removed. This allows the cell population to reach a "steady state" (i.e., growth rate and the total number of cells per milliliter of culture remain constant).

Two categories of continuous cultures can be distinguished *sensu* Fogg and Thake (1987):

- Turbidostat culture, in which fresh medium is delivered only when the cell density of the culture reaches some predetermined point, as measured by the extinction of light passing through the culture. At this point, fresh medium is added to the culture and an equal volume of culture is removed. The diluted culture increases the cell density until the process is repeated.
- Chemostat culture, in which a flow of fresh medium is introduced into the culture at a steady, predetermined rate. The latter adds a limiting vital nutrient (e.g., nitrate) at a fixed rate; in this way, the growth rate and not the cell density is kept constant. In a chemostat, the medium addition ultimately determines growth rate and cell density.

In many chemostat continuous culture systems, the nutrient medium is delivered to the culture at a constant rate by a peristaltic pump or solenoid gate system. The rate of media flow can be adjusted and is often set at approximately 20% of culture volume per day. Air is pumped into the culture vessel through a sterile filter. This bubbling air has three effects: it supplies CO_2 and O_2 to the culture, aids in circulation and agitation of the cultures; and pressurizes the head space of the culture vessel so as to provide the force to "remove" an amount of media (and cells) equal to the volume of inflowing media. The culture may be aseptically sampled by opening the clamp on a sample port. The magnetic stirrer and aeration help in preventing the cells from getting collected at the bottom of the culture vessel. A truly continuous culture will have the medium delivered at a constant volume per unit time. However, delivery systems such as peristaltic pumps or solenoid gates are inherently unreliable. In order to deliver exactly the same amounts of medium to several cultures growing at once, a "semicontinuous" approach can be taken.

The rate of flow of medium into a continuous culture system is known as the "dilution rate." When the number of cells in the culture vessel remains constant over time, the dilution rate is said to equal the rate of cell division in the culture, since the cells removed by the outflow of the medium are replaced by an equal number of cells through cell division in the culture. The principal advantage of continuous culture is that the rate of dilution controls the rate of microbial growth via the concentration of the growth-limiting nutrient in the medium. As long as the dilution rate is lower than the maximum growth rate attainable by the algal species, the cell density will increase to a point at which the cell division rate (birth rate) exactly balances the cell washout rate (death rate). This steady-state cell density is also characterized by a constancy of all metabolic and growth parameters. On the other hand, if the dilution rate exceeds the maximum cell division rate, then the cells are removed faster than they are produced and total washout of the entire cell population eventually occurs.

The disadvantages of the continuous system are its relatively high cost and complexity. The requirements for constant illumination and temperature mostly restrict continuous systems to indoors and this is only feasible for relatively small production scales. Continuous cultures have the advantages of producing algae of more predictable quality. Furthermore, they are amenable to technological control and automation, which in turn increases the reliability of the system and reduces the need for labor.

Semicontinuous Cultures

In a semicontinuous system, the fresh medium is delivered to the culture all at once, by simply opening a valve in the medium delivery line. Fresh medium flows into the culture vessel, and spent culture flows out into a collecting vessel. Once the required medium has entered the culture, the valve is closed, and the culture is allowed to grow for 24 h, when the procedure is repeated. The semicontinuous technique prolongs the use of large tank cultures by partial periodic harvesting followed immediately by topping up to the original volume and supplementing with nutrients to

achieve the original level of enrichment. The culture is grown up again, partially harvested, etc. Semicontinuous cultures may be indoors or outdoors, but usually their duration is unpredictable. Competitors, predators, and/or contaminants and metabolites eventually build up, rendering the culture unsuitable for further use. Since the culture is not harvested completely, the semicontinuous method yields more algae than the batch method for a given tank size.

Commercial-Scale Cultures

Existing commercial microalgae culture systems range in volume from about 10^2 L to more than 10^9 L. However, aside from the specialized small-scale culture systems (<1000 L), other types of culture systems predominate: large open ponds, circular ponds with a rotating arm to mix the cultures, raceway ponds, or large bags.

There are several considerations as to which culture system to use. Factors to be considered include: the biology of the alga, the cost of land, labor, energy, water, nutrients, climate (if the culture is outdoors), and the type of final product. The various large-scale culture systems also need to be compared on their basic properties such as their light utilization efficiency, ability to control temperature, the hydrodynamic stress placed on the algae, the ability to maintain the culture unialgal, and/or axenic and how easy they are to scale up from laboratory scale to large scale. The final choice of the system is almost always a compromise between all of these considerations to achieve an economically acceptable outcome. Successful further development of the industry requires significant improvements in the design and construction of the photobioreactors as well as a better understanding of the physiology and physical properties of the microalgae to be grown.

A common feature of most algal species currently produced commercially (i.e., *Chlorella, Spirulina*, and *Dunaliella*) is that they grow in highly selective environments, which means that they can be grown in open-air cultures and still remain relatively free of contamination by other algae and protozoa. Thus, *Chlorella* grows well in nutrient-rich media, *Spirulina* requires a high pH and bicarbonate concentration, and *Dunaliella salina* grows at very high salinity. Those species of algae that do not have this selective advantage must be grown in closed systems. This includes most of the marine algae grown as aquaculture feeds (e.g., *Skeletonema*, *Chaetoceros*, *Thalassiosira*, *Tetraselmis*, and *Isochrysis*) and the dinoflagellate *Crypthecodinium cohnii* grown as a source of long-chain polyunsaturated fatty acids, as well as almost all other species being considered for commercial mass culture. In the particular case of *C. cohnii*, a large-scale fermentation plant is operated by Martek Biosciences in Winchester (USA).

OUTDOOR PONDS

Different types of ponds have been designed and experimented with for microalgae cultivation, which vary in size, shape, materials used for construction, mixing device. Large outdoor ponds can be unlined, with a natural bottom, or lined with inexpensive materials such as clay, brick, or cement, or expensive plastics such as polyethylene, PVC sheets, glass fiber, or polyurethane. Unlined ponds suffer from silt suspension, percolation, and heavy contamination, and their use is limited to a few algal species, and to particular soil and environmental conditions.

Natural systems such as eutrophic lakes or small natural basins can also be exploited for microalgal production, provided suitable climatic conditions and sufficient nutrients are present. Examples are the numerous temporary or permanent lakes along the northeast border of Lake Chad, where *Arthrospira* sp. grows almost as monoculture, and is collected for human consumption by the Kanembou people inhabiting those areas. *Arthrospira* sp. naturally blooms also in old volcanic craters filled with alkaline waters in the Myanmar region. Production began at Twin Taung Lake in 1988, and by 1999 increased to 100 tons per year. About 60% is harvested from boats on the surface of the lake, and about 40% is grown in outdoor ponds alongside the lake. During the blooming season in the summer, when the cyanobacterium forms thick mats on the lake, people in boats collect a

dense concentration of *Arthrospira* in buckets. *Arthrospira* is harvested on parallel inclined filters, washed with freshwater, dewatered, and pressed again. This paste is extruded into noodle-like filaments that are dried in the sun on transparent plastic sheets. Dried chips are taken to a pharmaceutical factory in Yangon, pasteurized, and pressed into tablets ready to be sold.

Another cyanobacterium used as a food supplement is *Aphanizomenon flos-aquae*, which since the early 1980s has been harvested from Upper Klamath Lake, Oregon, and sold as a food and health food supplement by Cell Tech International. In 1998, the market for *A. flos-aquae* as a health food supplement was about $100 million with an annual production greater than 10^6 kg (dry weight). *A. flos-aquae* blooms are often biphasic, with a first peak in late June to early July, and a second peak late in September to mid-October. The harvested biomass is screened and centrifuged to remove small extraneous material. The algal concentrate is then gravity-fed into a vertical centrifuge that applies high centrifugal force to separate cells and colonies, removing about 90% of the remaining water. At this stage, the algal product is 6–7% solids. Once concentrated, the product is chilled to 2°C and stored before being pumped to the freezers. The frozen algae is then put into storage boxes and shipped to the freezer facility for storage. When needed, the frozen product is shipped to an external commercial freeze-drying facility to be freeze-dried into a powder containing 3–5% water content. This final product is processed into consumable products such as capsules or tablets.

Natural ponds that do not necessitate mixing, and need only minimal environmental control, represent other extensive cultivation systems.

The largest natural ponds used for commercial production of microalgae are *D. salina* lagoons in Australia. Western Biotechnology Ltd. operates 250 ha ponds (semiintensive cultivation) at Hutt Lagoon (Western Australia); Betatene Ltd., a division of Henkel Co. (Germany), operates 460 ha unmixed ponds (extensive cultivation) at Whyalla (South Australia). Both facilities produce biomass for β-carotene extraction. Other facilities use raceway culture ponds, such as those operated by Cyanotech Co. in Hawaii and Earthrise farms in California for the production of *Haematococcus* and *Artrosphira* biomass. In both cases, large raceway ponds from 1000 to 5000 m^2 are adopted, with stirring accomplished by one large paddle wheel per pond. Raceway ponds are also used for intensive cultivation of *D. salina* by Nature Beta Technologies Ltd. in Israel.

The nutrient medium for outdoor cultures is based on that used indoors, but agricultural-grade fertilizers are used instead of laboratory-grade reagents. However, fertilization of mass algal cultures in estuarine ponds and closed lagoons used for bivalve nurseries was not found to be desirable since fertilizers were expensive and induced fluctuating algal blooms, consisting of production peaks followed by total algal crashes. By contrast, natural blooms are maintained at a reasonable cell density throughout the year and the ponds are flushed with oceanic water whenever necessary. Culture depths are typically 0.25–1 m. Cultures from indoor production may serve as inoculum for monospecific cultures. Alternatively, a phytoplankton bloom may be induced in seawater from which all zooplankton has been removed by sand filtration. Algal production in outdoor ponds is relatively inexpensive, but it cannot be maintained for a prolonged period and is only suitable for a few, fast-growing species due to problems with contamination by predators, parasites, and more opportunistic algae that tend to dominate regardless of the species used as inoculum. Furthermore, outdoor production is often characterized by a poor batch-to-batch consistency and unpredictable culture crashes caused by changes in weather, sunlight, or water quality. As stated above, at present, large-scale commercial production of microalgae biomass is limited to *Dunaliella*, *Haematococcus*, *Arthrospira*, and *Chlorella*, which are cultivated in open ponds at farms located around the world (Australia, Israel, Hawaii, Mexico, China). These algae are a source for viable and inexpensive carotenoids, pigments, proteins, and vitamins that can be used for the production of nutraceuticals, pharmaceuticals, animal feed additives, and cosmetics. Mass algal cultures in outdoor ponds are applied in Taiwanese shrimp hatcheries where *Skeletonema costatum* is produced successfully in rectangular outdoor concrete ponds of 10–40 tons of water volume and a water depth of 1.5–2 m.

PHOTOBIOREACTORS

An alternative to open ponds for large-scale production of microalgal biomass are photobioreactors. The term "photobioreactor" is used to indicate only closed systems that do not allow for direct exchange of gases or contaminants between the algal culture they contain and the atmosphere. These devices provide a protected environment for cultivated species, relatively safe from contamination by other microrganisms, in which culture parameters such as pH, oxygen, and carbon dioxide concentration, and temperature can be better controlled, and provided in known amount. Moreover, they prevent evaporation and reduce water use, lower CO_2 losses due to outgassing, permit higher cell concentration, thus reducing operating costs, and attain higher productivity. However, these systems are more expensive to build and operate than ponds, due to the need of cooling, strict control of oxygen accumulation, and biofouling, and their use must be limited to the production of very high-value compounds from algae that cannot be cultivated in open ponds. Different categories of photobioreactors exist, such as axenic photobioreactors; tubular or flat photobioreactors; horizontal, inclined, vertical, or spiral; manifold or serpentine photobioreactors; air or pump mixed; single-phase, filled with culture suspension, with gas exchange taking place in a separate gas exchanger, or two-phase, with both the gas and the liquid phases contained in the photostage.

The use of these devices dates back to the late 1940s, as a consequence of the investigation on the fundamental of photosynthesis carried out with *Chlorella*. Open systems were considered inappropriate to guarantee the necessary degree of control and optimization of the continuous cultivation process. Since the first vertical tubular reactors set up in the 1950s for the culture of *Chlorella* under both artificial light and sunlight, several types of photobioreactors have been designed and experimented with. Most of these are small-scale systems, for which experimentation has been conducted mainly indoors, and only few have been scaled up to commercial level. Significantly higher photosynthetic efficiencies and a higher degree of system reliability have been achieved in recent years, thanks, in particular, to the progress in understanding the growth dynamic and requirements of microalgae under mass cultivation conditions. Notwithstanding these advances, there are only few examples of photobioreactor technology that has expanded from the laboratory to the market, proving to be commercially successful. In fact, the main obstacle remains the scaling-up phase, due to the difficulties of transferring a process developed at the laboratory scale to industrial scale in a reliable and efficient way. Two of the largest commercial systems in operation at present are the Klötze plant in Germany for the production of *Chlorella* biomass and the Algatechnologies plant in Israel in Arava desert for the production of *Haematococcus* biomass. Founded in 1998, Algatechnologies is a world leader in the production and supply of AstaPure, natural astaxanthin from *Haematococcus pluvialis*. The Algaltechnology closed system consists of a modular array of tubular photobioreactors based on glass tubes 300-km long set on 10 acres of arid desert land. Both plants utilize tubular, pump-mixed, single-phase photobioreactors; in particular, the Klötze plant consists of compact and vertically arranged horizontal running glass tubes of a total length of 500,000 m and a total PBR volume of 700 m^3. In a glasshouse requiring an area of only 10,000 m^2, an annual production of 130–150 tons of dry biomass was demonstrated to be economically feasible under Central European conditions.

Other industrial plants actually operating are the plant built in Maui, Hawaii (USA) by MicroGaia Ltd. (now BioReal, Inc., a subsidiary of Fuji Chemical Industry Co., Ltd.), which is based on a rather complex design, called BioDome™, for the cultivation of *Haematococcus*; the rigid, plastic tubes photobioreactor of AAPS (Addavita Ltd., UK) and the flexible, plastic tubes photobioreactor of the Mera Growth Module (Mera Pharmaceuticals, Inc., USA).

Culture of Sessile Microalgae

Farmers of abalone (*Haliotis* sp.) have developed special techniques to provide food for the juvenile stages that feed in nature by scraping coralline algae and slime off the surface of rocks using their

radulae. In culture operations, sessile microalgae are grown on plates of corrugated roofing plastic, which serve as substrate for settlement of abalone larvae. After metamorphosis, the spat graze on the microalgae until they become large enough to feed on macroalgae. The most common species of microalgae used on the feeder plates are pennate diatoms (e.g., *Nitzchia*, *Navicula*). The plates are inoculated by placing them in a current of sand-filtered seawater. Depending on the local conditions, the microalgae cultures on the plates take between 1 and 3 weeks to grow to a density suitable for settling the larvae. As the spat grow, their consumption rate increases and becomes greater than the natural production of the microalgae. At this stage, the animals are too fragile to be transferred to another plate, and algal growth may be enhanced by increasing illumination intensity and/or the addition of fertilizer.

QUANTITATIVE DETERMINATIONS OF ALGAL DENSITY AND GROWTH

Although tedious, time-consuming, and requiring an excellence in taxonomic identifications, the traditional counting of phytoplankton is still unsurpassed for quantifying plankton, especially at low limits of detection. The examination and counting of preserved material also allows for direct observation and assessment of cell condition. The fundamental issue that must be addressed prior to choosing a counting technique is whether samples must be concentrated. The three routine methods used to concentrate phytoplankton samples are centrifugation and filtration for live samples and sedimentation (gravitational settling) for preserved samples. Centrifugation and sedimentation are the most commonly used, although filtration onto membrane filters is an effective procedure for fluorescence microscopic enumerations. If the cell density is less than 10^5 cells L^{-1}, the sample needs to be concentrated; if cell density is too high to allow direct counting, the sample will be diluted. Dilution or concentration factors need to be taken into account for calculating the final cell concentration.

Species containing gas vacuoles (cyanobacteria) are unlikely to fully sediment despite the Lugol's fixation. Two methods are available for collapsing vacuoles to assist sedimentation. Samples can either be exposed to brief ultrasonication (<1 min, but may vary for different species) or alternatively, pressure can be applied to the sample by forcing it through a syringe with a fine needle; this will collapse the vacuoles and the cells will then settle through gravity.

If the water sample contains a sufficient number of algae and concentration is not required, a direct count can be undertaken. The sample is thoroughly mixed, treated with a few drops of Lugol's solution, mixed again, and allowed to stand for 30–60 min. The sample is mixed again and subsamples of it used for direct counting and taxonomic identification.

When concentration is required, a simple procedure for gravitational settling is to pour a well-mixed volume of the sample of water containing the microalgae in a measuring cylinder (100 mL), add Lugol's solution to it (1% by volume), and either allow the sample to stand overnight or use a centrifuge so that the cells sink. The iodine in Lugol's solution not only preserves and stains the cells, but also increases their density. When the column of water appears clear, the top 90 mL will be gently siphoned off without disturbing the sediment at the base of the cylinder. This leaves the cells concentrated in the bottom 10 mL. Subsamples of this sedimented fraction can be used for counting procedure and examined under the microscope for identification, keeping in mind that the cells of the original sample have been concentrated 10 times.

At present, there are many kinds of counting procedures available for enumerating phytoplankton, depending whether counting algae in mixtures, as from field sampling, or unialgal samples, such as in growth or bioassay experiments in a laboratory. Some techniques are relatively "low-tech," and can also be used in remote locations, other are "high-tech," and require an expensive instrument.

The Sedgewick–Rafter counting chamber (Figure 6.4) is a low-tech device routinely used for counting algae in mixed assemblages. This chamber limits the volume and area of the sample to enable easier counting and calculation of phytoplankton numbers. It consists of a brass or polystyrene rectangular frame mounted on a heavy glass slide from which a precise internal chamber has

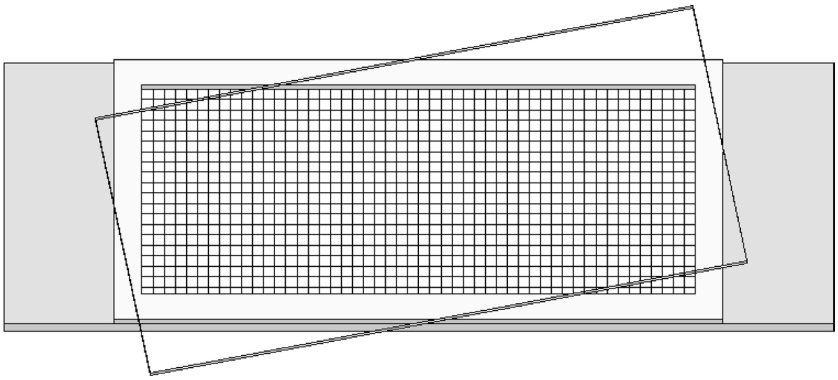

FIGURE 6.4 Schematic drawing of the Sedgewick–Rafter counting chamber.

been cut; its dimensions are $50 \times 20 \times 1$ mm^3, with an area of 1000 mm^2, and a volume of 1.0 mL. The base is ruled in a 1-mm grid. When the liquid sample is held in the cell by its large, rectangular glass coverslips, the grid subdivides 1-mL volume into microliters.

To fill the Sedgewick–Rafter chamber, the coverslip is placed on top of the chamber, diagonally across the cell, so that the chamber is only partially covered. This helps in preventing the formation of air bubbles in the cell corners. The coverslip will rotate slowly and cover the inner portion of the cell during filling. The coverslip should not float, nor should there be any air bubbles; the former results from over-filling, the latter from under-filling the chamber. In both cases, the depth of the chamber will be different from 1 mm, and the calculations will be invalidated. A large-bore pipette should be used to transfer the sample into the chamber; after filling, the coverslip is gently pushed to cover the chamber completely. The phytoplankton sample placed into the Sedgewick–Rafter counting chamber is allowed to stand on a flat surface for 20 min to enable the phytoplankton to settle. It is then transferred to the stage of an upright light microscope and securely positioned, ready for counting.

Counts are done with the 4× or (more usually) the 10× objectives of the compound microscope (depth of field and lens length preclude the use of higher magnification objectives). A Whipple disk is inserted into one of the ocular lenses in order to provide a sample grid. It is necessary to first determine the area (A) of the Whipple field for each set of ocular and objective lenses used. This is accomplished with a stage micrometer.

There are 50 fields in the length and 20 fields in the width of the chamber for a total of 1000 fields. A horizontal strip corresponds to 50 fields. All cells within randomly selected fields are counted. A convention needs to be followed for cells or units lying on a boundary line or field, such as all cells or units overlapping the right-hand and top boundaries are counted, but those overlapping the bottom and left-hand boundaries are not. The number of units per milliliter for each taxon is calculated according to following formula

$$\text{Number of cells mL}^{-1} = \frac{C \times 1000 \text{ mm}^3}{ADF} \tag{6.2}$$

where C is the number of cells counted, A the area of field in mm^2, D the depth of the field (Sedgewick–Rafter chamber depth) in mm, and F the number of fields counted.

For colonial taxa, multiply the count of units by the average number of cells per unit and use the resulting value as C in Equation 6.2. To adjust for sample concentration or dilution, the result is divided or multiplied by the appropriate factor. To obtain total cell density per milliliter, sum all counts of individual taxa.

If cell density is low (<10 units per field), counting of long transects to cover a large proportion of the chamber floor is more appropriate. Several transects with a width of a chamber field are counted. The number of strips depends on the required precision and the phytoplankton density. The number of cells per mm^3 is calculated according to the following formula:

$$\text{Number of cells mL}^{-1} = \frac{C \times 1000\ \text{mm}^3}{LDWS}, \tag{6.3}$$

where C is the number of cells counted, L the length of the strip in mm, D the depth of a field (Sedgewick–Rafter chamber depth) in mm, W the width of strip in mm, and S the number of strips counted.

To adjust for sample concentration or dilution, the result is divided or multiplied by the appropriate factor.

A "high-tech" alternative to counting algae in mixed assemblages with the Sedgewick–Rafter cell is the inverted microscope method. The expensive component here is the inverted microscope, whose great advantage is that settling chamber depth does not preclude use of high-magnification objective lenses. In 1931, Utermöhl solved the problem of concentrating and enumerating algae in mixed populations when he described a one-step settling and enumeration technique using the inverted microscope. The procedure involved the gravitational sedimentation of preserved phytoplankton into a counting chamber. This counting technique correctly assumed that phytoplankton would fall randomly to the bottom of the chamber and that counts would then be made on random fields or transects. The inverted microscope counting technique has gained broad popularity for phytoplankton enumeration. One of the advantages of this randomized counting technique is its ability to calculate error estimates to verify the accuracy of the enumeration. Through the years, many modified chambers have been designed and used with the inverted microscope.

Special and expensive "Utermöhl" chambers can be purchased, but cheaper ones can be constructed from large coverslips, and plastic syringe barrels. If a lens with a long focal-length is available, chambers may be constructed from glass slides.

A measured volume of preserved sample is added to the settling chamber and allowed to settle for at least an hour. Time periods as long as 24–48 h are preferred especially, if small algae are present in the sample (these will settle only very slowly). Upon settling, the upper portion of the chamber is removed and replaced with a glass plate. The sample is then transferred to an inverted microscope (condenser numerical aperture, 0.70; objectives, 25× and 40×; oculars, 12.5×) with phase-contrast optics.

The sample is initially enumerated at 500× using a random field technique. A minimum of 20 random fields and 200 individual cells are enumerated. Additional fields are counted until the minimum count is attained. When there are a large number of cells of a particular taxon in a sample, fewer than 20 random fields are enumerated with a minimum of five random fields examined for this taxon. Individual cells are enumerated, irrespective of whether in chains, filaments, or colonies. This allows for a more accurate estimate of biomass that is determined from the cell densities. Upon achieving 20 random fields and 200 individual cells, a low-magnification scan (25×) of 20 random fields is used to estimate the rarer, larger forms within the sample.

In the case of unialgal samples (unicells, small colonies, or relatively short filaments), chambers such as the haemacytometer, the Thoma chamber (Figure 6.5), the Fuchs–Rosenthal, or the Burker chambers are effective and commonly used for estimating the densities of cultures. The haemacytometer was developed for counting cells in blood samples (now this is mostly done with electronic particle counters). Most of these counting chambers have delicate, mirrored surfaces that must not be scratched. Each mirrored surface has a grid etched upon the surface. In the case of Thoma chamber, each grid is composed by 16 fields of 0.2-mm side, separated by three boundary lines (Figure 6.6).

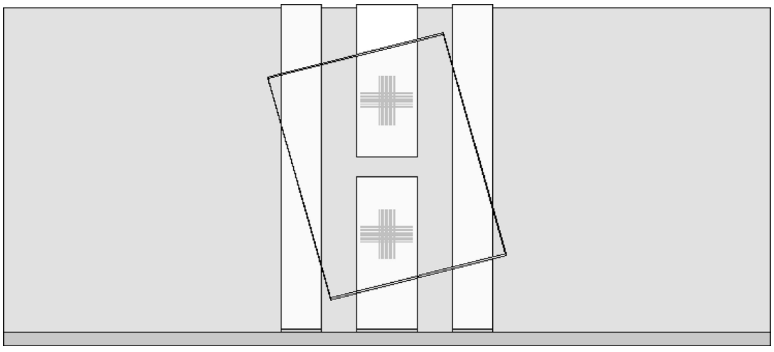

FIGURE 6.5 Schematic drawing of the Thoma counting chamber.

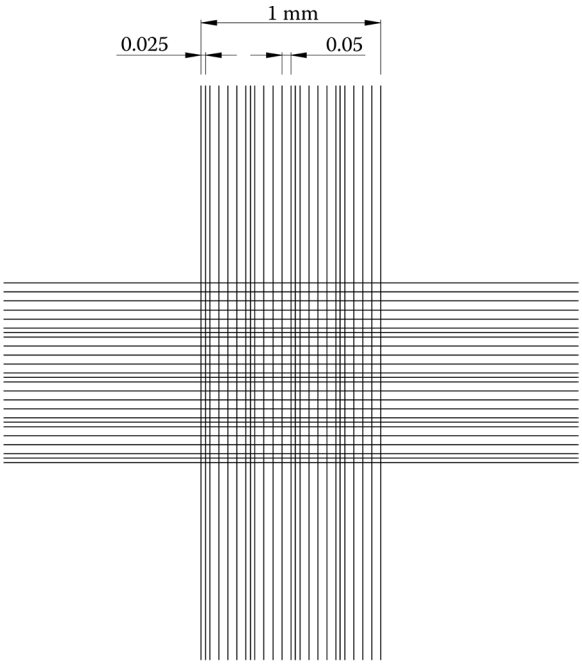

FIGURE 6.6 Schematic drawing of the Thoma chamber ruling.

These 16 fields are further subdivided into 16 smaller areas each, for a total of 256 counting fields. The chamber is 0.1-mm deep; hence each grid holds exactly 64×10^{-3} mL of sample. You have the choice of counting the algae in the entire grid; counting algae in only one of the 16 squares, then multiplying by 16; or counting algae in an even smaller area, and multiplying accordingly.

When counting cells in the entire grid, that is, 16 fields, the cell concentration is calculated according to the following formula:

$$\text{Number of cells mL}^{-1} = \frac{C \times 10^6}{64}, \tag{6.4}$$

where C is the number of cells counted.

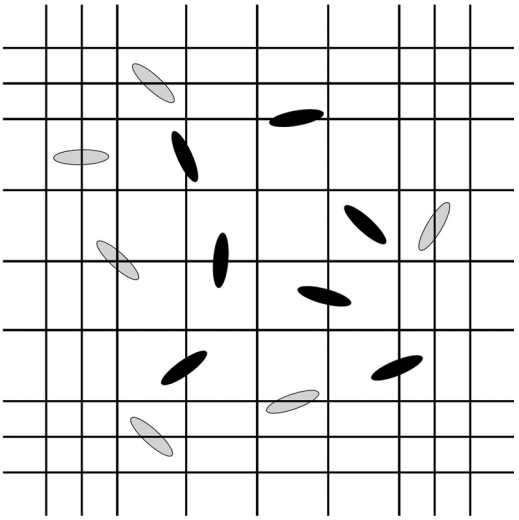

FIGURE 6.7 Schematic drawing of the counting convention: all cells overlapping the right-hand and top boundaries are counted (black cells), but those overlapping the bottom and left-hand boundaries are not (gray cells).

Counts of about 30 cells per field are desirable for accuracy. If there are more than 30 cells per field, dilute the sample, or count algae in a lower number of fields and multiply. As for the Sedgewick–Rafter, a convention needs to be followed for cells lying on a boundary line or field, such as all cells overlapping the right-hand and top boundaries are counted, but those overlapping the bottom and left-hand boundaries are not (Figure 6.7). The counting process has to be repeated at least 10 times to determine an accurate mean.

"High-tech" methods for counting unialgal samples are the electronic particle counter (e.g., Coulter counter) and the digital microscopy. In spite of relatively high cost, an electronic particle counter is highly recommended for doing growth or bioassay studies that require many counts and high accuracy. In addition, the instrument will provide particle size/biovolume distributions. The principle of operation is that particles, suspended in an electrolyte solution, are sized and counted by passing them though an aperture having a particular path of current flow for a given length of time. As the particles displace an equal volume of electrolyte in the aperture, they place resistance in the path of the current, resulting in current and voltage changes. The magnitude of the change is directly proportional to the volume of the particle; the number of changes per unit time is proportional to the number of particles in the sample. When opened, the stopcock introduces vacuum into the system, draws sample through the aperture, and unbalances the mercury in the manometer. The mercury flows past the "start" contact and resets the counter to zero. When the stopcock is closed, the mercury starts to return to its balanced position and draws sample through the aperture. Variously sized aperture tubes are available for use in counting variously sized particles; the aperture size is chosen to match that of particles.

Digital microscopy necessitates of a microscope equipped with a digital TV camera connected to a personal computer running dedicated application software for cell recognition and cell counting. It represents an automatic, reliable, and very fast approach to growth determination.

Growth Rate and Generation Time Determinations

Growth curves are prepared from cell density data obtained with a hemacytometer or electronic particle counter on cultures sampled at intervals, such as once a day, depending on the growth rate

of the alga. Plots of number of cells against time (in days) can be made, and specific growth rate or growth constant (μ) and division or generation time (T_g) can be calculated from these curves.

A typical growth curve will show a lag phase, an exponential or log phase, and a stationary or plateau phase, where increase in density has leveled off (Figure 6.3a). In the stationary phase, growth is likely limited by resources such as light or nutrients. Growth rate (μ) is calculated using

$$\mu = \frac{\ln(N_2/N_1)}{t_2 - t_1}, \tag{6.5}$$

where N_2 and N_1 are the number of cells at times t_1 and t_2.

When N_2 is twice N_1, for example, the population has undergone a doubling; the growth rate can be expressed as

$$\mu = \frac{\ln(2)}{T_g}, \tag{6.6}$$

where T_g is the generation time.

Since ln(2) is equal to 0.6931, generation time can be calculated with the following equation:

$$T_g = 0.6931\mu^{-1}. \tag{6.7}$$

SUGGESTED READING

Alverson, A. J., Manoylov, K. M. and Stevenson, R. J. Laboratory sources of error for algal community attributes during sample preparation and counting. *Journal of Applied Phycology*, 39, 1–13, 2003.

Andersen, P. and Throndsen, J. Estimating cell numbers. In Hallegraeff, G. M., Anderson, D. M., and Cembella, A. D. (Eds.). *Manual on Harmful Marine Algae*. IOC Manuals and Guides No. 33. UNESCO Publishing, Paris, France, pp. 99–129, 2003.

Andersen, R. A. (Ed.). *Algal Culturing Techniques*. Elsevier Academic Press, Burlington, USA, 2005.

Aparicio-González, A., Duarte, C. M., and Tovar-Sánchez, A. Trace metals in deep ocean waters: A review. *Journal of Marine Systems*, 100–101, 26–33, 2012.

Berges, J. A., Franklin, D. J., and Harrison, P. J. Evolution of an artificial seawater medium: Improvements in enriched seawater, artificial water over the last two decades. *Journal of Phycology*, 37, 1138–1145, 2001.

Bertrand, E. M. and Allen, A. E. Influence of vitamin B auxotrophy on nitrogen metabolism in eukaryotic phytoplankton. *Frontiers in Microbiology*, 3, 1–16, 2012.

Chen, C.-Y., Yeh, K.-L., Aisyah, R., Lee, D.-J., and Chang, J.-S. Cultivation, photobioreactor design and harvesting of microalgae for biodiesel production: A critical review. *Bioresource Technology*, 102(1), 71–81, 2011.

Chilsholm, S. W. Temporal patterns of cell division in unicellular algae. In Platt T. (Ed.). *Physiological Bases of Phytoplankton Ecology*. *Canadian Bulletin of Fishery and Acquatic Sciences*, 210, 150–181, 1981.

Coltelli, P., Barsanti, L., Evangelista, V., Frassanito, A. M., Passarelli, V., and Gualtieri, P. Automatic and real time recognition of microalgae by means of pigment signature and shape. *Environmental Science Progress and Impact* 15(7), 1397–1410, 2013.

Croft, M. T., Warren, M. J., and Smith, A. G. Algae need their vitamins. *Eukaryotic Cell*, 5(8), 1175–1183, 2006.

Day, J. G. Conservation strategies for algae. In: Benson E. E. (Ed.). *Plant Conservation Biotecnology*. Taylor and Francis, London, 1999, pp. 111–124.

Fogg, G. E. and Thake, B. *Algal Cultures and Phytoplankton Ecology*. University of Wisconsin Press, Madison, USA, 1987.

Giovannoni, S. J. Vitamins in the sea. *Proceedings of the National Academy of Sciences of the United States of America*, 109(35), 13888–13889, 2012.

Gualtieri, P. and Barsanti, L. Identification of cellular and subcellular features by means of digital microscopy. *International Journal of Biomedical Computing*, 20, 79–86, 1987.

Guillard, R. R. L. Culture methods. In Hallegraeff, G. M., Anderson, D. M., and Cembella, A. D. (Eds.). *Manual on Harmful Marine Algae*. IOC Manuals and Guides, No. 33, UNESCO Publishing, Paris, France, 2003, pp. 45–62.

Hamilton, P. B., Proulx, M., and Earle, C. Enumerating phytoplankton with an upright compound microscope using a modified settling chamber. *Hydrobiologia*, 444, 171–175, 2001.

http://www.epa.gov/glnpo/monitoring/

http://www.epa.gov/glnpo/monitoring/sop/

http://www.unep.or.jp/Ietc/Publications/Water_Sanitation/integrated_watershed_mgmt_manual/

Johnson, M. K., Johnson, E. J., MacElroy, R. D., Spencer, H. L., and Bruff, B. S. Effect of salt on the halophilic alga *Dunaliella viridis*. *Journal of Bacteriology* 95(4), 1461–1468, 1968.

Labeda, D. P. (Ed.). *Isolation of Biotechnological Organisms from Nature*. McGraw-Hill Publishing Company, New York, 1990.

Luo, Q., Gao, Y., Luo, J., Chen, C., Liang, J., and Yang, C. Automatic identification of diatoms with circular shape using texture analysis. *Journal of Software*, 6(3), 428–435, 2011.

Mansoor, H., Sorayya, M., Aishah, S., and Mogeeb, A. A. M. Automatic recognition system for some cyanobacteria using image processing techniques and ANN approach. *International Conference on Environmental and Computer Science*. Vol. 19. IACSIT Press, Singapore, 2011.

Mosleh, M., Manssor, H., Malek, S., Milow, P., and Salleh, A. A preliminary study on automated freshwater algae recognition and classification system. *BMC Bioinformatics*, 13(Suppl 17), S25, 2012.

Paxinos, R. and Mitchell, J. G. A rapid Utermohl method for estimating algal numbers. *Journal of Planktonic Research*, 22, 2255–2262, 2000.

Raoof, B., Kaushik, B. D., and Prasanna, R. Formulation of a low-cost medium for mass production of *Spirulina*. *Biomass and Bioenergy*, 30(6), 537–542, 2006.

Richmond, A. (Ed.). *Handbook of Microalgae Mass Culture and Biotechnology and Applied Phycology*. Blackwell Publishing, Malden, USA, 2004.

Sañudo-Wilhelmy, S. A., Cutter, L. S., Durazo, R., Smail, E. A., Gómez-Consarnau, L., Webb, E. A. et al. Multiple B-vitamin depletion in large areas of the coastal ocean. *Proceedings of the National Academy of Sciences of United States of America*, 109(35), 14041–14045, 2012.

Stein, R. S. (Ed.). *Culture Methods and Growth Measurements.* Cambridge University Press, Cambridge, UK, 1973.

Sunda, W. G. and Huntsman, S. A. Effects of pH, light, and temperature on Fe-EDTA chelation and Fe hydrolysis in seawater. *Marine Chemistry*, 84, 35–47, 2003.

Sunda, W. G. and Huntsman, S. A. Relationship among photoperiod, carbon fixation, growth, chlorophylla, and cellular iron and zinc in a costal diatom. *Limnology Oceanography*, 49, 1742–1753, 2004.

Tredici, M. R. Photobioreactors. In: Flinckinger, M. C., and Drew, S. W. (Eds.), *Encyclopedia of Bioprocess Technology: Fermentation, Biocatalysis and Bioseparation*. Wiley, New York, 1999, pp. 395–419.

Verikas, A., Gelzinis, A., Bacauskiene, M., Olenina, I., Olenin, S., and Vaiciukynas, E. Automated image analysis- and soft computing-based detection of the invasive dinoflagellate *Prorocentrum minimum* (Pavillard) Schiller. *Expert Systems with Applications*, 39(5), 6069–6077, 2012.

Warren, A., Day, J. G., and Brown, S. Cultivation of protozoa and algae. In Hurtst, C. J., Crawford, R. L., Knudsen, G. R., McInerney, M. J., and Stenzenbach, L. D. (Eds.). *Manual of Environmental Microbiology*. ASM Press, Washington, USA, 2002, pp. 71–83.

Zhang, L., Luo, Z., Wang, B., and Zhang, J. Comparative study of C–V active contour model and subdivision for micro algae image segmentation. *International Conference on Electric Information and Control Engineering* (ICEICE), 2011, pp. 1241–1244.

7 Algae Utilization

INTRODUCTION

Micro- and macroalgae have been utilized by human for over hundreds of years as food, fodder, remedies, and fertilizers. The earliest record of seaweed utilization dates back to 13,000 years at a Late Pleistocene settlement in Chile; remains of marine algae belonging to the genera *Durvillaea* (Ochrophyta, Phaeophyceae), *Porphyra* (Rhodophyta, Bangiophyceae), *Mazzaella* (Rhodophyta, Florideophyceae), *Sarcothalia* (Rhodophyta, Florideophyceae), *Gracilaria* (Rhodophyta, Florideophyceae), *Gigartina* (Rhodophyta, Florideophyceae), *Macrocystis* (Ochrophyta, Phaeophyceae), *Sargassum* (Ochrophyta, Phaeophyceae), and *Trentepohlia* (Chlorophyta, Ulvophyceae) were recovered from hearths and stone artifacts located in the remains of domestic huts at the archeological site of Monte Verde in southern Chile. All of the algae are edible and have important medicinal properties; hence, these findings suggest a strong reliance on coastal resources for food and medicine of early humans in the Americas.

Other records show that people collected macroalgae for food as early as 500 BC in China and one thousand years later in Europe. Here, the earliest recorded account of seaweed use is in a poem dates back to 563 AD, dealing with the collection of seaweed by the monks of Iona, in the west of Scotland, to provide food for themselves and the poor.

Microalgae such as *Arthrospira* (Cyanobacteria, Cyanophyceae) have a history of human consumption in Mexico and Africa. In the fourteenth century, the Aztecs harvested *Arthrospira* from Lake Texcoco and used to make a sort of dry cake called *tecuitlatl*, and very likely the use of this cyanobacterium as food in Chad dates back to the same period, or even earlier, to the Kanem Empire (ninth century).

Not only people migrated from countries such as China, Japan, and Korea, but also from Indonesia and Malaysia, where algae have always been used as food, have brought this custom with them, so that today there are many more countries all over the world where the consumption of algae is not unusual, including Europe.

On the east and west coasts of United States of America and Canada, around Maine, New Brunswick, Nova Scotia, and British Columbia, some companies have begun cultivating macroalgae onshore, in tanks, specifically for human consumption, and their markets are growing, in both countries and with exports to Japan. Ireland, Northern Ireland, and Scotland are showing a renewed interest in macroalgae that were once a traditional part of the diet, especially for the Irish people during the potato famine after 1846. In addition to direct consumption, agars and carrageenans extracted from red macroalgae and alginates from brown macroalgae and microalgae have been included in a remarkable array of prepared food products, serving mostly to modify viscosity or texture. Global utilization of macroalgae is on the increase and, in terms of harvested biomass per year, macroalgae are among the most important cultivated marine organisms.

Currently, only 31 countries and territories are recorded with algae farming production, and 99.6% of global cultivated algae production comes from just eight countries: China (58.4%, 11.1 million tons), Indonesia (20.6%, 3.9 million tons), the Philippines (9.5%, 1.8 million tons), the Republic of Korea (4.7%, 901,700 tons), Democratic People's Republic of Korea (2.3%, 444,300 tons), Japan (2.3%, 432,800 tons), Malaysia (1.1%, 207,900 tons), and the United Republic of Tanzania (0.7%, 132,000 tons). Global production has been dominated by marine macroalgae, grown in both marine and brackish waters. Aquatic algae production by volume increased at average annual rates of 9.5%

in the 1990s and 7.4% in the 2000s—comparable with the rates for farmed aquatic animals—with production increasing from 3.8 million tons in 1990 to 19 million tons in 2010. Cultivation has overshadowed production of algae collected from the wild, which accounted only for 4.5% of total algae production in 2010. The total value of farmed aquatic algae in 2010 was estimated at US $5.7 billion. A few species dominate algae culture, with 98.9% of world production in 2010 coming from Japanese kelp (*Saccharina japonica* syn. *Laminaria japonica*, Ochrophyta, Phaeophyceae) (mainly in the coastal waters of China), *Eucheuma* seaweeds (a mixture of *Kappaphycus alvarezii* (Rhodophyta, Florideophyceae), formerly known as *Eucheuma cottonii*, and *Eucheuma* spp.), *Gracilaria* spp., *nori/laver* (*Porphyra* spp.), *wakame* (*Undaria pinnatifida*, Ochrophyta, Phaeophyceae), and unidentified marine macroalgae species (3.1 million tons, mostly from China). The remainder consists of marine macroalgae species farmed in small quantities (such as *Caulerpa* spp., Chlorophyta, Ulvophyceae) and microalgae cultivated in freshwater. Large-scale commercial production of microalgae biomass is limited to *Arthrospira*, *Dunaliella* (Chlorophyta, Chlorophyceae), *Haematococcus* (Chlorophyta, Chlorophyceae), and *Chlorella* (Chlorophyta, Trebuxiophyceae), which are cultivated in open ponds at farms located around the world.

These algae are a source for viable and inexpensive carotenoids, pigments, proteins, and vitamins that can be used for the production of nutraceuticals, pharmaceuticals, animal feed additives, and cosmetics.

SOURCES AND USES OF ALGAE

Human Food

Cyanobacteria

Some *Nostoc* species are regionally being used as food and herbal ingredients. *Ge-Xian-Mi* has been regarded as *Nostoc sphaeroides*; however, its taxonomic identity remains controversial. This *Nostoc* species has been used as a delicacy for hundreds of years and is found in rice fields from December to May in Hubei, China. Colonies of *Ge-Xian-Mi* are dark green and pearl-shaped, develop from hormogonia, and can reach 2.5 cm in diameter. Dried *Nostoc* spp. balls are sold in Asian markets; they are stir-fried sautéed with oysters, and used in soups and as thickeners for other foods.

Another species is *Nostoc flagelliforme* Bornet et Flahault, a terrestrial cyanobacterium that naturally grows on arid and semiarid steppes in the Northern and the Northwestern parts of China, where it is considered an edible delicacy with significant medicinal and great economic values. The Chinese have used it as food for about 2000 years, as told in an old text dating back to the Jin Dynasty (AD 265–316). Its herbal values were recognized more than 400 years ago as recorded with other economic *Nostoc* species in "Compendium of Materia Medica" of 1578. *N. flagelliforme* is called *Fah Tsai* (hair vegetable) in Chinese because of its hair-like appearance. However, the pronunciation of *Fah Tsai* sounds like another Chinese word that means to be fortunate and get rich. Therefore, it symbolizes additionally good luck. *N. flagelliforme* has been consumed in China, especially in Guangdong, and among the overseas Chinese on account of its food and herbal values as well as its spiritual image.

Since this cyanobacterium has been collected and traded from old times, the resource is getting less and less, as the market demand increases with economic growth. People gather it by tools, which more or less destroy the vegetation, and in addition to this loss by harvesting, pasturing of cattle is rapidly diminishing the resource. On the other hand, exploitation of land has greatly reduced the area producing *N. flagelliforme*, and the quality of the product is degrading. Hence, recently the Chinese government has prohibited further collection for the sake of environmental protection.

Also *Arthrospira* has a history of human consumption, which can be located essentially in Mexico and in Africa. About 1300 AD, the Aztecs harvested *Arthrospira* from Lake Texcoco, near Tenochtitlan (today Mexico City) and used it to make a sort of dry cakes called *tecuitlatl*, which were sold in markets all over Mexico, and were commonly eaten with maize, and other cereals, or

in a sauce called *chilmolli* made with tomatoes, chilli peppers, and spices. Very likely the use of *Arthrospira* as food in Chad dates back to the same period, or even earlier, to the Kanem Empire (ninth century AD), indicating that two very different and very distant populations discovered independently the food properties of *Arthrospira*. Human consumption of this cyanobacterium in Chad was reported for the first time in 1940 by the French phycologist Dangeard in the little known *Journal of the Linnean Society of Bordeaux*. He wrote about an unusual food called *dihé* and eaten by the Kanembu of Chad, and concluded that it was a purée of the filamentous cyanobacterium *Arthrospira platensis*. However, at that time, his report failed to capture the attention it deserved because of the war. In 1966, the botanist Leonard, member of the 1964–1965 Belgian Trans-Saharan Expedition, confirmed the observations of Dangeard. He reported finding a greenish, edible substance being sold as dry cakes in the market of Fort-Lamy (today N'Djamena, the capital of Chad). His investigation revealed that these greenish cakes, called *dihé*, were a common component of the diet of the Kanembu populations of Chad and Niger, and that they were almost entirely composed of *Arthrospira*, blooming naturally in the saline-soda lakes of the region. Like *tecuitlatl*, *dihé* was commonly eaten as a thick, pungent sauce made of chilli peppers, and spices, poured over millet, the staple of the region. In 1976, Delpeuch and his collaborators of ORSTOM (Office de la Recherche Scientifique et Technique Outre-mer, Paris, France) carried out a study on the nutritional and economic importance of *dihé* for the populations of the Prefectures of Kanem and Lac in Chad. The use of *Arthrospira* by Kanembu was mentioned again in 1991 in a Canadian survey of food consumption and nutritional adequacy in wadi zones of Chad, which suggested that *dihé* makes a substantial contribution to vitamin A intake.

Arthrospira is still harvested and consumed by the Kanembu who live around Lake Kossorom, a soda lake at the irregular northeast fringe of Lake Chad, in the Prefecture of Lac. *Arthrospira* is harvested from Lake Kossorom throughout the year, with a minimum yield in December and January, and a maximum between June and September during the rainy season. The bloom is present as a thick bluish-green mat floating onto the surface of the lake only few hours a day, early in the morning. When the sun is high, the temperature of the water rises, and the bloom disperses, and therefore the harvesting begins at sunrise and it is over in about 2 h.

Only Kanembu women carry out the harvesting; men are banned from entering the water, since it is a deep-rooted belief that they would make the lake barren. The harvesting begins early in the morning, and the work is coordinated by an old woman (the captain), who is responsible for guarding the lake even when the harvesting is over. Just before harvesting begins, the women form a line along the shore at positions assigned to them by the captain according to the village they come from, so as to avoid overcrowding in areas where the alga bloom is more abundant and where trampling and muddying of the water would reduce the quality of *dihé*. The harvesting is carried out according to the rules and procedures handed down from mother to daughter from time immemorial. With their basins, the women skim off the bluish-green mat that floats at the surface of the water, especially along the shore, and pour it into twine baskets, which act as primary filters, or directly into jars (Figure 7.1a and b). In about 2 h, the harvesting is over, and the women move to sandy areas close to the lake for the filtration and drying of the alga. The women dig round holes, 40–50 cm in diameter and about 5-cm in deep, in the sand and line them with clean sand, which is patted to obtain a smooth, firm surface. The algal suspension is then carefully poured into the holes, and the surface of the biomass is smoothed with the palm of the hand. Within a few minutes, almost all of the extracellular water will have seeped out of the biomass, and the *dihé* is then cut into 8–10 cm squares, 1–1.5-cm thick, and removed from the holes as soon as it is firm enough for the squares to be handled without breaking (Figure 7.1c–f). The drying is completed on mats under the sunlight. *Dihé* is traded in the local markets, and in the markets of the main towns of Chad, from where it can also be taken across the borders of Chad to Nigeria, Cameroon, and other countries. It is estimated that about 40 tons of *dihé* are harvested from this lake Kossorom every year, corresponding to a local trading value of more than US $100,000, which represents an important contribution to the economy of one of the poorest nations in the world.

FIGURE 7.1 (a, b) Harvesting of *Artrosphyra* bloom from Lake Kossorom. (c–f) Drying of *Artrosphyra* and preparation of dihé on the shore of Lake Kossorom. (Courtesy of Dr. Gatuger Abdulqader.)

Dihé is mainly used to prepare *la souce*, a kind of vegetable broth served with corn, millet, or sorghum meal, which occasionally can have fish or meat as additional ingredients. Well-dried *dihé* is crumbled in a bowl either by hand or with a mortar and pestle; cold water is then added to disperse the lumps, and the suspension is strained through a fine sieve to remove such solid impurities as sticks, grass, and leaves. The suspension is poured away from most of the sand that settles to the bottom of the bowl. The cleaned *dihé* is cooked for 1–1.5 h, which further disperses the lumps, yielding a bluish-green broth that still contains small amounts of plant debris and sand. This broth is transferred into a bowl, left to settle for 5–10 min to allow for sedimentation of any residual sand, strained very carefully once more, and then poured over sautéed onions. Salt, chili peppers, bouillon cubes, and *gombo* (*Hibiscus esculentus*, Malvaceae) are added, and *la souce* is then simmered and occasionally stirred until cooked.

A minor utilization of *dihé* is as a remedy applied onto wounds to speed up the healing process, or as a poultice to soothe the pain and reduce the swelling of mumps.

Arthrospira biomass has a high content of protein, about 55–60% of the dry matter, with respect to other food such as milk, eggs, etc. The proteins are low in lysine and sulfured amino acids such as methionine and cysteine, but their amount is much higher than in other vegetables, including legumina. Phycobiliproteins represent a major portion of proteins, and among them phycocyanin can reach 7–13% of the dry matter; carbohydrates reach 10–20% of the dry weight and consist mainly of reserve products, whereas lipids account for 9–14% of the dry weight. The mineral fraction

represents 6–9% of the dry biomass, rich in K, P, Na, Ca, Mn, and Fe. Group A, B, and C vitamins are also present, with an average β-carotene content of 1.5 mg per gram of *Arthrospira*, corresponding to 0.25 μg of vitamin A. Considering a recommended dietary allowance (RDA) of vitamin A of about 800 μg, and taking into account a natural 20–30% decrease in β-carotene level due to *dihé* storing conditions, we can say that a daily consumption of 5 g of *dihé* would provide about 100% of RDA.

Rhodophyta

Porphyra (Bangiophyceae) is popularly known as *nori* in Japan, *Kim* in Korea, and "Zicai" in China (see Figures 1.1c and 1.33). It is among the most nutritious macroalgae, with a protein content of 25–50%, and about 75% of that is digestible. This alga is an excellent source of iodine, other trace minerals, and dietary fibers. Sugars are low (0.1%), and the vitamin content is very high, with significant amounts of vitamins A, B complex, and C, but the shelf life of vitamin C can be short in the dried product. During processing, to produce the sheets of *nori*, most salt is washed away, so the sodium content becomes low. The characteristic taste of *nori* is caused by the large amounts of three amino acids: alanine, glutamic acid, and glycine. It also contains taurine, which controls blood cholesterol levels. The alga is a preferred source of the red pigment R-phycoerythrin, which is utilized as a fluorescent "tag" in the medical diagnostic industry.

Porphyra has been cultivated in Japan and the Republic of Korea since the seventeenth century, because even at that time natural stocks were insufficient to meet demand. Today *Porphyra* is one of the largest aquaculture industries in Japan, Korea, and China. Because of its economic importance and other health benefits, *Porphyra* cultivation is now being expanded to other countries.

Porphyra species are primarily intertidal, occurring mainly in temperate zones around the world, but also in subtropical and sub-Arctic regions, as confirmed by its history of being eaten by the indigenous peoples of northwest America (Alaska) and Canada, Hawaii, New Zealand, and parts of the British Isles. *Porphyra abbottae* Krishnamurthy is a nutritionally and culturally important species of red alga used by First Peoples of coastal British Columbia and neighboring areas, down to northern California. This species, along with *Porphyra torta* and possibly others, is a highly nutritious food, still gathered in quantity today by the Coast Tsimshian, Haida, Heiltsuk, Kwakwaka'wakw, and other coastal peoples from wild populations in large quantities, dried, and processed, and served in a variety of ways: toasted as a snack, cooked with clams, salmon eggs, or fish in soup, or sprinkled on other foods as a condiment. Common linguistic origin of the majority of names for this species among some 16 language groups in five language families indicates widespread exchange of knowledge about this seaweed from southern Vancouver Island north to Alaska. The harvesting and preparation of this seaweed is exacting and time-intensive. It necessitates a wide range of knowledge and skills, including an understanding of weather patterns, tides, and currents; an appreciation of the growth and usable life stages of the seaweed; and knowledge of the optimum drying locations and techniques and of the procedures for secondary moistening, chopping, and drying to achieve the best flavors and greatest nutritional value. *P. abbottiae* is generally harvested in May. Though formerly a women's activity, as for dihé harvesting by Kanembu women, both genders now participate in seaweed gathering. The postharvest preparation and handling of the seaweed are fairly labor-intensive and detailed. Once processed, seaweed is considered "an expensive and prestigious food" and is valued as a gift or trade item that is often exchanged for equally valuable products from other groups, especially on the central and northern coasts of British Columbia and Alaska. *P. abbottiae* is valued also for its medicinal properties as a gastrointestinal aid, taken either as a decoction or applied as a poultice for any kind of sickness in the stomach, and also as an orthopedic aid applied on broken collar bones.

Nearly 133 species of *Porphyra* have been reported from all over the world, which includes 28 species from Japan, 30 from North Atlantic coasts of Europe and America, and 27 species from the Pacific coast of Canada and United States. Seven species have been reported from the Indian coast, but they are not exploited commercially.

Porphyra grows as a very thin, flat, blade, which can be yellow, olive, pink, or purple. It can be either round, round to ovate, obovate, linear or linear lanceolate, from 5 to 35 cm in length. The thalli are either one or two cells thick, and each cell has one or two stellate chloroplasts with a pyrenoid. *Porphyra* has a heteromorphic life cycle with an alternation between an aploid gametophyte consisting of a macroscopic foliose thallus, which is eaten, and a filamentous diploid sporophyte called conchocelis phase (see Figure 1.33). This diploid conchocelis phase in the life cycle was earlier thought to be *Conchocelis rosea*, a shell-boring independent organism. Understanding that these two phases were connected was a major research advance made in 1949 in Britain, when the British phycologist Kathleen Mary Drew-Baker demonstrated in culture that *P. umbilicalis* (L.) Kütz had a diploid conchocelis phase. Until this landmark work, cultivation of *Porphyra* was developed intuitively, by observing the seasonal appearance of spores, but nobody knew where the spores came from, so there was little control over the whole cultivation process. Drew's findings completely revolutionized and transformed the *Porphyra* industry in Japan and subsequently throughout Asia, allowing indoor mass cultivation of the filamentous form in sterilized oyster shells and the seeding of conchospores directly onto nets for out-planting in the sea. All Japanese species of *Porphyra* investigated so far produce the conchocelis phase, which can be maintained for long periods of time in free culture. It grows vegetatively under a wide range of temperature, irradiances, and photoperiods, and it is probably a perennial persistent stage in the life history on many species in nature as well.

Since Drew's time, cultivation has flourished, and now accounts for virtually all the production in China, Japan, and the Republic of Korea. Processing of wet *Porphyra* into dried sheets of *nori* has become highly mechanized, by an adaptation of the paper-making process. Wet *Porphyra* is rinsed, chopped into small pieces, and stirred in a slurry. It is then poured onto mats or frames, draining away most of the water, and the mats are run through a dryer. The sheets are peeled from the mats and packed in bundles of 10 for sale. This product is called *hoshi-nori*, which distinguishes it from *yaki-nori*, which is toasted. *Nori* is mainly used as a luxurious food. It is often wrapped around the rice ball of sushi, a typical Japanese food consisting of a small handful of boiled rice with a slice of raw fish on the top. It can be incorporated into soy sauce and boiled down to give an appetizing luxury sauce. It is also used as a raw material for jam and wine. In China, it is mostly used in soups and for seasoning fried foods. In the Republic of Korea, it has similar uses as that in Japan.

Dried *nori* is in constant oversupply in Japan and producers and dealers are trying to encourage its use in the USA and in other countries. Production and markets in China are expanding, although the quality of the product is not always as good as that from the Republic of Korea and Japan.

The fronds of the red alga *Palmaria* (*Rodimenia*) *palmata* (Florideophyceae) are known as *dulce* (see Figure 1.21); they are eaten raw as a vegetable substitute or dried and eaten as a condiment in North America and Europe (Brittany, Ireland and Iceland). Alaska natives consume the fronds fresh or singed on a hot stove, or add the air-dried fronds to soups and fish head stews. *Palmaria* is found in the eulittoral zone and sometimes the upper sublittoral. It is collected by hand by harvesters plucking it from the rocks at low tide. It is perennial and when either plucked or cut, new growth appears from the edge of the previous season's leaf. It is harvested mainly in Ireland and in the shores of the Bay of Fundy in eastern Canada, and is especially abundant around Grand Manan Island, situated in the Bay of Fundy, in a line with the Canadian–United States of America border between New Brunswick and Maine. The harvest season here is from mid-May to mid-October. After picking, fronds are laid out to sun-dry for 6–8 h; if the weather is not suitable, it can be stored in seawater for a few days, but it would soon deteriorate. Whole dulse is packed for sale in plastic bags, at 50 g per bag. Inferior dulse, usually because of poor drying, is broken into flakes or ground into powder for use as a seasoning. In Ireland, it is sold in packages and looks like dark-red bundles of flat leaves. It is eaten raw in Ireland, like chewing tobacco, or is cooked with potatoes, in soups, and in fish dishes.

Dulse is a good source of minerals, being very high in iron and containing all the trace elements needed in human nutrition, and also has a high vitamin content. In Canada, one company has

cultivated it in land-based systems (tanks) and promotes it as a sea vegetable with the trade name "Sea Parsley." It is a variant of normal dulse plants, but with small frilly outgrowths different from the normally flat plant. It was found by staff at the National Research Council of Canada's laboratories in Halifax, Nova Scotia, among samples from a commercial dulse harvester.

Chondrus crispus (Florideophyceae), the *Irish moss*, *carrageenan moss*, or *pioca*, has a long history of use in foods in Ireland and in some parts of Europe (Figure 7.2). It is not eaten as such, but used for its thickening quality when boiled in water, because of its carrageenan content. One such example is its use in making "blancmange," a traditional vanilla-flavored pudding. In eastern Canada, the Acadian Seaplants company is cultivating a strain of *C. crispus* and marketing it in Japan as *hana nori* (flower seaweed), a yellow macroalga that resembles the more traditional Japanese *nori* that is in limited supply from natural resources because of overharvesting and pollution. First introduced to the Japanese market in 1996, the dried product, to be reconstituted by the user, was reported to be selling well at the end of 1999, with forecasts of a market valued at tens of millions of US dollars. It is used in macroalgae salads, sushimi garnishings, and as a soup ingredient.

Fresh *Gracilaria* (Florideophyceae) has been collected and sold as a salad vegetable in Hawaii (USA) for several decades. It is known as *ogo*, *ogonori*, or *sea moss*. The mixture of ethnic groups in Hawaii (Hawaiians, Filipinos, Koreans, Japanese, Chinese) creates an unusual demand and supply has at times been limited by the stocks available from natural sources. Now, it is being successfully cultivated in Hawaii using an aerated tank system, producing up to 6 tons of fresh stock per week. Both *limu manauea* and *limu ogo* are sold as fresh vegetables, the latter usually mixed with raw fish. In Indonesia, Malaysia, the Philippines, and Viet Nam, species of *Gracilaria* are collected by coastal people for food. In southern Thailand, an education programme was undertaken to show people how it could be used to make jellies by boiling and making use of the extracted agar. In the West Indies, *Gracilaria* is sold in markets as *sea moss*; it is believed to possess aphrodisiac properties and is also used as a base for a nonalcoholic drink. *Gracilaria* sp. contain (wet weight basis): $6.9 \pm 0.1\%$ total protein, $24.7 \pm 0.7\%$ crude fiber, $3.3 \pm 0.2\%$ total lipid, and $22.7 \pm 0.6\%$ ash. It contains 28.5 ± 0.1 mg of vitamin C per 100 g of wet biomass, $5.2 \pm 0.4\%$ mg of β-carotene per 100 g of dry weight, which correspond to a vitamin A activity of 865 μg. According to the standard

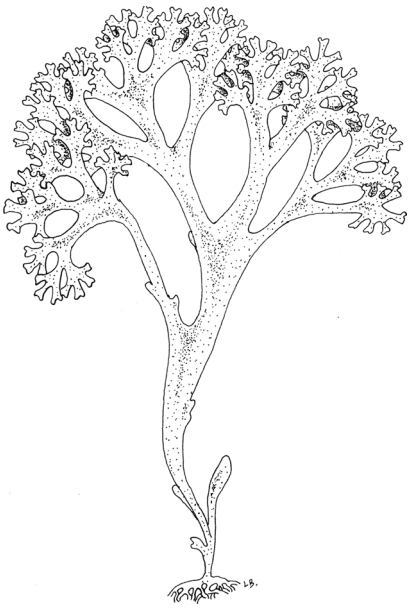

FIGURE 7.2 Frond of *Chondrus crispus*.

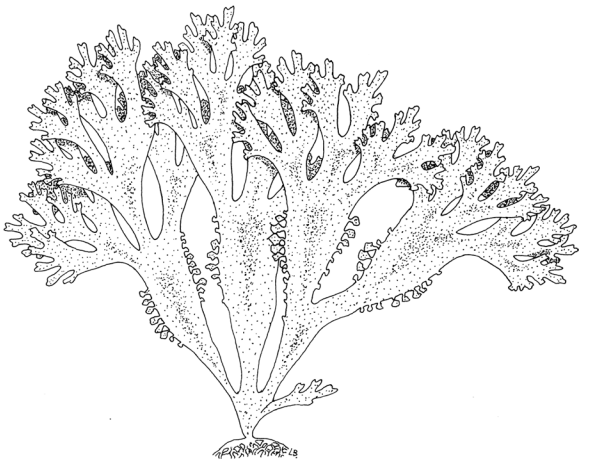

FIGURE 7.3 Frond of *Callophyllis variegata*.

classification adopted by AOAC (Association of Official Analytical Chemists), this can be considered a very high value of vitamin A activity for a food item, which makes *Gracilaria* a potential source of β-carotene for human consumption.

In Chile, the demand for edible macroalgae has increased, and *Gracilaria chilensis* and *Callophyllis variegata* (*carola*) (Florideophyceae) (Figure 7.3) are among the most popular. *G. chilensis* farming is profitable, which has stimulated the research activity in recent years. Several planting techniques have been developed to fasten *Gracilaria* to the substratum, which are commonly used by commercial farms in Chile. As *C. variegata*, this red macroalga has a promising future due to its high commercial value. However, knowledge of its biology is limited, and research projects have been funded for the management of the natural resources and opportunities for cultivation. Carpospores are available during winter, whereas tetraspores are available during spring. Natural populations of *C. variegata* are also being studied to develop management recommendations. From this perspective, it has been demonstrated that the holdfast of this species has a high regeneration capacity, which enables the harvested population to recover.

Ochrophyta (Phaeophyceae)

Alaria esculenta is a large brown kelp that grows in the upper limit of the sublittoral zone (Figure 7.4). It is known as winged kelp. It has a wide distribution in cold waters and does not survive above 16°C. Presumably due to this factor, and rising sea temperatures, this genus has largely disappeared from the English Channel in the past 100 years. It is found in areas such as coasts of the North Atlantic (France, Scotland, Ireland, Greenland, Iceland, northeastern United States, northeastern Canada), the North Sea (England, Norway, Netherlands), the Arctic Sea (Novaya Zemlya), and the North Pacific (Sakhalin and northern Hokkaido). *A. esculenta* is a colonizing species and can form the main canopy in the exposed rocky areas where it grows. Although it is typically not found at a depth more than 8–10 m, it has been recorded at depths over 20 m. Its highest seasonal growth rate can reach 20–25 cm per month. As all kelps, *Alaria* too demonstrate a heteromorphic, sporic life history, with a macroscopic, dominant sporophyte, and a microscopic gametophyte. The sporophyte comprises of a ramified holdfast, an unbranched stipe, and a blade with a percurrent, cartilaginous midrib. Unique to the genus *Alaria* is that the sori of the unilocular sporangia are restricted to certain blades, the sporophylls. Most species, such as *A. esculenta*, are perennial that can live up to 7 years in some locations; after reproduction, the blade sloughs off, leaving the stipe and meristem. The persisting meristem produces a new blade at the beginning of the next growing season.

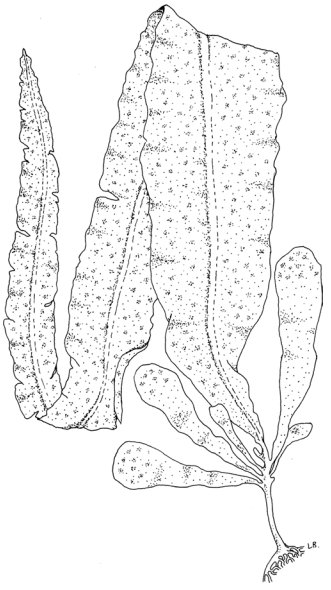

FIGURE 7.4 Frond of *Alaria esculenta*.

Being consumed in Ireland, Scotland (United Kingdom), and Iceland, either fresh or cooked, it is said to have the best protein among the kelps and is also rich in trace metals and vitamins, especially niacin. It is usually collected from the wild and eaten by local people, and although it has been successfully cultivated, this has not been extended to a commercial scale.

China is the largest producer of edible macroalgae, harvesting about 12 million wet tons annually. The greater part of this is for *haidai*, produced from hundreds of hectares of the brown macroalga *Laminaria japonica* (Figure 7.5). It is a large macroalga, usually 2–5-m long, but it can grow up to 10 m in favorable conditions. It requires water temperatures below 20°C. *Laminaria* was originally native to Japan and the Republic of Korea where it is being cultivated since 1730. It was introduced accidentally to China in 1927 probably by the importation of logs from Hokkaido

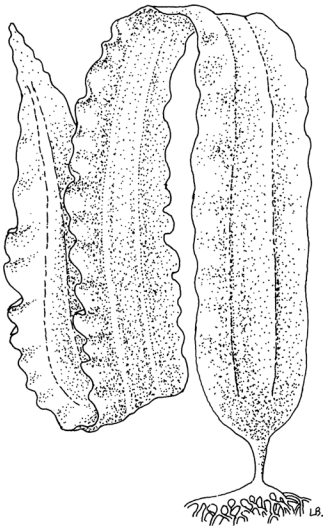

FIGURE 7.5 Frond of *Laminaria japonica*.

in Japan. Prior to that, China had imported its needs from the naturally growing resources in Japan and the Republic of Korea. In the 1950s, China developed a method for cultivating *Laminaria*; sporelings (seedlings) are grown in cooled water in greenhouses and later planted out in long ropes suspended in the ocean. This activity became a widespread source of income for large numbers of coastal families and made China self-sufficient in *Laminaria* leading also to a strong export market. Currently, the yield of kelp from 200,000 acres of farms is about 250,000 dry tons (equivalent to 2,000,000 wet tons) worth about 2 billion Yuan (~326 million US dollars).

In Japan, people consume a dried mixture of *Laminaria* species: *L. longissima*, *L. japonica*, *L. angustata*, *L. coriacea*, and *L. ochotensis.* These algae are all harvested from natural sources, mainly on the northern island of Hokkaido, with about 10% coming from the northern shores of Honshu. The plants grow on rocks and reefs in the sublittoral zone, from 2- to 15-m deep. They prefer calm water at temperatures between 3°C and 20°C. The naturally growing plants are biennial and are ready for harvesting after 20 months. Harvesting is from June to October, using boats. Hooks of various types are attached to long poles and used to twist and break the macroalgae from the rocky bottom. In the 1970s, forced cultivation was introduced, similar to the system developed in China in the early 1950s. Today, about one-third of Japan's requirements come from cultivation, with the remaining two-thirds still coming from natural resources.

For cultivation, *Laminaria* must go through its life cycle, involving an alternation of generations (see Figure 1.32). Seed stock is produced from meiospores released from wild or cultivated sporophytes, incubated in a cool, dark place for up to 24 h. The spores attach to a substratum within 24 h and develop into gametophytes. In 2 months, gametophytes release gametes, fertilization occurs, and sporophytes grow about 6-mm long. Seed stock is reared on horizontal or vertical strings, placed in sheltered waters for about 10 days; after this period, the strings are cut into small pieces that are inserted into the warp of the culture rope. The ropes with the young sporophytes are attached to floating rafts, which can be vertical-line rafts or horizontal-line rafts. The first type consists of a large-diameter rope, 60-m long, whose ends are anchored to a wooden peg driven into the sea bottom. Buoys fixed every 2–3 m keep the rope floating. The ropes with the young sporophytes attached hang down from this rope at 50-cm intervals. The second consists of three ropes laid out parallel, 5-m apart. The ropes with the young sporophytes are tied across two ropes so that they are more or less horizontal, and each of them has equal access to light.

In China, the largest region for *Laminaria* cultivation is in the Yellow Sea, where yields are increased by spray application of nitrogen fertilizer directly on the floating raft areas. In Japan, the cultivation is mainly in the waters between Honshu and Hokkaido islands, rich in nitrogen fertilizers. Harvesting takes place in the summer, from mid-June to early July, when the fronds are laid out in the sun to dry and then packed.

Laminaria species contain about 10% protein, 2% fat, and useful amounts of minerals and vitamins, though generally lower than those found in *nori*. For example, it has one-tenth the amounts of vitamins but three times the amount of iron compared with *nori*. Brown macroalgae also contain iodine, which is lacking in *nori* and other red macroalgae. In China, *haidai* is regarded as a health vegetable because of its mineral and vitamin content, especially in the north, where green vegetables are scarce in winter. It is usually cooked in soups with other ingredients. In Japan, it is used in everyday food, such as a seasoned and cooked *kombu* that is served with herring or sliced salmon.

Another exploited kelp is *Undaria* sp., which together with *Laminaria* sp. is one of the two most economically important edible algae. This alga has been a food item of high value and importance in Japan since 700 AD. Cultivation began in Japan at the beginning of the nineteenth century, when the demand exceeded the wild stock harvest, and was later followed in China. The Republic of Korea began the cultivation around the 1970s and today it is the largest producer of *wakame/quandai-cai* from *U. pinnatifida*, the main species cultivated (Figure 7.6). *U. pinnatifida* grows on rocky shores and bays in the sublittoral zone, down to about 7 m, indigenous to the northwest Pacific Ocean and the cold temperate coastal regions of Japan, China, Korea, and southeast Russia. It grows best between 5°C and 15°C, and stops growing if the water temperature rises above 25°C. *U. pinnatifida*

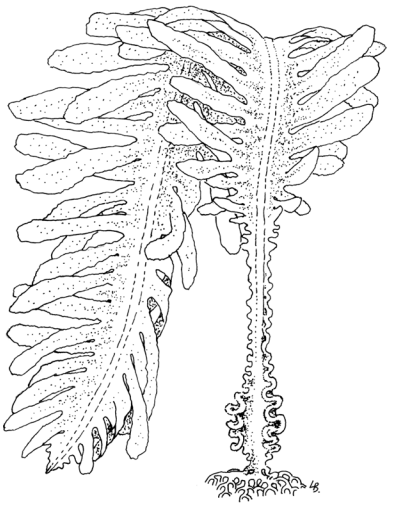

FIGURE 7.6 Frond of *Undaria pinnatifida*.

has been spread around the world by international shipping and mariculture and has extended its range to include four continents since the 1980s. It is now growing in the temperate Pacific Ocean (Australia and New Zealand), the southeastern temperate Indian ocean, the Mediterranean (France, Spain, Italy), and the temperate north and south Atlantic Ocean (United States, Mexico, Argentina, Great Britain, Belgium, and France).

Undaria is an annual plant with a life cycle similar to *Laminaria*. It has an alternation of generations with a large sporophyte and a microscopic gametophyte, and its cultivation method is similar to that of *Laminaria*. The ropes are immersed in seawater tanks containing fertile sporophytes in April–May, when the water temperature is 17–20°C, to let spores attaching to them. The ropes are then lashed to frames submerged in seawater tanks until September–November. When the young plants are 1–2 cm long, and the temperature falls below 15°C, the ropes are removed from the frames and wound around a rope that is suspended by floats and anchored to the bottom at each end. Harvesting begins by thinning out the plants by cutting them off at a point close to the rope. The remaining plants on the rope have plenty of space and continue to grow. Harvesting finishes in April.

After its accidental introduction, cultivation of *Undaria* has been undertaken also in France, where a new technique has been developed and applied. Once the spores have been collected in spring, they are cultivated in laboratories using techniques close to those used for the microalgae. Through precisely controlled light and temperature, the reproducing elements (gametes) are blocked, to the benefit of the cells that give them life (gametophytes). One month before out-planting, the gametophytes are brought to maturation. After fertilization, the solution with the suspended zygotes is sprayed onto a nylon line that is wound around a frame. The zygotes germinate, young sporophytes begin to grow on the frames, and are eventually out-planted on floating ropes in the usual way. It is then possible to produce large quantities of reproducing cells which can then be brought to maturity—any time of the year—to form gametes.

Undaria is processed into a variety of food products. After harvesting, the algae are washed (with seawater and then freshwater), the central midrib is removed, and the pieces are dried; this is *suboshi wakame*. To avoid fading of the color, the fresh fronds are mixed with ash from wood or straw, so that the alkalinity of the ash inactivates the enzymes responsible of the fading. After 2–3 days in the dark, the algae are washed to remove salt and ash (with seawater and then freshwater), the midrib is removed, and the pieces are dried. This is *haiboshi wakame*, which keeps its deep green color for a long time and retains the elasticity of the fresh fronds.

The major *wakame* product is salted *wakame*. Fresh fronds are heated into water at 80°C for 1 min, quickly cooled, dehydrated by 24-h incubation with salt (30% w/w), and then stored at –10°C. When ready for packaging, the midribs are removed, and the pieces placed in plastic bags for sale. It is a fresh green color and can be preserved for long periods when stored at low temperatures.

The crude protein content of *wakame* and *kombu* is 16.3 g% and 6.2 g%, respectively, and both algae contain all essential amino acids, which account for 47.1% of the total amino acid content in *wakame* and for 50.7% in *kombu*. *Wakame* and *kombu* have high contents of β-carotene, that is, 1.30 and 2.99 mg/100 g d.w. or 217 and 481 μg retinol/100 g d.w., respectively. The basic component in sea vegetables is iodine, an essential trace element, and an integral part of two hormones released by the thyroid gland. *Wakame* and *kombu* contain 26 and 170 mg/100 g d.w. of iodine, respectively. The recommended daily dose for adults is 150 μg, meaning that the consumption of 557 mg of *wakame* and 88 mg of *kombu* would satisfy the daily requirement for iodine. The toxic dose of iodine for adults is thought to be over 2000 μg per day. The intake of recommended amount of *wakame* and *kombu* per day would supply 0.94 and 6.29 mg of iodine, respectively, meaning that 1.18 g of *kombu* a day would not exceed the recommended safe dose of iodine. However, it is claimed that iodine supplements can be toxic only if taken in excess, while eating sea vegetables should cause no concern.

Hizikia fusiforme is another brown algae popular as food in Japan and the Republic of Korea known as *hiziki* (Figure 7.7). It grows at the bottom of the eulittoral and top of the sublittoral zones, on the southern shore of Hokkaido, all around Honshu, on the Korean peninsula, and most coasts of the China Sea. Up to 20,000 wet tons were harvested from natural beds in the Republic of Korea in 1984, when cultivation began. Since then, cultivation has steadily increased, on the southwest coast. This medium-dark brown macroalga grows to about 20–30 cm in length; the many-branched long central stipes give an appearance slightly reminiscent of conifer leaves, with a finer frond structure than *wakame* and *kombu*. The protein, fat, carbohydrate, and vitamin contents are similar to those found in *kombu*, although most of the vitamins are destroyed in the processing of the raw macroalgae. The iron, copper, and manganese contents are relatively high, certainly higher than in *kombu*. Like most brown macroalgae, its fat content is low (1.5%) but 20–25% of the fatty acid is eicosapentaenoic acid (EPA).

FIGURE 7.7 Frond of *Hizikia fusiforme*.

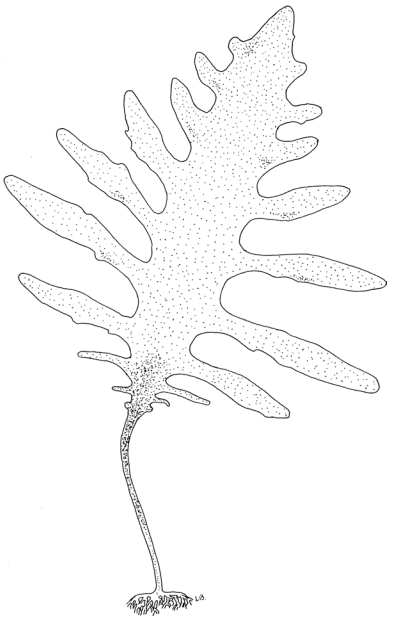

FIGURE 7.8 Frond of *Ecklonia cava*.

Cultivation process is very similar to that of *Undaria* and *Laminaria*. Young fronds collected from natural beds are inserted in a rope at 10-cm intervals. Seeding ropes are attached to the main cultivation rope, kept at a depth of 2–3 m using flotation buoys along the rope anchored to the seabed at each end. Cultivation is from November to May, and harvesting is in May–June.

The harvested fronds are washed with seawater, dried in the sun, and boiled with the addition of other brown macroalgae such as *Eisenia bicyclis* or *Ecklonia cava* (Figure 7.8), which helps removing phlorotannin, which gives *Hizikia* its astringent bitter taste. The resulting product is cut into short pieces, sun-dried, and sold packaged as *hoshi hiziki*. Typically, it is cooked in stir fries, with fried bean curd and vegetables such as carrot or it may be simmered with other vegetables.

Japan also produces *Cladosiphon okamuranus* cultivated around Okinawa Island. This brown macroalga is also harvested from natural populations around the southern islands of Japan and consumed as *mozuku*. It is characterized by a thallus with a stringy not turgid fronds and it can exceed 50 cm in length. *Cladosiphon* grows in the sublittoral zone, mainly at depths of 1–3 m. As *Undaria* and *Laminaria*, its life history involves an alternation of generations. Spores collected from the sporophytes are stored during the summer and used for seeding nets in fall. When young sporophytes have grown to 2–5 cm, the nets are moved to the main cultivation sites. The fronds are harvested after about 90 days, when they have grown to 50 cm. Harvesting is done by divers using a suction pump that draws the macroalgae up and into a floating basket beside the attending boat. The harvested macroalgae are washed, salted with 20–25% salt, and let to dehydrate for about 15 days. Drained fronds are sold in wet, salted form in packages.

Chlorophyta

Monostroma (Ulvophyceae) (Figure 7.9) and *Enteromorpha* (Ulvophyceae) (Figure 7.10) are two green macroalgae cultivated in Japan, and known as *aonori* or *green laver.*

Monostroma latissimum occurs naturally in the bays and gulfs of southern areas of Japan, usually in the upper eulittoral zone. The fronds are bright green in color, flat, and leafy consisting of a single cell layer. They are slender at the holdfast and growing wider toward the apex, often with a slight funnel shape that has splits down the side. *Monostroma* reproduces seasonally, usually during

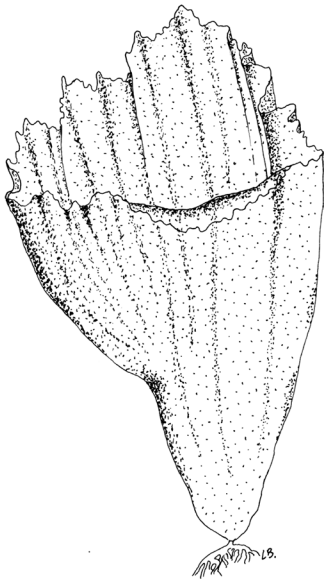

FIGURE 7.9 Frond of *Monostroma latissimum*.

tropical dry season or temperate spring. It is found in shallow seawater usually less than 1 m in depth; generally grows on rocks, coral, mollusk shells, or other hard substrates, but also grows as an epiphyte on sea plants including crops such as *Kappaphycus* and *Eucheuma*. It averages 20% protein and has a useful vitamin and mineral content. It has a life cycle involving an alternation of generations, one generation being the familiar leafy plant, and the other microscopic and approximately spherical. It is this latter generation that releases spores that germinate into the leafy frond. For cultivation, these spores are collected on rope nets by submerging the nets in areas where

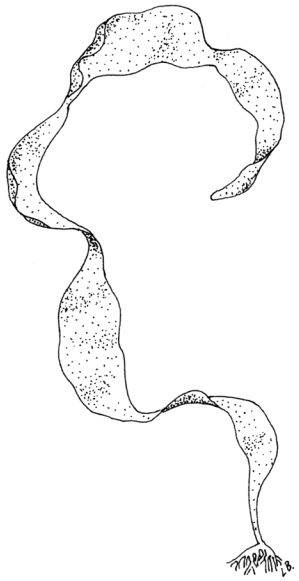

FIGURE 7.10 Frond of *Enteromorpha* sp.

natural *Monostroma* populations grow. The seeded nets are then placed in the bay or estuary, fixed to poles so that they are under water at high tide and exposed for about 4 h at low tide, or using floating rafts in deeper water. The nets are harvested every 3–4 weeks and the growing season allows about 3–4 harvests. The harvested macroalga is washed well in seawater and freshwater. It can then either be processed into sheets and dried, for sale in shops, or dried, either outside or in dryers, and then boiled with sugar, soy sauce, and other ingredients to make "*nori*-jam."

Enteromorpha prolifera and *Enteromorpha intestinalis* are found in bays and river mouths around Japan, and are also found in many other parts of the world, including Europe, North America, and Hawaii. They can thrive in both salt and brackish waters and are usually found at the top of the sublittoral zone. Fronds are usually flat, narrow, and bright green, and they can be attached to firm substrates in clear, shallow waters, and also occur as epiphyte on cultured red seaweeds such as *Kappaphycus*, *Eucheuma*, *Gracilaria*, *Gelidiella*, and others. They contain about 20% protein, little fat, low sodium, high iron, and calcium, and vitamin *B*-group content generally higher than most vegetables. The life history involves an alternation of generations with the same appearance of long, tubular filaments. As for *Monostroma*, rope nets are seeded with spores by submerging them in areas where *Enteromorpha* is growing naturally. Seed collection is from June to September depending on the country, and young plants are visible by early November. Harvesting, by hand or by machine, can be done 2–3 times during the growing period, and harvested fronds are washed in freshwater and dried in large trays.

Ulva sp. (see Figures 1.1r and 1.31) is known as sea lettuce, since fronds may be convoluted and have an appearance rather like lettuce. It is naturally found in shallow seawater usually <1 m in depth, where it grows on rocks, coral, mollusk shells, or other hard substrates but also as an epiphyte on other sea macroalgae. Bright green in color, it is slender at the holdfast and grows wider toward the ape; it reproduces seasonally, during tropical dry season or temperate spring. It can be collected from the wild and added to *Monostroma* and *Enteromorpha* as part of *aonori*. It has a higher protein content than the other two, but much lower vitamin content, except for niacin, which is double that of *Enteromorpha*.

Caulerpa lentillifera (Figure 7.11) and *C. racemosa* (Figure 1.20) are two edible green algae used in fresh salads and known as sea grapes or green caviar because of their appearance, such bunches of green grapes. These algae often produce "runners" under the substrate, which can produce several vertical branches extending above the substrate. They naturally grow on sandy or muddy bottom in shallow protected waters. *C. lentillifera* has been very successfully cultivated in enclosures similar to prawn ponds in the central Philippines, with water temperature ranging between 25°C and 30°C. Pond depth should be about 0.5 m and areas of about 0.5 ha are usual. Also some strains of *C. racemosa* give good yields under pond cultivation conditions.

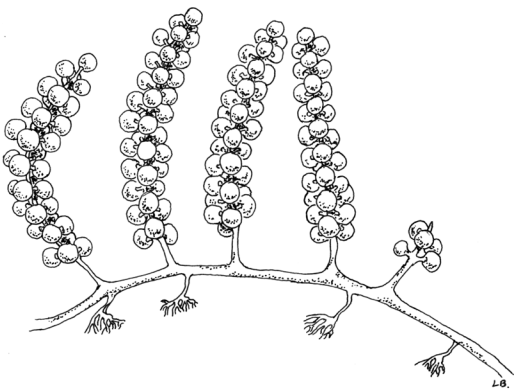

FIGURE 7.11 Frond of *Caulerpa lentillifera*.

TABLE 7.1
Summary of Edible Algae and the Corresponding Food Item

Scientific Name	Common Name	Class
Nostoc flagelliforme	*facai*	Cyanophyceae
Arthrospira sp.	*dihé/ttecuitlatl*	Cyanophyceae
Chondrus crispus	*pioca/irish moss*	Florideophyceae
Porphyra spp.	*nori/laber/zicai*	Bangiophyceae
Porphyra yezoensis	*kim/purple laver*	Bangiophyceae
Palmaria (Rodimenia) palmata	*dulce*	Florideophyceae
Callophyllis variegata	*carola*	Florideophyceae
Asparagopsis taxiformis	*limu kohu*	Florideophyceae
Gigartina spp.	*botelhas*	Florideophyceae
Gracilaria coronopifolia	*manauea*	Florideophyceae
Gracilaria parvisipora	*ogo*	Florideophyceae
Gracilaria verucosa	*ogo-nori/sea moss*	Florideophyceae
Ahnfeltiopsis concinna	*aki aki*	Florideophyceae
Sargassum echinocarpum	*kala*	Pheophyceae
Dictyopteris plagiogramma	*lipoa*	Pheophyceae
Undaria pinnatifida	*wakame/sea mustard/miyeok*	Pheophyceae
Laminaria spp.	*kombu*	Pheophyceae
Nereocystis spp.	*black kelp*	Pheophyceae
Hizikia fusiforme	*hiziki/hijiki*	Pheophyceae
Alaria esculenta	*oni-wakame*	Pheophyceae
Cladosiphon okamuranus	*mozuku*	Pheophyceae
Codium edule	*wawale'iole*	Bryopsidophyceae
Enteromorpha prolifera	*'ele'ele/green laver*	Ulvophyceae
Ulva fasciata	*palahalaha*	Ulvophyceae
Monostroma nitidum	*aonori*	Ulvophyceae
Caulerpa lentillifera	*eka*	Charophyceae

Planting is done by hand, pushing the small plants into the soft bottom of the pond at 0.5–1 m intervals. Two months after, fronds are harvested, leaving about 25% of the plants as seed for the next harvest. Depending on growth rates, harvesting can then be done every 2 weeks. The harvested plants are washed thoroughly in seawater to remove all sand and mud, then sorted and placed in 100–200-g packages; these will stay fresh for 7 days if chilled and kept moist.

Table 7.1 summarizes edible algae and the corresponding food item.

Animal Feed

Microalgae are utilized in aquaculture as live feeds for all growth stages of bivalve molluscs (e.g., oysters, scallops, clams, and mussels), for the larval/early juvenile stages of abalone, crustaceans, and some fish species, and for zooplankton used in aquaculture food chains. Over the last four decades, several hundred microalgae species have been tested as food, but probably <20 have gained widespread use in aquaculture. Microalgae must possess a number of key attributes to be useful aquaculture species. They must be of an appropriate size for ingestion, for example, from 1 to 15 μm for filter feeders and 10–100 μm for grazers and readily digested. They must have rapid growth rates, be amenable to mass culture, and also be stable in culture to any fluctuations in temperature, light, and nutrients as may occur in hatchery systems. Finally, they must

have a good nutrient composition, including an absence of toxins that might be transferred up the food chain.

Successful strains for bivalve culture included *Isochrysis galbana* (Haptophyta, Coccolitophyceae), *Isochrysis* sp. (T.ISO) (Haptophyta, Coccolitophyceae), *Pavlova lutheri* (Haptophyta, Pavlovophyceae) (see Figure 1.1ag), *Tetraselmis suecica* (Chlorophyta, Chlorodendrophyceae) (see Figure 1.1p), *Pseudoisochrysis paradoxa* (Haptophyta, Coccolitophyceae), *Chaetoceros calcitrans* (Ochrophyta, Bacillariophyceae), and *Skeletonema costatum* (Ochrophyta, Bacillariophyceae).

Isochrysis sp. (T.ISO), *P. lutheri*, and *C. calcitrans* are the most common species used to feed the larval, early juvenile, and broodstock (during hatchery conditioning) stages of bivalve molluscs; these are usually fed together as a mixed diet. Many of the strains successfully used for bivalves are also used as direct feed for crustaceans (especially shrimp) during the early larval stages, especially diatoms such as *Skeletonema* spp. and *Chaetoceros* spp. Benthic diatoms such as *Navicula* spp. and *Nitzschia* are commonly mass-cultured and then settled onto plates as a diet for grazing juvenile abalone. *Isochrysis* sp. (T.ISO), *P. lutheri*, *T. suecica*, or *Nannochloropsis* spp. (see Figure 1.1am) are commonly fed to the brine shrip *Artemia* or rotifers, which are then fed on to later larval stages of crustacean and fish larvae.

Microalgal species can vary significantly in their nutritional value, and this may also change under different culture conditions. Nevertheless, a carefully selected mixture of microalgae can offer an excellent nutritional package for larval animals, either directly or indirectly (through enrichment of zooplankton). Microalgae that have been found to possess good nutritional properties—either as monospecies or within a mixed diet—include *C. calcitrans*, *C. muelleri*, *P. lutheri*, *Isochrysis* sp. (T.ISO), *T. suecica*, *S. costatum*, and *Thalassiosira pseudonana* (Ochrophyta, Bacillariophyceae). Several factors can contribute to the nutritional value of a microalga, including its size and shape, digestibility (related to cell-wall structure and composition), biochemical composition (e.g., nutrients, enzymes, toxins if present), and the requirements of the animal feeding on the alga. Since the early reports that demonstrated biochemical differences in gross composition between microalgae and fatty acids, many studies have attempted to correlate the nutritional value of microalgae with their biochemical profile. However, results from feeding experiments that have tested microalgae differing in a specific nutrient are often difficult to interpret because of the confounding effects of other microalgal nutrients. Nevertheless, from examining all the literature data, including experiments where algal diets have been supplemented with compounded diets or emulsions, some general conclusions can be reached.

Microalgae grown to late-logarithmic growth phase typically contain 30–40% protein, 10–20% lipid, and 5–15% carbohydrate. When cultured through to the stationary phase, the proximate composition of microalgae can change significantly; for example, when nitrate is limiting, carbohydrate levels can double at the expense of protein. There does not appear to be a strong correlation between the proximate composition of microalgae and nutritional value, though algal diets with high levels of carbohydrate are reported to produce the best growth for juvenile oysters (*Ostrea edulis*) and larval scallops (*Patinopecten yessoensis*) provided polyunsaturated fatty acids (PUFAs) are also present in adequate proportions. In contrast, high dietary protein provided best growth for juvenile mussels (*Mytilus trossulus*) and Pacific oysters (*Crassostrea gigas*). PUFAs derived from microalgae, that is, docosahexaenoic acid (DHA), EPA, and arachidonic acid (AA) are known to be essential for various larvae.

The fatty acid content showed systematic differences according to the taxonomic group, although there were examples of significant differences between microalgae from the same class. Most microalgal species have moderate to high percentages of EPA (7–34%). Haptophytes (e.g., *Pavlova* spp. and *Isochrysis* sp. (T.ISO)) and cryptomonads are relatively rich in DHA (0.2–11%), whereas eustigmatophytes (*Nannochloropsis* spp.) and diatoms have the highest percentages of AA (0–4%). Chlorophytes (*Dunaliella* spp. and *Chlorella* spp.) are deficient in both C20 and C22 PUFAs, although some species have small amounts of EPA (up to 3.2%). Because of this PUFA deficiency, chlorophytes generally have low nutritional value and are not suitable as a single species diet.

Chlorodendrophyceae as *Tetraselmis* spp. and Mamiellophyceae as *Micromonas* spp. contain significant proportions of C20 or C22, respectively. In the late-logarithmic phase, prymnesiophytes, on average, contain the highest percentages of saturated fats (33% of total fatty acids), followed by diatoms and eustigmatophytes (27%), prasinophytes, and chlorophytes (23%) and cryptomonads (18%). The content of saturated fats in microalgae can also be improved by culturing under high light conditions.

The content of vitamins can vary between microalgae. Ascorbic acid shows the greatest variation, that is, 16-fold (1–16 mg g^{-1} dry weight). Concentrations of other vitamins typically show a two- to four-fold difference between species, that is, β-carotene, 0.5–1.1 mg g^{-1}; niacin, 0.11–0.47 mg g^{-1}; α-tocopherol, 0.07–0.29 mg g^{-1}; thiamin, 29–109 μg g^{-1}; riboflavin, 25–50 μg g^{-1}; pantothenic acid, 14–38 μg g^{-1}; folates, 17–24 μg g^{-1}; pyridoxine, 3.6–17 μg g^{-1}; cobalamin, 1.8–7.4 μg g^{-1}; biotin, 1.1–1.9 μg g^{-1}; retinol, ≤2.2 μg g^{-1}; and vitamin D, <0.45 μg g^{-1}. To put the vitamin content of the microalgae into context, data should be compared with the nutritional requirements of the consuming animal. Unfortunately, nutritional requirements of larval or juvenile animals that feed directly on microalgae are, at best, poorly understood. However, the requirements of the adult are far better known and, in the absence of information to the contrary, will have to serve as a guide for the larval animal. These data suggest that a carefully selected, mixed-algal diet should provide adequate concentrations of the vitamins for aquaculture food chains.

The amino acid composition of the protein of microalgae is very similar between species and relatively unaffected by the growth phase and light conditions. Further, the composition of essential amino acids in microalgae is very similar to that of protein from oyster larvae (*C. gigas*). This indicates that it is unlikely that the protein quality is a factor contributing to the differences in nutritional value of microalgal species.

Sterols, minerals, and pigments also may contribute to nutritional differences of microalgae.

A common procedure during the culture of both larval fish and prawns is to add microalgae (i.e., "green water") to intensive culture systems together with the zooplankton prey. Addition of the microalgae to larval tanks can improve the production of larvae, though the exact mechanism of action is unclear. Theories advanced include (a) light attenuation (i.e., shading effects), which have a beneficial effect on larvae, (b) maintenance of the nutritional quality of the zooplankton, (c) an excretion of vitamins or other growth-promoting substances by algae, and (d) a probiotic effect of the algae. Most likely, the mechanism may be a combination of several of these possibilities. Maintenance of NH_3 and O_2 balance has also been proposed, though this has not been supported by experimental evidence. The most popular algae species used for green water applications are *N. oculata* and *T. suecica*. More research is needed on the application of other microalgae, especially those species rich in DHA, to green water systems. Green water may also be applied to extensive outdoor production systems by fertilizing ponds to stimulate microalgal growth, and correspondingly, zooplankton production, as food for larvae introduced into the ponds.

For a long time, animals such as sheep, cattle, and horses that lived in coastal areas have eaten macroalgae, especially in those European countries where large brown macroalgae were washed ashore. Today, the availability of macroalgae for animals has been increased with the production of macroalgae meal: dried macroalgae that has been milled to a fine powder. In the early 1960s, Norway was among the early producers of macroalgae meal, using *Ascophyllum nodosum* (Ochrophyta, Phaeophyceae) (see Figure 1.1aq), a macroalga that grows in the eulittoral zone so that it can be cut and collected when exposed at low tide. France has used *Laminaria digitata*, Iceland both *Ascophyllum* and *Laminaria* species, and the United Kingdom, *Ascophyllum*.

Because *Ascophyllum* is so accessible, it is the main raw material for macroalgae meal, and most experimental work to measure the effectiveness of macroalgae meal has been done on this macroalgae. The macroalgae used for meal must be freshly cut, as drift macroalgae is low in minerals and usually becomes infected with mold. The wet macroalgae is passed through hammer mills with progressively smaller screens to reduce it to fine particles. These are passed through a drum dryer

starting at 700–800°C and exiting at no more than 70°C. It should have a moisture level of about 15%. It is milled and stored in sealed bags because it picks up moisture if exposed to air. It can be stored for about a year. Analysis shows that it contains useful amounts of minerals (potassium, phosphorus, magnesium, calcium, sodium, chlorine, and sulfur), trace elements, and vitamins. Trace elements are essential elements needed by humans and other mammals in smaller quantities than iron (approximately 50 mg/kg body weight), and include zinc, cobalt, chromium, molybdenum, nickel, tin, vanadium, fluorine, and iodine. Because most of the carbohydrates and proteins are not digestible, the nutritional value of macroalgae has traditionally been assumed to be in its contribution of minerals, trace elements, and vitamins to the diet of animals. In Norway, it has been assessed as having only 30% of the feeding value of grains.

Ascophyllum is a very dark macroalga due to a high content of phenolic compounds. It is likely that the protein is bound to the phenols, giving insoluble compounds that are not attacked by bacteria in the stomach or enzymes in the intestine. *Alaria esculenta* is another large brown macroalgae, but much lighter in color and in some experimental trials it has been found to be more effective than *Ascophyllum* meal. It is this lack of protein digestibility that is a distinct drawback to *Ascophyllum* meal providing useful energy content. In preparing compound feedstuffs, farmers may be less concerned about the price per kilogram of an additive; the decisive factor is more likely to be the digestibility and nutritive value of the additive.

In feeding trials with poultry, adding *Ascophyllum* meal had no benefit except to increase the iodine content of the eggs. With pigs, addition of 3% *Ascophyllum* meal had no effect on the meat yield. However, there have been some positive results reported with cattle and sheep. An experiment for 7 years with dairy cows (seven pairs of identical twins) showed an average increase in milk production of 6.8% that lead to 13% more income. A trial involving two groups each of 900 ewes showed that those fed macroalgae meal over a 2-year period maintained their weight much better during winter feeding and also gave greater wool production.

The results of trials reported above and in the suggested reading below leave the impression that macroalgae meal is probably only really beneficial to sheep and cattle. Certainly, the size of the industry has diminished since the late 1960s and early 1970s, when Norway alone was producing about 15,000 tons of macroalgae meal annually. Australia, Canada, Ireland, Norway, United Kingdom, and United States of America use macroalgae meal as a feed additive for sheep, cattle, horses, poultry, goats, dogs, cats, emus, and alpacas. In fish farming, wet feed usually consists of meat waste and fish waste mixed with dry additives containing extra nutrients, all formed together in a doughy mass. When thrown into the fish ponds or cages, it must hold together and not disintegrate or dissolve in the water. A binder is needed; sometimes a technical grade of alginate is used. It has also been used to bind formulated feeds for shrimp and abalone. However, still cheaper is the use of finely ground macroalgae meal made from brown macroalgae; the alginate in the macroalgae acts as the binder. The binder may be a significant proportion of the price of the feed, so macroalgae meal is a much better choice. However, since the trend is to move to dry feed rather than wet, this market is not expected to expand.

There is also a market for fresh macroalgae as a feed for abalone. In Australia, the brown macroalgae *Macrocystis pyrifera* (Ochrophyta, Phaeophyceae) (Figure 7.12) and the red macroalgae *Gracilaria edulis* (Rhodophyta, Florideophyceae) have been used. In South Africa, *Porphyra* (Rhodophyta, Bangiophyceae) is in demand for abalone feed, and recommendations have been made for the management of the wild population of the macroalgae. Pacific *dulse* (*Palmaria mollis*, Rhodophyta, Florideophyceae) has been found to be a valuable food for the red abalone, *Haliotis rufescens*, and development of land-based cultivation has been undertaken with a view to producing commercial quantities of the macroalgae. The green macroalgae, *Ulva lactuca* (Chlorophyta, Ulvophyceae), has been fed to *Haliotis tuberculata* and *H. discus*. Feeding trials showed that abalone growth is greatly improved by high protein content and this is attained by culturing the macroalgae with high levels of ammonia present.

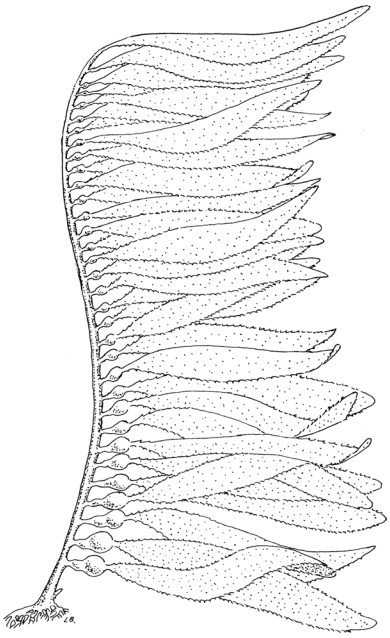

FIGURE 7.12 Frond of *Macrocystis pyrifera*.

Extracts

The principal commercial seaweed extracts continue to be the three hydrocolloids: agar, alginates (derivative of alginic acid), and carrageenans, which are extracted from various red and brown macroalgae. A hydrocolloid is a noncrystalline substance with very large molecules, which dissolves in water to give a thickened (viscous) solution. The processed food industry is still the primary market for the seaweed hydrocolloids where they serve as texturing agents and stabilizers of certain products, such as ice-cream (they inhibit the formation of large ice crystals, allowing the ice-cream to retain a smooth texture); agar and its derivative products agarose and bacteriological agar have long enjoyed attractive markets such as microbiological and electrophoresis media, respectively. Alginates continue to be used in textile printing, paper coating, and other relatively low-margin industrial applications, but their use in restructured meat products for pet and human foods offer better profit margins. Interest is growing in the use of alginate beads for controlled drug release and this could develop into a profitable niche market. Carrageenan has long enjoyed a small share of the personal care toothpaste binder market and has started to make inroads into cosmetics and pharmaceuticals, for example, drug capsules and excipient formulations.

The use of macroalgae as a source of these hydrocolloids dates back to 1658, when the gelling properties of agar, extracted with hot water from a red macroalgae, were first discovered in Japan. Extracts of Irish moss (*Chondrus crispus*; Figure 7.2), another red macroalgae, contain carrageenan and were popular as thickening agents in the nineteenth century. It was not until the 1930s that extracts of brown macroalgae, containing alginate, were produced commercially and sold as thickening and gelling agents. Industrial uses of macroalgae extracts expanded rapidly after the Second World War, but were sometimes limited by the availability of raw materials. Once again, research into life cycles has led to the development of cultivation industries that now supply a high proportion of the raw materials for some hydrocolloids. Today, approximately 1 million tons of wet macroalgae are harvested annually and extracted to produce the above three hydrocolloids. In 2009, total hydrocolloid sales volume was about 87,000 tons, for a value of more than 1000 million US dollars.

There are a number of artificial products reputed to be suitable replacements for macroalgae gums but none have the exact gelling and viscosity properties of macroalgae gums and it is very unlikely that macroalgae will be replaced as the source of these polysaccharides in the near future.

Agar

Agar, a general name for polysaccharides extracted from some red algae, is built up of alternating D- and L-galactopyranose units. The name agar is derived from a Malaysian word *agar-agar*, which literally means "macroalgae." As the gelling agent *kanten*, it is known from Japan since the 17th century; extracts from red macroalgae were carried up the mountains to freeze overnight so that water and other impurities could be extracted from the material. Agar finds its widest use as a solid microbiological culture substrate. Modern agar is a purified form consisting largely of the neutral fraction known as agarose; the nonionic nature of the latter makes it more suitable for a range of laboratory applications. Agar in a crude or purified form also finds wide usage in the food industry where it is used in various kinds of ices, canned foods, and bakery products.

The higher-quality agar (bacteriological-grade agar) is extracted from species of the red algal genera *Pterocladia* (Florideophyceae) and *Gelidium* (Florideophyceae) (Figure 7.13), which are harvested by hand from natural populations in Spain, France, Portugal, Morocco, the Azores, California, Mexico, New Zealand, South Africa, India, Indonesia, the Republic of Korea, Chile, and Japan. Agars of lesser quality (food-grade agar) are extracted from *Gracilaria* and *Hypnea* (Florideophyceae) species. *Gelidium* is a small, slow-growing alga and, while efforts to cultivate it in tanks and ponds have been biologically successful, they have generally proved uneconomic. *Gracilaria* species were once considered unsuitable for agar production because the quality of the agar was poor. In the 1950s, it was found that pretreatment of the macroalgae with alkali before extraction lowered the yield but gave a good-quality agar. This allowed expansion of the agar industry, which had been previously limited by the available supply of *Gelidium*, and led to the harvesting of a variety of wild species of *Gracilaria* in countries such as Argentina, Chile, Indonesia, and Namibia. Chilean *Gracilaria* was especially useful, but evidence of over-harvesting of the wild crop

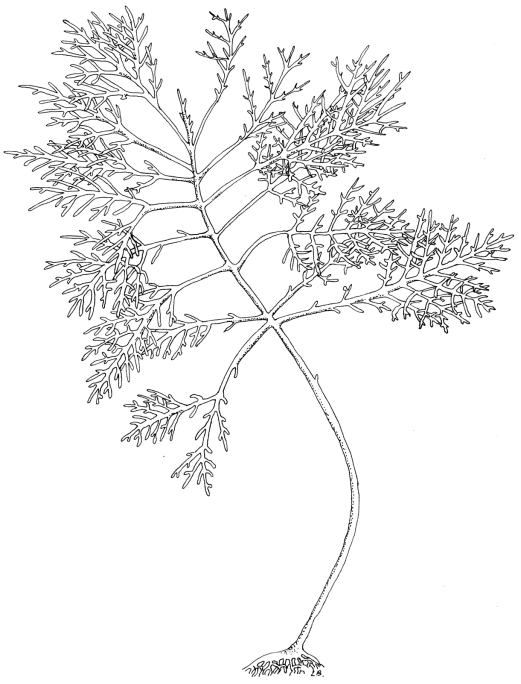

FIGURE 7.13 Frond of *Gelidium* sp.

soon emerged. Cultivation methods were then developed, both in ponds and in the open waters of protected bays. These methods have since spread beyond Chile to other countries, such as China, Indonesia, the Republic of Korea, Namibia, the Philippines, and Vietnam, usually using species of *Gracilaria* native to each particular country. *Gracilaria* species can be grown in both cold and warm waters. Today, the supply of *Gracilaria* still derives mainly from the wild, with the extent of cultivation depending on price fluctuations.

Strong-gelling agar is extracted directly from *Gelidium* with a dilute acid solution to break down cell walls in a pressure cooker, whereas extracting strong-gelling agar from *Gracilaria* requires the use of a boiling alkali solution. The alkali treatment converts the galactose 6-SO_4 to 3,6-anhydrogalactose, well-known chemistry that "de-kinks" the polygalactose molecules and enhances the gelling process. These process differences explain why it is difficult to optimize the production of agar from both seaweeds in the same process line.

Currently, two companies have emerged as undisputed leaders within the industry: Algas Marinas in Chile and Agarindo Bogatama in Indonesia; between them, they are producing about 3600 tons $year^{-1}$ or about 38% of current production. Other strong producers are Setexam in Morocco, MSC Co. in Korea, Hispanagar in Spain, and Huey Shyang Seaweed Industrial Company in China. These six companies account for about 5500 tons $year^{-1}$ of production/sales or 57% of current total market. Some European producers have also chosen to expand production outside their home country. B & V from Italy has production interests in Indonesia and Morocco (although production there has been recently curtailed). Hispanagar, with some existing overseas operations, has started up activities in China as well.

Alginates

Alginates are cell-wall constituents of brown algae (Phaeophyceae). They are chain-forming heteropolysaccharides made up of blocks of mannuronic acid and guluronic acid. Composition of the blocks depends on the species being used for extraction and the part of the thallus from which extraction is made. Extraction procedures probably also affect alginate quality. Alginates of one kind or another seem to be present in most species of brown algae but they occur in exploitable quantities (30–45% d.w.) only in the larger kelps and wracks (Laminariales and Fucales). The more useful brown macroalgae grow in cold waters, thriving best in waters up to about 20°C. Brown macroalgae are also found in warmer waters, but these are less suitable for alginate production and are rarely used as food. A wide variety of species are used, harvested in both the Northern and Southern hemispheres.

Alginates of commerce are primarily the alkali or alkaline earth salts of alginic acid, the sodium salt being the most widely used in foods. The only other derivative of alginic acid that is used in the food industry is propylene glycol alginate. The ammonia and alkali metal salts of alginic acid readily dissolve in cold water at low concentrations to give viscous solutions. Alginates, especially sodium alginate, are widely used in the textile industry because they form an excellent dressing and polishing material. Calcium alginate, which is insoluble in water, has been used in the manufacture of a medical dressing very suitable for burns and extensive wounds where a normal dressing would be extremely difficult to remove; calcium alginate is extruded to make a fiber which is then woven into a gauze-like product; alginates with a high proportion of guluronic acid blocks are most suitable for this purpose. When applied to either a wound or burn, a network is formed around which a healthy scab may form; the bandage may be removed with a sodium chloride solution, which renders the alginate soluble in water. Alginates are also used as a thickening paste for colors in printing textiles, as a hardener and thickener for joining threads in weaving; the alginates may subsequently be dissolved away, giving special effects to the material. Other uses include glazing and sizing paper, special printers' inks, paints, cosmetics, insecticides, and pharmaceutical preparations. In the USA, alginates are frequently used as stabilizers in ice-cream, giving a smooth texture and body, and also as a suspending agent in milk shakes. Alginates take up atomically heavy metals in a series of affinities; for example, lead and other heavy metals will be taken up in preference to sodium, potassium, and other "lighter" metals; accordingly, alginates are useful in lead and strontium-90 poisoning.

Twenty-five to thirty years ago, almost all extraction of alginates took place in Europe, USA, and Japan. The major change in the alginates industry over the last decade has been the emergence of producers in China in the 1980s. Initially, production was limited to low-cost, low-quality alginate for the local industrial markets produced from locally cultivated *Laminaria* (Saccharina) *japonica*. By the 1990s, producers in China were competing in Western industrial markets for alginates, primarily based on low cost.

Some 35,000 tons of alginates per annum are extracted worldwide. Alginate manufacturing in the USA has ceased to exist, whereas Europe (mainly Scotland and Norway) is still able to maintain a fairly substantial part of their alginate industry even though Europe is a high-cost production region. This is primarily due to FMC company's ability to increase their market share of high-quality, specialty grades of alginates being sold in developed countries. Of the 8900 tons $year^{-1}$ of alginates still being produced in Europe, two-thirds is being produced by FMC in its Norway facility. Asia-Pacific, on the other hand, is where the real capacity growth has taken place, but at the same time markets for this capacity is mostly in the Asia-Pacific region.

About 15 years ago, *Ascophyllum nodosum* and *Macrocystis pyrifera* accounted for 58% of the harvest, while today *Laminaria* and *Lessonia* species are dominant, accounting for 81% of the world harvest. Ireland, Scotland, Iceland, France, and Canada possess substantial resources of *A. nodosum* seaweed, but this species is now relatively costly to harvest, and the extract quality is not competitive with other species, so hardly any is being used today. In addition, special *A. nodosum* extracts are finding new, more profitable markets as a source of animal and plant nutrients and growth promoters. The giant kelp *M. pyrifera* was in the past an important raw material for the alginate industry, particularly Kelco in San Diego (Figure 7.12); it was harvested from large offshore beds off the coasts of California and Mexico. *Macrocystis* has the distinction of being the largest macroalga in the world; the largest attached plant recorded was 65-m long and the plants are capable of growing at up to 50 cm per day.

A. nodosum and *Laminaria hyperborea* are used in Norway and Scotland. *Ascophyllum* is sustainably harvested in Ireland to produce macroalgae meal that is exported to Scotland for alginate extraction. Norway processes *Laminaria hyperborea*, manufacturing high-quality alginates.

Carrageenan

Of the three categories of hydrocolloids under consideration, carrageenan is the most difficult to characterize, mainly because of its chemical complexity. This polysaccharide built up from D-galactopyranose units only, has many chemical forms: the brittle gel-forming kappa, the elastic gel-forming iota, and the nongelling, but commercially unavailable, lambda. To replace lambda in cold soluble applications, the mu/nu hybrids obtained from Chilean *Gigartina* (Rhodophyta, Florideophyceae) and *Sarcothalia* (Rhodophyta, Florideophyceae) species are used. Alkali treatment of these extracts yields kappa/iota hybrids that find use in dairy and toothpaste products. Kappa carrageenan today is almost exclusively obtained from farmed *Kappaphycus alvarezii* (Rhodophyta, Florideophyceae) and iota from farmed *Eucheuma denticulatum* (Rhodophyta, Florideophyceae).

The word carrageenan is derived from the colloquial Irish name for this macroalgae, carrageen (from the Irish place name, probably Carrigeen Head in Co. Donegal, Carraigín; "little rock") and the use of this macroalgae to extract a gel is known in Ireland since 1810. *Chondrus crispus* (Irish moss, Figure 7.2) used to be the sole source of carrageenan, but species of *Eucheuma*, *Ahnfeltia* (Rhodophyta, Florideophyceae), and *Gigartina* are now commonly used. About 50,000 tons of carrageenan are manufactured worldwide, and although *Chondrus* is no longer the unique source, it is still the principal one. Modern carrageenan is a branded product designed, by mixing various types of carrageenan, to give a gel with particular qualities. Most of the *Chondrus* that is used in the carrageenan industry comes from the Maritime Provinces of Canada (Nova Scotia, etc.), where *C. crispus* is harvested from natural populations. The bulk of the harvest is collected using long-handled rakes and dredges from small boats. The macroalgae is then dried, either by spreading and air-drying or by using rotary dryers, and exported to the USA and Denmark for processing.

Carrageenan production was originally dependent on wild macroalgae, especially *C. crispus*, with a limited resource base in France, Ireland, Portugal, Spain, and the east coast provinces of Canada. As the carrageenan industry expanded, the demand for raw material began to strain the supply from natural resources. However, since the early 1970s, the industry has expanded rapidly following the availability of other carrageenan-containing macroalgae that have been successfully cultivated in warm-water countries with low labor costs.

The seaweeds for production of carrageenan are dominated by the warm water species *K. alvarezii* (*cottonii*) and *E. denticulatum* (*spinosum*). Both are being cultivated by vegetative growth primarily in the Philippines and Indonesia with smaller amounts from Tanzania. The other seaweeds being used are cold water species: *Sarcothalia crispata* and *Gigartina skottsbergii* (*Gigartina radula* of commerce) coming mainly from Chile with smaller amounts from Mexico. *C. crispus*, another cold-water carrageenophyte, comes predominantly from Maritimes Canada with smaller amounts from France but is declining in availability and use. None of these cold-water weeds is cultivated, so supply depends entirely on the natural harvest. These cold-water weeds are needed to supply specific types of carrageenan that cannot be obtained from the cultivated, warm water weeds.

Twenty-five years ago, almost all carrageenan extraction took place in Western Europe and USA with the remainder taking place in Asia-Pacific and Latin America. Since then, the situation has changed considerably and in particular with the introduction of human food-grade semi-refined carrageenan (PES). From its start in the mid-1970s, PES has progressively reconfigured the geographic distribution of production facilities as well as increasing the percent of PES being produced.

Table 7.2 summarizes commercially exploited algae and the corresponding extract.

TABLE 7.2
Summary of Commercially Exploited Algae and the Corresponding Extracts

Scientific Name	Class	Extracts
Gracilaria chilensis	Florideophyceae	Agar
Gelidium lingulatum	Florideophyceae	Agar
Pterocladia spp.	Florideophyceae	Agar
Hypnea spp.	Florideophyceae	Agar
Laminaria hyperborea	Phaeophyceae	Alginates
Laminaria digitata	Phaeophyceae	Alginates
Laminaria japonica	Phaeophyceae	Alginates
Laminaria saccarina	Phaeophyceae	Alginates
Macrocystis pyrifera	Phaeophyceae	Alginates
Ascophyllum nodosum	Phaeophyceae	Alginates
Durvillea potatorum	Phaeophyceae	Alginates
Ecklonia spp.	Phaeophyceae	Alginates
Lessonia nigrescens	Phaeophyceae	Alginates
Lessonia trabiculata	Phaeophyceae	Alginates
Ahnfeltia spp.	Florideophyceae	Carrageenan
Chondrus crispus	Florideophyceae	Carrageenan
Gigartina skottsbergii	Florideophyceae	Carrageenan
Gigartina canaliculata	Florideophyceae	Carrageenan
Mazzaella laminaroides	Florideophyceae	Carrageenan
Sarcothalia crispata	Florideophyceae	Carrageenan
Kappaphycus alvarezii	Florideophyceae	Carrageenan
Eucheuma denticulatum	Florideophyceae	Carrageenan
Iridaea spp.	Florideophyceae	Carrageenan

Fertilizers

There is a long history of coastal people using macroalgae, especially the large brown macroalgae, to fertilize nearby land. Wet macroalgae is heavy, so it was not usually carried very far inland, although on the west coast of Ireland enthusiasm was such that it was transported several kilometers from the shore. Generally drift macroalgae or beach-washed macroalgae is collected, although in Scotland farmers sometimes cut *Ascophyllum* exposed at low tide. In Cornwall, UK, the practice was to mix the macroalgae with sand, let it rot, and then dig it in. For over a few hundred kilometers of the coast line around Brittany, France, the beach-cast, brown macroalgae is regularly collected by farmers and used on fields up to a kilometer inland. Similar practices can be reported for many countries around the world. For example, in a more tropical climate like the Philippines, large quantities of *Sargassum* have been collected, used wet locally, but also sun-dried and transported to other areas. In Puerto Madryn, Argentina, large quantities of green macroalgae are cast ashore every summer and interfere with recreational uses of beaches. Part of this algal mass has been composted and then used in trials for growing tomato plants in various types of soil. In all cases, the addition of the compost increased water-holding capacity and plant growth, so composting simultaneously solved environmental pollution problems and produced a useful organic fertilizer.

Macroalgae meal is dried, milled macroalgae, and again it is usually based on the brown macroalgae because they are the most readily available in large quantities. Species of *Ascophyllum*, *Ecklonia*, and *Fucus* (Ochrophyta, Pheophyceae) are the common ones. They are sold as soil additives and function as both fertilizers and soil conditioners. They have a suitable content of nitrogen and potassium, but are much lower in phosphorus than traditional animal manures and the typical N:P:K ratios in chemical fertilizers. The large amounts of insoluble carbohydrates in brown macroalgae act as soil conditioners (improve aeration and soil structure, especially in clay soils) and have good moisture-retention properties. Their effectiveness as fertilizers is also sometimes attributed to the trace elements they contain, but the actual contribution they make is very small compared to normal plant requirements. One company in Ireland that produces milled macroalgae for the alginate industry is developing applications for macroalgae meal in Mediterranean fruit and vegetable cultivation. "Afrikelp" is another example of a commercially available dried macroalgae, sold as a fertilizer and soil conditioner; it is based on the brown macroalgae *Ecklonia maxima* that is washed up on the beaches of the west coast of Africa and Namibia. Like all brown macroalgae, *Ascophyllum* contains alginate, a carbohydrate composed of long chains. When calcium is added to alginate, it forms strong gels. By composting the dried, powdered *Ascophyllum* under controlled conditions for 11–12 days, the alginate chains are broken into smaller chains and these chains still form gels with calcium but they are weaker. The composted product is a dark brown, granular material containing 20–25% of water and it can be easily stored and used in this form. Steep slopes are difficult to cultivate with conventional equipment and are likely to suffer soil loss by runoff. Spraying such slopes with composted *Ascophyllum*, clay, fertilizer, seed, mulch, and water has given good results, even on bare rock. Plants quickly grow and topsoil forms after a few years. The spray is thixotropic, that is, it is fluid when a force is applied to spread it but it sets to a weak gel when standing for a time and sticks to the sloping surface. It holds any soil in place and retains enough moisture to allow the seeds to germinate. Composted *Ascophyllum* has been used after the construction of roads in a number of countries and has found other uses as well.

Maerl is the common name of a fertilizer derived from calcareous red algae; *maerl* beds are characterized by accumulations of living and dead unattached nongeniculate calcareous Florideophyceae (mostly Corallinales such as *Phymatolithon calcareum* and *Lithothamnion corallioides*). Also known as rhodolith beds, these habitats occur in tropical, temperate, and polar environments. In Europe, they are known from throughout the Mediterranean and along most of the Western Atlantic coast from Portugal to Norway, although they are rare in the English Channel, Irish Sea, North Sea, and Baltic Sea. *Maerl* beds are often found in subdued light conditions and their depth limit depends primarily on the degree of light penetration. In the northeast Atlantic, *maerl* beds occur from low in

the intertidal to about 30-m depth; in the West Mediterranean, they are found down to 90–100 m, while in the East they occur down to depths of about 180 m. *Maerl* beds in subtidal waters have been utilized over a long period in Britain, with early references dating back to 1690. In France also, *maerl* has been used as a soil fertilizer for several centuries. Extraction of *maerl*, either from beds where live thalli are present or where the *maerl* is dead or semifossilized, has been carried out in Europe for hundreds of years. Initially, the quantities extracted were small, being dug by hand from intertidal banks, but in the 1970s about 600,000 tons of *maerl* was extracted per annum in France alone. Amounts have declined to about 500,000 tons per annum since then, though *maerl* extraction still forms a major part of the French seaweed industry, both in terms of quantity and value of harvest. Live *maerl* extraction is obviously very problematic with regard to growth rates for replacement. Dead *maerl* extraction is liable to lead to muddy plumes and excessive sediment load in water that later settles out and smothers surrounding communities.

The *maerl* is marketed mainly for use as an agricultural fertilizer, for soil improvement in horticulture, mainly to replace lime as an agricultural soil conditioner. There are conflicting reports on the benefits of *maerl* use as opposed to the use of dolomite or calcium carbonate limestone. Other uses include: as an animal food additive, for biological denitrification and in neutralization of acidic water in the production of drinking water, aquarium gravel as well as in the pharmaceutical, cosmetics, nuclear, and medical industries. These uses are all related to the chemical composition of *maerl*, which is primarily composed of calcium and magnesium carbonates. It is occasionally used for miscellaneous other purposes such as hardcore for filling roads and surfacing garden paths.

Maerl beds are analogous to the sea-grass beds or kelp forests in that they are structurally and functionally complex perennial habitats formed by marine algae that support a very rich biodiversity. The high biodiversity associated with *maerl* grounds is generally attributed to their complex architecture. Long-lived *maerl* thalli and their dead remains build up on underlying sediments to produce deposits with a three-dimensional structure that is intermediate in character between hard and soft grounds. *Maerl* thalli grow very slowly such that *maerl* deposits may take hundreds of years to develop, especially in high latitudes. One of the most obvious threats is commercial extraction, as this has led to the wholesale removal of *maerl* habitats (e.g., from five sites around the coasts of Brittany), while areas adjacent to extraction sites show significant reductions in diversity and abundance. Even if the proportion of living *maerl* in commercially collected material is low, extraction has major effects on the wide range of species present in both live and dead *maerl* deposits. Brittany is the main area for *maerl* extraction with about 500,000 tons extracted annually; smaller amounts are extracted in southwest England and southwest Ireland. *Maerl* beds represent a nonrenewable resource as extraction and disruption far out-strips their slow rate of accumulation. In France, *maerl* extraction is now considered to be "mining" which implies more constraints for the extractors and more controls on the impact of extraction. Scientists, managers, and policy makers have been slow to react to an escalating degradation of these habitats such that there is now an urgent need to protect these systems from severe human impacts.

Macroalgae extracts and suspensions have achieved a broader use and market than macroalgae and macroalgae meal. They are sold in concentrated form, are easy to transport, dilute, and apply, and act more rapidly. They are all made from brown macroalgae, although the species varies between countries. Some are made by alkaline extraction of the macroalgae and anything that does not dissolve is removed by filtration; others are suspensions of very fine particles of macroalgae.

Macroalgae extracts have given positive results in many applications. There are probably other applications where they have not made significant improvements, but these receive less, if any, publicity. However, there is no doubt that macroalgae extracts are now widely accepted in the horticultural industry. When applied to fruit, vegetable, and flower crops, some improvements have included higher yields, increased uptake of soil nutrients, increased resistance to some pests such as red spider mite and aphids, improved seed germination, and more resistance to frost. There have

been many controlled studies to show the value of using macroalgae extracts, with mixed results. For example, they may improve the yield of one cultivar of potato but not another grown under the same conditions. No one is really sure about why they are effective, despite many studies having been made. The trace element content is insufficient to account for the improved yields, etc. It has been shown that most of the extracts contain several types of plant growth regulators such as cytokinins, auxins, and betaines, but even here there is no clear evidence that these alone are responsible for the improvements. Finally, there is the question, are macroalgae extracts an economically attractive alternative to NPK fertilizers? Perhaps not when used on their own, but when used with NPK fertilizers they improve the effectiveness of the fertilizers, so less can be used, with a lowering of costs. Then there are always those who prefer an "organic" or "natural" fertilizer, especially in horticulture, so macroalgae extracts probably have a bright future.

The use of macroalgae as fertilizers dates back at least to the nineteenth century. Early usage was by coastal dwellers, who collected storm-cast macroalgae, usually large brown macroalgae, and dug it into local soils. The high fiber content of the macroalgae acts as a soil conditioner and assists moisture retention, whereas the mineral content is a useful fertilizer and a source of trace elements. In the early twentieth century, a small industry developed based on the drying and milling of mainly storm-cast material, but it dwindled with the advent of synthetic chemical fertilizers. Today, with the rising popularity of organic farming, there has been some revival of the industry, but not yet on a large scale; the combined costs of drying and transportation have confined usage to sunnier climates where the buyers are not too distant from the coast. Liquid macroalgae extracts are the growth area in macroalgae fertilizers. These can be produced in concentrated form for dilution by the user. Several can be applied directly onto plants or they can be watered in, around the root areas. Several scientific studies have proved the effectiveness of these products, and macroalgae extracts are now widely accepted in the horticultural industry. No one is really sure of the reasons for their effectiveness: the trace element content is insufficient to account for the improved yields, for example. In 1991, it was estimated that about 10,000 tons of wet macroalgae were used annually to make 1000 tons of macroalgae extracts with a value of US $5 million. However, since that time the market has probably doubled as the usefulness of these products has become more widely recognized and organic farming has increased in popularity.

Cosmetics

To date, microalgal extracts can be found in many face and skin-care products, for example, anti-aging cream, refreshing, or regenerative care products, sun cream, emollient, and anti-irritant in peelers. Dermochlorella is actually extracted from *Chlorella vulgaris*, which can stimulate collagen synthesis in skin-supporting tissue regeneration and wrinkle reduction. Protulines is a protein-rich extract from *Arthrospira* (*Spirulina*), which helps combat early skin aging, exerting a tightening effect, and preventing wrinkle formation.

More generally, extracts of algae are often found on the list of ingredients on cosmetic packages, particularly in face, hand, and body creams or lotions, but the use of algae themselves in cosmetics, rather than extracts of them, is rather limited.

Milled macroalgae, packed in sachets, are sold as an additive to bath water, sometimes with essential oils being added. Bath salts with macroalgae meal are also sold. Thalassotherapy has come into fashion in recent years, especially in France. In thalassotherapy, macroalgae pastes, made by cold-grinding or freeze-crushing, are applied to the person's body and then warmed under infrared radiation. This treatment, in conjunction with seawater hydrotherapy, is said to provide relief for rheumatism and osteoporosis. Mineral-rich seawater is used in a range of therapies, including hydrotherapy, massage, and a variety of marine mud and algae treatments. One of the treatments is to cover a person's body with a paste of fine particles of macroalgae, sometimes wrap them in cling wrap, and warm the body with infrared lamps. It is said to be useful in various ways, including relief of rheumatic pain or the removal of cellulite. Paste mixtures are also used in massage creams, with

promises to rapidly restore elasticity and suppleness to the skin. The macroalgae pastes are made by freeze-grinding or crushing. The macroalgae is washed, cleaned, and then frozen in slabs. The slabs are either pressed against a grinding wheel or crushed, sometimes with additional freezing with liquid nitrogen that makes the frozen material more brittle and easier to grind or crush. The result is a fine green paste of macroalgae.

There appears to be no shortage of products with ingredients and claims linked to macroalgae: creams, face masks, shampoos, body gels, bath salts, and even a do-it-yourself body wrap kit. The efficacy of these products must be judged by the user. One company recently pointed out that the lifetime of cosmetic products has reduced over the years and now rarely exceeds 3 or 4 years. Perhaps the macroalgae products that are really effective will live longer than this.

Cosmetic products, such as creams and lotions, sometimes show on their labels that the contents include "marine extract," "extract of alga," "macroalgae extract," or similar. This usually means that one of the hydrocolloids extracted from macroalgae has been added. Alginate or carrageenan could improve the skin moisture-retention properties of the product.

FUNCTIONAL FOODS AND NUTRACEUTICALS

There is a strong body of science underpinning health benefits from foods, and new, different, natural sources of so-called "functional foods" and "nutraceuticals" are continuously investigated and tested for their applicability in improving health and reduce risk through prevention. A working definition of functional food was proposed by EC Concerted Action on Functional Food Science in Europe (FUFOSE): a food that beneficially affects one or more target functions in the body beyond adequate nutritional effects in a way that is relevant to either an improved state of health and well-being and/or reduction of risk of disease. It is consumed as part of a normal food pattern. It is not a pill, a capsule, or any form of dietary supplement. A working definition has been recently suggested also for the portmanteau word "nutraceutical," coined in 1989 by Dr. S. De Felice from the terms "nutrition" and "pharmaceutical": a nutraceutical is a food or a part of a food for oral administration with demonstrated safety and health benefits beyond the basic nutritional functions to supplement diet, presented in a nonfood matrix or nonconventional food formats, in such a quantity that exceeds those that could be obtained from normal foods and with such frequency as required to realize such properties, and is labeled as a "nutraceutical." Despite the different definitions, the boundary between functional foods and nutraceuticals is not always clear and the main difference is the format in which they are consumed: functional foods are always consumed as ordinary foods, while nutraceuticals are consumed as pills, tablets, etc.

In this perspective, algae, both micro- and macroalgae (seaweed), are a largely untapped reservoir still to be explored. As already said in the Introduction, algae have a history of consumption all over the world and have made base of eastern countries, such as Japan, Korea, China, Philippines, and Indonesia, diet since prehistorical period, with the earliest recorded use dating back to 2700 BC. In Japan, about 50 species of algae are used as foods, with an estimated annual consumption per person of 1.4 kg. This ancient tradition and everyday habit has made possible a large number of epidemiological researches showing the health benefits linked to algae consumption. Observational data collected in South East Asian populations give a strong indication of the association between algae intake, reduced disease risk, and health outcomes. The Japanese, in particular, have one of the lowest rates of obesity in the world, a life expectancy very long (83 years), low rate of heart-related deaths, and an extraordinarily low rate of certain types of cancer. In contrast, highly caloric diets typical of Western developed countries together with a decrease in physical activity due to a modified sedentary lifestyle have caused an increase in the incidence of obesity and associated comorbidities at an epidemic rate.

Algae can be considered both functional food because of their high-quality nutritional value (protein content, presence of all of the essential amino acids in level sufficient to meet normal nutritional requirements) and nutraceuticals, because of their content in bioactive ingredient, such

as ω-3 essential PUFA (e.g., DHA, EPA), sterols, minerals (e.g., Na, K, Ca, Mg, and iodine), carotenoids (e.g., β-carotene, astaxanthin), essential vitamins (e.g. A, B_1, B_2, C, D, E), polyphenols, and polysaccharides (e.g., alginate, fucoidan, β-glucan). Many of these bioactive ingredients have been tested in clinical trials or are under validation to assess their efficacy in tackling vitality issues, especially in the field of lipid metabolism, oxidative cellular stress, cancer, and neurological and cardiovascular diseases. For example, some of the general effects of algal PUFAs include anti-arteriosclerosis, antihypertension, antiinflammation, and immunoregulation. Pigments and polyphenols have shown bioactivity effect toward cancer, as antioxidant and antiinflammatory; algal polysaccharides, most of which cannot be digested in the human gastrointestinal tract, act as a good source of dietary fibers, which stimulate human health, by creating a better intestinal environment, or because of their hypocholesterolemic and hypolipidemic properties. Because of their precious content of high-value compounds, algae are systematically screened for these substances as exploitable functional food, nutraceutical. Many of these compounds have been tested also as therapeutic supplement.

Table 7.3 shows the main bioactive compounds present in algae, with the corresponding health effects. In the following, details will be given on some of these algal compounds.

Among prokaryotic microalgae, the cyanobacterium *Arthrospira* sp. has undergone numerous and rigorous toxicological studies that have highlighted its potential therapeutic applications in the area of immunomodulation, anticancer, antiviral, and cholesterol-reduction effects. A number of extracts were found to be remarkably active in protecting human lymphoblastoid T-cells from the cytopathic effects of HIV infection.

Active agents consisting of sulfolipids with different fatty acid esters were isolated also from *Lyngbya lagerheimii* and *Phormidium tenue*. Additional cultured cyanobacterial extracts with inhibitory properties were also found in *Phormidium cebennse*, *Oscilatoria raciborskii*, *Scytonema burmanicum*, *Calotrix elenkinii*, and *Anabaena variabilis*. A protein called cyanovirin, isolated from an aqueous cellular extract of *Nostoc elipsosporum* prevents the *in vitro* replication and citopathicity of primate retroviruses. Cryptophycin 1, an active compound isolated from *Nostoc* strain GSV224, exerts antiproliferative and antimitotic activity by binding to the ends of the microtubules, thus blocking the cell cycle at the metaphase of mitosis. Cryptophycin 1 is the most potent suppressor of microtubule dynamics yet described. It belongs to the family of cryptophycins, potent anticancer agents at picomolar concentrations, which exert their cytotoxic effects in both alkaloid- and taxol-resistant cancer cells that contribute to the proliferation of drug-resistant tumors.

Other studies using water-soluble extracts of cyanobacteria have found a novel sulfated polysaccharide, calcium spirulan to be an antiviral agent. This compound appears to be selectively inhibiting the penetration of enveloped viruses into host cells, thereby preventing the replication. Using specific assays for the quantification of viral replication *in vitro*, spirulan exhibited strong inhibition of human cytomegalovirus, herpes simplex virus type 1, human herpes virus type 6, and human immunodeficiency virus type 1.

Among eukaryotic microalgae, a polypeptide has been separated from *Chlorella pyrenoidosa*, which exhibited inhibitory activity on human liver cancer HepG2 cells. It has been named CPAP (*C. pyrenoidosa* antitumor polypeptide).

Apart from these very specific compounds, as already stated, the general beneficial effect of microalgae is attributed to their content in pigments, carotenoids, in particular, PUFAs and polysaccharides. Carotenoids (both carotenes and xanthophylls) are tetraterpenoid organic pigments that serve two key roles in algae: they absorb light energy for use in photosynthesis and they protect chlorophyll from photodamage. There has been much interest in carotenoids, especially their effect on human health, because they have a market value of several hundred million Euros. Their chemical synthesis is still a demanding challenge for chemists. The major dietary source of vitamin A (essential for cell growth, embryonic development, vision, and immune system functioning) for mammals, including humans, is derived from carotenoids.

TABLE 7.3
Example of Bioactive Compounds Present in Algae, with the Corresponding Health Effects

Category	Specific Product	Source	Effects
Carotenoids	Astaxanthin	*Haematococcus* sp.	Antioxidant/Antihypertensive
	β-carotene	*Dunaliella* sp.	Antioxidant/Antimutagenic
		Porphyra tenera	
	Fucoxanthin	*Hizikia fusiforme*	Antiangiogenic/
		Fucus serratus	Retinol deficiency protection/
		Padina tetrastomatic	Antioxidant/
		Laminaria japonica	Photoprotective
	Zeaxanthin	*Ascophyllum nodosum*	Eyes diseases remediation
	Lutein	*Porphyra tenera*	Antimutagenic
	Siphonoxanthin	*Codium fragile*	Anticancer/Antiangiogenic
PUFA	AA	*Gracilaria verrucosa*	Antioxidant
	DHA	*Schizochytrium limacinum*	Antioxidant
	EPA	*Nannochloropsis sp.*	Antioxidant
Polyphenol	Flavonoids	*Palmaria palmata*	Antioxidant
	Cathechins	*Halimedia* sp.	Antimicrobial
	Phlorotannins	*Ecklonia cava*	Anti-inflammatory/Lipid metabolism control
Polysaccharide	Alginic acid	*Undaria pinnatifida*	Anticancer/Antibacterial
		Saccarina latissima	
	Carrageenan	*Chondrus crispus*	Anticoagulant/Antiviral/
		Euchema cottoni	Stimulation collagen biosynthesis
		Gigartina skottsbergii	
	Fucoidan	*Macrocistis* sp.	AntiHIV/Antiarteriosclerosis
		Laminaria japonica	Lipid metabolism control/
		Undaria pinnatifida	Reduction of interleukin production
	β-glucan	*Euglena gracilis*	Immunostimulant/Antiviral
	Laminaran	*Laminaria* sp.	Antihypertensive/ Anticoagulant /
		Fucus vesicolotus	Dietary fibre/Wound repair
	Ulvan	*Ulva lactuca*	Gastric ulcer repair
		Monostroma sp.	
	Porphyran	*Porphyra* sp.	Anticoagulant/ Antihypercholesterolemic
Vitamins	Tocopherol	*Fucus* sp.	Antioxidant
		Laminaria sp.	
		Cappaficus sp.	
	Ascorbic acid	*Chondrus crispus*	Antioxidant
		Sargassum sp.	
Extracts	Methanolic extract	*Hypnea valentiae*	Acetylcholinesterase inhibition/Cytotoxic activity
		Padina pavonia	

Carotenoids by their quenching action on reactive oxygen species carry intrinsic antiinflammatory properties, whereas PUFAs exhibit antioxidant activity and polysaccharides act as immunostimulators.

A major bottleneck in the exploitation of microalgal biomass for the production of high-value compounds is low productivity of the culture, both in terms of biomass and product formation. One fundamental reason for this is slow cell growth rates owing to inefficient use of strong light. Furthermore, most microalgal products are secondary metabolites that are produced when growth is limited. One solution to this bottleneck could be to milk the secondary metabolites from the microalgae. This involves continuous removal of secondary metabolites from cells, thereby enabling the biomass to be reused for the continuous production of high-value compounds.

Recently, a new method was developed for milking β-carotene from *Dunaliella salina* in a two-phase bioreactor. In this technique, cells are first grown under normal growth conditions and then stressed by excess light to produce larger amounts of β-carotene. At this stage, the second, biocompatible organic phase is added and the β-carotene is extracted selectively via continuous recirculation of a biocompatible organic solvent (lipophilic compound) through the aqueous phase containing the cells. Because the cells continue to produce β-carotene, the extracted product is continuously replaced by newly produced molecules. Therefore, the cells are continuously reused and do not need to be grown again. In contrast to existing commercial processes, this method does not require the harvesting, concentrating, and destroying of cells for extraction of the desired product. Furthermore, purification of the product is simple owing to the selectivity of the extraction process. The general application of this process would facilitate the commercialization of microalgal biotechnology and development of microalgal products.

The properties of the cell membrane play an important role in the contact between biocompatible lipophilic solvents, and hydrophobic parts of the cell membrane might be prevented by the presence of a cell wall and/or hydrophilic parts of the outer membrane. Physiological properties of the cells, such as their capacity for continuous endo- and exo-cytosis, might also play a role in the milking process. Other considerations are the location and way in which the product accumulates inside the cells and the function of that product inside the cells. A product such as chlorophyll would be difficult to extract owing to its location in thylakoid membranes and because it is bound strongly to other cell components. The extraction of a product with a protective effect on the cells (e.g., β-carotene) will enhance its synthesis. The milking process can also be applied to other algae and other products besides *D. salina*, for example, in *Haematococcus pluvialis* for the recovery astaxanthin, and marine microalgae for PUFAs.

In addition to its use in aquaculture (e.g., to give salmon a pink color), astaxanthin has also been described as having nutraceutical importance related to free-radical scavenging, immunomodulation, and cancer prevention. *H. pluvialis* can produce and accumulate astaxanthin to concentrations of 1–8% of the dry weight. This concentration within the cell would make milking of *H. pluvialis* more successful compared with *D. salina*. However, cultivation of *H. pluvialis* is more complex than *D. salina*, and productivity is lower. Furthermore, extraction, purification, and concentration are a heavy burden on the production cost. As the final product cost is also sensitive to algal productivity and duration of the growth period, this process is not economically feasible at present.

PUFAs are gaining increasing importance as valuable pharmaceutical products and ingredients of food owing to their beneficial effect on human health. DHA (22:6 ω3) and EPA (20:5 ω3), in particular, are important in the development and functioning of brain, retina, and reproductive tissues both in adults and infants. They can also be used in the treatment of various diseases and disorders, including cardiovascular problems, a variety of cancers, and inflammatory disease. At present, PUFAs are produced commercially from fish oil, but this is an insufficient source of these products, and microalgae provide an optimal lipid source of PUFAs. Microalgal-derived PUFAs, such as AA (arachidonic acid) and DHA, are added as fortifications to infant formulae—an industry that is worth $10 billion per annum alone.

Microalgae are the primary producers of EPA and DHA that are eventually accumulated through the various trophic levels. Changes in microalgal lipid content are carried on up the food chain, impacting the growth and dietary make-up of zooplankton, crustacean larvae, mollusc, and some fish. This subsequently affects the accumulation of EPA and DHA fatty acids in higher organisms and humans. Consequently, lipid profiles in microalgae play a vital role in maintaining the integrity of the world's aquatic food webs.

Several heterotrophic microalgae have been used as biofactories for omega-3 fatty acids commercially, but a strong interest also in autotrophic microalgae has emerged in recent years. To date, the ω-3 fatty acid content of numerous microalgae strains have been studied. Strains from the genera *Phaeodactylum*, *Nannochloropsis*, *Thraustochytrium*, and *Schizochytrium* have demonstrated high accumulation of EPA and/or DHA. *Phaeodactylum tricornutum* and *Nannochloropsis* sp. demonstrated an EPA content of up to 39% of total fatty acids, while strains

such as *Thraustochytrium* and *Schizochytrium limacinum* contained a DHA percentage of between 30% and 40% of total fatty acids when grown heterotrophically. High biomass and commercially acceptable EPA and DHA productivities are achieved with microalgae grown in media with optimized carbon and nitrogen concentrations and controlled pH and temperature conditions. High oil production, including DHA from *Schizochytrium* (50% w/w), can be obtained as a result of high growth rate by controlling nutrients such as glucose, nitrogen, sodium, and some other environmental factors, such as oxygen concentration as well as temperature and pH, achieving high cell densities and DHA productivities.

The heterotrophic marine dinoflagellate *Crypthecodinium cohnii* has a lipid content greater than 20% d.w. and is known for its ability to accumulate fatty acids that have a high fraction (30–50%) of DHA. Lipids are not only important components of algal cell membranes, but also accumulate in globules in other parts of the cells. Microalga growth and fatty acid formation are affected by medium composition and environmental conditions (e.g., carbon sources). Lipid production occurs under growth-limiting conditions; during linear growth, the cells are stressed owing to nutrient limitation and therefore produce more lipids. Also the concentration of DHA, hence the lipid quality, is negatively affected by increases in lipid concentration. The highest quality lipid is obtained when glucose is used as the carbon source, and when the cell concentration and lipid content of the cells are the lowest.

Milking can also be used for DHA production by *C. cohnii*. In this process, cells are first grown under the correct conditions for growth, after which they are stressed to produce higher concentrations of DHA. A biocompatible organic solvent is added during the DHA production stage to extract the product. This process enables the production of high-quality lipid, thereby reducing extraction and purification costs. Furthermore, higher amounts of DHA are produced by substitution of extracted lipids by newly synthesized lipid, increasing the productivity of the system.

An EPA production potential has also been found in the genus *Nitzschia* (especially *N. alba* and *N. laevis*). It was reported that the oil content of *N. alba* was as high as 50% of cell dry weight and the EPA comprised 4–5% of the oil. *N. laevis* could utilize glucose or glutamate as single substrate for heterotrophic growth, and the cellular EPA content of the alga in heterotrophic conditions was also higher than that in photoautotrophic conditions, suggesting that this diatom is a good heterotrophic EPA producer.

From a production point of view, an increase in microalgal lipid content can be induced by a sudden change of growth conditions. The accumulation of starch and/or lipids reserves is considered a survival mechanism in response to growth-limiting stresses, such as UV radiation, temperature, and shock or nutrient deprivation, as long as light conditions are present that still allow for efficient photosynthesis. For example, during nutritional deprivation (e.g., nitrogen) and under the provision of light, cellular division of many marine or brackish microalgae is put on hold and cells begin to accumulate lipids, leading to a 2–3-fold increase in lipid content. Both total lipid and omega-3 fatty acid production can be adjusted by varying growth conditions. The diatom *P. tricornutum* can be induced to increase its lipid level from 81.2 mg/g of culture dry weight to 168.5 mg/g dry weight, and *Nannochloropsis* sp. and *Dunaliella* sp. can achieve a total lipid content of up to 47% and 60% of dry ash weight by modifying the light intensity, temperature, and salinity levels.

ω-3 fatty acid biosynthesis can be stimulated by a number of environmental stresses, such as low temperature, change of salinity, or UV radiation. For example, *Pavlova lutheri* increased its relative EPA content from 20.3 to 30.3 M% when the culture temperature is reduced to 15°C. Similarly, *P. tricornutum* had a higher EPA content when the temperature is shifted from 25°C to 10°C for 12 h.

Salinity may also regulate PUFA biosynthesis; for example, *C. cohnii* increases its total DHA content up to 56.9% of total fatty acids when cultured in 9 g/L NaCl. Other treatments that cause the generation of reactive oxygen species and lipid peroxidation also result in higher PUFA contents. For example, *P. tricornutum* increased its EPA content up to 19.84% when stressed with UV light. Some of the increased PUFAs are used to repair membrane damage but as PUFAs contain many double bonds, these also act as an antioxidant by scavenging free radicals.

Apart from external stresses, metabolic engineering is another promising approach to increase the production of fatty acids in microalgae. Genes encoding key enzymes involved in the fatty acid biosynthesis have been identified in *Ostreococcus tauri*, *Thalassiosira pseudonana*, *P. tricornutum*, and *Chlamydomonas reinhardtii*.

As to macroalgae, extracts from several species may prove to be a source of effective antiviral agents; although the tests have been either *in vitro* (in test tubes or similar) or on animals, with few advancing to trials involving people. A notable exception is Carraguard, a mixture of carrageenans similar to those extracted from Irish moss. Carraguard has been shown to be effective against human immunodeficiency virus (HIV) *in vitro* and against herpes simplex virus in animals. Testing advanced to Phase 3 clinical trial in South Africa, with the Contribution of Bill and Melinda Gates Foundation. This was the first Phase-3 trial of a novel candidate microbicide to be conducted among a general population of 6000 women and completed as planned in 4 years without any safety concerns. The trial did not show that Carraguard is effective in preventing HIV transmission during vaginal sex, but confirmed its safety that could make it a potentially useful vehicle for future microbicides.

Extracts from the brown macroalga *Undaria pinnatifida* have also shown antiviral activity; an Australian company is involved in several clinical trials, in Australia and the United States, of such an extract against HIV and cancer. Because antiviral substances in macroalgae are composed of very large molecules, it was thought they would not be absorbed by eating macroalgae. However, it has been found in one survey that the rate of HIV infection in macroalgae-eating communities can be markedly lower than it is elsewhere. This has led to some small-scale trials in which people infected with HIV ate powdered *Undaria*, with a resulting decrease of 25% in the viral load.

Fucoxanthin, a carotenoid commonly distributed in brown algae, such as *U. pinnatifida*, *Scytosiphon lomentaria*, *Petalonia binghamiae*, and *Laminaria religiosa*, is a potent drug candidate and can be utilized as an excellent supplement such as astaxanthin, since it acts as an antioxidant and inhibits GOTO cells of neuroblastoma and colon cancer cells. Recently, apoptosis activity of fucoxanthin against HL-60 (human leukema) and Caco-2 (cancer colon) cells has been reported.

Algae, especially marine algae, contain a large amount of structural polysaccharides (e.g., cellulose, hemicellulose), storage polysaccharides (e.g., glucan, fucoidan, agar, carrageenan), and mucopolysaccharides (e.g., porphyran). Most of these polysaccharides are not digested by humans and therefore can be defined as functional fibers, that is, physiologically beneficial nondigestible carbohydrates. These polysaccharides may be a constituent of the cell wall as in unicellular red algae as *Porphyridium* sp. and *Rhodella* sp., or be present inside the cell, as in the Euglenophyceae. The polysaccharides of Rhodophyta are highly sulfated and consist mainly of xylose, glucose, and galactose. These compounds selectively inhibit reverse transcriptase (RT) enzyme of human immunodeficiency virus (HIV) and its replication *in vitro*. Rodents fed with a diet supplemented with biomass and polysaccharide derived from *Porphyridium* results in a decrease in blood cholesterol concentration (by 22% and 29%, respectively) and triglyceride levels, increased feces weight (by 130% and 196%, respectively) and bile acid excretion (5.1- and 3.2-folds more). Moreover, algal biomass or polysaccharide increased the length of both the small intestine (by 17% and 30%, respectively) and the colon (by 8.5% and 32%, respectively).

Also β-glucans in algae are present as storage polysaccharides or wall components. The have been identified as water-soluble polysaccharides in brown algae (laminaran, also called laminarin), diatoms (chrysolaminarin), chrysophytes (chrysolaminarin, also called leucosin), and other ochrophytes. Laminarans are maybe among the most investigated glucans; these polymers are extracted from kelps (*Laminaria* sp., *Eicenia* sp.) as a by-product from production of alginic acid. They consist of glucopyranosyl residues linked by β-1,3-D-glycosidic bonds or β-1,6-D branched β-1,3-D-glycosidic bonds; laminaran from *Eicenia bicyclis* has a molecular weight of 6.17 kDa, while laminaran from *L. digitata* weights 5.85 kDa. Laminarans are easily soluble in neutral water, and can be fermented by human fecal bacteria easier than other brown algal polysaccharides, such as alginate, fucoidan, and cellulose.

Paramylon is the term used for the reserve β-glucans of *Euglena* and euglenoids in general. Its granules appearing in various locations inside the cell; in many species, they are scattered throughout the cytoplasm, but others can be massed together or few, but large, and located in a fairly constant position. Their shape and size differ markedly, and together with their distribution inside the cell, represent a taxonomic feature. Paramylon from *Euglena gracilis* can be considered a quite particular case. *E. gracilis* non-photosynthetic WSLZ mutant can accumulate large amounts of paramylon, up to 95% of the cell mass, when grown in the presence of adequate carbon sources under heterotrophic growth conditions (Figure 7.14a). Paramylon has an unusual high crystallinity as natural macromolecule. Its high crystallinity is an advantage, in that paramylon granules can be isolated in a very low cost and efficient manner by simply disrupting the cells and purifying the granules by successive washing with a low concentration of detergent (Figure 7.14b and c). It can be easily solubilized in concentrated alkaline solution (Figure 7.14d). It consists of pure β-glucan, as shown in the NMR spectrum, which indicates that it consists of 100% glucose (Figure 7.14e). Paramylon crystallinity is due to higher-order aggregates of microfibrils, measuring 4–10 nm, composed of unbranched triple helices of β-(1,3)-D-glucan chains (Figure 7.14f). For these characteristics, *Euglena* could represent an alternative source of β-glucan to *Saccharomyces cerevisiae* (Baker's yeast), which is currently exploited industrially for its extraction.

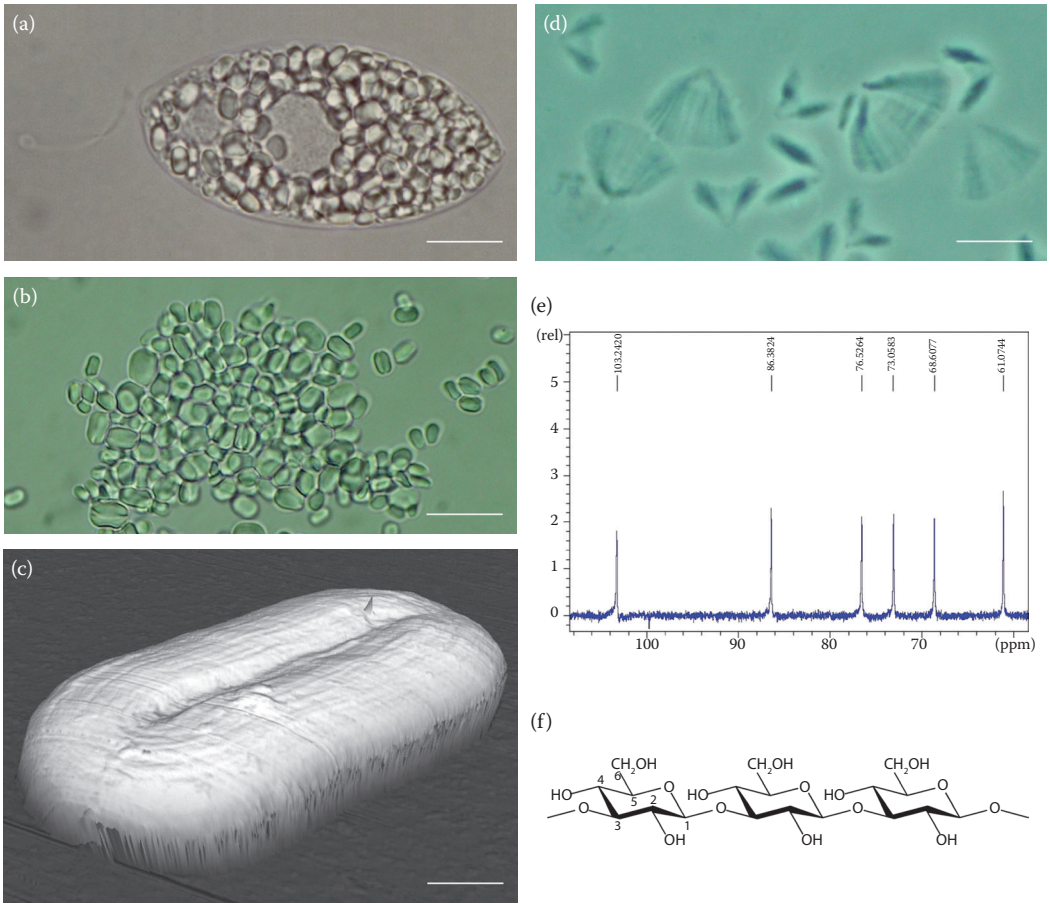

FIGURE 7.14 *Euglena gracilis* nonphotosynthetic WSLZ mutant cell rich in paramylon granules (a); paramylon granules extracted from *Euglena* cell (b); single paramylon granule (c); granules dissolving in alkaline solution (d); NMR spectrum of paramylon (e); and paramylon chemical structure (f).

Paramylon was proved to potentiate the resistance of the brine shrimp *Artemia* sp. to stress conditions resulting from poor growth medium quality and daily handling, and to enhance reproductive success of the shrimps. Moreover, glucose-tolerant tests performed in diabetic mice 5 weeks after diabetes induction showed blood glucose concentration lower in animal fed with paramylon-added food with respect to control animals. Though the mechanisms by which β-glucan improves markers of glucose and insulin metabolism is poorly understood, the leading theory is that it increases the viscosity of the intestinal content, causing reduced postprandial insulin and glucose levels. Over time, lower ambient insulin level improves cellular insulin sensitivity, resulting in improved glucose metabolism. The effect of β-glucan to reduce blood glucose could also be mediated by delaying stomach emptying so that dietary glucose is absorbed more gradually. After ingestion of the glucans, the peak of the blood glucose level is much smoothed and the shape of the plasma glucose response curve is much flatter. These changes reduce the feeling of hunger caused by rapid decrease in blood glucose. Thus, β-glucans may decrease appetite and reduce food intake.

β-glucan from *Euglena* paramylon has successfully been used in aquaculture to strengthen the nonspecific defence of many important species of fishes and shrimps by injection, immersion, or in the feed. It acts as a nonspecific immune system stimulant, by binding to a specific receptor on monocytes/macrophages and granulocytes.

Other results have demonstrated that the oral administration of paramylon exhibits protective action on acute hepatic injury induced by CCl_4 via an antioxidative mechanism and also inhibits the development of atopic dermatitis-like symptoms in mice, providing an effective alternative therapy to prednisolone. All these results support the potential use of paramylon in different fields of application.

Toxins

Toxins are all compounds that are either synthesized by the algae or formed by the composition of metabolic products and hence represent an intrinsic characteristic of the organism. Of the million species of microalgae, those that produce specific toxins scarcely exceed a hundred. These occur in both salt and freshwaters and while most are planktonics, some are benthic or floating at water surface. Toxins can attract particular attention when they cause the death of livestock that has drunk water containing them or fish and shellfish in the sea, or humans who consume them.

Algae which seem to be a direct producer of toxic substances mostly belong to three taxonomic groups: Cyanobacteria, Haptophyta, and Dynophyceae (Myzozoa). As well as these there are some groups which include one or two toxic members. Species of *Chattonella* and *Heterosygma*, belonging to the Raphidophyceae (Ochrophyta), form toxic red tides in Japanese waters and a few diatoms of the genus *Peusdonitzschia* (Ochrophyta, Bacillariophyceae) produce domoic acid (DA), a low-molecular amino acid causing amnesic shellfish poisoning.

Among the 50 freshwater existing cyanobacteria genera, 12 are capable of producing toxins. While blue-green algae have significant taste and odor constituents, representing a moldy smell, their toxic metabolites have no taste, odor, or color. The risk of exposure to algal toxins may come from drinking water, recreational water, dietary supplements, or residue on products irrigated with contaminated water and consumption of animal tissue. Avoiding cyanobacterial toxins is not as easy as avoiding a harmful algal bloom as toxins may be present in fish, shellfish, and water even after the bloom has dissipated. Cyanobacterial toxins are responsible for a variety of health effects such as skin irritations, respiratory ailments, neurological effects, and carcinogenic effects. The three major classes of these compounds are:

- *Hepatotoxic cyclic peptides*. The most frequently occurring and widespread are nodularins and microcystins. *Nodularia*, a well-known cyanobacterium, produces nodularins and is primarily a concern in marine and brackish waters, thus creating a risk to recreational swimmers. The 65 variants of microcystins, however, are isolated from freshwaters worldwide and are produced by *Microcystis* (the most commonly identified cyanobacteria in

human and animal poisonings), *Anabaena*, and other algae. They are very stable in the environment and resistant to heat, hydrolysis, and oxidation. Both toxins have an affinity for the liver. Other symptoms of exposure to microcystins may range from weakness, loss of appetite, vomiting, and diarrhea to cancer.

- *Neurotoxic alkaloids.* These toxins are divided into two main classes, that is, anatoxins and saxitoxins, produced by the genera *Anabaena*, *Planktothrix*, and *Aphanizomenon*. Anatoxins may affect the nervous system, skin, liver, or gastrointestinal tract. These neurotoxins can cause symptoms of diarrhea, shortness of breath, convulsions, and death, in high doses, due to respiratory failure. Saxitoxins are the cause of paralytic shellfish poisonings (PSPs) in humans consuming contaminated shellfish. There are no reports of similar poisonings via the drinking water route. Another alkaloid toxin is cylindrospermopsin produced by the filamentous cyanobacteria *Cylindrospermopsis raciborskii*, *Anabaena bergii*, and *Aphanizomenon flos-aquae*.
- *Endotoxic lipopolysaccharides*. These compounds are common constituents of the outer cell walls of Cyanobacteria, similar to the cell-wall toxin found in *Salmonella* bacteria, but less toxic.

The physicochemical nature of the water source can have an effect on not only the growth, but also the toxicity of the algal bloom. For example, some algae increase in toxicity when blooms are iron-deficient. In general, temperature, sunlight, and nutrient loads have a substantial impact on the proliferation of the bloom.

Haptophyta contain a few toxic species. One of them, *Prymnesium parvum*, produces a mixture of toxins collectively named prymnesins, which exhibit potent cytotoxic, hemolytic, neurotoxic, and ichthyotoxic effects. Another flagellate *Chrysochromulina polylepis* produces and excretes two compounds, one hemolytic and one ichthyotoxic. The major hemolytic compound is a galactolipid, 1-acyl-3-digalacto-glycerol. These toxins cause osmoregulatory failure similar to that brought about by *P. parvum*. Another widely distributed marine haptophyte *Phaeocystis* sp. is familiar to fishermen in the form of extensive blooms of mucilaginous colonies which are avoided by herring. It produces large quantities of acrylic acid, which has strong bactericidal properties. Seventy years ago, *Phaeocystis pouchetii* was suspected to cause avoidance of herring. Later, it was demonstrated that copepods avoided gracing on healthy *P. pouchetii* colonies; food intake and growth were reduced in sea cage-cultivated salmon during the spring bloom of *P. pouchetii*, and water from *P. pouchetii* cultures acted toxic toward cod larvae. Species belonging to the genus *Phaeocystis* are important in all oceans, and *P. pouchetii* is an important component of the spring bloom of phytoplankton in northern waters. Its life cycle is only partly resolved but is known to be polymorphic consisting of at least two solitary and one colonial stage. *P. pouchetii* has been reported to produce a polyunsaturated aldehyde (PUA) as diatoms, namely the 2-*trans*-4-*trans*-decadienal. This compound is known to interfere with the proliferation of different cell types, both prokaryotic and eukaryotic. As mechanical stress is known to induce the release of PUAs in other phytoplankton species, the release of 2-*trans*-4-*trans*-decadienal has been suggested to be a mean of deterring grazers, for example, zooplankton or fish larvae. *P. pouchetii* is a common component of northern and temperate spring blooms, is grazed by zooplankton at normal rates, and can also be a diet preferable to diatoms. Copepods may avoid gracing on healthy colonies of *P. pouchetii*, thus, the production and excretion of PUAs seem to be depending on the state of the cells or on environmental factors, or both. It has been reported that this PUA can be released into the sea in the absence of grazers, indicating that it may serve as an allelochemical, that is, a compound that gives *P. pouchetii* a competitive advantage over phytoplankton species blooming at the same time by inhibiting their growth.

Dynophyceae includes about a dozen genera, with at least 30 species, producing water and lipid-soluble, low-molecular weight, neuroactive secondary metabolites that are among the most potent non-proteinaceous poisons known. In general, these toxins have been shown to block the influx of sodium

through excitable nerve membranes, thus preventing the formation of action potentials. The toxins are accumulated and sometimes metabolized by the shellfish that feed upon these dinoflagellates, causing different types of shellfish poisoning, such as paralytic shellfish poisoning (PSP), diarrheic shellfish poisoning (DSP), neurotoxic shellfish poisoning (NSP), ciguatera fish poisoning (CFP), and amnesic shellfish poisoning (ASP).

Ingestion of contaminated shellfish results in a wide variety of symptoms, depending on the toxin(s) present, their concentrations in the shellfish, and the amount of contaminated shellfish consumed. In the case of PSP, caused by toxin of *Alexandrium* spp., the effects are predominantly neurological and include tingling, burning, numbness, drowsiness, incoherent speech, and respiratory paralysis. Less well characterized are the symptoms associated with DSP and NSP.

DSP is caused by okadaic acid (OA), a lyposoluble cyclic polyether with a carboxylic function. OA is a diarrhoeic shellfish toxin and tumor promoter found in many dinoflagellates of the genera *Dinophysis* and in *Prorocentrum lima*. DSP is primarily observed as a generally mild gastrointestinal disorder, that is, nausea, vomiting, diarrhoea, and abdominal pain accompanied by chills, headache, and fever.

Both gastrointestinal and neurological symptoms characterize NSP, including tingling and numbness of lips, tongue, and throat, muscular aches, dizziness, reversal of the sensations of hot and cold, diarrhoea, and vomiting. The NSP toxins are brevetoxins produced by *Gymnodinium breve*.

Another syndrome caused by dinoflagellate toxins is the CFP, connected with eating contaminated tropical reef fish. Ciguatoxins (CTXs) that cause CFP are actually produced by *Gambierdiscus toxicus*, a photosynthetic dinoflagellate that normally grows as an epiphyte and has a relatively slow growth rate of approximately one division every 3 days. In its coral reef habitat, *G. toxicus* is biflagellate and swims if disturbed, but is usually motionless and attached to certain macroalgae. The dinoflagellate may also be associated with macroalgal detritus on the seafloor. Some scientists believe that the diverse symptoms of CFP are a result of a combination of several toxins and/or their metabolites, produced by one or more dinoflagellates. However, *G. toxicus*, which is found on a variety of macroalgae eaten by herbivorous fish, is now widely considered the single-celled source of CTXs and the potential cause of CFP. *G. toxicus* produces two classes of polyether toxins, the CTXs and maitotoxins (MTXs). The CTXs are lipophilic and are accumulated in fish through food web transfer. More than 20 CTX congeners have been isolated; however, only a few have been fully characterized structurally. The MTXs are transfused ladder-like polyether toxins, but are somewhat more polar, due to the presence of multiple sulfate groups. MTX was originally identified as a water-soluble toxin in the viscera of surgeon fish, and later found to be the principal toxin produced by *G. toxicus*. MTXs have not been demonstrated to bioaccumulate is fish tissues, possibly due to their more polar structure. Thus, if MTX is involved in CFP, it may be implicated only in CFPs derived from herbivorous fishes. The toxic potency of MTX exceeds that of CTX (respectively, 10 and 50 ng kg^{-1} in mice). Its mode of action has not been fully elucidated. Its biological activity is strictly calcium-dependent and causes both membrane depolarization and calcium influx in many different cell types. These toxins become progressively concentrated as they move up the food chain from small fish to large fish that eat them, and reach particularly high concentrations in large predatory tropical reef fish. Barracuda are commonly associated with CFP, but eating grouper, sea bass, snapper, mullet, and a number of other fish that live in oceans between latitude 35°N and 35°S has caused the disease. These fish are typically caught by sport fishermen on reefs in Hawaii, Guam and other South Pacific islands, the Virgin Islands, and Puerto Rico. CTX usually causes symptoms within a few minutes to 30 h after eating contaminated fish, and occasionally it may take up to 6 h. Common nonspecific symptoms include nausea, vomiting, diarrhea, cramps, excessive sweating, headache, and muscle aches. The sensation of burning or "pins-and-needles," weakness, itching, and dizziness can occur. Patients may experience reversal of temperature sensation in their mouth (hot surfaces feeling cold and vice versa), unusual taste sensations, nightmares, or hallucinations. CFP is rarely fatal. Symptoms usually clear in 1–4 weeks.

In its typical form, CFP is characterized initially by the onset of intense vomiting, diarrhea, and abdominal pain within hours of ingestion of toxic fish. Within 12–14 h of onset, a prominent neurological disturbance develops, characterized by intense paraesthesia (tingling, crawling, or burning sensation of the skin) and dysanesthesia (painful sensation) in the arms, legs and perioral region, myalgia, muscle cramping, and weakness. During this stage of the illness, pruritus and sweating are commonly experienced.

Pseudonitzschia spp. are among several other marine algae that can produce DA, the cause of ASP. DA was first isolated in Japan from the macroalgae species *Chondria armata* in 1958 and was consequently called after the Japanese word for macroalgae, which is "domoi." Its identification in 1987 as a neurotoxin was first treated with skepticism, because this water-soluble 3-carboxylic amino acid was known as a folk medicine in Japan to treat intestinal pinworm infestations when used in very small doses. Production of DA by algae seems to be a genetic property for a secondary metabolite with no known function in defense or primary metabolism.

DA can enter the marine food chain via uptake by shellfish such as mussels that filter their food out of the water. This water can contain both diatoms themselves and the toxin, which is released to the water column (although there is no evidence yet that the toxin can be taken up directly). The toxin accumulates in the digestive gland and certain tissues of shellfish, and it appears to have no effect on the animals. DA may be metabolized by bacteria (e.g., of the genera *Alteromonas* and *Pseudomonas*) present in tissue of blue mussels (*Mytilus edulis*). Scallops are reported not to contain these elimination bacteria. Anchovies can also contain DA in their guts, by feeding on toxic *Pseudonitzschia* spp.; this toxin affects their behavior and survival. Effects are also seen in seals. In humans, consumption of contaminated seafood mostly affected the elderly or infirm. Heat does not destroy DA, although shellfish toxicity can decrease during cooking or freezing via DA transfer from the meats to the surrounding liquid. The sea otter is the only animal known to be able to avoid intoxication, probably recognizing toxic prey by their odor. The mechanism of DA toxicity is explained by its structural similarity with the excitatory neurotransmitter glutamic acid and its analogs, but with a much stronger receptor affinity. DA is three times more potent than its analog kainic acid and up to 100 times more potent than glutamic acid itself. After exposure, DA binds predominately to *N*-methyl-D-aspartate (NMDA) receptors in the central nervous system, causing depolarization of the neurones. Subsequently, the intercellular calcium concentration increases, resulting in sustained activation of calcium-sensitive enzymes, eventually leading to depletion of energy, neuronal swelling, and cell death. The affected neurones are mainly located in the hippocampus, explaining the most striking effect of DA poisoning, which is short-term memory loss, observed in 25% of the affected persons in the 1987 contaminated mussel event. Other symptoms are confusion, nausea, vomiting, gastroenteritis, cramps, and diarrhea, all within 24 h. Neurological complaints, including ataxia, headache, disorientation, difficulty in breathing, and coma, develop 48 h after consumption. Permanent brain damage can also be caused by DA intoxication. Effects of chronic low-level ingestion are unknown. DA from mussels is more neurotoxic than the chemically pure compound. This increase is due to DA potentiation, caused by high concentrations of glutamic and aspartic acids present in mussel tissue. This neurotoxic synergism occurs through a reduction in the voltage-dependent Mg_2 block at the receptor-associated channel, following activation of non-NMDA receptors, in addition to the NMDA receptor activation by DA itself.

Intensive research over the last years has revealed a new class of phytotoxins produced by diatoms with more subtle and less specific effects, a discovery that has drawn a lot of attention since the diatoms have traditionally been regarded as a key component of the food chain. Three closely related PUAs have been isolated from *Thalassiosira rotula*, *Skeletonema costatum*, and *Pseudonitzschia delicatissima*, namely 2-*trans*-4-*cis*-7-*cis*-decatrienal, 2-*trans*-4-*trans*-7-*cis*-decatrienal, and 2-*trans*-4-*trans*-decadienal. In the same study, these aldehydes were found to inhibit cleavage of sea urchin embryos and reduce growth of $CaCO_2$ cells and hatching of copepod eggs. The structural element shared by these compounds, the unsaturated aldehyde group, is able to form adducts with nucleophiles

TABLE 7.4
Summary of Toxic Algae and the Corresponding Metabolites

Scientific Name	Class	Toxin
Nodularia spp.	Cyanophyceae	Nodularin
Microcystis spp.	Cyanophyceae	Microcystin
Anabaena spp.	Cyanophyceae	Microcystin
Planktothrix spp.	Cyanophyceae	Anatoxin
Cylindrospermopsis raciborskii	Cyanophyceae	Brevetoxin
Aphanizomenon flos-aquae	Cyanophyceae	Brevetoxin
Prymnesium parvum	Haptophyceae	Prymnesins
Chrysochromulina polylepis	Haptophyceae	Toxic galactolipid
Phaeocystis pouchetii	Haptophyceae	PUA
Alexandrium spp.	Dinophyceae	Saxitoxin/Brevetoxin
Dinophysis spp.	Dinophyceae	Okadaic acid
Prorocentrum lima	Dinophyceae	Okadaic acid
Gymnodinium breve	Dinophyceae	Brevetoxin
Gambierdiscus toxicus	Dinophyceae	Ciguatoxin/Maitotoxin
Chondria armata domoi	Florideophyceae	Domoic acid
Pseudonitzschia spp.	Bacillariophyceae	Domoic acid
Thalassiosira rotula	Bacillariophyceae	PUA
Skeletonema costatum	Bacillariophyceae	PUA
Pseudonitzschia delicatissima	Bacillariophyceae	PUA

and is thus capable of inducing reactions that are toxic to the cell. The harmful effects of PUAs have been demonstrated at the organism level as inducers of apoptosis in sea urchin embryos, at the cell level as cytotoxicity in human cell lines, and at the protein level by deactivation of enzymes.

Table 7.4 summarizes toxic algae and the corresponding metabolite.

SELECTED READING

Abdulquader, G., Barsanti L., and Tredici, M. R. Harvest of *Artrosphira platensis* from Lake Kossorom (Chad) and its household usage among the Nanembu. *Journal of Applied Phycology*, 12, 493–498, 2000.

Amin, I. and Hong, T. S. S. Antioxidant activity of selected commercial seaweeds. *Malaysian Journal of Nutrition*, 8, 167–177, 2002.

Arunkumar, E., Bhuvaneswari, S., and Anuradha, C. V. An intervention study in obese mice with astaxanthin, a marine carotenoid—Effects on insulin signaling and pro-inflammatory cytokines. *Food & Function*, 3(2), 120–126, 2012.

Barbera, C., Bordehore, C., Borg, J. A., Glemarec, M., Grall, J., Hall-Spencer, J. M. et al. Conservation and management of northeast Atlantic and Mediterranean maerl beds. *Aquatic Conservation: Marine and Freshwater Ecosystems*, 13, s65–s76, 2003.

Barsanti, L., Bastianini, A., Passarelli, V., Tredici, M. R., and Gualtieri, P. Fatty acid content in wild type and WZSL mutant of *Euglena gracilis*. *Journal of Applied Phycology*, 12, 515–520, 2000.

Barsanti, L., Vismara, R., Passarelli, V., and Gualtieri, P. Paramylon(β-1,3-glucan) content in wild type and WZSL mutant of *Euglena gracilis*: Effects of growth conditions. *Journal of Applied Phycology*,13, 59–65, 2001.

Barsanti, L., Passarelli, V., Evangelista, V., Frassanito, A. M., and Gualtieri, P. Chemistry, physico-chemistry and applications linked to biological activities of β-glucans. *Natural Products Reports* 28(3), 457–466, 2011.

Becker, W. Microalgae in human and animal nutrition. In: Richmond, A. (Ed.). *Handbook of Microalgae Mass Culture and Biotechnology and Applied Phycology*. Blackwell Publishing, Malden, USA, 2004.

Blas-Valdivia, V., Ortiz-Butron, R., Rodriguez-Sanchez, R., Torres-Manzo, P., Hernandez-Garcia, A., and Cano-Europa, E. Microalgae of the Chlorophyceae class: Potential nutraceuticals reducing oxidative

stress intensity and cellular damage. In: Lushchak, V. (Ed.). *Oxidative Stress and Diseases*. InTech, Rijeka, Croatia, 2012.

Blouin, N. A., Brodie, J. A., Grossman, A. C., Xu, P., and Brawley, S. H. *Porphyra*: A marine crop shaped by stress. *Trends in Plant Science*, 16(1), 29–37, 2011.

Brown, M. R., Mular, M., Miller, I., Farmer, C., and Trenerry, C. The vitamin content of microalgae used in aquaculture. *Journal of Applied Phycology*, 11, 247–255, 1999.

Brownlee, I., Fairclough, A., Hall, A., and Paxman, J. The potential health benefits of seaweed and seaweed extract. In: Pomin, V.H. (Ed.). *Seaweed: Ecology, Nutrient Composition and Medicinal Uses*. Nova Science Publishers, Hauppauge, New York, 2012.

Buchholz, C. M., Krause, G., and Buck, B. H. Seaweed and man. In: Wiencke, C., and Bischof, K. (Eds.). *Seaweed Biology, Ecological Studies.* Springer-Verlag, Berlin, Heidelberg, 2012.

Buschmann, A. H., Correaa, J. A., Westermeier, R., Hernandez-Gonzales, M. C., and Norambuena, R. Red algal farming in Chile: A review. *Aquaculture*, 194, 203–220, 2001.

But, P. P., Cheng, L., Chan, P. K., Lau, D. T., and But, J. W. *Nostoc flagelliforme* and faked items retailed in Hong Kong. *Journal of Applied Phycology*, 14, 143–145, 2002.

Chini-Zittelli, G., Rodolfi, L., and Tredici, M. R. Mass cultivation of *Nannochloropsis* sp. in annular reactors. *Journal of Applied Phycology*, 15, 107–114, 2003.

Cohen, Z. (Ed.). *Chemicals from Microalgae*. Taylor and Francis, London, 1999.

Cornish, M. L. and Garbary, D. J. Antioxidants from macroalgae: Potential applications in human health and nutrition. *Algae*, 25(4), 155–171, 2010.

Daranas, A. H., Norte, M., and Fernandez, J. J. Toxic marine microalgae. *Toxicon*, 39, 1101–1132, 2001.

Delisle, H., Allasoumgue, F., Begin, K. N., and Lasorsa, C. Household food consumption and nutritional adequacy in wadi zones of Chad. *Ecology Food Nutrition*, 25, 229–248, 1991.

Delpeuch, F., Joseph, A., and Cavalier, C. Consommation alimentaire et apport nutritionnel des algues bleues chez quelques populations du Kanem (Chad). *Annales Nutrition Alimentation,* 29, 497–516, 1976.

Dettmar P. W., Strugala, V., and Craig Richardson, J. The key role alginates play in health. *Food Hydrocolloids*, 25(2), 263–266, 2011.

Dillehay, T. D., Ramírez, C., Pino, M., Collins, M. B., Rossen, J., and Pino-Navarro, J. D. Monte Verde: Seaweed, food, medicine, and the peopling of South America. *Science*, 320(5877), 784–786, 2008.

Dungeard, P. Su rune algue bleue alimentaire pour l'homme. *Actes Society Linnean Bordeaux,* 91, 39–41, 1940.

Evangelista, V., Barsanti, L., Frassanito, A. M., Passarelli, V., and Gualtieri, P. (Eds.). *Algal Toxins: Nature, Occurrence, Effect and Detection*. NATO Series A: Chemistry and Biology. Springer Science, Dordrecht, The Netherlands, 2008.

Farra, W. V. Tecuitlatl: A glimpse of Aztec food technology. *Nature*, 211, 341–342, 1966.

Faulkner, D. J. Marine natural products. *Natural Products Reports*, 18, 1–49, 2001.

Fitzgerald, C., Gallagher, E., Tasdemir, D., and Hayes, M. Heart health peptides from macroalgae and their potential use in functional foods. *Journal of Agricultural and Food Chemistry*, 59(13), 6829–6836, 2011.

Funaki, M., Nishizawa, M., Sawaya, T., Inoue, S., and Yamagishi, T. Mineral composition in the holdfast of three brown algae of the genus *Laminaria*. *Fisheries Science*, 67, 295–300, 2001.

Gao, K. Chinese studies on the edible blue-green alga, *Nostoc flagelliforme*: A review. *Journal of Applied Phycology*, 10, 37–49, 1998.

Gao, K. and Ai, H. Relationship of growth and photosynthesis with colony size in an edible cyanobacterium, Ge-Xian-Mi (*Nostoc*). *Journal of Phycology*, 40, 523–526, 2004.

Georg Jensen, M., Pedersen, C., Kristensen, M., Frost, G., and Astrup, A. Review: Efficacy of alginate supplementation in relation to appetite regulation and metabolic risk factors: Evidence from animal and human studies. *Obesity Reviews*, 14(2), 129–144, 2013.

Hallegraeff, G. M., Anderson, D. M., and Cembella, A. D. (Eds.). *Manual on Harmful Marine Algae*. IOC Manuals and Guides, No. 33, UNESCO Publishing, Paris, France, 2003.

Harel, M., Koven, W., Lein, I., Bar, Y., Behrens, P., Stubblefield, J., Zohar, Y., and Place, A. R. Advanced DHA, EPA and ARA enrichment materials for marine aquaculture using single cell heterotrophs. *Aquaculture*, 213, 347–362, 2002.

Hetland, G., Ohno, N., Aaberge, I. S., and Lovik, M. Protective effect of β-glucan against systemic *Streptococcus pneumoniae* infection in mice. *FEMS*, 27, 111–116, 2000.

Holdt, S. and Kraan, S. Bioactive compounds in seaweed: Functional food applications and legislation. *Journal of Applied Phycology*, 23(3), 543–597, 2011.

http://www.fao.org/docrep/016/i2727e/i2727e.pdf

http://www.aqua-in-tech.com

http://www.marlin.ac.uk/species/Lithothamnioncorallioides.htm

http://www.mumm.ac.be/SUMARE
http://www.scotland.gov.uk/cru/kd01/orange/sdsp-06.asp
Irianto, A. and Austin, B. Probiotics in aquaculture. *Journal of Fish Diseases*, 25, 633–642, 2002.
Jacobson, T. A., Glickstein, S. B., Rowe, J. D., and Soni, P. N. Effects of eicosapentaenoic acid and docosahexaenoic acid on low-density lipoprotein cholesterol and other lipids: A review. *Journal of Clinical Lipidology*, 6(1), 5–18, 2012.
Jyonouchi, H., Sun, S., Iijima, K., and Gross, M. D. Antitumor activity of astaxanthin and its mode of action. *Nutrition and Cancer*, 36, 59–65, 2000.
Khan, S. and Satam, S. B. Seaweed marine culture: Scope and potential in India. *Aquaculture Asia*, 8, 26–29, 2003.
Kusmic, C., Barsacchi, R., Barsanti, L., Gualtieri, P., and Passarelli, V. *Euglena gracilis* as source of the antioxidant vitamin E. Effects of culture conditions in the wild type strain in the *Euglena* natural mutant WZSL. *Journal of Applied Phycology*, 10, 555–559, 1999.
Lee, Y. Microalgal mass culture systems and methods: Their limitation and potential. *Journal of Applied Phycology*, 13, 307–315, 2001.
Leonard, J. The 1964–1965 Belgian Trans-Saharan expedition. *Nature*, 209, 126–128, 1966.
Leonard, J. and Compere, P. *Spirulina platensis* algue bleue de grande valeur alimentatire par sa richesse en proteins. *Bulletin Jarden Botanique Naturelle Belgique*, 37, 3–23, 1967.
Lordan, S., Ross, R. P., and Stanton, C. Marine bioactives as functional food ingredients: Potential to reduce the incidence of chronic diseases. *Marine Drugs*, 9(6), 1056–1100, 2011.
Lourenço, S. O., Barbarino, E., De-Paula, J. C., da S. Pereira, L. O., and Marquez, U. M. L. Amino acid composition, protein content and calculation of nitrogen-to-protein conversion factors for 19 tropical Seaweeds. *Phycological Research*, 50, 233–241, 2002.
Lu, C., Rao, K., Hall, D., and Vonshak, A. Production of eicosapentaenoic acid (EPA) in *Monodus subterraneus* grown in a helical tubular photobioreactor as affected by cell density and light intensity. *Journal of Applied Phycology*, 13, 517–522, 2001.
Luning, K. and Pang, S. Mas cultivation of seaweeds: Current aspects and approaches. *Journal of Applied Phycology*, 15, 115–119, 2003.
Malloch, S. Marine plant management and opportunities in British Columbia. Fisheries, Sustainable Economic Development Branch, Victoria, BC, 2000.
McHugh, D. J. *A Guide to the Seaweed Industry*. FAO Fisheries Technical Paper. No. 441. FAO, Rome, Italy, 2003.
Mhadhebi, L., Laroche-Clary, A., Robert, J., and Bouraoui, A. Anti-inflammatory, anti-proliferative and antioxidant activities of organic extracts from the Mediterranean seaweed, *Cystoseira crinita*. *African Journal of Biotechnology*, 10(73), 16682–16690, 2011.
Murakami, T., Ogawa, H., Hayashi, M., and Yoshizumi, H. Effect of *Euglena* cells on blood pressure, cerebral peripheral vascular changes and life-span in stroke-prone spontaneously hypertensive rats. *Journal Japanese Society Nutrition Food Science*, 41, 115–125, 1998.
Nagai, T. and Yukimoto, T. Preparation and functional properties of beverages made from sea algae. *Food Chemistry*, 81, 327–332, 2003.
Neff, L. M., Culiner, J., Cunningham-Rundles, S., Seidman, C., Meehan, D., Maturi, J. et al. Algal docosahexaenoic acid affects plasma lipoprotein particle size distribution in overweight and obese adults. *The Journal of Nutrition*, 141(2), 207–213, 2011.
Norziah, M. H. and Ching, C. Y. Nutritional composition of edible seaweed *Gracilaria changgi*. *Food Chemistry*, 68, 69–76, 2000.
Palthur, M. P., Palthur, S. S., and Chitta, S. K. Nutraceuticals: A conceptual definition. *International Journal of Pharmacy and Pharmaceutical Sciences*, 2(3), 19–27, 2010.
Pangestuti, R. and Kim, S. K. Biological activities and health benefit effects of natural pigments derived from marine algae. *Journal of Functional Foods*, 3(4), 255–266, 2011a.
Pangestuti, R. and Kim, S. K. Neuroprotective effects of marine algae. *Marine Drugs*, 9(5), 803–818, 2011b.
Park M. K., Jung, U., and Roh, C. Fucoidan from marine brown algae inhibits lipid accumulation. *Marine Drugs*, 9(8), 1359–1367, 2011.
Park, E. Y., Kim, E. H., Kim, M. H., Seo, Y. W., Lee, J. I., and Jun, H. S. Polyphenol-rich fraction of brown alga *Ecklonia cava* collected from Gijang, Korea, reduces obesity and glucose levels in high-fat diet-induced obese mice. *Evidence-Based Complementary and Alternative Medicine*, 1–11 2012.
Parker, N. S., Negri, A. P., Frampton, D. M. F., Rodolfi, L., Tredici, M. R., and Blackburn, S. I. Growth of the toxic dinoflagellate *Alexandrium minutum* (Dinophyceae) using high biomass culture systems. *Journal of Applied Phycology*, 14, 313–324, 2002.

Patel, S. Therapeutic importance of sulfated polysaccharides from seaweeds: Updating the recent findings. *3 Biotech*, 2(3), 171–185, 2012.

Pereira, H., Barreira, L., Figueiredo, F., Custódio, L., Vizetto-Duarte, C., Polo, C. et al. Polyunsaturated fatty acids of marine macroalgae: Potential for nutritional and pharmaceutical applications. *Marine Drugs*, 10(9), 1920–1935, 2012.

Richmond, A. Microalgal biotechnology at the turn of the millennium: A personal view. *Journal of Applied Phycology*, 12, 441–451, 2000.

Ridolfi, L., Chini-Zitelli, G., Barsanti, L., Rosati, G., and Tredici, M. R. Growth medium recycling in *Nannochloropsis* sp. mass cultivation. *Biomolecular Engineering*, 20, 243–248, 2003.

Shields, R. J. and Lupatsch, I. Algae for aquaculture and animal feeds. *Technikfolgenabschätzung-Theorie und Praxis*, 21, 23–37, 2012.

Steneck, R. S., Graham, M. H., Bourque, B. J., Corbett, D., Erlandson, J. M., Estes, J. A., and Tegner, M. J. Kelp forest ecosystems: Biodiversity, stability, resilience and future. *Environmental Conservation*, 29, 436–459, 2002.

Stepp, J. R. and Moerman, D. E. The importance of weed in ethnopharmacology. *Journal of Ethnopharmacology*, 75, 19–23, 2001.

Takaichi, S. Carotenoids in algae: Distributions, biosyntheses and functions. *Marine Drugs*, 9(6), 1101–1118, 2011.

Takeyama, H. K., Yoshino, Y., Kakuta, H., Kawamura, Y., and Matsunaga, T. Production of antioxidant vitamins, β-carotene, vitamin C, vitamin E, by two-step culture of *Euglena gracilis* Z. *Biotechnology and Bioengineering*, 53, 185–190, 1997.

Talyshinsky, M. M., Souprun, Y. Y., and Huleihel, M. M. Anti-viral activity of red microalgal polysaccharides against retroviruses. *Cancer Cell International*, 2, 8–15, 2002.

Tani, Y., and Tsumura, H. Screening for tocopherol-producing microorganisms and α-tocopherol production by *Euglena gracilis* Z. *Agriculture Biological Chemistry*, 53, 305–312, 1989.

Tseng, C. K. Algal biotechnology industries and research activities in China. *Journal Applied Phycology*, 13, 375–380, 2001.

Turner, N. J. The ethnobotany of edible seaweeds (*Porphyra abbotae*) and its use by First Nations on the Pacific Coast of Canada. *Canadian Journal of Botany*, 81, 283–293, 2003.

Vicente, M. F., Basilio, A., Cabello, A., and Pelaez, F. Microbial natural products as a source of antifungals. *Clinical Microbiology and Infectious Disease*, 9, 15–32, 2003.

Vismara, R., Vestri, S., Kusmic, C., Barsanti, L., and Gualtieri, P. Natural vitamin E enrichment of *Artemia salina* fed freshwater and marine microalgae. *Journal of Applied Phycology*, 15, 75–80, 2003a.

Vismara, R., Vestri, S., Barsanti, L., and Gualtieri, P. Diet-induced variations in fatty acid content and composition of two on-grown stages of *Artemia* sp. *Journal Applied Phycology*, 15, 477–483, 2003b.

Vismara, R., Vestri, S., Frassanito, A. M., Barsanti, L., and Gualtieri, P. Stress resistance induced by paramylon treatment in *Artemia* sp. *Journal of Applied Phycology*, 16, 61–67, 2004.

Wang, B., Zarka, A., Trebst, A., and Boussiba, S. Astaxanthin accumulation in *Haematococcus pluvialis* as an active photoprotective process under high irradiance. *Journal of Phycology*, 39, 1116–1124, 2003.

Wilson, S., Blake, C., Berges, J. A., and Maggs, C. A. Environmental tolerances of free-living coralline algae (maerl): Implication for European marine conservation. *Biological Conservation*, 120, 283–293, 2004.

8 Oddities and Curiosities in the Algal World

The profound diversity of size, shape, habitat, metabolic traits, and growth strategies of algae makes this heterogeneous assemblage of prokaryotic and eukaryotic species an almost unlimited source of curious and unusual features.

The algal world is affected by both abiotic (physiochemical) and biotic factors. Abiotic factors are light, temperature, salinity, and nutrient availability, whereas biotic factors are, for example, competition within and between species for space, light, and nutrient or any limiting source, and associations/relations with other organisms.

Under the pressure of abiotic factors, algae display an incredible adaptability to most environments and provide an excellent system for testing hypotheses concerning the evolution of ecological tolerance. In fact, they are not limited to temperate waters, but can survive at very low depths and very low irradiances, and thrive beneath polar ice sheets. Upon adaptation to life on land, algae have colonized surprising places, such as catacombs, tree trunks, and hot springs, and can also resist desiccation in the desert regions of the world.

Algae also relate and interact with other organisms and face the problems connected to these interactions. A variety of relations exists, which includes epiphytism, parasitism, and symbiosis. Algae can share their life with animals, growing on sloth hair, inside the jelly capsule of amphibian eggs, upon the carapaces of turtles or shells of mollusks, camouflaging the dorsal scute of harvestmen. They can also establish pathogenic association and cause infections in animals and humans.

The interactions between all these different factors can both hide and reveal odd traits and unusual characteristics of algae, providing a different perspective of discussion.

IN THE REALM OF DARKNESS

Among the factors that limit the rate of primary production through photosynthesis in aquatic systems (light, nutrients, CO, temperature), light is the one that shows the most extreme variation within the aquatic medium. Light decreases with depth down to levels that cannot support photosynthesis, with a marked change also in spectral distribution (refer to section "Light" in Chapter 3). Furthermore, to a much greater extent than the other limiting factors, light availability varies with time: both within the day—from darkness to the full noon sun—and as clouds pass across the sun, and with the seasons during the course of the year. Hence, low-light ecosystems are among the most challenging environments for photosynthetic organisms and relatively few algae thrive at the lower limits of the photic zone. Notwithstanding the constraints that restrict photosynthesis and growth at low photon flux density, deep-water algal populations are far more diverse and extensive than expected, and exploration associated to submersible collection of this diversity are continuously leading to an increase in the number of recorded species.

The depth receiving 1% of surface irradiance has typically been cited as the average compensation depth and the lower limit of the euphotic zone, but we will see that many are the deviations from this figure.

The dependence of benthic primary production on irradiance can be defined by three distinct compensation irradiances (refer to Chapter 4):

- $E_{c\ phot}$, compensation irradiance for photosynthesis, the irradiance at which net photosynthesis is zero, that is, the rates of gross photosynthesis and autotrophic respiration are equal.
- $E_{c\ growth}$, compensation irradiance for growth, the irradiance at which gross primary production balances the carbon losses (respiration, grazing, exudation of dissolved organic carbon, reproduction) for a particular organism.
- $E_{c\ comm}$, compensation irradiance for community metabolism, the irradiance at which gross community primary production balances the respiratory carbon loss for the entire community.

$E_{c\ phot}$ is by far the most often reported measure of compensation irradiance and is an important physiological trait, but does not have a direct translation into the distribution and long-term production of benthic organisms. It approximates $E_{c\ growth}$ only when measurements are obtained from individuals collected close to the depth limit of a particular species or acclimated at an irradiance close to that found at the depth limit. These conditions are not frequently met. $E_{c\ growth}$, for which there is a reasonable empirical basis, is the relevant parameter for estimating the areal extent of benthic primary producers (the area receiving irradiances $\geq E_{c\ growth}$). $E_{c\ comm}$ represents the threshold irradiance above which benthic communities are autotrophic and can contribute to net production of organic carbon in coastal ecosystems.

$E_{c\ growth}$ and $E_{c\ comm}$ are the ecologically and biogeochemically relevant irradiance thresholds for benthic communities. These thresholds, respectively, delineate the deepest extent of benthic primary producers and the depth over which these communities act as sources of organic carbon to coastal ecosystems.

The maximum depth of distribution of primary producers, both microalgae (planktonic and benthic) and benthic macroalgae, which represents an estimate of $E_{c\ growth}$, ranges from 90 to 268 m corresponding to 11 to 0.0005% of incident surface radiation.

The first example of oceanic deep-water dwelling microalga is *Prochlorococcus*, a small (about 0.7 μm) planktonic cyanobacterium recorded in the Arabian Sea, growing at a depth of 120–160 m, at photon fluxes averaging 0.04% of surface incident radiation. This microalga is adapted to this extremely low light largely through increased light absorption capabilities, that is, very high levels of accessory pigments per cell, namely chlorophyll *b*-related pigments, and high ratios of accessory pigments to chlorophyll *a* (high A_{480}/A_{450} and A_{450}/A_{680}). It displays exceptional photosynthetic efficiencies, averaging 0.107 mg C (mg chlorophyll *a*)$^{-1}$ h^{-1} (μmol photons m^{-2} s^{-1})$^{-1}$, biomass-normalized photosynthetic rates, P^B, between 0.48 and 3.84 mg C (mg chlorophyll *a*)$^{-1}$ h^{-1}, and saturating irradiance, E_k, as low as 9.2 μmol m^{-2} s^{-1}.

Much less is known about the ecological limits of benthic microalgae, *in situ* light requirements or maximum depth of distribution. Limited field studies of benthic microalgae distributions and assessments of their photophysiology under low-light conditions suggest the potential for depth and light limits similar to those of phytoplankton and benthic macroalgae. Significant concentrations of chemically intact chlorophyll *a* have been reported from sediments in outer shelf and upper slope habitats in several locations globally and, offshore from North Carolina, to depths as great as 222 m, which could suggest the presence of benthic microalgae in this very low-light environment.

Recently, obligate benthic diatoms were discovered living on the upper continental slope offshore from North Carolina, in waters as deep as 191 m. A total of 126 species were identified from prepared samples, more than 90% of which are obligate benthic forms. Species of the epipsammic, monoraphid genus *Cocconeis* were dominating in samples collected at bottom depths from 67 to 191 m. This discovery substantially extends the known depth range of these primary producers and holds significant implications for oceanic productivity and biogeochemical cycling. Midday, near

bottom, photosynthetically active radiation values recorded at the 191-m site averaged 0.106 μmol m^{-2} s^{-1}, representing about 0.028% of surface incident radiation and resulting from a water column attenuation coefficient of 0.0446 m^{-1} (refer to Equation 3.2). The presence of active benthic microalgae in these extremely low-light conditions suggests the development of special light-harvesting adaptations including elevated levels of the blue-light absorbing accessory pigment, fucoxanthin.

The maximum depth of macroalgae distribution is 268 m where dark-purple crustose coralline algae (Rhodophyta) grow on the primary basement substratum of San Salvador Island, Bahamas. Crustose corallines have adopted the ideal strategy for life in deep water; they can survive in spite of slow growth, they tolerate a wide range of nutrients, and they are well protected against grazing by herbivores. Their thallus structure represents a horizontal light receiver with no self-shading by a single cell layer which enhances light absorption. These algae have an increased content of accessory pigments, including carotenoids, xantophylls, and phycobiliproteins, which absorb light in spectral regions different from those of the green chlorophylls *a* and *b*, and channel it to chlorophyll *a*, which is the only molecule capable of converting sunlight energy into chemical energy. Moreover, they show an increased photosynthetic antenna size, which in turn increases the chance of photon absorption.

Depending on to the clarity of water and the annual sum of photosynthetic active radiation impinging at the water surface, the lower depth limit of crustose coralline algae shifts with lower latitude from several meters in cold temperate waters (e.g., 15 m on Helgoland Island, North Sea) to several hundred meters in tropical waters (e.g., 268 m Bahamas). The annual sum of impinging irradiance must support at least the annual need of energy for maintenance metabolism, measured by the maintenance respiration rate and guarantee a minimum of energy surplus for the establishment of growth and reproduction. Compared to cold-temperate regions, Caribbean algae are able to survive in such extreme depths due to the higher solar irradiance, a 12-h period of daylight and the clear water conditions. For algae with a more complex, even erected thallus and the presence of non-photosynthetic tissue as typically found in kelps, the need for light energy increases and the algae have to grow in more shallow waters as the amount of respiration and self-shading areas increases.

At the depth of crustose corallines, the red part of the sunlight spectrum is filtered out from the water, the faint residual light is blue-green, and its amount is approximately 0.0005% of the surface value. Considering that "full sun" (i.e., irradiance in the middle of the day) shines approximately 10^4 mol m^{-2} $year^{-1}$ on the earth surface, 0.0005% is equivalent to a photon flux of only 5 mol m^{-2} $year^{-1}$ during full sunlight at its maximum zenith. At this low photon flux density, there are a number of constraints that restrict photosynthesis and growth in the form of energy-consuming processes whose rates are invariant with photon flux density, and thus consume a large fraction of adsorbed photons at lower photon flux densities. Among these processes are the redox back reactions of reaction center II, the leakage of H^+ through thylakoid membranes, and the turnover of photosynthetic proteins. The first process limits the rate of linear transport and ADP phosphorylation, whereas the second consumes ATP. These energy-consuming processes are sequential, so that their effects in constraining photosynthetic and growth rates are multiplicative. It is still difficult to explain how algae that can grow at less than 1 μmol m^{-2} s^{-1} cope with these energy-consuming reactions, which use an increasing fraction of the energy input as the photon flux density decreases.

Also green and brown algae occur in depths comparable with those of red algae. In San Salvador Island, Bahamas, above the depth of crustose coralline algae, around 210 m, trace amounts of the rock-boring green alga *Ostreobium* sp. have been found, followed at 155 m by *Rhipiliopsis profunda*, another green alga. In the same location, the brown alga *Lobophora variegata* has been collected at 140 m, but many other ochrophytes and chlorophytes have been observed in different locations of coastal oceans between 100 and 157 m (Table 8.1).

Recently, particular attention has been paid to a group of little-known chlorophytes persisting in deep, low-light, benthic marine habitats, where grazing pressure and competition for space are highly reduced. This group forms the early diverging chlorophytic lineage of the Palmophyllales, which includes the three genera of *Palmophyllum*, *Verdigellas*, and *Palmoclathrus. Verdigellas* has mostly been recorded at depths between 60 and 120 m, whereas *Palmophyllum* and *Palmoclathrus*

TABLE 8.1
Maximum Depth of Deep-Water Microalgae

Maximum Depth (m)	Genus	Phylum	Class
40	*Derbesia*	Chlorophyta	Ulvophyceae
45	*Nereocystis*	Ochrophyta	Phaeophyceae
50	*Callophyllis*	Rhodophyta	Florideophyceae
60	*Avrainvillea*	Chlorophyta	Ulvophyceae
65	*Hydrolithon*	Rhodophyta	Florideophyceae
70	*Cladophora*	Chlorophyta	Ulvophyceae
75	*Halimeda*	Chlorophyta	Ulvophyceae
80	*Lithophyllum*	Rhodophyta	Florideophyceae
85	*Mesophyllum*	Rhodophyta	Florideophyceae
90	*Microdictium*	Chlorophyta	Ulvophyceae
95	*Laminaria*	Ochrophyta	Phaeophyceae
100	*Anadyomene*	Chlorophyta	Ulvophyceae
	Palmophyllum	Chlorophyta	Incertae sedis
105	*Mesophyllum*	Rhodophyta	Florideophyceae
110	*Codium*	Chlorophyta	Ulvophyceae
115	*Dictyota*	Ochrophyta	Phaeophyceae
120	*Verdigellas*	Chlorophyta	Incertae sedis
125	Endosymbiotic *Symbiodinium*	Myzozoa	Dinophyceae
130	*Halimeda*	Chlorophyta	Ulvophyceae
135	*Caulerpa*	Chlorophyta	Ulvophyceae
140	*Lobophora*	Ochrophyta	Phaeophyceae
150	*Corallinales*	Rhodophyta	Florideophyceae
	Peyssonnelia	Rhodophyta	Florideophyceae
155	*Rhipiliopsis*	Chlorophyta	Ulvophyceae
160	*Prochlorococcus*	Cyanobacteria	Cyanophyceae
170	*Lithothamnion*	Rhodophyta	Florideophyceae
175	*Hydrolithon*	Rhodophyta	Chloridophyceae
180	*Peyssonnelia*	Rhodophyta	Florideophyceae
190	*Cocconeis*	Ochrophyta	Bacillariophyceae
210	*Ostreobium*	Chlorophyta	Ulvophyceae
220	*Corallinales*	Rhodophyta	Florideophyceae
268	Crustose red algae	Rhodophyta	Florideophyceae

species occur in shallower water, between 40 and 100 m. These algae are characterized by a unique type of multicellularity, forming firm, well-defined microscopic thalli composed of isolated spherical cells morphologically and ultrastructurally identical in a gelatinous matrix (palmelloid organization). Several members have evolved relatively large, erect thalli with specialized gross morphological features. Individuals of the deep-water genus *Verdigellas* attach to substrate by means of one or more distinct holdfast structures, from which thalli expand above, yielding an umbrella-like morphology well adapted to maximally capture the sparse light penetrating from the sea surface and reflected from the underlying substratum. *Palmoclathrus*, a genus from seasonally changing temperate waters, features a stout, perennial holdfast system consisting of a basal disk and one to several cylindrical stalks from which seasonal peltate blades grow. *Palmophyllum* is morphologically simpler, forming irregular lobed crusts that are tightly attached to the substrate.

Motile stages and their accompanying basal bodies and flagellar roots have never been observed. These algae lack the green light-harvesting photosynthetic pigments siphonoxanthin and siphonein typically found in other low-light adapted green algae, but adapt to low-light conditions by maintaining high concentration of chlorophyll *b*, which absorbs the blue-green light of deeper water more efficiently than chlorophyll *a*.

The interest in the Palmophyllales is strictly connected to their deep-branching position, which raises questions about the nature of the green plant ancestor, generally accepted to be a unicellular flagellate. The molecular phylogenetic evidence that the nonflagellate Palmophyllales form a distinct and early diverging lineage of green algae indicates that the green plant ancestor could have been a nonmotile unicellular organism, maybe possessing transient motile stages.

A separate mention has to be reserved for other benthic primary producers, thriving at very dimly lit deep-water habitats, that is, corals, invertebrates in intimate endosymbiosis with photosynthetic dinoflagellates of the genus *Symbiodinium* (zooxanthellae). The deepest known hermatypic coral reefs are mainly located in Jamaica and Bahamas, at a depth of around 70 m. Recently, a deep-water coral community has been discovered at Pulley Ridge off the southwest coast of Florida, in waters 58–75 m deep. At these depths, large areas with up to 60% live coral coverage are present; the zooxanthellate scleractinian coral *Agaricia* sp. is one of the most abundant hermatypic corals in southern Pulley Ridge, forming tan-brown plates up to 50 cm in diameter. The corals generally appear to be healthy, with no obvious evidence of coral bleaching or disease, though they appear to be thriving on 1–2% (5–30 μmol m^{-2} s^{-1}) of the available surface light (PAR) and about 5% of the light typically available to shallow-water reefs (500–1000 μmol m^{-2} s^{-1}).

Besides zooxanthellate corals, the deepest portion of the photic zone also hosts antiphatarians, commonly known as black corals. These organisms have traditionally been considered an exclusive azooxanthellate order of anthozoan hexacorals, a trait thought to reflect their preference for low-light environments that do not support photosynthesis. They occur in dimly lit to dark areas in both shallow water, where they are present in shaded microenvironments, and deep water, where they are effectively shaded by light intensities decreasing with depth. ITS2 genotyping and histology performed on antiphatarian species collected from the Hawaian Islands and Johnston Atoll at depths between 10 and 396 m detected *Symbiodinium* cells in all the samples collected down to below the compensation depth for photosynthesis in Hawaian waters (approx. 125 m). This study represents the deepest record for *Symbiodinium*, indicating that at least some members of this dinoflagellate genus have incredibly diverse habitat preferences and broad environmental ranges. Moreover, these findings suggest that the carbon demand of these dinoflagellate is either reduced by dormancy or met by means other than photosynthesis, such as by self-digestion or by heterothrophic feeding on an external carbon source. Heterotrophic endosymbiont feeding has been suggested in zooxanthellate invertebrates that are seasonally exposed to environmental conditions that do not support photosynthesis, and these modes of nutrition would make sense for *Symbiodinium* populations located below the compensation depth for photosynthesis.

Low-light habitats are not limited to aquatic environments, but they are present also in subaerial locations, such as hypogea. The most comprehensive studies of subaerial biofilms have been carried out on the three catacomb sites dedicated to St. Domitilla, St. Callistus, and Priscilla in Rome, Italy, and on Maltese paleo-Christian catacombs situated in Rabat and Paola.

Micro-environmental parameters (light intensity/photoperiod, degree of wetness of the surface, relative humidity, temperature) determine which microorganisms prevail in a specific hypogeum, but the undisputed phototrophic protagonists in subaerial biofilms are filamentous cyanobacteria. Different species of terrestrial epilithic cyanobacteria belonging to the genera *Eucapsis* Clements et Shantz 1909, *Leptolyngbya* Anagnostidis et Komárek 1988, *Scytonema* Agardh ex Bornet et Flahault 1887, and *Fischerella* lahault Gomont 1895 occur as dominant organisms in these phototrophic microbial communities.

Some of these taxa have never been recorded outside of these habitats and for this reason are defined as "troglobitic," that is, obligate cavernicole taxa unable to survive outside of caves

or other low-light environments. Subaerophytic troglobitic cyanobacteria belonging to the genus *Leptolyngbya* are particularly abundant in phototrophic biofilms present in both Roman and Maltese hypogea. These cyanobacteria live under extremely low photon fluxes, rarely exceeding 10 μmol m^{-2} s^{-1}, similar to deep-water algae. At this extremely low photon fluxes, these algae can grow because of the presence of phycobiliproteins organized in phycobilisomes in the thylakoid membranes inside the cell that transfer their absorbed extra energy to chlorophylls. They sense the light direction by means of a photoreceptive apparatus that is located in the apical portion of the tip cell, which is composed by a carotenoid-containing screening device and a light detector based on rhodopsin-like proteins (refer to Chapter 2).

ALGAE–ANIMAL INTERACTION: RIDING A SLOTH, SWINGING ON A SPIDER WEB, SWIMMING IN A JELLY . . .

Algae are involved into complex relationships with very different animals. They have been reported to grow epizoic on sloths, polar bears, seals, frogs and salamanders, arthropods, and turtles. In the following, we will describe the most unusual associations between these quite distant biological groups.

A very particular symbiosis is that between sloths and green algae. Sloths are slow-moving arborean mammals inhabiting tropical rainforest in Central and South America, represented by two genera, *Bradypus*, the three-toed sloths, and *Chaelopus*, the two-toed sloths. A versatile small-scale ecosystem that includes algae, ciliates, and fungi thrives in the sloth fur. The greenish color of the hair, especially evident in *Bradypus* species, is due to green algae belonging to the algal classes Ulvophyceae and Trebouxiophyceae. These algae effectively turn these animals green, giving them excellent camouflage among the leaves. The camouflage is crucial to the sloth's survival, because its inability to move quickly makes it an easy target for predators such as the harpy eagle (*Harpia harpyja*). Among the many odd features of these interesting animals, perhaps the oddest of all is their hair which, with its peculiar structure and its algal presence, is unlike the hair of any other mammal. Sloth hair is long and coarse and that of the two living species belonging to the genus *Chaelopus* is unique in having a number of deep groves running the length of each hair, whereas the hair of the four species belonging to genus *Bradypus* has irregular transverse cracks that increase in number and size with age. During the dry season, the hair of sloths usually has a dirty brown coloration, but during a long period of rain it may show very appreciable greenish tinges brought about by the increased presence of symbiotic algae.

Recently, the genetic diversity of the eukaryotic community present in the fur of sloths belonging to all six extant species was investigated. The majority of the green algal sequences obtained from the hair samples formed a clade of their own within the green algal class Ulvophyceae (Chlorophyta). This group received high support (100%) for its monophyly in all phylogenetic analyses that were employed. This clade, consisting of small (3–13 μm) thick-walled cells without pyrenoids, is likely to correspond to the green algal genus *Trichophilus*, whose first description dates back to 1887. The clade was subdivided into three subclades that received moderate-to-high internal node support. Two subclades, A and C, were formed by rRNA gene clones originating from *Choloepus hoffmanni* hair samples. Clones in the clade B originated from the hair of *Bradypus* species. Within clade B, the sequences from *Bradypus tridactylus* were different from those of *B. variegatus* and *B. pygmaeus*.

Trichophilus spp. was the only green alga in the hair of the brown-throated sloth *B. variegatus* and the pygmy three-toed sloth *B. pygmaeus*. These species were also found on Hoffmann's two-toed sloth *C. hoffmanni* and the pale-throated sloth *B. tridactylus*, together with terrestrial green algae from their surroundings, such as *Trentepohlia* (Ulvophyceae, Chlorophyta) and *Myrmecia* (Trebouxiophyceae, Chlorophyta), while the maned three-toed sloth *B. torquatus* hosted a variety of purely terrestrial algae.

The algae have a distinct distribution patterns in *Choloepus* and *Bradypus*, lying longitudinally along the grooves in the former and in short lateral tongue or lines in the latter. The algae found on the

coat of *B. tridactylus* lie between the cuticle scales and the hair changes with age in apparently all species of *Bradypus*. Young hairs are white, gray, brownish, or black and do not possess the deep cracks seen in older hairs. The first traces of algae appear on these young hairs as tiny dots or extremely narrow transverse lines. Older hairs have larger, wider algal colonies and obvious deep transverse cracks. When wet, these cracks close considerably, but when dry give the effects of beads on a string. The oldest hairs are badly deteriorated with the spongy cuticle worn off on one side exposing the full length of the cortex. In the older hairs, living algae are absent. It was suggested that either the algae colonize the very narrow cracks in young hairs or the algae themselves initiate the cracks. The hair of all the three *Bradypus* species readily absorbs water, but those of *Choloepus* do not.

No evidence of algae were found in babies still at the age of clinging to their mothers, suggesting that at least *Trichophilus* is gained in childhood, most likely from the mother. This observation is supported by an earlier study noting that sloths gain the algae and other parasites by the time they are a few weeks old, which could provide them a protective camouflage.

Lack of healthy algal colonies has been observed in *Bradypus* kept in captivity; since they do not survive long under these conditions, algae have been suggested to provide nutrition or a particular trace element essential for the health of the animals.

Algae have reported to grow also on the fur of polar bears (*Thalarctos maritimus*). These animals normally have creamy-white fur, presumably an adaptation for camouflage in a snowy environment. However, cases are being reported of polar bears kept in captivity in different American and Japanese zoos, which turned green as a result of algae growing on their fur. The coloration was particularly evident on the flanks, on the outer fur of the legs, and in a band across the rump. This coloration was clearly attributable to the presence of algae inside the hairs, specifically in the hollow medullae of many of the wider (50–200 μm), stiffer guard hairs of the outer coat. The thinner (<20 μm) hairs of the undercoat, which were not hollow, were colorless. The fact that some of these lumina were in connection with the external air or water could explain how the algal cells could have entered the hairs in the first place, and how exchange of O_2 and CO_2 and uptake of water and mineral salts would be facilitated and could permit growth of the algae if suitably illuminated. Such a habitat has certain advantages, being warm and protected from most kind of potential predators. The algae isolated from the polar bear hairs and cultured under controlled conditions were identified as cyanobacteria.

Algal occurrence on turtle carapacians is another common associative phenomenon often reported in literature. The green algal genus *Basicladia* Hoffman and Tilden (Ulvophyceae, Chlorophyta) contains species, which are specifically epizoic on carapaces of turtles or shells of mollusks. Closely related to the genus *Cladophora*, the genus *Basicladia* is mainly distinguished by its epizoic nature. Five species are recognized and all are known only from freshwater turtles or snails. *Basicladia crassa* and *B. chelonum* have been reported from freshwater turtles in several states of the Rocky Mountains and the Caribbean. Outside the USA, *B. sinensis* was described from the back of a turtle brought from China to an aquarium in California, and *B. ramulosa*, an exceptionally large species, is known from Australian turtles. The fifth taxon, *B. vivipara* is known only from the freshwater snail, *Viviparus malleatus* Reeve. In 1975, *B. crassa* was reported for the first time from Virginia on the carapace of a red-bellied turtle *Chrysemis rubriventris*. The algae are characterized by a thallus with siphonocladous organization, with single, unbranched, sometimes twisted filaments. Rhizoids at the basal part are usually round and they attach to the turtle shell. These algae are usually restricted to the turtle carapace, where they form a wide band thickly covering the marginals and ventral half of the pleural scutes, but thinning as it extended dorsally. The rugose carapacial surface of this turtle is well suited for the attachment of algal rhizoids, but the basking habit of the turtle may account for the absence of most carapacial algae since they are subject to increased desiccation and solar radiation above the water level. Also *C. rubiventris* sheds the epidermal scutes of its carapace periodically, thus freeing itself of any algae attached. However, it is not uncommon to find "moss-back" red-bellies in the spring, especially just after emergence from hibernation when air temperature is still too cool for much basking. *B. crassa* and *B. chelonum*

are able to survive periods of basking desiccation and even more heat than the turtles themselves. It is possible that repeated exposure to the sun's ultraviolet (UV) rays and the drying effect through frequent basking associated with the grazing action of herbivorous fish or amphipods would at least limit the growth of these algae.

Another mutualistic association with algae occurs in some amphibians. All amphibians lay eggs with a capsule, although the form and thickness of the capsule vary widely. Some amphibians, including the spotted salamander *Ambystoma maculatum* and the pickerel frog *Rana palustris*, embed their eggs in large masses of relatively firm jelly, which are attached to vegetation in ponds. Other amphibians, including the wood frog *Rana sylvatica* and the spotted marsh frog *Lymnodynastes tasmaniensis*, lay their eggs in masses that float at the surface of the pond or are loosely attached to vegetation. The capsule, at least in aquatically developing amphibians, protects the eggs from predators and it also resists exchange of respiratory gases. Amphibian egg masses in the wild are often inhabited by algae, as, for example, egg masses of *A. maculatum*. The algae were first noted by Orr in 1888, who speculated that they must have considerable influence on the respiration of the embryos. It is now well established that this relationship is symbiotic. The alga *Oophila ambystomatis* (Chlorophyceae, Chlorophyta) is found exclusively in amphibian egg masses, mostly in those of *A. maculatum* (it derives its name from this association), but also in those of *R. sylvatica* and some other species.

Individual egg capsules appear green due to dense accumulations of algae surrounding the embryo. In *A. maculatum*, algae primarily enter salamander embryos through the blastopore before the formation of a patent stomodeum and therefore before active feeding is possible. The embryonic association of the *Ambystoma*–alga symbiosis may indicate an inefficient immune system or an adaptive immune response that would otherwise remove invading intracellular algae. Some algal cells are also embedded within epithelial or mesenchymal tissues that are far from the alimentary canal, consistent with algae having entered salamander embryos directly by penetrating their embryonic integument. Molecular data are consistent with a process of oviductal transmission of algae from one salamander generation to the other, but horizontal transmission could be present as well, with the algae deriving from the environment. Algal cells leave direct sunlight by entering opaque salamander tissues. Behavioral stimuli, such as gradients of nitrogenous waste, which may instigate algal proliferation, could serve as the behavioral cue for tissue and cellular invasion against this light gradient.

The mutual benefit of this facultative association has been clearly established through exclusion experiments. Clutches raised in the dark do not accrue detectable algae. The presence of algae in these experiments correlates with earlier hatching, decreased embryonic mortality, more synchronous hatching, and reaching a larger size, and later developmental stage at hatching. Additionally, algal growth is minimal in egg capsules after embryos are removed, indicating that the embryos, and not the egg capsules, aid algal growth. Intracapsular algae are thought to benefit from nitrogenous wastes released by the embryos, whereas salamander embryos benefit from the net increase of oxygen produced by the algae. Most intracellular algae, and algae of the alimentary canal, disappear by early larval stages. Their possible absorption may confer a further metabolic benefit to their host. Presence of algae also correlates with decreased cilium-mediated rotation of early-stage embryos and increased muscular contractions during later embryonic stages, both of which may be secondary effects of modulated oxygen levels. The reciprocal benefits of hatchling survival and growth to the embryo, and population growth to the algae, reveal that this symbiosis is a true mutualism.

Algae are also important for tadpoles of other amphibians, establishing an ecologically important mutualism that is conditional and provides partner species with novel options for adjusting to a changing environment. It is well known that organisms reaching their critical thermal maximum (CTM; the minimal high deep-body temperature that is lethal to an animal) are incapable of escaping the lethal conditions. This holds especially true for aquatic organisms in thermally uniform systems, which have no refuge from heat stress; further, temperature increases within such systems decrease

the concentration of the necessary oxygen and carbon dioxide gases. Aquatic organisms that are stressed for these gases for respiration and photosynthesis would benefit from fortuitous mutualistic interactions in which the "by-product" gases evolved by metabolism can be absorbed reciprocally. Observations were conducted on numerous tadpoles of the dwarf American toad, *Bufo americanus charlesmithi* in a shallow temporary pool subjected to extended exposure to solar radiation, located in Ashley County (Arkansas, USA). The water became very warm by mid-afternoon, and some of the tadpoles possessed an atypical greenish color. The tadpoles were late stage, and some of them exhibited well-developed legs. Microscopic examination of live tadpoles from the pool revealed cluster of biflagellated green algae identified as *Chlorogonium* (Chlorophyceae, Chlorophyta) scattered as greenish blotches over the skin. Individuals of this alga were observed actively flagellating to maintain a position oriented to the skin of the tadpole. The distribution of the alga generally followed the pattern of cutaneous blood vessels on the dorsal surfaces of the legs, tail, and lateral body wall.

The high CTM of toads help them survive in warmer conditions and shortens the time required for development, thereby promoting metamorphosis prior to desiccation of the habitat. Rates of oxygen consumption in tadpoles increase with higher temperatures, but water at higher temperature holds a lower concentration of gases. Although tadpoles are tolerant of warmer temperatures, the O_2 deficits can lead to respiratory distress and death. Under conditions of low O_2, tadpoles of some species can supplement oxygen intake by gulping air, but the late development of the lungs precludes this in *Bufo*. Consumption of O_2 increases sharply prior to metamorphosis. Thus, the warmer water contains less O_2 at a time when more may be needed. Even after acclimatization to warmer temperatures, the CTM of tadpoles of most anuran species is 38–40°C, with a few exceptions above 41°C in species that develop in xeric (with very little moisture) or tropical habitats. On the other hand, the rate of photosynthesis tends to increase with increases in temperature up to an optimum, after which it decreases rapidly, partly limited by the availability of inorganic carbon. Growth rate of algae slows in stagnant cultures because the rate of diffusion of CO_2 from the air becomes limiting, partly because CO_2 diffuses 10^4 times faster in air than in water. Green algae (Chlorophyta, including *Chlorogonium*) tend to dominate in temperatures of 15–30°C, but are replaced by cyanobacteria above 30°C. Thermophilic algae thrive best in waters rich in CO_2, where conditions necessary to maintain high rates of photosynthesis are met. The pattern of association and distribution of *Chlorogonium* over the skin of tadpoles allows maximum potential for uptake of otherwise limiting CO_2 released via cutaneous respiration by tadpoles. The relatively small size of *Chlorogonium* specimens also could indicate stress. The mean length of the cells taken from the tadpoles was 13.4 μm (range 7–22 μm), and width ranged only between 1.5 and 3 μm. The normal measurements from species known to occur in the USA ranges from 19 to 59 μm in length and 5 to 18 μm in width. Smaller cells result in a higher surface-to-volume ratio, which could help maximize absorption in a CO_2-limited environment.

The CTM at which tadpoles of *Bufo americanus* could survive independently is 39.5°C. In a heat-stress-inducing environment, however, the CTM could be expanded by over 4°C (to about 43°C) in the presence of a photosynthetic, mutualistic alga such as *Chlorogonium*. Considering these phenomena, it is hypothesized that the *Chlorogonium* and tadpoles are exhibiting a facultative symbiosis in which tadpoles gain O_2 produced via photosynthesis adjacent to the skin, and concomitantly *Chlorogonium* received the metabolic CO_2 evolved from the tadpoles. Similar algal accumulations have been found on tadpoles of gray tree frogs (*Hyla versicolor*) and cricket frog (*Acris crepitans*) at other locations within Arkansas, USA.

Arthropods are also good hosts for algae. Cyanobacteria were reported to grow epizoically on the dorsal scute of the harvestman *Neosadocus* sp. (Arachnida, Opiliones), on Cardoso Island, southeast Brazil. The epizoic algae almost fully covered the harvestmen's back, giving the animals a greenish coloration contrasting markedly with the brownish body and appendages. The growth of the algae did not affect behavior and locomotion of the animals, which would benefit from the presence of the photosynthetic organism by being camouflaged and thus protected from visual diurnal predators.

Arachnids are also exploited by green algae. Very recently, a species of the well-known genus of green unicellular alga *Dunaliella* (Chlorophyceae, Chlorophyta) was found on the walls of a cave located in the Coastal Range hills of the Atacama Desert (Chile). The cave, situated about 75 m above sea level, is about 170-m deep, with an average height of 50 m, and its entrance directly confronts the Pacific Ocean, less than 200 m away from it. The alga grows upon spider webs attached to the walls of the entrance-twilight transition zone of the cave. All previously reported members of this genus are found in extremely saline aquatic environments, and hence this is the first *Dunaliella* species able to thrive in a subaerial habitat. The identity of this alga as a new species, *Dunaliella atacamensis*, was assessed by molecular and morphological methods.

The Coastal Range, which separates the hyperarid Atacama Desert plateau from the Pacific Ocean, acts as a topographic barrier to clouds and moisture-rich marine air moving from the ocean. Thus, fog-originated water allows the presence of "fog oases" in this region, with a daily cycle with a maximum expansion over the coastal hills during the night and early morning hours. The cave interior acts like a funnel that continuously captures the incoming water-rich air of oceanic origin, in particular, the south-facing walls exposed to the moisture-rich prevailing winds, the only area of the cave where the alga grows. This area is about 20 m away from the entrance, where the light is about 1.4% of the outside incident light. The alga grows mostly as colonies of green cells covering spider webs attached to the cave walls and not on the underlying rocks. The colonized spider webs are constantly subjected to the flow of the humid-rich air moving through them, condensing water droplets especially during the night and early morning hours. Condensation of water onto the hygroscopic threads of spider webs is a well-known phenomenon. An alternative source of water could be dew, whose formation is induced by substrates with temperatures below the dew point of the ambient air. As the exposed surfaces of the cave cool by radiating heat during the late afternoon and night, atmospheric moisture could condense at a rate greater than that at which it can evaporate, resulting in the formation of water droplets on the spider-web threads at the early hours of the morning as observed.

D. atacamensis cells are nonmotile, mostly round or ovoid, with a diameter of 6 μm; they possess one cup-shaped chloroplast with a single pyrenoid surrounded by several starch bodies. Though no flagellum appears to be present, the cells possess small stub-like structures reminiscent of flagella. These stub-like structures are comparable to the short flagella previously described in a *D. salina* mutant and could have the function of primary "clinging" devices attaching the cell to the spider-web thread.

The cells form tetrads which join into colony-like structures in irregular clumps reminiscent of palmelloid stages of other *Dunaliella* species under reduced salinity conditions (≤10% NaCl). In the palmella stage, the cells usually lose their flagella and eyespot, become more rounded and excrete a layer of exopolysaccharides (EPSs) in which they repeatedly divide, thus forming colonies of green cells. All these morphological characteristics are present in *D. atacamensis* cells.

Another interesting feature is the well-developed layer of EPSs, which in *D. salina* strains are produced in response to the environmental stress caused by increasing salt concentrations. EPSs have been shown to be involved in the efficient capture and retention of ambient water by cyanobacteria in extreme environments, suggesting a similar role for the cave inhabiting *D. atacamensis*. Since the thick layer of EPSs could lower CO_2 diffusion in the cells, a pyrenoid might be advantageous in a subaerial habitat for carbon fixation in this extreme environment.

Different features previously evolved by *Dunaliella* species for living in hypersaline environments (i.e., colonial growth, pigments for avoiding photodamage, salt tolerance, glycerol production, EPS production) result highly advantageous for adapting to a subaerial environment with reduced water availability and perhaps different light regimes than those experienced by its aquatic ancestors. This process recapitulates the adaptations evolved by green algae for the sea-to-land transition, that is, from aquatic algae to land plants. As algae moved to land, they could make an efficient use of resources by exploiting a range of previously evolved traits that are likely to have played a key role in this successful process of extending the habitability range. These include

cell-wall biochemistry, desiccation resistance and tolerance, structural complexity, as well as various reproductive strategies. Many of these traits characterize the enormous physiological variability of *Dunaliella* species, and *D. atacamensis* represents a beautiful example of this assertion.

Algae can also establish pathogenic association with both animals and humans. Among the genera most intensely investigated are *Prototheca*, which infect only vertebrates, and *Helicosporidium* (Trebouxiophyceae, Chlorophyta), which are known so far to invade only invertebrates.

Algae of the genus *Prototheca* are achlorophyllic unicells, spherical to oval in shape, ranging from 3 to 30 μm in diameter. Phylogenetic studies indicate that *Prototheca* spp. cluster with the photosynthetic alga *Auxenochlorella protothecoide* (Trebouxiophyceae, Chlorophyta), and *Helicosporidium*. Therefore, protothecal species are closely related to the green algae *Chlorella* (Trebouxiophyceae, Chlorophyta) but lack chloroplasts and possess a two-layered, instead of three-layered, cell wall; they are heterotrophic and require an external source of organic carbon and nitrogen. The life cycle is similar to that of algae of the genus *Chlorella*; reproduction is asexual by internal septation and irregular cleavage, with subsequent rupture and release of 2-to-16 autospores through a characteristic split in the cell wall of the parent cell. Released autospores then go on to develop into mature cells. The taxonomic status of the genus *Prototheca* has changed during the last decades and currently the following five species are assigned to this genus: *P. zopfii*, *P. wickerhamii*, *P. stagnora*, *P. ulmea*, and *P. blaschkeae*. A sixth species, *P. moriformis*, is not generally accepted. Only two of these species have been documented to cause infections in humans and animals, that is, *P. zopfii* and *P. wickerhamii*.

These algae are globally ubiquitous and can be isolated from various reservoirs, such as environment, animals, and food. Typical sources of *Prototheca* species are the slime flux of trees, fresh and marine waters, soil and sewage, stables and animal buildings, excrement, various animals (cattle, deer, dogs), and food items such as butter, potato peels, bananas, and cow milk.

In 1952, *P. zopfii* was first identified as a pathogen of bovine mastitis associated with reduced milk production characterized by thin watery secretion with white flakes. This form of mastitis now occurs endemic in the most countries of the world and represents a serious problem since the affected animals must be culled from their herds to halt transmission of the disease.

Prototheca produce disease also in humans, and the clinical conditions caused by this alga are generally referred to as protothecosis. The first case of human infection was diagnosed in 1961 in Sierra Leone on a rice farmer; it took the form of a verrucose foot lesion from which *P. zopfii* was isolated as an etiological agent. Over the following years, the number of documented cases of protothecosis rose continuously, with about four new cases being diagnosed every year over the past decade.

Only a few cases of systemic disease have been reported. Most infections are likely due to traumatic implantation of organisms, but a few cases of opportunistic infection have also been reported. Protothecosis has also been diagnosed among other very different species such as dogs, cats, sheep, deer, Atlantic salmon, carp, and flying foxes.

Despite its nonphotosynthetic, obligate heterotrophic nature, *Prototheca* is known to have retained a plastid with starch granules; recent data indicate that several metabolic pathways (e.g., carbohydrate, amino acid, lipid, and isoprenoid) are located in this nonphotosynthetic plastid. The reconstruction of this complex metabolic network could represent a new approach in the treatment of protothecosis.

Algae of the genus *Helicosporidium* are obligate parasites of invertebrates, especially arthropods (insects, mites, crustaceans, and trematodes), which support the growth and development of the parasite in their hemolymph. This alga features three different life stages: cysts, filamentous cells, and vegetative cells. The life cycle begins with an orally transmitted cyst stage that is comprised of three ovoid cells and a coiled, elongate filamentous cell enclosed within an outer pellicle. Within the gut of the host, cysts burst, open, and release a filamentous cell with surface barbs along with three egg-shaped accessory cells. The barbed filaments proceed to invade the gut cells, penetrating them and emerging into the hemolymph. Vegetative cells have been observed to replicate within

the phagocytic hemocytes and to develop extracellularly in the hemolymph. After multiple 2–4 cell autosporogenic cell divisions, a portion of the hemolymph-borne vegetative cells differentiate into cysts. Generally, the infection leads to the death of the host, but the exact mode of transmission remains poorly known.

Also Helicosporidia contain plastids, and although they have not yet been visually identified, molecular evidence has confirmed their existence. The *Helicosporidium* plastid genome is one of the smallest known (37.5 kb). Its reduced size results from loss of many genes commonly found in plastids of other plants and algae (including all proteins that function in photosynthesis), elimination of duplicated genes and redundant tRNA isoacceptors, and minimization of intergenic spaces. The *Helicosporidium* plastid genome is also highly structured, with each half of the circular genome containing nearly all genes on one strand. Both the structure and content of the plastid genome and the deduced function of the organelle show parallels with the relict plastid found in the apicomplexan malaria parasite, *Plasmodium falciparum*.

The apicomplexa and *Helicosporidium* are not closely related; indeed, among plastid types, they could hardly be more different: the apicoplast is a secondary plastid derived from a red alga, whereas the *Helicosporidium* plastid is a primary green algal plastid. The cryptic *Helicosporidium* plastid is probably also metabolically more diverse and retains several pathways that have been lost by *Plasmodium*, such as amino acid metabolic pathways. A possible explanation is that *Helicosporidium* can survive in a cyst form outside its host and thus might need more metabolic autonomy than *Plasmodium*, which is entirely host associated throughout its life cycle.

These unrelated organisms each evolved from photosynthetic ancestors, and the convergence in form and function of their relict plastids suggest that common forces shape plastid evolution, following the switch from autotrophy to parasitism. If plastid reduction is a continuous process, then *Plasmodium* may simply be further along in the process of reducing a full functioning plastid to the highly specialized relict we see today.

SOME LIKE IT COLD . . .

Other unusual and extreme habitats for algae are represented by very cold environments, such as platelet ice layer, the snowfield, and the glaciers. Algal cells adapting to cold temperatures have to take care of the following three processes:

- Changing the ratio of saturated and unsaturated fatty acids in the lipids of the cell membranes to maintain membrane fluidity
- Adjusting the permeability of the cell membrane for water to react to osmotic changes of the outer medium
- When exposed to freezing temperatures, reducing the water content of the cell interior to prevent ice crystal formation

Adaptive features include pigments, polyols (sugar alcohols, e.g., glycerin), sugars and lipids (oils), mucilage sheaths, motile stages, and spore formation. Moreover, since the algae living in regions that receive full solar exposure are adapted to high UV light environment, they can augment their UV protection capacity especially during summer months by producing secondary metabolites including phenylpropanoids, carotenoids, xanthophylls, and mycosporine amino acids.

In some Antarctic coastal areas, a semi-consolidated layer of platelet ice (flat, disk-shaped ice crystals mixed with seawater, approximately 20% ice and 80% seawater by volume, approximately 0.1 m in diameter and 10 mm in thickness), ranging from a few centimeters to several meters in thickness, occurs under sea ice located adjacent to floating ice shelves. The platelet ice is intermediate between the relatively impermeable congelation ice above and the water column below and it is characterized by quite rapid nutrient exchanges. Because it is submerged beneath 1–2 m of consolidated ice, irradiance reaching the platelet ice is first attenuated by the overlying snow cover, sea ice

crystals and brine inclusions, particles, and soluble material, resulting in a light field that is reduced in magnitude and restricted in spectral distribution. Nevertheless, reports of high algal production and biomass accumulation in the platelet ice of the Weddell and Ross Seas (Antarctica) attest to the success of the platelet ice microalgal community at growth in these low light conditions. The algae inhabiting the platelet ice layer are extremely shade adapted, typically attaining maximum photosynthetic rates at an irradiance of ≤ 20 μmol m^{-2} s^{-1}.

Platelet ice provides a much larger surface area for algal attachment and growth than the skeletal layer where most of the biomass within the congelation ice is concentrated. For example, a 0.02-m thick skeletal layer with ice crystals spaced 0.6 mm apart provides approximately 67 m^2 of surface area per m^2 of horizontal surface, with relatively little interstitial space for seawater exchange. In contrast, a platelet layer 0.6–0.7-m thick would have a surface area of approximately 400 m^2 per m^2 of horizontal surface, with a large amount of interstitial space.

In addition, the fixed position of the platelets provides a stable substrate that isolates the algae from vertical mixing and holds them in a higher and less variable light field than that available within the underlying water column. Vertical compression of the biomass also reduces the fraction of PAR absorbed by the ice/water milieu of the platelet layer and increases the fraction absorbed by the algae for use in photosynthesis. Ice microbial communities are dominated by microalgae, primarily diatom species, such as *Nitzschia stellata*, *Pinnularia quadreata*, *Fragilariopsis sublineata*, and *Melosira arctica* (Bacyllariophyceae, Ochrophyta). The latter diatom has extensively been studied for the effect that its abundant secretion of mucus-like EPSs might have on sea ice formation and durability. *M. arctica*, together with other unicellular algae, small crustaceans, and bacteria, inhabits the brine channels present in the platelet ice, in which the brine expelled from the ice crystals remains trapped. The particularly potent exopolymers of *M. arctica* lead to more disordered ice crystals, greater pore density, more complex pore geometries, and greater salt retention by the newly formed ice. Exopolymer-enhanced retention of salt in growing sea ice translates to greater retention of other source water impurities, including EPS-producing microalgae. The benefits of ice entrainment to algae include stable positioning to capture more light energy for photosynthesis and refuge from predation. By altering ice physical properties, EPSs precondition the bottom ice layer for optimal habitability, as well as for later survival as the growing ice front becomes colder interior ice with smaller pores of more concentrated brine and biologically protective EPSs. The survival benefits extend to Bacteria and Archaea ubiquitous in cold winter ice. For filamentous ice algae that cross the ice–water interface, accessing nutrients in underlying waters, the EPS-mediated geometric complexities of the ice pore space may help anchor filaments.

Sea ice that retains more salt will also retain more of the dissolved constituents of the source water, from carbon dioxide and other greenhouse gases to iron and other nutrients essential to primary production. Their retention, alteration, and eventual release determine the biogeochemical imprint of sea ice on the surface ocean (and atmosphere). The reduction of ice permeability by EPSs must also influence the role of sea ice as an inorganic carbon pump from atmosphere to underlying ocean, as well as its seeding and fertilization of surface waters during the melt season.

True snow algae are defined as those that grow and reproduce wholly within the water retained by snow during snowmelt. During summer months, large blooms occur, which can reach cell concentration of 10^6 cells mL^{-1} and color whole snow banks red, orange, green, or gray depending on the species and habitat conditions. Most snow algae belong to Chlorophyta, such as *Chloromonas rubroleosa* (Chlorophyceae) and *Chlamydomonas nivalis* (Chlorophyceae). These algae color the snow red, due to the excess of carotenoids and xantophylls. Species from other algal groups are also important, and the dominant alga in many of the glaciers around the world is the saccoderm desmid *Mesotaenium berggrenii* (Conjugatophyceae, Chlorophyta), an alga that colors the snow grey, due to its iron tannin compounds.

Snow algae go through a complex life history, involving motile vegetative stages that undergo syngamy and thick-walled resting spores and zygotes. The latter allow them to survive the time when the snow has completely melted, and probably to be spread by wind. Many of these algae

possess vegetative and/or motile cells that are usually green in color and immotile spores or cysts that may be red, orange, or yellowish-green in color. The green vegetative cells color the snow green, whereas the red and orange snow are generally caused by the spore stages though some snow algae may be red-pigmented in their vegetative state. The spores usually have thick walls and large amounts of lipid reserves, polyols, and sugars. They are able to withstand subzero temperatures in winter and also high soil temperatures and desiccation in summer, which would kill normal vegetative cells. The motile stages enable them to recolonize the snow from germinating spores left behind on the soil as well as to position themselves at the optimum depth for photosynthesis in the snow/ice column. The cells of some species also secrete copious amounts of mucilage which enable them to adhere to one another and to snow crystals and prevent the cells from being washed away by melt water. The mucilage also forms a protective coat and delays desiccation, and it may have an additional function as a UV shield. A few species are common worldwide, but others are restricted to either the Northern or Southern hemispheres.

Snow algae sustain a highly diverse microbial community on snowfields and glaciers, which is composed of bacteria, heterotrophic flagellates, and ciliates. These organisms in turn sustain a community of cold-adapted animal species, such as midges, copepods, and snow fleas on Himalayan glaciers, and ice worms and collembolas on North American glaciers. Blooms of snow algae can reduce the surface albedo (i.e., the ratio of reflected to incident light) of snow and ice, and largely affect their melting.

The ecology of snow algae is important for understanding the glacial ecosystem since they can be used as indicators to date ice cores drilled from glaciers. Their biomass and community structure inside ice cores may also provide information on the paleo-environment.

SOME LIKE IT HOT . . .

Another example of ecological diversification of algae is the colonization of thermal environments. In these complex, high-temperature systems, the microbial and geochemical interactions are highly interwoven, providing many of the basic constituents for the primordial synthesis of organic molecules and for the evolution of fundamental metabolic processes. Present-day hydrothermal venting occurs in both terrestrial and marine environments, primarily as a direct result of geothermal activity associated to plate tectonic movement. Spreading centers, subduction zones, and hot spot release heat from the crust and generate high-temperature water. Wherever fissures develop around hydrothermal vents, water can percolate into the crust and react with the surrounding rock, heating the fluid and altering its chemistry. The altered water will eventually be forced back convectively to the surface as superheated, highly reduced, hydrothermal fluid rich in gases and minerals. The hydrothermal fluid chemistry is a record of its path within the earth's crust and differs as a function of the underlying rock composition and the residence time of the fluid in the subsurface.

Thermal waters are widely distributed over the face of the earth, although springs are often concentrated in restricted areas. The antiquity of many individual springs is noteworthy. Historical records of springs in the Mediterranean go back to the ancient Greeks and Romans. The largest concentrations of hot springs and fumaroles are found in Yellowstone National Park (USA), Iceland, New Zealand, Japan, and the USSR. Temperatures of hot springs range from 30°C up to boiling (90–100°C depending on the altitude).

Despite the geochemical constraints (physical and chemical parameters) defining the environmental conditions of hydrothermal systems, these systems do support a plethora of unicellular microalgae (microorganisms). The pH of the habitat defines the composition of phototrophic communities, which greatly differ between alkaline and acidic reaches.

Alkaline hot spring habitats across western North America, Asia, Africa, and possibly Europe have been studied for several decades for understanding the composition, structure, and function of microbial communities of thermal environments. Hot spring outflows typically exhibit marked temperature gradients, and microbial communities containing *Synechococcus* (Cyanophyceae,

Cyanobacteria) generally develop in these systems at temperatures between about 45°C and 73°C, which is the thermal maximum for photosynthetic life. Studies on the behavior of *C*-phycocyanin from *Synechoccocus lividus* showed that purified *C*-phycocyanin is stable up to least 70°C and it is highly aggregated with identical spectroscopic behaviors at 20°C and 70°C. For these characteristics, it is termed temperature-resistant protein.

Thermoacidic environments are scattered disparately throughout the earth, but cluster mainly in volcanic areas that have constant geothermal activity and low pH levels, due primarily to the presence of sulfuric acid as a result of the biological and abiological oxidation of elemental sulfur or hydrogen sulfide. The biology of acid hot springs is quite different from that of the neutral/alkaline springs. Though most thermo-acidophiles are prokaryotes (Archea and Bacteria), photosynthetic prokaryotes, such as cyanobacteria, are completely absent from acid water even when the temperature has dropped to quite low values. The photosynthetic microorganisms of such acid water are rare kinds of eukaryotes found nowhere else on earth, the Cyanidiales (Cyanidiophyceae, Rhodopyta), a group of asexual unicellular red algae. Members of this rhodophytan order are able to live in extreme environments that combine low pH levels (~0.2–4.0) and moderately high temperatures of 40–56°C throughout the globe. These algae often form well-developed mats in acidic geothermal locations. How this important physiological resistance is achieved is still not understood, though a strong proton pump or low proton membrane permeability are possibilities.

Three genera, that is, *Cyanidium*, *Galdieria*, and *Cyanidioschyzon,* are recognized. The genera *Cyanidium* and *Cyanidioschyzon* are thought to include a single species each, *Cyanidium caldarium* and *Cyanidioschyzon merolae*, respectively, whereas the genus *Galdieria* has been classified into four species, *Galdieria sulphuraria*, *Galdieria maxima*, *Galdieria partita*, and *Galdieria daedala*, based on cell morphology. The three genera have been distinguished morphologically, based on reproductive patterns, chloroplast, and mitochondrion shapes, the presence or absence of a vacuole, cell size, and the presence or absence of a cell wall. Strains of the genus *Cyanidioschyzon* are smaller (usually 1 or 2 μm in breadth), with an oval, club-like shape. They reproduce by binary cytokinesis and lack rigid cell walls. *Galdieria* and *Cyanidium* have more spherical shapes, possess rigid cell walls, and reproduce through the formation of 4–32 small daughter cells within a mother cell. Chloroplasts vary from a multilobed shape in *G. sulphuraria* to a spherical shape in *Cyanidium*. These algae are not red, but blue-green, due to their predominant pigments, C-phycocyanin, and chlorophyll *a*. As in the case of *Synechococcus*, C-phycocyanin from *Cyanidium* fits the characteristics of a temperature-resistant protein. Its hallmark for stability is to remain inflexible toward structural change over a wide range of temperatures from 10°C to 50°C. The protein denatures irreversibly at the temperature at which the alga is no longer viable between 60°C and 65°C.

Geothermal environments are well known not only for their high temperature and their extremely acidic or basic pH, but also for their elevated content of toxicants such as arsenic and copper. Among the Cyanidiales, *Cyanidioschyzon* has been shown to influence arsenic cycling at elevated temperatures by oxidizing arsenite As(III) to arsenate As(V), and to methylate arsenic. The ability of this alga to transform arsenic represents a major mechanism for tolerance to high concentration of arsenic in acidic geothermal settings and contributes to the ecological fitness and ability of this red alga to flourish in such surroundings.

Also diatoms have been proved to be thermophilous and acidophilous and are able to survive in a toxic environment. An epipelic community of diatoms inhabits arsenic-rich hydrous ferric oxide mats that coat the sandy substratum of Beowulf Spring, Yellowstone National Park, USA, a strongly acidic (pH < 3) and thermophilous (temperature >50°C) environment with potentially toxic concentrations of dissolved metals. Diatoms are present mainly in the regions of the spring characterized by a temperature of 67°C, brown arsenic-rich mats, and a pH of 2.26. The diatom flora in this area is dominated by a deme within the *Nitzschia thermalis* complex, in association with *N. ovalis*, *Pinnularia acoricola*, and *Eunotia exigua*. The success of this community may be due to low diatom diversity, hence reduced interspecific competition, and absence of predators, coupled to the potential metabolism of toxic metals.

SOME LIKE IT DRY . . .

Crusts can be defined as microbiotic assemblages formed by living organisms and their by-products, creating a complex surface structure of soil particles bound together by organic material. Some crusts are characterized by their marked increase in surface topography, often referred to as pinnacles or pedicles. Other crusts are merely rough or smooth and flat. The process of creating surface topography, or pinnacling, is due largely to the presence of filamentous cyanobacteria and green algae. These organisms swell when wet, migrating out of their sheaths. After each migration, new sheath material is exuded, thus extending sheath length. Repeated swelling leaves a complex network of empty sheath material that maintains soil structure after the organisms have dehydrated and decreased in size.

Algal crusts of desert regions have been suggested to retard soil erosion, which generally includes rain and wind erosion. Although the erodibility of soil with and without crusts has been quantified, only a few studies have been focused on the specific effects of different algae in stabilization of sand dunes. The recovery rate of cryptogamic crusts (i.e., a thin crust made up of mosses, lichens, algae, and bacteria) in natural and artificial conditions has been examined, as well as the effect of the wind regime (including wind force and types), moisture, crust development, soil texture, vegetation coverage, season, and human activity on algal crust integrity. Most algal crust formation in arid areas is initiated by the growth of cyanobacteria during episodic events of available moisture with subsequent entrapment of mineral particles by the mechanical net of cyanobacterial filaments and glue of extracellular slime. Algal crusts are critical to the ecosystem in which they occur. Evidence has shown that they may play important roles in the stabilization of soil surfaces and the improvement of soil structure, contributing significantly to soil fertility of these regions through processes such as nitrogen fixation, excretion of extracellular substances, and retention of soil particles, organic matter, and moisture. Nitrogen fixation by cyanobacteria and lichens (due to their symbiotic cyanobacteria) comprising the crusts is the primary source of nitrogen input in many of the arid ecosystems on a worldwide basis. The fascinating points herein are why and how the algal crusts, only a few millimeters thick, play such important roles, and how the relevant organisms survive and even flourish in such a harsh environment with extreme desiccation, strong radiation, and large fluctuation of temperature.

Systematic investigations of algal crusts conducted in the Tengger Desert (China) have provided data on the vertical microdistribution of cyanobacterial and algal species within samples aged 42, 34, 17, 8, and 4 years. This vertical distribution was distinctly laminated into an inorganic layer with few algae (0.00–0.02 mm), an algae-dense-layer relatively compact and densely inhabited with algae (0.02–1.0 mm), and an algae-sparse layer (1.0–5.0 mm). Owing to extremely high irradiation, the surface of the inorganic layer was the harshest microenvironment of the desert crusts, and therefore was colonized only with the cyanobacteria *Scytonema javanicum*, and *Nostoc flagelliforme*, desiccation-tolerant species possessing high UV screening pigments. These two heterocystous, diazotrophic species were the only algae found at the depth of approximately 0.02–0.05 mm, while around 0.05–0.10 mm, the coccoid green alga *Desmococcus olivaceus* (Trebuxiophyceae, Chlorophyta), characterized by strong resistance to stressful environments, was the dominant species. The biggest algal biovolume was present at 0.10–0.15 mm, with the dominance of *Microcoleus vaginatus* (Cyanophyceae, Cyanobacteria), a sheath-forming and polysaccharide-excreting cyanobacterium capable of stabilizing sand grains. The diversity of algal species was the largest in all the crust samples at the depth of approximately 0.15–0.50 mm. Filamentous (*Anabaena azotica*, *Phormidium tenue*, and *Lyngbya cryptovaginatus*) and unicellular cyanobacteria (*Gloeocapsa* sp. and *Synechocystis pevalekii*), unicellular coccoid green algae (*Chlamydomonas* sp.), *Chlorococcum humicola* (Chlorophyceae), *Chlorella vulgaris* and *Palmellococcus miniatus* (Trebuxiophyceae), diatoms (*Navicula cryptocephala*, *Diatoma vulgare* var. *ovalis* and *Hantzschia amphioxys*), and euglenoids (*Euglena* spp.) were present. Within the range of approximately 0.50–1.00 mm, there were much more green algae and euglenoids than in the other strata. Because the upper 1 mm of the crust was the euphotic zone (i.e., the zone where enough light penetrates for photosynthesis to occur), more than 96% algal biovolume was distributed in this algae-dense layer (0.02–1.0 mm). By

the algae-sparse layer, dramatically reduced irradiance was inadequate for efficient photosynthesis and therefore this layer had only about 4% of the total algal biovolume. At 1.0–2.0 mm, species usually found were *L. cryptovaginatus*, *M. vaginatus*, *P. tenue*, *S. pevalekii*, *N. cryptocephala*, and *H. amphioxys*. At the depth of approximately 2.0–3.0 mm, *P. tenue* was the dominant species together with diatoms, mainly *N. cryptocephala* and *H. amphioxys*. At the depth of approximately 3.0–4.0 mm, only diatoms were present. Existence of a diatom layer at the crust base might be the result of downward seepage of water and the high motility of these algae.

The older the crusts, the nearer to the surface were *Nostoc* sp., *C. vulgaris*, *M. vaginatus*, *N. cryptocephala* and fungi, which might be less resistant to the surface stresses. This might reflect the slow but effective process of algal crust development at early stages, and this process might be beneficial to the transformation from algal crusts to lichen crusts at later stages in consideration of the integration of cyanobacteria and green algae, such as *Nostoc*, with fungi to form lichen.

SELECTED READING

Aponte N.E. and D.L. Ballantine. Depth distribution of algal species on the deep insular fore reef at Lee Stocking Island, Bahamas. *Deep Sea Research Part I: Oceanographic Research Papers*, 48(10), 2185–2194, 2001.

Arrigo K.R., D.K. Perovich, R.S. Pickart, Z.W. Brown, G.L. van Dijken, K.E Lowry et al. Massive phytoplankton blooms under Arctic Sea ice. *Science*, 336(6087), 1408, 2012.

Azúa-Bustos A., C. González-Silva, L. Salas, R.E. Palma, and R. Vicuña. A novel subaerial *Dunaliella* species growing on cave spiderwebs in the Atacama Desert. *Extremophiles*, 14(5), 443–452, 2010.

Ballantine D.L. and N.E. Aponte. An annotated checklist of deep-reef benthic marine algae from Lee Stocking Island, Bahamas (western Atlantic), I. *Chlorophyta and Heterokontophyta. Nova Hedwigia*, 76(1–2), 113–127, 2003.

Becraft E.D., F.M. Cohan, M. Kühl, S.I. Jensen, and D.M. Ward. Fine-scale distribution patterns of *Synechococcus.* Ecological diversity in microbial mats of mushroom spring, Yellowstone National Park. *Applied and Environmental Microbiology*, 77(21), 7689–7697, 2011.

Conen F., J. Leifeld, B. Seth, and C. Alewell. Warming mineralises young and old soil carbon equally. *Biogeosciences Discussions*, 3(4), 489–513, 2006.

De Wever A., F. Leliaert, E. Verleyen, P. Vanormelingen, K. Van der Gucht, D.A. Hodgson et al. Hidden levels of phylodiversity in Antarctic green algae: Further evidence for the existence of glacial refugia. *Proceedings of the Royal Society B: Biological Sciences*, 276(1673), 3591–3599, 2009.

Eiseman N.J. and S.A. Earle. *Johnson-sea-linkia profunda*, a new genus and species of deep-water Chlorophyta from the Bahamas Islands. *Phycologia*, 22(1), 1–6, 1983.

Fujii M., Y. Takano, H. Kojima, T. Hoshino, R. Tanaka, and M. Fukui. Microbial community structure, pigment composition, and nitrogen source of red snow in Antarctica. *Microbial Ecology*, 59(3), 466–475, 2010.

Gattuso, J.P., B. Gentili, C.M. Duarte, J.A. Kleypas, J.J. Middelburg, and D. Antoine. Light availability in the costal ocean: Impact on the distribution of benthic photosynthetic organisms and their contribution to primary production. *Biogeoscience*, 3, 489–513, 2006.

Hobbs W.O., A.P. Wolfe, W.P. Inskeep, L. Amskold, and K.O. Konhauser. Epipelic diatoms from an extreme acid environment: Beowulf Spring, Yellowstone National Park, USA. *Nova Hedwigia Beiheft*, 135, 71–83, 2009.

Jarrett B.D., A.C. Hine, R.B. Halley, D.F. Naar, S.D. Locker, A.C. Neumann et al. Strange bedfellows—A deep-water hermatypic coral reef superimposed on a drowned barrier island; southern Pulley Ridge, SW Florida platform margin. *Marine Geology*, 214, 295–307, 2005.

Johnson Z., M.L. Landry, R.R. Bidigare, S.L. Brown, L. Campbell, J. Gunderson et al. Energetics and growth kinetics of a deep *Prochlorococcus* spp. population in the Arabian Sea. *Deep Sea Research, Part II: Topical Studies in Oceanography*, 46(8–9), 1719–1743, 1999.

Karthikeyan C.V. and G. Gopalaswamy. Studies on acid stress tolerant proteins of cyanobacterium. *International Journal of Biological Chemistry*, 3(1), 1–10, 2009.

Kerney R., E. Kim, R.P. Hangarter, A.A. Heiss, C.D. Bishop, and B.K. Hall. Intracellular invasion of green algae in a salamander host. *PNAS*, 108(16), 6497–6502, 2011.

Krembs C., H. Eicken, and J.W. Deming. Exopolymer alteration of physical properties of sea ice and implications for ice habitability and biogeochemistry in a warmer Arctic. *Proceedings of the National Academy of Sciences*, 108(9), 3653–3658, 2011.

Lass-Flörl C. and A. Mayr. Human protothecosis. *Clinical Microbiology Reviews*, 20(2), 230–242, 2007.

Littler M.M, D.S. Littler, S.M. Blair, and J.N. Norris. Deepest known plant life discovered on an uncharted seamount. *Science*, 1, 57–59, 1985.

Littler M.M, D.S. Littler, S.M. Blair, and J.N. Norris. Deep-water plant communities from an uncharted seamount off from San Salvador Island, Bahamas: Distribution, abundance, and primary productivity. *Deep Sea Research*, 33(7), 881–892, 1986.

Markager S. and K. Sand-Jensen. Requirements and depth zonation of marine macro algae. *Marine Ecology Progress Series*, 88, 83–92, 1992.

Mayorga J., J.F. Barba-Gómez, A.P. Verduzco-Martínez, V.F. Muñoz-Estrada, and O. Welsh. Protothecosis. *Clinics in Dermatology*, 30(4), 432–436, 2012.

McGee D., R.A. Laws, and L.B. Cahoon. Live benthic diatoms from the upper continental slope: Extending the limits of marine primary production. *Marine Ecology Progress Series*, 356, 103–112, 2008.

Mrozińska T., J. Czerwik-Marcinkowska, and M. Webb-Janich. *Basicladia chelonum* (Collins) W.E. Hoffmann et Tilden (Chlorophyta, Cladophorophyceae) from Cuba (Caribbean): New observation of the ultrastructure of its vegetative cells. *Acta Societatis Botanicorum Poloniae*, 78(1), 63–67, 2009.

Oren A., D. Ionescu, M. Hindiyeh, and H. Malkawi. Morphological, phylogenetic and physiological diversity of cyanobacteria in the hot springs of Zerka Ma. *BioRisk*, 3, 69–82, 2009.

Qin J., C.R. Lehr, C. Yuan, X.C. Le, T.R. McDermott, and B.P. Rosen. Biotransformation of arsenic by a Yellowstone thermoacidophilic eukaryotic alga. *Proceedings of the National Academy of Sciences*, 106(13), 5213–5217, 2009.

Reysenbach A.L. and S.L. Cady. Microbiology of ancient and modern hydrothermal systems. *Trends in Microbiology*, 9(2), 79–86, 2001.

Runcie J.W., C.F.D. Gurgel, and K.J. McDermid. In situ photosynthetic rates of tropical marine macroalgae at their lower depth limit. *European Journal of Phycology*, 43(4), 377–388, 2008.

Sansón M., J. Reyes, J. Afonso-Carrillo, and E Muñoz. Sublittoral and deep-water red and brown algae new from the Canary Islands. *Botanica Marina*, 45, 35–49, 2002.

Skinner S., N. FitzSimmons, and T.J. Entwisle. The moss-back alga (Cladophorophyceae, Chlorophyta) on two species of freshwater turtles in the Kimberleys. *Telopea*, 12(2), 279–284, 2008.

Spalding H., M.S. Foster, and J.N. Heine. Composition, distribution, and abundance of deep-water (>30 m) macroalgae in central California. *Journal of Phycology*, 39(2), 273–284, 2003.

Spijkerman E., A. Wacker, G. Weithoff, and T. Leya. Elemental and fatty acid composition of snow algae in arctic habitats. *Frontiers in Microbiology*, 3, 2012.

Su Y., X. Zhao, A. Li, and X. Li, G. Huang. Nitrogen fixation in biological soil crusts from the Tengger Desert, northern China. *European Journal of Soil Biology*, 47(3), 182–187, 2011.

Suutari M., M. Majaneva, D. Fewer, B. Voirin, A. Aiello, T. Friedl et al. Molecular evidence for a diverse green algal community growing in the hair of sloths and a specific association with *Trichophilus welckeri* (Chlorophyta, Ulvophyceae). *BMC Evolutionary Biology*, 10(1), 86, 2010.

Tattersall, G.J. and N. Spiegelaar. Embryonic motility and hatching success of *Ambyostoma maculatum* are influenced by a symbiotic algae. *Canadian Journal of Zoology*, 86, 1289–1298, 2008.

Tumlison R. and S.E. Trauth. A novel facultative mutualistic relationship between bufonid tadpoles and flagellated green algae. *Herpetological Conservation and Biology*, 1(1), 51–55, 2006.

Wagner, D., X. Pochon, L. Irwin, R.J. Toonen, and R.D. Gates. Azooxanthellate? Most Hawaiian black coral contain *Symbiodinium*. *Proceedings of Royal Society B*, 278, 1323–1328, 2011.

Wang G., K. Chen, L. Chen, C. Hu, D. Zhang, and Y. Liu. The involvement of the antioxidant system in protection of desert cyanobacterium *Nostoc* sp. against UV-B radiation and the effects of exogenous antioxidants. *Ecotoxicology and Environmental Safety*, 69(1), 150–157, 2008.

Ward D.M., M.M. Bateson, M.J. Ferris, M. Kühl, A. Wieland, A. Koeppel et al. Cyanobacterial ecotypes in the microbial mat community of Mushroom Spring (Yellowstone National Park, Wyoming) as species-like units linking microbial community composition, structure and function. *Philosophical Transactions of the Royal Society B: Biological Sciences*, 361(1475), 1997–2008, 2006.

Yan-Gui S., L. Xin-Rong, C. Ying-Wu, Z. Zhi-Shan, and L. Yan. Carbon fixation of cyanobacterial–algal crusts after desert fixation and its implication to soil organic carbon accumulation in desert. *Land Degradation & Development*, 24(4), 342–349, 2013.

Zammit G., D. Billi, E. Shubert, J. Kaštovsk, and P. Albertano. The biodiversity of subaerophytic phototrophic biofilms from *Maltese hypogea*. *Fottea*, 11(1), 187–201, 2011.

Zhao J., B. Zhang, and Y. Zhang. Chlorophytes of biological soil crusts in Gurbantunggut Desert, Xinjiang Autonomous Region, China. *Frontiers of Biology in China*, 3(1), 40–44, 2008.

" ... stands out for its in-depth information on structural and mechanical anatomy, with flagella as the most prominent example. The meticulous and elegant drawings of algal apparatuses and their mechanics make it easy to understand complex structures and functions, as well as constitutes another outstanding feature of this book."
—Senjie Lin, Marine Sciences, University of Connecticut, Groton, *The Quarterly Review of Biology*, Vol. 81, December 2006

" ... the authors concentrate on highlighting interesting and illuminating topics, with the idea of inciting the sort of wonder and curiosity that will encourage further outstanding research."
—Willem F. Prud'homme van Reine, *Blumea*, 2006, Vol. 51, No.3

A single-source reference on the biology of algae, **Algae: Anatomy, Biochemistry, and Biotechnology, Second Edition** examines the most important taxa and structures for freshwater, marine, and terrestrial forms of algae. Its comprehensive coverage goes from algae's historical role through its taxonomy and ecology to its natural product possibilities.

The authors have gathered a significant amount of new material since the publication of the first edition. This completely revised second edition contains many changes and additions including the following:

- All revised and rewritten tables, plus new figures, many in color
- A fascinating new chapter: Oddities and Curiosities in the Algal World
- Expanded information on algal anatomy
- Absorption spectra from all algal divisions, chlorophylls, and accessory pigments
- Additional information on collection, storage, and preservation of algae
- Updated section on algal toxins and algal bioactive molecules

The book's unifying theme is on the important role of algae in the earth's self-regulating life support system and its function within restorative models of planetary health. It also discusses algae's biotechnological applications, including potential nutritional and pharmaceutical products. Written for students as well as researchers, teachers, and professionals in the field of phycology and applied phycology, this new full-color edition is both illuminating and inspiring.

K13023

ISBN: 978-1-4398-6732-7
90000
9 781439 867327

CRC Press
Taylor & Francis Group
an informa business
www.crcpress.com

6000 Broken Sound Parkway, NW
Suite 300, Boca Raton, FL 33487
711 Third Avenue
New York, NY 10017
2 Park Square, Milton Park
Abingdon, Oxon OX14 4RN, UK